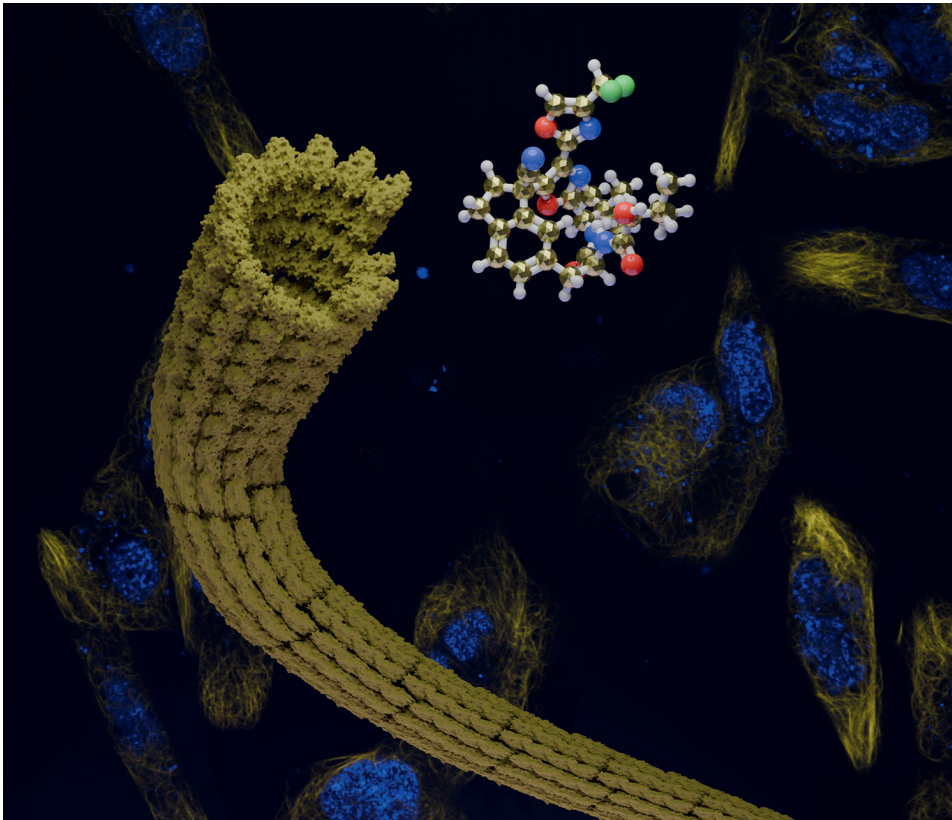# UNIVERSITY OF LATVIA

Viktorija Vitkovska

SIMPLIFIED ANALOGS OF DIAZONAMIDE A AS ANTICANCER AGENTS

Doctoral Thesis

Riga 2024

UNIVERSITY
OF LATVIA

FACULTY OF MEDICINE AND LIFE SCIENCES

Viktorija Vitkovska

SIMPLIFIED ANALOGS OF DIAZONAMIDE A AS ANTICANCER AGENTS

DOCTORAL THESIS

Submitted for the PhD degree in Natural Science
Field of chemistry
Subfield of organic chemistry

Supervisor: Prof., Dr. chem. Edgars Sūna

Riga 2024

The development of the doctoral thesis was carried out at the Latvian Institute of Organic Synthesis from 2019 to 2024.

The thesis comprises the following sections: Introduction, Literature Review, Results and Discussion, Experimental Part, Conclusions and 4 Appendices. Form of the thesis: dissertation in chemistry, organic chemistry.

Supervisor: Prof., Dr. chem. **Edgars Sūna**.

Reviewers:
1) Dr. **Pāvels Arsenjans** (reviewer of the doctoral committee; Latvian Institute of Organic Synthesis, University of Latvia);
2) Prof. Dr. **Marc Nazaré** (Leibniz-Institute for Molecular Pharmacology, Germany).
3) Prof. Dr. **Fredrik Björkling** (University of Copenhagen, Denmark)

The thesis will be defended at the public session of the Doctoral Committee of chemistry, University of Latvia, at 14.00 on November 15, 2024 at the Academic Center of Natural Science of the University of Latvia, Riga, Jelgavas street 1.

The thesis is available at the Library of the University of Latvia, Raiņa blvd. 19.

Chairman of the Doctoral Committee _____/*Edgars Sūna*/

Secretary of the Doctoral Committee _____/*Vita Rudoviča*/

ABSTRACT

Simplified analogs of diazonamide A as anticancer agents. Vitkovska V., supervisor Prof., Dr. chem. Suna E. Doctoral thesis, 94 pages, 15 tables, 56 figures, 97 references, 4 appendices. In English.

Structurally simplified analogs of diazonamide A were developed as anticancer agents by truncation of the synthetically challenging tetracyclic subunit. The thesis comprises three chapters, and each of them focuses on a distinct series of simplified diazonamide A analogs. First chapter covers the synthesis of aliphatic chain-containing macrocycles and describes their *in-vitro* antiproliferative activity against several cancer cell lines and tubulin binding affinity. The second chapter reports the development of oxindole-containing macrocycle series, describing their synthesis, SAR, *in vitro* cell viability data, functional activity (inhibition of tubulin polymerization), and mechanism of action studies. Finally, the third chapter deals with indane-containing series of diazonamide A analogs with particular focus on the development of metabolically stable compounds suitable for *in-vivo* proof-of-concept studies.

Keywords: DIAZONAMIDE A, ANTICANCER AGENTS, MACROCYCLE, TUBULIN, MICROTUBULES.

TABLE OF CONTENTS

ABBREVIATIONS

1A9	–	human ovarian endometrioid adenocarcinoma cell line
A2780	–	human ovarian endometrioid adenocarcinoma cell line
A2058	–	human amelanotic melanoma cell line
A549	–	human lung adenocarcinoma cell line
ADMET	–	Absorption Distribution Metabolism Excretion Toxicity
acac	–	acetylacetone
Alk	–	alkyl
Ali	–	aliphatic
ATP	–	adenosine 5'-triphosphate disodium salt hydrate
9-BBN	–	9-borabicyclo(3.3.1)nonane
B-16	–	mouse melanoma cell line
BME	–	2-mercaptoethanol
Boc	–	*tert*-butyloxycarbonyl
cat.	–	catalyst
Cbz	–	benzyloxycarbonyl
coe	–	cyclooctene
Cy	–	cyclohexyl
DAST	–	diethylaminosulfur trifluoride
dba	–	dibenzylideneacetone
DBU	–	1,8-diazabicyclo(5.4.0)undec-7-ene
DCE	–	1,2-dichloroethane
DCM	–	dichloromethane
DIPEA	–	*N,N*-diisopropylethylamine
DMF	–	dimethylformamide
DMAP	–	4-dimethylaminopyridine
DMP	–	Dess-Martin periodinane
DMSO	–	dimethylsulfoxide
dr	–	diastereomeric ratio
EDC	–	1-ethyl-3-(3-dimethylamino-propyl)carbodiimide
EDTA	–	ethylenediaminetetraacetic acid
EGTA	–	ethylene glycol bis(β-aminoethyl)-*N,N,N',N'*-tetraacetic acid
equiv.	–	equivalents
FACS	–	fluorescence activated cell sorting
FDA	–	Food and Drug Administration
GDP	–	guanosine-5'-diphosphate disodium salt
GI_{50}	–	half-maximal growth inhibition
GM08402	–	human fibroblast primary cells
GTP	–	guanosine 5'-triphosphate
H1299	–	human lung large cell carcinoma cell line
HCC-44	–	human lung adenocarcinoma cell line
HCT-116	–	human colorectal carcinoma cell line
Hek293	–	human embryonic kidney cells
HOBt	–	hydroxybenzotriazole

Hoechst 33342	–	bisbenzimide
HMDS	–	bis(trimethylsilyl)amide
HPLC	–	high performance liquid chromatography
HRMS	–	high resolution mass spectrometer
IC_{50}	–	half-maximal inhibitory concentration
K_d	–	dissociation constant
LC	–	liquid chromatography
LC_{50}	–	half-maximal lethal concentration
MCF-7	–	human invasive breast carcinoma cell line
m-CPBA	–	meta-chloroperoxybenzoic acid
MDA-MB-231	–	human breast adenocarcinoma cell line
MDA-MB-231-LM2	–	human breast adenocarcinoma cell line with lung metastasis
MDA-MB-435	–	human amelanotic melanoma cell line
MiaPaCa-2	–	human pancreatic ductal adenocarcinoma cell line
Ms	–	methanesulfonyl
MS	–	mass spectrometry
MTT	–	3-(4,5-dimethylthiazol-2-yl)-2,5-diphenyltetrazolium bromide
ND	–	not determined
NMR	–	nuclear magnetic resonance spectroscopy
o-tol	–	ortho-tolyl
ODmax	–	maximum optical density
PANC-1	–	human pancreatic ductal adenocarcinoma cell line
PC-3	–	human prostate carcinoma cell line
PI	–	propidium iodide
PIPES	–	piperazine-N,N'-bis(2-ethanesulfonic acid)
ppm	–	parts per million
py	–	pyridine
r.t.	–	room temperature
RNA	–	ribonucleic acid
SDS-PAGE	–	sodium dodecyl sulfate-polyacrylamide gel electrophoresis
SEM	–	standard error of the mean
S_N2	–	nucleophilic substitution reaction
S_NAr	–	nucleophilic aromatic substitution
SPhos	–	2-dicyclohexylphosphino-2′,6′-dimethoxybiphenyl
T_2R-TTL	–	complex of α/β tubulin, stathmin-like domain of RB3 and tubulin tyrosine ligase
TBS	–	*tert*-butyldimethylsilyl
Tf	–	trifluoromethanesulfonyl
TFA	–	trifluoroacetic acid
TFAA	–	trifluoroacetic acid anhydride
TFE	–	2,2,2-trifluoroethanol
TGI	–	total growth inhibition
THF	–	tetrahydrofuran
TMAO	–	trimethylamine N-oxide
Ts	–	toluenesulfonyl
U937	–	human histicytic lymphoma cell line
UPLC	–	ultra-high performance liquid chromatography
UV	–	ultraviolet

INTRODUCTION

According to World Health Organization data in 2020, cancer is leading cause of death worldwide, where every sixth death is from the malignant tumors.[1] Cancer is rapidly emerging disease with more than 2.7 million new cases diagnosed in 2022 in European Union.[2] Growing incidence and high mortality together with increasing multidrug resistance towards cancer therapeutics[3] puts the development of new effective anticancer treatment among top priorities worldwide. In Latvia cancer is second leading cause of death.[4] To this day at the drug market there is not a single anticancer drug known, that does not cause additional health problems or dangerous side effects. Nowadays chemotherapeutics are the most effective means for the treatment of tumors. However, most of the cancer chemotherapeutic agents currently used in clinics develops resistance over time. Therefore, there still is high medical need for effective anticancer chemotherapeutic medicines.

A considerable number of anticancer medications used now in clinics have originated from natural sources. Thus, about one third of small molecule anticancer drugs approved from 1981 to 2019 for clinical use are natural products and natural product derivatives.[5] Among them, microtubule-targeting agents (MTA) such as vinca alkaloids (vinorelbine, vincristine) and taxanes (paclitaxel, docetaxel) have become a standard-of-care treatment in combination chemotherapy regimens.[6]

A notable representation of naturally-occurring MTA is diazonamide A that has been the target of intense and sustained synthetic interest for nearly two decades, when many total syntheses were published.[7–10] First isolated in 1991 from marine ascidian *Diazona angulata* diazonamide A is a marine metabolite that exerts nanomolar cytotoxicity against a range of human tumor cell lines.[11] However, none of the published total syntheses allowed to obtain the compound in sufficient quantities to continue its development as a new potent anticancer drug. Several patents were published after, where structure-activity relationships (SAR) of diazonamide A analogs were studied.[12,13] Later, Harran developed first simplified analog of diazonamide A – DZ-2384 by removing right-hand heteroaromatic macrocycle (Figure 1).[14,15] New compound binds to vinca site of tubulin and exhibits 100-fold lower IC_{50} values against cancer cell lines than diazonamide A.[16] The example of DZ-2384 has opened up a new path towards the potential successful simplification of the core structure of diazonamide A. However, the synthesis of DZ-2384 remains challenging, particularly in relation to the remaining tetracyclic hemiaminal subunit. The simplification of the tetracyclic moiety of diazonamide A has never been studied in detail before.
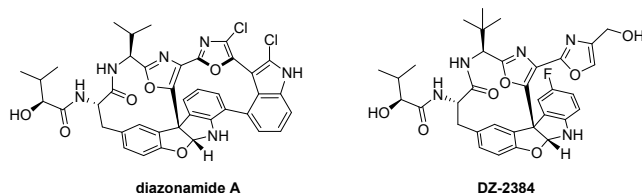

*Figure 1.* **Structures of diazonamide A and DZ-2384**

Aim of the doctoral thesis is the development of structurally simplified analogs of diazonamide A as microtubule targeting agents (MTA) by truncation of the synthetically challenging tetracyclic subunit of diazonamide A.

Objectives of the doctoral thesis

1. Development of methods for the synthesis of simplified diazonamide Analogs;
2. Determination of functional activity (inhibition of tubulin polymerization) and antiproliferative potency of the MTA;
3. Establishing structure-activity relationship (SAR) of the synthesized MTA series;
4. Optimization of ADMET properties for the best analog.

The novelty of the doctoral thesis

For the first time, the highly complex marine metabolite diazonamide A has been structurally simplified by replacing the tetracyclic hemiaminal subunit with chiral quaternary center-containing indolin-2-one or indoline core structures, while retaining its mechanism of action and high antiproliferative activity. As a main result of the thesis, a patent-protected analog was identified for *in vivo* proof-of-concept studies.
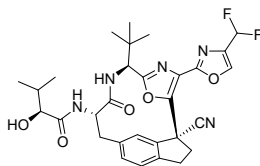
Practical significance of the doctoral thesis

Microtubule-targeting agents (MTAs) such as vinca alkaloids (vinorelbine, vincristine) and taxanes (paclitaxel, docetaxel) have become a standard-of-care treatment in combination chemotherapy regimens. However, MTA are associated with several important drawbacks that are addressed in the Doctoral Thesis research:

1. Since the majority of MTA (vinca alkaloids, taxanes) are of natural origin, they feature a remarkable structural complexity that limits their availability due to highly challenging chemical synthesis and difficulties with large-scale synthesis. We have designed simplified and easy-to-synthesize analogs of natural MTA agent diazonamide And its synthetic analog DZ-2384. The designed series are potent MTA that have a good potential for their development into anticancer medications.
2. Most of clinically used MTA cause severe side-effects such as nausea, vomiting, diarrhea, hair loss and pain. These side-effects are a result of undesired cytotoxicity toward normal cells. A notable feature of diazonamide A and it's synthetic analog DZ-2384 is considerably reduced systemic toxicity observed in animal models. Since the developed macrocycle series represent structural analogs of diazonamide A and DZ-2384, it is expected that the structural similarity may endow the new series with reduced systemic toxicity. Indeed, the best congeners of the developed series feature up to 100-fold selectivity of toxicity against non-malignant cells.
3. Most anticancer drugs tend to develop resistance over time. To overcome this obstacle, there is a high demand for new anticancer drugs. The development of an easy-to-synthesize diazonamide Analog has a potential for the development of new anticancer agent.

Overall, the Doctoral Thesis work provides important contribution to the development of anticancer medication and improvement of human health worldwide.

Research of the doctoral thesis has been published in the following articles and patent applications

1. Vitkovska, V., Zogota, R., Kalnins, T., Zelencova, D., Suna, E. Aliphatic Chain-Containing Macrocycles as Diazonamide A Analogs. *Chem Heterocycl Comp* **2020**, *56* (5), 586–602 (contribution: 85%).
2. Kalnins. T.; Vitkovska, V.; Kazak, M.; Zelencova-Gopejenko, D.; Ozola, M.; Narvaiss, N.; Makrecka-Kuka, M.; Domraceva, I.; Kinens, A.; Gukalova, B.; Konrad, N.; Aav, R.; Bonato, F.; Lucena-Agell, D.; Díaz, J. F.; Liepinsh, E.; Suna, E. Development of Potent Microtubule Targeting Agent by Structural Simplification of Natural Diazonamide. *J. Med. Chem.* **2024**, *67*, 9227–9259 (contribution: 35%).
3. Suna, E.; Kalnins, T.; Kazak, M.; Vitkovska, V.; Narvaiss N.; Zelencova D.; Jaudzems K. Structurally Simplified Diazonamide Analogs as Antimitotic Agents. WO2021130515A1, Jul. 1, 2021.
4. Vitkovska V., Kazak M., Suna E. Macrocyclic Tubulin Polymerization Inhibitors as Anticancer Agents. Application number: PCT/IB2024/059899, Oct. 10, 2024.

Poster presentations at conferences

1. <u>V. Vitkovska</u>, M. Kazak. *Synthesis of Simplified Analogues of Diazonamide A*. Paul Walden Symposium. Poster Session. Riga, Latvia, 2019 (Best poster prize).
2. <u>V. Vitkovska</u>, T. Kalnins, M. Kazak. *Structurally Simplified Diazonamide A Analogs as Anticancer Agents*. Paul Walden Symposium. Poster Session (D-16). Riga, Latvia, 2021 (Best poster prize).
3. <u>V. Vitkovska</u>, E. Suna. *Structurally Simplified Diazonamide A Analogs as Anticancer Agents*. 22nd Tetrahedron Symposium. Poster Session (P1.08). Lisbon, Portugal, 2022.
4. <u>V. Vitkovska</u>, E. Suna. *Structurally Simplified Diazonamide A Analogs as Anticancer Agents*. 17th Belgian Organic Synthesis Symposium. Poster Session (P001). Namur, Belgium, 2022.
5. <u>V. Vitkovska</u>, M. Kazak, T. Kalnins, E. Suna. *Structurally Simplified Diazonamide A Analogs as Anticancer Agents*. Drug Discovery Conference. Poster Session (PO 52). Riga, Latvia, 2022 (Best poster prize).
6. <u>V. Vitkovska</u>, T. Kalnins, M. Kazak, D. Zelencova-Gopejenko, M. Ozola, M. Makrecka-Kuka, E. Liepinsh, E. Suna. *Discovery of Diazonamide A Analogs as Potent Tubulin Polymerization Inhibitors*. 23rd Tetrahedron Symposium. Poster Session (P1.O49). Gothenburg, Sweden, 2023.

Funding

Acknowledgments

1. LITERATURE REVIEW

1.1. Tubulin and Microtubule Targeting Agents

Microtubules play an essential role in every eukaryotic cell as part of the cytoskeleton, providing structural support and shaping the cell. They are also integral to several crucial cellular processes, one of which is cell division. During the cell division, microtubules become the primary components of the mitotic spindle, responsible for separating eukaryotic chromosomes.[17]

Microtubules are composed of α,β-tubulin dimers and microtubule-associated proteins (MAPs). α,β-Tubulin is a globular protein composed of two subunits. Each of the tubulin subunit is characterized by a sequence of approximately 450 amino acids and has a molecular weight of about 55 kD. α- and β-Tubulin monomers combine into heterodimers in a head-to-tail arrangement to form protofilaments (Figure 1.1). The polymerized protofilaments assemble into microtubules. Each microtubule consists of 13 protofilaments and has a diameter of 25 nm. Microtubules are stabilized by MAPs such as Tau, MAP1, MAP2 and MAP4 proteins. Additionally, MAPs assist tubulin dissociation, and also acts as motor proteins for transporting substances along microtubules (e.g., kinesin and dyneins).[18]
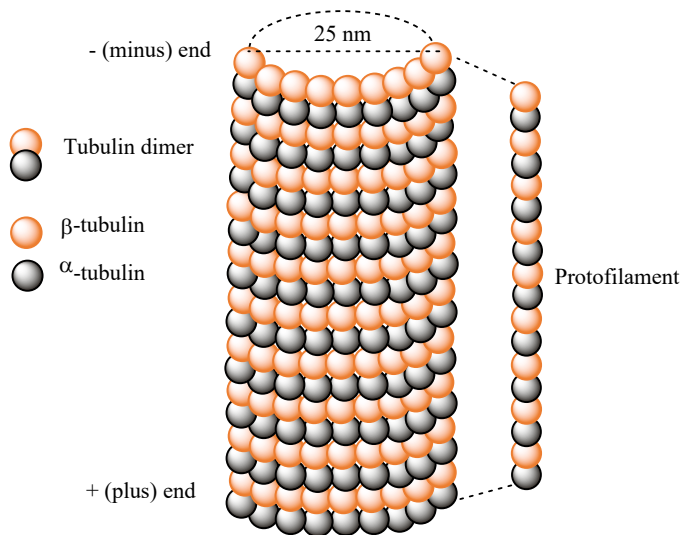
Figure 1.1. **Structure of the microtubule**

Microtubules are highly dynamic polymers and their function can be determined by polymerization dynamics. Tubulin can polymerize from both ends, but the rate of polymerization is not equal. The rapidly polymerizing end is called 'plus end' and the opposite slowly polymerizing end is 'minus end'. During the polymerization,

α- and β-tubulin dimers bind to GTP and assemble at the 'plus end' of microtubules while in their GTP-bound state. The β-tubulin subunit is exposed at the 'plus end' of the microtubule, while the α-tubulin subunit is exposed at the 'minus end'.[19] The GTP molecule bound to the α-tubulin subunit remains non-hydrolyzed throughout the entire polymerization process. In the cell, the 'minus end' is often anchored at microtubule-organizing centers, whereas the 'plus end' is unbound and grows into the cytoplasm. The assembly of protofilaments into microtubules is more efficient at the 'plus end' rather than at 'minus end'. During the assembly, α,β-tubulin subunits are removed from one end and added to the other. This process is called treadmilling. In the meantime, a process, when the length of the microtubule is changing primarily at the 'plus end', is called dynamic instability. This process depends on GTP tubulin cap, that protects microtubule from disassembly. Upon hydrolysis of GTP to GDP occurs at microtubule end, a rapid depolymerization and shrinkage begins. The process from growth to shrinking of microtubule is called 'catastrophe'. The shrinking is stopped by the addition of GTP-bound tubulin to the tip of the microtubule. The new cap protects the microtubule from shrinking in a process called a 'rescue' (Figure 1.2).[18,20]
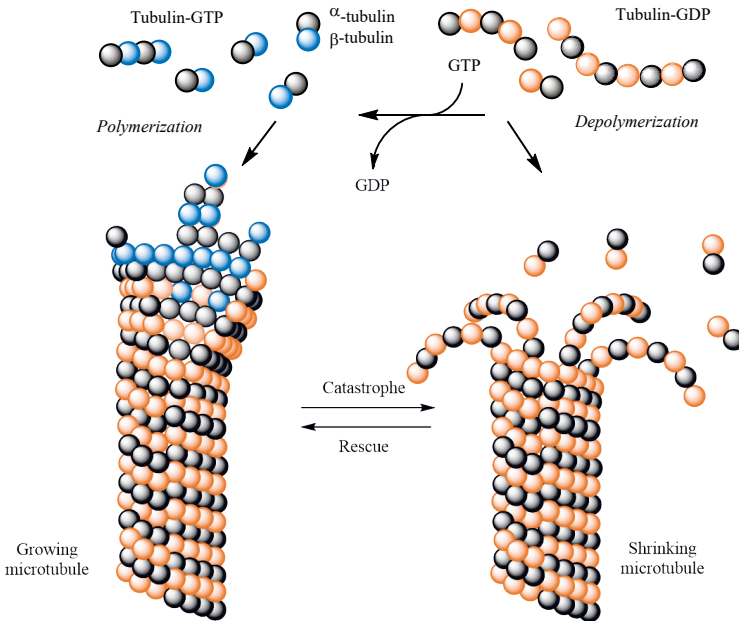
Figure 1.2. **Dynamic instability of the microtubule**

The dynamic instability of microtubules is responsible for reversible mitotic spindle formation during cell division. The mitotic spindle is a self-organized bipolar arrangement of microtubules. The mitotic spindle mainly consists of microtubules, centrosomes at the spindle poles. Chromosomes at the center of the spindle are attached to the microtubules via kinetochores (Figure 1.3). The spindle is organized in a way that the minus end of the microtubule is located in the spindle poles and the plus end is directed towards the center of the spindle, where it overlaps with microtubules from

the opposite poles. Three types of microtubules are formed: astral microtubules (A-MT), kinetochore microtubules (K-MT) and non-kinetochore microtubules (nK-MT). Astral microtubules are positioned away from the spindle. They interact with the cell cortex and control the spindle orientation. Kinetochore microtubules attach chromosomes to the spindle poles moving apart the sister chromatids. Non-kinetochore microtubules provide stability to the spindle. They come from opposing poles of the spindle, but do not bind to the kinetochore during the mitosis (Figure 1.3).[21]
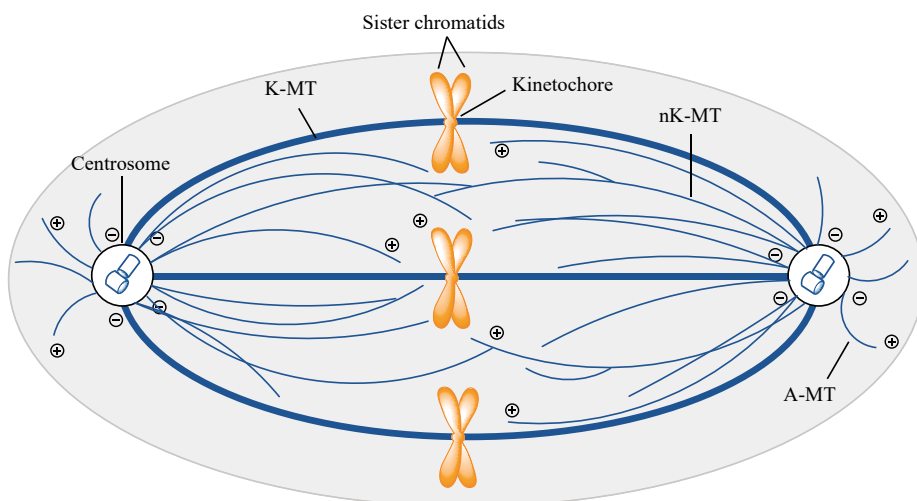
Figure 1.3. **Mitotic spindle**

The mitotic spindle and, in particular, microtubules has long been an attractive target for the development of new drugs, that could interfere with cell division process. Compounds that bind to microtubules and affect their properties and function, are called microtubule targeting agents (MTAs). The first MTAs were vinca alkaloids vinblastine (1961) and vincristine (1963) that were approved by FDA for treatment of lymphomas and several solid tumors.[22] Both drugs bind to the dedicated (vinca) binding site between two tubulin heterodimers (Figure 1.4). Later, additional tubulin binding sites were discovered by studying interaction between tubulin and various natural products such as paclitaxel, colchicine, pironetin, laulimalide and maitansine. Nowadays, 27 distinct binding sites of tubulin have been identified using combined computational and crystallographic fragment screening approach. These findings identify a framework for the design and development of novel MTAs.[23]

The majority of MTAs are natural compounds or their synthetic derivatives. All MTAs are divided into two groups based on their effect on microtubules at high concentrations: microtubule stabilizing agents (MSAs) and microtubule destabilizing agents (MDAs). Both groups bind to tubulin dimer at the specific site and perturb microtubule dynamics leading to cell arrest in mitosis and promotion of apoptotic cell death. However, mechanisms of action of MSAs and MDAs are different. MTAs that bind to the taxane and laulimalide/peloruside site stabilize microtubules, while molecules targeting colchicine, vinca, pironetin or maitansine site destabilize microtubules.
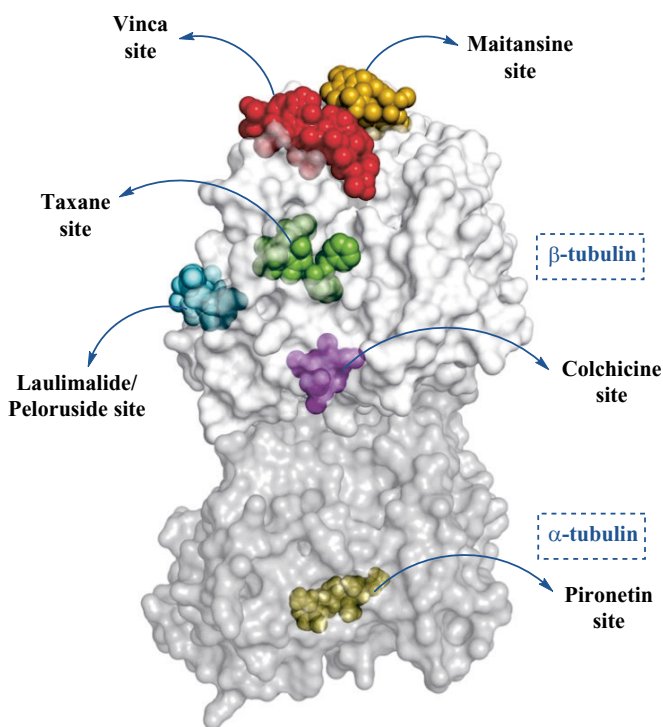
Figure 1.4. **Tubulin binding sites[6]**

MSAs promote microtubule assembly acting as a 'lock' to strengthen interactions across protofilaments in the growing microtubule. As a result, stabilized microtubule lattice is formed, which could not undergo further disassembly. In contrast, MDAs impede microtubule formation. For example, vinca alkaloids such as vinorelbine bind to tubulin site between two heterodimers and acts as a 'wedge', which prevents it from further incorporation into microtubule, or forming ring-like oligomers, which are incompatible with straight microtubule protofilament structure.[6]

Vinca alkaloids bind to tubulin at the site close to the GTP-binding site. This results in increase of microtubule depolymerization leading to the termination of mitotic spindle and initiation of cell apoptosis. The binding of vinca alkaloids to the tubulin depends on the concentration of the drug and leads to different outcomes. At lower concentrations vinca alkaloids inhibit tubulin polymerization, and decrease in microtubule dynamics is observed.[24] At higher concentrations, vinca alkaloids promote formation of oligomers, rings or spirals.[25] At high drug concentrations even precipitation of oligomers may occur. However, the exact concentrations required to achieve either of the effects are not well defined.[26]

Even though MTAs have been broadly used in clinics as chemotherapeutic agents, the treatment with MTAs often is associated with undesired adverse effects and the development of resistance. One of the main side effects of vinca alkaloids is peripheral neuropathy that causes the development of axonal degeneration, neuropathic pain, motor dysfunction, ataxia, and paralysis. To battle side effects, novel drugs were introduced to the clinics including antibody-drug conjugates (ADCs). ADCs improve

the delivery of potent and toxic MTAs, by incorporating antibodies to target specific antigens expressed on cancer cells.[27] Additionally, novel drug delivery systems were developed to overcome drug resistance mechanisms, increase the uptake of the drug or to overcome its low stability. Such drug delivery systems are microspheres, nanoparticles, and liposomes.[28–30] For instance, a liposomal formulation of vincristine (sphingomyelin and cholesterol-based nanoparticles) has been recently approved by FDA[31] to overcome the toxicity limitations of standard vincristine.[32] To overcome resistance, novel MTAs have been administered in combination with other drugs having different mechanism of action, where dosage of MTAs is reduced.[33]

1.2. Determination of Binding Affinity

A robust and reproducible method for the studying of interactions between tubulin and MDAs is a key in drug discovery. When novel MDAs are synthesized, it is advantageous to establish in-house assays to evaluate drug-target interactions and functional effects MDAs induce in tubulin. In recent years, the screening efficiency of new tubulin polymerization inhibitors has been greatly improved.[34] Below we summarized the most frequently used methods to evaluate tubulin polymerization inhibitors.

Potential MDAs could be assessed by the effect on tubulin polymerization, measuring binding affinity to tubulin or observing morphology of microtubules. Screening methods based on the observation of microtubule structure can provide the most direct evidence of changes in microtubule morphology. These methods require specialized equipment, are only qualitative and are often used after other methods mentioned above. Example of those methods are transmission electron microscopy[35,36] and immunofluorescence staining assay.[37] Methods based on binding affinity are most reliable methods for primary screening of potential tubulin polymerization inhibitors.

Isothermal titration calorimetry (ITC)[38] is an indirect method used to study drug-tubulin interactions and determine binding affinity (association constant, K_a), as it allows access to all the thermodynamic parameters of the interaction.[39,40] The interaction of molecules, such as ligand-tubulin binding, typically involves heat exchange. ITC is a method that relies solely on the exchange of heat during the interaction between tubulin and a ligand. Therefore, it serves as a tool to monitor binding of ligand to tubulin independent of spectroscopic changes that may occur during these interactions. During the titration, heat is measured as a function of the molar ratio of interacting molecules. By measuring the heat emitted during injections of the ligand into the tubulin solution, the calorimeter can plot an isotherm of binding after a single one-hour experiment. Fitting experimental data with theoretical model enables one to determine all thermodynamic parameters of interaction: stoichiometry (N), association constant (K_a), enthalpy of binding (ΔH) and calculate free Gibbs energy (ΔG) and entropy of binding (ΔS). A typical titration involved injections of test ligand at time intervals into the sample cell containing tubulin in buffer solution.[41–43] ITC has been used to investigate tubulin interaction with a number of drugs, including vinca alkaloids. For example, it was used to demonstrate that stathmin dramatically increases the affinity of vinblastin to tubulin and vice versa.[44]

Another way, how binding affinity could be determined, are competition experiments, that allows for determination of tubulin binding site and dissociation constant

(K_d) for an inhibitor by using the competitive binding of MDA and corresponding known radiolabeled or fluorescent drug analog.[45] The high-affinity binding sites of tubulin, as discussed earlier (Figure 1.4), are ligand-selective, meaning that many drugs or metabolites with similar structures and physicochemical properties may compete for the same binding site. When two or more drugs are used simultaneously, the competitive binding phenomenon can occur if both bind to the same tubulin binding site. A drug with a high binding affinity may displace a drug with a lower binding affinity from the tubulin binding site.[46] Various methods are known for calculating binding affinity and determining the binding site on tubulin. In addition to X-ray crystallography of the ligand and tubulin complex[47], competition experiments also offer methods for determining the binding site. Competitive binding experiments can also be performed without fluorescent or radiolabeled probes, using known tubulin binders such as paclitaxel, vinblastine, or colchicine. This is done by measuring the concentration of unbound ligand by the LC-MS/MS method to determine tubulin-ligand covalent binding.[48] The method involves measuring the concentration of unbound ligand by LC-MS/MS with the internal standard after incubating the ligand with tubulin, which was previously incubated with a known drug binding to a same binding site.[49]

Turbidity assay is the most employed extracellular method for monitoring tubulin polymerization. It is simple, quantifiable and requires readily available equipment such as UV spectrophotometer. Method is based on occurring turbidity when dimeric tubulin assembles into polymers at the buffered conditions. The turbidity of the solution increases as more insoluble tubulin polymers are formed. As soluble tubulin dimers assemble into polymers, the solution scatters more light, which can be detected through increased optical density (OD) in a spectrophotometer.[50,51] Tubulin polymerization inhibitors typically bind to dedicated sites on tubulin, hindering the assembly of microtubules. This results in disruption of tubulin polymerization and polymers disassemble back into tubulin dimers. To characterize these changes in tubulin polymerization, polymerization curves can be generated (Figure 1.5). Typically, a polymerization curve for ligand free tubulin includes a lag time, a period of net growth, and a steady state (plateau). An increase in the amount of polymerized tubulin is associated with an increase in the maximum slope and plateau of the curve. Thus, the curve serves not only for qualitative analysis of inhibitor binding but also for quantitative analysis of inhibitory activity by measuring the curve's slope. However, when the potent tubulin polymerization inhibitor is added, optical density does not change overtime, as no polymerization occurs.[50]

In a standard polymerization assay, the reagent list includes a buffer system (with Mg^{2+} and GTP), purified active tubulin (amount of polymerization-competent tubulin), and polymerization promoters. These promoters have the capacity to enhance polymerization to achieve greater OD_{max} values for polymerization curves, while using same amount of tubulin in the assay (Figure 1.5).[50] This makes the comparison of different tested inhibitors with similar potency more convenient. Paclitaxel and MAPs are often employed to promote polymerization at concentrations compatible with tubulin concentration used in the assay, given their specific binding sites. Organic osmolytes such as glycerol, glutamate and TMAO can also stimulate polymerization at micromolar to molar concentrations by promoting polymerization by 'molecular crowding' or water-exclusion effects.
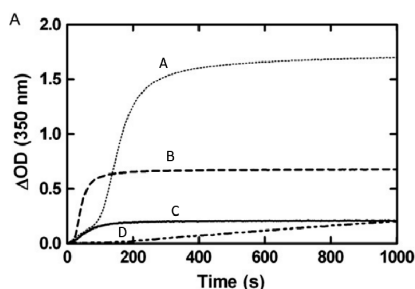
Figure 1.5. **Polymerization curved in the presence of different polymerization promoters (A: 1 M glutamate; B: 1 M TMAO; C: 10 μM paclitaxel; D: 1 M glycerol).** *Reprinted with permission from Elsevier Inc.*

In addition, fluorescence enhancement upon polymerization could be measured by spectrofluorometer and provides sensitive method for measuring tubulin polymerization. Polymerization is followed by fluorescence enhancement due to the incorporation of a fluorescent reporter (such as 4',6-diamidino-2-phenylindole (DAPI)[52,53] into microtubules as polymerization occurs. When tubulin polymerization is induced with GTP, it results in an enhancement of DAPI binding and, consequently, increases fluorescence intensity. DAPI, with a binding site distinct from that of colchicine, vinblastine, or taxol, did not significantly interfere with microtubule polymerization.[50]

Some polymerization protocols use commercially available lyophilized tubulin and it is included also in commercial kits. However, it is important to note that commercial lyophilized tubulin may lose some activity over time or during transportation. Consequently, polymerization assay results may not be reproducible when different batches of commercial tubulin are used, as they may contain a varying amount of active tubulin. Using freshly isolated and purified tubulin is advantageous for polymerization experiments due to its high purity and activity, especially when the protein is used immediately after purification.

Several methods exist for tubulin isolation and purification. Some of them are based on tubulin isolation from mammalian brains (usually porcine or bovine)[54–56] while other methods comprise tubulin expression from mammalian or unicellular eukaryote cells.[56,57] The purification of mammalian-derived tubulin involves homogenizing brain material, followed by GTP-facilitated polymerization-centrifugation-depolymerization cycles. This process capitalizes on tubulin's unique property to form microtubules, which allows for the isolation of soluble tubulin from brain cell membranes and non-MAPs. The resulting solution comprises soluble tubulin along with MAPs, which is then subjected to ion exchange chromatography to remove all remaining MAPs. The purified tubulin can be stored for years as a frozen stock in buffer. Prior to its use, an additional polymerization-centrifugation-depolymerization cycle has to be performed to ensure that only active tubulin is present.[56]

1.3.   Diazonamide A and DZ-2384

Diazonamide A (**1.1**) is a secondary metabolite first isolated from rare marine sponge *Diazona angulata* in 1991 by Fenical *et. al.* The natural product features remarkable

17

in vitro cytotoxicity against carcinoma HCT-116 and melanoma B-16 cancer cell lines (IC$_{50}$ < 20 nM).[11] Diazonamide A (**1.1**) had also showed antiproliferative activity against various human cancer cell lines (1A9, PC-3, MCF-7 and A549) as well as drug resistant tumor cell lines (A2780/AD10 with a multidrug resistant phenotype and 1A9/PTX10 Taxol-resistant cells) with IC$_{50}$ values in the low nanomolar range (2–5 nM).[58] Since its isolation, diazonamide A (**1.1**) had also attracted attention of many researcher groups due to its highly complex molecular structure. Because diazonamide A is difficult to collect from natural sources, sheer effort was directed at its total synthesis. Within a decade since isolation, four total syntheses of diazonamide A were published.[7–10,58,59] Unfortunately, none of them were suitable for preparative scale as they required many synthetic steps and featured low overall yields. The most efficient 19 step synthesis with 1% overall yield was published by P. Haran.[10] However, the synthesis was not scalable, which rendered diazonamide A further development as anticancer agent.

Synthesized milligrams together with tiny amounts obtained from natural sources allowed several groups to study biological activity of diazonamide A and its mechanism of action.[60–62] Flow cytometry analysis of cell cycle showed that diazonamide A causes cell arrest in mitosis by preventing formation of the mitotic spindle.[62] Diazonamide A (**1.1**) also inhibits microtubule assembly in the same way as does marine anticancer peptide dolastatin 10 (Dol-10). Taken together, these findings suggest that diazonamide A interacts with tubulin and acts as MTA. Later, it had been proved that diazonamide A does not compete for binding to tubulin with so-called vinca-site binders such as [3H] dolastatin-10 and also [3H]vinblastine.[62] Further experiments with [3H]diazonamide also suggested that it likely binds to larger aggregates of tubulin rather than α,β-tubulin dimer.[60] These data indicated that diazonamide A may have a different binding site at α,β-tubulin dimer and their mechanism of action in terms of binding site is unclear. On the other hand, G. Wang et al. proposed that diazonamide A interacts with mitochondrial enzyme ornithine δ-amino transferase, an enzyme that is involved in mitotic cell division in human cancer cells.[61] Taken together, the above-mentioned studies generated somewhat controversial data on the mechanism of antitumor activity of diazonamide A (**1.1**).

Later in 2015, P. Haran designed a simplified analog **1.2** of diazonamide A (Figure 1.6) with improved cytotoxicity profile.[15] The removal of indole moiety, the replacement of isopropyl group next to oxazole ring by *tert*-butyl moiety, and also the attachment of fluorine atom to the tetracyclic hemiaminal allowed for enhancement in antiproliferative activity as compared to the parent diazonamide A (**1.1**). In the meantime, the new analog DZ-2384 (**1.2**) lacks right-hand macrocycle and hence it is much easier to synthesize. The total synthesis of DZ-2384 (**1.2**) has been accomplished in 13 steps with 4.8% overall yield. Interestingly, the assembly of tetracyclic hemiaminal moiety

diazonamide A (1.1)   **DZ-2384 (1.2)**
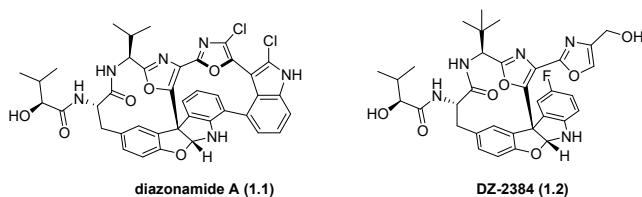
Figure 1.6. **Structures of diazonamide A (1.1) and DZ-2384 (1.2)**

has been achieved by electrochemical macrocyclization that proceeded with rather moderate yields (35%) and low diastereoselectivity (2:1 dr).

A genome-wide RNA interference screen has helped to identify cell cycle and mitosis as potential targets for DZ-2384 (**1.2**) in H1299 cells.[16] SPR experiments provided an evidence that DZ-2384 (**1.2**) interacts specifically with the vinca domain of tubulin.[16] Thus, pre-incubation of tubulin with vinorelbine (vinca alkaloid) led to an inhibition of binding of biotinylated DZ-2384 in a dose-response manner. The vinca-site binding of DZ-2384 (**1.2**) was later confirmed by X-ray crystallographic analysis of a complex between **1.2** and stabilized tubulin tetramer (T$_2$R-TTL).[16] Furthermore, the X-ray data showed that DZ-2384 (**1.2**) binds at the interface between α and β subunits of tubulin (Figure 1.7). Investigations of the binding mode and a superimposed model with vinblastine revealed that these two structures share similar binding interactions at the interdimer interface.[16]
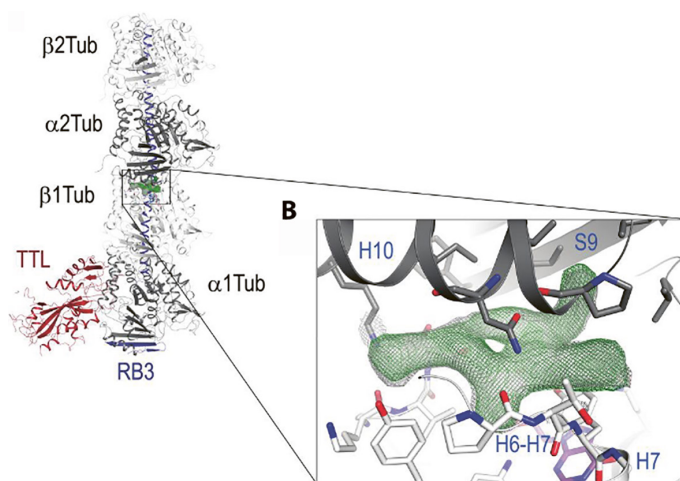
Figure 1.7. **X-ray crystal structure of T$_2$R-TTL complex with DZ-2384 (1.2).**[16] *Reprinted with permission from American Association for the Advancement of Science.*

Synthetic availability of DZ-2384 (**1.2**) allowed for its extensive preclinical testing.[16] Studies of DZ-2384 (**1.2**) in mice xenograft models (subcutaneous injection) revealed that the drug caused complete tumor regression in adenocarcinoma MIAPaCa-2 model within 3 months of treatment. In addition, experimental model of breast cancer MDA-MB-231-LM2 in immunocompromised mice showed regression of all lung metastases at the lowest dose tested, where some animals were tumor-free up to 106 days after initial treatment with DZ-2384 (**1.2**).[16] Importantly, an analysis of the safety profile for DZ-2384 (**1.2**) in mice indicated that it has a much wider safety margin than vinorelbine, a clinically used MTA.

Cumulative peripheral neuropathy is a major toxicity issue for many MTAs used in clinics. An examination of extended DZ-2384 (**1.2**) treatment on nerve function revealed that it had no signs of peripheral neuropathy at concentrations 13 times to 28 times higher than those needed for antitumor activity in mice. The data suggested that DZ-2384 (**1.2**) does not cause neuropathy in rats at doses that are effective in

cancer models.[16] The decreased toxicity of **1.2** was attributed to distinct changes in microtubule dynamics as compared to those when other MTA such as dolastatin 10, eribulin, and vincristine (vinca alkaloid) are used.[16] Specifically, it has been suggested that DZ-2384 (**1.2**) increases the microtubule rescue frequency. More frequent rescues help to rebuild microtubule cytoskeleton and improve survival of DZ-2384-treated non-malignant cells.[16] Overall, the ability of DZ-2384 to interrupt the cell cycle coupled with its remarkable safety profile suggested that sensitivity to the drug was increased in actively dividing cells.[63] DZ-2384 (**1.2**) has entered preclinical studies in 2016, however no results have been published thus far pointing to possibly unsuccessful outcome of the preclinical investigations. This prompted us to initiate a program toward design of simplified diazonamide analogs, for which an in-depth analysis of the SAR around diazonamide A (**1.1**) and DZ-2384 (**1.2**) was instrumental.

1.4. Analogs of Diazonamide A

Several patents were published, where SAR of diazonamide A (**1.1**) and DZ-2384 (**1.2**) have been explored.[12–14] The first patent on diazonamide A (**1.1**) analogs by Harran and co-workers was primarily focused on SAR around (*S*)-2-hydroxy-3-methylbutanoyl moiety in the left-hand macrocycle (position R^1) of diazonamide A (see Figure 1.8).[12] More than 90 diazonamide A analogs were synthesized with linear or branched alkyl chain-containing fragments of different length at the R^1 position and tested against two cancer cell lines A2058 (melanoma) and U937 (lymphoma). In addition, cycloalkyl-, aryl-, amine, carbonate, carbamate, and aryl sulfonyl substituents-containing groups at the R^1 position were also evaluated in the *in-vitro* assay (Figure 1.8). Finally, minor substitution at the indole (R^3, R^4, R^5), the oxazole (R^2) and the tetracyclic hemiaminal (R^6) subunits were also made, however scaffold hopping was not attempted (Figure 1.8).

The SAR study returned the only fragment that would afford similar antiproliferative activity to the (*S*)-2-hydroxy-3-methylbutanoyl substituent in the diazonamide A (**1.1**) structure is 2-hydroxy-2-ethylbutanoyl substituent in compound **1.3d**. It was also found that the introduction of a halogen atom at the R^6 position has no major impact on the antiproliferative effect. Similarly, chlorine at the R^3 position was found to be unnecessary for cytotoxic effect. The addition of hydroxyl (OH) or methoxy (OMe) groups at the R^5 position of the indole fragment also did not alter the antiproliferative effect. Interestingly, a methyl ester at the R^2 position demonstrated cytotoxicity equal to that of halides (Cl, Br) or hydrogen (H). Other synthesized analogs exhibited reduced potency, with IC_{50} values exceeding 100 nM. The explored SAR underscores the importance of the (*S*)-2-hydroxy-3-methylbutanoic acid residue for high cytotoxicity, and indicates that chlorine atoms at the R^2 and R^3 positions, as present in the original diazonamide A (**1.1**) structure, apparently do not contribute to the antiproliferative effect of diazonamide A.[12] The most cytotoxic analogs **1.3a–d** of diazonamide A (**1.1**) are depicted in Figure 1.8.

In the second patent[13] Harran and co-workers described the SAR of analogs, where the removal of the right-hand macrocycle in the diazonamide A (**1.1**) structure was applied. They also explored alternatives to the bioxazole subunit (R^2 position in Figure 1.9). In addition to these structural variations, the authors also briefly surveyed various substituents at the left-hand macrocycle (position R^1) and at the tetracyclic

Figure 1.8. **Diazonamide A (1.1) analogs SAR 1**

hemiaminal moiety (position R^3). Altogether, more than 90 analogs have been synthesized and tested *in vitro* against melanoma A2058 and lymphoma U937 cancer cell lines.

The main finding in the patent is that the presence of right-hand polyaromatic macrocycle including indole subunit is not required for high antiproliferative effect. The replacement of one oxazole ring at position R^2 in the bioxazole subunit by secondary amides, imidazole or oxadiazole led to drop in cytotoxicity, so the bioxazole subunit obviously is important for the antiproliferative activity. In the meantime, the introduction of carboxylic esters at position R^4 of oxazole led to analogs **1.4b–d** with comparable or even superior IC_{50} values (1–77 nM) to those of diazonamide A (57–86 nM). Other tested substituents at position R^4 such as amides, ether, methyl or hydroxymethyl led to significant drop in antiproliferative effect. Introduction of Me substituent at position R^5 at the oxazole did not affect antiproliferative activity of analogs. Additionally, alkyl chains of different lengths as well as aryl moieties were tested as alternatives to (S)-2-hydroxy-3-methylbutanoic acid substituent at the R^1 position of the left-hand macrocycle. As anticipated from the previous patent, (S)-2-hydroxy-3-methylbutanoic acid substituent at the R^1 position was superior, however 2-hydroxy-2-ethylbutanoyl substituent in **1.4a**, (S)-2-hydroxy-3,3-dimethylbutanoyl substituent in **1.4f** and 2-cyclohexyl-2-hydroxyacetyl substituent in **1.4e** showed similar antiproliferative effects, when methyl ester was at position R^4. Finally, aryl, heteroaryl (pyridinyl, indolyl), alkyl and bromine were also tested at the R^3 position. This resulted in significant drop in the antiproliferative effect of the analogs. Introduction of substituents at R^3 position was not necessary for cytotoxic effect of the compound. The analogs **1.4** with the most significant antiproliferative effects are those featuring

an unsubstituted tetracyclic hemiaminal fragment, an R^1 fragment containing an alcohol functional group and various alkyl substituents at the end of the chain, and a bioxazole moiety with carboxylic esters at R^4 and methyl substituent or no substituents at R^5. Other synthesized analogs exhibited reduced potency, with IC_{50} values exceeding 80 nM.[13] The most potent diazonamide A analogs **1.4a–f** are disclosed in Figure 1.9.
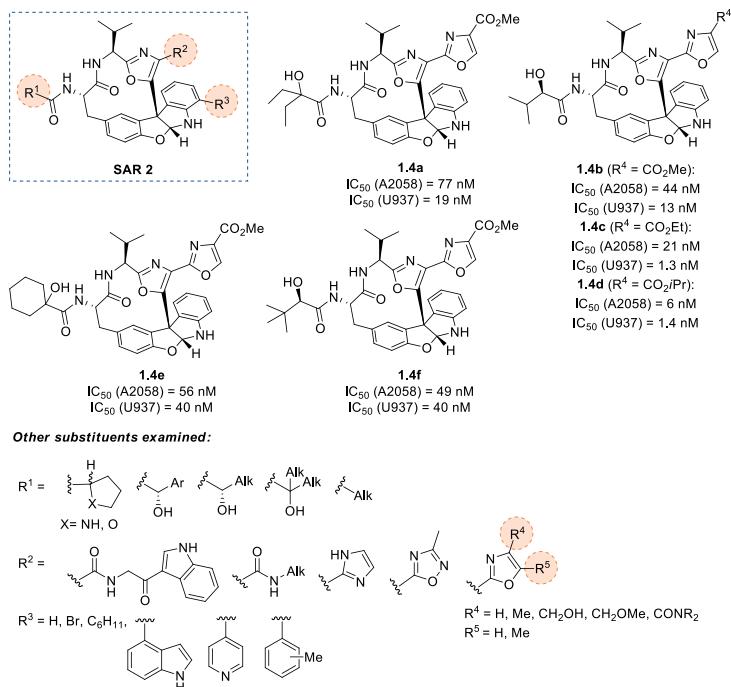

Figure 1.9. **Diazonamide A (1.1) analogs SAR 2**

In the last patent[14] related to SAR of diazonamide A (**1.1**) analogs the inventors extended the SAR presented in the previous patent[13] by introducing substituents at various positions within the structural framework **SAR 3** (Figure 1.10). Subsequently, more than 80 analogs were synthesized, which underwent *in vitro* testing against two cancer cell lines, namely, A2058 (melanoma) and U937 (lymphoma). While the tetracyclic hemiaminal moiety and the macrocyclic core of the structure remained intact, multiple substitutions were made at positions R^1 to R^{10}. Notably, this work marked the first synthesis of 13-membered macrocyclic diazonamide A (**1.1**) analogs, allowing for a comparison with the previously established 12-membered analogs. At the R^1 position, in conjunction with the (*S*)-2-hydroxy-3-methylbutanoic acid fragment, additional aliphatic or hydroxyaliphatic fragments were incorporated, as in the previous patent.[13] While the majority of analogs featured an oxazole moiety at the R^2, some other heterocycles and a phenyl substituent were also introduced at this position. Diverse substitutions were made at the tetracyclic hemiaminal fragment, affecting the R^3, R^8, and R^9 positions. Both amides were substituted separately or in the one analog with methyl groups (R^6 and R^{10}). The R^7 position was also subject to exploration, leading to the introduction of various aliphatic fragments and a benzyl moiety. The primary

focus of this research centered on the substitutions at the R^4 position, where a variety of functional groups, including carboxylic esters, amides, amines, nitriles, and alcohols, were incorporated. Some examples of these substitutions can be found in Figure 1.10.[14]

The compounds with the most potent antiproliferative effects are illustrated in Figure 1.10. In comparison to the findings in the previous patent[13], the cytotoxicity of the synthesized analogs has significantly improved. Analogs with subnanomolar IC_{50} values were obtained, showing that simplification of diazonamide A (**1.1**) structure can result in analogs with improved antiproliferative effect. Interestingly, it was found that the size of the macrocycle is not a critical factor if the stereochemistry of the tetracyclic moiety and quaternary stereogenic center of the macrocycle remain unchanged. The macrocycle **1.5a** showed lowest IC_{50} values among all tested analogs ($IC_{50} <0.1$ nM). Moreover, the introduction of a methyl substituent at the R^{10} position did not diminish the activity of the analog such as in compound **1.5c**. Similarly, the substitution of isopropyl or *tert*-butyl groups at the R^7 positions exhibited equivalent potency. However, the role of substituents at the R^4 position was observed to be of critical significance, as it resulted in a shift of IC_{50} values from subnanomolar to micromolar ranges. The most effective choices among these substituents were compounds **1.5a–c** and **1.2** with methyl ester (**1.5a** and **1.5c**), hydroxymethyl (**1.2**), or cyano (**1.5b**) groups. Fluorine atom at R^3 position also improves the antiproliferative effect. In contrast, other synthesized analogs demonstrated reduced potency, with IC_{50} values exceeding 10 nM.
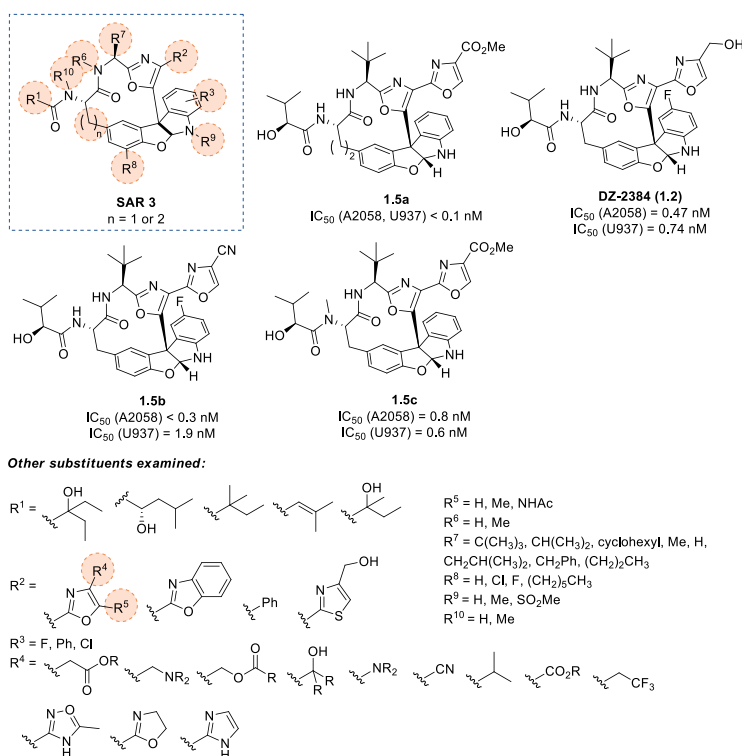
Figure 1.10. **DZ-2384 (1.2) and its analogs SAR 3**

Three patents were published featuring over 250 analogs of diazonamide A, with modifications at different sites of the structure. However, no SAR around the tetracyclic moiety has been studied. Among all the analogs, the lowest IC_{50} values were observed when the analog contained the tetracyclic hemiaminal subunit with a chiral quaternary stereogenic center as well as a bioxazole moiety. As a result, the necessity of the tetracyclic fragment for maintaining high activity against cancer cells remains unknown.

2. RESULTS AND DISCUSSION

The thesis comprises three chapters, and each of them describes a distinct series of simplified diazonamide A analogs. *Chapter 2.1* focuses on aliphatic chain-containing macrocycles and discloses their synthesis, *in-vitro* antiproliferative activity against several cancer cell lines and tubulin binding affinity, measured by isothermal titration calorimetry (ITC) method. *Chapter 2.2* delves into oxindole-containing macrocycle series, and describes their synthesis, SAR, *in vitro* cell viability data, functional activity (inhibition of tubulin polymerization), and mechanism of action studies. Finally, *Chapter 2.3* discloses indane-containing series of diazonamide A analogs, with particular focus on the development of metabolically stable compounds suitable for *in-vivo* proof-of-concept studies.

2.1. Aliphatic Chain-Containing Macrocycles as Diazonamide A Analogs

Synthesis of analog series

The structurally simplified diazonamide A analog **1.2** lacks indole subunit and heteroaromatic macrocycle as compared to the parent natural product **1.1** (see Introduction). Considering further structural modifications, the substitution of the difficult-to-synthesize tetracyclic subunit by less complex linker is highly attractive from the synthetic viewpoint. To verify the importance of the tetracyclic subunit for the binding of cytotoxic agents diazonamide A (**1.1**) and DZ-2384 (**1.2**) to tubulin, a series of diazonamide analogs **2.1–2.4** that feature the replacement of the tetracyclic subunit by aliphatic chain of various length were designed and synthesized (Figure 2.1). Binding energy of the synthesized analogs **2.1–2.4** with tubulin has been measured by ITC assay.
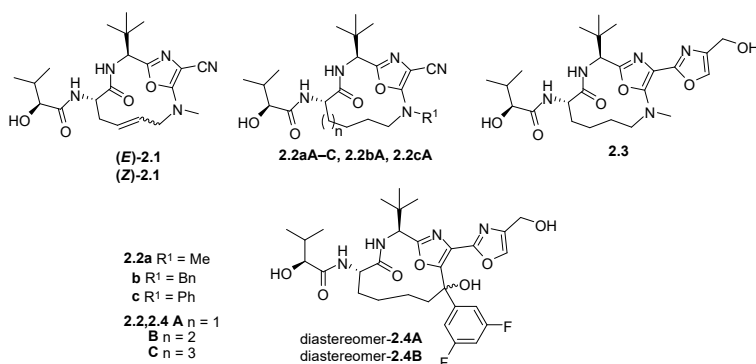

Figure 2.1. **Structures of diazonamide A analogs 2.1–2.4**

The retrosynthetic analysis of diazonamide A analogs **2.2–2.4** is depicted in Figure 2.2. We envisioned that macrocycles **2.5** could be constructed from the parent bisalkene intermediates **2.6** using the ring-closing metathesis (RCM) as the key step. The allyl moieties in the key intermediates **2.6** (X = NR^2) could be installed by amide coupling with chiral unsaturated amino acids and by the C–N bond formation in the S$_N$Ar-type reaction of bromooxazole **2.8** and allyl amines. In addition, the allyl moiety could be also attached to the oxazole subunit in the key intermediate **2.6** (X = C(OH)Ar) by the nucleophilic addition of allyl metal species to ketone **2.9**. The latter is accessible by regioselective lithiation of bioxazole **2.10**,[64] followed by the *in situ* addition of lithiated species to aryl ketones.
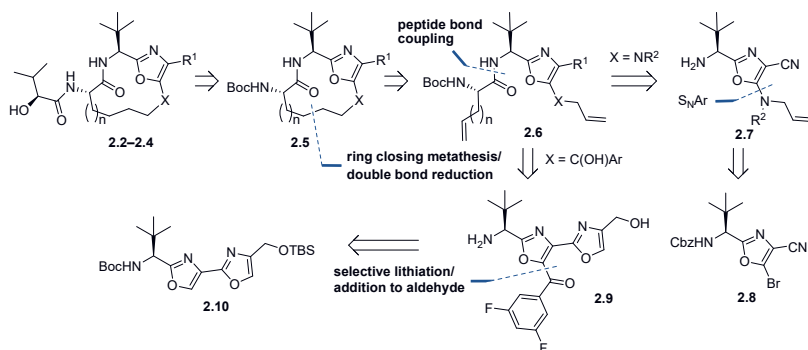

Figure 2.2. **Retrosynthetic analysis of macrocycles 2.2–2.4**

The synthesis of macrocycles **2.2–2.4** commenced by the preparation of bromooxazole **2.8** and amino acids **2.14B** and **2.14C** using literature methods (Figure 2.3). Thus, bromooxazole **2.8** was synthesized from the commercially available Cbz-protected (*S*)-*tert*-leucine **2.11** and 2-aminomalononitrile **2.12**, followed by exchange of amine to bromide in compound **2.13** under the Sandmeyer reaction conditions.[65] The synthesis of unsaturated amino acid **2.14C** started with the formation of ester **2.15A** from the corresponding acid **2.14A**. Subsequent reaction sequence included the hydroboration of ester **2.15A** with 9-BBN, which was followed by Suzuki cross coupling between the in situ generated boronate and vinyl bromide to afford ester **2.15C**. The hydrolysis of the ester moiety afforded acid **2.14C** in good yield.[66] The synthesis of amino acid **2.14B** required the preparation of organozinc species from iodide **2.16**. The intermediate *N*-Boc-protected organozinc species were cross-coupled with allyl bromide in the presence of stoichiometric amounts of copper bromide.[67] The formed aminohexenoate **2.15B** was converted into corresponding acid **2.14B** by saponification with LiOH (Figure 2.3).[68]

Macrocycles **2.1–2.2** were prepared starting from oxazole **2.8** (Figure 2.4). The allylamine moiety was installed in bromooxazole **2.8** or it's *N*-deprotected derivative by S$_N$Ar-type nucleophilic substitution of bromide in the presence of TEA as a general base.[69] For the less nucleophilic aniline, the generation of the corresponding potassium anilide by KHMDS was required to effect the desired nucleophilic substitution of bromide in compound **2.8**. The cleavage of *N*-Cbz protection was accomplished by HBr solution, and higher yield of **2.17** was achieved if morpholine was added to trap the formed benzyl bromide and to avoid the alkylation side reactions. The amide bond formation with *N*-Boc-protected amino acids **2.14A–C** gave the corresponding
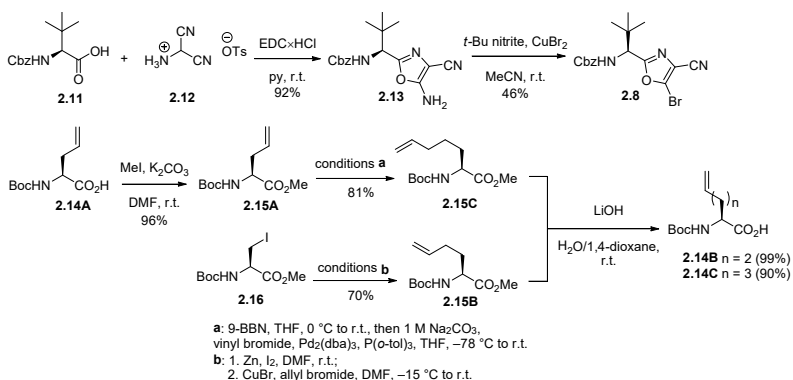
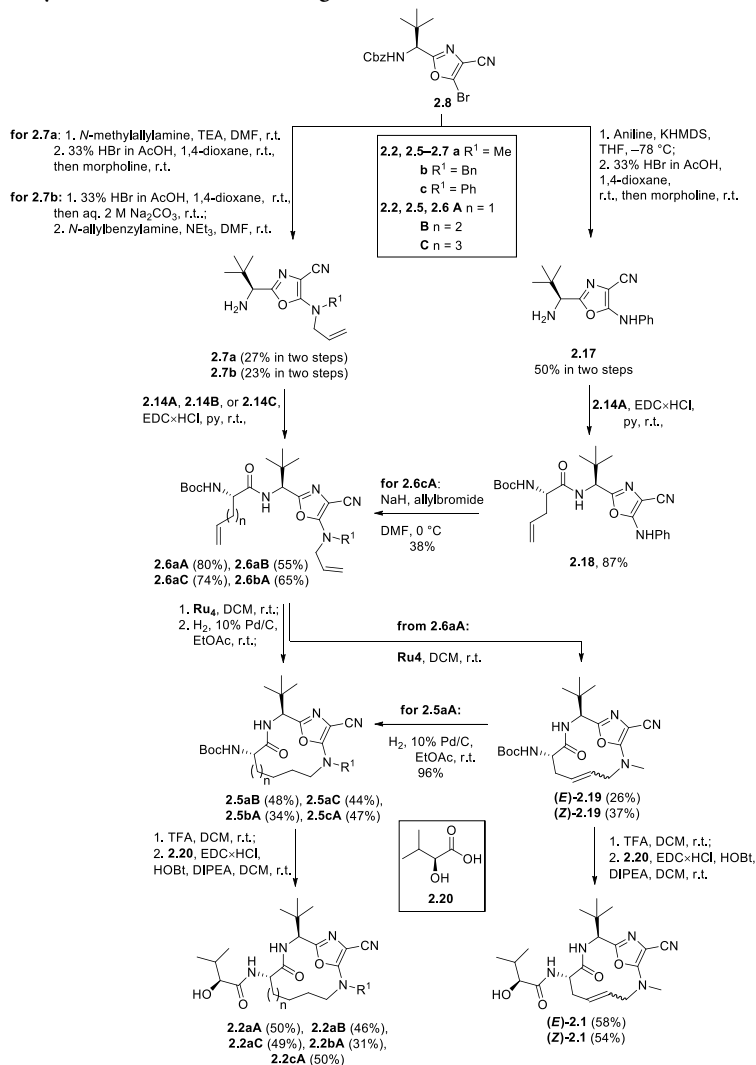**Figure 2.3.** Synthesis of oxazole building block **2.8** and amino acids **2.14B-C**

Scheme conditions (Figure 2.3):

- **2.11** CbzHN–CH(t-Bu)–COOH + **2.12** (H$_3$N$^+$–CH(CN)–CN · OTs$^-$) → EDC×HCl, py, r.t., 92% → **2.13** (CbzHN oxazole, CN, NH$_2$)
- **2.13** → t-Bu nitrite, CuBr$_2$, MeCN, r.t., 46% → **2.8** (CbzHN oxazole, CN, Br)
- **2.14A** (BocHN–CH(CO$_2$H)) → MeI, K$_2$CO$_3$, DMF, r.t., 96% → **2.15A** (BocHN–CH(CO$_2$Me))
- **2.15A** → conditions **a**, 81% → **2.15C** (BocHN CO$_2$Me)
- **2.16** (BocHN–CH(CO$_2$Me)–CH$_2$I) → conditions **b**, 70% → **2.15B** (BocHN CO$_2$Me)
- **2.15C / 2.15B** → LiOH, H$_2$O/1,4-dioxane, r.t. → **2.14B** n = 2 (99%), **2.14C** n = 3 (90%)

a: 9-BBN, THF, 0 °C to r.t., then 1 M Na$_2$CO$_3$, vinyl bromide, Pd$_2$(dba)$_3$, P(o-tol)$_3$, THF, –78 °C to r.t.
b: 1. Zn, I$_2$, DMF, r.t.;
2. CuBr, allyl bromide, DMF, –15 °C to r.t.

Figure 2.4. Synthesis of analogs **2.1** and **2.2aA–C,bA,cA**

Scheme text (Figure 2.4):

2.8 (CbzHN oxazole, CN, Br)

for **2.7a**: 1. N-methylallylamine, TEA, DMF, r.t.
2. 33% HBr in AcOH, 1,4-dioxane, r.t., then morpholine, r.t.

for **2.7b**: 1. 33% HBr in AcOH, 1,4-dioxane, r.t., then aq. 2 M Na$_2$CO$_3$, r.t.;
2. N-allylbenzylamine, NEt$_3$, DMF, r.t.

2.2, 2.5–2.7 a R^1 = Me
b R^1 = Bn
c R^1 = Ph
2.2, 2.5, 2.6 A n = 1
B n = 2
C n = 3

1. Aniline, KHMDS, THF, –78 °C;
2. 33% HBr in AcOH, 1,4-dioxane, r.t., then morpholine, r.t.

2.7a (27% in two steps)
2.7b (23% in two steps)

2.17 50% in two steps

2.14A, 2.14B, or 2.14C, EDC×HCl, py, r.t.

2.14A, EDC×HCl, py, r.t.

for **2.6cA**: NaH, allylbromide, DMF, 0 °C, 38%

2.6aA (80%), **2.6aB** (55%), **2.6aC** (74%), **2.6bA** (65%)

2.18, 87%

1. **Ru$_4$**, DCM, r.t.;
2. H$_2$, 10% Pd/C, EtOAc, r.t.;

from **2.6aA**: **Ru4**, DCM, r.t.

for **2.5aA**: H$_2$, 10% Pd/C, EtOAc, r.t., 96%

2.5aB (48%), **2.5aC** (44%), **2.5bA** (34%), **2.5cA** (47%)

(E)-**2.19** (26%), (Z)-**2.19** (37%)

1. TFA, DCM, r.t.;
2. **2.20**, EDC×HCl, HOBt, DIPEA, DCM, r.t.

2.20

1. TFA, DCM, r.t.;
2. **2.20**, EDC×HCl, HOBt, DIPEA, DCM, r.t.

2.2aA (50%), **2.2aB** (46%), **2.2aC** (49%), **2.2bA** (31%), **2.2cA** (50%)

(E)-**2.1** (58%), (Z)-**2.1** (54%)

dienes **2.6aA**–**CbA**. *N*-Phenyl diene **2.6cA** was prepared by the initial amide coupling of intermediate **2.17** with amino acid **2.14A**, followed by regioselective allylation of the most nucleophilic nitrogen in the deprotonated compound **2.18** (Figure 2.4).

Next, the reaction conditions for the RCM step were optimized using diene **2.6aA** as a model substrate (0.1 M solution in DCM) at 50 °C[70] (Table 2.1). Initial attempts to effect the formation of the desired macrocycle **2.5aA** using **Ru1** catalyst[71] were not successful: incomplete conversion of the starting diene **2.6aA** was observed, and macrocycle **2.5aA** was not formed (entry 1). The lack of the RCM product and the incomplete conversion of diene **2.6aA** pointed to a low catalytic activity of **Ru1** that resulted in slow reaction and concomitant decomposition of the starting material under the tested conditions. Catalyst **Ru2** was also inefficient (entry 2),[72] however it was shown that the catalytic activity of **Ru2** complex could be increased by introduction of a strong electron-withdrawing group in the 2-isopropoxystyrene ligand.[73] Indeed, the nitro-substituted catalyst **Ru3** and the corresponding sulfonamide **Ru4** afforded 39 and 41%, respectively, of the desired macrocycle **2.5aA** together with ca. 20% of unidentified side products with the balance corresponding to 61–63% conversion (entries 3 and 4). We speculated that the metathesis-polymerization side reaction might account for the formation of the side products. Indeed, two-fold increase of the dilution and prolonged reaction time has helped to increase the yield of macrocycle **2.5aA** to 63% isolated yield (entry 5). It should be noted that macrocycle **2.5aA** was formed as a 2:3 mixture of *E*:*Z* isomers that was anticipated for a medium-sized (12-membered) macrocycles.[74,75]

Table 2.1

Optimization of ring closing metathesis reaction conditions
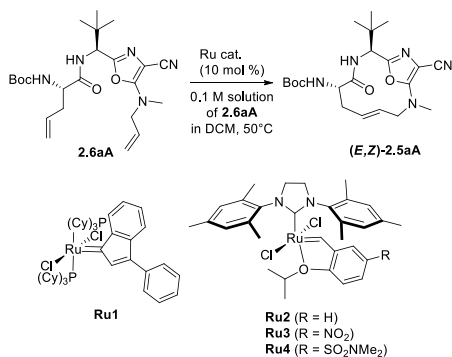
No.	Conditions	Conversion*, %	Yield*, %
1	**Ru1**, 22 h	30	0
2	**Ru2**, 22 h	100	0
3	**Ru3**, 22 h	61	39
4	**Ru4**, 22 h	63	41
5**	**Ru4**, 72 h	83	76 (63***)

* Determined by UPLC-MS.

** 0.05 M solution in DCM.

*** Isolated yield.

With the optimized cyclization conditions in hand, dienes **2.6aA–CbA,cA** were subjected to RCM in the presence of **Ru4** catalyst (5 mol%) (Figure 2.4). Isolation of the RCM products was accomplished only for diene **2.6aA** to afford unsaturated macrocycles (*E*)-**2.19** and (*Z*)-**2.19** as individual isomers after column chromatography. The other macrocyclization products were obtained as mixtures of *E*- and *Z*-isomers and directly converted into saturated macrocycles **2.5aA–C,bA,cA** under Pd-catalyzed hydrogenation conditions. The end-game of the synthesis involved *N*-Boc deprotection, followed by amide bond formation with (*S*)-2-hydroxy-3-methylbutanoic acid (**2.20**) to afford unsaturated macrocycles (*E*)-**2.1** and (*Z*)-**2.1** as well as their saturated analogs **2.2aA–C,bA,cA** (Figure 2.4).

Bioxazole-containing analog **2.3** was prepared by analogy to the synthesis of macrocycles **2.1**, **2.2** (Figure 2.5). Thus, the *N*-Boc deprotection of compound **2.21**[4] was followed by the nucleophilic substitution of bromide with allyl-*N*-methylamine. Subsequent amide coupling with amino acid **2.14A** afforded diene **2.22**. Disappointingly, the optimized RCM conditions (Table 2.1, entry 5) turned out to be unsuitable for the RCM of diene **2.22** as the formation of the desired macrocycle was not observed. We hypothesized that the chelation of catalytically active Ru species by substrate may be responsible for the inhibition of the catalytic cycle. It has been demonstrated that the addition of certain Lewis acids such as Ti(IV) species helps to avoid the deactivation of the Ru catalyst.[76] Indeed, the addition of stoichiometric amounts of Ti(O*i*Pr)$_4$ improved the reaction rate and allowed for the formation of the unsaturated macrocycle, which was converted into the saturated analog **2.23** by Pd-catalyzed hydrogenation. The endgame of the synthesis involved reduction of the ester moiety, *N*-deprotection, and amide bond formation sequence to give macrocycle **2.3** (Figure 2.5).
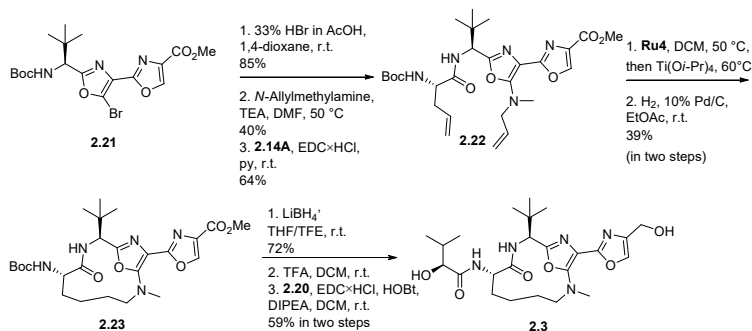

Figure 2.5. **Bioxazole containing synthesis of analog 2.3**

The synthesis of macrocycle **2.4** was started by regioselective lithiation of bioxazole **2.10**,[4] followed by the addition of the lithiated intermediate to 3,5-difluorobenzaldehyde to form alcohol **2.24** as a 1:1 mixture of diastereomers (Figure 2.6). Subsequent oxidation with Dess-Martin periodinane[77] provided ketone **2.25**, which further reacted with allylmagnesium bromide to afford tertiary alcohol **2.26** (1:1 mixture of diastereomers). The cleavage of both *N*-Boc and OTBS protecting groups under acidic conditions was followed by the amide bond formation using acid **2.14A** to give diene **2.27**. The resulting diene was subjected to Ru-catalyzed RCM under the optimized conditions (Table 2.1, entry 5). The unsaturated macrocyclization product was formed as a 2:1 *E:Z* mixture

of isomers in high (82%) yield. The mixture of isomers was hydrogenated to form macrocycle **2.28**. At this point, the stage was set for the *N*-deprotection/amide bond formation sequence. However, the cleavage of *N*-Boc protecting group in macrocycle **2.28** by trifluoroacetic acid resulted in the concomitant trifluoroacetoxylation of the tertiary alcohol-derived transient carbocation. After some experimentation, it was found that the ester side product can be hydrolyzed back to the tertiary alcohol by aqueous LiOH. Subsequent amide bond formation with (*S*)-2-hydroxy-3-methylbutanoic acid (**2.20**) furnished macrocycle **6** as a mixture of diastereomers **2.4A** and **2.4B**. Individual diastereomers were obtained after separation by chromatography, however, the configuration of the quaternary stereogenic center could not be assigned for the individual diastereomers **2.4A,B** (Figure 2.6).
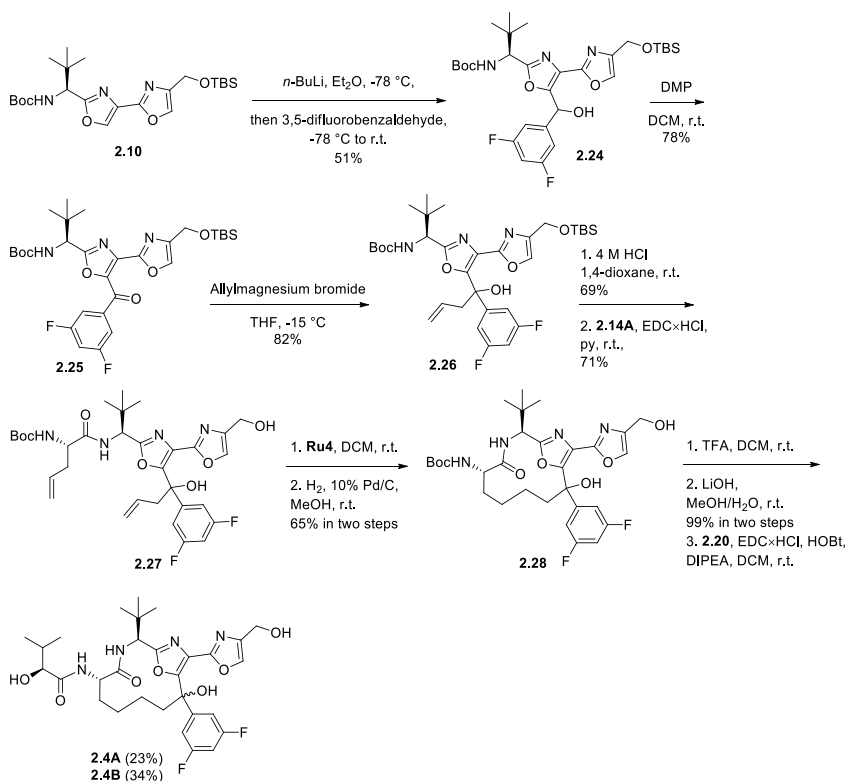

Figure 2.6. **Synthesis of macrocycles 2.4**

Determination of binding affinity and cell viability data[a]

The heat effect of binding (dissociation constants, Kd values) between all synthesized diazonamide A analogs **2.1**–**2.4** and α,β-tubulin tetramer (T_2R-TTL complex) have been measured by ITC method (Table 2.2). No heat effect of the binding has

---

been observed for the most of the synthesized analogs (Table 2.2, entries 1–4, 7, 8). Low micromolar binding was observed for diazonamide A analogs **2.2aC**, **2.2bA** and both diastereomers of compound **2.4** (entries 5, 6, 9, and 10, respectively). However, the measured heat effects of binding are 100-fold lower than that of DZ-2384 (**1.2**) (Kd 0.05 μM). Hence, the ITC results provided strong evidence that the presence of the tetracyclic subunit in the natural product and the synthetic derivative is important for the binding of these antimitotic agents to the α,β-tubulin tetramer.

Table 2.2

Dissociation constants measured by ITC

No.	Compound	Kd, μM
1	(*E*)-**2.1**	No heat observed
2	(*Z*)-**2.1**	No heat observed
3	**2.2aA**	No heat observed
4	**2.2aB**	No heat observed
5	**2.2aC**	2.52±0.83
6	**2.2bA**	3.38
7	**2.2cA**	No heat observed
8	**2.3**	No heat observed
9	**2.4A**	4.10
10	**2.4B**	1.52

All synthesized macrocycles **2.1**–**2.4** were evaluated for their *in vitro* antiproliferative activity against four cancer cell lines (carcinoma PANC-1 and MiaPaCa-2, adenocarcinoma MCF-7 and MDA-MB-231) by the MTT assay with vinorelbine as the positive control. However, none of the compound showed antiproliferative effect at the tested concentration range (up to 100 μM).

In summary, a series of structurally simplified macrocyclic analogs of diazonamide A (**1.1**) and DZ-2384 (**1.2**) have been synthesized in 7 to 9 linear steps from chiral, enantiomerically pure 5-bromooxazole building block. Ruthenium-catalyzed ring-closing metathesis was employed to construct 12–14-membered macrocycles. The addition of stoichiometric amounts of Ti(O*i*Pr)$_4$ has helped to avoid the chelation of catalytically active Ru species by bioxazole subunit-containing RCM substrates. The starting chiral 5-bromooxazole building block was prepared from (*S*)-*tert*-leucine in a straightforward two-step synthesis. Several of the synthesized diazonamide analogs showed weak (low micromolar) binding with α,β-tubulin tetramer (T$_2$R-TTL complex), and the measured heat effects were considerably lower than that of DZ-2384 (**1.2**). Furthermore, cell viability experiments showed no antiproliferative activity of the compounds on several cancer cell lines. These data provided an evidence that the presence of the tetracyclic subunit in diazonamide A (**1.1**) and its synthetic derivative DZ-2384 (**1.2**) is important for the binding to the α,β-tubulin tetramer. We believe that this finding will have implications in the design of diazonamide A analogs as antimitotic agents.

2.2. Oxindole-Containing Simplified Analogs of Diazonamide A

Despite the notable example of successful structural simplification of highly complex diazonamide A (**1.1**) by truncation of the right-hand polyaromatic macrocycle, the presence of difficult-to-synthesize tetracyclic hemiaminal subunit with chiral quaternary stereogenic center in the simplified analog DZ-2384 (**1.2**) renders its synthesis highly challenging, especially on preparative scale. Since the substitution of tetracyclic subunit by aliphatic chain resulted in significant loss of biological activity (Section 2.1), we hypothesized that truncation of the tetracyclic hemiaminal would afford less complex and easier-to-synthesize analogs with improved drug-like properties. Accordingly, we envisioned replacing the tetracycle by chiral quaternary center-containing indolin-2-one core, while retaining both bioxazole subunit and peptide macrocycle. The respective design is exemplified by macrocycles **2.29** and **2.30** (Figure 2.7). Exploration of SAR around macrocycle **2.30** allowed for the development of potent analogs of cytotoxic natural diazonamide A (**1.1**) as shown below.
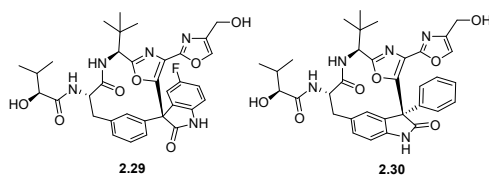

Figure 2.7. **Oxindole-containing analogs 2.29 and 2.30**

Synthesis of analog series

The synthesis of macrocycle series **2.30** capitalized on an approach developed by *Sammakia* and co-workers in their formal total synthesis of diazonamide A (**1.1**), where diastereoselective intramolecular S_NAr-type arylation of 3-aryl indolin-2-one moiety with 5-bromooxazole-4-carbonitrile subunit was employed to create the quaternary center in **2.31** with *S* absolute configuration (Figure 2.8).[78] We realized that the base-mediated diastereoselective macrocyclization with concomitant quaternary center formation would be the most efficient strategy toward **2.32** provided that bromobioxazole subunit in intermediate **2.33** is sufficiently reactive under S_NAr conditions. We also hypothesized that the desired *S* configuration at the quaternary center could be secured by the stereogenic centers in the peptide backbone. The cyclization precursor **2.33** can be readily assembled from 3-substituted indolin-2-one **2.35** and bromobioxazole **2.34**[64] (Figure 2.8). We also envisioned that simplified diazonamide analog **2.29** could be obtained using the same macrocyclization strategy.

The synthesis of the macrocycle **2.30** commenced by Negishi cross-coupling[79] of known 3-phenyl-substituted 5-iodoindolin-2-one **2.36** with freshly prepared alkylzinc iodide **2.37** to afford amino acid ester **2.35** in excellent yield (Figure 2.9). Saponification of the ester was followed by EDC-mediated amide coupling with **2.34** to furnish amide **2.38**. With amide **2.38** in hand, the macrocyclization reaction was addressed. We were pleased to find that bromobioxazole subunit in **2.38** is sufficiently reactive to undergo S_NAr-type substitution of bromine by oxindole enolate (formed *in situ* upon
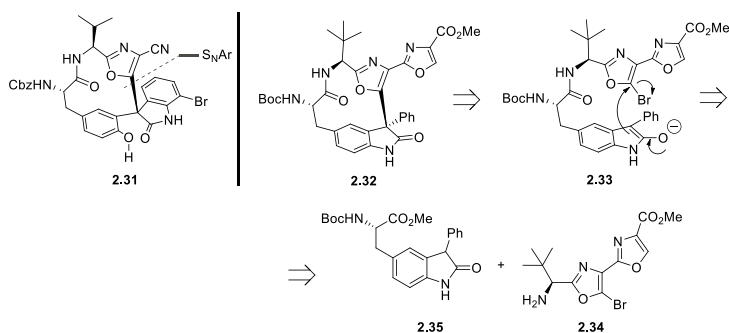
Figure 2.8. **Retrosynthesis of macrocycle 2.32**

the addition of Na$_2$CO$_3$) at elevated temperatures. Under these conditions macrocycle **2.32** was obtained in 65% yield. Notably, the macrocyclization proceeded with excellent diastereoselectivity (99:1 dr; determined by UPLC-UV/MS assay for the crude reaction mixture) and the corresponding 12-membered macrocycle **2.32** was obtained as single diastereomer after purification by flash column chromatography. The desired *S* configuration at the quaternary stereogenic center was confirmed for the macrocycle **2.40** by single crystal X-ray analysis.[b] The reduction of methyl ester in **2.32** to alcohol **2.39** with LiBH$_4$ was followed by two-step sequence comprising *N*-Boc cleavage and amide bond formation with (*S*)-(+)-2-hydroxy-3-methylbutyric acid (**2.20**) to afford the target macrocycle **2.30**.
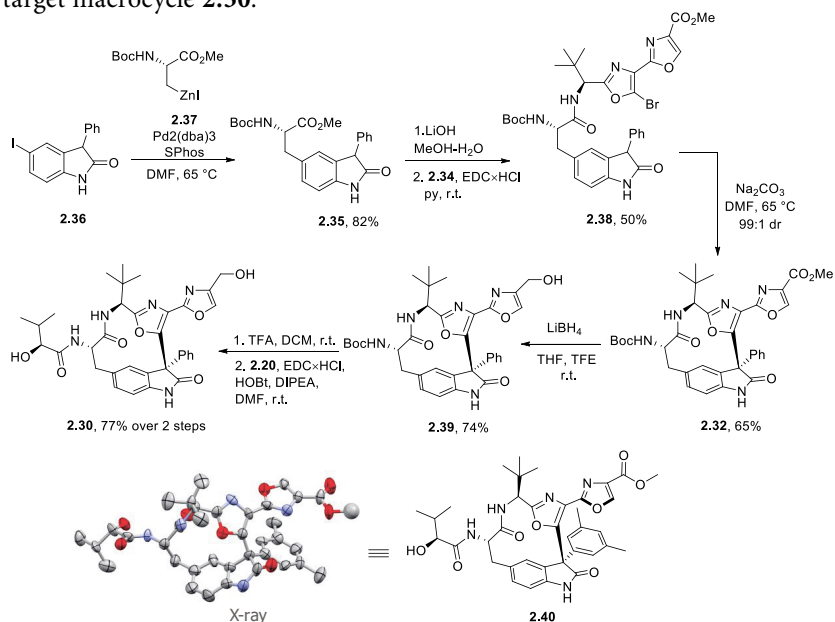

Figure 2.9. **Synthesis of macrocycle 2.30**

---

[b] Synthesis and crystallization of **2.40** was performed by Mihail Kazak and X-ray analysis was performed by Dr. Sergey Belyakov.

Macrocycle **2.29** was also synthesized using *Sammakia*'s approach (Figure 2.10).[78] Accordingly, magnesium phenoxide (prepared from **2.41** and MeMgBr) was added to unprotected isatin **2.42** to furnish adduct **2.43** in 74% yield (1:1 dr). Subsequent conversion of phenol **2.43** into triflate **2.44** by *N*-phenyl-bis(trifluoromethanesulfonim ide) (75% yield) was followed by Pd-catalyzed reductive cleavage of triflate (H₂, Pd/C, TEA, EtOAc) and hydrogenolysis of tertiary alcohol (H₂, Pd/C, MeOH) to deliver ester **2.45** (68%, 1:1 dr). Saponification with LiOH and coupling with bromobioxazole **2.34** provided macrocyclization precursor **2.46** (63% over two steps). The macrocyclization under *Sammakia*'s conditions (Na₂CO₃ as a base in DMF) afforded the desired 12-membered macrocycle **2.47** as 85:15 mixture of diastereomers (69% yield). Major diastereomer was obtained after chromatography, and absolute configuration at the quaternary stereogenic center was assigned *R* by analogy to *Sammakia*'s work. The synthesis endgame involved the reduction of ester moiety in **2.47** to alcohol **2.48**, *N*-Boc cleavage and amide bond formation with carboxylic acid **2.20**.
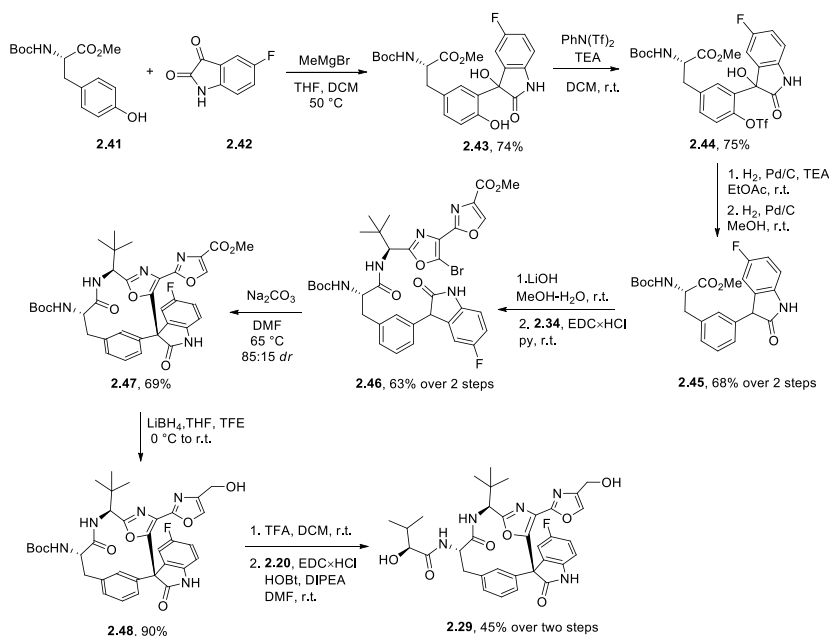

Figure 2.10. **Synthesis of macrocycle 2.29**

Antiproliferative potency of the two synthesized macrocycles **2.29** and **2.30** was tested *in vitro* against several cancer cells lines: carcinoma PANC-1 and MiaPaCa-2, adenocarcinoma MCF-7 and MDA-MB-231 by the MTT assay with vinorelbine (VNB) as assay positive control (see Table 2.3). Macrocycles **2.29** and **2.30** turned out to be several orders of magnitude less potent than vinorelbine against selected cancer cell lines (entries 2,3 vs. 1, Table 2.3). However, macrocycle **2.30** possessed slightly higher antiproliferative activity against MiaPaCa-2 and MCF-7 cancer cell lines than compound **2.29** (entry 3 vs. 2), and therefore the oxindole-bearing macrocycle **2.30** was chosen for further development and SAR studies.

34

Table 2.3

Cell viability data[c]

entry	cmpd	GI$_{50}$, μM			
		PANC-1	MiaPaCa-2	MCF-7	MDA-MB-231
1	VNB	0.00303 ± 0.00038	0.000789 ± 0.000034	0.00385 ± 0.00035	0.00450 ± 0.00042
2	**2.29**	>100	45 ± 9	96 ± 6	>100
3	**2.30**	68 ± 6	20 ± 5	16 ± 4	95 ± 11

SAR studies around macrocycle **2.30** commenced by variation of substituents at oxazole substituent R^3 taking advantage of methyl ester moiety at the bioxazole sub-unit in **2.32** that is well-suited for various synthetic transformations (Figure 2.11). As a result, analogs **2.49–2.65** with various functional groups at the oxazole were synthesized. *In-vitro* antiproliferative activity (GI$_{50}$ values) against four cancer cell lines (PANC-1, MiaPaCa-2, MCF-7 and MDA-MB-231) was used as the readout.
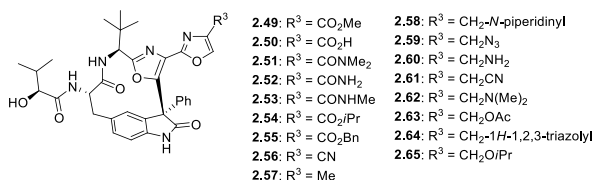

Figure 2.11. **Analogs 2.49–2.65**

Accordingly, methyl ester **2.49** was obtained from macrocycle **2.32** after *N*-Boc deprotection, followed by amide bond formation with acid **2.20**. Next, the saponification of the ester in **2.49** afforded carboxylic acid **2.50**, that was further converted into amide **2.51**. In the meantime, direct aminolysis of ester **2.49** afforded amides **2.52** and **2.53**. Esters **2.54** and **2.55** were also obtained from **2.49** by titanium iso-propoxide-mediated transesterification (Figure 2.12). Aminolysis/amide dehydratation sequence allowed for the synthesis of cyanobioxazole **2.66** from ester **2.32**. Subsequent TFA-mediated *N*-Boc cleavage and amide bond formation with acid **2.20** yielded cyano-bioxazole **2.56**.

The reduction of methyl ester to hydroxymethyl intermediate and subsequent mesylation afforded key intermediate **2.67** that was used in the synthesis of analogs series **2.58–2.63** (Figure 2.13). Thus, methylene-bridged piperidine, azide, dimethyl-amine, cyano and acetoxymethyl-moieties were installed in one step from mesylate **2.67** under S$_N$2 reaction conditions to afford macrocycles **2.68–2.72**. Subsequent TFA-mediated *N*-Boc cleavage and amide bond formation with acid **2.20** yielded *N*-piperidinylmethylene-oxazole **2.58**, azidomethylene-oxazole **2.59**, cyanomethyl-ene-oxazole **2.61**, dimethylaminomethylene-oxazole **2.62**, acetoxymethyly-oxazole **2.63** and in moderate yields. Hydrogenation of azide **2.59** afforded aminomethyl-ene-oxazole **2.60** (Figure 2.13).

---

[c] Cell viability experiments in this section were performed by Dr. Ilona Domraceva.
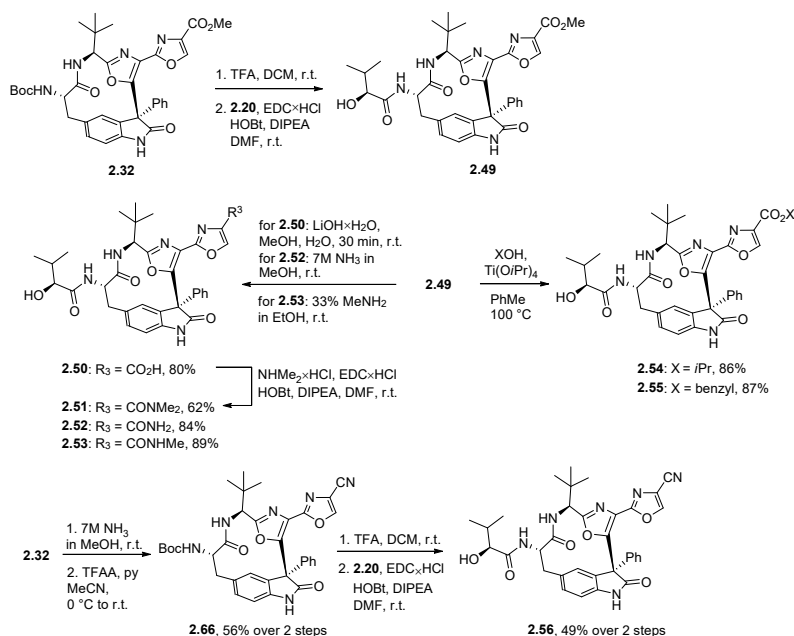
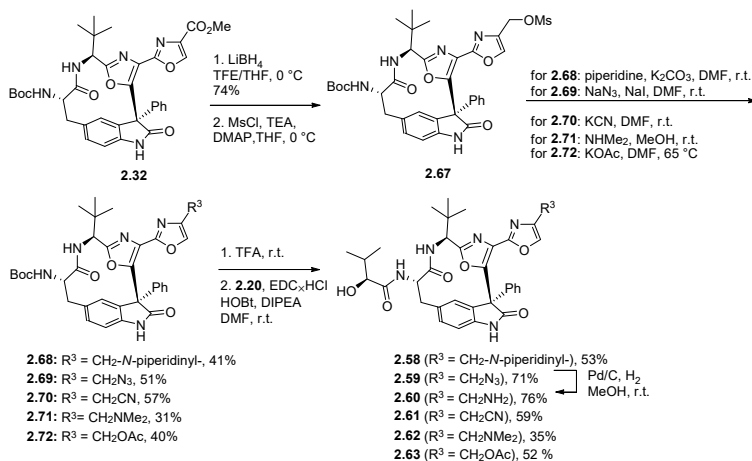*Figure 2.12.* **Synthesis of macrocycles 2.49–2.56**

Figure 2.13. **Synthesis of amines 2.58, 2.60 and 2.62, azide 2.59, nitrile 2.61 and ester 2.63**

Additional diazonamide analogs **2.57**, **2.64** and **2.65** were also obtained (Figure 2.14). Thus, the reduction of mesylate **2.67** with sodium borohydride at elevated temperature afforded methyl-substituted bioxazole **2.73**. Tetrazole fragment-containing macrocycle **2.74** was obtained from azide **2.69** under Cu-catalyzed „click" reaction conditions. Alkylation of primary alcohol **2.39** with isopropyl iodide under basic reaction conditions yielded ether **2.75**. *N*-Boc deprotection and amide bond formation with carboxylic acid **2.20** gave macrocycles **2.57**, **2.64** and **2.65** (Figure 2.14).
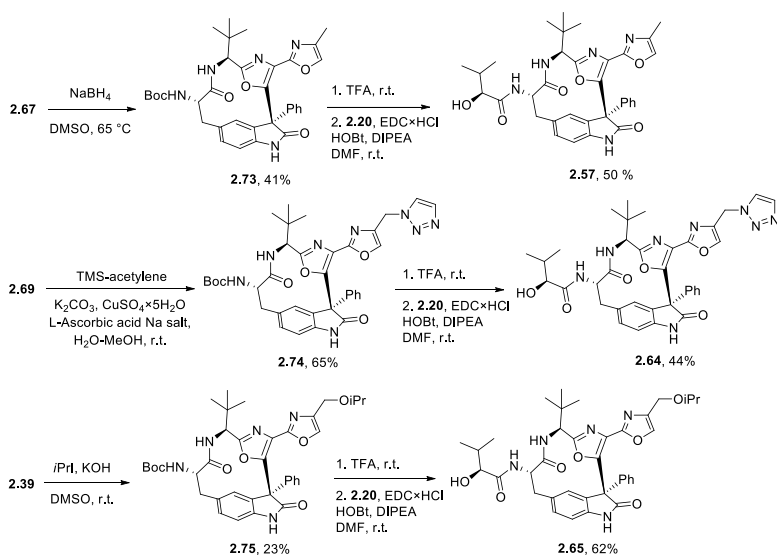
Figure 2.14. **Synthesis of analogs 2.57, 2.64 and 2.65**

Antiproliferative activity of macrocycles **2.49–2.65** is summarized in Table 2.4. The compounds with the highest antiproliferative effect tuned out to be methyl ester **2.49**, isopropyl ester **2.54** and benzyl ester **2.55** (entries 2, 6 and 8) with GI_{50} values in submicromolar range. Antiproliferative effects of cyanobioxazole **2.56**, azidomethylbioxazole **2.59** and acetoxymethylbioxazole **2.63** (entries 9, 12 and 16) were similar with GI_{50} values in the low micromolar range. The rest of the tested compounds possessed no antiproliferative effect or antiproliferative activity in micromolar range. Amides **2.51–2.53**, amines **2.58**, **2.60**, **2.62**, carboxylic acid **2.50**, cyanomethyl-analog **2.61**, tetrazole **2.64** and ether **2.65** at the oxazole (R^3) provided macrocycles with low or no antiproliferative effects.

Table 2.4

Cell viability data
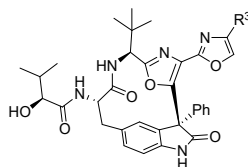
entry	cmpd	R^3	GI_{50}, µM			
			PANC-1	MiaPaCa-2	MCF-7	MDA-MB-231
1	VNB	–	0.00324 ± 0.00031	0.000765 ± 0.000039	0.00411 ± 0.00045	0.00422 ± 0.00032
2	**2.49**	CO_2Me	12 ± 2	0.67 ± 0.05	1.2 ± 0.3	8 ± 2
3	**2.50**	CO_2H	>100	38 ± 3	49 ± 1	93 ± 11
4	**2.51**	$CONMe_2$	>100	56 ± 3	74 ± 13	99 ± 1

entry	cmpd	R³	GI₅₀, µM			
			PANC-1	MiaPaCa-2	MCF-7	MDA-MB-231
5	**2.52**	CONH₂	>100	>100	98 ± 2	99 ± 1
6	**2.53**	CONHMe	>100	89 ± 13	44 ± 8	88 ± 5
7	**2.54**	CO₂iPr	6.0 ± 2.1	0.36 ± 0.03	0.42 ± 0.05	0.77 ± 0.04
8	**2.55**	CO₂Bn	1.17 ± 0.06	0.15 ± 0.01	0.26 ± 0.11	2.1 ± 0.5
9	**2.56**	CN	23 ± 3	1.9 ± 0.4	2.2 ± 0.1	6.1 ± 0.3
10	**2.57**	Me	39 ± 4	6.5 ± 0.9	12 ± 2	78 ± 4
11	**2.58**	CH₂-N-piperidinyl	>100	>100	>100	99 ± 2
12	**2.59**	CH₂N₃	42 ± 5	9.1 ± 1.3	6.7 ± 0.4	25 ± 3
13	**2.60**	CH₂NH₂	>100	>100	>100	>100
14	**2.61**	CH₂CN	80 ± 6	8 ± 2	20 ± 4	47 ± 6
15	**2.62**	CH₂NMe₂	>100	>100	>100	>100
16	**2.63**	CH₂OAc	39 ± 2	2.1 ± 0.2	3.7 ± 0.3	39 ± 3
17	**2.64**	CH₂-1H-1,2,3-triazolyl	>100	>100	>100	>100
18	**2.65**	CH₂OiPr	>100	51 ± 3	43 ± 6	>100

Next, we briefly explored SAR in the peptidic part of the macrocycle by introducing various carboxylic acids possessing both longer and shorter alkyl chains (Figure 2.15). This was achieved by an initial TFA cleavage of N-Boc protecting group in macrocycle **2.32**, followed by amide bond formation with alkyl carboxylic acid **2.76a**, hydroxyl carboxylic acids **2.76c-e** and N-Cbz-protected amino acid **2.76b**. N-Cbz amine in **2.77b** was then deprotected under hydrogenation reaction conditions to give amino acid **2.78**. Since methyl ester **2.49** exhibited high antiproliferative potency compared to other tested functional groups at R³ position and was easily accessible among other active carboxylic esters (R³ = CO₂iPr, CO₂Bn), we have selected macrocycle **2.32** as our starting material.
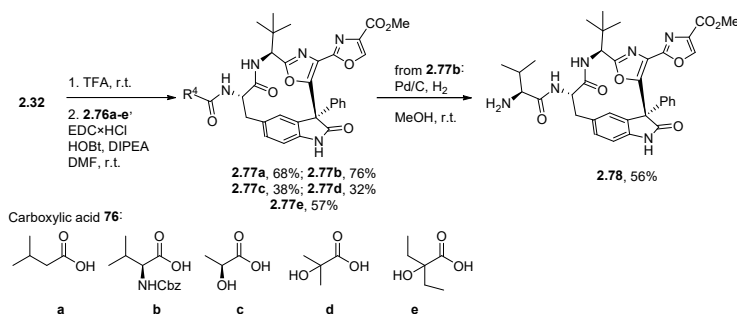

*Figure 2.15.* **Synthesis of analogs 2.77 and 2.78**

All synthesized compounds in Figure 2.15 were tested against four cancer cell lines and the results were depicted in Table 2.5. The compound with the lowest GI₅₀ value was **2.77e** (entry 6) with diethyl group and no stereocenter at the tertiary alcohol

fragment. Shorter alkyl chain- carrying macrocycles **2.77c–d** (entries 4 and 5) showed no antiproliferative effect. Macrocycle **2.77a** bearing alkyl chain and amino-substituted macrocycle **2.78** showed similar moderate antiproliferative activity (entries 2 and 3, respectively). However, none of the synthesized analog were superior to the analog **2.49** with (*S*)-2-hydroxy-3-methylbutanoic fragment at R^4 position (Table 2.4, entry 2) originally present in diazonamide A (**1.1**) structure.

Table 2.5

Cell viability data
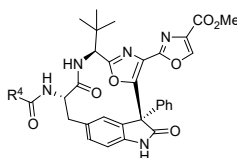
entry	cmpd	R^4	GI$_{50}$, µM			
			PANC-1	MiaPaCa-2	MCF-7	MDA-MB-231
1	VNB	–	0.00308 ± 0.00029	0.000772 ± 0.000037	0.00389 ± 0.00041	0.00459 ± 0.00047
2	**2.77a**		32 ± 3	8.8 ± 0.8	10 ± 2	98 ± 5
3	**2.78**		33 ± 3	8.4 ± 0.6	8.7 ± 0.8	96 ± 5
4	**2.77c**		>100	>100	>100	>100
5	**2.77d**		>100	>100	>100	>100
6	**2.77e**		65.8 ± 9.5	3.33 ± 0.33	9.31 ± 2.31	19.9 ± 1.0

Finally, SAR studies modifying substituents at the quaternary stereocenter were performed. A range of substituents with different steric demands were introduced at quaternary stereogenic center, including sterically small primary alkyl substituents such as methyl and ethyl groups as well as more hindered benzyl and isopropyl moieties (Figure 2.16). Macrocycles **2.79a,b** contain a hydrogen bond donor (N-H) at the oxindole nitrogen instead of a hydrogen bond acceptor (oxygen atom) as found in the tetracyclic hemiaminal moiety of the diazonamide A. To avoid the presence of hydrogen bond donor, *N*-methyl-substituted macrocycles **2.79c–f** were synthesized. We envisioned that the two series should help to determine influence of the hydrogen bond donor on binding to tubulin and, consequently, antiproliferative activity (Figure 2.16).
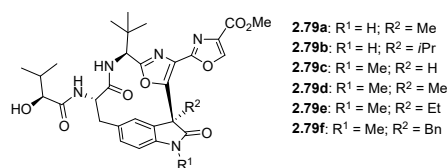
2.79a: $R^1 = H$; $R^2 = Me$
2.79b: $R^1 = H$; $R^2 = iPr$
2.79c: $R^1 = Me$; $R^2 = H$
2.79d: $R^1 = Me$; $R^2 = Me$
2.79e: $R^1 = Me$; $R^2 = Et$
2.79f: $R^1 = Me$; $R^2 = Bn$

Figure 2.16. **Analogs 2.79a–f**

The synthesis of macrocycles **2.79a–b** required an access to 3-substituted 5-iodoindolin-2-ones **2.81a–b** that were prepared by the addition of Grignard reagent to unprotected isatin **2.80**, followed by reductive deoxygenation using previously described methods[80,81] (Figure 2.17). To avoid the need of excess Grignard reagent due to the presence of the acidic N-H, 5-iodoisatin **2.80** was deprotonated with NaH prior to the Grignard addition. Formation of the anion also prevented addition of the Grignard to the carbonyl moiety of the amide and made the reaction more selective. Then, the freshly prepared Grignard reagent was added to the anion, forming aryl- or alkyl-substituted tertiary alcohols. The latter were then reduced in the presence of stoichiometric tin(II) chloride to alkyl-oxindoles **2.81a–b**. 5-Iodo-1-methyl-oxindole **2.81c** was obtained by *N*-alkylation of oxindole followed by reduction of ketone with hydrazine hydrate[82] (Figure 2.17).
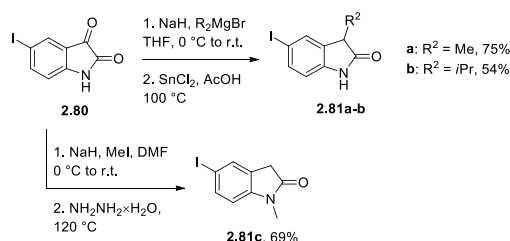

Figure 2.17. **Synthesis of oxindoles 2.81 from isatin 2.80**

The synthesis of the macrocycles **2.79a–c** commenced by Negishi cross-coupling[43] of 3-alkyl-substituted 5-iodoindolin-2-ones **2.81a–c** with freshly prepared alkylzinc iodide **2.37** to afford amino acid esters **2.82a–c** in good yields (Figure 2.18). Saponification of the methyl ester moiety was followed by EDC-mediated amide coupling with **2.34** to furnish amides **2.83a–c**. With amides **2.83a–c** in hand, the macrocyclization reaction was carried out. The S_NAr-type substitution of bromine by oxindole enolate at elevated temperatures in the presence of Na_2CO_3 afforded macrocycles **2.84a–c** in high yields and high diastereoselectivity (99:1 dr for **2.84a,b** and 93:7 dr for **2.84c**). Since *S* configuration at the quaternary stereogenic center was confirmed for the macrocycle **2.40** by single crystal X-ray analysis (Figure 2.9), *S* configuration was assigned by analogy for all macrocycles **2.84a–c**. The latter were converted into target structures **2.79a–c** in a two-step sequence comprising *N*-Boc cleavage and amide bond formation with carboxylic acid **2.20**.

40

The highly diastereoselective intramolecular S$_N$Ar-type arylation of oxindoles **2.83a–c** prompted us to examine the C-alkylation of macrocycle **2.84c** as a convenient approach to the late-stage formation of quaternary stereogenic center.
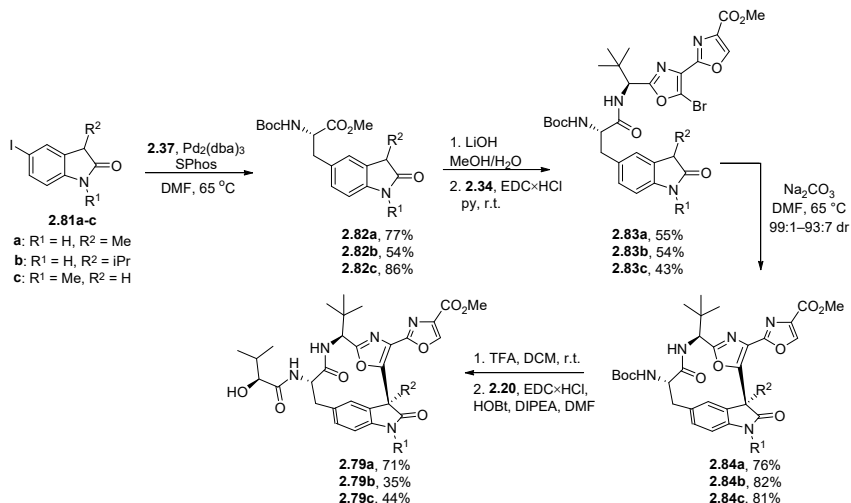

Figure 2.18. **Synthesis of macrocycles 2.79**

Gratifyingly, the alkylation of **2.84c** sodium enolate with various alkylating agents proceeded with high diastereoselectivity (from 86:14 dr to 92:8 dr; see Figure 2.19). The formation of *S* epimer was later confirmed by the counter synthesis of **2.84d** by *N*-methylation of (*S*)-**2.84a**. Identical NMR spectra for **2.84d** prepared either from (*S*)-**2.84a** or by the alkylation of **2.84c** provided compelling evidence for the formation of *S* isomers in the diastereoselective alkylation of **2.84c** sodium enolate.
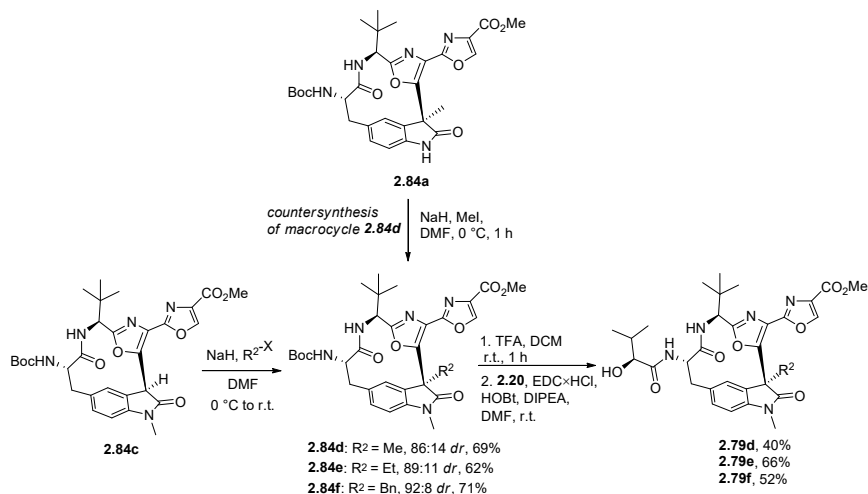

Figure 2.19. **Alkylation of macrocycle 2.84c and counter synthesis of 2.84d**

All synthesized macrocycles **2.79a–f** were tested against the four cancer cell lines (Table 2.6). Compounds **2.79a** and **2.79d** with methyl substituent at the quaternary center (entries 2 and 5) showed several orders of magnitude stronger antiproliferative effect than analogs **2.79b,f** possessing sterically more demanding substituents, and ethyl-substituted macrocycle **2.79e** was somewhat less potent. The compound **2.79a** showed even higher GI_{50} values against all tested cancer cell lines than phenyl-bearing substituent at quaternary center **2.49** (Table 2.4, entry 2). Surprisingly, tertiary stereogenic center-containing macrocycle **2.79c** ($R^2 = H$) was found to be inferior to **2.79a,d**, so the observed SAR apparently is not related to steric effects only. At the same time, the substitution pattern at oxindole nitrogen ($R^1 = H$ or Me) did not affect the antiproliferative activity.

Table 2.6

Cell viability data
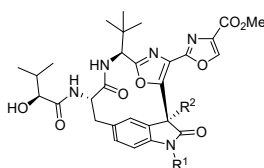
entry	cmpd	R^1	R^2	GI_{50}, µM			
				PANC-1	MiaPaCa-2	MCF-7	MDA-MB-231
1	VNB	–	–	0.00303 ± 0.00038	0.000789 ± 0.000034	0.00385 ± 0.00035	0.00450 ± 0.00042
2	**2.79a**	H	Me	11 ± 2	0.68 ± 0.09	0.53 ± 0.09	1.4 ± 0.3
3	**2.79b**	H	iPr	>100	39 ± 3	>100	98 ± 11
4	**2.79c**	Me	H	>100	54 ± 2	63 ± 7	>100
5	**2.79d**	Me	Me	4.5 ± 1.4	0.55 ± 0.02	0.75 ± 0.07	2.50 ± 0.14
6	**2.79e**	Me	Et	13 ± 1	3.50 ± 0.62	2.86 ± 0.31	19 ± 4
7	**2.79f**	Me	Bn	>100	95 ± 5	82 ± 1	54 ± 9

Previously obtained results of SAR indicated that small non-aromatic substituent at the quaternary stereocenter is necessary for higher antiproliferative activity of the compound (Table 2.6, entries 2, 5). Also, from Table 2.4 we observed that carboxylic esters **2.54–2.55** (entries 7 and 8) were the most active among other analogs with different substituents at R^3 position. Considering all the previously obtained data, we also have synthesized ester-containing compounds **2.85** and **2.86** from macrocycle **2.79a** carrying methyl group at the quaternary stereogenic center (Figure 2.20). Corresponding carboxylic acid **2.87** was synthesized from **2.86** by hydrolysis of ester group in high yield.
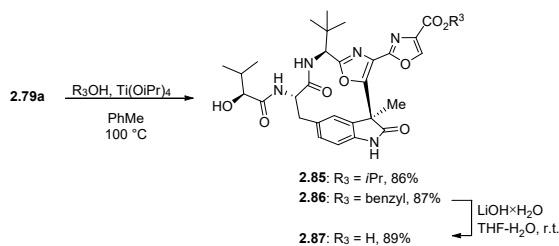
Figure 2.20. **Synthesis of esters 2.85–2.86 and carboxylic acid 2.87**

Newly obtained esters **2.85–2.86** and carboxylic acid **2.87** were tested against four cancer cell lines (Table 2.7). Benzylic ester **2.86** (entry 3) was found to be the most active against three of four tested cancer cell lines with the GI_{50} values against pancreatic carcinoma (MiaPaCa-2) and estrogen positive breast adenocarcinoma (MCF-7) in sub-micromolar range. Benzyl ester **2.86** turned out to be the compound with the highest antiproliferative effect. Carboxylic acid **2.87** was tested only against one cancer cell line and possessed almost no effect (entry 4).
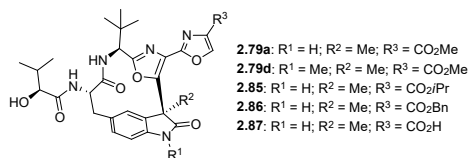
Table 2.7

Cell viability data

entry	cmpd	GI_{50}, µM			
		PANC-1	MiaPaCa-2	MCF-7	MDA-MB-231
1	VNB	0.00312 ± 0.00040	0.000752 ± 0.000027	0.00384 ± 0.00039	0.00411 ± 0.00051
2	**2.85**	2.6 ± 0.1	0.18 ± 0.04	0.24 ± 0.01	21.8 ± 2.3
3	**2.86**	6.5 ± 1.8	0.081 ± 0.006	0.044 ± 0.015	0.73 ± 0.17
4	**2.87**	ND	ND	ND	67.1 ± 1.1

In-vitro antiproliferative activity

The efficacy of the best performing macrocycles thorough the series **2.79a, 2.79d, 2.85–2.86** and carboxylic acid **2.87** as the assay negative control was further evaluated in a series of additional cancer cell lines (lymphoma U937, melanoma A2058 and adenocarcinoma HCC-44) using the MTT assay (see Table 2.8). Gratifyingly, benzyl ester **2.86** demonstrated the highest antiproliferative activity with GI_{50} values in low nanomolar range across all three cell lines (entry 5). The corresponding isopropyl ester **2.85** (R^3 = *i*-Pr; entry 4) was slightly less efficient, whereas methyl esters **2.79a**, **2.79d** were less efficient (entries 2–3, Table 2.8). As anticipated, carboxylic acid **2.87** exerted up to 1000-fold lower antiproliferative activity than benzyl ester **2.86**.

The selectivity of toxicity for macrocycles **2.79a, 2.79d, 2.85** and **2.86** was also evaluated using non-malignant cell lines such as HEK-293 and GM08402 (see Table 2.8). Surprisingly, *N*-methyl indoline derivative **2.79d** showed poor selectivity of toxicity with GI_{50} values against HEK-293 cell line comparable to those against cancer cell lines PANC-1 and HCC-34 (see entry 3, Table 2.8). In contrast, N-H indolines **2.79a, 2.85** and **2.86** featured at least 100-fold lower antiproliferative effect against non-malignant cells as compared to tumor cell lines. Similarly, high selectivity of toxicity was also observed for all macrocycles when human dermal fibroblast cells GM08402 were used.

Table 2.8

In vitro antiproliferative activities of selected analogs

2.79a: R^1 = H; R^2 = Me; R^3 = CO$_2$Me
2.79d: R^1 = Me; R^2 = Me; R^3 = CO$_2$Me
2.85: R^1 = H; R^2 = Me; R^3 = CO$_2$iPr
2.86: R^1 = H; R^2 = Me; R^3 = CO$_2$Bn
2.87: R^1 = H; R^2 = Me; R^3 = CO$_2$H

Entry	cmpd	GI$_{50}$, µM				
		U937	A2058	HCC-44	Hek293	GM08402
1	VNB	0.00407 ± 0.00051	0.00241 ± 0.00021	0.00534 ± 0.00030	0.048 ± 0.011	>100
2	**2.79a**	0.084 ± 0.007	0.35 ± 0.01	2.38 ± 0.07	44 ± 8	53
3	**2.79d**	0.098 ± 0.011	0.48 ± 0.01	1.52 ± 0.01	0.19 ± 0.01	>100
4	**2.85**	0.031 ± 0.004	0.049 ± 0.005	0.22 ± 0.02	3.05 ± 0.02	>100
5	**2.86**	0.011 ± 0.001	0.0095 ± 0.0004	0.035 ± 0.002	1.67 ± 0.19	33 ± 3
6	**2.87**	12.3 ± 1.2	26.2 ± 1.3	ND	43.4 ± 1.2	ND

Further, 12-membered macrocycles **2.79a** and **2.86** were submitted to dose-response screening assay against 60 human tumor cell line panel NCI-60 (US National Cancer Institute) at five concentrations (ranging from 0.01 to 100 µM).[83] Macrocycle **2.86** displayed submicromolar average GI$_{50}$ value whereas **2.79a** exhibited mean inhibitory activity at the micromolar range (Table 2.9, entries 1–2). Gratifyingly, despite considerable structural simplification, macrocycle **2.86** appears to be only ca. 10-fold less active than the natural diazonamide **1.1** as well as marketed MTA vinorelbine and paclitaxel as evidenced by their mean GI$_{50}$ values in NCI-60 panel (entry 2 vs. entries 3–5). Moreover, antiproliferative activity within the same order of magnitude was observed for macrocycle **2.86** and diazonamide **1.1** against 19 out of 60 cell lines in the NCI panel (see SI for complete NCI data[84]). Overall, the results in dose-response screening assay against NCI-60 panel cell lines (Table 2.9) are in line with our data (Tables 2.7 and 2.8) and point to the high antiproliferative potency of macrocycle **2.86**.

A difference between toxic concentrations of **2.86** (mean LC$_{50}$ > 100 µM) and the concentration required for total growth inhibition (mean TGI > 11 µM) suggests that macrocycle **2.86** possibly possesses cytostatic rather than cytotoxic properties (entry 3, Table 2.9).[85–88] Similar differences between LC$_{50}$ and TGI concentrations have been determined for marketed tubulin-targeting agents vinorelbine and paclitaxel (entries 3 and 4, Table 2.9) that are inherently cytostatic because interference with microtubule dynamics leads to proliferation arrest.[89] Hence, NCI-60 data suggest that macrocycle **2.86** might act in a similar manner. In addition, macrocycle **2.86** demonstrated a differential cytotoxicity pattern, which was highly similar to that of paclitaxel and vinblastine (correlation coefficients 0.79 and 0.77, respectively as indicated by COMPARE algorithm).[83] Overall, the cytotoxicity pattern for macrocycle **2.86** and marketed MTA paclitaxel and vinblastine suggests that the measured antiproliferative activity of macrocyclic series is associated with their effect on microtubule dynamics.

Table 2.9

NCI-60 Dose-Response Data

entry	Compound	NSC number	Mean GI$_{50}$, μM	Mean TGI, μM	Mean LC$_{50}$, μM
1	**2.79a**	NSC #830922	4.1	>100[a]	>100[a]
2	**2.86**	NSC #831032	0.19	>11[b]	>100[a]
3	vinorelbine[c]	NSC #608210	0.018	4.2	52
4	paclitaxel[c]	NSC #125973	0.025	3.9	75
5	diazonamide **1.1**[d]	NSC #700089	0.011	>10[e]	>10[e]

[a] TGI and LC$_{50}$ values exceeded the upper concentration limit (100 μM) for more than half of NCI-60 cell lines; [b] TGI values for 11 out of 59 cell lines exceeded the upper concentration limit of 100 μM; [c] Data from ref. [90]; [d] Data from ref. [91]; [e] TGI values exceeded the upper concentration limit (10 μM) for more than half and LC$_{50}$ for 90% of cell lines in NCI-60 panel

Tubulin polymerization assay[d]

An *in vitro* tubulin polymerization assay was performed to evaluate the effect of macrocycles on microtubule dynamics and stability (Figure 2.21.A).[e] In the assay, paclitaxel-induced self-polymerization of soluble α/β-tubulin heterodimer to microtubules under buffered conditions was monitored in the presence of the desired ligands by measuring changes in light scattering at 340 nm. A slope was calculated for the linear growth phase of the tubulin polymerization curves to render a comparison vs the positive assembly control containing 10 μM paclitaxel (Table 2.10). Paclitaxel-induced self-polymerization was measured in the presence of macrocyclic esters **2.79a**, **2.79d**, **2.85**, **2.86**. In addition, macrocycles with weak antiproliferative activity such as amides **2.52**, **2.53** as well as carboxylic acid **2.87** were also examined to verify the correlation between antiproliferative activity of the macrocycles and effect they exert on tubulin polymerization dynamics. Finally, vinorelbine was also tested as the assay positive control.

Table 2.10

Tubulin polymerization assay results

Entry	Ligand[a]	Slope[b]	R^2 fit	Time span of R^2 fit, s
1	control	1.000	0.99	290–740
2	vinorelbine	0.023	0.83	110–6420
3	**2.79a**	0.060	0.95	110–5500
4	**2.79d**	0.120	0.99	316–6420
5	**2.52**	0.750	0.97	470–920
6	**2.53**	0.700	0.98	470–1835
7	**2.85**	0.060	0.97	110–6420
8	**2.86**	0.036	0.94	110–6420
9	**2.87**	0.035	0.94	110–6420

[a] at 2:1 tubulin:ligand ratio;
[b] Slope values are relative to that of control (entry 1)

[d] The assay was conducted following Enhancer Control Polymerization Assay Method from Tubulin Polymerization Assay Kit manual by Cytoskeleton, Inc. (https://www.cytoskeleton.com/pdf-storage/datasheets/bk004p.pdf).

[e] Polymerization experiments were performed with the assistance of Dr. Diana Zelencova-Gopejenko.
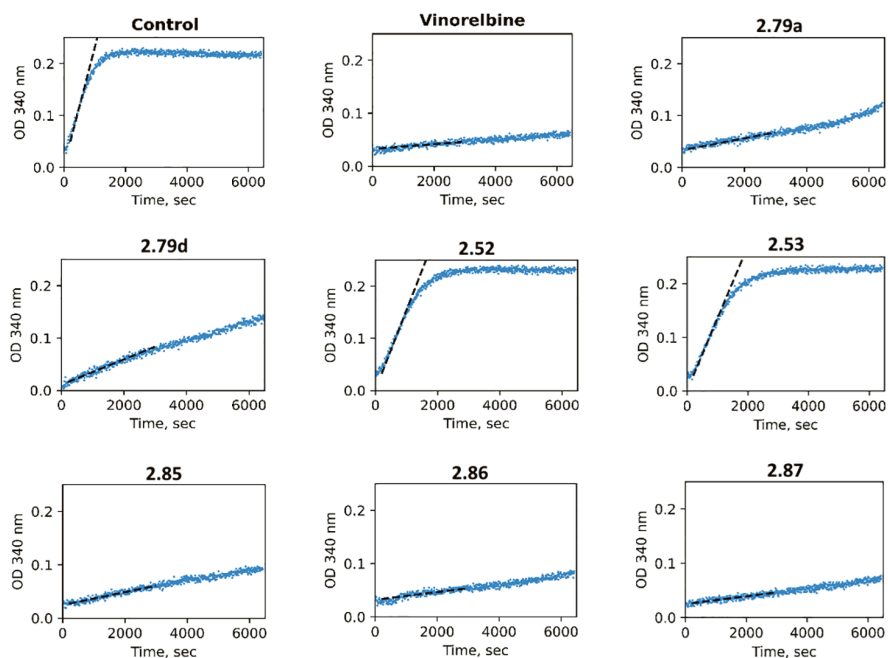
Figure 2.21.A. **Enhancer control tubulin self-polymerization assay results for macrocycles 2.79a, 2.79d, 2.52, 2.53, 2.85, 2.86, 2.87 and vinorelbine**
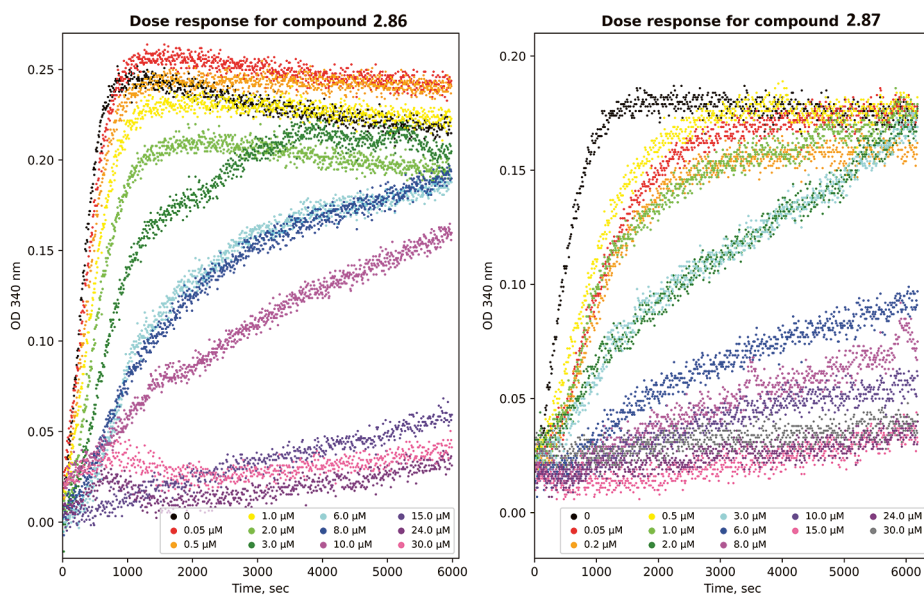

Figure 2.21. B. **Dose-dependent inhibition of tubulin polymerization by benzyl ester 2.86;** *C.* **dose-dependent inhibition of tubulin polymerization by carboxylic acid 2.87**

A good correlation between the inhibition of tubulin polymerization and *in vitro* antiproliferative activity was observed for macrocycles **2.79a**, **2.79d**, **2.85–2.86** (Table 2.10). Thus, the most active macrocycle **2.86** in cell viability experiments turned out to be the most potent inhibitor of tubulin polymerization across the series (entry 8). Structurally related 12-membered macrocyclic esters **2.79a, 2.85** (entries 3 and 7) also inhibited polymerization, albeit they were less efficient than macrocycle **2.86**. Further drop of inhibitory efficiency was observed for macrocycle **2.79d** (entry 4), and this observation is consistent with its reduced antiproliferative effect (Table 2.8). Not surprisingly, amides **56–57** with weak antiproliferative effects were measured to be the least potent inhibitors in a series (entries 5 and 6, respectively). In a striking contrast, acid **2.87** showed inhibitory effect similar to that of the most efficient macrocycle **2.86** (entry 9 vs entry 8) despite the acid **2.87** displayed lowest *in vitro* antiproliferative activity among all tested macrocycles (Table 2.8). The high inhibitory efficiency of tubulin polymerization observed both for ester **2.86** and the corresponding acid **2.87** prompted us to perform dose-dependent tubulin polymerization assay for both macrocycles (Figure 2.21.B and 2.21.C). From the assay data, we were able to estimate IC_{50} values for ester **2.86** (IC_{50} = 2.30 μM) and acid **2.87** (IC_{50} = 2.74 μM). The similar calculated IC_{50} values confirm that both ester **2.86** and acid **2.87** are equally potent inhibitors of tubulin polymerization. The apparent lack of correlation between *in vitro* antiproliferative activity and efficiency in the tubulin polymerization assay for acid **2.87** lead us to hypothesize that poor cell permeability could be responsible for lack of *in vitro* activity. Finally, vinorelbine strongly inhibited the polymerization of tubulin (entry 2; Table 2.10). Overall, the observed inhibition of tubulin polymerization in the presence of macrocycles **2.79a**, **2.79d**, **2.85–2.86** provide evidence that *in vitro* antiproliferative effects are to be attributed to binding tubulin and inhibiting the assembly of microtubule networks within cells.

Determination of the tubulin binding site[f]

Differential cytotoxicity pattern data (determined from NCI-60 panel by the COMPARE algorithm), tubulin polymerization assays and A2058 cell cycle analysis results provided evidence that the antiproliferative effect for the structurally simplified diazonamide analog series is exerted through the inhibition of tubulin function in cells. In order to confirm the binding site of the macrocycles to tubulin, competition experiments of vinblastine with **2.79a** and **2.79d** were performed using ultracentrifugation/ HPLC assay. We found that the macrocycles weakly compete with vinblastine. This data is in agreement with previous reports of biotinylated diazonamide analog DZ-2384 (**1.2**) binding to tubulin being blocked in a dose-responsive manner by vinca domain MTA vinorelbine,[16] and the structural analysis showing the apparent overlapping binding sites for DZ-2384 (**1.2**) and vinorelbine was confirmed by X-ray crystal structure of DZ-2384 (**1.2**) bound at vinca domain of the tubulin heterodimer.[16] In collaboration with Dr. Andrea Prota from Paul Scherrer Institut we also attempted the analysis of the binding site by X-ray crystallography. Unfortunately, very poor diffraction or poorly defined electron density at the tubulin interdimer interface was observed for crystals of T_2R-TTL (two α/β-tubulin dimers in complex with the stathmin-like protein RB3

---

[f] This work was performed by Francesca Bonato, Dr. Daniel Lucena-Agell and Dr. J. Fernando Díaz.

and tubulin tyrosine ligase) that were soaked for different times with the most efficient macrocycle **2.86**. Although the density highlights perturbation at the vinca site, it is poorly defined and does not allow modeling of the correct pose of the compounds.

Evaluation of the compound-induced effects on apoptosis[g]

In the MTT assay, we observed a time-dependent loss of cell viability. We have evaluated apoptotic and necrotic cell death using PI and annexin staining and FACS counting (Figure 2.22A). In the control cells without treatment, 5% necrotic and 15% apoptotic cells were counted. In the presence of 2.86 and vinorelbine necrotic cell count gradually increased reaching 10% after 24 h incubation. This indicated that the antiproliferative effect of 2.86 was not related to the induction of necrotic cell death. Furthermore, incubation with compounds increased both early and late apoptotic cell count in a time-dependent manner. Thus, at the 24 h time point, apoptotic cells were about 40% (10% early and 30% late) of the total cell number in both treatment groups (Figure 2.22B,C). These results confirm that similarly to vinorelbine at equitoxic concentration (10 nM) the antiproliferative effect of 2.86 occurs due to inhibited cell division and induction of apoptotic cell death due to arrested cell cycle. The data are presented as the mean ± SEM of three independent experiments in triplicate.
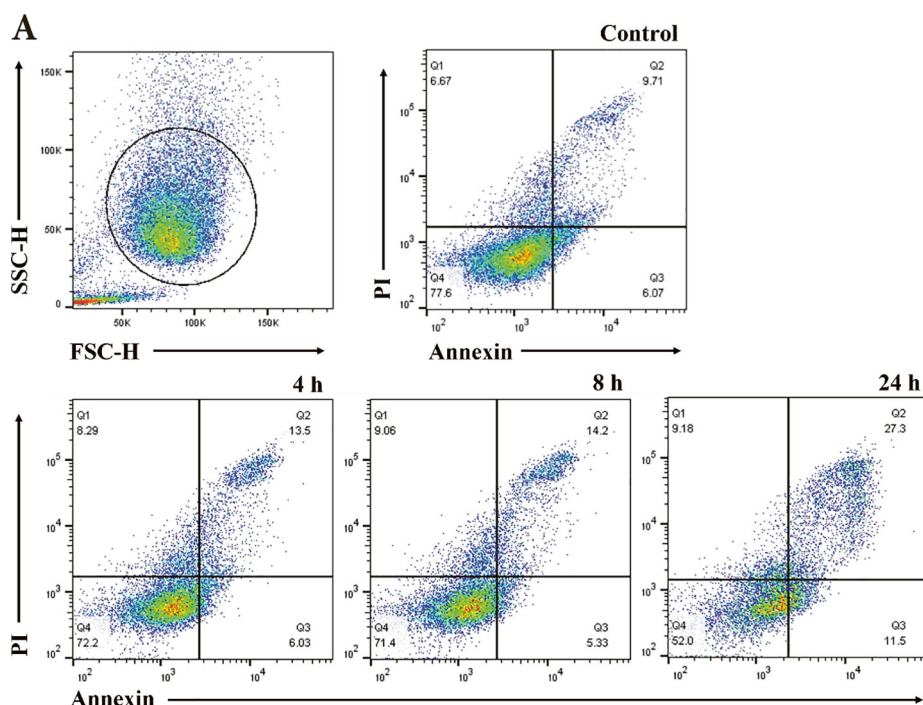

Figure 2.22. A. **Representative plots from flow cytometry analysis of apoptosis after incubation with compound 2.86 (200 nM) for time points up to 24 h in A2058 cells**

---

[g] Flow cytometry analysis was performed by Dr. Edgars Liepinsh, Dr. Marina Makrecka-Kuka and Dr. Melita Ozola.
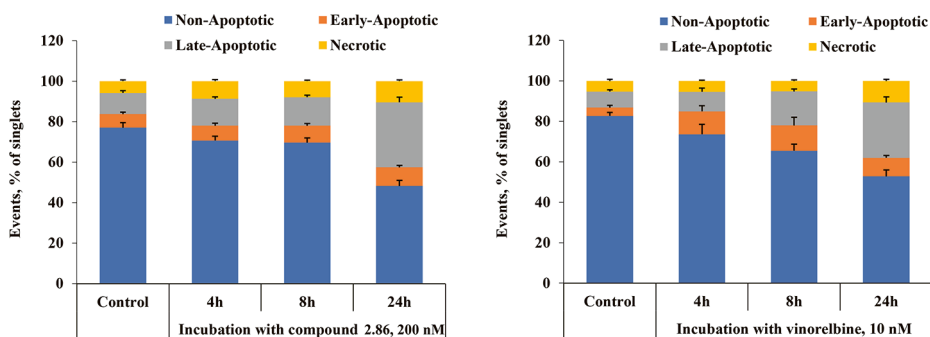
Figure 2.22. B. **Effects of compound 2.86 on induction of apoptosis (*C*) in comparison with equitoxic concentration (10 nM) of vinorelbine**

Evaluation of the compound effect on the cell cycle[h]

To investigate the antiproliferative mechanisms of **2.86**, the time-dependent effect on cell cycle distribution in melanoma A2058 cells was examined (Figure 2.23A). In the control group, relative cell count at G1, S and G2 phases remained unchanged over 24 h period. The treatment with **2.86** and vinorelbine caused strong cell cycle arrest in the G2/M phase. The arrest of the cell cycle induced by both compounds was also time dependent. A higher number of G2/M cells were evident already after 4 h treatment with **2.86** while two times more G2/M cells were counted after 24 h incubation period. Thus, after 24 h incubation in the presence of **2.86** and vinorelbine, approximately 40–50% of cells were arrested at the G2/M phase (Figure 2.23B,C). Overall, compound **2.86** (at 200 nM concentration) and vinorelbine (at 10 nM concentration) induced similar effects on the cell cycle. The data are presented as the mean ± SEM of three independent experiments in triplicate.

---

[h] This work was performed by Dr. Edgars Liepinsh, Dr. Marina Makrecka-Kuka and Dr. Melita Ozola.
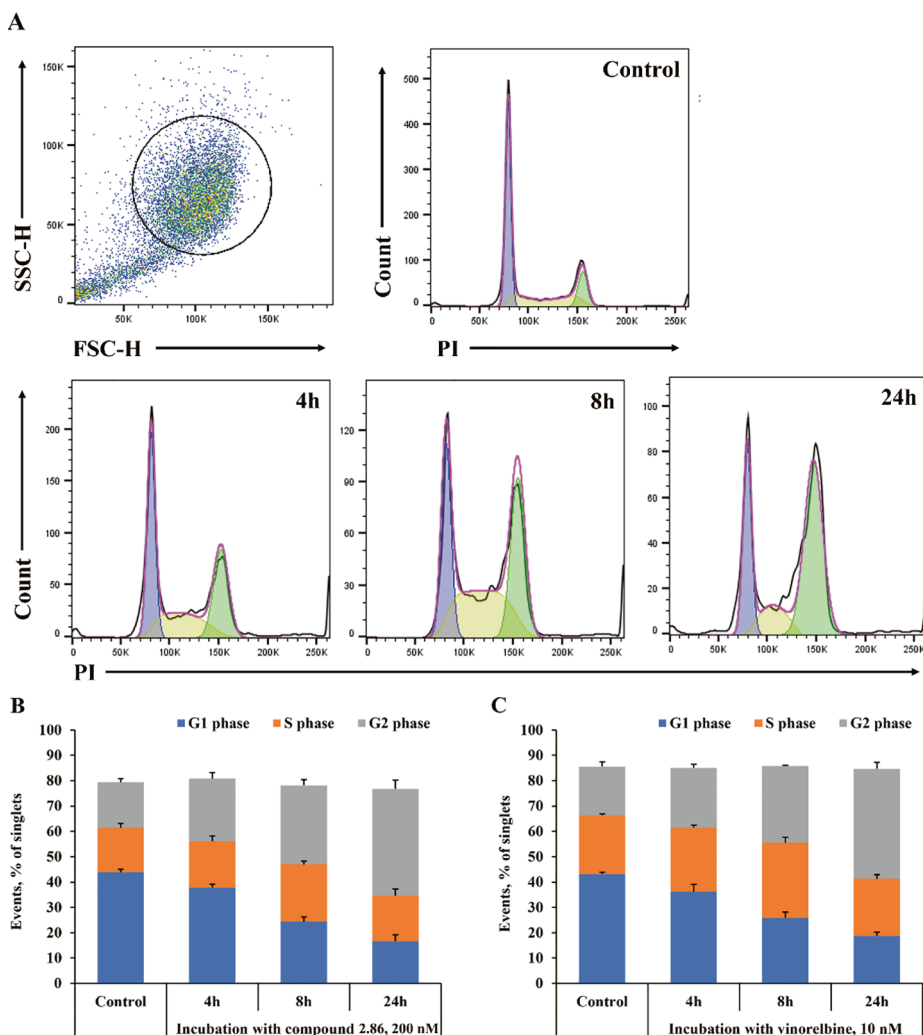
Figure 2.23. A. **Flow cytometry analysis of cell cycle progression of A2058 cells after incubation with compound 2.86 (200 nM) for up to 24 h.** *B.* **Quantitative results of the effects of compound 2.86 on cell distribution among phases of the cell cycle (C) in comparison with equitoxic concentration (10 nM) of vinorelbine**

Evaluation of macrocycle 2.86 effect on cell morphology[i]

To further investigate the antiproliferative activity of macrocycle **2.86** and vinorelbine, morphological changes were examined in melanoma A2058 cells. Initially, cells were stained for tubulin (yellow) and cell nuclei (blue) (Figure 2.24). When treated with **2.86** and vinorelbine, the cells detached and became rounded. In the treatment groups, a substantially higher number of cells were stuck in metaphase which further

---

[i] This work was performed by Dr. Edgars Liepinsh, Dr. Marina Makrecka-Kuka and Dr. Melita Ozola.

results in apoptosis and degradation (Figure 2.24). Thus **2.86** and vinorelbine halted cell proliferation, and the cells entering the cell division phase became apoptotic within 4–48 h after the beginning of treatment (see also Figure 2.23). The remaining cells attached to the plate became substantially larger while polymerized tubulin structure remained intact. Overall, the arrest of the cell cycle and induction of apoptosis were similar in **2.86**- and vinorelbine-treated cells. Further, the effects of compounds on mitochondria were tested using MitoTracker™ Deep Red. Both compounds **2.86** and vinorelbine did not affect the number of mitochondria and their morphology despite substantially increased cell size.

Cells were stained with SPY555-tubulin (yellow) and Hoechst 33342 (blue) after 24 h incubation with and without compounds. Confocal images show attached cell (Figure 2.24, A) and floating cell (Figure 2.24, B) morphology. In the third panel (Figure 2.24, C), cells were stained with MitoTracker™ Deep Red (red) to evaluate changes in the number of mitochondria and their structure.
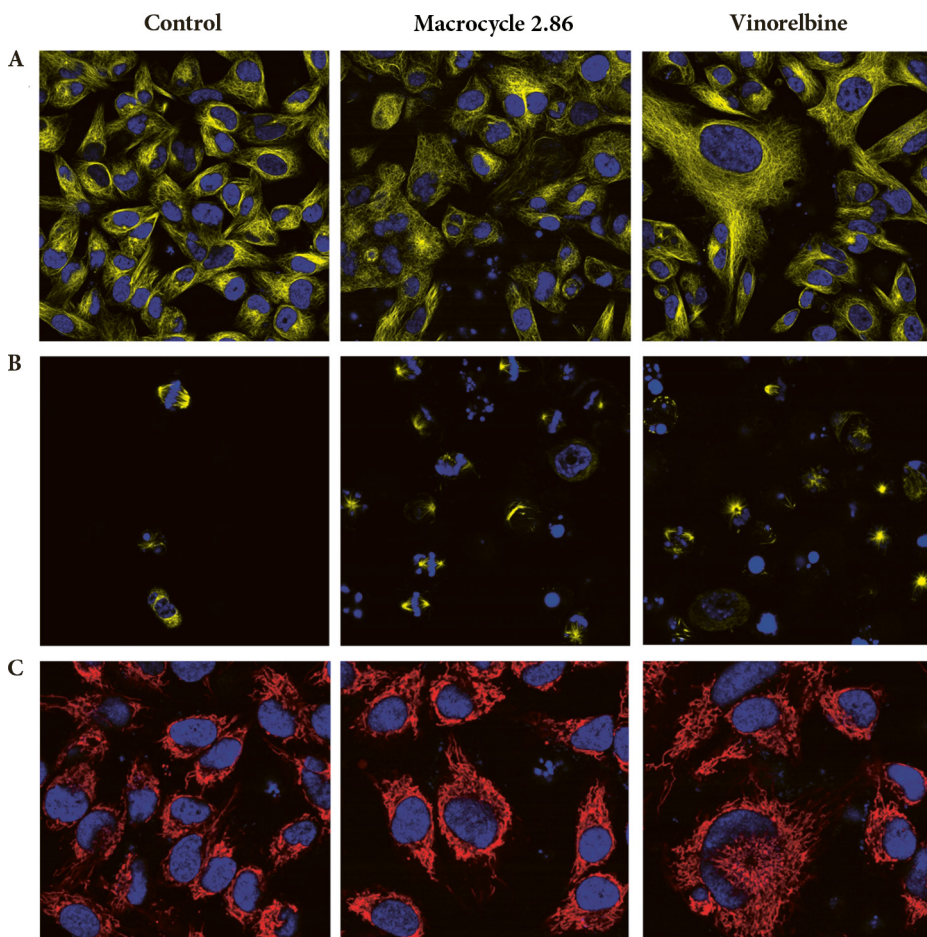
Figure 2.24. **Melanoma A2058 cell morphology analysis after incubation with compound 2.86 (200 nM) and vinorelbine (10 nM)**

Evaluation of intracellular uptake, metabolism and efflux[j]

Intracellular uptake of macrocyclic benzyl ester **2.86** and the corresponding acid **2.87** was evaluated to address the observed lack of correlation between *in vitro* antiproliferative activity and efficiency in the tubulin polymerization assay for **2.87** (Table 2.8 vs. Figure 2.21.C). To this end, melanoma A2058 cells were incubated with ester **2.86** or acid **2.87** for up to 16 h. Already during the first 4 h of incubation with ester **2.86**, acid **2.87** reached high intracellular levels that decreased gradually over the 16 h incubation period. In sharp contrast, incubation with acid **2.87** at five-fold higher concentration (1000 nM) resulted in very low intracellular levels. The limited cellular uptake of acid **2.87** explains its poor antiproliferative effect. On the other hand, two to three-fold higher intracellular concentration of the acid **2.87** as compared to that of the parent benzyl ester **2.86** at all time points suggests that metabolization of ester **2.86** to acid **2.87** occurs *inside* the melanoma A2058 cells that were incubated with ester **2.86** (Figure 2.25.A). In the meantime, a gradual decrease of intracellular acid **2.87** concentration points to its slow metabolic degradation. In addition, slow efflux of ester **2.86** and acid **2.87** from A2058 cells to cell media was also observed (Figure 2.25.B). Importantly, the increase in the concentration of acid **2.87** in cell media over 4 h is larger than the decrease of ester **2.86** concentration. This observation rules out the possibility that acid **2.87** concentration increases only because of ester **2.86** hydrolysis in cell media. Overall, the metabolism of ester **2.86** into acid **2.87** did not reduce the antiproliferative effect of **2.86** because both **2.86** and **2.87** exert a similar effect on tubulin polymerization. Obviously, the acid **2.87** is an active metabolite of benzyl ester **2.86**.

Intracellular uptake of **2.86** and **2.87** was measured after incubation with compounds **2.86** (200 nM) and **2.87** (1000 nM) for 4–16 h in A2058 cells (Figure 2.25. A). In the uptake experiment for **2.86**, metabolism was also evaluated by measuring the concentration of **2.87** as the main metabolite of **2.86**. Efflux from A2058 cells was measured in cell media at 1–4 h time points after incubation with ester **2.86** for 4 h, washing and addition of fresh cell media (without **2.86**) (Figure 2.25.B). The data are presented as the mean ± SEM of three parallels.
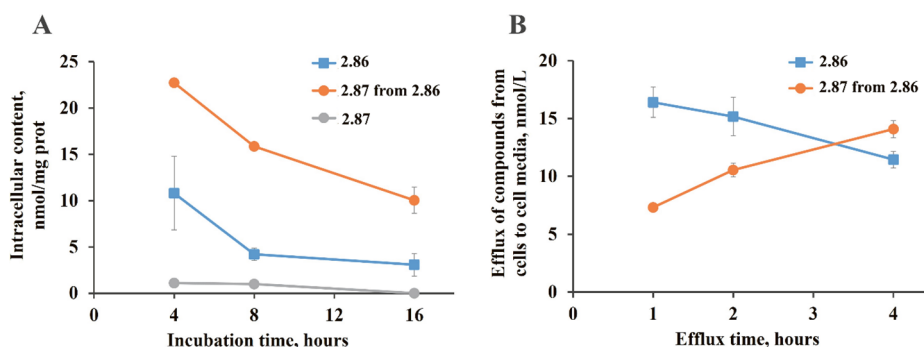

Figure 2.25. A. **Intracellular uptake of 2.86 and 2.87 and the metabolism of 2.86.**
B. **Efflux from A2058 cells**

In summary, a series of structurally simplified analogs of highly complex natural product diazonamide A was developed by removing the right-hand heteroaromatic macrocycle and truncation of the challenging-to-synthesize tetracyclic subunit by quaternary center-containing indolin-2-one. The explored SAR around oxindole-containing macrocycle series led to the development of potent analogs of natural diazonamide A (**1.1**). A highly diastereoselective alkylation of oxindole **2.83c** was developed and used as a convenient approach for the late-stage construction of quaternary stereogenic center in macrocycles **2.84d–f** (86:14–92:8 dr).

Based on the cell viability data, ester **2.86** was chosen as a *hit* compound of the series. The macrocycle **2.86** is relatively easy to synthesize, it was obtained in 13 linear steps from *tert*-Leucine with excellent diastereoselectivity (99:1 dr) in the key macrocyclization step. Despite the considerably reduced structural complexity, macrocycle **2.86** possesses nanomolar antiproliferative activity against a range of tumor cell lines. In the meantime, **2.86** featured at least 100-fold lower selectivity of toxicity against non-malignant cells such as HEK-293 and GM08402. Macrocycle **2.86** is a potent inhibitor of tubulin assembly, and it exerts similar effects to the marketed MTA vinorelbine on the cell cycle progression and induction of apoptosis in A2058 cell lines. Even though in melanoma A2058 cells macrocyclic ester **2.86** metabolizes into the corresponding acid **2.87**, the latter shows tubulin assembly inhibitory potency similar to that of the parent ester **2.86**. Taken together, our data provide strong evidence that the antiproliferative effect for the developed structurally simplified diazonamide A analog series is to be attributed to binding tubulin and inhibiting the assembly of microtubule networks within cells. As such, our work demonstrates that a highly complex natural product can be structurally simplified while retaining the mechanism of action and high antitumor potency. Macrocycle **2.86** is a promising compound that deserves further development as a potential anticancer agent.

2.3. Indane-Containing Simplified Analogs of Diazonamide A

Despite its high antiproliferative activity, macrocycle **2.86** possess low stability in cell lysate during intracellular uptake and metabolism assay (cf. Figure 2.25). Only carboxylic acid **2.87** could be detected indicating that the hydrolysis of the ester moiety to be the main metabolic degradation pathway. With the weak points of macrocycle **2.86** identified, we aimed to design a novel series of diazonamide A analogs with improved metabolic stability and to explore the structure-activity relationship (SAR) around the indane-containing series of diazonamide A analogs (Figure 2.26).
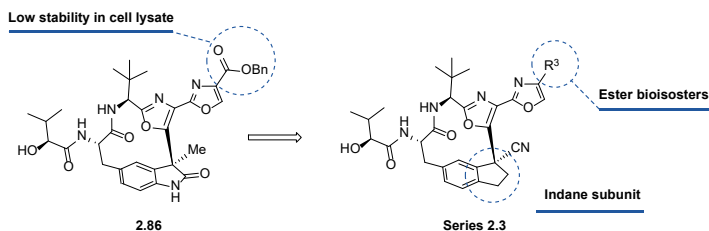

Figure 2.26. **Optimization of the structure of 2.86**

Synthesis of analog series

The design of a novel series involved the substitution of the oxindole moiety by an indane fragment. The primary objective was to maintain the same synthetic pathway used in the oxindole series, particularly the key S_NAr-type macrocyclization step. We also aimed at preserving the high cyclization diastereoselectivity. To facilitate anion generation for the S_NAr-type macrocyclization step, electron-withdrawing cyano substituent was installed instead of the methyl group at the quaternary stereogenic center (Figure 2.26). We envisioned that comparable steric of cyano and methyl substituents should secure similar functional activity for oxindoles and indane series.

The synthesis began with Pd-catalyzed Negishi cross-coupling of nitrile **2.88** with freshly prepared organozinc species **2.37** to afford amino acid ester **2.89** in almost quantitative yield. Ester hydrolysis in **2.89** was followed by amide coupling with corresponding amine **2.34** resulting in amide **2.90** formation. The key macrocyclization step in the presence of K_3PO_4 furnished macrocycle **2.91** with excellent diastereoselectivity (98:2 dr; determined by UPLC-UV/MS assay for the crude reaction mixture). The desired *S* configuration at the quaternary stereogenic center was confirmed for the macrocycle **2.93** by single crystal X-ray analysis.[k] After *N*-Boc cleavage with TFA, the resulting amine was coupled with (*S*)-2-hydroxy-3-methylbutanoic acid (**2.20**) to give macrocycle **2.91** (Figure 2.27).
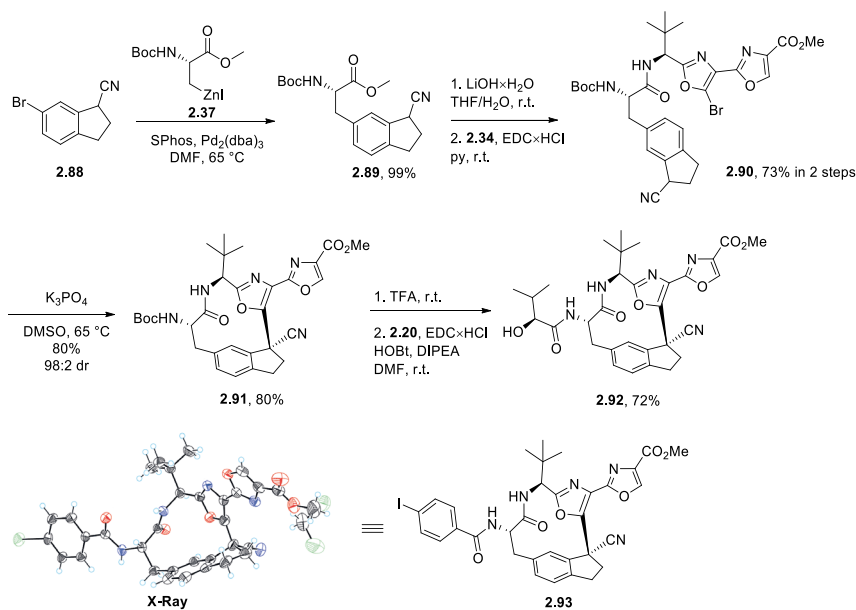

Figure 2.27. **Synthesis of macrocycle 2.92**

In vitro antiproliferative effect of **2.92** was determined in four cancer cell lines: melanoma A2058, lymphoma U937, adenocarcinomas MDA-MB-231 and HCC-44. The measured GI_{50} values of methyl ester **2.92** were compared to those of

---

k   X-ray analysis was performed by Dr. Sergey Belyakov.

oxindole-containing methyl ester **2.79a** (Figure 2.18) to evaluate the effect of oxindole substitution by indane (Table 2.11). We were pleased to see that indane-containing macrocycle **2.92** showed much superior GI_{50} values to those of oxindole **2.79a** against all tested cancer cell lines. Encouraged by these data, we proceeded with bioisosteric replacement of the ester moiety. Additional SAR study of the ester moiety was also performed to verify whether the SAR of the oxindole series can be translated the indane-containing macrocycles.

Table 2.11

Cell viability data

		GI_{50}, nM			
#	Compound	A2058	U937	MDA-MB-231	HCC-44
1	VNB	2.51 ± 0.28	4.84 ± 0.58	4.42 ± 0.39	5.56 ± 0.22
2	**2.79a**	350 ± 8	84.2 ± 7.1	1400 ± 300	2383 ± 68
3	**2.92**	12.9 ± 1.9	1.93 ± 0.7	131 ± 21	40.2 ± 0.5

Primary alcohol-containing macrocycle **2.95** was prepared in three steps from methyl ester **2.91**. The ester reduction by $LiBH_4$ and *N*-Boc cleavage afforded crude amine that was coupled with (*S*)-2-hydroxy-3-methylbutanoic acid (**2.20**) to give the desired **2.95**. Nitrile-containing macrocycle **2.97** was prepared in four steps from ester **2.91**. Thus, methyl ester first was converted into amide by liquid ammonia in MeOH. Then, the resulting amide was dehydrated to nitrile **2.96** by TFAA in pyridine. The synthesis of macrocycle **2.97** was completed by *N*-Boc cleavage and amide coupling with acid **2.20** (Figure 2.28).

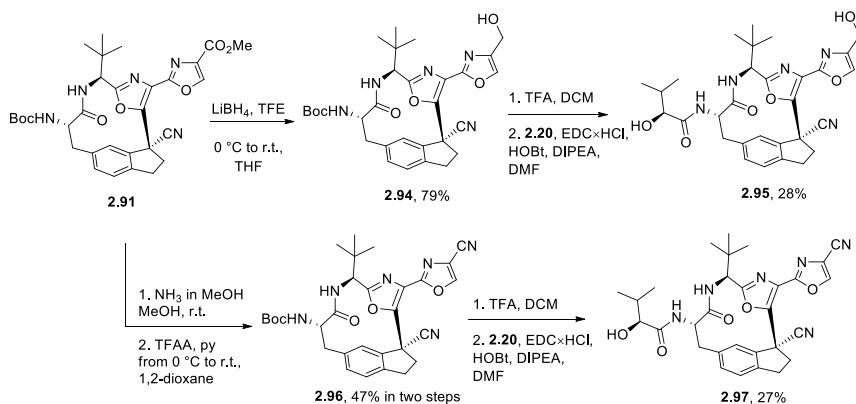*Figure 2.28.* **Synthesis of hydroxymethylbioxazole 2.95 and cyanobioxazole 2.97**

Owing to their stability towards hydrolysis, 1,2,4-oxadiazoles are broadly used in drug discovery as bioisosters of esters and amides.[92] 1,2,4-Oxadiazole-containing analogs **2.99–2.101** were prepared from methyl ester **2.92** and the corresponding hydroxyamidine **2.98** in the presence of K_2CO_3 (Figure 2.29).
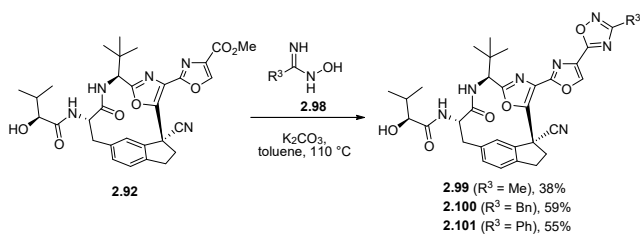
Figure 2.29. **Synthesis of 1,2,4-oxadiazoles 2.99–2.101**

Next, the synthesis of acetal esters **2.105** and **2.106** as prodrugs of carboxylic acid **2.104** was addressed because oxindole-containing carboxylic acid **2.87** showed tubulin polymerization inhibitory activity like that of benzyl ester **2.86** (cf. Figure 2.21). However, acid **2.87** possessed considerably lower *in-vitro* antiproliferative activity as compared to ester **2.86**, likely because of reduced cellular uptake. Furthermore, hydrolysis of ester **2.86** to acid **2.87** was observed inside the melanoma A2058 cells that were incubated with ester **2.86**. These data led us to conclude that ester **2.86** serves as a prodrug of carboxylic acid **2.87** (cf. Figure 2.25). To test the prodrug hypothesis, esters **2.105** and **2.106** were prepared by alkylation of carboxylic acid **2.104** with iodomethyl pivalate to give ester **2.105** or with 1-bromoethyl acetate to give analog **2.106** (Figure 2.30).
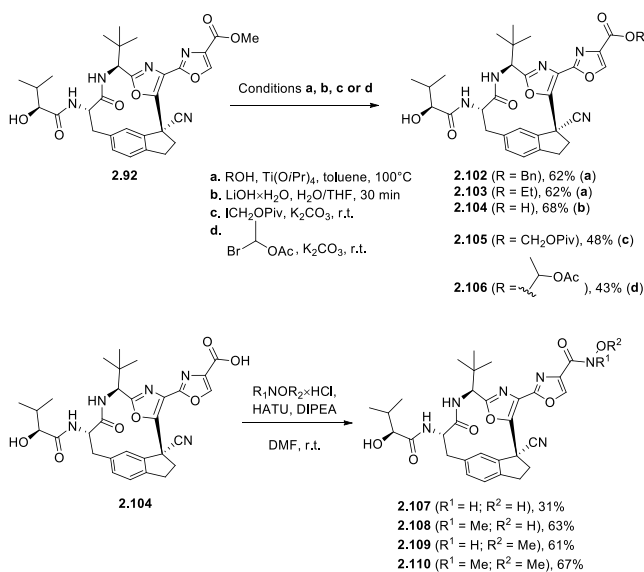
Figure 2.30. **Synthesis of esters 2.102–2.103, 2.105–2.106, carboxylic acid 2.104, hydroxamic acid 2.107 and its derivatives 2.108–2.110**

Hydroxamic acids are utilized as carboxylic acid bioisosteres.[93] Even though hydroxamic acids may undergo rapid hydrolysis *in-vitro* to the corresponding carboxylic acids, their hydrolytic stability is higher than that of esters. Furthermore, their stability can be improved by introducing substituents at the nitrogen atom.[94] To test

suitability of hydroxamic acids as bioisosteres of carboxylic acid, macrocycles **2.108**–**2.110** with methyl group at nitrogen and/or oxygen atoms alongside hydroxamic acid **2.107** were prepared by amide bond formation between acid **2.104** and the corresponding hydroxylamine/alkoxyamines (Figure 2.30). To compare the antiproliferative effects of bioisosters of carboxylic esters and acid corresponding esters **2.102** and **2.10**, along with acid **2.104**, were synthesized for the series. Benzyl and ethyl esters **2.102** and **2.103**, respectively, were prepared from methyl ester **2.92** in Lewis acid-catalyzed transesterification reaction. The basic hydrolysis of **2.92** afforded carboxylic acid **2.104** (Figure 2.30).

Since ester-containing macrocycles possessed the best antiproliferative activity in oxindole series, we decided to synthesize *tert*-butyl ester **2.117** in the hope that it will be more stable towards hydrolysis than methyl or benzyl esters (Figure 2.31). The synthesis of *tert*-butyl ester **2.117** commenced from acid **2.111**[95] and involved amide coupling with L-serine *tert*-butyl ester in the presence of EDC hydrochloride, followed by DAST-mediated cyclization of **2.112** to bioxazole **2.113** in the presence of DBU and BrCCl3 (Figure 2.31). The final step of the synthesis was the cleavage of *N*-Boc protecting group under mild conditions. At this stage, the use of TFA was not feasible because it would also hydrolyze the *tert*-butyl ester in **2.113**. To prevent this, we employed MsOH in the *N*-Boc deprotection reaction, which led to the almost selective deprotection of the amine, yielding building block **2.114**. Ester hydrolysis in **2.89** was followed by amide coupling with corresponding amine **2.114** giving amide **2.115**. The key macrocyclization step in the presence of K_3PO_4 furnished macrocycle **2.116** with diastereomeric ratio 97:3. After *N*-Boc cleavage with MsOH the resulting amine was coupled with (*S*)-2-hydroxy-3-methylbutanoic acid (**2.20**) to give macrocycle **2.117** (Figure 2.31).
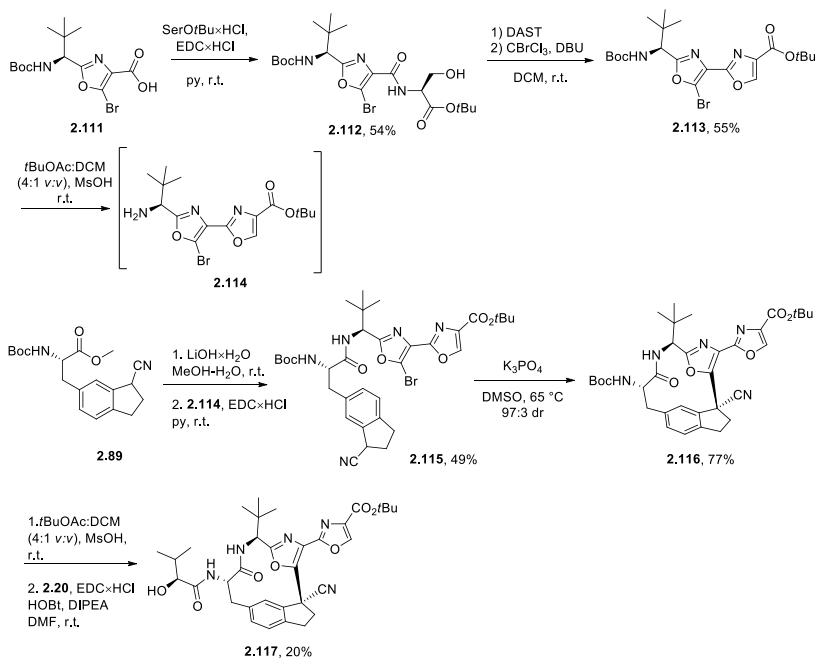

Figure 2.31. **Synthesis of *tert*-butyl ester 2.117**

Carbonate **2.120** was prepared from alcohol **2.94** in reaction with methyl chloro-formate **2.118** under basic conditions, followed by *N*-Boc deprotection and amidation reaction sequence. Unsaturated aliphatic ester-containing analog **2.123** was prepared from alcohol **2.94** by oxidation to the aldehyde and subsequent Horner-Wadsworth-Emmons reaction with phosphonate **2.121** to give *E*-alkene **2.122**. The latter was converted into macrocycle **2.123** by *N*-Boc cleavage and coupling with (*S*)-2-hydroxy-3-methylbutanoic acid (**2.20**). Saturated aliphatic ester-containing analog **2.124** was obtained from **2.123** by Pd-catalyzed hydrogenation (Figure 2.32).
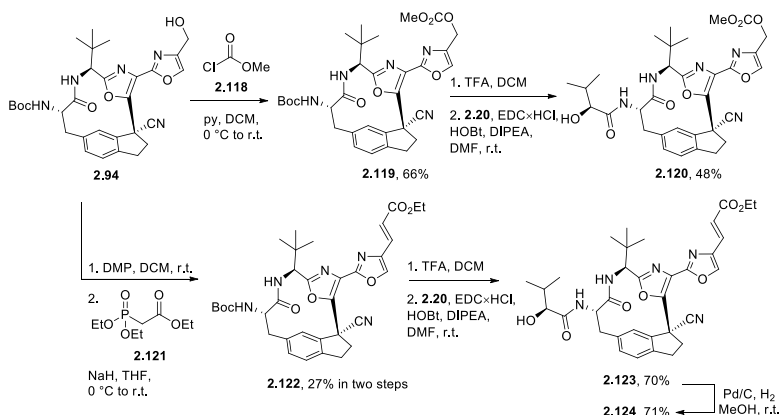

Figure 2.32. **Synthesis of carbonate 2.120 and esters 2.123–2.124**

To further explore SAR fluorinated analogs were also synthesized as bioisosters of hydroxymethyl oxazole **2.95** (Figures 2.33 and 2.34). This approach aimed to enhance the necessary lipophilicity compared to compound **2.95**, therefore improving penetration into the cell membrane[96] to potentially enhance the desired antiproliferative effect. However, often fluorine atom in the final structure may help boost permeability or increase binding in hydrophobic pockets of protein.[97] The synthesis of fluorinated analogs is depicted in Figure 2.33. Mono-fluorinated macrocycle **2.126** was obtained from the corresponding alcohol **2.94** by an S_N2-type reaction of intermediate mesylate with TBAF. Then, fluoromethyl substituted macrocycle **2.125** was subjected to *N*-Boc deprotection and amide bond formation with acid **2.20**. The synthesis of difluormethyl macrocycle **2.128** involved oxidation of alcohol **2.94** to aldehyde by DMP and subsequent treatment with DAST to furnish difluoromethyl substituted macrocycle **2.127**. After *N*-Boc cleavage with TFA, the resulting amine was coupled with (*S*)-2-hydroxy-3-methylbutanoic acid (**2.20**) to furnish **2.128** (Figure 2.33).

Trifluormethyl substituted macrocycle **2.136** was obtained from ester **2.89** (Figure 2.34). Its hydrolysis with LiOH×H₂O produced carboxylic acid, which was coupled with amine **2.130** (prepared from carboxylic acid **2.11**)[95] to give amide **2.131**. The base-mediated macrocyclization of **2.131** proceeded with excellent diastereoselectivity (99:1 dr). Methyl ester moiety in the macrocycle **2.132** was then hydrolyzed and coupled with 2-amino-3,3,3-trifluoropropan-1-ol (**2.133**) to furnish amide **2.134**. DMP oxidation of primary alcohol in **2.134** was followed by the oxazole ring formation in the presence of PPh₃ and 1,2-dibromotetrachloroethane under basic conditions to give bioxazole **2.135**. After *N*-Boc cleavage with TFA, the resulting amine was coupled with (*S*)-2-hydroxy-3-methylbutanoic acid (**2.20**) to afford macrocycle **2.136**.
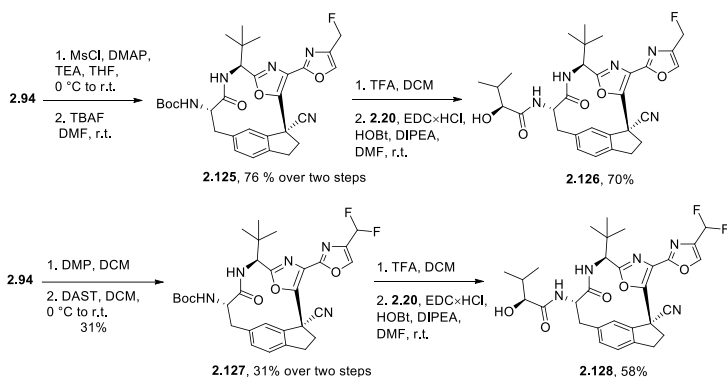
Figure 2.33. **Synthesis of fluorine-containing analogs 2.126, 2.128**
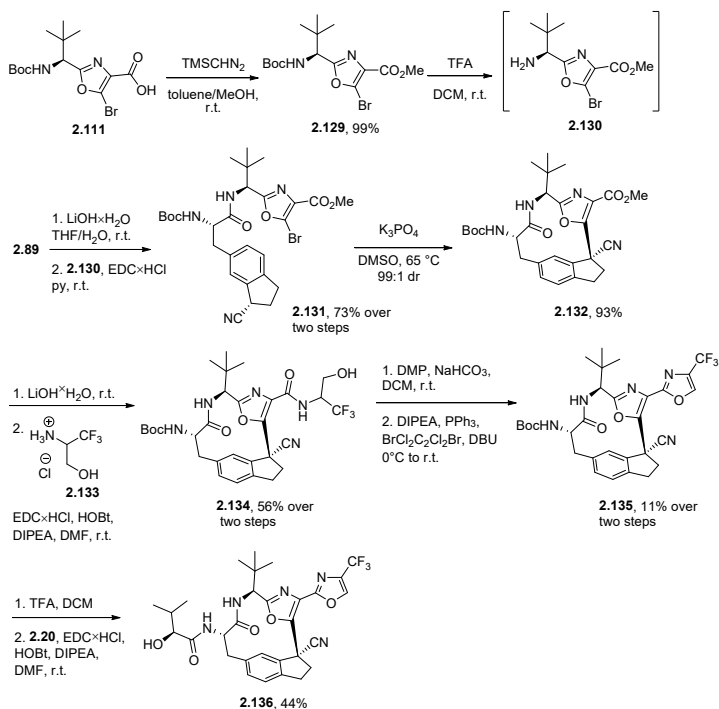
Figure 2.34. **Synthesis of trifluorooxazole analog 2.136**

To explore SAR around indane moiety, we incorporated the fluorine atom into the benzene ring of the indane and obtained analog **2.142** (Figure 2.35). The synthesis of **2.142** capitalized on the key S_NAr-type macrocyclization step as depicted in Figure 2.27. Accordingly, ketone **2.137** was transformed into nitrile **2.138** in the presence of TosMIC and KO*t*Bu, and the resulting nitrile **2.138** was further reacted with freshly prepared organozinc species **2.37** in Pd-catalyzed Negishi cross-coupling. Ester hydrolysis in **2.139** was followed by amide bond formation with amine **2.34** to afford **2.140**. Subsequent macrocyclization step in the presence of K_3PO_4 furnished macrocycle **2.141** with 98:2 diastereomer ratio. After *N*-Boc cleavage with TFA, the resulting amine was coupled with acid **2.20** to give the target macrocycle **2.142**.
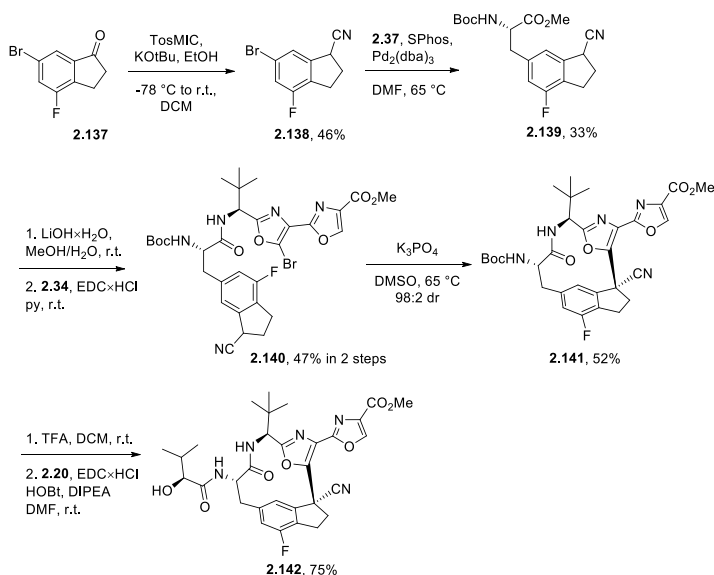
Figure 2.35. **Synthesis of macrocycle 2.142**

The cyano substituent at the quaternary center is well-suited for further synthetic transformations to explore SAR. Our modifications involved hydrolysis or reduction of the nitrile moiety in **2.91** into amide or primary amine, respectively (Figure 2.36). Accordingly, amide **2.143** was obtained from the corresponding macrocycle **2.91** after nitrile hydrolysis with hydrogen peroxide in the presence of K_2CO_3. The resulting amide **2.143** was elaborated into macrocycle **2.144** by *N*-Boc cleavage and amide coupling with carboxylic acid **2.20**. Primary amine-containing analog **2.145** was obtained from ester **2.92** by the reduction of nitrile with $NaBH_4$ in the presence of $InCl_3$.
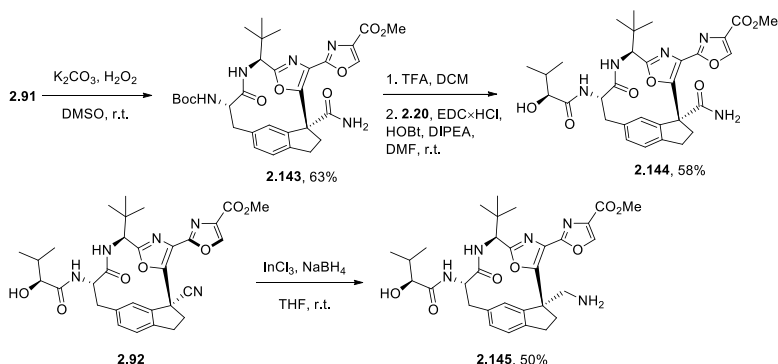
Figure 2.36. **Synthesis of macrocycles 2.144 and 2.145**

Considering the structure of the heteroatom-rich tetracyclic hemiaminal subunit in the natural diazonamide A (**1.1**), we were interested in examining the effect of

a heteroatom at the benzylic position of indane. To this end, the synthesis of several heteroatom-containing indane analogs such as indoline, dihydrobenzofuran, or dihydrobenzothiophene was attempted. Unfortunately, their synthesis proved challenging due to inherent property to aromatize into benzofurans, indoles, and benzothiophenes, respectively. In attempt to synthesize 2,3-dihydro-1-benzofuran-3-carbonitrile **2.147** only benzofuran **2.148** was obtained in moderate yield (Figure 2.37).
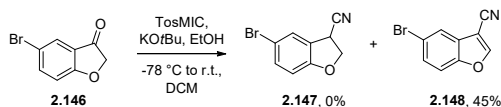
Figure 2.37. **Unsuccessful synthesis of 2.147**

In contrast, the corresponding six-membered heterocycles such as chromane, tetralin, and thiochromane could be readily incorporated into macrocycles (Figure 2.38). Thus, ketones **2.149** were converted into corresponding nitriles **2.150–2.152** by TosMIC and KO*t*Bu, and then reacted with freshly prepared organozinc species **2.37** under Pd-catalyzed Negishi cross-coupling conditions. Ester hydrolysis in **2.153–2.155** was followed by amide coupling with corresponding amine **2.34**, and the formed amides **2.156–2.158** were subjected to K_3PO_4-mediated cyclization. Gratifyingly, the macrocycles **2.159–2.161** were formed with excellent diastereoselectivity that ranged from 96:4 to 99:1 dr. After *N*-Boc cleavage with TFA, the resulting amines were coupled with (*S*)-2-hydroxy-3-methylbutanoic acid (**2.20**) to give analogs **2.162–2.164**. In addition, thiochromane-1,2-dioxide **2.165** was obtained from **2.164** after oxidation with *m*CPBA.
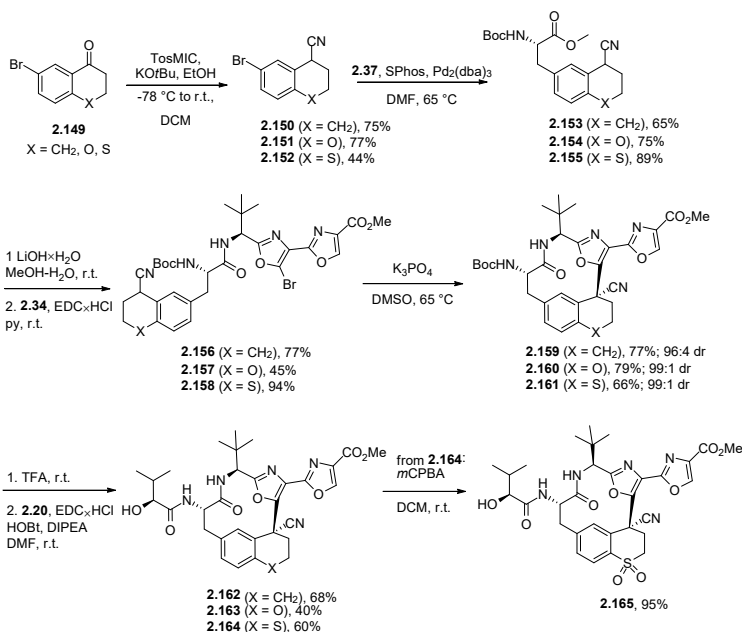
Figure 2.38. **Synthesis of analogs 2.162–2.165**

Cell viability data[1]

In vitro antiproliferative activity against several human tumor cell lines such as melanoma A2058, lymphoma U937, adenocarcinoma MDA-MB-231, melanoma MDA-MB-435 as well as non-malignant HEK-293 was determined for all macrocycles by the MTT assay with vinorelbine (VNB) as the positive control (Table 2.12). In analogy to the oxindole-containing series, macrocycles bearing ester group at the oxazole moiety showed the highest antiproliferative activity against all tested cancer cell lines. Among them, methyl ester **2.92** showed low nanomolar activity against melanoma A2058 and lymphoma U937 cell lines (entry 2). However, methyl ester **2.92** also featured low selectivity of toxicity as evidenced by low GI_{50} values against non-malignant cell line HEK-293. Interestingly, only carbonate **2.120** and difluoromethyl substituted macrocycle **2.128** showed antiproliferative activity comparable to that of the ester-containing analogs **2.92**, **2.102**, **2.103** and **2.117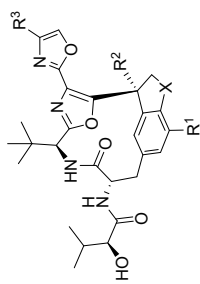** (entries 18, 22 vs. entries 2, 8, 9 and 17, respectively). Not only macrocycles **2.120** and **2.128** showed high antiproliferative activity against cancer cells, but they also demonstrated low antiproliferative activity against non-malignant cell line HEK-293. Fluoro substituted indane **2.142** was found to be inferior to ester **2.92** in terms of antiproliferative activity (entry 24 vs. entry 2). Likewise, oxadiazoles **2.99–2.101** featured poor antiproliferative properties (entries 5–7), so they turned out to be unsuitable as ester bioisosters. As anticipated, carboxylic acid **2.104** did not show any activity (entry 10) possibly because of poor intracellular uptake. Carboxylic ester bioisosters such as hydroxamic acid and its derivatives **2.107–2.110** (entries 13–16) also possessed low or no antiproliferative activity against all tested cancer cell lines. Disappointingly, lack of antiproliferative activity was observed for prodrugs of carboxylic acid **2.105–2.106** (entries 11–12). The lack of activity likely is to be attributed to the rapid hydrolysis of acylals **2.105** and **2.106** under aqueous buffered conditions to poorly cell-permeable carboxylic acid during the relatively long incubation period (48 h). Thus, the most promising compounds with the highest GI_{50} values were **2.128** (entry 22) and **2.120** (entry 18), which have been selected as *hit* compounds for the series. Further, any modifications in the indane subunit in compounds **2.162–2.165** (entries 25–26) and at the chiral quaternary stereogenic center in compounds **2.144–2.145** led to significant drop of antiproliferative activity (entries 27–30).

---

[1] Cell viability experiments were performed by Dr. Melita Ozola.

Cell viability data

Table 2.12

No.	Compound	R¹	R²	R³	X	GI₅₀, nM				
						A2058	U937	MDA-MB-231	MDA-MB-435	HEK-293
1	VNB	–	–	–	–	2.41 ± 0.21	4.21 ± 0.61	4.50 ± 0.42	ND	48.0 ± 11.3
2	2.92	H	CN	CO_2Me	CH_2	12.9 ± 1.9	1.9 ± 0.7	131 ± 21	40.1 ± 6.0	191 ± 24
3	2.95	H	CN	CH_2OH	CH_2	167 ± 17	64.9 ± 9.3	>1000	299 ± 60	>1000
4	2.97	H	CN	CN	CH_2	643 ± 92	692 ± 20	>1000	ND	>1000
5	2.99	H	CN	oxazole–Me	CH_2	156 ± 18	110 ± 8	ND	ND	>1000
6	2.100	H	CN	oxazole–Bn	CH_2	186 ± 16	157 ± 2	ND	ND	>1000
7	2.101	H	CN	oxazole–Ph	CH_2	687 ± 79	729 ± 75	ND	ND	>1000
8	2.102	H	CN	CO_2Bn	CH_2	20.4 ± 1.3	22.2 ± 1.2	ND	ND	>1000
9	2.103	H	CN	CO_2Et	CH_2	12.4 ± 1.5	9.7 ± 2.1	290 ± 43	ND	325 ± 79
10	2.104	H	CN	CO_2H	CH_2	>1000	>1000	>1000	>1000	>1000
11	2.105	H	CN	CH_2OPiv	CH_2	>1000	>1000	>1000	ND	ND
12	2.106	H	CN	OAc ester	CH_2	>1000	ND	>1000	ND	ND

GI$_{50}$, nM

No.	Compound	R^1	R^2	R^3	X	A2058	U937	MDA-MB-231	MDA-MB-435	HEK-293
13	**2.107**	H	CN	C(=O)NH–OH	CH$_2$	>1000	ND	>1000	ND	>1000
14	**2.108**	H	CN	C(=O)N(–)–OH	CH$_2$	212 ± 55	ND	>1000	ND	>1000
15	**2.109**	H	CN	C(=O)NH–O–	CH$_2$	865 ± 191	ND	>1000	ND	>1000
16	**2.110**	H	CN	C(=O)N(–)–O–	CH$_2$	221 ± 52	ND	>1000	ND	>1000
17	**2.117**	H	CN	CO$_2$tBu	CH$_2$	68.2 ± 10.8	22.5 ± 4.6	ND	ND	540 ± 67
18	**2.120**	H	CN	CH$_2$OCO$_2$Me	CH$_2$	60.1 ± 8.9	ND	433 ± 55	62.1 ± 8.9	>1000
19	**2.123**	H	CN	CO$_2$Et	CH$_2$	541 ± 182	94.7 ± 17.5	>1000	ND	ND
20	**2.124**	H	CN	CO$_2$Et	CH$_2$	203 ± 53	136.3 ± 45.0	>1000	ND	ND
21	**2.126**	H	CN	CH$_2$F	CH$_2$	235 ± 35	ND	526.7 ± 57.2	130.5 ± 19.2	>1000
22	**2.128**	H	CN	CHF$_2$	CH$_2$	90.8 ± 16.5	ND	ND	80.8 ± 10.9	>1000
23	**2.136**	H	CN	CF$_3$	CH$_2$	480 ± 87	ND	ND	403 ± 86	903 ± 189
24	**2.142**	F	CN	CO$_2$Me	CH$_2$	100.3 ± 10.0	ND	736 ± 176	ND	ND
25	**2.145**	H	CH$_2$NH$_2$	CO$_2$Me	CH$_2$	793 ± 223	40.9 ± 10.3	>1000	ND	ND
26	**2.144**	H	C(O)NH$_2$	CO$_2$Me	CH$_2$	>1000	ND	>1000	ND	>1000
27	**2.162**	H	CN	CO$_2$Me	CH$_2$CH$_2$	959 ± 130	214 ± 47	>1000	ND	>1000
28	**2.163**	H	CN	CO$_2$Me	OCH$_2$	>1000	261 ± 66	>1000	ND	>1000
29	**2.164**	H	CN	CO$_2$Me	SCH$_2$	574 ± 76	100.8 ± 22.6	ND	ND	>1000
30	**2.165**	H	CN	CO$_2$Me	SO$_2$CH$_2$	>1000	>1000	ND	ND	>1000

Tubulin polymerization assay[m]

An *in vitro* tubulin polymerization assay was performed to evaluate the effect of macrocycle series on microtubule dynamics and stability (Figure 2.39). In the assay, paclitaxel-induced self-polymerization of soluble α,β-tubulin heterodimer to microtubules under buffered conditions was monitored in the presence of macrocycles and vinorelbine by measuring changes in light scattering at 340 nm.[50] A slope was calculated for the linear growth phase of the tubulin polymerization curves to render a comparison vs. the positive assembly control containing 10 μM paclitaxel (Table 2.13). Paclitaxel-induced self-polymerization was measured in the presence of the compounds **2.92**, **2.95**, **2.120**, **2.126**, **2.128**, **2.142**, **2.136** and **2.145** that showed high or medium antiproliferative activity. In addition, macrocycles with weak antiproliferative effects such **2.106**, **2.107**, **2.162**, **2.165** as well as carboxylic acid **2.104** were also examined to verify the correlation between antiproliferative activity of the macrocycles and effect they exert on tubulin polymerization dynamics. Finally, vinorelbine was also tested as the assay positive control. Tubulin was obtained from porcine brain and purified as described in Experimental Section.[56]

Table 2.13

Tubulin polymerization assay results

Entry	Ligand[a]	Slope[b]	R^2 fit
1	Control	1.000	0.999
2	VNB	0.010	0.999
3	**2.92**	0.021	0.999
4	**2.95**	0.061	0.998
5	**2.104**	0.019	0.999
6	**2.106**	0.020	0.999
7	**2.107**	0.040	0.999
8	**2.120**	0.040	0.999
9	**2.126**	0.198	0.999
10	**2.128**	0.007	0.999
11	**2.136**	0.046	0.979
12	**2.142**	0.033	0.999
13	**2.145**	0.075	0.999
14	**2.162**	0.058	0.998
15	**2.165**	0.551	0.999

[a] 2:1 tubulin:ligand ratio;
[b] Slope values are relative to that of control (entry 1)

---

[m] Polymerization experiments were performed with the assistance of Dr. Diana Zelencova-Gopejenko.
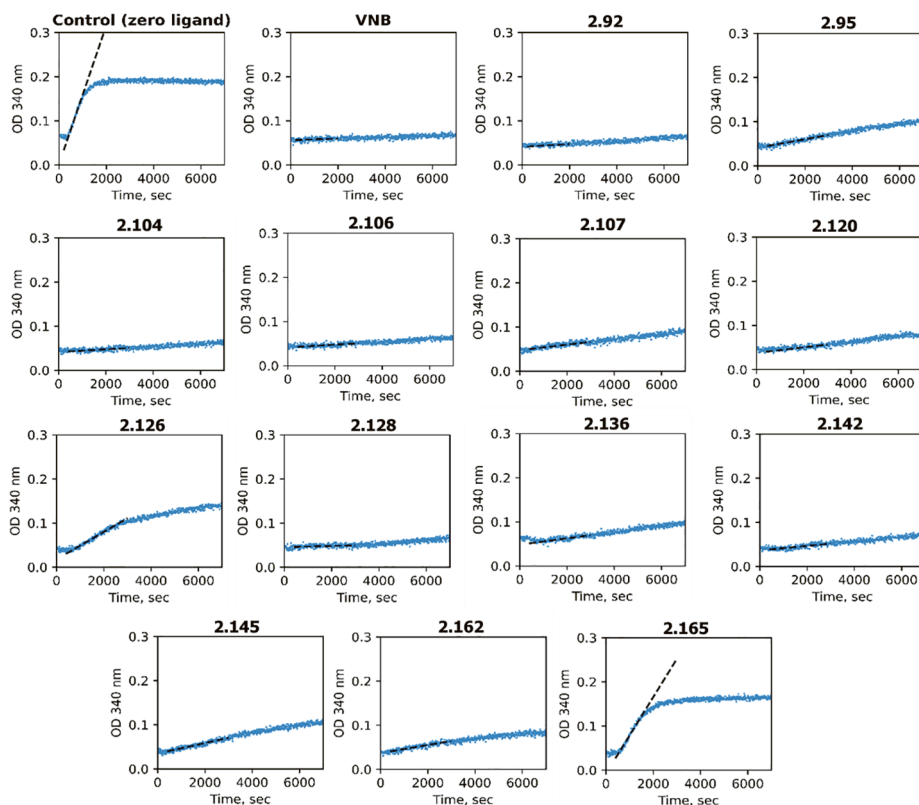
Figure 2.39. **Enhancer control tubulin self-polymerization assay results for macrocycles 2.92, 2.95, 2.104, 2.106, 2.107, 2.120, 2.126, 2.128, 2.136, 2.142, 2.145, 2.162, 2.165 and vinorelbine**

A strong correlation between the inhibition of tubulin polymerization and *in vitro* antiproliferative activity was observed for most of the tested macrocycles, such as **2.92**, **2.95**, **2.107**, **2.120**, **2.126**, **2.128**, **2.136**, **2.142**, **2.145**, **2.162** and **2.165** (Table 2.13). The macrocycles with the lowest GI_{50} values in Table 2.13 also exhibited the lowest slope values of the polymerization curve, indicating that their *in vitro* antiproliferative effects is likely to be attributed to the disruption of microtubule dynamics. However, some of the macrocycles in the series did not exhibit a correlation between GI_{50} values and tubulin polymerization inhibition potency. As expected, one of these compounds was carboxylic acid **2.104**, which demonstrated no antiproliferative activity against cancer cells, despite having a polymerization curve slope comparable to that of methyl ester **2.92**. A similar lack of correlation was observed for acylal **2.106**. The apparent lack of correlation for acid **2.104** and acylal **2.106** led us to hypothesize that poor cell permeability for the former and low stability in cell medium for the latter (leading to **2.106** hydrolysis to **2.104**) could be responsible for the lack of *in vitro* activity.

Plasma stability assay[n]

Compounds **2.128**, **2.120**, **2.117**, **2.95**, **2.92** as well as benzyl ester **2.86** from the oxindole series were tested for their stability in mouse plasma (Table 2.14). Verapamil and propantheline bromide were used as the assay negative and positive controls (entries 1 and 2). The most stable compound among all tested analogs was macrocycle **2.128**. After incubation of **2.128** in mouse plasma for 2 h, 96.2% of the compound remains in the medium (entry 3). Carbonate **2.120** as well as methyl ester **2.92** and benzyl ester from oxindole series **2.86** were unstable (entries 4, 6 and 7). Likewise, only half of *tert*-butyl ester **2.117** was measured in the medium after incubation in mouse plasma for 15 min (entry 5). Consequently, high antiproliferative effects, functional effect on tubulin polymerization and high stability in mouse plasma taken together, difluoromethyl-substituted macrocycle **2.128** was selected as a front-runner of the series.

Table 2.14

Plasma stability data

Entry		% of a compound found				
		0 min	15 min	30 min	60 min	120 min
1	Verapamil	100.0	93.6	99.1	96.1	99.3
2	Propantheline bromide	100.0	80.7	55.3	21.8	2.8
3	% of **2.128** found	100.0	95.8	94.2	96.9	96.4
4	% of **2.120** found	100.0	0.2	–	–	–
5	% of **2.117** found	100.0	55.3	27.6	10.2	1.0
6	% of **2.92** found	100.0	–	–	–	–
7	% of **2.86** found	100.0	–	–	–	–

In summary, a series of structurally simplified analogs of highly complex natural product diazonamide A with improved metabolic stability was developed. Thus, the replacement of an ester moiety by difluoromethyl substituent and oxindole subunit by indane fragment allowed for the improvement of mouse plasma stability. Difluoromethyl-substituted macrocycle **2.128** is relatively easy-to-synthesize (13 linear steps from *tert*-Leucine with 4% overall yield), and the macrocyclization proceeds with excellent diastereoselectivity (99:1 dr). The compound showed strong inhibition of tubulin polymerization with slope value comparable to vinorelbine. Macrocycle **2.128** possesses low nanomolar antiproliferative activity against melanoma cancer cell lines A2058 and MDA-MB-435, while being inactive against non-malignant cell line HEK-293. Overall, macrocycle **2.128** has good development potential as anticancer agent and is suitable for further preclinical testing.

---

[n] Plasma stability assay was performed by Dr. Solveiga Grinberga and Baiba Gukalova.

3. EXPERIMENTAL PART

General information

All reactions were caried out under argon atmosphere. All chemicals were obtained from commercial sources. Reactions were monitored with either analytical TLC (pre-coated silica gel F-254 plates (Merck)) or UPLC-MS (Waters Acquity H-series with SQ-2 detector; column: Acquity BEH C18 1.7 μm, 2.1 × 50 mm; eluent: 9 : 1 to 5 : 95 0.01% aqeous TFA : MeCN). Flash column chromatography was performed on Armen Instrument systems with either silica gel (Zeochem ZEOprep 60 40–63 μm) or C18 silica gel (Biotage Sfar C18 D 100 Å 30 μm). Preparative HPLC purification was performed on Shimadzu LC-8A system with SPD-20A UV/Vis detector and Waters Xbridge BEH C18 OBD 5 μm, 10 × 150 mm or Atlantis T3 Prep 5 μm, 30 × 100 mm columns. Column chromatography was perfomed using Acros silicagel (0.060–0.200 nm). All NMR spectra were recorded on Bruker Avance Neo 600, Avance Neo 400 or Fourier 300 instruments at 600, 400 or 300 MHz for ^{1}H-NMR and 151, 101 or 75 MHz for ^{13}C-NMR. Chemical shifts are reported in parts per million (ppm) relative to TMS or with the residual solvent peak as an internal reference. High-resolution mass spectra (HRMS) were recorded on Waters Synapt G2-Si instrument using ESI ionization technique. Optical rotation ($[\alpha]D^{20}$) was measured on Kruess P3000 polarimeter. Prior to biological testing procedures, all compounds were determined to be > 95% pure by UPLC-MS method.

Synthesis of compounds **2.1–2.4** is described in: Vitkovska, V., Zogota, R., Kalnins, T., Zelencova, D., Suna, E. Aliphatic Chain-Containing Macrocycles as Diazonamide A Analogs. *Chem. Heterocycl. Compd.* **2020**, *56* (5), 586–602 (see appendix I).

Synthesis of compounds **2.29–2.30**, **2.79a–f**, **2.51–2.53**, **2.55–2.56**, **2.85–2.87** is described in: Kalnins. T.; Vitkovska, V.; Kazak, M.; Zelencova-Gopejenko, D.; Ozola, M.; Narvaiss, N.; Makrecka-Kuka, M.; Domraceva, I.; Kinens, A.; Gukalova, B.; Konrad, N.; Aav, R.; Bonato, F.; Lucena-Agell, D.; Díaz, J. F.; Liepinsh, E.; Suna, E. Development of Potent Microtubule Targeting Agent by Structural Simplification of Natural Diazonamide. *J. Med. Chem.* **2024**, *67*, 9227–9259 (see appendix II).

Synthesis of all compounds is described in: Vitkovska V., Kazak M., Suna E. Macrocyclic Tubulin Polymerization Inhibitors as Anticancer Agents. Application number: PCT/IB2024/059899, Oct. 10, 2024. (see appendix IV).

Synthesis of compounds

General Method A. *N*-Boc protected macrocycle was dissolved in dry DCM and TFA (10 equiv.) was added dropwise at room temperature. The yellow solution was stirred for 1–2 h and the reaction mixure was evaporated. The residue was dissolved in dry DCM and washed with saturated aqueous $NaHCO_3$. Organics were washed with brine, dried over Na_2SO_4, filtered through cotton plug and evaporated. Crude amine (1 equiv.) was used in the next reaction without additional purification. Crude amine was dissolved in dry DMF and carboxylic acid (1.5 equiv.), EDC×HCl (3 equiv.), HOBt

(3 equiv.) were added followed by DIPEA (6 equiv.). The resulting solution was stirred at room temperature for 1 h. The reaction mixture was diluted with EtOAc and washed with saturated aqueous NH_4Cl, water and brine. Organics were dried over anhydrous Na_2SO_4, filtered through cotton plug and evaporated. The residue was purified with reverse phase flash chromatography (from 10% to 50% MeCN in 0.01% TFA in water).

General Method B. In MW vial methyl ester (1 equiv.) was dissolved in dry toluene and DMF (10:1, v/v) and alcohol (40 equiv.) was added dropwise followed by Ti(O*i*Pr)$_4$ (1 equiv.). The vial was closed with aluminum cap and stirred at 100 °C in mineral oil bath for 18 h. Then the vial was cooled to room temperature and quenched by the addition of aqueous 1N HCl. The resulting mixture was extracted with EtOAc (two times), organic layers were combined and washed with brine. Organics were dried over anhydrous Na_2SO_4, filtered through cotton plug and evaporated. The residue was purified with reverse phase flash chromatography (from 10% to 50% MeCN in 0.01% TFA in water).
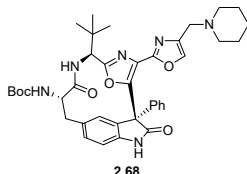

2.67
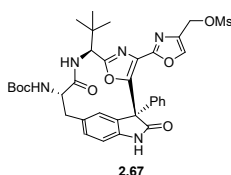
***tert*-Butyl *N*-[(1*S*,6*S*,9*S*)-6-*tert*-butyl-3-{4-[(methanesulfonyloxy)methyl]-1,3-oxazol-2-yl}-8,16-dioxo-1-phenyl-19-oxa-4,7,15-triazatetracyclo[9.5.2.1²,⁵.0¹⁴,¹⁷]nonadeca-2,4,11,13,17-pentaen-9-yl]carbamate (2.67).** Alcohol **2.32** (215 mg, 0.34 mmol, 1 equiv.) was dissolved in dry THF (3 mL) and TEA (96 µL, 0.69 mmol, 2 equiv.) was added dropwise at room temperature followed by DMAP (1 mg, 0.01 mmol, 0.03 equiv.). The solution was cooled to 0 °C in ice bath and MsCl (40 µL, 0.51 mmol, 1.5 equiv.) was added dropwise. The resulting yellow solution was stirred at the same temperature for 30 minutes. The solution was diluted with EtOAc and washed with aqueous 1N HCl, water and brine. Organic layer was dried over anhydrous Na_2SO_4, filtered through cotton plug and evaporated. The residue (yellow oil) was used in the next reaction without additional purification.
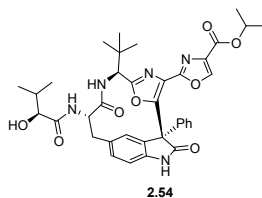
2.54

Propan-2-yl 2-[(1*S*,6*S*,9*S*)-6-*tert*-butyl-9-[(2*S*)-2-hydroxy-3-methylbutanamido]-8,16-dioxo-1-phenyl-19-oxa-4,7,15-triazatetracyclo[9.5.2.1²,⁵.0¹⁴,¹⁷]nonadeca-2,4,11,13,17-pentaen-3-yl]-1,3-oxazole-4-carboxylate (2.54). The compound **2.54** was obtained from macrocycle **2.49** (100 mg, 0.15 mmol), *i*PrOH (470 µL, 6.1 mmol) and Ti(O*i*Pr)$_4$ (45 µL, 0.15 mmol) following General Method B to give ester **2.54** (85 mg, 82%) as a white amorphous solid. ^{1}H NMR (400 MHz, MeOD) δ 8.37 (d, J = 0.7 Hz, 1H), 7.48–7.40 (m, 2H), 7.40–7.30 (m, 3H), 7.27 (d, J = 7.3 Hz, 2H), 6.98–6.89 (m, 1H), 5.21 (hept, J = 6.3 Hz, 1H), 4.97 (s, 1H), 4.44 (dd, J = 11.7, 3.7 Hz, 1H), 3.86 (d, J = 3.7 Hz, 1H), 3.19 (t, J = 12.2 Hz, 1H), 2.81 (dd, J = 12.6, 3.8 Hz, 1H),

2.08 (sept d, *J* = 6.9, 3.8 Hz, 1H), 1.35 (d, *J* = 6.2 Hz, 6H), 1.07 (s, 9H), 1.00 (d, *J* = 6.9 Hz, 3H), 0.89 (d, *J* = 6.9 Hz, 3H). ^{13}C NMR (101 MHz, MeOD) δ 176.1, 175.8, 174.0, 164.5, 161.8, 156.4, 152.2, 146.4, 141.7, 137.2, 135.4, 133.4, 132.2, 131.4, 130.6, 130.0, 129.4, 128.7, 127.3, 112.0, 76.8, 70.3, 60.4, 58.2, 56.7, 39.3, 34.1, 33.1, 26.7, 22.0, 19.6, 16.3. HRMS (ESI/Q-TOF) m/z: found: 684.3033. Calculated for $C_{37}H_{42}N_5O_8$ [M+H]$^+$: 684.3033. [α] D^{20} –234 (c 1.0, MeOH).

2.68

***tert*-Butyl *N*-[(1*S*,6*S*,9*S*)-6-*tert*-butyl-8,16-dioxo-1-phenyl-3-{4-[(piperidin-1-yl) methyl]-1,3-oxazol-2-yl}-19-oxa-4,7,15-triazatetracyclo[9.5.2.1^{2,5}.0^{14,17}]nonade-ca-2,4,11,13,17-pentaen-9-yl]carbamate (2.68).** Mesylate **2.67** (135 mg, 0.19 mmol, 1 equiv.) was dissolved in dry DMF (2 mL) and piperidine (189 μL, 1.91 mmol, 10 ekv.) was added dropwise followed by K$_2$CO$_3$ (132 mg, 0.96 mmol, 5 equiv.). Resulting yellow suspension was stirred for 1 h at room temperature. Then the reaction mixture was diluted with EtOAc and washed with aqueous 1N HCl (×2). Organic layers were combined, washed with brine, dried over anhydrous Na$_2$SO$_4$, filtered through cotton plug and evaporated. The resulting yellow oil was purified with reverse phase flash chromatography (from 10% to 70% MeCN in water) to give amine **2.68** (55 mg, 41%) as a white amorphous solid. ^{1}H NMR (400 MHz, CDCl$_3$) δ 11.32 (br. s., 1H), 10.64 (br.s., 1H), 8.52 (s, 1H), 7.54 (s, 1H), 7.38–7.32 (m, 2H), 7.29–7.22 (m, 3H), 7.04 (dd, *J* = 7.9, 1.8 Hz, 1H), 6.78 (d, *J* = 8.8 Hz, 1H), 6.70 (d, *J* = 7.9 Hz, 1H), 5.30 (d, *J* = 9.1 Hz, 1H), 4.99 (d, *J* = 8.8 Hz, 1H), 4.08–3.93 (m, 2H), 3.72 (d, *J* = 13.8 Hz, 1H), 3.11 (t, *J* = 12.1 Hz, 1H), 3.03–2.84 (m, 3H), 2.77 (dd, *J* = 12.6, 3.6 Hz, 1H), 1.82–1.72 (m, 4H), 1.53–1.39 (m, 11H), 1.05 (s, 9H). ^{13}C NMR (101 MHz, CDCl$_3$) δ 175.1, 172.2, 168.5, 162.8, 155.2, 154.9, 150.1, 140.4, 140.1, 136.1, 132.7, 132.3, 130.9, 129.7, 128.9, 128.2, 127.7, 126.9, 110.8, 80.2, 59.3, 58.0, 56.9, 52.5, 51.1, 41.0, 38.3, 33.3, 28.4, 26.5, 23.4, 22.5. HRMS (ESI/Q-TOF) m/z: found: 695.3579. Calculated for $C_{39}H_{47}N_6O_6$ [M+H]$^+$: 695.3557. [α] D^{20} –190.0 (c 1.0, CHCl$_3$).
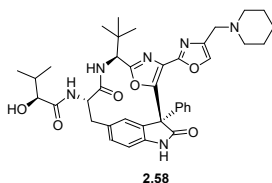
2.58

(2*S*)-*N*-[(1*S*,6*S*,9*S*)-6-*tert*-Butyl-8,16-dioxo-1-phenyl-3-{4-[(piperidin-1-yl) methyl]-1,3-oxazol-2-yl}-19-oxa-4,7,15-triazatetracyclo[9.5.2.1^{2,5}.0^{14,17}]nonade-ca-2,4,11,13,17-pentaen-9-yl]-2-hydroxy-3-methylbutanamide (2.58). Compound **2.58** was obtained from macrocycle **2.68** (55 mg, 0.79 mmol), TFA (61 μL, 0.79 mmol) in dry DCM (1 mL) and from (*S*)-(+)-2-hydroxy-3-methylbutyric acid (14 mg, 0.12 mmol), EDC×HCl (30 mg, 0.16 mmol), HOBt (32 mg, 0.24 mmol) and DIPEA (68 μL, 0.40 mmol) in dry DMF (1 mL) following General method A. White amorphous solid (29 mg, 53%). ^{1}H NMR (400 MHz, MeOD) δ 7.93 (s, 1H),

7.44–7.40 (m, 2H), 7.39–7.31 (m, 3H), 7.28 (dd, J = 8.1, 1.8 Hz, 1H), 7.21 (d, J = 1.8 Hz, 1H), 6.93 (d, J = 8.1 Hz, 1H), 4.91 (s, 1H), 4.47 (dd, J = 11.8, 3.9 Hz, 1H), 4.10–3.96 (m, 2H), 3.86 (d, J = 3.9 Hz, 1H), 3.16 (t, J = 12.1 Hz, 1H), 3.09–2.95 (m, 4H), 2.84 (dd, J = 12.6, 3.9 Hz, 1H), 2.08 (septd, J = 6.9, 3.9 Hz, 1H), 1.82–1.73 (m, 4H), 1.64 –1.55 (m, 2H), 1.06 (s, 9H), 1.00 (d, J = 6.9 Hz, 3H), 0.89 (d, J = 6.9 Hz, 3H). ^{13}C NMR (101 MHz, MeOD) δ 176.4, 175.8, 174.0, 164.1, 156.3, 151.5, 141.9, 141.6, 137.7, 133.9, 133.7, 132.3, 131.4, 130.7, 129.9, 129.3, 128.6, 128.2, 112.0, 76.8, 60.6, 58.6, 56.7, 54.1, 52.6, 39.3, 34.2, 33.2, 26.7, 24.8, 23.1, 19.5, 16.3. HRMS (ESI/Q-TOF) m/z: found: 695.3553. Calculated for $C_{39}H_{47}N_6O_6$ [M+H]$^+$: 695.3557. [α]D^{20} –168.0 (c 1.0, MeOH).
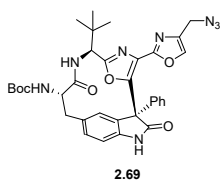
2.69

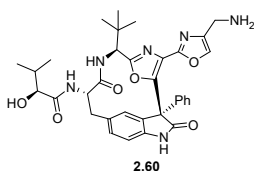*tert*-**Butyl *N*-[(1*S*,6*S*,9*S*)-3-[4-(azidomethyl)-1,3-oxazol-2-yl]-6-*tert*-butyl-8,16-dioxo-1-phenyl-19-oxa-4,7,15-triazatetracyclo[9.5.2.1^{2,5}.0^{14,17}]nonadeca-2,4,11,13,17-pentaen-9-yl]carbamate (2.69).** Mesylate **2.67** (215 mg, 0.31 mmol, 1 equiv.) was dissolved in dry DMF (2 mL) and NaN$_3$ (59 mg, 0.91 mmol, 3 equiv.) was added dropwise followed by K$_2$CO$_3$ (211 mg, 1.52 mmol, 5 equiv.) and NaI (5 mg, 0.03 mmol, 0.1 equiv.). Resulting yellow suspension was stirred for 1 h at room temperature. Then the reaction mixture was diluted with EtOAc and washed with saturated aqueous NH$_4$Cl (×2). Organic layers were combined, washed with brine, dried over anhydrous Na$_2$SO$_4$, filtered through cotton plug and evaporated. The resulting yellow oil was purified with reverse phase flash chromatography (from 10% to 70% MeCN in water) to give azide **2.69** (102 mg, 51%) as a white amorphous solid. ^{1}H NMR (400 MHz, CDCl$_3$) δ 8.72 (s, 1H), 7.46–7.37 (m, 2H), 7.32 (s, 1H), 7.29–7.24 (m, 3H), 7.14 (d, J = 1.6 Hz, 1H), 7.06 (dd, J = 8.0, 1.6 Hz, 1H), 6.72 (d, J = 8.0 Hz, 1H), 6.17 (d, J = 8.2 Hz, 1H), 5.32 (d, J = 9.3 Hz, 1H), 4.86 (d, J = 8.2 Hz, 1H), 4.28 (s, 2H), 3.98 (ddd, J = 12.4, 9.3, 3.6 Hz, 1H), 3.14 (t, J = 12.1 Hz, 1H), 2.81 (dd, J = 12.4, 3.6 Hz, 1H), 1.45 (s, 9H), 1.03 (s, 9H). ^{13}C NMR (101 MHz, CDCl$_3$) δ 174.9, 172.0, 162.3, 155.4, 155.1, 149.9, 139.4, 136.8, 135.6, 133.1, 131.4, 130.0, 129.5, 128.9, 128.4, 128.3, 127.4, 111.0, 80.6, 59.0, 58.3, 57.8, 46.3, 38.2, 33.4, 28.4, 26.6. HRMS (ESI/Q-TOF) m/z: found: 653.2825. Calculated for $C_{34}H_{37}N_8O_6$ [M+H]$^+$: 653.2836. [α]D^{20} –130.0 (c 1.0, CHCl$_3$).

2.59
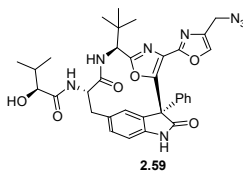
(2*S*)-*N*-[(1*S*,6*S*,9*S*)-3-[4-(Azidomethyl)-1,3-oxazol-2-yl]-6-*tert*-butyl-8,16-dioxo-1-phenyl-19-oxa-4,7,15-triazatetracyclo[9.5.2.1^{2,5}.0^{14,17}]nonadeca-2,4,11,13,17-pentaen-9-yl]-2-hydroxy-3-methylbutanamide (2.59). Compound **2.59** was obtained from macrocycle **2.69** (81 mg, 0.12 mmol), TFA (95 µL, 1.24 mmol) in dry DCM (1 mL) and from (S)-(+)-2-hydroxy-3-methylbutyric acid (22 mg, 0.19 mmol), EDC×HCl (48 mg, 0.25 mmol), HOBt (51 mg, 0.38 mmol) and DIPEA (110 µL, 0.62 mmol) in dry DMF (1 mL) following General method A. White amorphous solid (58 mg, 71%).

^{1}H NMR (400 MHz, MeOD) δ 7.74 (s, 1H), 7.46–7.39 (m, 2H), 7.37–7.29 (m, 3H), 7.27 (dd, *J* = 8.0, 1.8 Hz, 1H), 7.21 (d, *J* = 1.8 Hz, 1H), 6.92 (d, *J* = 8.0 Hz, 1H), 4.89 (s, 1H), 4.47 (dd, *J* = 11.7, 3.9 Hz, 1H), 4.26 (s, 2H), 3.86 (d, *J* = 3.9 Hz, 1H), 3.16 (t, *J* = 12.1 Hz, 1H), 2.82 (dd, *J* = 12.6, 3.9 Hz, 1H), 2.08 (sept d, *J* = 6.9, 3.8 Hz, 1H), 1.05 (s, 9H), 1.00 (d, *J* = 6.9 Hz, 3H), 0.89 (d, *J* = 6.9 Hz, 3H). ^{13}C NMR (101 MHz, MeOD) δ 176.4, 175.8, 174.0, 164.3, 156.3, 151.8, 141.7, 139.1, 138.0, 137.3, 134.1, 132.2, 131.3, 130.5, 129.9, 129.3, 128.7, 128.3, 112.0, 76.8, 60.5, 58.7, 56.6, 46.5, 39.2, 34.2, 33.1, 26.7, 19.6, 16.3. HRMS (ESI/Q-TOF) m/z: found: 653.2852. Calculated for $C_{34}H_{37}N_8O_6$ [M+H]$^{+}$: 653.2836. [α]D^{20} –240.0 (c 1.0, MeOH).
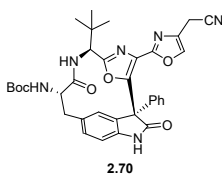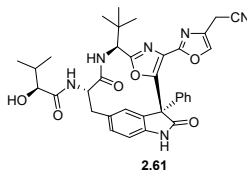

2.60

(2*S*)-*N*-[(1*S*,6*S*,9*S*)-3-[4-(Aminomethyl)-1,3-oxazol-2-yl]-6-*tert*-butyl-8,16-dioxo-1-phenyl-19-oxa-4,7,15-triazatetracyclo[9.5.2.1²,⁵.0¹⁴,¹⁷]nonadeca-2,4,11,13,17-pentaen-9-yl]-2-hydroxy-3-methylbutanamide (2.60). Azide **2.59** (40 mg, 0.061 mmol, 1 equiv.) was dissolved in dry MeOH (1 mL) and 10% Pd/C (7 mg, 0.0061 mmol, 0.1 equiv.) was added in one portion. Hydrogen gas was barbotated through the black suspension for 1 h at room temperature. Then the suspension was filtrated through Celite® and washed the filter with MeOH (×2). The resulting filtrate was evaporated and purified with reverse phase flash chromatography (from 10% to 50% MeCN in aqueous 0.1% TFA) to give amine **2.60** (29 mg, 76%) as a white amorphous solid. ^{1}H NMR (400 MHz, MeOD) δ 7.83 (s, 1H), 7.44–7.39 (m, 2H), 7.37–7.30 (m, 3H), 7.28 (dd, *J* = 8.0, 1.7 Hz, 1H), 7.20 (d, *J* = 1.7 Hz, 1H), 6.94 (d, *J* = 8.0 Hz, 1H), 4.87 (s, 2H), 4.48 (dd, *J* = 11.7, 3.9 Hz, 1H), 3.95 (s, 1H), 3.87 (d, *J* = 3.8 Hz, 1H), 3.15 (t, *J* = 12.2 Hz, 1H), 2.84 (dd, *J* = 12.6, 3.9 Hz, 1H), 2.08 (sept d, *J* = 6.9, 3.8 Hz, 1H), 1.05 (s, 9H), 1.00 (d, *J* = 6.9 Hz, 3H), 0.89 (d, *J* = 6.9 Hz, 3H). ^{13}C NMR (101 MHz, MeOD) δ 176.6, 175.8, 174.0, 164.2, 156.2, 151.5, 141.6, 139.3, 137.5, 136.8, 134.1, 132.3, 131.4, 130.6, 129.9, 129.2, 128.6, 128.4, 112.1, 76.8, 60.6, 58.8, 56.6, 39.2, 35.9, 34.2, 33.2, 26.7, 19.5, 16.3. HRMS (ESI/Q-TOF) m/z: found: 627.2942. Calculated for $C_{34}H_{39}N_6O_6$ [M+H]$^{+}$: 627.2931. [α]D^{20} –196.0 (c 1.0, MeOH).

2.70

***tert*-Butyl *N*-[(1*S*,6*S*,9*S*)-6-*tert*-butyl-3-[4-(cyanomethyl)-1,3-oxazol-2-yl]-8,16-dioxo-1-phenyl-19-oxa-4,7,15-triazatetracyclo[9.5.2.1²,⁵.0¹⁴,¹⁷]nonadeca-2,4,11,13,17-pentaen-9-yl]carbamate (2.70).** Mesylate **2.67** (62 mg, 0.09 mmol, 1 equiv.) was dissolved in dry DMF (1 mL) and NaCN (43 mg, 0.88 mmol, 10 equiv.) was added in one portion at room temperature. Resulting yellow suspension was stirred for 1 h. Then the reaction mixture was diluted with EtOAc and washed with saturated aqueous NH₄Cl (×2). Organic layers were combined, washed with brine, dried over anhydrous Na₂SO₄, filtered through cotton plug and evaporated. The resulting yellow

oil was purified with reverse phase flash chromatography (from 10% to 50% MeCN in aqueous 0.1% TFA) to give nitrile **2.70** (102 mg, 51%) as a white amorphous solid. ^{1}H NMR (400 MHz, CDCl$_3$) δ 10.03 (s, 1H), 7.47–7.29 (m, 7H), 7.17 (d, J = 7.9 Hz, 1H), 6.79 (d, J = 7.9 Hz, 1H), 6.59 (d, J = 9.3 Hz, 1H), 5.27 (d, J = 9.2 Hz, 1H), 5.08 (d, J = 9.2 Hz, 1H), 4.02–3.79 (m, 2H), 3.52 (d, J = 19.1 Hz, 1H), 3.15 (t, J = 12.1 Hz, 1H), 2.82 (dd, J = 12.6, 3.4 Hz, 1H), 1.44 (s, 9H), 1.10 (s, 9H). ^{13}C NMR (101 MHz, CDCl$_3$) δ 175.9, 172.3, 163.3, 155.5, 155.1, 149.7, 139.4, 136.2, 135.5, 132.6, 131.7, 131.7, 130.3, 130.0, 129.1, 128.7, 128.0, 126.3, 115.9, 110.6, 80.2, 59.8, 57.8, 56.1, 38.7, 33.4, 28.4, 26.4, 15.9. HRMS (ESI/Q-TOF) m/z: found: 637.2783. Calculated for C$_{35}$H$_{37}$N$_6$O$_6$ [M+H]$^+$: 637.2775. [α]D^{20} –222 (c 1.0, CHCl$_3$).

2.61

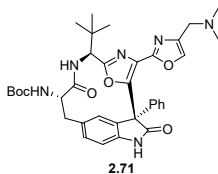**(2S)-N-[(1S,6S,9S)-6-*tert*-Butyl-3-[4-(cyanomethyl)-1,3-oxazol-2-yl]-8,16-dioxo-1-phenyl-19-oxa-4,7,15-triazatetracyclo[9.5.2.1^{2,5}.0^{14,17}]nonadeca-2,4,11,13,17-pentaen-9-yl]-2-hydroxy-3-methylbutanamide (2.61).** Compound **2.61** was obtained from macrocycle **2.70** (65 mg, 0.10 mmol), TFA (78 μL, 1.02 mmol) in dry DCM (1 mL) and from (S)-(+)-2-hydroxy-3-methylbutyric acid (18 mg, 0,15 mmol), EDC×HCl (39 mg, 0.21 mmol), HOBt (42 mg, 0.31 mmol) and DIPEA (89 μL, 0.51 mmol) in dry DMF (1 mL) following General method A. White amorphous solid (14 mg, 22%). ^{1}H NMR (400 MHz, MeOD) δ 7.73 (s, 1H), 7.44–7.40 (m, 2H), 7.37–7.30 (m, 3H), 7.27 (dd, J = 8.0, 1.8 Hz, 1H), 7.22 (d, J = 1.8 Hz, 1H), 6.92 (d, J = 8.0 Hz, 1H), 4.90 (s, 1H), 4.47 (dd, J = 11.7, 3.9 Hz, 1H), 3.86 (d, J = 3.9 Hz, 1H), 3.79 (d, J = 1.1 Hz, 2H), 3.16 (t, J = 12.1 Hz, 1H), 2.82 (dd, J = 12.6, 3.9 Hz, 1H), 2.08 (sept d, J = 6.9, 3.7 Hz, 1H), 1.05 (s, 9H), 1.00 (d, J = 6.9 Hz, 3H), 0.89 (d, J = 6.9 Hz, 3H). ^{13}C NMR (101 MHz, MeOD) δ 176.3, 175.8, 174.0, 164.3, 156.3, 151.8, 141.7, 138.6, 137.2, 134.0, 133.6, 132.2, 131.3, 130.6, 129.9, 129.3, 128.7, 128.2, 117.7, 112.0, 76.8, 60.5, 58.6, 56.6, 39.2, 34.2, 33.1, 26.7, 19.6, 16.3, 15.7. HRMS (ESI/Q-TOF) m/z: found: 637.2775. Calculated for C$_{35}$H$_{37}$N$_6$O$_6$ [M+H]$^+$: 637.2775. [α]D^{20} –249 (c 1.0, MeOH).

2.71

***tert*-Butyl *N*-[(1S,6S,9S)-6-*tert*-butyl-3-{4-[(dimethylamino)methyl]-1,3-oxazol-2-yl}-8,16-dioxo-1-phenyl-19-oxa-4,7,15-triazatetracyclo[9.5.2.1^{2,5}.0^{14,17}]nonadeca-2,4,11,13,17-pentaen-9-yl]carbamate (2.71).** Mesylate **2.67** (242 mg, 0.34 mmol, 1 equiv.) was dissolved in dimethylamine in MeOH (2M, 2.6 mL) at room temperature. The resulting yellow solution was stirred for 1 h and evaporated. The residual yellow oil was purified with reverse phase flash chromatography (from 10% to 50% MeCN in aqueous 0.1% TFA) to give amine **2.71** (70 mg, 31%) as a white amorphous solid. ^{1}H NMR (400 MHz, CDCl$_3$) δ 10.21 (s, 1H), 7.41–7.33 (m, 3H), 7.26–7.22 (m, 2H), 7.15 (d, J = 1.7 Hz, 1H), 7.00 (dd, J = 8.0, 1.8 Hz, 1H), 6.70 (d, J = 8.0 Hz, 1H), 6.36 (d, J = 8.3 Hz,

1H), 5.34–5.25 (m, 1H), 4.89 (d, J = 8.3 Hz, 1H), 4.02 (ddd, J = 12.6, 9.4, 3.8 Hz, 1H), 3.60 (q, J = 13.8 Hz, 2H), 3.09 (t, J = 12.1 Hz, 1H), 2.96–2.87 (m, 1H), 2.78 (dd, J = 12.5, 3.8 Hz, 1H), 2.46 (s, 6H), 1.46 (s, 9H), 1.05 (s, 9H). ^{13}C NMR (101 MHz, CDCl$_3$) δ 175.1, 172.1, 162.2, 155.4, 154.8, 149.7, 140.2, 138.3, 136.1, 132.9, 130.8, 129.9, 129.6, 128.9, 128.1, 127.9, 127.5, 111.0, 80.5, 77.2, 59.2, 58.0, 57.5, 53.5, 44.4, 38.3, 33.4, 28.5, 26.6. HRMS (ESI/Q-TOF) m/z: found: 655.3257. Calculated for C$_{36}$H$_{43}$N$_6$O$_6$ [M+H]$^+$: 655.3244. [α]D^{20} –206.0 (c 1.0, CHCl$_3$).
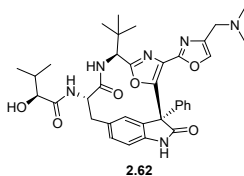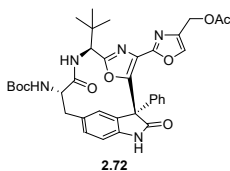

2.62

(2S)-N-[(1S,6S,9S)-6-$tert$-Butyl-3-{4-[(dimethylamino)methyl]-1,3-oxazol-2-yl}-8,16-dioxo-1-phenyl-19-oxa-4,7,15-triazatetracyclo[9.5.2.1^{2,5}.0^{14,17}]nonadeca-2,4,11,13,17-pentaen-9-yl]-2-hydroxy-3-methylbutanamide (2.62). Compound **2.62** was obtained from macrocycle **2.71** (58 mg, 0.09 mmol), TFA (68 µL, 0.89 mmol) in dry DCM (1 mL) and from (S)-(+)-2-hydroxy-3-methylbutyric acid (16 mg, 0.13 mmol), EDC×HCl (34 mg, 0.18 mmol), HOBt (36 mg, 0.27 mmol) and DIPEA (76 µL, 0,44 mmol) in dry DMF (1 mL) following General method A. White amorphous solid (20 mg, 35%). ^{1}H NMR (400 MHz, MeOD) δ 7.93 (s, 1H), 7.45–7.38 (m, 2H), 7.37–7.30 (m, 3H), 7.28 (dd, J = 8.0, 1.7 Hz, 1H), 7.23 (d, J = 1.7 Hz, 1H), 6.93 (d, J = 8.0 Hz, 1H), 4.92 (s, 1H), 4.47 (dd, J = 11.7, 3.8 Hz, 1H), 4.05–3.91 (s, 2H), 3.86 (d, J = 3.8 Hz, 1H), 3.16 (t, J = 12.2 Hz, 1H), 2.83 (dd, J = 12.6, 3.8 Hz, 1H), 2.66 (s, 6H), 2.08 (sept d, J = 6.9, 3.8 Hz, 1H), 1.06 (s, 9H), 1.00 (d, J = 6.9 Hz, 3H), 0.89 (d, J = 6.9 Hz, 3H). ^{13}C NMR (101 MHz, MeOD) δ 176.3, 175.8, 174.0, 164.2, 151.6, 141.6, 137.6, 134.5, 133.8, 132.2, 131.4, 130.6, 129.9, 129.3, 128.6, 128.2, 112.0, 101.4, 76.8, 60.5, 58.5, 56.7, 53.2, 43.6, 40.4, 39.2, 34.2, 33.2, 26.7, 19.5, 16.3. HRMS (ESI/Q-TOF) m/z: found: 655.3256. Calculated for C$_{36}$H$_{43}$N$_6$O$_6$ [M+H]$^+$: 655.3244. [α]D^{20} –223 (c 1.0, MeOH).

2.72

{2-[(1S,6S,9S)-9-{[($tert$-Butoxy)carbonyl]amino}-6-$tert$-butyl-8,16-dioxo-1-phenyl-19-oxa-4,7,15-triazatetracyclo[9.5.2.1^{2,5}.0^{14,17}]nonadeca-2,4,11,13,17-pentaen-3-yl]-1,3-oxazol-4-yl}methyl acetate (2.72). Mesylate **2.67** (80 mg, 0.11 mmol, 1 equiv.) was dissolved in dry DMF (0.5 mL) and KOAc (56 mg, 0.57 mmol, 5 equiv.) was added in one portion at room temperature. Then the MW vial was closed with aluminium cap and stirred at 65 °C for 1 h. The vial was cooled to room temperature and quenched by the addition of saturated aqueous NH$_4$Cl. The resulting mixture was extracted with EtOAc (×2), organic layers were combined and washed with brine, dried over anhydrous Na$_2$SO$_4$, filtered through cotton plug and evaporated. The resulting dark yellow oil was purified with reverse phase flash chromatography (10% to 70% MeCN in water) to give **2.72** (30 mg, 40%) as a white amorphous solid. ^{1}H NMR (400 MHz, CDCl$_3$) δ 10.08 (s, 1H), 7.55 (s, 1H), 7.43 (s, 1H), 7.39–7.29 (m, 5H),

7.15 (d, J = 9.3 Hz, 1H), 7.08 (dd, J = 8.0, 1.7 Hz, 1H), 6.72 (d, J = 8.0 Hz, 1H), 5.26 (d, J = 9.3 Hz, 1H), 5.13 (d, J = 9.2 Hz, 1H), 4.71–4.47 (m, 2H), 3.98–3.89 (m, 1H), 3.20 (t, J = 12.2 Hz, 1H), 2.78 (dd, J = 12.7, 3.3 Hz, 1H), 2.06 (s, 3H), 1.44 (s, 9H), 1.11 (s, 9H). ^{13}C NMR (101 MHz, CDCl$_3$) δ 176.1, 172.3, 171.4, 163.1, 155.1, 154.2, 149.1, 139.7, 137.3, 137.2, 135.8, 132.0, 131.8, 129.8, 129.5, 129.1, 128.5, 127.9, 126.7, 110.6, 80.1, 59.53, 59.47, 57.9, 56.3, 38.8, 33.4, 28.4, 26.5, 21.2. HRMS (ESI/Q-TOF) m/z: found: 670.2892. Calculated for C$_{36}$H$_{40}$N$_5$O$_8$ [M+H]$^+$: 670.2877. [α]D^{20} –264 (c 1.0, CHCl$_3$).
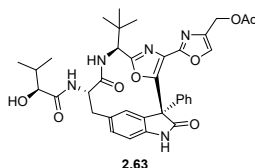
2.63

{2-[(1S,6S,9S)-6-*tert*-Butyl-9-[(2S)-2-hydroxy-3-methylbutanamido]-8,16-dioxo-1-phenyl-19-oxa-4,7,15-triazatetracyclo[9.5.2.1^{2,5}.0^{14,17}]nonadeca-2,4,11,13,17-pentaen-3-yl]-1,3-oxazol-4-yl}methyl acetate (2.63). Compound **2.63** was obtained from macrocycle **2.72** (30 mg, 0.05 mmol), TFA (34 µL, 0.5 mmol) in dry DCM (0.5 mL) and from (S)-(+)-2-hydroxy-3-methylbutyric acid (9 mg, 0.08 mmol), EDC×HCl (19 mg, 0.10 mmol), HOBt (20 mg, 0.15 mmol) and DIPEA (43 µL, 0.25 mmol) in dry DMF (1 mL) following General method A. White amorphous solid (16 mg, 52%). ^{1}H NMR (400 MHz, MeOD) δ 7.75 (s, 1H), 7.44–7.39 (m, 2H), 7.36–7.29 (m, 3H), 7.26 (dd, J = 8.0, 1.8 Hz, 1H), 7.22 (d, J = 1.8 Hz, 1H), 6.91 (d, J = 8.0 Hz, 1H), 4.99 (d, J = 0.9 Hz, 2H), 4.91 (s, 1H), 4.46 (dd, J = 11.7, 3.8 Hz, 1H), 3.86 (d, J = 3.8 Hz, 1H), 3.16 (t, J = 12.2 Hz, 1H), 2.82 (dd, J = 12.6, 3.8 Hz, 1H), 2.12–2.04 (m, 1H), 2.07 (s, 3H), 1.06 (s, 9H), 1.00 (d, J = 6.9 Hz, 3H), 0.89 (d, J = 6.9 Hz, 3H). ^{13}C NMR (101 MHz, MeOD) δ 176.3, 175.8, 174.0, 172.3, 164.3, 156.0, 151.7, 141.7, 139.9, 138.1, 137.3, 133.9, 132.2, 131.3, 130.5, 129.9, 129.3, 128.7, 128.2, 112.0, 76.8, 60.5, 58.6, 58.5, 56.7, 39.3, 34.2, 33.1, 26.7, 20.7, 19.6, 16.3. HRMS (ESI/Q-TOF) m/z: found: 670.2901. Calculated for C$_{36}$H$_{40}$N$_5$O$_8$ [M+H]$^+$: 670.2877. [α]D^{20} –270 (c 1.0, MeOH).
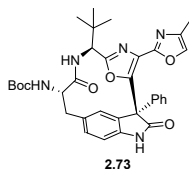
2.73

***tert*-Butyl N-[(1S,6S,9S)-6-*tert*-butyl-3-(4-methyl-1,3-oxazol-2-yl)-8,16-dioxo-1-phenyl-19-oxa-4,7,15-triazatetracyclo[9.5.2.1^{2,5}.0^{14,17}]nonadeca-2,4,11,13,17-pentaen-9-yl]carbamate (2.73).** Mesylate **2.67** (120 mg, 0.17 mmol, 1 equiv.) was dissolved in dry DMSO (2 mL) and NaBH$_4$ (32 mg, 0.85 mmol, 5 equiv.) was added in one portion at room temperature. Then the MW vial was closed with aluminium cap and stirred at 65 °C for 1 h. The vial was cooled to room temperature and quenched by the addition of saturated aqueous NH$_4$Cl. The resulting dark mixture was extracted with EtOAc (×2), organic layers were combined and washed with brine, dried over anhydrous Na$_2$SO$_4$, filtered through cotton plug and evaporated. The resulting dark yellow oil was purified with reverse phase flash chromatography (10% to 70% MeCN in aqueous 0.1% TFA) to give **2.73** (35 mg, 34%) as a white amorphous solid. ^{1}H NMR (400 MHz, CDCl$_3$) δ 9.10 (s, 1H), 7.50–7.34 (m, 2H), 7.23 (m, 3H), 7.08 (d, J = 1.7 Hz, 1H),

7.03–6.94 (m, 2H), 6.65 (d, J = 7.9 Hz, 1H), 6.30 (d, J = 8.2 Hz, 1H), 5.46 (d, J = 9.2 Hz, 1H), 4.82 (d, J = 8.2 Hz, 1H), 4.05 (ddd, J = 12.5, 9.2, 3.6 Hz, 1H), 3.13 (t, J = 12.1 Hz, 1H), 2.80 (dd, J = 12.5, 3.6 Hz, 1H), 2.12 (s, 3H), 1.45 (s, 9H), 1.01 (s, 9H). ^{13}C NMR (101 MHz, CDCl$_3$) δ 175.1, 172.1, 162.0, 155.5, 154.1, 149.1, 139.7, 137.6, 135.8, 135.1, 133.5, 131.2, 129.9, 129.3, 129.1, 128.7, 128.1, 127.4, 111.0, 80.5, 59.0, 58.3, 57.9, 38.3, 33.4, 28.4, 26.6, 11.6. HRMS (ESI/Q-TOF) m/z: found: 612.2838. Calculated for C$_{34}$H$_{38}$N$_5$O$_6$ [M+H]$^+$: 612.2822. [α]D^{20} –142 (c 1.0, CHCl$_3$).
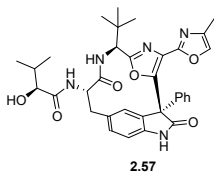
2.57

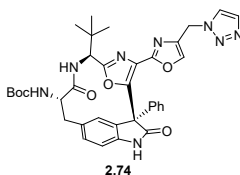**(2S)-N-[(1S,6S,9S)-6-*tert*-Butyl-3-(4-methyl-1,3-oxazol-2-yl)-8,16-dioxo-1-phenyl-19-oxa-4,7,15-triazatetracyclo[9.5.2.1^{2,5}.0^{14,17}]nonadeca-2,4,11,13,17-pentaen-9-yl]-2-hydroxy-3-methylbutanamide (2.57).** Compound **2.57** was obtained from macrocycle **2.73** (30 mg, 0.05 mmol), TFA (38 μL, 0.5 mmol) in dry DCM (0.5 mL) and from (S)-(+)-2-hydroxy-3-methylbutyric acid (9 mg, 0.07 mmol), EDC×HCl (19 mg, 0.10 mmol), HOBt (20 mg, 0.15 mmol) and DIPEA (42 μL, 0.24 mmol) in dry DMF (1 mL) following General method A. White amorphous solid (15 mg, 50%). ^{1}H NMR (400 MHz, MeOD) δ 7.45 (s, 1H), 7.43–7.38 (m, 2H), 7.36–7.28 (m, 3H), 7.26 (dd, J = 8.0, 1.8 Hz, 1H), 7.23 (d, J = 1.8 Hz, 1H), 6.91 (d, J = 8.0 Hz, 1H), 4.95–4.89 (m, 1H), 4.46 (dd, J = 11.7, 3.8 Hz, 1H), 3.86 (d, J = 3.8 Hz, 1H), 3.16 (t, J = 12.1 Hz, 1H), 2.81 (dd, J = 12.6, 3.8 Hz, 1H), 2.13 (s, 3H), 2.08 (sept d, J = 6.9, 3.5 Hz, 1H), 1.06 (s, 9H), 1.00 (d, J = 6.9 Hz, 3H), 0.89 (d, J = 6.9 Hz, 3H). ^{13}C NMR (101 MHz, MeOD) δ 176.3, 175.8, 174.0, 164.2, 155.4, 151.3, 141.7, 138.4, 137.4, 137.1, 133.9, 132.1, 131.3, 130.5, 129.8, 129.2, 128.7, 128.4, 111.9, 76.8, 60.5, 58.5, 56.7, 39.3, 34.2, 33.1, 26.7, 19.6, 16.3, 11.1. HRMS (ESI/Q-TOF) m/z: found: 612.2851. Calculated for C$_{34}$H$_{38}$N$_5$O$_6$ [M+H]$^+$: 612.2822. [α]D^{20} –270 (c 1.0, MeOH).

2.74

tert-Butyl N-[(1S,6S,9S)-6-*tert*-butyl-8,16-dioxo-1-phenyl-3-{4-[(1H-1,2,3-triazol-1-yl)methyl]-1,3-oxazol-2-yl}-19-oxa-4,7,15-triazatetracyclo[9.5.2.1^{2,5}.0^{14,17}]nonadeca-2,4,11,13,17-pentaen-9-yl]carbamate (2.74). Azide **2.69** (34 mg, 0.05 mmol, 1 equiv.), K$_2$CO$_3$ (14 mg, 0.10 mmol, 2 equiv.), CuSO$_4$×5H$_2$O (3 mg, 0.01 mmol, 0.2 equiv.) and sodium ascorbate (4 mg, 0.02 mmol, 0.4 equiv.) were dissolved in MeOH-H$_2$O mixture (1:1 v/v, overall 2 mL) at room temperature. Then trimethyl-silylacetylene (15 μL, 0.10 mmol, 2 equiv.) was added dropwise. The resuling brown suspension was stirred for 18 at the same temperature and then diluted with EtOAc. The mixture was washed with water (×2), organic layers were combined, washed with brine, dried over anhydrous Na$_2$SO$_4$, filtered through cotton plug and evaporated. The resulting yellow oil was purified with direct phase flash chromatography (0% to 10% MeOH in DCM) to give **2.74** (23 mg, 65%) as a white amorphous solid. ^{1}H NMR

(400 MHz, MeOD) δ 8.02 (s, 1H), 7.88 (s, 1H), 7.73 (d, J = 1.1 Hz, 1H), 7.41–7.37 (m, 2H), 7.32–7.25 (m, 3H), 7.27–7.19 (m, 2H), 6.89 (d, J = 8.0 Hz, 1H), 5.55 (s, 2H), 4.91 (s, 1H), 4.04 (dd, J = 11.8, 3.6 Hz, 1H), 3.10 (t, J = 12.1 Hz, 1H), 2.78 (dd, J = 12.6, 3.6 Hz, 1H), 1.43 (s, 9H), 1.06 (s, 9H). ^{13}C NMR (101 MHz, MeOD) δ 176.3, 174.9, 164.5, 157.2, 156.4, 151.7, 141.6, 139.9, 137.4, 137.0, 134.6, 133.7, 132.7, 131.3, 130.6, 129.8, 129.3, 128.7, 128.0, 126.1, 111.9, 80.5, 60.5, 58.5, 46.2, 38.8, 34.2, 28.7, 26.7. HRMS (ESI/Q-TOF) m/z: found: 679.2999. Calculated for $C_{36}H_{39}N_8O_6$ [M+H]$^+$: 679.2993. [α]D^{20} –235 (c 1.0, MeOH).
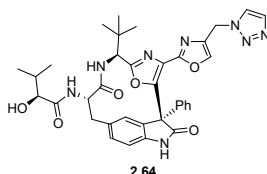
2.64

(2S)-N-[(1S,6S,9S)-6-*tert*-Butyl-8,16-dioxo-1-phenyl-3-{4-[(1H-1,2,3-triazol-1-yl)methyl]-1,3-oxazol-2-yl}-19-oxa-4,7,15-triazatetracyclo[9.5.2.1²,⁵.0¹⁴,¹⁷]nonadeca-2,4,11,13,17-pentaen-9-yl]-2-hydroxy-3-methylbutanamide (2.64). Compound **2.64** was obtained from macrocycle **2.74** (32 mg, 0.05 mmol), TFA (36 µL, 0.5 mmol) in dry DCM (0.5 mL) and from (*S*)-(+)-2-hydroxy-3-methylbutyric acid (8 mg, 0.07 mmol), EDC×HCl (18 mg, 0.09 mmol), HOBt (19 mg, 0.14 mmol) and DIPEA (49 µL, 0.28 mmol) in dry DMF (1 mL) following General method A. White amorphous solid (14 mg, 44%). ^{1}H NMR (400 MHz, MeOD) δ 8.01 (d, J = 1.1 Hz, 1H), 7.86 (d, J = 1.1 Hz, 1H), 7.74 (d, J = 1.1 Hz, 1H), 7.44–7.35 (m, 2H), 7.34–7.23 (m, 4H), 7.20 (d, J = 1.7 Hz, 1H), 6.91 (d, J = 8.0 Hz, 1H), 5.54 (s, 2H), 4.89 (s, 1H), 4.46 (dd, J = 11.7, 3.9 Hz, 1H), 3.85 (d, J = 3.9 Hz, 1H), 3.15 (t, J = 12.2 Hz, 1H), 2.82 (dd, J = 12.6, 3.9 Hz, 1H), 2.08 (sept d, J = 6.9, 3.9 Hz, 1H), 1.04 (s, 9H), 1.00 (d, J = 6.9 Hz, 3H), 0.89 (d, J = 6.9 Hz, 3H). ^{13}C NMR (101 MHz, MeOD) δ 176.3, 175.8, 174.0, 164.3, 156.3, 151.8, 141.7, 139.9, 137.3, 137.0, 134.6, 134.0, 132.2, 131.3, 130.6, 129.9, 129.3, 128.6, 128.2, 126.1, 112.0, 76.8, 60.5, 58.6, 56.6, 46.2, 39.2, 34.2, 33.2, 26.7, 19.5, 16.3. HRMS (ESI/Q-TOF) m/z: found: 679.2988. Calculated for $C_{36}H_{39}N_8O_6$ [M+H]$^+$: 679.2993. [α]D^{20} –244 (c 0.8, MeOH).
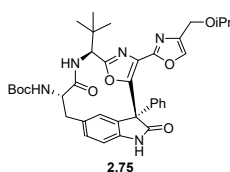
2.75

tert-Butyl N-[(1S,6S,9S)-6-*tert*-butyl-8,16-dioxo-1-phenyl-3-{4-[(propan-2-yloxy)methyl]-1,3-oxazol-2-yl}-19-oxa-4,7,15-triazatetracyclo[9.5.2.1²,⁵.0¹⁴,¹⁷]nonadeca-2,4,11,13,17-pentaen-9-yl]carbamate (2.75). Alcohol **2.39** (120 mg, 0.19 mmol, 1 equiv.) and 2-iodopropane (96 µL, 0.96 mmol, 5 equiv.) were dissolved in dry DMSO (0.5 mL) and then KOH (11 mg, 0.19 mmol, 1 equiv.) was added in one portion. The resulting suspension was stirred for 2 h at room temperature. The reaction mixture was quenched by the addition of aqueous saturated NH₄Cl and extracted with EtOAc (×2). Organic layers were combined, washed with brine, dried over anhydrous Na₂SO₄, filtered through cotton plug and evaporated. The resulting yellow oil was purified with direct phase flash chromatography (0% to 10% MeOH in DCM) to give

2.75 (30 mg, 23%) as a yellow amorphous solid. ^{1}H NMR (400 MHz, CDCl$_3$) δ 7.42–7.36 (m, 3H), 7.33–7.26 (m, 4H), 7.22 (d, J = 1.8 Hz, 1H), 7.18 (dd, J = 8.1, 1.8 Hz, 1H), 6.95 (d, J = 8.1 Hz, 1H), 5.67 (d, J = 8.1 Hz, 1H), 5.16 (d, J = 9.0 Hz, 1H), 4.86 (d, J = 8.1 Hz, 1H), 4.58–4.48 (m, 3H), 3.87 (ddd, J = 12.3, 9.0, 3.6 Hz, 1H), 3.14 (t, J = 12.1 Hz, 1H), 2.83 (dd, J = 12.3, 3.6 Hz, 1H), 1.50–1.41 (m, 15H), 1.02 (s, 9H). ^{13}C NMR (101 MHz, CDCl$_3$) δ 172.6, 171.8, 162.1, 155.2, 154.7, 150.0, 141.4, 141.0, 136.2, 135.5, 132.9, 131.0, 129.9, 129.4, 128.9, 128.2, 127.5, 110.8, 80.5, 58.7, 58.5, 57.4, 57.1, 45.0, 38.0, 33.4, 28.4, 26.5, 19.5, 19.4. HRMS (ESI/Q-TOF) m/z: found: 670.3245. Calculated for C$_{37}$H$_{44}$N$_5$O$_7$ [M+H]$^+$: 670.3241. [α]D^{20} –170 (c 0.5, CHCl$_3$).
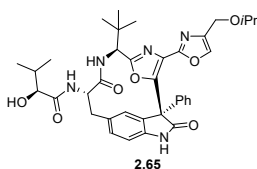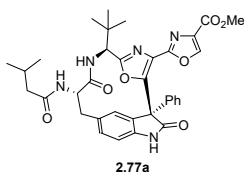

2.65

(2S)-N-[(1S,6S,9S)-6-*tert*-Butyl-8,16-dioxo-1-phenyl-3-{4-[(propan-2-yloxy) methyl]-1,3-oxazol-2-yl}-19-oxa-4,7,15-triazatetracyclo[9.5.2.1^{2,5}.0^{14,17}]nonadeca-2,4,11,13,17-pentaen-9-yl]-2-hydroxy-3-methylbutanamide (2.65). Compound **2.65** was obtained from macrocycle **2.75** (30 mg, 0.05 mmol), TFA (34 µL, 0.5 mmol) in dry DCM (0.5 mL) and from (S)-(+)-2-hydroxy-3-methylbutyric acid (8 mg, 0.07 mmol), EDC×HCl (18 mg, 0.09 mmol), HOBt (19 mg, 0.14 mmol) and DIPEA (49 µL, 0.28 mmol) in dry DMF (1 mL) following General method A. White amorphous solid (19 mg, 62%). ^{1}H NMR (400 MHz, MeOD) δ 7.69 (t, J = 1.1 Hz, 1H), 7.39–7.31 (m, 7H), 7.15 (d, J = 8.6 Hz, 1H), 4.95 (s, 1H), 4.51–4.41 (m, 2H), 4.50 (d, J = 1.05 Hz, 2H), 3.86 (d, J = 3.8 Hz, 1H), 3.18 (t, J = 12.1 Hz, 1H), 2.83 (dd, J = 12.6, 3.8 Hz, 1H), 2.09 (sept d, J = 6.9, 3.8 Hz, 1H), 1.42 (dd, J = 12.1, 7.0 Hz, 6H), 1.06 (s, 9H), 1.00 (d, J = 6.9 Hz, 3H), 0.89 (d, J = 6.9 Hz, 3H). ^{13}C NMR (101 MHz, MeOD) δ 175.8, 173.9, 173.9, 164.4, 155.6, 151.3, 143.3, 142.1, 137.8, 137.5, 133.2, 132.4, 131.2, 130.6, 129.9, 129.3, 128.7, 128.0, 112.2, 76.8, 60.1, 58.2, 57.2, 56.6, 46.3, 39.1, 34.1, 33.1, 26.7, 19.6, 19.4, 16.3. HRMS (ESI/Q-TOF) m/z: found: 670.3249. Calculated for C$_{37}$H$_{44}$N$_5$O$_7$ [M+H]$^+$: 670.3241. [α]D^{20} –214 (c 1.0, MeOH).

2.77a

Methyl 2-[(1S,6S,9S)-6-*tert*-butyl-9-(3-methylbutanamido)-8,16-dioxo-1-phenyl-19-oxa-4,7,15-triazatetracyclo[9.5.2.1^{2,5}.0^{14,17}]nonadeca-2,4,11,13,17-pentaen-3-yl]-1,3-oxazole-4-carboxylate (2.77a). Compound **2.77a** was obtained from macrocycle **2.32** (150 mg, 0.23 mmol), TFA (176 µL, 2.29 mmol) in dry DCM (0.5 mL) and from 3-methylbutanoic acid **2.76a** (24 µL, 0.22 mmol), EDC×HCl (55 mg, 0.29 mmol), HOBt (58 mg, 0.43 mmol) and DIPEA (150 µL, 0.86 mmol) in dry DMF (1 mL) following General method A. White amorphous solid (63 mg, 68%). ^{1}H NMR (400 MHz, MeOD) δ 8.42 (s, 1H), 7.44–7.39 (m, 2H), 7.39–7.29 (m, 4H), 7.24 (dd, J = 8.0, 1.8 Hz, 1H), 6.90 (d, J = 8.0 Hz, 1H), 4.98 (s, 1H), 4.34 (dd, J = 11.9, 3.6 Hz, 1H), 3.88 (s, 3H), 3.21 (t, J = 12.3 Hz, 1H), 2.77 (dd, J = 12.7, 3.6 Hz, 1H), 2.10–2.01 (m, 3H),

1.08 (s, 9H), 0.95 (d, J = 6.3 Hz, 3H), 0.92 (d, J = 6.3 Hz, 3H). ^{13}C NMR (101 MHz, MeOD) δ 176.1, 174.8, 174.2, 164.7, 162.6, 156.5, 152.2, 146.6, 141.7, 137.3, 134.8, 133.3, 132.6, 131.4, 130.6, 129.9, 129.3, 128.7, 127.1, 111.9, 60.4, 58.1, 57.3, 52.6, 45.9, 38.6, 34.1, 27.7, 26.7, 22.7, 22.6. HRMS (ESI/Q-TOF) m/z: found: 640.2777. Calculated for $C_{35}H_{38}N_5O_7$ [M+H]$^+$: 640.2771. [α]D^{20} –256 (c 1.0, MeOH).

2.77c

Methyl 2-[(1S,6S,9S)-6-*tert*-butyl-9-[(2S)-2-hydroxypropanamido]-8,16-dioxo-1-phenyl-19-oxa-4,7,15-triazatetracyclo[9.5.2.1^{2,5}.0^{14,17}]nonadeca-2,4,11,13,17-pen-taen-3-yl]-1,3-oxazole-4-carboxylate (2.77c). Compound **2.77c** was obtained from Boc-deprotected macrocycle **2.32** (60 mg, 0.11 mmol), (S)-lactic acid **2.76c** (15 mg, 0.16 mmol), EDC×HCl (41 mg, 0.22 mmol), HOBt (44 mg, 0.32 mmol) and DIPEA (112 μL, 0.65 mmol) in dry DMF (1 mL) following General method A. White amor-phous solid (26 mg, 36%). ^{1}H NMR (400 MHz, MeOD) δ 8.50 (d, J = 8.6 Hz, 1H), 8.41 (s, 1H), 7.45–7.38 (m, 2H), 7.38–7.29 (m, 3H), 7.29–7.22 (m, 2H), 6.91 (dd, J = 7.8, 0.7 Hz, 1H), 4.98 (d, J = 8.7 Hz, 1H), 4.46–4.36 (m, 1H), 4.13 (q, J = 6.9 Hz, 1H), 3.88 (s, 3H), 3.19 (t, J = 12.2 Hz, 1H), 2.82 (dd, J = 12.7, 3.7 Hz, 1H), 1.35 (d, J = 6.9 Hz, 3H), 1.06 (s, 9H). ^{13}C NMR (101 MHz, MeOD) δ 176.9, 176.1, 174.1, 164.5, 162.6, 156.4, 152.3, 146.6, 141.7, 137.2, 134.8, 133.4, 132.2, 131.4, 130.6, 129.9, 129.4, 128.7, 127.3, 112.0, 68.9, 60.4, 58.3, 56.7, 52.6, 39.1, 34.1, 26.7, 21.2. HRMS (ESI/Q-TOF) m/z: found: 628.2407. Calculated for $C_{33}H_{34}N_5O_8$ [M+H]$^+$: 628.2407. [α]D^{20} –262 (c 1.0, MeOH).

2.77d

Methyl 2-[(1S,6S,9S)-6-*tert*-butyl-9-(2-hydroxy-2-methylpropanamido)-8,16-dioxo-1-phenyl-19-oxa-4,7,15-triazatetracyclo[9.5.2.1^{2,5}.0^{14,17}]nonadeca-2,4,11,13,17-pen-taen-3-yl]-1,3-oxazole-4-carboxylate (2.77d). Compound **2.77d** was obtained from Boc-deprotected macrocycle **2.32** (40 mg, 0.07 mmol), 2-hydroxy-2-methylbutanoic acid **2.76d** (11 mg, 0.11 mmol), EDC×HCl (28 mg, 0.14 mmol), HOBt (29 mg, 0.22 mmol) and DIPEA (75 μL, 0.43 mmol) in dry DMF (1 mL) following General method A. White amorphous solid (15 mg, 33%). ^{1}H NMR (400 MHz, MeOD) δ 8.43 (s, 1H), 7.45–7.39 (m, 2H), 7.39–7.31 (m, 3H), 7.31–7.24 (m, 2H), 6.91 (d, J = 8.0 Hz, 1H), 5.00 (s, 1H), 4.36 (dd, J = 11.8, 3.7 Hz, 1H), 3.89 (s, 3H), 3.17 (t, J = 12.2 Hz, 1H), 2.83 (dd, J = 12.7, 3.7 Hz, 1H), 1.38 (s, 3H), 1.33 (s, 3H), 1.07 (s, 9H). ^{13}C NMR (101 MHz, MeOD) δ 178.9, 176.0, 174.2, 164.5, 162.6, 156.4, 152.3, 146.6, 141.8, 137.3, 134.8, 133.3, 132.3, 131.4, 130.6, 130.0, 129.4, 128.8, 127.2, 112.0, 73.7, 60.4, 58.1, 56.9, 52.6, 40.4, 39.1, 34.1, 27.7, 26.7. HRMS (ESI/Q-TOF) m/z: found: 642.2595. Calculated for $C_{34}H_{36}N_5O_8$ [M+H]$^+$: 642.2564. [α]D^{20} –240 (c 1.0, MeOH).
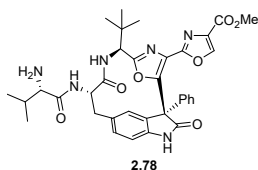
2.77e

Methyl 2-[(1S,6S,9S)-6-*tert*-butyl-9-(2-ethyl-2-hydroxybutanamido)-8,16-dioxo-1-phenyl-19-oxa-4,7,15-triazatetracyclo[9.5.2.1^{2,5}.0^{14,17}]nonadeca-2,4,11,13,17-pentaen-3-yl]-1,3-oxazole-4-carboxylate (2.77e). Compound **2.77e** was obtained from Boc-deprotected macrocycle **2.32** (51 mg, 0.09 mmol), 2-ethyl-2-hydroxybutanoic acid **2.76e** (18 mg, 0.14 mmol), EDC×HCl (35 mg, 0.18 mmol), HOBt (37 mg, 0.28 mmol) and DIPEA (95 μL, 0.55 mmol) in dry DMF (1 mL) following General method A. White amorphous solid (35 mg, 57%). ^{1}H NMR (400 MHz, MeOD) δ 8.43 (s, 1H), 7.45–7.38 (m, 2H), 7.38–7.31 (m, 3H), 7.31 (d, J = 1.7 Hz, 1H), 7.27 (dd, J = 8.0, 1.7 Hz, 1H), 6.91 (d, J = 8.0 Hz, 1H), 5.00 (s, 1H), 4.43 (dd, J = 11.8, 3.7 Hz, 1H), 3.89 (s, 3H), 3.21 (t, J = 12.2 Hz, 1H), 2.79 (dd, J = 12.7, 3.7 Hz, 1H), 1.88–1.71 (m, 2H), 1.60–1.47 (m, 2H), 1.07 (s, 9H), 0.91 (t, J = 7.4 Hz, 3H), 0.79 (t, J = 7.4 Hz, 3H). ^{13}C NMR (101 MHz, MeOD) δ 176.9, 176.0, 174.2, 164.5, 162.6, 156.4, 152.2, 146.6, 141.7, 137.3, 134.8, 133.2, 132.3, 131.4, 130.5, 130.0, 129.4, 128.7, 127.1, 112.0, 79.5, 60.4, 58.1, 56.7, 52.6, 39.4, 34.1, 33.5, 33.4, 26.7, 8.2, 8.1. HRMS (ESI/Q-TOF) m/z: found: 670.2883. Calculated for $C_{36}H_{40}N_5O_8$ [M+H]$^+$: 670.2877. [α]D^{20} –244 (c 1.0, MeOH).
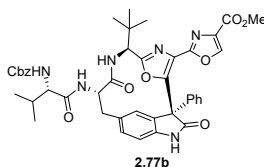
2.77b

Methyl 2-[(1S,6S,9S)-9-[(2S)-2-{[(benzyloxy)carbonyl]amino}-3-methylbutanamido]-6-*tert*-butyl-8,16-dioxo-1-phenyl-19-oxa-4,7,15-triazatetracyclo[9.5.2.1^{2,5}.0^{14,17}]nonadeca-2,4,11,13,17-pentaen-3-yl]-1,3-oxazole-4-carboxylate (2.77b). Compound **2.77b** was obtained from Boc-deprotected macrocycle **2.32** (85 mg, 0.15 mmol), carbobenzyloxy-L-valine **2.76b** (58 mg, 0.23 mmol), EDC×HCl (59 mg, 0.31 mmol), HOBt (62 mg, 0.46 mmol) and DIPEA (159 μL, 0.92 mmol) in dry DMF (1 mL) following General method A. White amorphous solid (92 mg, 76%). ^{1}H NMR (400 MHz, MeOD) δ 8.41 (s, 1H), 7.44–7.39 (m, 2H), 7.39–7.31 (m, 8H), 7.31–7.27 (m, 1H), 7.23 (dd, J = 8.0, 1.8 Hz, 1H), 6.89 (d, J = 8.0 Hz, 1H), 5.08 (s, 2H), 4.99 (s, 1H), 4.37 (dd, J = 11.9, 3.6 Hz, 1H), 3.97 (d, J = 7.4 Hz, 1H), 3.88 (s, 3H), 3.24 (t, J = 12.3 Hz, 1H), 2.79 (dd, J = 12.7, 3.6 Hz, 1H), 2.04–1.90 (m, 1H), 1.06 (s, 9H), 0.91 (t, J = 6.6 Hz, 6H). ^{13}C NMR (101 MHz, MeOD) δ 176.0, 174.0, 173.5, 164.6, 162.6, 158.5, 156.5, 152.2, 146.6, 141.7, 138.2, 137.4, 134.8, 133.2, 132.5, 131.4, 130.6, 130.0, 129.5, 129.4, 129.0, 128.8, 128.7, 127.1, 111.9, 67.7, 61.7, 60.4, 58.0, 57.2, 52.5, 38.5, 34.1, 32.4, 26.7, 19.6, 18.8. HRMS (ESI/Q-TOF) m/z: found: 789.3259. Calculated for $C_{43}H_{45}N_6O_9$ [M+H]$^+$: 789.3248. [α]D^{20} –214 (c 1.0, MeOH).

2.78

Methyl 2-[(1S,6S,9S)-9-[(2S)-2-amino-3-methylbutanamido]-6-*tert*-butyl-8,16-dioxo-1-phenyl-19-oxa-4,7,15-triazatetracyclo[9.5.2.1²,⁵.0¹⁴,¹⁷]nonadeca-2,4,11,13,17-pentaen-3-yl]-1,3-oxazole-4-carboxylate (2.78). Cbz-protected amine **2.77b** (75 mg, 0.10 mmol, 1 equiv.) was dissolved in dry MeOH (1 mL) and 10% Pd/C (10 mg, 0.0095 mmol, 0,1 equiv.) was added in one portion. Hydrogen gas was barbotated through the black suspension for 1 h at room temperature. Then the suspension was filtrated through Celite® and washed the filter with MeOH (×2). The resulting filtrate was evaporated to give amine **2.78** (35 mg, 56%) as a white amorphous solid. ^{1}H NMR (400 MHz, MeOD) δ 8.42 (s, 1H), 7.44–7.38 (m, 2H), 7.38–7.29 (m, 4H), 7.24 (dd, *J* = 8.0, 1.8 Hz, 1H), 6.91 (d, *J* = 8.0 Hz, 1H), 4.98 (s, 1H), 4.38 (dd, *J* = 11.9, 3.6 Hz, 1H), 3.88 (s, 3H), 3.23 (t, *J* = 12.3 Hz, 1H), 3.16 (d, *J* = 6.0 Hz, 1H), 2.80 (dd, *J* = 12.7, 3.6 Hz, 1H), 2.00–1.84 (m, 1H), 1.07 (s, 9H), 0.93 (d, *J* = 6.9 Hz, 3H), 0.91 (d, *J* = 6.9 Hz, 3H). ^{13}C NMR (101 MHz, MeOD) δ 176.0, 175.4, 174.0, 164.6, 162.6, 156.5, 152.2, 146.6, 141.7, 137.3, 134.8, 133.3, 132.4, 131.4, 130.5, 130.0, 129.4, 128.7, 127.2, 112.0, 61.1, 60.4, 58.1, 57.1, 52.6, 38.7, 34.1, 33.8, 26.7, 19.5, 18.1. HRMS (ESI/Q-TOF) m/z: found: 655.2887. Calculated for $C_{35}H_{39}N_6O_7$ [M+H]$^+$: 655.2880. [α]D^{20} –284 (c 1.0, MeOH).

Tubulin Purification from Porcine Brains[o]

Tubulin was purified following the protocol.[56] Porcine brains were collected at the nearest slaughterhouse and transferred into the bags filled with PBS ice cubes in chilled PBS buffer until transported to the cold room. In the lab, brains were weighted (~ 500 g), cut into smaller pieces and diluted with ice-cold blending buffer (1 L: 100 mM PIPES-KOH pH 6.85, 0.1 mM EDTA, 2.0 mM EGTA, 0.5 mM MgCl₂; 1 mM ATP, and 0.1% (v/v) BME supplemented with *SigmaFAST*™ protease inhibitor cocktail). The resulting suspension was homogenized in a blender (1.5 L *Stollar*, *STB550*) using short pulses, so the suspension did not warm up. The resulting homogenate (Figure 3.1, A) was clarified using *Beckmann Avanti* (J-E series; JLA-10.500 rotor, 12 000×g) centrifuge at 4 °C for 15 min, filtered through cotton pads, and resulted in reddish suspension (Figure 3.1, B). Afterwards, supernatant was clarified again with *Beckmann Avanti* (J-E series; JLA-25.500 rotor, 33 000×g) centrifuge at 4 °C for 60 min. The resulting supernatant was subjected into polymerization step.

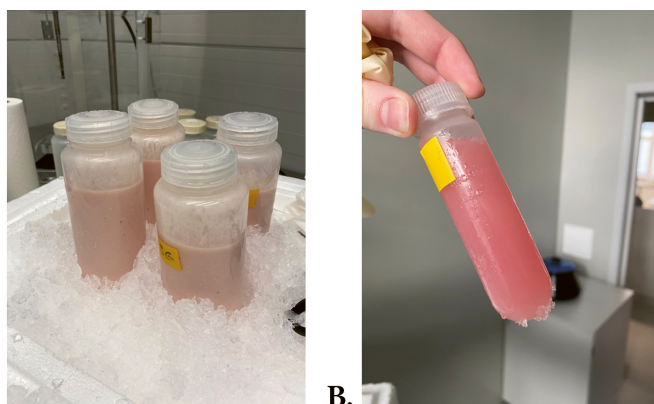[o] Conducted with the assistance of Dr. Diana Zelencova-Gopejenko

Figure 3.1. **A. Brain homogenate after homogenization step. B. Brain homogenate after first centrifugation**

Tubulin solution (~900 mL) was transferred to 2 L Erlenmeyer flask (Figure 3.2, A) and GTP, ATP and $MgCl_2$ were added (final concentrations: 1.0 mM GTP, 1.5 mM ATP, 4.0 mM $MgCl_2$, respectively) followed by addition of pre-warmed glycerol (33 % (v/v), ~300 mL). The flask was quickly warmed up to 30 °C in the water bath at 55 °C and then transferred to the water bath at 37 °C to let tubulin to polymerize. The polymerization mixture was occasionally stirred, and the temperature monitored continuously for 60 min. Temperature was controlled with electronic thermometer. The solution became turbid and more viscous after 1 hour. Afterwards, viscous solution (Figure 3.2, B) was transferred to the pre-warmed centrifugation tubes and clarified with *Beckmann Avanti* (J-E series; JA-25.50 rotor, 50 000×g) centrifuge at 37 °C for 120 min. Supernatant was discarded.
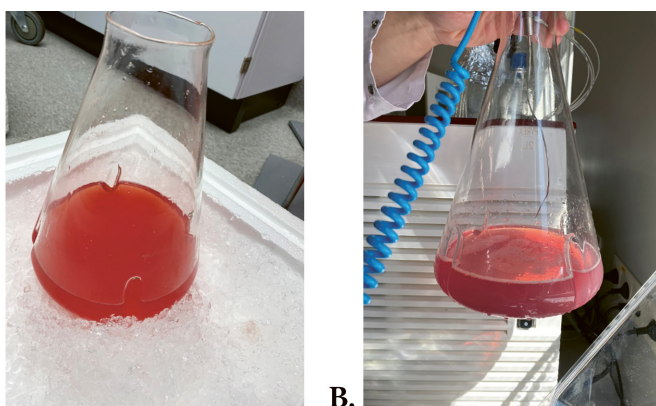
Figure 3.2. **A. Tubulin solution before the polymerization step. B. Tubulin solution after the polymerization step**

Tubulin was sedimented as pellets together with MAPs at this stage (Figure 3.3, A). The pellets were combined, cooled on ice and resuspended in the depolymerization buffer (overall 50 mL: 100 mM PIPES-KOH pH 6.85, 0.1 mM EDTA, 2.0 mM EGTA, 0.5 mM $MgCl_2$ and 0.1% (v/v) BME). The resulting suspension was homogenized using

douncer (*IKA RW 20 digital*) to give pale pink solution (Figure 3.3, B) and incubated on ice for 30 min for complete tubulin depolymerization. The solution was then clarified with *Beckman Coulter L-100XP* (SW 32 Ti rotor; 132 000×g) ultracentrifuge at 4 °C for 30 min. Supernatant was collected and used for the second polymerization step.
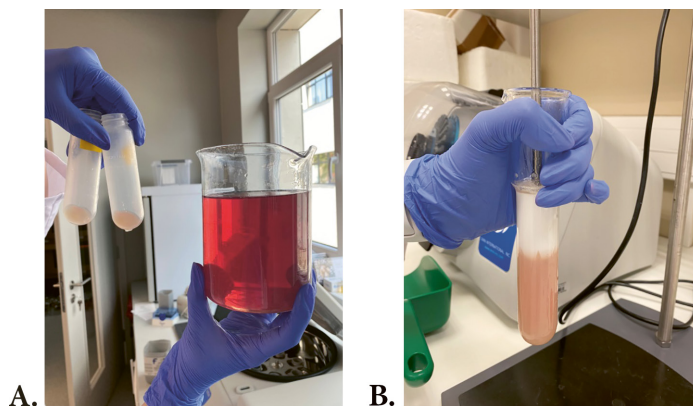
Figure 3.3. **A. Tubulin pellets (on the left). B. Microtubule homogenization**

Next, the pale tubulin solution was subjected into the second polymerization step following the same procedure: addition of GTP, ATP, $MgCl_2$, and glycerol. Second polymerization also continued at 37 °C for 60 min. The solution becomes viscous and the precipitation was observed (Figure 3.4, A–B).
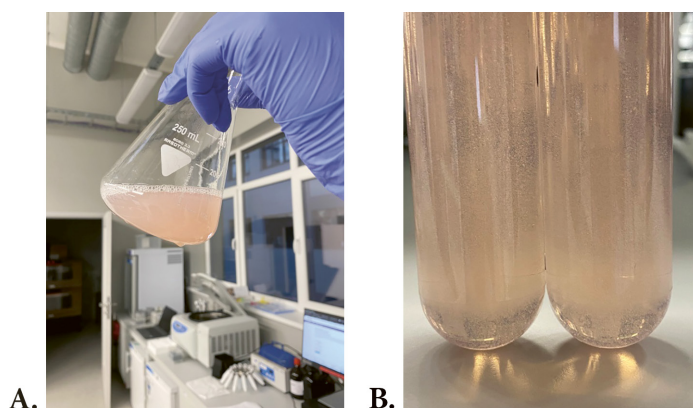
Figure 3.4. **A–B. Tubulin after second polymerization step**

After incubation viscous solution was transferred to the pre-warmed centrifuge tubes and clarified using *Beckman Coulter L-100XP* (SW 32 Ti rotor; 230 000×g) ultracentrifuge at 37 °C for 60 min. Supernatant was discarded and at this stage tubulin with MAPs (overall ~8 mL of pellets; Figure 3.5) was snap-frozen in liquid nitrogen and stored at -80 °C overnight.

Figure 3.5. **Tubulin with MAPs after second warm centrifugation**

The next day tubulin pellets were half-thawed in the water bath at 37 °C and then transferred to ice. Afterwards, completely thawed pellets were resuspended in the ice-cold column buffer (overall 15 mL; 50 mM PIPES-KOH pH 6.85, 1.0 mM EGTA, 0.2 mM $MgCl_2$). The suspension was homogenized using douncer (*IKA RW 20 digital*) and incubated on ice for 30 min for complete depolymerization of tubulin. The resulting mixture was clarified with *Beckman Coulter L-100XP* (SW 32 Ti rotor; 200 000×g) ultracentrifuge at 4 °C for 30 min. Supernatant was recovered and purified on *GE AKTA Purifier* (10 FPLC System w/ UPC-900) at 4 °C using *HiTrap™ SP HP* (4×5 mL) columns (*Cytiva*, Marlborough, MA, USA) equilibrated in the column buffer. Tubulin was eluted in the flow through while MAPs were eluted by increasing the ionic strength of the column buffer by applying gradient of 1 M KCl in the column buffer from 0 % to 50 %. Column was regenerated by washing with 100% of column buffer + 0.1% NaN_3. The flow through and the eluted fractions were analyzed by SDS-PAGE. Tubulin fraction was purified up to 95+% (Figure 3.6, 12). Tubulin concentration in the flow through was determined on *NanoDrop 2000c* UV-VIS spectrometer by Bradford assay[p] using BSA as the standard and reached 4.7 mg/mL. The tubulin concentration was below recommended 10 mg/mL, so the purified tubulin was concentrated using *Amicon® Ultra-15 Centrifugal Filter Units* (30K NWCO, Merck Milipore) at 4 °C and 5 000×g using 5–7 min cycles to prevent tubulin from precipitation. Final concentration of tubulin determined by Bradford assay was 9.3 mg/mL (overall 5.5 mL). The tubulin solution was aliquoted by 500 µL, fast-frozen in liquid nitrogen, and stored at –80 °C.

---

[p] https://www.bio-rad.com/webroot/web/pdf/lsr/literature/4110065A.pdf
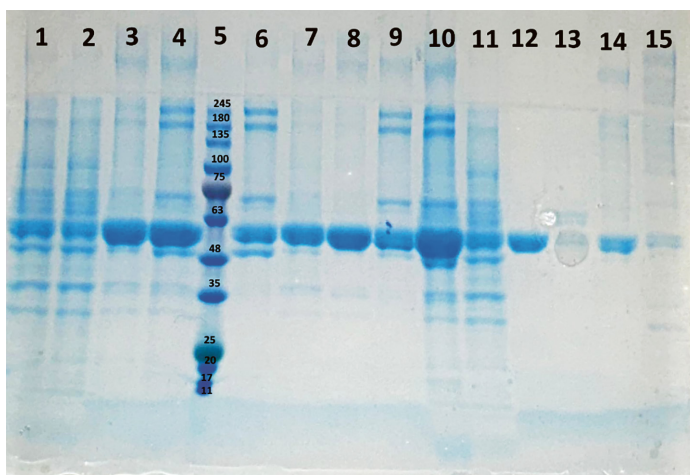
Figure 3.6. **SDS-PAGE analysis showing the protein content at every stage during tubulin purification. (1) Mixture before first polymerization step. (2) Supernatant after first polymerization step. (3) Mixture before second polymerization step. (4) Pellet after the first warm spin; (5) BLUeye Prestained Protein Ladder; (6) Pellets after the second warm spin; (7) Supernatant after second warm spin; (8) Tubulin solution before purification on the column; (9) Discarded pellet before the column; (10) Pellet (microtubules + MAPs); (11) Second supernatant; (12) Flow-through from the column; (13) Fraction 1; (14) Fraction 2; (15) Fraction 3.**

CONCLUSIONS

1. A highly complex marine metabolite diazonamide A can be structurally simplified by truncating right-hand macrocycle and replacement of tetracyclic hemiaminal subunit by chiral quaternary center-containing indolin-2-one or indane moieties while retaining the mechanism of action and high antiproliferative activity. Simple aliphatic alkyl chain as well as *meta*-substituted benzene linker are not suitable as substitutes of the tetracyclic subunit.

GI$_{50}$, μM (MDA-MB-231)   0.015 (NCI-60)   0.19 (NCI-60)   0.73 ± 0.17   0.13 ± 0.02

diazonamide A

GI$_{50}$, μM (MDA-MB-231)   >100   >100
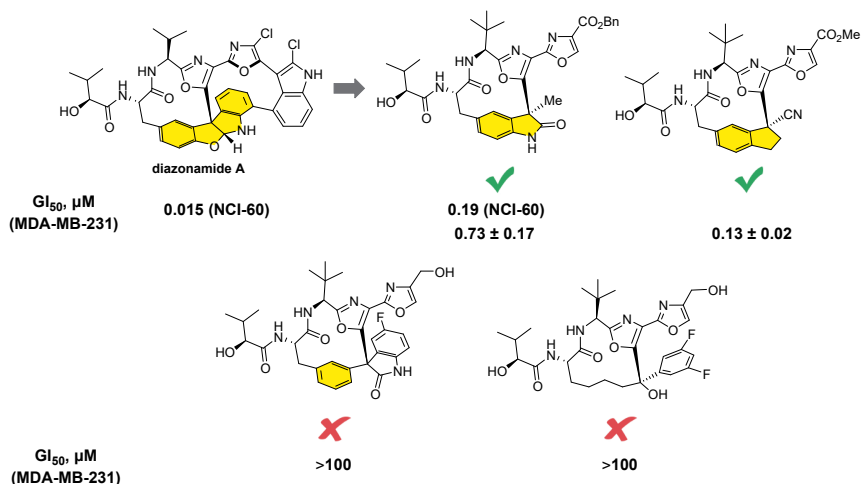
2. Benzyl and methyl esters exert the highest antiproliferative activities in both oxindole and indane series, respectively. GI$_{50}$ values for the best oxindole congener are comparable to those of diazonamide A against 19 cancer cell lines. In addition, compounds exert at least 100-fold lower antiproliferative activity against non-malignant cells as compared to tumor cell lines. However, carboxylic esters feature unfavorable ADME properties such as low stability in cell lysate and in mouse plasma.

GI$_{50}$, nM (A2058)   9.5±0.4   12.9±1.9
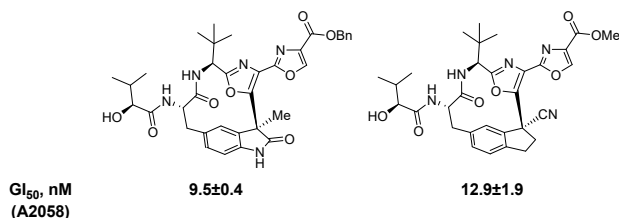
3. In the indane series, a bioisosteric relationship between the difluoromethyl moiety and the hydroxymethyl group has been demonstrated by comparable antiproliferative activity and efficiency in the tubulin polymerization assay for both macrocycles.

GI$_{50}$, nM
(A2058)   **90.8±16.5**   **167.4±16.5**
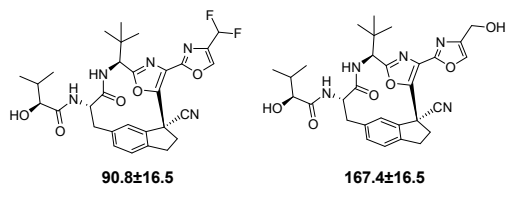
4. Difluormethyl group-containing macrocycle with indane as the core subunit exhibits high plasma stability (96.4% of compound remains after 2 h). Although its antiproliferative activity is inferior to that of the parent diazonamide A, this is compensated by easier synthetic accessibility. The difluormethyl group-substituted macrocycle is the most suitable candidate for *in vivo* proof-of-concept studies.

5. Comparable efficacy in the tubulin polymerization assay for oxindole-containing benzyl ester and carboxylic acid combined with the lack of the *in vitro* antiproliferative activity for the latter suggests that the carboxylic acid serves as the active metabolite of the benzyl ester. The intracellular formation of the acid was confirmed by the intracellular uptake experiment.

GI$_{50}$, nM
(A2058)   **9.5±0.4**   **>1000**
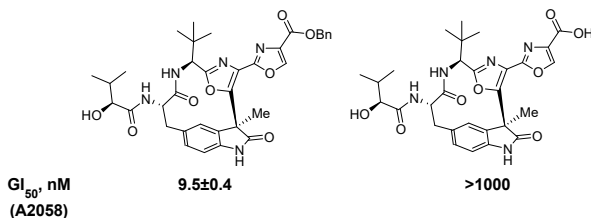
6. Late-stage alkylation of oxindole macrocycle represents an efficient approach to construction of quaternary stereogenic center with excellent diastereoselectivity and high yields.

R^1 = Me, Et, Bn,
86:14-92:8 *dr*,
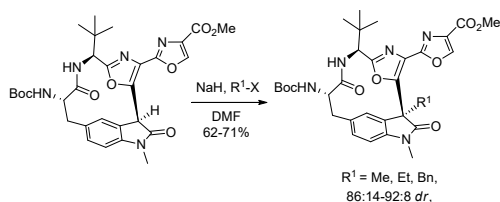
REFERENCES

(1) *WHO data about cancer*. https://www.who.int/news-room/fact-sheets/detail/cancer (accessed 2024-01-05).

(2) *European Cancer Information System*. https://ecis.jrc.ec.europa.eu/factsheets_2022.php (accessed 2023-12-04).

(3) Vaidya, F. U.; Sufiyan Chhipa, A.; Mishra, V.; Gupta, V. K.; Rawat, S. G.; Kumar, A.; Pathak, C. Molecular and Cellular Paradigms of Multidrug Resistance in Cancer. *Cancer Rep.* **2022**, *5* (12). https://doi.org/10.1002/cnr2.1291.

(4) European Comission. State of Health in the EU. Latvia. Country Health Profile 2021. https://health.ec.europa.eu/system/files/2021-12/2021_chp_lv_english.pdf.

(5) Newman, D. J.; Cragg, G. M. Natural Products as Sources of New Drugs over the Nearly Four Decades from 01/1981 to 09/2019. *J. Nat. Prod.* **2020**, *83* (3), 770–803. https://doi.org/10.1021/acs.jnatprod.9b01285.

(6) Steinmetz, M. O.; Prota, A. E. Microtubule-Targeting Agents: Strategies To Hijack the Cytoskeleton. *Trends Cell Biol.* **2018**, *28* (10), 776–792. https://doi.org/Pelletier.

(7) Nicolaou, K. C.; Chen, D. Y.-K.; Huang, X.; Ling, T.; Bella, M.; Snyder, S. A. Chemistry and Biology of Diazonamide A: First Total Synthesis and Confirmation of the True Structure. *J. Am. Chem. Soc.* **2004**, *126* (40), 12888–12896. https://doi.org/10.1021/ja040092i.

(8) Knowles, R. R.; Carpenter, J.; Blakey, S. B.; Kayano, A.; Mangion, I. K.; Sinz, C. J.; MacMillan, D. W. C. Total Synthesis of Diazonamide A. *Chem. Sci.* **2011**, *2* (2), 308–311. https://doi.org/10.1039/C0SC00577K.

(9) Nicolaou, K. C.; Bheema Rao, P.; Hao, J.; Reddy, M. V.; Rassias, G.; Huang, X.; Chen, D. Y.-K.; Snyder, S. A. The Second Total Synthesis of Diazonamide A. *Angew. Chem. Int. Ed.* **2003**, *42* (15), 1753–1758. https://doi.org/10.1002/anie.200351112.

(10) Burgett, A. W. G.; Li, Q.; Wei, Q.; Harran, P. G. A Concise and Flexible Total Synthesis of (−)-Diazonamide A. *Angew. Chem. Int. Ed.* **2003**, *42* (40), 4961–4966. https://doi.org/10.1002/anie.200352577.

(11) Lindquist, N.; Fenical, W.; Van Duyne, G. D.; Clardy, J. Isolation and Structure Determination of Diazonamides A and B, Unusual Cytotoxic Metabolites from the Marine Ascidian Diazona Chinensis. *J. Am. Chem. Soc.* **1991**, *113* (6), 2303–2304. https://doi.org/10.1021/ja00006a060.

(12) Hanson, G. J.; Zhou, M.; Wei, Q.; Caldwell, C. Diazonamide Analogs. US 8,153,619 B2, April 10, 2012.

(13) Hanson, G. J.; Wei, Q.; Caldwell, C.; Zhou, M.; Wang, L.; Harran, S. Indoline Anti-Cancer Agents, October 18, 2012.

(14) Wei, Q.; Zhou, M.; Xu, X.; Caldwell, C.; Harran, S.; Wang, L. Diazonamide Analogs. US8846734B2, September 30, 2014. https://patents.google.com/patent/US8846734B2/en (accessed 2023-10-20).

(15) Ding, H.; DeRoy, P. L.; Perreault, C.; Larivée, A.; Siddiqui, A.; Caldwell, C. G.; Harran, S.; Harran, P. G. Electrolytic Macrocyclizations: Scalable Synthesis of a Diazonamide-Based Drug Development Candidate. *Angew. Chem. Int. Ed.* **2015**, *54* (16), 4818–4822. https://doi.org/10.1002/anie.201411663.

(16) Wieczorek, M.; Tcherkezian, J.; Bernier, C.; Prota, A. E.; Chaaban, S.; Rolland, Y.; Godbout, C.; Hancock, M. A.; Arezzo, J. C.; Ocal, O.; Rocha, C.; Olieric, N.; Hall, A.; Ding, H.; Bramoulle, A.; Annis, M. G.; Zogopoulos, G.; Harran, P. G.; Wilkie, T. M.; Brekken, R. A.; Siegel, P. M.; Steinmetz, M. O.; Shore, G. C.; Brouhard, G. J.; Roulston, A. The Synthetic Diazonamide DZ-2384 Has Distinct Effects on Microtubule Curvature and Dynamics without Neurotoxicity. *Sci. Transl. Med.* **2016**, *8* (365), 365ra159-365ra159. https://doi.org/10.1126/scitranslmed.aag1093.

(17) Wittmann, T.; Hyman, A.; Desai, A. The Spindle: A Dynamic Assembly of Microtubules and Motors. *Nat. Cell Biol.* **2001**, *3* (1), E28–E34. https://doi.org/10.1038/35050669.

(18) Stanton, R. A.; Gernert, K. M.; Nettles, J. H.; Aneja, R. Drugs That Target Dynamic Microtubules: A New Molecular Perspective. *Med. Res. Rev.* **2011**, *31* (3), 443–481. https://doi.org/10.1002/med.20242.

(19) Liu, Y.-M.; Chen, H.-L.; Lee, H.-Y.; Liou, J.-P. Tubulin Inhibitors: A Patent Review. *Expert Opin. Ther. Pat.* **2014**, *24* (1), 69–88. https://doi.org/10.1517/13543776.2014.859247.

(20) Desai, A.; Mitchison, T. J. Microtubule Polymerization Dynamics. *Annu. Rev. Cell Dev. Biol.* **1997**, *13* (1), 83–117. https://doi.org/10.1146/annurev.cellbio.13.1.83.

(21) Prosser, S. L.; Pelletier, L. Mitotic Spindle Assembly in Animal Cells: A Fine Balancing Act. *Nat. Rev. Mol. Cell Biol.* **2017**, *18* (3), 187–201. https://doi.org/10.1038/nrm.2016.162.

(22) Škubník, J.; Pavlíčková, V. S.; Ruml, T.; Rimpelová, S. Vincristine in Combination Therapy of Cancer: Emerging Trends in Clinics. *Biology* **2021**, *10* (9), 849. https://doi.org/10.3390/biology10090849.

(23) Mühlethaler, T.; Gioia, D.; Prota, A. E.; Sharpe, M. E.; Cavalli, A.; Steinmetz, M. O. Comprehensive Analysis of Binding Sites in Tubulin. *Angew. Chem. Int. Ed.* n/a (n/a). https://doi.org/10.1002/anie.202100273.

(24) Toso, R. J.; Jordan, M. A.; Farrell, K. W.; Matsumoto, B.; Wilson, L. Kinetic Stabilization of Microtubule Dynamic Instability in Vitro by Vinblastine. *Biochemistry* **1993**, *32* (5), 1285–1293. https://doi.org/10.1021/bi00056a013.

(25) Himes, R. H. Interactions of the Catharanthus (Vinca) Alkaloids with Tubulin and Microtubules. *Pharmacol. Ther.* **1991**, *51* (2), 257–267. https://doi.org/10.1016/0163-7258(91)90081-V.

(26) Rai, S. S.; Wolff, J. Vinblastine-Induced Formation of Tubulin Polymers Is Electrostatically Regulated and Nucleated. *Eur. J. Biochem.* **1997**, *250* (2), 425–431. https://doi.org/10.1111/j.1432-1033.1997.0425a.x.

(27) Drago, J. Z.; Modi, S.; Chandarlapaty, S. Unlocking the Potential of Antibody–Drug Conjugates for Cancer Therapy. *Nat. Rev. Clin. Oncol.* **2021**, *18* (6), 327–344. https://doi.org/10.1038/s41571-021-00470-8.

(28) Marinina, J.; Shenderova, A.; Mallery, S. R.; Schwendeman, S. P. Stabilization of Vinca Alkaloids Encapsulated in Poly(Lactide-Co-Glycolide) Microspheres. *Pharm. Res.* **2000**, *17* (6), 677–683. https://doi.org/10.1023/A:1007522013835.

(29) Chen, J.; Li, S.; Shen, Q. Folic Acid and Cell-Penetrating Peptide Conjugated PLGA–PEG Bifunctional Nanoparticles for Vincristine Sulfate Delivery. *Eur. J. Pharm. Sci.* **2012**, *47* (2), 430–443. https://doi.org/10.1016/j.ejps.2012.07.002.

(30) O'Brien, S.; Schiller, G.; Lister, J.; Damon, L.; Goldberg, S.; Aulitzky, W.; Ben-Yehuda, D.; Stock, W.; Coutre, S.; Douer, D.; Heffner, L. T.; Larson, M.; Seiter, K.; Smith, S.; Assouline, S.; Kuriakose, P.; Maness, L.; Nagler, A.; Rowe, J.; Schaich, M.; Shpilberg, O.; Yee, K.; Schmieder, G.; Silverman, J. A.; Thomas, D.; Deitcher, S. R.; Kantarjian, H. High-Dose Vincristine Sulfate Liposome Injection for Advanced, Relapsed, and Refractory Adult Philadelphia Chromosome–Negative Acute Lymphoblastic Leukemia. *J. Clin. Oncol.* **2013**, *31* (6), 676–683. https://doi.org/10.1200/JCO.2012.46.2309.

(31) Silverman, J. A.; Deitcher, S. R. Marqibo® (Vincristine Sulfate Liposome Injection) Improves the Pharmacokinetics and Pharmacodynamics of Vincristine. *Cancer Chemother. Pharmacol.* **2013**, *71* (3), 555–564. https://doi.org/10.1007/s00280-012-2042-4.

(32) Boehlke, L.; Winter, J. N. Sphingomyelin/Cholesterol Liposomal Vincristine: A New Formulation for an Old Drug. *Expert Opin. Biol. Ther.* **2006**, *6* (4), 409–415. https://doi.org/10.1517/14712598.6.4.409.

(33) Kavallaris, M. Microtubules and Resistance to Tubulin-Binding Agents. *Nat. Rev. Cancer* **2010**, *10* (3), 194–204. https://doi.org/10.1038/nrc2803.

(34) Zhu, T.; Wang, S.-H.; Li, D.; Wang, S.-Y.; Liu, X.; Song, J.; Wang, Y.-T.; Zhang, S.-Y. Progress of Tubulin Polymerization Activity Detection Methods. *Bioorg. Med. Chem. Lett.* **2021**, *37*, 127698. https://doi.org/10.1016/j.bmcl.2020.127698.

(35) Burton, P.; Himes, R. Electron Microscope Studies of pH Effects on Assembly of Tubulin Free of Associated Proteins. Delineation of Substructure by Tannic Acid Staining. *J. Cell Biol.* **1978**, *77* (1), 120–133. https://doi.org/10.1083/jcb.77.1.120.

(36) Zhang, Y.-L.; Li, B.-Y.; Yang, R.; Xia, L.-Y.; Fan, A.-L.; Chu, Y.-C.; Wang, L.-J.; Wang, Z.-C.; Jiang, A.-Q.; Zhu, H.-L. A Class of Novel Tubulin Polymerization Inhibitors Exert Effective Anti-Tumor Activity via Mitotic Catastrophe. *Eur. J. Med. Chem.* **2019**, *163*, 896–910. https://doi.org/10.1016/j.ejmech.2018.12.030.

(37) Ozono, Y.; Tamura, A.; Nakayama, S.; Herawati, E.; Hanada, Y.; Ohata, K.; Takagishi, M.; Takahashi, M.; Imai, T.; Ohta, Y.; Oshima, K.; Sato, T.; Inohara, H.; Tsukita, S. Daple Deficiency Causes Hearing Loss in Adult Mice by Inducing Defects in Cochlear Stereocilia and Apical Microtubules. *Sci. Rep.* **2021**, *11* (1), 20224. https://doi.org/10.1038/s41598-021-96232-8.

(38) Bastos, M.; Abian, O.; Johnson, C. M.; Ferreira-da-Silva, F.; Vega, S.; Jimenez-Alesanco, A.; Ortega-Alarcon, D.; Velazquez-Campoy, A. Isothermal Titration Calorimetry. *Nat. Rev. Methods Primer* **2023**, *3* (1), 1–23. https://doi.org/10.1038/s43586-023-00199-x.

(39) Tsvetkov, P. O.; Barbier, P.; Breuzard, G.; Peyrot, V.; Devred, F. Chapter 18 – Microtubule-Associated Proteins and Tubulin Interaction by Isothermal Titration Calorimetry. In *Methods in Cell Biology*; Correia, J. J., Wilson, L., Eds.; Microtubules,; Academic Press, 2013; Vol. 115, pp 283–302. https://doi.org/10.1016/B978-0-12-407757-7.00018-9.

(40) Tsvetkov, P. O.; Kulikova, A. A.; Devred, F.; Zernii, E. Yu.; Lafitte, D.; Makarov, A. A. Thermodynamics of Calmodulin and Tubulin Binding to the Vinca-Alkaloid Vinorelbine. *Mol. Biol.* **2011**, *45* (4), 641–646. https://doi.org/10.1134/S0026893311040108.

(41) Gupta, S.; Chakraborty, S.; Poddar, A.; Sarkar, N.; Das, K. P.; Bhattacharyya, B. BisANS Binding to Tubulin: Isothermal Titration Calorimetry and the Site-Specific Proteolysis Reveal the GTP-Induced Structural Stability of Tubulin. *Proteins Struct. Funct. Bioinforma.* **2003**, *50* (2), 283–289. https://doi.org/10.1002/prot.10292.

(42) Zhao, W.; Bai, J.-K.; Li, H.-M.; Chen, T.; Tang, Y.-J. Tubulin Structure-Based Drug Design for the Development of Novel 4β-Sulfur-Substituted Podophyllum Tubulin Inhibitors with Anti-Tumor Activity. *Sci. Rep.* **2015**, *5* (1), 10172. https://doi.org/10.1038/srep10172.

(43) Banerjee, M.; Poddar, A.; Mitra, G.; Surolia, A.; Owa, T.; Bhattacharyya, B. Sulfonamide Drugs Binding to the Colchicine Site of Tubulin: Thermodynamic Analysis of the Drug–Tubulin Interactions by Isothermal Titration Calorimetry. *J. Med. Chem.* **2005**, *48* (2), 547–555. https://doi.org/10.1021/jm0494974.

(44) Devred, F.; Tsvetkov, P. O.; Barbier, P.; Allegro, D.; Horwitz, S. B.; Makarov, A. A.; Peyrot, V. Stathmin/Op18 Is a Novel Mediator of Vinblastine Activity. *FEBS Lett.* **2008**, *582* (17), 2484–2488. https://doi.org/10.1016/j.febslet.2008.06.035.

(45) Marzullo, P.; Boiarska, Z.; Pérez-Peña, H.; Abel, A.-C.; Álvarez-Bernad, B.; Lucena-Agell, D.; Vasile, F.; Sironi, M.; Altmann, K.-H.; Prota, A. E.; Díaz, J. F.; Pieraccini, S.; Passarella, D. Maytansinol Derivatives: Side Reactions as a Chance for New Tubulin Binders. *Chem. – Eur. J.* **2022**, *28* (2), e202103520. https://doi.org/10.1002/chem.202103520.

(46) Montecinos, F.; Loew, M.; Chio, T. I.; Bane, S. L.; Sackett, D. L. Interaction of Colchicine-Site Ligands With the Blood Cell-Specific Isotype of β-Tubulin—Notable Affinity for Benzimidazoles. *Front. Cell Dev. Biol.* **2022**, *10*. https://doi.org/10.3389/fcell.2022.884287.

(47) Steinmetz, M. O.; Prota, A. E. Structure-Based Discovery and Rational Design of Microtubule-Targeting Agents. *Curr. Opin. Struct. Biol.* **2024**, *87*, 102845. https://doi.org/10.1016/j.sbi.2024.102845.

(48) Li, C.-M.; Lu, Y.; Ahn, S.; Narayanan, R.; Miller, D. D.; Dalton, J. T. Competitive Mass Spectrometry Binding Assay for Characterization of Three Binding Sites of Tubulin. *J. Mass Spectrom.* **2010**, *45* (10), 1160–1166. https://doi.org/10.1002/jms.1804.

(49) Field, J. J.; Calvo, E.; Northcote, P. T.; Miller, J. H.; Altmann, K.-H.; Díaz, J. F. Chapter 19 – Methods for Studying Microtubule Binding Site Interactions: Zampanolide as a Covalent Binding Agent. In *Methods in Cell Biology*; Correia, J. J., Wilson, L., Eds.; Microtubules,; Academic Press, 2013; Vol. 115, pp 303–325. https://doi.org/10.1016/B978-0-12-407757-7.00019-0.

(50) Mirigian, M.; Mukherjee, K.; Bane, S. L.; Sackett, D. L. Measurement of In Vitro Microtubule Polymerization by Turbidity and Fluorescence. In *Methods in Cell Biology*; Elsevier, 2013; Vol. 115, pp 215–229. https://doi.org/10.1016/B978-0-12-407757-7.00014-1.

(51) Hamel, E. Evaluation of Antimitotic Agents by Quantitative Comparisons of Their Effects on the Polymerization of Purified Tubulin. *Cell Biochem. Biophys.* **2003**, *38* (1), 1–21. https://doi.org/10.1385/CBB:38:1:1.

(52) Bane, S. L.; Ravindra, R.; Zaydman, A. A. High-Throughput Screening of Microtubule-Interacting Drugs. In *Microtubule Protocols*; Zhou, J., Ed.; Methods in Molecular Medicine™; Humana Press: Totowa, NJ, 2007; pp 281–288. https://doi.org/10.1007/978-1-59745-442-1_19.

(53) Bonne, D.; Heuséle, C.; Simon, C.; Pantaloni, D. 4′,6-Diamidino-2-Phenylindole, a Fluorescent Probe for Tubulin and Microtubules. *J. Biol. Chem.* **1985**, *260* (5), 2819–2825. https://doi.org/10.1016/S0021-9258(18)89437-6.

(54) Andreu, J. M. Large Scale Purification of Brain Tubulin With the Modified Weisenberg Procedure. In *Microtubule Protocols*; Zhou, J., Ed.; Methods in Molecular Medicine™; Humana Press: Totowa, NJ, 2007; pp 17–28. https://doi.org/10.1007/978-1-59745-442-1_2.

(55) Castoldi, M.; Popov, A. V. Purification of Brain Tubulin through Two Cycles of Polymerization–Depolymerization in a High-Molarity Buffer. *Protein Expr. Purif.* **2003**, *32* (1), 83–88. https://doi.org/10.1016/S1046-5928(03)00218-3.

(56) Gell, C.; Friel, C. T.; Borgonovo, B.; Drechsel, D. N.; Hyman, A. A.; Howard, J. Purification of Tubulin from Porcine Brain. In *Microtubule Dynamics: Methods and Protocols*; Straube, A., Ed.; Methods in Molecular Biology; Humana Press: Totowa, NJ, 2011; pp 15–28. https://doi.org/10.1007/978-1-61779-252-6_2.

(57) Fourest-Lieuvin, A. Purification of Tubulin from Limited Volumes of Cultured Cells. *Protein Expr. Purif.* **2006**, *45* (1), 183–190. https://doi.org/10.1016/j.pep.2005.05.011.

(58) Nicolaou, K. C.; Hao, J.; Reddy, M. V.; Rao, P. B.; Rassias, G.; Snyder, S. A.; Huang, X.; Chen, D. Y.-K.; Brenzovich, W. E.; Giuseppone, N.; Giannakakou, P.; O'Brate, A. Chemistry and Biology of Diazonamide A: Second Total Synthesis and Biological Investigations. *J. Am. Chem. Soc.* **2004**, *126* (40), 12897–12906. https://doi.org/10.1021/ja040093a.

(59) Nicolaou, K. C.; Bella, M.; Chen, D. Y.-K.; Huang, X.; Ling, T.; Snyder, S. A. Total Synthesis of Diazonamide A. *Angew. Chem. Int. Ed.* **2002**, *41* (18), 3495–3499. https://doi.org/10.1002/1521-3773(20020916)41:18<3495::AID-ANIE3495>3.0.CO;2-7.

(60) Bai, R.; Cruz-Monserrate, Z.; Fenical, W.; Pettit, G. R.; Hamel, E. Interaction of Diazonamide A with Tubulin. *Arch. Biochem. Biophys.* **2020**, *680*, 108217. https://doi.org/10.1016/j.abb.2019.108217.

(61) Wang, G.; Shang, L.; Burgett, A. W. G.; Harran, P. G.; Wang, X. Diazonamide Toxins Reveal an Unexpected Function for Ornithine δ-Amino Transferase in Mitotic Cell Division. *Proc. Natl. Acad. Sci. U. S. A.* **2007**, *104* (7), 2068–2073. https://doi.org/10.1073/pnas.0610832104.

(62) Cruz-Monserrate, Z.; Vervoort, H. C.; Bai, R.; Newman, D. J.; Howell, S. B.; Los, G.; Mullaney, J. T.; Williams, M. D.; Pettit, G. R.; Fenical, W.; Hamel, E. Diazonamide A and a Synthetic Structural Analog: Disruptive Effects on Mitosis and Cellular Microtubules and Analysis of Their Interactions with Tubulin. *Mol. Pharmacol.* **2003**, *63* (6), 1273–1280. https://doi.org/10.1124/mol.63.6.1273.

(63) Allred, T. K.; Manoni, F.; Harran, P. G. Exploring the Boundaries of "Practical": De Novo Syntheses of Complex Natural Product-Based Drug Candidates. *Chem. Rev.* **2017**, *117* (18), 11994–12051. https://doi.org/10.1021/acs.chemrev.7b00126.

(64) Kazak, M.; Vasilevska, A.; Suna, E. Preparative Scale Synthesis of Functionalized Bioxazole. *Chem. Heterocycl. Compd.* **2020**, *56* (3), 355–364. https://doi.org/10.1007/s10593-020-02667-8.

(65) Jeong, S.; Chen, X.; Harran, P. G. Macrocyclic Triarylethylenes via Heck Endocyclization: A System Relevant to Diazonamide Synthesis. *J Org Chem* **1998**, *63* (24), 8640–8641. https://doi.org/10.1021/jo981791e.

(66) Atmuri, N. D. P.; Lubell, W. D. Insight into Transannular Cyclization Reactions To Synthesize Azabicyclo[*X* . *Y* . *Z*]Alkanone Amino Acid Derivatives from 8-, 9-, and 10-Membered Macrocyclic Dipeptide Lactams. *J. Org. Chem.* **2015**, *80* (10), 4904–4918. https://doi.org/10.1021/acs.joc.5b00237.

(67) Mangold, S. L.; Grubbs, R. H. Stereoselective Synthesis of Macrocyclic Peptides via a Dual Olefin Metathesis and Ethenolysis Approach. *Chem. Sci.* **2015**, *6* (8), 4561–4569. https://doi.org/10.1039/C5SC01507C.

(68) Kaul, R.; Surprenant, S.; Lubell, W. D. Systematic Study of the Synthesis of Macrocyclic Dipeptide *β* -Turn Mimics Possessing 8-, 9-, and 10-Membered Rings by Ring-Closing Metathesis. *J. Org. Chem.* **2005**, *70* (12), 4901–4902. https://doi.org/10.1021/jo056027o.

(69) Shibata, K.; Yoshida, M.; Doi, T.; Takahashi, T. Derivatization of a Tris-Oxazole Using Pd-Catalyzed Coupling Reactions of a 5-Bromooxazole Moiety. *Tetrahedron Lett.* **2010**, *51* (13), 1674–1677. https://doi.org/10.1016/j.tetlet.2010.01.064.

(70) Topolovčan, N.; Panov, I.; Kotora, M. Synthesis of 1,2-Disubstituted Cyclopentadienes from Alkynes Using a Catalytic Haloallylation/Cross-Coupling/Metathesis Relay. *Org. Lett.* **2016**, *18* (15), 3634–3637. https://doi.org/10.1021/acs.orglett.6b01682.

(71) Fürstner, A.; Guth, O.; Düffels, A.; Seidel, G.; Liebl, M.; Gabor, B.; Mynott, R. Indenylidene Complexes of Ruthenium: Optimized Synthesis, Structure Elucidation, and Performance as Catalysts for Olefin Metathesis—Application to the Synthesis of the ADE-Ring System of Nakadomarin A. *Chem. – Eur. J.* **2001**, *7* (22), 4811–4820. https://doi.org/10.1002/1521-3765(20011119)7:22<4811::AID-CHEM4811>3.0.CO;2-P.

(72) Scholl, M.; Ding, S.; Lee, C. W.; Grubbs, R. H. Synthesis and Activity of a New Generation of Ruthenium-Based Olefin Metathesis Catalysts Coordinated with 1,3-Dimesityl-4,5-Dihydroimidazol-2-Ylidene Ligands §. *Org. Lett.* **1999**, *1* (6), 953–956. https://doi.org/10.1021/ol990909q.

(73) Grela, K.; Harutyunyan, S.; Michrowska, A. A Highly Efficient Ruthenium Catalyst for Metathesis Reactions. *Angew. Chem. Int. Ed.* **2002**, *41* (21), 4038–4040. https://doi.org/10.1002/1521-3773(20021104)41:21<4038::AID-ANIE4038>3.0.CO;2-0.

(74) Gradillas, A.; Pérez-Castells, J. Macrocyclization by Ring-Closing Metathesis in the Total Synthesis of Natural Products: Reaction Conditions and Limitations. *Angew. Chem. Int. Ed.* **2006**, *45* (37), 6086–6101. https://doi.org/10.1002/anie.200600641.

(75) Ojima, I.; Lin, S.; Inoue, T.; Miller, M. L.; Borella, C. P.; Geng, X.; Walsh, J. J. Macrocycle Formation by Ring-Closing Metathesis. Application to the Syntheses of Novel Macrocyclic Taxoids. *J. Am. Chem. Soc.* **2000**, *122* (22), 5343–5353. https://doi.org/10.1021/ja000293w.

(76) Muthusamy, S.; Azhagan, D. Titanium Isopropoxide Promoted Tandem Self-Cross and Ring-Closing Metathesis Approach for the Synthesis of Macrotetralides: Tandem Self-Cross and Ring-Closing Metathesis. *Eur. J. Org. Chem.* **2014**, *2014* (2), 363–370. https://doi.org/10.1002/ejoc.201301239.

(77) Barrett, A. G. M.; Hamprecht, D.; Ohkubo, M. Dess–Martin Periodinane Oxidation of Alcohols in the Presence of Stabilized Phosphorus Ylides: A Convenient Method for the Homologation of Alcohols via Unstable Aldehydes. *J. Org. Chem.* **1997**, *62* (26), 9376–9378. https://doi.org/10.1021/jo971569u.

(78) Mai, C.-K.; Sammons, M. F.; Sammakia, T. A Concise Formal Synthesis of Diazonamide A by the Stereoselective Construction of the C10 Quaternary Center. *Angew. Chem. Int. Ed.* **2010**, *49* (13), 2397–2400. https://doi.org/10.1002/anie.200906318.

(79) Ross, A. J.; Lang, H. L.; Jackson, R. F. W. Much Improved Conditions for the Negishi Cross-Coupling of Iodoalanine Derived Zinc Reagents with Aryl Halides. *J. Org. Chem.* **2010**, *75* (1), 245–248. https://doi.org/10.1021/jo902238n.

(80) Deng, Y.-H.; Zhang, X.-Z.; Yu, K.-Y.; Yan, X.; Du, J.-Y.; Huang, H.; Fan, C.-A. Bifunctional Tertiary Amine-Squaramide Catalyzed Asymmetric Catalytic 1,6-Conjugate Addition/ Aromatization of Para-Quinone Methides with Oxindoles. *Chem. Commun.* **2016**, *52* (22), 4183–4186. https://doi.org/10.1039/C5CC10502A.

(81) Ghosh, S.; Chaudhuri, S.; Bisai, A. Oxidative Dimerization of 2-Oxindoles Promoted by KOtBu-I2: Total Synthesis of (±)-Folicanthine. *Org. Lett.* **2015**, *17* (6), 1373–1376. https://doi.org/10.1021/acs.orglett.5b00032.

(82) Zhang, J.-Q.; Li, S.-M.; Wu, C.-F.; Wang, X.-L.; Wu, T.-T.; Du, Y.; Yang, Y.-Y.; Fan, L.-L.; Dong, Y.-X.; Wang, J.-T.; Tang, L. The Synthesis of Symmetrical 3,3-Disubstituted Oxindoles by Phosphine-Catalyzed γ/γ-Addition of Oxindoles with Allenoates. *Catal. Commun.* **2020**, *138*, 105838. https://doi.org/10.1016/j.catcom.2019.105838.

(83) Shoemaker, R. H. The NCI60 Human Tumour Cell Line Anticancer Drug Screen. *Nat. Rev. Cancer* **2006**, *6* (10), 813–823. https://doi.org/10.1038/nrc1951.

(84) Kalnins, T.; Vitkovska, V.; Kazak, M.; Zelencova-Gopejenko, D.; Ozola, M.; Narvaiss, N.; Makrecka-Kuka, M.; Domračeva, I.; Kinens, A.; Gukalova, B.; Konrad, N.; Aav, R.; Bonato, F.; Lucena-Agell, D.; Díaz, J. F.; Liepinsh, E.; Suna, E. Development of Potent Microtubule Targeting Agent by Structural Simplification of Natural Diazonamide. *J. Med. Chem.* **2024**, *67* (11), 9227–9259. https://doi.org/10.1021/acs.jmedchem.4c00388.

(85) Cree, I. A.; Charlton, P. Molecular Chess? Hallmarks of Anti-Cancer Drug Resistance. *BMC Cancer* **2017**, *17* (1), 10. https://doi.org/10.1186/s12885-016-2999-1.

(86) Sisco, E.; Barnes, K. L. Design, Synthesis, and Biological Evaluation of Novel 1,3-Oxazole Sulfonamides as Tubulin Polymerization Inhibitors. *ACS Med. Chem. Lett.* **2021**, *12* (6), 1030–1037. https://doi.org/10.1021/acsmedchemlett.1c00219.

(87) Krause, W. Resistance to Anti-Tubulin Agents: From Vinca Alkaloids to Epothilones. *Cancer Drug Resist.* **2019**, *2* (1), 82–106. https://doi.org/10.20517/cdr.2019.06.

(88) Cortes, J.; Vidal, M. Beyond Taxanes: The next Generation of Microtubule-Targeting Agents. *Breast Cancer Res. Treat.* **2012**, *133* (3), 821–830. https://doi.org/10.1007/s10549-011-1875-6.

(89) Rixe, O.; Fojo, T. Is Cell Death a Critical End Point for Anticancer Therapies or Is Cytostasis Sufficient? *Clin. Cancer Res.* **2007**, *13* (24), 7280–7287. https://doi.org/10.1158/1078-0432.CCR-07-2141.

(90) Holbeck, S. L.; Collins, J. M.; Doroshow, J. H. Analysis of Food and Drug Administration–Approved Anticancer Agents in the NCI60 Panel of Human Tumor Cell Lines. *Mol. Cancer Ther.* **2010**, *9* (5), 1451–1460. https://doi.org/10.1158/1535-7163.MCT-10-0106.

(91) *National Cancer Institute, publicly accessible database of NCI-60 panel screening results and COMPARE analysis;* https://dtp.cancer.gov/public_compare/ (accessed 2024-01-05).

(92) Camci, M.; Karali, N. Bioisosterism: 1,2,4-Oxadiazole Rings. *ChemMedChem* **2023**, *18* (9), e202200638. https://doi.org/10.1002/cmdc.202200638.

(93) Lassalas, P.; Gay, B.; Lasfargeas, C.; James, M. J.; Tran, V.; Vijayendran, K. G.; Brunden, K. R.; Kozlowski, M. C.; Thomas, C. J.; Smith, A. B. I.; Huryn, D. M.; Ballatore, C. Structure Property Relationships of Carboxylic Acid Isosteres. *J. Med. Chem.* **2016**, *59* (7), 3183–3203. https://doi.org/10.1021/acs.jmedchem.5b01963.

(94) Ballatore, C.; Huryn, D. M.; Smith III, A. B. Carboxylic Acid (Bio)Isosteres in Drug Design. *ChemMedChem* **2013**, *8* (3), 385–395. https://doi.org/10.1002/cmdc.201200585.

(95) Kazak, M.; Vasilevska, A.; Suna, E. Preparative Scale Synthesis of Functionalized Bioxazole. *Chem. Heterocycl. Compd.* **2020**, *56* (3), 355–364. https://doi.org/10.1007/s10593-020-02667-8.

(96) Liu, X.; Testa, B.; Fahr, A. Lipophilicity and Its Relationship with Passive Drug Permeation. *Pharm. Res.* **2011**, *28* (5), 962–977. https://doi.org/10.1007/s11095-010-0303-7.

(97) Richardson, P. Applications of Fluorine to the Construction of Bioisosteric Elements for the Purposes of Novel Drug Discovery. *Expert Opin. Drug Discov.* **2021**, *16* (11), 1261–1286. https://doi.org/10.1080/17460441.2021.1933427.

APPENDICES

Appendix I – ALIPHATIC CHAIN-CONTAINING MACROCYCLES AS DIAZONAMIDE A ANALOGS

Vitkovska, V., Zogota, R., Kalnins, T., Zelencova, D., Suna, E.

Aliphatic chain-containing macrocycles as diazonamide A analogs

**Viktorija Vitkovska[1], Rimants Zogota[1], Toms Kalnins[1],
Diana Zelencova[1], Edgars Suna[1]***

[1] *Latvian Institute of Organic Synthesis,
21 Aizkraukles St., Riga LV-1006, Latvia; e-mail: edgars@osi.lv*
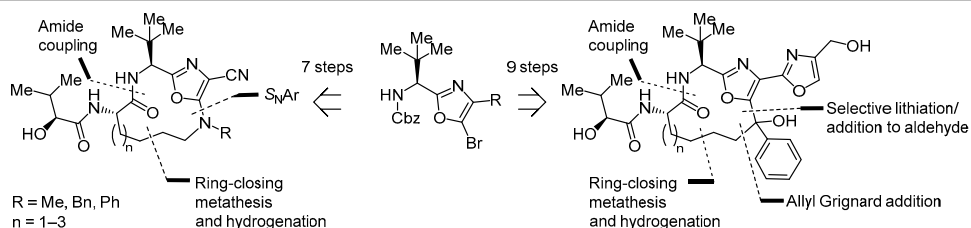
Aliphatic alkyl chain-containing 12–14-membered macrocycles have been designed as structural analogs of antimitotic natural product diazonamide A. Macrocycles were synthesized from 5-bromooxazole in 7 to 9 linear steps using Ru-catalyzed ring-closing metathesis as the key transformation. Heat effect of binding to α,β-tubulin tetramer (T4-RB3 complex) has been measured for the synthesized macrocycles by isothermal titration calorimetry method.

Keywords: diazonamide A, anticancer agents, macrocycles, ring-closing metathesis.

Chemotherapeutics are the most efficient means for the treatment of metastatic tumors. However, a majority of cancer chemotherapeutic agents cause side effects such as nausea, vomiting, diarrhea, hair loss, and pain. These side effects result from undesired cytotoxicity toward normal cells.[1] A notable exception among cancer chemotherapeutic agents is marine metabolite diazonamide A (**1**) (Fig. 1), which does not cause systemic toxicity typical for other antimitotic drugs, while exerting nanomolar cytotoxicity against a range of human tumor cell lines.[2] The greatly reduced systemic toxicity renders diazonamide A (**1**) a highly attractive cancer chemotherapeutic agent. Unfortunately, highly complex structure of the natural product **1** is an important hurdle for its use in the cancer treatment. The decrease of the structural complexity of diazonamide A (**1**) without affecting the anticancer activity is possible, as was demonstrated by the development of anticancer agent DZ-2384 (**2**) (Fig. 1).[3] It has been shown that both natural product **1** and synthetic analog **2** are microtubule-targeting agents.[2,3]

The structurally simplified diazonamide A analog **2** lacks CD subunit and heteroaromatic macrocycle as compared to the parent natural product **1** (Fig. 1). Considering further structural modifications, the substitution of the difficult to synthesize tetracyclic subunit EFGH by less complex linker is highly attractive from the synthetic viewpoint. To verify
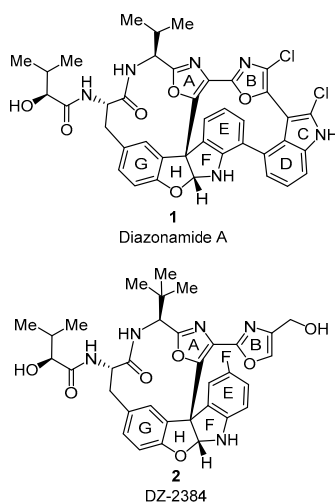

Figure 1. Antimitotic diazonamide A (**1**) and the structurally simplified synthetic analog **2**.
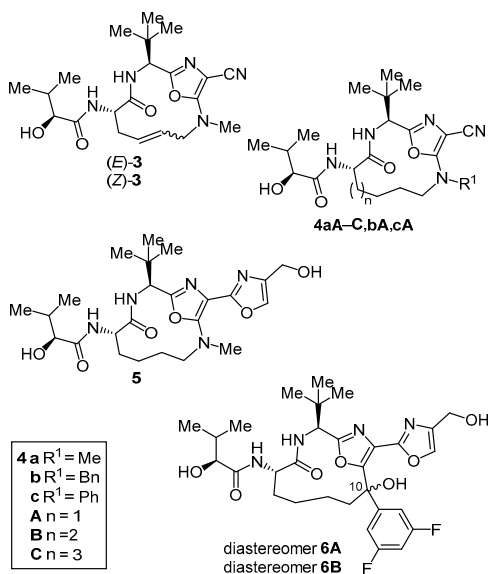
Figure 2. Structure of diazonamide A analogs **3**–**6**.

Figure 3. Retrosynthetic analysis of macrocycles **4**–**6**.

the importance of the tetracyclic subunit EFGH for the binding of cytotoxic agents **1**, **2** to tubulin, a series of diazonamide analogs **3**–**6** that feature the replacement of the EFGH subunit by aliphatic chain of various length were designed and synthesized (Fig. 2). Binding energy of the synthesized analogs **3**–**6** with tubulin has been measured by isothermal titration calorimetry (ITC) assay.

The retrosynthetic analysis of diazonamide A analogs **3**–**6** is depicted in Figure 3. We envisioned that macrocycles **7** could be constructed from the parent bisalkene inter-mediates **8** using the ring-closing metathesis (RCM) as the key step. The allyl moieties in the key intermediates **8** (X = NR[2]) could be installed by amide coupling with chiral unsaturated amino acids and by the C–N bond formation in the S_NAr-type reaction of bromooxazole **10** and allyl amines. In addition, the allyl moiety could be also attached to the oxazole subunit in the key intermediate **8** (X = C(OH)Ar) by the nucleophilic addition of allyl metal species to ketone **11**. The latter is accessible by regio-selective lithiation of bioxazole **12**,[4] followed by the *in situ* addition of lithiated species to aryl ketones.

The synthesis of macrocycles **4**–**6** commenced with the preparation of bromooxazole **10** and amino acids **16B** and **16C** using literature methods (Scheme 1). Thus, bromo-oxazole **10** was synthesized from the commercially available Cbz-protected (*S*)-*tert*-leucine **13** and 2-aminomalononitrile tosylate **14**, followed by amine-bromide exchange in compound **15** under the Sandmeyer reaction conditions.[5] The synthesis of unsaturated amino acid **16C** started with the formation of ester **17A** from the corresponding acid **16A**. Subsequent reaction sequence included the hydro-boration of ester **17A** with 9-BBN, which was followed by Suzuki cross coupling between the *in situ* generated
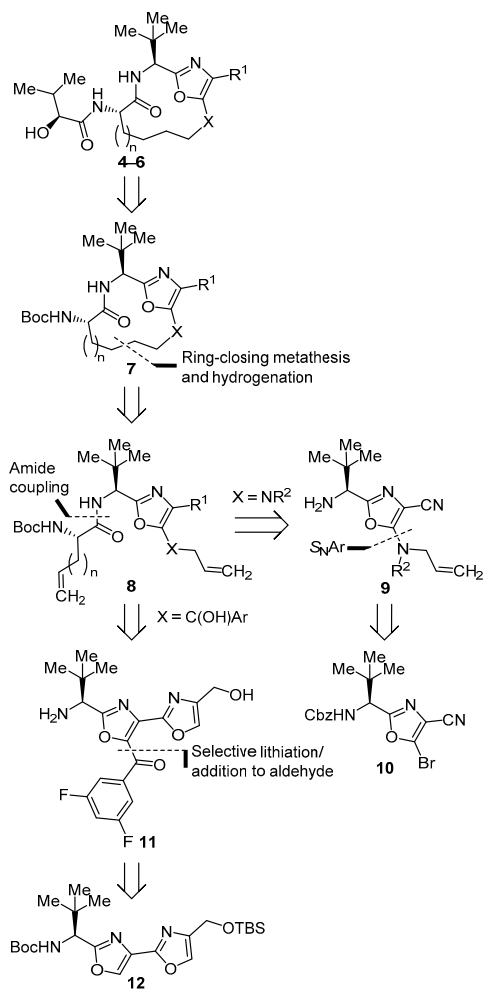
boronate and vinyl bromide to afford ester **17C**. The hydrolysis of the ester moiety afforded acid **16C** in good yield.[6] The synthesis of amino acid **16B** required the preparation of organozinc species from iodide **18**. The intermediate *N*-Boc-protected organozinc species were cross-coupled with allyl bromide in the presence of stoichiometric amounts of copper bromide.[7] The formed aminohexenoate **17B** was converted into corresponding acid **16B** by saponification with LiOH (Scheme 1).[8]

Macrocycles **3**–**4** were prepared starting from oxazole **10** (Scheme 2). The allylamine moiety was installed in bromooxazole **10** or its *N*-deprotected derivative by S_NAr-type nucleophilic substitution of bromide in the presence of a general base such as NEt₃.[9] For the less

Scheme 1. Synthesis of oxazole building block **10** and amino acids **16B,C**
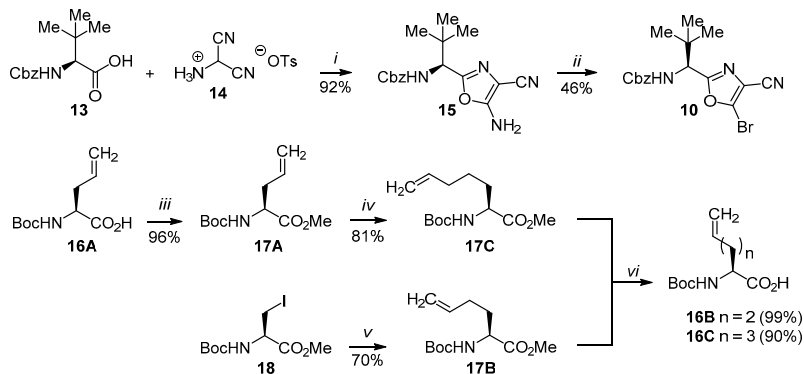
i: EDC·HCl, pyridine, rt, 24 h
ii: *t*-BuONO, CuBr$_2$, MeCN, rt, 1 h
iii: MeI, K$_2$CO$_3$, rt, DMF, 18 h
iv: 9-BBN, THF, 0°C to rt, 3 h, then aq 1 M Na$_2$CO$_3$, CH$_2$=CHBr, Pd$_2$(dba)$_3$ (2 mol %), P(*o*-tol)$_3$ (10 mol %), THF, −78°C to rt, 20 h
v: 1. Zn powder, I$_2$, DMF, rt, 3 h; 2. CuBr, CH$_2$=CHCH$_2$Br, −15°C to rt, DMF, 20 h
vi: LiOH, H$_2$O–1,4-dioxane, 1:1, rt, 3 h

nucleophilic aniline, the generation of the corresponding potassium anilide by KHMDS was required to effect the desired nucleophilic substitution of bromide in compound **10**. The cleavage of *N*-Cbz protection was accomplished by HBr solution, and higher yields were achieved if morpholine was added to trap the formed benzyl bromide and to avoid the alkylation side reactions. The amide bond formation with *N*-Boc-protected amino acids **16A–C** gave the corresponding dienes **8aA–C,bA**. *N*-Phenyl diene **8cA** was prepared by the initial amide coupling of intermediate **19** with amino acid **16A**, followed by regioselective allylation of the most nucleophilic nitrogen in the deprotonated compound **20** (Scheme 2).

Next, the reaction conditions for the RCM step were optimized using diene **8aA** as a model substrate (0.1 M solution in CH$_2$Cl$_2$) at 50°C[10] (Table 1). Initial attempts to effect the formation of the desired macrocycle **7aA** using catalyst **Ru1**[11] were not successful: incomplete conversion of the starting diene **8aA** was observed, and macrocycle **7aA** was not formed (entry 1). The lack of the RCM product and the incomplete conversion of diene **8aA** pointed to a low catalytic activity of **Ru1** that resulted in slow reaction and concomitant decomposition of the starting material under the tested conditions. Catalyst **Ru2** was also inefficient (entry 2),[12] however it was shown that the catalytic activity of complex **Ru2** could be increased by introduction of a strong electron-withdrawing group in the 2-isopropoxystyrene ligand.[13] Indeed, the nitro-substituted catalyst **Ru3** and the corresponding sulfonamide **Ru4** afforded 39 and 41%, respectively, of the desired macrocycle **7aA** together with ca. 20% of unidentified side products with the balance corresponding to 61–63% conversion (entries 3 and 4). We speculated that the metathesis-polymerization side reaction might account for the formation of the side products. Indeed, twofold increase of the dilution and prolonged reaction time has helped to increase the yield of

macrocycle **7aA** to 63% isolated yield (entry 5). It should be noted that macrocycle **7aA** was formed as a 2:3 mixture of *E*:*Z* isomers that was anticipated for a medium-sized (12-membered) macrocycles.[14,15]

Table 1. Screening of conditions for the RCM*

Entry	Conditions	Conversion**, %	Yield**, %
1	**Ru1**, 50°C, 22 h	30	0
2	**Ru2**, 50°C, 22 h	100	0
3	**Ru3**, 50°C, 22 h	61	39
4	**Ru4**, 50°C, 22 h	63	41
5***	**Ru4**, 50°C, 72 h	83	76 (63*[4])

* 0.1 M solution of diene **8aA** in CH$_2$Cl$_2$ at 50°C.
** Determined by UPLC-MS assay.
*** 0.05 M solution.
*[4] Isolated yield.

Scheme 2. Synthesis of analogs **3** and **4aA–C,bA,cA**
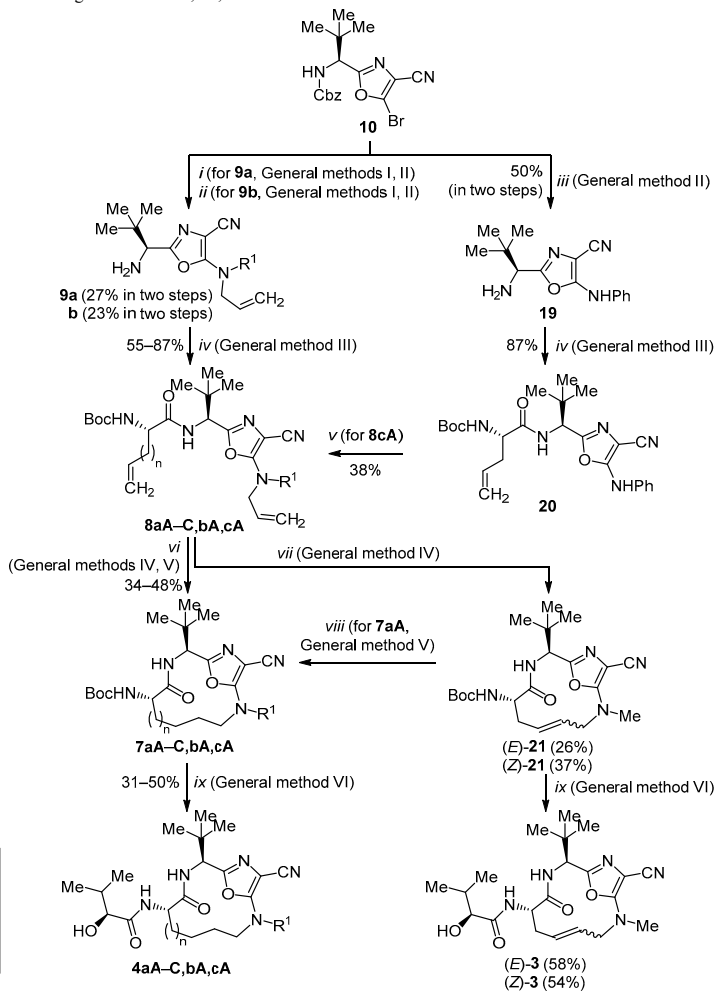
i: 1. *N*-Methylallylamine (2 equiv), NEt$_3$ (3 equiv), DMF, rt, 18 h (General method I); 2. 33% HBr in AcOH (40 equiv), 1,4-dioxane, rt, 10 min, then morpholine, rt, 1 h (General method II)

ii: 1. 33% HBr in AcOH (40 equiv), 1,4-dioxane, rt, 10 min (General method II), then aqueous 2 M Na$_2$CO$_3$, rt; 2. *N*-allylbenzylamine (2 equiv), NEt$_3$ (3 equiv), DMF, rt, 18 h (General method I)

iii: 1. Aniline (2 equiv), KN(SiMe$_3$)$_2$ (3.5 equiv), THF, –78°C, 30 min; 2. 33% HBr in AcOH (40 equiv), 1,4-dioxane, rt, 10 min, then morpholine, rt, 1 h (General method II)

iv: Acid **16A**, **16B**, or **16C** (1.5 equiv), EDC·HCl (2 equiv), pyridine, rt, 18 h, 80% (**8aA**), 55% (**8aB**), 74% (**8aC**), 65% (**8bA**), 87% (**20**) (General method III)

v: NaH (3 equiv), allyl bromide (1 equiv), DMF, 0°C, 1 h

vi: 1. Catalyst **Ru4** (5 mol %), anhydrous CH$_2$Cl$_2$ (50 ml per mmol of alkene), rt, 30–48 h (General method IV); 2. H$_2$ (1 atm), 10% Pd/C (1 mol %), EtOAc, rt, 18–24 h (General method V); yield of the two-step process: 48% (**7aB**), 44% (**7aC**), 34% (**7bA**), 47% (**8cA**)

vii: 1. Catalyst **Ru4** (5 mol %), alkene **8aA**, CH$_2$Cl$_2$ (50 ml per mmol of alkene), rt, 30 h (General method IV); 2. Separation of *E*/*Z*-isomers by chromatography

viii: H$_2$ (1 atm), 10% Pd/C (1 mol %), EtOAc, rt, 18 h (General method V)

ix: 1. CF$_3$CO$_2$H (50 equiv), CH$_2$Cl$_2$, rt, 5 h; 2. (*S*)-2-hydroxy-3-methylbutanoic acid (1.5 equiv), EDC·HCl (3 equiv), HOBt (3 equiv), DIPEA (6 equiv), CH$_2$Cl$_2$, rt, 12 h (General method VI), 54% ((*Z*)-**3**), 58% ((*E*)-**3**), 50% (**4aA**), 46% (**4aB**), 49% (**4aC**), 31% (**4bA**), 50% (**4cA**)

Scheme 3. Synthesis of analog **5**
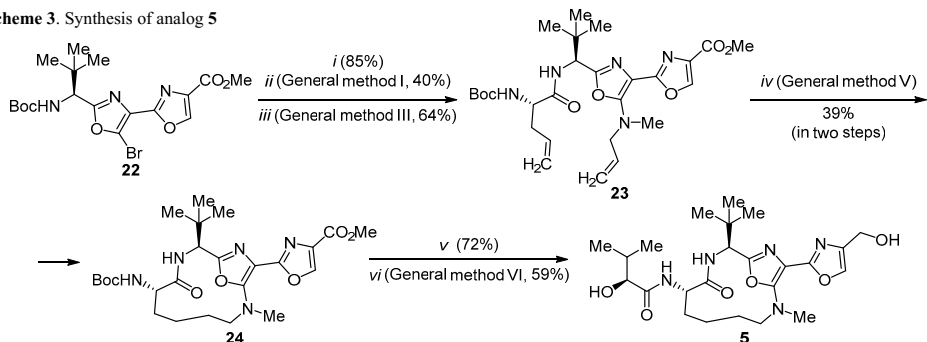
i. 33% HBr in AcOH (20 equiv), 1,4-dioxane, rt, 15 min
ii: *N*-Methylallylamine (1.6 equiv), NEt$_3$ (2 equiv), DMF, 50°C, 24 h (General method I)
iii: Acid **16A** (1.7 equiv), EDC·HCl (2 equiv), pyridine, rt, 3 h (General method III)
iv: 1. Catalyst **Ru4** (10 mol %), anhydrous CH$_2$Cl$_2$ (50 ml per mmol of alkene), 50°C, 24 h, then Ti(O*i*-Pr)$_4$ (1 equiv), 60°C, 5 days;
    2. H$_2$ (1 atm), 10% Pd/C (1 mol %), EtOAc, rt, 20 h (General method V)
v: LiBH$_4$ (5 equiv), THF–CF$_3$CH$_2$OH, 10:1, rt, 20 h
vi: 1. CF$_3$CO$_2$H (50 equiv), CH$_2$Cl$_2$, rt, 3 h; 2. (S)-2-Hydroxy-3-methylbutanoic acid (1.5 equiv), EDC·HCl (3 equiv), HOBt (3 equiv),
DIPEA (6 equiv), CH$_2$Cl$_2$, rt, 18 h (General method VI)

With the optimized cyclization conditions in hand, dienes **8aA**–**C**,**bA**,**cA** were subjected to RCM in the presence of catalyst **Ru4** (5 mol %) (Scheme 2). Isolation of the RCM products was accomplished only for diene **8aA** to afford unsaturated macrocycles (*E*)-**21** and (*Z*)-**21** as individual isomers after column chromatography. The other macrocyclization products were obtained as mixtures of *E*- and *Z*-isomers and directly converted into saturated macrocycles **7aA**–**C**,**bA**,**cA** under Pd-catalyzed hydrogenation conditions. The end-game of the synthesis involved *N*-Boc deprotection, followed by amide bond formation with (S)-2-hydroxy-3-methylbutanoic acid to afford unsaturated macrocycles (*E*)-**3** and (*Z*)-**3** as well as their saturated analogs **4aA**–**C**,**bA**,**cA** (Scheme 2).
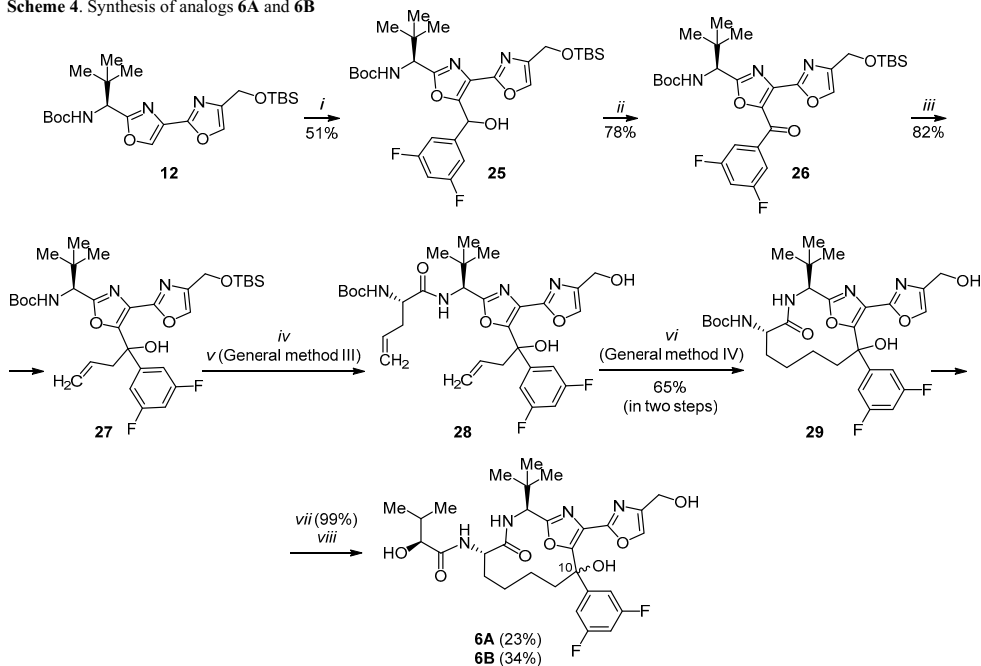
Bioxazole-containing analog **5** was prepared by analogy to the synthesis of macrocycles **3**, **4** (Scheme 3). Thus, the *N*-Boc deprotection of compound **22**[4] was followed by the nucleophilic substitution of bromide with *N*-methylallylamine. Subsequent amide coupling with amino acid **16A** afforded diene **23**. Disappointingly, the optimized RCM conditions (Table 1, entry 5) turned out to be unsuitable for the RCM of diene **23**, as the formation of the desired macrocycle was not observed. We hypothesized that the chelation of catalytically active Ru species by substrate may be responsible for the inhibition of the catalytic cycle. It has been demonstrated that the addition of certain Lewis acids such as Ti(IV) species helps to avoid the deactivation of the Ru catalyst.[16] Indeed, the addition of stoichiometric amounts of Ti(O*i*-Pr)$_4$ improved the reaction rate and allowed for the formation of the unsaturated macrocycle, which was converted into the saturated analog **24** by Pd-catalyzed hydrogenation. The end-game of the synthesis involved reduction of the ester moiety, *N*-deprotection, and amide bond formation sequence to give macrocycle **5** (Scheme 3).

The synthesis of macrocycle **6** was started by regioselective lithiation of bioxazole **12**,[4] followed by the addition of the lithiated intermediate to 3,5-difluorobenzaldehyde to form alcohol **25** as a 1:1 mixture of diastereomers (Scheme 4). Subsequent oxidation with Dess–Martin periodinane[17] provided ketone **26**, which further reacted with allylmagnesium bromide to afford tertiary alcohol **27** (1:1 mixture of diastereomers). The cleavage of both *N*-Boc and OTBS protecting groups under acidic conditions was followed by the amide bond formation using acid **16A** to give diene **28**. The resulting diene was subjected to Ru-catalyzed RCM under the optimized conditions (Table 1, entry 5). The unsaturated macrocyclization product was formed as a 2:1 *E*:*Z* mixture of isomers in high (82%) yield. The mixture of isomers was hydrogenated to form macrocycle **29**. At this point, the stage was set for the *N*-deprotection/ amide bond formation sequence. However, the cleavage of *N*-Boc protecting group in macrocycle **29** by trifluoroacetic acid resulted in the concomitant trifluoroacetoxylation of the tertiary alcohol-derived transient carbocation. After some experimentation, it was found that the ester side product can be hydrolyzed back to the tertiary alcohol by aqueous LiOH. Subsequent amide bond formation with (S)-2-hydroxy-3-methylbutanoic acid furnished macrocycle **6** as a mixture of diastereomers **6A** and **6B**. Individual diastereomers were obtained after separation by chromatography, however, the configuration of the quaternary stereogenic center could not be assigned for the individual diastereomers **6A**,**B** (Scheme 4).

The heat effect of binding (dissociation constants, K_d values) between all synthesized diazonamide A analogs **3**–**6** and α,β-tubulin tetramer (T4-RB3 complex) has been measured by isothermal titration calorimetry (ITC) method (Table 2). No heat effect of the binding has been observed for most of the synthesized analogs (Table 2, entries 1–4, 7, 8). Low micromolar binding was observed for diazonamide A analogs **4aC**,**bA** and both diastereomers of compound **6** (entries 5, 6, 9, and 10, respectively). However, the measured heat effects of binding are 2 orders

Scheme 4. Synthesis of analogs **6A** and **6B**

i: *n*-BuLi (2.1 equiv), Et$_2$O, –78°C, 10 min, then 3,5-difluorobenzaldehyde (2.4 equiv), –78°C to rt, 30 min
ii: Dess–Martin periodinane (1.5 equiv), CH$_2$Cl$_2$, rt, 1 h
iii: Allylmagnesium bromide (2.5 equiv), THF, –15°C, 30 min
iv: 4 M HCl in 1,4-dioxane, rt, 18 h, 69%
v: Acid **16A** (1.5 equiv), EDC·HCl (1.1 equiv), pyridine, rt, 3 h, 71% (General method III)
vi: 1. Catalyst **Ru4** (12.5 mol %), anhydrous CH$_2$Cl$_2$ (50 ml per mmol of alkene), rt, 44 h (General method IV);
2. H$_2$ (5 atm), 10% Pd/C (50 mol %), MeOH, rt, 5 days
vii: 1. CF$_3$CO$_2$H (65 equiv), CH$_2$Cl$_2$, rt, 3 h; 2. LiOH (5 equiv), THF–MeOH–H$_2$O, 1:1:1, rt, 1 h
viii: 1. (S)-2-Hydroxy-3-methylbutanoic acid (1.1 equiv), EDC·HCl (1.1 equiv), HOBt (1.1 equiv), DIPEA (3 equiv), CH$_2$Cl$_2$, rt, 18 h;
2. Separation of diastereomers by chromatography

of magnitude lower than that of DZ-2384 (**2**) (K_d 0.05 μM). Hence, the ITC results provided strong evidence that the presence of the tetracyclic subunit GHFE in the natural product **1** and the synthetic derivative **2** is important for the

Table 2. Heat effect of binding between compounds **3**–**6** and α,β-tubulin tetramer (T4-RB3 complex) measured by ITC method

Entry	Compound	K_d, μM*
1	(*E*)-**3**	No heat observed
2	(*Z*)-**3**	No heat observed
3	**4aA**	No heat observed
4	**4aB**	No heat observed
5	**4aC**	2.52 ± 0.83**
6	**4bA**	3.38
7	**4cA**	No heat observed
8	**5**	No heat observed
9	**6A**	4.10
10	**6B**	1.52

* Single ITC experiment.
** Duplicate ITC run.

binding of these antimitotic agents to the α,β-tubulin tetramer.

A series of structurally simplified macrocyclic analogs of marine metabolite diazonamide A and synthetic antimitotic agent DZ-2384 have been synthesized in 7 to 9 linear steps from chiral, enantiomerically pure 5-bromooxazole building block. Ruthenium-catalyzed ring-closing metathesis was employed to construct 12–14-membered macrocycles. The addition of stoichiometric amounts of Ti(*i*-OPr)$_4$ has helped to avoid the chelation of catalytically active Ru species by bioxazole subunit-containing RCM substrates. The starting chiral 5-bromooxazole building block was prepared from (*S*)-*tert*-leucine in a straightforward two-step synthesis. Several of the synthesized diazonamide analogs showed weak (low micromolar) binding with α,β-tubulin tetramer (T4-RB3 complex), and the measured heat effects were considerably lower than that of DZ-2384. These data provided an evidence that the presence of the tetracyclic subunit GHFE in diazonamide A and its synthetic derivative DZ-2384 is important for the

binding to the α,β-tubulin tetramer. We believe that this finding will have implications in the design of diazonamide A analogs as antimitotic agents.

Experimental

^{1}H and ^{13}C NMR spectra were recorded on a Bruker Avance Neo spectrometer with a 5-mm Double-Resonance Broadband CryoProbe Prodigy probe (400 and 101 MHz, respectively) using TMS or the residual solvent peaks as internal reference (CDCl$_3$: 7.26 ppm for ^{1}H nuclei and 77.2 ppm for ^{13}C nuclei; DMSO-d_6: 2.50 ppm for ^{1}H nuclei and 39.5 ppm or ^{13}C nuclei; CD$_3$OD: 3.31 ppm for ^{1}H nuclei and 49.0 ppm for ^{13}C nuclei). Assignments in ^{13}C NMR spectra of compounds **20**, (*Z*)-**3**, **4bA** and **6B** were made based on the COSY, ^{1}H–^{13}C HSQC, and ^{1}H–^{13}C HMBC experiments. High-resolution mass spectra were recorded on a Waters Synapt G2-Si TOF MS instrument using ESI technique. Specific rotation was recorded on a Kruss P3000 instrument. Analytical thin-layer chromatography (TLC) was performed on precoated silica gel F-254 plates (Merck).

All chemicals were used as obtained from commercial sources and all reactions were performed under argon atmosphere in an oven-dried (120°C) glassware, unless noted otherwise. Anhydrous PhMe, Et$_2$O, THF, and CH$_2$Cl$_2$ were obtained by passing commercially available solvent through activated alumina columns.

General method I. Allylamine (2 equiv), followed by NEt$_3$ (3 equiv), was dropwise added to a solution of bromo-oxazole or bromobioxazole (1 equiv) in DMF (6 ml/mmol) at room temperature. The orange solution was stirred for 18–24 h at room temperature or at 50°C. Then the reaction mixture was diluted with EtOAc (10 ml/mmol) and washed with H$_2$O (10 ml/mmol) two times. The organic layers were washed with brine, dried over anhydrous Na$_2$SO$_4$, filtered, and concentrated under reduced pressure. The residue was purified by column chromatography on silica gel using gradient elution from pure hexane to 30% EtOAc in hexane or from pure CH$_2$Cl$_2$ to 10% MeOH in CH$_2$Cl$_2$.

General method II. 33% HBr solution in AcOH (60 equiv) was added dropwise to a solution of Cbz-protected aminooxazole (1 equiv) in 1,4-dioxane (3 ml/mmol) at room temperature. The yellow solution was stirred for 10 min, then cooled to 0°C (crushed ice batch), and 2 M aqueous Na$_2$CO$_3$ solution was carefully added (*Caution! Intense gas evolution!*) until the mixture medium reached pH 7–9. The mixture was extracted with EtOAc (10 ml/mmol) four times. The combined organic layers were washed with brine, dried over anhydrous Na$_2$SO$_4$, and filtered. Morpholine (neat, 10 equiv) was added, and after stirring for 1 h at room temperature, all volatiles were removed under reduced pressure.

General method III. *N*-Boc-protected carboxylic acid **16** (1.5 equiv) was added at room temperature to a solution of amine **9a,b**, **19**, **22**, **27** (1 equiv) and EDC·HCl (2 equiv) in anhydrous pyridine (15 ml/mmol). The yellow solution was stirred for 3–18 h at room temperature, then pyridine was evaporated under reduced pressure. The residue was dissolved in EtOAc (10 ml/mmol) and washed with 0.1 M aqueous HCl solution two times. The organic layers were washed with brine, dried over anhydrous Na$_2$SO$_4$, filtered,

and concentrated under reduced pressure. The residue was purified by column chromatography on silica gel using gradient elution from pure hexane to 40% EtOAc in hexane.

General method IV. Catalyst **Ru4** (0.05 equiv) and diene **8aA–C,bA,cA**, **28** (1 equiv) were weighed in an oven-dried ACE glass pressure tube, and anhydrous CH$_2$Cl$_2$ (50 ml/mmol) was added. The resulting green solution was stirred at 60°C for 30–48 h whereupon the color gradually changed to dark-brown. The reaction mixture was cooled to room temperature and concentrated under reduced pressure.

General method V. 10% Pd on carbon (0.01 equiv) was added to a solution of macrocyclic alkene (from General method III or IV) in EtOAc (15 ml/mmol) under argon atmosphere. The argon atmosphere was replaced by hydrogen atmosphere and the black suspension was stirred for 18–24 h at room temperature. Then the suspension was filtered through a pad of Celite®, and the filtrate was concentrated under reduced pressure. The residue was purified by reversed-phase column chromatography on silica gel using gradient elution from pure H$_2$O to 95% MeCN in H$_2$O.

General method VI. CF$_3$CO$_2$H (50 equiv) was dropwise added to a solution of macrocycle **7aA–C,bA,cA**, (*Z*)-**21**, or (*E*)-**21** (1 equiv) in CH$_2$Cl$_2$ (10 ml/mmol) at 0°C. The resulting solution was warmed to room temperature and stirred for 3–5 h, whereupon all volatiles were concentrated under reduced pressure. The resulting crude amine was used in the next step without further purification. Thus, (*S*)-2-hydroxy-3-methylbutanoic acid (1.5 equiv), EDC·HCl (3 equiv), and HOBt (3 equiv) were added to a solution of the above crude amine in CH$_2$Cl$_2$ (15 ml/mmol). Then DIPEA (6 equiv) was added dropwise and the resulting yellow solution was stirred at room temperature for 12–18 h, whereupon the mixture was washed with 1 M aqueous HCl (10 ml/mmol) two times. The organic layers were washed with brine, dried over anhydrous Na$_2$SO$_4$, and concentrated under reduced pressure. The residue was purified by reversed-phase column chromatography on silica gel using gradient elution from pure H$_2$O to 95% MeCN in H$_2$O.

Benzyl *N*-[(1*S*)-1-(5-amino-4-cyano-1,3-oxazol-2-yl)-2,2-dimethylpropyl]carbamate (15). EDC·HCl (16.3 g, 85.2 mmol, 1.2 equiv) was added to a solution of (2*S*)-2-{([benzyloxy)carbonyl]amino}-3,3-dimethylbutanoic acid (**13**)[5,18] (18.8 g, 71.0 mmol, 1 equiv) and amino-malononitrile *p*-toluenesulfonate (**14**) (19.8 g, 78.1 mmol, 1.1 equiv) in pyridine (200 ml). The resulting orange solution was stirred for 24 h at room temperature, whereupon pyridine was evaporated under reduced pressure. The residue was dissolved in EtOAc and washed with H$_2$O three times. The organic layers were washed with brine, dried over anhydrous Na$_2$SO$_4$, filtered, and evaporated under reduced pressure. The crude product was used in the next reaction without additional purification. Yield 21.5 g (92%), brown amorphous solid, [α]$_D^{20}$ –41.4° (*c* 1.0, MeOH). ^{1}H NMR spectrum (CDCl$_3$), δ, ppm (*J*, Hz): 7.38–7.32 (5H, m, H Ph); 5.34 (1H, d, *J* = 9.8, NH); 5.12–5.09 (2H, m, CH$_2$); 4.81 (2H, s, NH$_2$); 4.58 (1H, d, *J* = 9.8, CH); 0.98 (9H, s, C(CH$_3$)$_3$). ^{13}C NMR spectrum (DMSO-d_6), δ, ppm: 162.3; 156.7; 151.9; 137.3; 128.8; 128.7; 128.2; 115.9; 82.8; 66.1; 58.2; 35.0; 26.7. Found, *m/z*: 329.1614 [M+H]$^+$. C$_{17}$H$_{21}$N$_4$O$_3$. Calculated, *m/z*: 329.1614.

Benzyl ***N*-[(1*S*)-1-(5-bromo-4-cyano-1,3-oxazol-2-yl)-2,2-dimethylpropyl]carbamate (10)**. *tert*-Butylnitrite (1.2 ml, 10.1 mmol, 1.1 equiv) was added to a suspension of CuBr$_2$ (4.1 g, 18.3 mmol, 2 equiv) in MeCN (80 ml) at room temperature under argon atmosphere. The resulting solution was stirred for 5 min whereupon a solution of amine **15** (3.0 g, 9.1 mmol, 1 equiv) in MeCN (30 ml) was added dropwise at room temperature. *Gas evolution was observed!* The reaction mixture was stirred for 1 h at room temperature. Then Et$_2$O and H$_2$O were added and layers were separated. The organic layer was washed with 1 M aqueous HCl solution (3×20 ml), then with brine, dried over anhydrous Na$_2$SO$_4$, filtered, and concentrated under reduced pressure. The residue was purified by reversed-phase column chromatography on silica gel using gradient elution from 40 to 85% MeCN in H$_2$O to give product as a brown oil, which was additionally purified by direct-phase column chromatography on silica gel using gradient elution from pure hexane to 30% EtOAc in hexane. Yield 1.6 g (46%), colorless oil, $[\alpha]_D^{20}$ –17.7° (*c* 1.0, CHCl$_3$). ^{1}H NMR spectrum (CDCl$_3$), δ, ppm (*J*, Hz): 7.40–7.29 (5H, m, H Ph); 5.40 (1H, d, *J* = 9.7, NH); 5.10 (2H, s, CH$_2$); 4.76 (1H, d, *J* = 9.7, CH); 1.00 (9H, s, C(CH$_3$)$_3$). ^{13}C NMR (CDCl$_3$), δ, ppm: 166.0; 155.9; 135.8; 130.9; 128.6; 128.4; 128.2; 116.0; 110.8; 67.5; 58.1; 35.5; 26.1. Found, *m/z*: 392.0603 [M+H]$^+$. C$_{17}$H$_{19}$BrN$_3$O$_3$. Calculated, *m/z*: 392.0610.

Methyl (2*S*)-2-[(*tert*-butoxycarbonyl)amino]hex-5-enoate (17B). An oven-dried Schlenk flask (50 ml) was charged with Zn powder (2.2 g, 34.0 mmol, 4 equiv) and attached to high vacuum system (0.1 Torr). The flask was heated with heatgun and then cooled back to room temperature. The heating/cooling sequence was repeated three times. Then the flask was disconnected from the vacuum, filled with argon, and I$_2$ (533 mg, 2.1 mmol, 0.3 equiv) was added. The flask was heated again with the heatgun until evaporation of I$_2$ has started (red steam appeared). The flask was cooled to room temperature under argon atmosphere, and anhydrous DMF (10 ml) was added dropwise, whereupon color of the suspension slowly (within 1 min) changed from dark-brown to colorless. The resulting suspension was cooled to 0°C (crushed ice), and a solution of methyl (2*R*)-2-[(*tert*-butoxycarbonyl)amino]-3-iodopropanoate (**18**) (2.3 g, 7.0 mmol, 1 equiv) in anhydrous DMF (7 ml) was added dropwise. The resulting yellow suspension was warmed to room temperature and stirred for 3 h, whereupon the stirring was stopped to let the solid settle to the bottom. The supernatant containing organozinc species (~0.5 M, 8.4 ml, 4.2 mmol, 1 equiv) was then carefully transferred by a syringe to a well-stirred suspension of CuBr (301 mg, 2.1 mmol, 0.5 equiv) and allyl bromide (0.7 ml, 8.4 mmol, 2 equiv) in anhydrous DMF (5 ml) at –15°C (NaCl–ice bath). After the addition was completed, the cooling bath was removed and the stirring was continued for 20 h. Then, EtOAc (25 ml) was added to the reaction mixture and stirring was continued for 15 min. The mixture was washed with H$_2$O (20 ml), the organic layer was washed with aqueous 1 M Na$_2$S$_2$O$_3$ (2×20 ml), then with H$_2$O (20 ml) and brine. After drying over anhydrous Na$_2$SO$_4$ and concentration under reduced pressure, the residue was purified by column chromatography on silica gel using gradient elution from

pure hexane to 10% EtOAc in hexane. Yield 716 mg (70%), colorless oil. ^{1}H NMR spectrum (CDCl$_3$), δ, ppm (*J*, Hz): 5.79 (1H, ddt, *J* = 16.9, *J* = 10.2, *J* = 6.5, CH$_2$=C$\underline{H}$); 5.09–5.04 (1H, m, CH); 5.04–4.95 (2H, m, =CH$_2$); 4.30–4.28 (1H, m, NH); 3.74 (3H, s, OCH$_3$); 2.19–2.00 (2H, m, CH$_2$); 1.95–1.89 (1H, m, CH$_2$); 1.78–1.56 (1H, m, CH$_2$); 1.63 (9H, s, C(CH$_3$)$_3$). NMR data are in agreement with the literature reported.[7]

Methyl (2*S*)-2-[(*tert*-butoxycarbonyl)amino]hept-6-enoate (17C). Anhydrous K$_2$CO$_3$ (2.7 g, 19.5 mmol, 3 equiv) and MeI (1.2 ml, 19.5 mmol, 3 equiv) were added to a solution of (2*S*)-2-[(*tert*-butoxycarbonyl)amino]pent-4-enoic acid (**16A**) (1.4 g, 6.5 mmol, 1 equiv) in anhydrous DMF (30 ml) at room temperature. The yellow suspension was stirred for 18 h, whereupon it was diluted with Et$_2$O (50 ml), washed with H$_2$O (2×50 ml), then with aqueous 10% CuSO$_4$ solution (50 ml) and brine. The organic layer was dried over anhydrous Na$_2$SO$_4$ and concentrated under reduced pressure to give methyl ester **17A** as a yellow oil, yield 1.4 g (96%), which was used in the next step without additional purification.

A solution of 9-BBN in THF (0.5 M, 26 ml, 13.1 mmol, 2.5 equiv) was added to a solution of methyl ester **17A** (1.2 g, 5.2 mmol, 1 equiv) in anhydrous THF (20 ml) at 0°C (crushed ice). The mixture was warmed to room temperature, stirred for 3 h, and then quenched with aqueous 1 M Na$_2$CO$_3$ solution (18 ml, 18.3 mmol, 3.5 equiv) while passing a stream of argon through the resulting solution. Vinyl bromide (1 M solution in THF, 21 ml, 20.9 mmol, 4 equiv), followed by a degassed solution of boronate from above was added to a stirred suspension of Pd$_2$(dba)$_3$ (96 mg, 0.1 mmol, 0.02 equiv) and tri-*o*-tolylphosphine (159 mg, 0.5 mmol, 0.1 equiv) in THF at −78°C (dry ice/Me$_2$CO bath). The resulting mixture was warmed to room temperature and stirred for 20 h, whereupon the dark-brown solution was diluted with H$_2$O (50 ml) and extracted with EtOAc (3×50 ml). The organic extracts were combined, washed with brine, dried over anhydrous Na$_2$SO$_4$, and concentrated under reduced pressure. The residue was purified by column chromatography on silica gel using gradient elution from pure hexanes to 10% EtOAc in hexane. Yield 1.1 g (81%), colorless oil. ^{1}H NMR spectrum (CDCl$_3$), δ, ppm (*J*, Hz): 5.83–5.68 (1H, m, C$\underline{H}$=CH$_2$); 5.05–4.91 (3H, m, C$\underline{H}_2$=CH, CH); 4.30–4.28 (1H, m, NH); 3.73 (3H, s, OCH$_3$); 2.11–2.01 (2H, m, CH$_2$); 1.90–1.75 (1H, m, CH$_2$); 1.70–1.60 (1H, m, CH$_2$); 1.55–1.38 (11H, m, C(CH$_3$)$_3$, CH$_2$). NMR data are in agreement with the literature reported.[6]

(2*S*)-2-[(*tert*-Butoxycarbonyl)amino]hex-5-enoic acid (16B). A solution of LiOH (44 mg, 1.9 mmol, 1 equiv) in H$_2$O (10 ml) was added to a solution of ester **17B** (450 mg, 1.9 mmol, 1 equiv) in 1,4-dioxane (10 ml). The colorless mixture was stirred at room temperature for 3 h and concentrated under reduced pressure. The residue was partitioned between H$_2$O (20 ml) and EtOAc (20 ml). The aqueous phase was acidified with 1 M HCl to pH 4 and extracted with EtOAc (2×20 ml). The combined organic layers were washed with brine, dried over anhydrous Na$_2$SO$_4$, and concentrated under reduced pressure. Yield 424 mg (99%), colorless oil. ^{1}H NMR (CDCl$_3$), δ, ppm (*J*, Hz): 7.89 (1H, br. s, OH); 5.76–5.68 (1H, m, C$\underline{H}$=CH$_2$); 5.03–4.89 (3H, m, C$\underline{H}_2$=CH, CH); 4.27–4.23 (1H, m, NH);

2.12–2.03 (2H, m, CH$_2$); 1.92–1.84 (1H, m, CH$_2$); 1.74–1.68 (1H, m, CH$_2$); 1.39 (9H, s, C(CH$_3$)$_3$). NMR data are in agreement with the literature reported.[8]

(2*S*)-2-[(*tert*-Butoxycarbonyl)amino]hept-6-enoic acid (16C). A solution of LiOH (101 mg, 4.2 mmol, 1 equiv) in H$_2$O (25 ml) was added to a solution of ester **17C** (1.08 g, 4.2 mmol, 1 equiv) in 1,4-dioxane (25 ml). The colorless mixture was stirred at room temperature for 3 h and evaporated under reduced pressure. The residue was partitioned between H$_2$O (50 ml) and EtOAc (50 ml). The aqueous phase was acidified with 1 M HCl to pH 4 and extracted with EtOAc (2×20 ml). The combined organic layers were washed with brine, dried over anhydrous Na$_2$SO$_4$, and concentrated under reduced pressure. Yield 922 mg (90%), colorless oil. ^{1}H NMR spectrum (CDCl$_3$), δ, ppm (*J*, Hz): 9.53 (1H, br. s, OH); 5.85–5.69 (1H, m, CH=CH$_2$); 5.06–4.93 (3H, m, CH$_2$=CH, CH); 4.34–4.30 (1H, m, NH); 2.13–2.03 (2H, m, CH$_2$); 1.95–1.76 (1H, m, CH$_2$); 1.73–1.59 (1H, m, CH$_2$); 1.56–1.37 (11H, m, C(CH$_3$)$_3$, CH$_2$). NMR data are in agreement with the literature reported.[6]

2-((1*S*)-1-Amino-2,2-dimethylpropyl)-5-[methyl(prop-2-en-1-yl)amino]-1,3-oxazole-4-carbonitrile (9a) was obtained in a two-step sequence from benzyl *N*-[(1*S*)-1-(5-bromo-4-cyano-1,3-oxazol-2-yl)-2,2-dimethylpropyl]carbamate (**10**).

Step 1. **Benzyl *N*-[(1*S*)-1-{4-cyano-5-[methyl(prop-2-en-1-yl)amino]-1,3-oxazol-2-yl}-2,2-dimethylpropyl]carbamate** was obtained from bromooxazole **10** (6.0 g, 15.2 mmol), *N*-methylallylamine (2.8 ml, 30.8 mmol), and NEt$_3$ (6.4 ml, 46.0 mmol) in anhydrous DMF following the general method I. The crude product was purified by column chromatography on silica gel using gradient elution from pure hexanes to 30% EtOAc in hexane to afford the subtitle compound. Yield 4.80 g (82%), yellow oil. [α]$_D^{20}$ –30.6° (*c* 1.0, CHCl$_3$). ^{1}H NMR spectrum (CDCl$_3$), δ, ppm (*J*, Hz): 7.39–7.27 (5H, m, H Ph); 5.86–5.73 (1H, m, CH=CH$_2$); 5.43 (1H, d, *J* = 9.8, CH(NH)); 5.31–5.20 (2H, m, CH$_2$=); 5.10 (2H, s, CH$_2$O); 4.57 (1H, d, *J* = 9.8, NH(CH)); 3.97 (2H, dq, *J* = 14.0, *J* = 5.7, NCH$_2$); 3.10 (3H, s, CH$_3$); 0.97 (9H, s, C(CH$_3$)$_3$). ^{13}C NMR spectrum (CDCl$_3$), δ, ppm: 160.0; 156.1; 152.1; 136.1; 131.1; 128.5; 128.2; 118.9; 116.0; 84.5; 67.2; 57.4; 53.9; 36.3; 35.7; 26.1. Found, *m/z*: 383.2083 [M+H]$^+$. C$_{21}$H$_{27}$N$_4$O$_3$. Calculated, *m/z*: 383.2092.

Step 2. **2-((1*S*)-1-Amino-2,2-dimethylpropyl)-5-[methyl-(prop-2-en-1-yl)amino]-1,3-oxazole-4-carbonitrile (9a)** was obtained from benzyl *N*-[(1*S*)-1-{4-cyano-5-[methyl-(prop-2-en-1-yl)amino]-1,3-oxazol-2-yl}-2,2-dimethylpropyl]-carbamate (step 1) (3.57 g, 9.3 mmol) and 33% HBr in AcOH (96 ml, 560.1 mmol) in 1,4-dioxane, followed by the addition of morpholine (8.1 ml, 93.3 mmol) by the general method II. Yield 762 mg (33%), orange oil. The crude amine **9a** was used in the next step without additional purification.

tert-Butyl *N*-{(1*S*)-1-[((1*S*)-1-{4-cyano-5-[methyl(prop-2-en-1-yl)amino]-1,3-oxazol-2-yl}-2,2-dimethylpropyl)-carbamoyl]but-3-en-1-yl}carbamate (8aA) was obtained from crude amine **9a** (254 mg, 1.0 mmol), EDC·HCl (292 mg, 2.0 mmol), and acid **16A** (330 mg, 1.5 mmol) in anhydrous pyridine following the general method III. Yield 365 mg (80%), colorless oil, [α]$_D^{20}$ –33.5° (*c* 1.3, CHCl$_3$). ^{1}H NMR spectrum (CDCl$_3$), δ, ppm (*J*, Hz): 6.91 (1H, br. s, NH);

5.86–5.68 (2H, m, 2CH=CH$_2$); 5.31–5.20 (2H, m, CH=CH$_2$); 5.19–5.10 (2H, m, CH=CH$_2$); 4.95 (1H, br. s, NH); 4.84 (1H, d, *J* = 9.4, CH–oxazole); 4.16–4.08 (1H, m, 2CH$_2$); 4.05–3.90 (2H, m, NCH$_2$); 3.11 (3H, s, CH$_3$); 2.57–2.43 (2H, m, CHCH$_2$); 1.44 (9H, s, C(CH$_3$)$_3$); 0.95 (9H, s, C(CH$_3$)$_3$). ^{13}C NMR spectrum (CDCl$_3$), δ, ppm: 171.1; 160.0; 155.7; 151.7; 133.0; 131.1; 119.2; 118.9; 116.0; 84.5; 80.6; 55.0; 53.9; 36.3; 35.8; 28.3; 26.1. Found, *m/z*: 446.2771 [M+H]$^+$. C$_{23}$H$_{36}$N$_5$O$_4$. Calculated, *m/z*: 446.2767.

tert-Butyl *N*-{(1*S*)-1-[((1*S*)-1-{4-cyano-5-[methyl(prop-2-en-1-yl)amino]-1,3-oxazol-2-yl}-2,2-dimethylpropyl)-carbamoyl]pent-4-en-1-yl}carbamate (8aB) was obtained from crude amine **9a** (250 mg, 1.0 mmol), acid **16B** (231 mg, 1.0 mmol), and EDC·HCl (232 mg, 1.2 mmol) in anhydrous pyridine following the general method III. Yield 253 mg (55%), yellow oil, [α]$_D^{20}$ –42.5° (*c* 1.0, CHCl$_3$). ^{1}H NMR spectrum (CDCl$_3$), δ, ppm (*J*, Hz): 6.80 (1H, d, *J* = 9.0, CHNH); 5.87–5.69 (2H, m, 2CH=CH$_2$); 5.32–5.18 (2H, m, CH=CH$_2$); 5.09–4.97 (2H, m, CH=CH$_2$); 4.95 (1H, d, *J* = 7.4, NHCOO); 4.84 (1H, d, *J* = 9.0, CH–oxazole); 4.07–3.89 (3H, m, CH$_2$–CH=, CHCO); 3.11 (3H, s, CH$_3$); 2.17–2.06 (2H, m, CH$_2$); 1.99–1.85 (1H, m, CH$_2$); 1.76–1.63 (1H, m, CH$_2$); 1.44 (9H, s, C(CH$_3$)$_3$); 0.96 (9H, s, C(CH$_3$)$_3$). ^{13}C NMR spectrum (CDCl$_3$), δ, ppm: 171.6; 160.1; 155.7; 151.7; 137.1; 131.1; 118.9; 116.0; 115.9; 84.5; 80.4; 55.0; 54.2; 53.9; 36.4; 35.8; 30.7; 29.8; 28.3; 26.1. Found, *m/z*: 460.2925 [M+H]$^+$. C$_{24}$H$_{38}$N$_5$O$_4$. Calculated, *m/z*: 460.2924.

tert-Butyl *N*-{(1*S*)-1-[((1*S*)-1-{4-cyano-5-[methyl(prop-2-en-1-yl)amino]-1,3-oxazol-2-yl}-2,2-dimethylpropyl)-carbamoyl]hex-5-en-1-yl}carbamate (8aC) was obtained from crude amine **9a** (350 mg, 1.4 mmol), acid **16C** (343 mg, 1.4 mmol), and EDC·HCl (324 mg, 1.7 mmol) in anhydrous pyridine following the general method III. Yield 495 mg (74%), yellow oil, [α]$_D^{20}$ –42.3° (*c* 1.0, CHCl$_3$). ^{1}H NMR spectrum (CDCl$_3$), δ, ppm (*J*, Hz): 6.78 (1H, d, *J* = 8.8, CHNH); 5.88–5.68 (2H, m, 2CH=CH$_2$); 5.31–5.20 (2H, m, CH=CH$_2$); 5.05–4.92 (2H, m, CH=CH$_2$); 4.91–4.87 (1H, m, NHCOO); 4.84 (1H, d, *J* = 9.5, CH–oxazole); 4.07–3.88 (3H, m, CH$_2$–CH=, CHCO); 3.11 (3H, s, CH$_3$); 2.11–2.00 (2H, m, CH$_2$); 1.87–1.81 (1H, m, CH$_2$); 1.71–1.55 (1H, m, CH$_2$); 1.49–1.42 (11H, m, C(CH$_3$)$_3$, CH$_2$); 0.98 (9H, s, C(CH$_3$)$_3$). ^{13}C NMR spectrum (CDCl$_3$), δ, ppm: 171.8; 160.2; 151.9; 138.1; 131.3; 119.1; 116.1; 115.3; 84.7; 54.8; 55.1; 54.1; 36.5; 36.0; 33.4; 32.2; 31.2; 28.5; 26.4; 26.3; 25.1. Found, *m/z*: 474.3086 [M+H]$^+$. C$_{25}$H$_{40}$N$_5$O$_4$. Calculated, *m/z*: 474.3080.

2-((1*S*)-1-Amino-2,2-dimethylpropyl)-5-[benzyl(prop-2-en-1-yl)amino]-1,3-oxazole-4-carbonitrile (9b) was obtained in a two-step sequence from benzyl *N*-[(1*S*)-1-(5-bromo-4-cyano-1,3-oxazol-2-yl)-2,2-dimethylpropyl]carbamate (**10**).

Step 1. **2-((1*S*)-1-Amino-2,2-dimethylpropyl)-5-bromo-1,3-oxazole-4-carbonitrile**. 33% HBr solution in AcOH (28 ml, 163 mmol, 40 equiv) was added dropwise to a solution of bromooxazole **10** (1.6 g, 4.1 mmol, 1 equiv) in 1,4-dioxane (15 ml) at room temperature. The yellow solution was stirred for 10 min, and cooled (0°C) 2 M Na$_2$CO$_3$ aqueous solution was added till the mixture medium reached pH 7–9. The mixture was extracted with EtOAc (4×50 ml). The organic layers were combined and washed with 1 M HCl aqueous solution (2×50 ml). Aqueous layers were combined, and solid Na$_2$CO$_3$ was added till the medium reached pH 9. Aqueous layer was

extracted with EtOAc (3×50 ml). The organic layers were combined, washed with brine, dried over anhydrous Na$_2$SO$_4$, and evaporated under reduced pressure. The crude subtitle product was obtained as orange oil, yield 700 mg (67%), and used in the next reaction without additional purification.

Step 2. **2-((1*S*)-1-Amino-2,2-dimethylpropyl)-5-[benzyl-(prop-2-en-1-yl)amino]-1,3-oxazole-4-carbonitrile (9b)** was obtained from 2-[(1*S*)-1-amino-2,2-dimethylpropyl]-5-bromo-1,3-oxazole-4-carbonitrile (700 mg, 2.7 mmol), *N*-allylbenzylamine (0.8 ml, 5.4 mmol), and NEt$_3$ (1.1 ml, 8.1 mmol) in anhydrous DMF 50°C (72 h) following the general method I. Purification by column chromatography on silica gel using gradient elution from pure hexane to 30% EtOAc in hexane afforded compound **9b**. Yield 295 mg (34%), yellow oil. Compound **9b** was used in the next reaction without additional purification.

***tert*-Butyl *N*-{(1*S*)-1-[((1*S*)-1-{5-[benzyl(prop-2-en-1-yl)amino]-4-cyano-1,3-oxazol-2-yl}-2,2-dimethylpropyl)-carbamoyl]but-3-en-1-yl}carbamate (8bA)** was obtained from compound **9b** (295 mg, 0.9 mmol), acid **16A** (196 mg, 0.9 mmol), and EDC·HCl (209 mg, 1.1 mmol) in anhydrous pyridine following the general method III. Yield 310 mg (65%), yellow oil, [α]$_D^{20}$ –28.0° (*c* 1.0, CHCl$_3$). ^{1}H NMR spectrum (CDCl$_3$), δ, ppm (*J*, Hz): 7.40–7.20 (5H, m, H Ph); 6.97–6.86 (1H, m, NH); 5.88–5.66 (2H, m, 2CH=CH$_2$); 5.32–5.23 (2H, m, CH=CH$_2$); 5.21–5.09 (2H, m, CH=CH$_2$); 4.98–4.89 (1H, m, NH); 4.84 (1H, d, *J* = 9.5, CH–oxazole); 4.69–4.48 (2H, m, CH$_2$Ph); 4.17–4.06 (1H, m, CHCO); 4.05–3.87 (2H, m, CH$_2$–CH=); 2.59–2.40 (2H, m, CH$_2$–CH=); 1.44 (9H, s, C(CH$_3$)$_3$); 0.92 (9H, s, C(CH$_3$)$_3$). ^{13}C NMR spectrum (CDCl$_3$), δ, ppm: 171.1; 159.9; 155.7; 151.8; 135.5; 133.0; 131.2; 128.9; 128.1; 127.7; 119.2; 155.7; 84.8; 80.6; 55.0; 53.9; 52.4; 51.1; 35.9; 29.7; 28.3; 26.1. Found, *m/z*: 522.3083 [M+H]$^+$. C$_{29}$H$_{40}$N$_5$O$_4$. Calculated, *m/z*: 522.3080.

2-((1*S*)-1-Amino-2,2-dimethylpropyl)-5-(phenylamino)-1,3-oxazole-4-carbonitrile (19) was obtained in a two-step sequence from benzyl *N*-[(1*S*)-1-(5-bromo-4-cyano-1,3-oxazol-2-yl)-2,2-dimethylpropyl]carbamate (10).

Step 1. **Benzyl *N*-{(1*S*)-1-[4-cyano-5-(phenylamino)-1,3-oxazol-2-yl]-2,2-dimethylpropyl}carbamate**. Aniline (0.4 ml, 4.2 mmol, 2 equiv) was added dropwise to a solution of bromooxazole **10** (815 mg, 2.1 mmol, 1 equiv) in anhydrous THF (20 ml) at room temperature. Then the orange solution was cooled to –78°C (dry ice/Me$_2$CO) and KHMDS (1 M solution in THF (7.3 ml, 7.3 mmol, 3.5 equiv)) was added dropwise. The resulting dark solution was stirred for 30 min at –78°C and quenched by the addition of aqueous saturated NH$_4$Cl solution. The organic layer was diluted with EtOAc (50 ml), washed with aqueous 1 M HCl (2×40 ml), brine, and dried over anhydrous Na$_2$SO$_4$. Filtration and evaporation under reduced pressure afforded the subtitle compound as a yellow amorphous solid, yield 760 mg (90%), [α]$_D^{20}$ –7.6° (*c* 1.0, CHCl$_3$). ^{1}H NMR spectrum (CDCl$_3$), δ, ppm (*J*, Hz): 7.50 (1H, br. s, NHPh); 7.40–7.27 (7H, m, H Ph); 7.22–7.08 (3H, m, H Ph); 5.45 (1H, d, *J* = 9.8, CH(NH)); 5.14–5.09 (2H, m, CH$_2$); 4.69 (1H, d, *J* = 9.8, NH(CH)); 1.02 (9H, s, C(CH$_3$)$_3$). ^{13}C NMR spectrum (CDCl$_3$), δ, ppm: 156.9; 156.1; 154.0; 137.6; 136.0; 129.6; 128.6; 128.3; 128.2; 124.1; 118.3; 113.9; 89.2; 67.4; 57.8; 35.7; 26.2. Found, *m/z*: 405.1928 [M+H]$^+$. C$_{23}$H$_{25}$N$_4$O$_3$. Calculated, *m/z*: 405.1927.

Step 2. **2-((1*S*)-1-Amino-2,2-dimethylpropyl)-5-(phenyl-amino)-1,3-oxazole-4-carbonitrile (19)** was obtained from benzyl *N*-{(1*S*)-1-[4-cyano-5-(phenylamino)-1,3-oxazol-2-yl]-2,2-dimethylpropyl}carbamate (step 1) (1.05 g, 2.6 mmol), 33% HBr solution in AcOH (27 ml, 156 mmol), and morpholine (2.3 ml, 26.0 mmol) in 1,4-dioxane following the general method II. The crude amine **19** was used in the next step without additional purification. Yield 390 mg (56%), yellow oil.
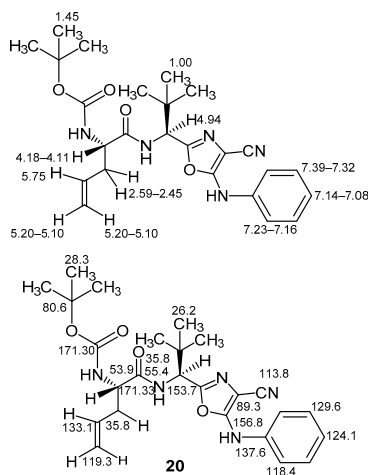
***tert*-Butyl [(1*S*)-1-({(1*S*)-1-[4-cyano-5-(phenylamino)-1,3-oxazol-2-yl]-2,2-dimethylpropyl}carbamoyl)but-3-en-1-yl]carbamate (20)** was obtained from aminooxazole **19** (390 mg, 1.4 mmol), EDC·HCl (553 mg, 2.9 mmol), and acid **16A** (466 mg, 2.2 mmol) in anhydrous pyridine following the general method III. Yield 585 mg (87%), colorless oil, [α]$_D^{20}$ –28.0° (*c* 1.0, CHCl$_3$). ^{1}H NMR spectrum (CDCl$_3$), δ, ppm (*J*, Hz): 7.39–7.32 (2H, m, H Ph); 7.23–7.16 (2H, m, H Ph); 7.14–7.08 (1H, m, H Ph); 5.75 (1H, ddd, *J* = 17.3, *J* = 10.0, *J* = 7.2, CH=CH$_2$); 5.20–5.10 (2H, m, CH=CH$_2$); 4.94 (1H, d, *J* = 9.3, CH–*t*-Bu); 4.18–4.11 (1H, m, CHNHCOO); 2.59–2.45 (2H, m, CH$_2$–CH=); 1.45 (9H, s, C(CH$_3$)$_3$); 1.00 (9H, s, C(CH$_3$)$_3$). ^{13}C NMR spectrum (CDCl$_3$), δ, ppm: 171.3; 170.3; 156.8; 153.7; 137.6; 133.1; 129.6; 124.1; 119.3; 118.4; 113.8; 89.3; 80.6; 55.4; 53.9; 35.8; 28.3; 26.2. Found, *m/z*: 490.2426 [M+Na]$^+$. C$_{25}$H$_{33}$NaN$_5$O$_4$. Calculated, *m/z*: 490.2430.

***tert*-Butyl *N*-{(1*S*)-1-[((1*S*)-1-{4-cyano-5-[phenyl(prop-2-en-1-yl)amino]-1,3-oxazol-2-yl}-2,2-dimethylpropyl)-carbamoyl]but-3-en-1-yl}carbamate (8cA)**. 60% NaH in mineral oil (116 mg, 2.9 mmol) was added to a solution of phenylaminooxazole **20** (450 mg, 1.0 mmol) in anhydrous DMF (10 ml) at 0°C. After the hydrogen evolution was ceased, the resulting yellow suspension was stirred for 15 min, whereupon allyl bromide (0.08 ml, 1.0 mmol) was added dropwise. The resulting solution was stirred for 1 h at 0°C, quenched by the addition of H$_2$O, and extracted with EtOAc (3×50 ml). The combined organic extracts were washed with brine, dried over anhydrous Na$_2$SO$_4$, and

concentrated under reduced pressure. The residue was purified by column chromatography on silica gel using gradient elution from pure hexane to 30% EtOAc in hexane to afford the title compound **8cA**. Yield 185 mg (38%), yellow oil, $[\alpha]_D^{20}$ –36.0° (*c* 1.0, CHCl$_3$). ^{1}H NMR spectrum (CDCl$_3$), δ, ppm (*J*, Hz): 7.45–7.27 (3H, m, H Ph); 7.25–7.08 (2H, m, H Ph); 6.96–6.90 (1H, m, NH); 5.98–5.88 (1H, m, C$\underline{H}$=CH$_2$); 5.79–5.71 (1H, m, C$\underline{H}$=CH$_2$); 5.30–5.23 (2H, m, CH=C$\underline{H}_2$); 5.19–5.11 (2H, m, CH=C$\underline{H}_2$); 5.01–4.92 (1H, m, C$\underline{H}$NHCOO); 4.86 (1H, d, *J* = 9.4, C$\underline{H}$–oxazole); 4.40 (2H, ddt, *J* = 16.5, *J* = 6.8, *J* = 1.4, C$\underline{H}_2$–CH=); 4.18–4.08 (1H, m, NH); 2.58–2.44 (2H, m, C$\underline{H}_2$–CH=); 1.45 (9H, s, C(CH$_3$)$_3$); 0.95 (9H, s, C(CH$_3$)$_3$). ^{13}C NMR spectrum (CDCl$_3$), δ, ppm: 171.3; 158.7; 155.8; 153.1; 141.6; 133.2; 132.1; 129.8; 127.5; 125.2; 119.4; 118.8; 114.0; 88.7; 80.7; 55.2 (2C); 54.0; 36.0; 35.9; 28.4; 26.3. Found, *m/z*: 508.2921 [M+H]$^+$. C$_{28}$H$_{38}$N$_5$O$_4$. Calculated, *m/z*: 508.2924.

***tert*-Butyl *N*-((4*Z*,7*S*,10*S*)-10-*tert*-butyl-13-cyano-2-methyl-8-oxo-14-oxa-2,9,12-triazabicyclo[9.2.1]tetradeca-1(13),4,11-trien-7-yl)carbamate (21)**, obtained as a mixture of *E*/*Z*-isomers in 59:41 ratio. Compound **21** was synthesized from amide **8aA** (350 mg, 0.8 mmol) and ruthenium metathesis catalyst **Ru4** (29 mg, 0.04 mmol) in anhydrous CH$_2$Cl$_2$ following the general method IV. Purification of the crude product by column chromatography on silica gel using gradient elution from pure CH$_2$Cl$_2$ to 5% MeOH in CH$_2$Cl$_2$ afforded product **21**. Yield 220 mg (65%), yellow amorphous solid. Individual isomers were obtained after separation by silica gel column chromatography using CH$_2$Cl$_2$–EtOAc, 9:1 as eluent.

Compound (*Z*)-21. Yield 121 mg (37%), white amorphous solid, $[\alpha]_D^{20}$ –294.8° (*c* 1.0, MeOH). ^{1}H NMR spectrum (CDCl$_3$), δ, ppm (*J*, Hz): 6.36 (1H, d, *J* = 6.9, N$\underline{H}$–CO); 5.64–5.53 (2H, m, NH, CH=); 5.43–5.33 (1H, m, CH=); 4.44 (1H, d, *J* = 6.9, C$\underline{H}$–C(CH$_3$)$_3$); 4.41–4.30 (1H, m, NH–C$\underline{H}$–CH$_2$); 4.15–4.05 (1H, m, CH$_2$); 3.67–3.59 (1H, m, CH$_2$); 3.23 (3H, s, CH$_3$); 2.55–2.47 (1H, m, CH$_2$); 2.39–2.28 (1H, m, CH$_2$); 1.39 (9H, s, C(CH$_3$)$_3$); 1.03 (9H, s, C(CH$_3$)$_3$). ^{13}C NMR spectrum (CDCl$_3$), δ, ppm: 172.2; 160.5; 155.2; 150.9; 130.4; 128.0; 115.9; 86.2; 80.0; 57.7; 57.0; 53.8; 39.3; 36.4; 33.5; 28.3; 26.5. Found, *m/z*: 418.2494 [M+H]$^+$. C$_{21}$H$_{32}$N$_5$O$_4$. Calculated, *m/z*: 418.2454.

Compound (*E*)-21. Yield 84 mg (26%), beige amorphous solid, $[\alpha]_D^{20}$ –226.7° (*c* 0.6, MeOH). ^{1}H NMR spectrum (CDCl$_3$), δ, ppm (*J*, Hz): 5.96 (1H, d, *J* = 6.2, NHCO); 5.74 (1H, t, *J* = 11.1, CH=); 5.65 (1H, d, *J* = 6.2, C$\underline{H}$–CH=); 5.59–5.52 (1H, m, CH=); 5.28 (1H, s, NH); 4.54–4.43 (3H, m, CH$_2$, NH–C$\underline{H}$–CH$_2$); 3.23 (3H, s, CH$_3$); 2.84 (1H, t, *J* = 13.1, CH$_2$); 2.60–2.52 (1H, m, CH$_2$); 1.41 (9H, s, C(CH$_3$)$_3$); 1.05 (9H, s, C(CH$_3$)$_3$). ^{13}C NMR spectrum (CDCl$_3$), δ, ppm: 171.6; 160.1; 155.0; 151.1; 128.2; 123.8; 115.8; 86.1; 80.0; 57.8; 52.6; 49.8; 37.8; 33.7; 31.1; 28.3; 26.5. Found, *m/z*: 418.2489 [M+H]$^+$. C$_{21}$H$_{32}$N$_5$O$_4$. Calculated, *m/z*: 418.2441.

***tert*-Butyl *N*-((7*S*,10*S*)-10-*tert*-butyl-13-cyano-2-methyl-8-oxo-14-oxa-2,9,12-triazabicyclo[9.2.1]tetradeca-1(13),11-dien-7-yl)carbamate (7aA)** was obtained by the hydrogenation of alkene (*Z*)-**21** (88 mg, 0.2 mmol) in the presence of 10% Pd on carbon (23 mg, 0.02 mmol) following the general method V. Yield 85 mg (96%), yellow oil, $[\alpha]_D^{20}$ –63.0° (*c* 1.0, CHCl$_3$). ^{1}H NMR spectrum

(CDCl$_3$), δ, ppm (*J*, Hz): 5.88 (1H, d, *J* = 7.6, NHCO); 5.51 (1H, d, *J* = 7.6, C$\underline{H}$C(CH$_3$)$_3$); 4.59–4.48 (2H, m, C$\underline{H}$CH$_2$, NHCOO); 3.84 (1H, t, *J* = 14.5, CH$_2$); 3.17 (3H, s, CH$_3$); 3.00 (1H, dt, *J* = 14.5, *J* = 3.1, CH$_2$); 2.02–1.76 (3H, m, CH$_2$); 1.61–1.49 (1H, m, CH$_2$); 1.48–1.36 (10H, m, CH$_2$, C(CH$_3$)$_3$); 1.33–1.21 (1H, m, CH$_2$); 1.06 (9H, s, C(CH$_3$)$_3$). ^{13}C NMR spectrum (CDCl$_3$), δ, ppm: 172.9; 160.1; 155.3; 150.1; 116.4; 83.5; 79.9; 58.9; 53.4; 49.1; 36.4; 33.6; 31.0; 28.5; 26.7; 25.4. Found, *m/z*: 442.2415 [M+Na]$^+$. C$_{21}$H$_{33}$NaN$_5$O$_4$. Calculated, *m/z*: 442.2430.

***tert*-Butyl *N*-((8*S*,11*S*)-11-*tert*-butyl-14-cyano-2-methyl-9-oxo-15-oxa-2,10,13-triazabicyclo[10.2.1]pentadeca-1(14),12-dien-8-yl)carbamate (7aB)** was obtained in a two-step sequence from amide **8aB** (200 mg, 0.4 mmol) and ruthenium metathesis catalyst **Ru4** (16 mg, 0.02 mmol) in anhydrous CH$_2$Cl$_2$ following the general method IV. The crude mixture of *E*/*Z*-isomers in 2:1 ratio of the resulting macrocycle was hydrogenated in the presence of 10% Pd on carbon (46 mg, 0.04 mmol) following the general method V. Yield in two steps 90 mg (48%), white amorphous solid, $[\alpha]_D^{20}$ –59.7° (*c* 1.0, CHCl$_3$). ^{1}H NMR spectrum (CDCl$_3$), δ, ppm (*J*, Hz): 6.17 (1H, d, *J* = 9.3, NHCO); 5.50 (1H, d, *J* = 7.5, NHCOO); 4.88 (1H, d, *J* = 9.3, C$\underline{H}$C(CH$_3$)$_3$); 4.36–4.27 (1H, m, C$\underline{H}$CH$_2$); 3.63–3.56 (1H, m, CH$_2$); 3.19–3.07 (4H, m, CH$_3$, CH$_2$); 1.94–1.83 (1H, m, CH$_2$); 1.64–1.48 (2H, m, CH$_2$); 1.44–1.30 (13H, m, CH$_2$, C(CH$_3$)$_3$); 1.15–1.03 (10H, m, CH$_2$, C(CH$_3$)$_3$). ^{13}C NMR spectrum (CDCl$_3$), δ, ppm: 171.7; 160.2; 155.3; 149.7; 116.7; 83.3; 79.9; 55.7; 53.9; 49.5; 36.1; 33.8; 32.9; 28.5; 26.5; 25.8; 24.6; 20.8. Found, *m/z*: 456.2574 [M+Na]$^+$. C$_{22}$H$_{35}$NaN$_5$O$_4$. Calculated, *m/z*: 456.2587.

***tert*-Butyl *N*-((9*S*,12*S*)-12-*tert*-butyl-15-cyano-2-methyl-10-oxo-16-oxa-2,11,14-triazabicyclo[11.2.1]hexadeca-1(15),13-dien-9-yl)carbamate (7aC)** was obtained in a two-step sequence from amide **8aC** (350 mg, 0.7 mmol) and ruthenium metathesis catalyst **Ru4** (27 mg, 0.04 mmol) in anhydrous CH$_2$Cl$_2$ following the general method IV. The crude mixture of *E*/*Z*-isomers in 2:1 ratio of the resulting macrocycle was hydrogenated in the presence of 10% Pd on carbon (88 mg, 0.08 mmol) following the general method V. Yield in two steps 161 mg (44%), white amorphous solid, $[\alpha]_D^{20}$ –144.6° (*c* 1.0, MeOH). ^{1}H NMR spectrum (CDCl$_3$), δ, ppm (*J*, Hz): 6.54 (1H, br. s, NHCO); 5.25 (1H, br. s, NHCOO); 4.82 (1H, d, *J* = 9.2, C$\underline{H}$C(CH$_3$)$_3$); 4.19–4.10 (1H, m, C$\underline{H}$CH$_2$); 3.68–3.58 (1H, m, CH$_2$); 3.19–3.11 (4H, m, CH$_3$, CH$_2$); 1.90–1.76 (2H, m, CH$_2$); 1.70–1.58 (2H, m, CH$_2$); 1.48–1.38 (11H, m, CH$_2$, C(CH$_3$)$_3$); 1.38–1.28 (2H, m, CH$_2$); 1.23–1.15 (2H, m, CH$_2$); 1.03 (9H, s, C(CH$_3$)$_3$). ^{13}C NMR spectrum (CDCl$_3$), δ, ppm: 171.4; 160.2; 155.6; 149.8; 116.4; 84.0; 80.1; 55.7; 54.0; 49.5; 35.8; 34.8; 31.3; 28.3; 26.3; 26.0; 25.2; 24.8; 24.4. Found, *m/z*: 448.2924 [M+H]$^+$. C$_{23}$H$_{38}$N$_5$O$_4$. Calculated, *m/z*: 448.2924.

***tert*-Butyl *N*-((7*S*,10*S*)-2-benzyl-10-*tert*-butyl-13-cyano-8-oxo-14-oxa-2,9,12-triazabicyclo[9.2.1]tetradeca-1(13),11-dien-7-yl)carbamate (7bA)** was obtained in a two-step sequence from amide **8bA** (280 mg, 0.54 mmol) and ruthenium metathesis catalyst **Ru4** (20 mg, 0.03 mmol) in anhydrous CH$_2$Cl$_2$ following the general method IV. The crude mixture of *E*/*Z*-isomers in 2:1 ratio of the resulting macrocycle was hydrogenated in the presence of 10% Pd

on carbon (57 mg, 0.05 mmol) following the general method V. Yield in two steps 90 mg (34%), white amorphous solid, $[\alpha]_D^{20}$ –30.3° (*c* 1.0, CHCl$_3$). ^{1}H NMR spectrum (CDCl$_3$), δ, ppm (*J*, Hz): 7.40–7.26 (5H, m, H Ph); 5.87 (1H, d, *J* = 7.5, NHCO); 5.51 (1H, d, *J* = 7.5, CHC(CH$_3$)$_3$); 4.81 (1H, d, *J* = 15.6, NHCOO); 4.60–4.43 (3H, m, CH$_2$Ph, CHCH$_2$); 3.73 (1H, t, *J* = 15.6, CH$_2$); 3.05 (1H, dt, *J* = 15.6, *J* = 3.3, CH$_2$); 2.05–1.96 (1H, m, CH$_2$); 1.88–1.70 (2H, m, CH$_2$); 1.58–1.37 (11H, m, CH$_2$, C(CH$_3$)$_3$); 1.24–1.12 (1H, m, CH$_2$); 1.08 (9H, s, C(CH$_3$)$_3$). ^{13}C NMR spectrum (CDCl$_3$), δ, ppm: 172.9; 160.1; 155.3; 150.0; 135.6; 129.1; 128.4; 127.9; 116.0; 83.7; 79.9; 58.8; 53.4; 52.3; 46.1; 33.7; 31.1; 28.5; 26.7; 25.8; 18.2. Found, *m/z*: 496.2921 [M+H]$^+$. C$_{27}$H$_{38}$N$_5$O$_4$. Calculated, *m/z*: 496.2924.

tert-Butyl ***N*-((7*S*,10*S*)-10-*tert*-butyl-13-cyano-8-oxo-2-phenyl-14-oxa-2,9,12-triazabicyclo[9.2.1]tetradeca-1(13),11-dien-7-yl)carbamate (7cA)** was obtained in a two-step sequence from amide **8cA** (185 mg, 0.4 mmol) and ruthenium metathesis catalyst **Ru4** (14 mg, 0.02 mmol) in anhydrous CH$_2$Cl$_2$ following the general method IV. The crude mixture of *E/Z*-isomers in 2:1 ratio of the resulting macrocycle was hydrogenated in the presence of 10% Pd on carbon (39 mg, 0.04 mmol) following the general method V. Yield in two steps 82 mg (47%), white amorphous solid, $[\alpha]_D^{20}$ –126.9° (*c* 0.6, CHCl$_3$). ^{1}H NMR spectrum (CDCl$_3$), δ, ppm (*J*, Hz): 7.49–7.27 (5H, m, H Ph); 5.91 (1H, d, *J* = 7.5, NHCO); 5.56 (1H, d, *J* = 7.5, CHC(CH$_3$)$_3$); 4.62–4.57 (2H, m, CHCH$_2$, NHCOO); 4.12 (1H, t, *J* = 14.4, CH$_2$); 3.51 (1H, dt, *J* = 14.4, *J* = 3.2, CH$_2$); 2.13–2.01 (1H, m, CH$_2$); 1.98–1.85 (2H, m, CH$_2$); 1.68–1.56 (1H, m, CH$_2$); 1.43 (9H, s, C(CH$_3$)$_3$); 1.32–1.23 (1H, m, CH$_2$); 1.19–1.06 (10H, m, CH$_2$, C(CH$_3$)$_3$). ^{13}C NMR spectrum (CDCl$_3$), δ, ppm: 172.9; 159.3; 155.2; 150.4; 139.9; 130.1; 128.7; 127.5; 113.6; 85.8; 79.8; 58.8; 53.3; 50.1; 33.6; 31.1; 28.4; 26.6; 26.2; 17.9. Found, *m/z*: 482.2759 [M+H]$^+$. C$_{26}$H$_{36}$N$_5$O$_4$. Calculated, *m/z*: 482.2767.

(2*S*)-*N*-((4*Z*,7*S*,10*S*)-10-*tert*-Butyl-13-cyano-2-methyl-8-oxo-14-oxa-2,9,12-triazabicyclo[9.2.1]tetradeca-1(13),4,11-trien-7-yl)-2-hydroxy-3-methylbutanamide ((*Z*)-3) was obtained from compound (*Z*)-**21** (110 mg, 0.3 mmol), CF$_3$CO$_2$H (1.0 ml, 13.2 mmol), (*S*)-2-hydroxy-3-methyl-butanoic acid (47 mg, 0.4 mmol), EDC·HCl (152 mg, 0.8 mmol), HOBt (107 mg, 0.8 mmol), and DIPEA (0.28 ml, 1.6 mmol) following the general method VI. Yield 60 mg (54%), white amorphous solid, $[\alpha]_D^{20}$ –264.1° (*c* 0.7, CD$_3$OD). ^{1}H NMR spectrum (CD$_3$OD), δ, ppm (*J*, Hz): 5.84–5.75 (1H, m, CH=); 5.42 (1H, dddd, *J* = 11.4, *J* = 10.2, *J* = 2.8, *J* = 2.8, CH=); 4.80 (1H, dd, *J* = 11.4, *J* = 5.4, CHCH$_2$); 4.36 (1H, s, CHC(CH$_3$)$_3$); 4.14–4.05 (1H,

(Z)-**3**
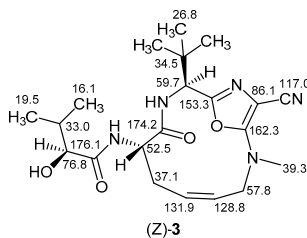
m, CH$_2$); 3.84 (1H, d, *J* = 3.5, CHOH); 3.73 (1H, dq, *J* = 14.7, *J* = 2.8, CH$_2$); 3.25 (3H, s, NCH$_3$); 2.54 (1H, dddd, *J* = 13.1, *J* = 5.4, *J* = 5.4, *J* = 2.8, CH$_2$); 2.28 (1H, ddd, *J* = 13.1, *J* = 11.4, *J* = 11.4, CH$_2$); 2.07 (1H, sept d, *J* = 6.9, *J* = 3.4, CH(CH$_3$)$_2$); 1.08 (9H, s, C(CH$_3$)$_3$); 0.99 (3H, d, *J* = 6.9, CH$_3$CH); 0.83 (3H, d, *J* = 6.9, CH$_3$CH). ^{13}C NMR spectrum (CD$_3$OD), δ, ppm: 176.1; 174.2; 162.3; 153.3; 131.9; 128.8; 117.0; 86.1; 76.8; 59.7; 57.8; 52.5; 39.3; 37.1; 34.5; 33.0; 26.8; 19.5; 16.1. Found, *m/z*: 418.2455 [M+H]$^+$. C$_{21}$H$_{32}$N$_5$O$_4$. Calculated, *m/z*: 418.2454.

(2*S*)-*N*-((4*E*,7*S*,10*S*)-10-*tert*-Butyl-13-cyano-2-methyl-8-oxo-14-oxa-2,9,12-triazabicyclo[9.2.1]tetradeca-1(13),4,11-trien-7-yl)-2-hydroxy-3-methylbutanamide ((*E*)-3) was obtained from compound (*E*)-**21** (83 mg, 0.2 mmol), CF$_3$CO$_2$H (0.76 ml, 9.9 mmol), (*S*)-2-hydroxy-3-methylbutanoic acid (35 mg, 0.3 mmol), EDC·HCl (114 mg, 0.6 mmol), HOBt (81 mg, 0.6 mmol), and DIPEA (0.21 ml, 1.2 mmol) following the General method VI. Yield 48 mg (58%), beige amorphous solid, $[\alpha]_D^{20}$ –190.7° (*c* 1.0, MeOH). ^{1}H NMR spectrum (CD$_3$OD), δ, ppm (*J*, Hz): 5.71–5.57 (2H, m, 2CH=); 4.92 (1H, dd, *J* = 5.3, *J* = 2.4, CHCH$_2$); 4.59–4.49 (1H, m, CH$_2$); 3.89 (1H, d, *J* = 3.3, CHOH); 3.38 (1H, s, CHC(CH$_3$)$_3$); 3.35 (1H, s, CH$_2$); 3.25 (3H, s, NCH$_3$); 3.14–3.04 (1H, m, CH$_2$); 2.58–2.47 (1H, m, CH$_2$); 2.18–2.07 (1H, m, CH(CH$_3$)$_2$); 1.09 (9H, s, C(CH$_3$)$_3$); 1.01 (3H, d, *J* = 6.9, CH$_3$CH); 0.85 (3H, d, *J* = 6.9, CH$_3$CH). ^{13}C NMR spectrum (CD$_3$OD), δ, ppm: 174.6; 172.8; 160.8; 151.8; 130.5; 127.4; 115.5; 84.7; 75.3; 58.3; 56.3; 51.0; 37.9; 35.7; 33.1; 31.5; 25.3; 18.1; 14.7. Found, *m/z*: 418.2477 [M+H]$^+$. C$_{21}$H$_{32}$N$_5$O$_4$. Calculated, *m/z*: 418.2454.
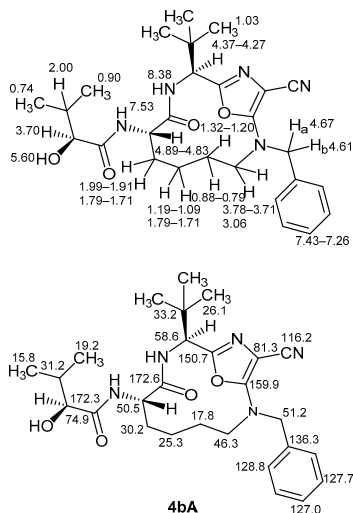
(2*S*)-*N*-((7*S*,10*S*)-10-*tert*-Butyl-13-cyano-2-methyl-8-oxo-14-oxa-2,9,12-triazabicyclo[9.2.1]tetradeca-1(13),11-dien-7-yl)-2-hydroxy-3-methylbutanamide (4aA) was obtained from compound **7aA** (80 mg, 0.2 mmol), CF$_3$CO$_2$H (0.73 ml, 9.5 mmol), (*S*)-2-hydroxy-3-methylbutanoic acid (34 mg, 0.3 mmol), EDC·HCl (108 mg, 0.6 mmol), HOBt (76 mg, 0.6 mmol), and DIPEA (0.2 ml, 1.1 mmol) following the General method VI. Yield 39 mg (50%), white amorphous solid, $[\alpha]_D^{20}$ –109.5° (*c* 1.0, MeOH). ^{1}H NMR spectrum (CD$_3$OD), δ, ppm (*J*, Hz): 4.41 (1H, s, CHC(CH$_3$)$_3$); 3.95–3.86 (1H, m, CHCH$_2$); 3.86 (1H, d, *J* = 3.2, CHOH); 3.18 (3H, s, NCH$_3$); 3.09 (1H, dt, *J* = 14.7, *J* = 3.2, CH$_2$); 2.16–2.02 (2H, m, CH$_2$, CH(CH$_3$)$_2$); 2.00–1.86 (2H, m, CH$_2$); 1.50–1.37 (1H, m, CH$_2$); 1.32–1.21 (1H, m, CH$_2$); 1.09 (9H, s, C(CH$_3$)$_3$); 1.05–1.01 (1H, m, CH$_2$); 1.00 (3H, d, *J* = 6.9, CH$_3$CH); 0.93–0.85 (1H, m, CH$_2$); 0.83 (3H, d, *J* = 6.9, CH$_3$CH). ^{13}C NMR spectrum (CD$_3$OD), δ, ppm: 175.8; 174.7; 161.6; 152.5; 117.4; 83.0; 76.8; 60.7; 52.6; 49.8; 36.4; 34.4; 32.9; 31.4; 26.7; 26.3; 19.6; 19.1. Found, *m/z*: 420.2599 [M+H]$^+$. C$_{21}$H$_{34}$N$_5$O$_4$. Calculated, *m/z*: 420.2611.
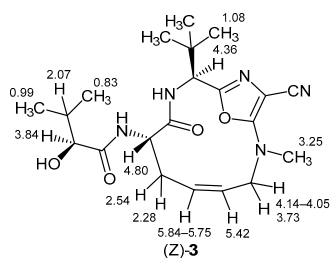
(2*S*)-*N*-((8*S*,11*S*)-11-*tert*-Butyl-14-cyano-2-methyl-9-oxo-15-oxa-2,10,13-triazabicyclo[10.2.1]pentadeca-1(14),12-dien-8-yl)-2-hydroxy-3-methylbutanamide (4aB) was obtained from compound **7aB** (90 mg, 0.2 mmol), CF$_3$CO$_2$H (1.0 ml, 12.5 mmol), (*S*)-2-hydroxy-3-methylbutanoic acid (37 mg, 0.3 mmol), EDC·HCl (119 mg, 0.6 mmol), HOBt (84 mg, 0.6 mmol), and DIPEA (0.2 ml, 1.2 mmol) following the general method VI. Yield 41 mg (46%), white amorphous solid, [α]$_D^{20}$ –88.9° (*c* 1.1, MeOH). ^{1}H NMR spectrum (CD$_3$OD), δ, ppm (*J*, Hz): 4.79 (1H, s, CHC(CH$_3$)$_3$); 4.59 (1H, t, *J* = 5.3, CHCH$_2$); 3.88 (1H, d, *J* = 3.3, CHOH); 3.58–3.48 (1H, m, CH$_2$); 3.41–3.34 (1H, m, CH$_2$); 3.19 (3H, s, NCH$_3$); 2.15–2.02 (1H, m, CH(CH$_3$)$_2$); 1.79–1.71 (2H, m, CH$_2$); 1.70–1.56 (2H, m, CH$_2$); 1.49–1.37 (2H, m, CH$_2$); 1.36–1.18 (2H, m, CH$_2$); 1.15 (9H, s, C(CH$_3$)$_3$); 1.02 (3H, d, *J* = 6.9, CH$_3$CH); 0.86 (3H, d, *J* = 6.9, CH$_3$CH). ^{13}C NMR spectrum (CD$_3$OD), δ, ppm: 175.9; 173.7; 161.7; 151.5; 117.6; 83.4; 76.8; 57.6; 53.3; 50.3; 36.2; 34.6; 33.4; 33.0; 26.8; 26.7; 25.8; 21.9; 19.6; 16.1. Found, *m/z*: 434.2772 [M+H]$^+$. C$_{22}$H$_{36}$N$_5$O$_4$. Calculated, *m/z*: 434.2767.

(2*S*)-*N*-((9*S*,12*S*)-12-*tert*-Butyl-15-cyano-2-methyl-10-oxo-16-oxa-2,11,14-triazabicyclo[11.2.1]hexadeca-1(15),13-dien-9-yl)-2-hydroxy-3-methylbutanamide (4aC) was obtained from compound **7aC** (113 mg, 0.3 mmol), CF$_3$CO$_2$H (1.2 ml, 15.1 mmol), (*S*)-2-hydroxy-3-methyl-butanoic acid (45 mg, 0.4 mmol), EDC·HCl (146 mg, 0.8 mmol), HOBt (103 mg, 0.8 mmol), and DIPEA (0.3 ml, 1.5 mmol) following the general method VI. Yield 56 mg (49%), white amorphous solid, [α]$_D^{20}$ –183.4° (*c* 1.0, CHCl$_3$). ^{1}H NMR spectrum (CD$_3$OD), δ, ppm (*J*, Hz): 4.84 (1H, s, CHC(CH$_3$)$_3$); 4.57 (1H, dd, *J* = 10.4, *J* = 4.8, CHCH$_2$); 3.86 (1H, d, *J* = 3.7, CHOH); 3.83–3.74 (1H, m, CH$_2$); 3.34–3.25 (1H, m, CH$_2$); 3.18 (3H, s, NCH$_3$); 2.13–2.05 (1H, m, CH(CH$_3$)$_2$); 1.87–1.69 (3H, m, CH$_2$); 1.69–1.61 (2H, m, CH$_2$); 1.45–1.36 (2H, m, CH$_2$); 1.34–1.23 (1H, m, CH$_2$); 1.19–1.10 (2H, m, CH$_2$); 1.08 (9H, s, C(CH$_3$)$_3$); 1.01 (3H, d, *J* = 6.9, CH$_3$CH); 0.86 (3H, d, *J* = 6.9, CH$_3$CH). ^{13}C NMR spectrum (CD$_3$OD), δ, ppm: 175.9; 173.6; 162.0; 151.6; 117.4; 84.2; 76.8; 57.1; 53.4; 50.5; 36.1; 36.0; 33.3; 33.0; 27.3; 26.8; 26.2; 25.7; 25.4; 19.6; 16.2. Found, *m/z*: 448.2937 [M+H]$^+$. C$_{23}$H$_{38}$N$_5$O$_4$. Calculated, *m/z*: 448.2924.

(2*S*)-*N*-((7*S*,10*S*)-2-Benzyl-10-*tert*-butyl-13-cyano-8-oxo-14-oxa-2,9,12-triazabicyclo[9.2.1]tetradeca-1(13),11-dien-7-yl)-2-hydroxy-3-methylbutanamide (4bA) was obtained from compound **7bA** (80 mg, 0.2 mmol), CF$_3$CO$_2$H (0.7 ml, 9.7 mmol), (*S*)-2-hydroxy-3-methylbutanoic acid (29 mg, 0.2 mmol), EDC·HCl (93 mg, 0.5 mmol), HOBt (66 mg, 0.5 mmol), and DIPEA (0.2 ml, 1.0 mmol) following the general method VI. Yield 25 mg (31%), white amorphous solid, [α]$_D^{20}$ –52.0° (*c* 1.0, DMSO-*d*$_6$). ^{1}H NMR spectrum (DMSO-*d*$_6$), δ, ppm (*J*, Hz): 8.38 (1H, d, *J* = 6.7, NHCO); 7.53 (1H, d, *J* = 7.6, NHCOO); 7.43–7.26 (5H, m, H Ph); 5.60 (1H, d, *J* = 5.7, OH); 4.89–4.83 (1H, m, CHCH$_2$); 4.67 (1H, d, *J* = 17.4, CH$_2$Ph); 4.61 (1H, d, *J* = 16.8, CH$_2$Ph); 4.37–4.27 (1H, m, CHC(CH$_3$)$_3$); 3.78–3.71 (1H, m, CH$_2$N); 3.70 (1H, dd, *J* = 5.6, *J* = 3.2, CHOH); 3.06 (1H, d, *J* = 15.0, CH$_2$); 2.00 (1H, sept d, *J* = 6.8, *J* = 3.2, CH(CH$_3$)$_2$); 1.99–1.91 (1H, m, CH$_2$); 1.79–1.71 (2H, m, CH$_2$); 1.32–1.20 (1H, m, CH$_2$); 1.19–1.09 (1H, m, CH$_2$); 1.03 (9H, s,

C(CH$_3$)$_3$); 0.90 (3H, d, *J* = 6.9, CH$_3$CH); 0.88–0.79 (1H, m, CH$_2$); 0.74 (3H, d, *J* = 6.9, CH$_3$CH). ^{13}C NMR spectrum (DMSO-*d*$_6$), δ, ppm: 172.6; 172.3; 159.9; 150.7; 136.3; 128.8; 127.7; 127.0; 116.2; 81.3; 74.9; 58.6; 51.2; 50.5; 46.3; 33.2; 31.2; 30.2; 26.1; 25.3; 19.2; 17.8; 15.8. Found, *m/z*: 496.2921 [M+H]$^+$. C$_{27}$H$_{38}$N$_5$O$_4$. Calculated, *m/z*: 496.2924.

(2*S*)-*N*-((7*S*,10*S*)-10-*tert*-Butyl-13-cyano-8-oxo-2-phenyl-14-oxa-2,9,12-triazabicyclo[9.2.1]tetradeca-1(13),11-dien-7-yl)-2-hydroxy-3-methylbutanamide (4cA) was obtained from compound **7cA** (80 mg, 0.2 mmol), CF$_3$CO$_2$H (0.6 ml, 8.3 mmol), (*S*)-(+)-2-hydroxy-3-methylbutanoic acid (30 mg, 0.3 mmol), EDC·HCl (96 mg, 0.5 mmol), HOBt (68 mg, 0.5 mmol), and DIPEA (0.2 ml, 1.0 mmol) following the general method VI. Yield 40 mg (50%), white amorphous solid, [α]$_D^{20}$ –111.0° (*c* 1.0, MeOH). ^{1}H NMR spectrum (CD$_3$OD), δ, ppm (*J*, Hz): 7.55–7.46 (2H, m, H Ph); 7.44–7.37 (3H, m, H Ph); 4.97–4.90 (1H, m, CHC(CH$_3$)$_3$); 4.50 (1H, d, *J* = 6.7, CH$_2$); 4.28–4.18 (1H, m, CHCH$_2$); 3.90 (1H, d, *J* = 3.3, CHOH); 3.57 (1H, d, *J* = 15.0, CH$_2$); 2.24–2.08 (2H, m, CH$_2$); 2.08–1.96 (1H, m, CH$_2$); 1.96–1.85 (1H, m, CH$_2$); 1.58–1.46 (1H, m, CH(CH$_3$)$_2$); 1.36–1.24 (1H, m, CH$_2$); 1.24–1.17 (1H, m, CH$_2$); 1.14 (9H, s, C(CH$_3$)$_3$); 1.03 (3H, d, *J* = 7.0, CH$_3$CH); 0.87 (3H, d, *J* = 7.0, CH$_3$CH). ^{13}C NMR spectrum (CD$_3$OD), δ, ppm: 175.9; 175.0; 161.1; 153.0; 141.6; 131.1; 129.7; 128.8; 114.8; 85.5; 76.8; 60.9; 52.7; 51.2; 34.6; 32.9; 31.6; 27.1; 26.8; 19.6; 19.0; 16.2. Found, *m/z*: 482.2765 [M+H]$^+$. C$_{26}$H$_{36}$N$_5$O$_4$. Calculated, *m/z*: 482.2767.

Methyl 2-{2-[(1*S*)-1-((2*S*)-2-{[(*tert*-butoxy)carbonyl]amino}pent-4-enamido)-2,2-dimethylpropyl]-5-[methyl-(prop-2-en-1-yl)amino]-1,3-oxazol-4-yl}-1,3-oxazole-4-carboxylate (23) was synthesized in a three-step sequence from bioxazole **22**.

Step 1. **Methyl 2-[2-((1*S*)-1-amino-2,2-dimethylpropyl)-5-bromo-1,3-oxazol-4-yl]-1,3-oxazole-4-carboxylate**. 33% HBr solution in AcOH (2.6 ml, 15.0 mmol, 20 equiv) was added to a solution of bioxazole **22** (370 mg, 0.8 mmol,

1 equiv) in 1,4-dioxane (2 ml). The reaction mixture was stirred at room temperature for 15 min. Then Et$_2$O (20 ml) was added to the reaction mixture and white precipitate was formed. The resulting suspension was decanted, and the precipitate was washed with Et$_2$O (2×40 ml) and evaporated under reduced pressure to provide crude oxazole as a yellow oil, yield 280 mg (85%), which was used in the next reaction without additional purification.

Step 2. **Methyl 2-{2-((1***S***)-1-amino-2,2-dimethylpropyl)-5-[methyl(prop-2-en-1-yl)amino]-1,3-oxazol-4-yl}-1,3-oxazole-4-carboxylate** was obtained from methyl 2-[2-((1*S*)-1-amino-2,2-dimethylpropyl)-5-bromo-1,3-oxazol-4-yl]-1,3-oxazole-4-carboxylate (step 1) (280 mg, 0.8 mmol), *N*-methyl-allylamine (0.1 ml, 1.3 mmol), and NEt$_3$ (0.3 ml, 1.9 mmol) in anhydrous DMF at 50°C following the general method I. The crude product was purified by column chromatography on silica gel using gradient elution from pure CH$_2$Cl$_2$ to 10% MeOH in CH$_2$Cl$_2$ to obtain product as a yellow oil, yield 110 mg (40%), which was used in the next reaction without additional purification.

Step 3. **Methyl 2-{2-[(1***S***)-1-((2***S***)-2-{[(***tert***-butoxy)-carbonyl]amino}pent-4-enamido)-2,2-dimethylpropyl]-5-[methyl(prop-2-en-1-yl)amino]-1,3-oxazol-4-yl}-1,3-oxazole-4-carboxylate (23)** was obtained from methyl 2-{2-((1*S*)-1-amino-2,2-dimethylpropyl)-5-[methyl(prop-2-en-1-yl)amino]-1,3-oxazol-4-yl}-1,3-oxazole-4-carboxylate (step 2) (110 mg, 0.3 mmol), acid **16A** (102 mg, 0.5 mmol), and EDC·HCl (121 mg, 0.6 mmol) in anhydrous pyridine following the general method III. Yield 110 mg (64%), yellow oil, [α]$_D^{20}$ –48.0° (*c* 1.0, CHCl$_3$). ^{1}H NMR spectrum (CDCl$_3$), δ, ppm (*J*, Hz): 8.19 (1H, s, H oxazole); 6.90 (1H, d, *J* = 9.6, NHCO); 5.94–5.66 (2H, m, 2C*H*=CH$_2$); 5.26–5.05 (4H, m, 2CH=C*H*$_2$); 5.02–4.97 (1H, m, NHCOO); 4.96 (1H, d, *J* = 9.6, C*H*C(CH$_3$)$_3$); 4.19–4.04 (3H, m, C*H*CH$_2$, CH$_2$); 3.89 (3H, s, OCH$_3$); 3.10 (3H, s, NCH$_3$); 2.55–2.40 (2H, m, CH$_2$); 1.42 (9H, s, C(CH$_3$)$_3$); 0.98 (9H, s, C(CH$_3$)$_3$). ^{13}C NMR spectrum (CDCl$_3$), δ, ppm: 171.1; 162.1; 157.7; 155.4; 152.8; 142.7; 133.9; 133.3; 132.9; 119.1; 118.4; 103.3; 80.4; 60.5; 55.3; 54.0; 52.1; 37.7; 36.2; 28.4; 26.4; 26.3. Found, *m/z*: 546.2932 [M+H]$^+$. C$_{27}$H$_{40}$N$_5$O$_7$. Calculated, *m/z*: 546.2928.

Methyl 2-((7*S***,10***S***)-7-{[(***tert***-butoxy)carbonyl]amino}-10-*tert*-butyl-2-methyl-8-oxo-14-oxa-2,9,12-triazabicyclo-[9.2.1]tetradeca-1(13),11-dien-13-yl)-1,3-oxazole-4-carb-oxylate (24)**. Alkene **23** (90 mg, 0.2 mmol, 1 equiv) was added to a solution of ruthenium metathesis catalyst **Ru4** (12 mg, 0.02 mmol, 0.1 equiv) in anhydrous CH$_2$Cl$_2$ (100 ml). After stirring at 50°C for 24 h, neat Ti(O*i*-Pr)$_4$ (0.05 ml, 0.2 mmol, 1 equiv) was added dropwise. The stirring was continued for 5 days at 60°C, whereupon the reaction mixture was cooled to room temperature and concentrated under reduced pressure. The crude unsaturated macrocycle (as a mixture of *E/Z*-isomers) was hydrogenated in the presence of 10% Pd on carbon (18 mg, 0.02 mmol) following the general method V to afford product **24** as a white amorphous solid, yield 33 mg (39%), [α]$_D^{20}$ –160.0° (*c* 1.0, CHCl$_3$). ^{1}H NMR spectrum (CDCl$_3$), δ, ppm (*J*, Hz): 8.17 (1H, s, H oxazole); 5.81 (1H, d, *J* = 7.5, NHCO); 5.51 (1H, d, *J* = 7.5, C*H*C(CH$_3$)$_3$); 4.60 (1H, d, *J* = 15.4, NHCOO); 4.59–4.53 (1H, m, C*H*CH$_2$); 3.89 (3H, s, OCH$_3$); 3.89–3.83 (1H, m, CH$_2$); 3.27 (3H, s, NCH$_3$); 3.05–3.00 (1H, m,

CH$_2$); 2.08–1.95 (2H, m, CH$_2$); 1.93–1.83 (1H, m, CH$_2$); 1.55–1.38 (10H, m, CH$_2$, C(CH$_3$)$_3$); 1.29–1.18 (1H, m, CH$_2$); 1.08 (9H, s, C(CH$_3$)$_3$); 1.03–0.91 (1H, m, CH$_2$). ^{13}C NMR spectrum (CDCl$_3$), δ, ppm: 172.9; 162.2; 158.1; 155.3; 154.8; 150.3; 142.7; 133.5; 100.1; 79.9; 58.8; 53.4; 52.1; 49.4; 37.0; 33.8; 31.5; 28.5; 26.8; 25.1; 18.0. Found, *m/z*: 520.2772 [M+H]$^+$. C$_{25}$H$_{38}$N$_5$O$_7$. Calculated, *m/z*: 520.2771.

(2*S***)-*N*-{(7***S***,10***S***)-10-*tert*-Butyl-13-[4-(hydroxymethyl)-1,3-oxazol-2-yl]-2-methyl-8-oxo-14-oxa-2,9,12-triazabicyclo-[9.2.1]tetradeca-1(13),11-dien-7-yl}-2-hydroxy-3-methyl-butanamide (5)**. CF$_3$CH$_2$OH (0.1 ml) was added to a solution of compound **24** (25 mg, 0.05 mmol, 1 equiv) in anhydrous THF (1 ml). The flask was cooled to 0°C (crushed ice bath), and LiBH$_4$ (5 mg, 0.2 mmol, 5 equiv) was added in one portion. The resulting mixture was warmed to room temperature and stirred for 20 h, whereupon it was quenched by addition of aqueous saturated NH$_4$Cl solution to 10% and extracted with EtOAc (3×10 ml). The combined organic extracts were washed with brine, dried over anhydrous Na$_2$SO$_4$, filtered, and concentrated under reduced pressure to afford crude alcohol as colorless oil, yield 17 mg (72%), which was used in the next step without additional purification.

The title compound **5** was obtained from the crude alcohol (17 mg, 0.03 mmol), CF$_3$CO$_2$H (0.1 ml, 1.6 mmol), (*S*)-2-hydroxy-3-methylbutanoic acid (8 mg, 0.07 mmol), EDC·HCl (14 mg, 0.07 mmol), HOBt (15 mg, 0.08 mmol), and DIPEA (0.03 ml, 0.4 mmol) following the general method VI. Yield 10 mg (59%), white amorphous solid, [α]$_D^{20}$ –154.8° (*c* 1.0, CHCl$_3$). ^{1}H NMR spectrum (CD$_3$OD), δ, ppm (*J*, Hz): 7.75 (1H, s, H oxazole); 4.53 (2H, s, C*H*$_2$OH); 4.51 (1H, s, C*H*C(CH$_3$)$_3$); 4.00–3.90 (1H, m, C*H*CH$_2$); 3.87 (1H, d, *J* = 3.3, C*H*OH); 3.17 (3H, s, NCH$_3$); 3.09 (1H, dt, *J* = 14.9, *J* = 3.3, CH$_2$); 2.18–1.88 (4H, m, CH$_2$, C*H*(CH$_3$)$_2$); 1.47–1.35 (1H, m, CH$_2$); 1.34–1.21 (2H, m, CH$_2$); 1.12 (9H, s, C(CH$_3$)$_3$); 1.05–0.93 (4H, m, C*H*$_3$CH, CH$_2$); 0.85 (3H, d, *J* = 6.8, C*H*$_3$CH). ^{13}C NMR spectrum (CD$_3$OD), δ, ppm: 175.9; 174.6; 158.8; 155.6; 152.8; 142.5; 135.6; 101.0; 76.8; 60.6; 57.3; 52.7; 50.0; 37.4; 34.6; 32.9; 31.8; 26.9; 26.3; 19.6; 19.1; 16.1. Found, *m/z*: 492.2818 [M+H]$^+$. C$_{24}$H$_{38}$N$_5$O$_6$. Calculated, *m/z*: 492.2822.

tert*-Butyl *N*-((1S***)-1-{4-(4-{[(***tert***-butyldimethylsilyl)-oxy]methyl}-1,3-oxazol-2-yl)-5-[(3,5-difluorophenyl)-(hydroxy)methyl]-1,3-oxazol-2-yl}-2,2-dimethylpropyl)-carbamate (25)**. *n*-BuLi (1.6 M solution in hexane, 1.17 ml, 1.88 mmol, 2.05 equiv) was added gradually (within 20 min) to a solution of bioxazole (*S*)-**12**^{4} (427 mg, 0.92 mmol, 1.0 equiv) in anhydrous Et$_2$O (9 ml) at –78°C. The color of the solution slowly changed from yellow to dark-brown. After 10 min of the stirring at –78°C, a solution of 3,5-difluoro-benzaldehyde (313 mg, 2.20 mmol, 2.4 equiv) in anhydrous Et$_2$O (2 ml) was added dropwise. The resulting solution was stirred for 10 min at –78°C, slowly warmed to room temperature, stirred for 30 min, and cooled back to 0°C. Aqueous saturated NH$_4$Cl solution (20 ml) was added, and the mixture was extracted with Et$_2$O (3×20 ml). Combined organic extracts were washed with brine, dried over anhydrous Na$_2$SO$_4$, and concentrated under reduced pressure. The residue was purified by column chromatography on silica gel using gradient elution from 5% EtOAc in hexane to 50% EtOAc in hexane to afford alcohol **25** as

a mixture of diastereomers, yield 284 mg (51%), colorless oil, which was used in the next reaction without additional purification.

***tert*-Butyl *N*-{(1*S*)-1-[4-(4-{[(*tert*-butyldimethylsilyl)-oxy]methyl}-1,3-oxazol-2-yl)-5-(3,5-difluorobenzoyl)-1,3-oxazol-2-yl]-2,2-dimethylpropyl}carbamate (26)**. Dess–Martin periodinane (290 mg, 0.68 mmol, 1.5 equiv) was portionwise added to a solution of crude alcohol **25** (277 mg, 0.46 mmol, 1.0 equiv) in anhydrous CH_2Cl_2 (9 ml). The resulting white suspension was stirred at room temperature for 1 h, whereupon all volatiles were removed under reduced pressure. The residue was purified by flash chromatography using gradient elution from pure hexane to 60% EtOAc in hexane. Yield 215 mg (78%), white amorphous solid, $[\alpha]_D^{20}$ –42.0° (*c* 1.0, $CHCl_3$). ^{1}H NMR spectrum ($CDCl_3$), δ, ppm (*J*, Hz): 7.61 (1H, dd, *J* = 1.4, *J* = 1.4, H Ar); 7.48–7.41 (2H, m, H Ar); 7.07 (1H, tt, *J* = 8.4, *J* = 2.4, H Ar); 5.45 (1H, d, *J* = 9.8, NH); 4.84 (1H, d, *J* = 9.8, C$\underline{H}$NH); 4.74 (2H, s, C$\underline{H}_2$OH); 1.43 (9H, s, OC(CH₃)₃); 1.05 (9H, s, C(CH₃)₃); 0.92 (9H, s, C(CH₃)₃); 0.10 (6H, s, 2CH₃Si). ^{13}C NMR spectrum ($CDCl_3$), δ, ppm (*J*, Hz): 179.3; 166.1; 163.0 (dd, *J* = 251.6, *J* = 11.8); 155.4; 153.8; 144.8; 144.2; 139.2 (t, *J* = 8.2); 136.7; 134.5; 112.9–112.5 (m); 109.1 (t, *J* = 25.2); 80.5; 59.2; 36.2; 31.7; 28.4; 26.4; 26.0; –5.3. Found, *m/z*: 606.2810 [M+H]⁺. $C_{30}H_{42}F_2N_3O_6Si$. Calculated, *m/z*: 606.2811.

***tert*-Butyl *N*-((1*S*)-1-{4-(4-{[(*tert*-butyldimethylsilyl)-oxy]methyl}-1,3-oxazol-2-yl)-5-[1-(3,5-difluorophenyl)-1-hydroxybut-3-en-1-yl]-1,3-oxazol-2-yl}-2,2-dimethyl-propyl)carbamate (27)**. Allylmagnesium bromide (1 M solution in Et_2O, 0.88 ml, 0.88 mmol, 2.5 equiv) was drop-wise added to a solution of ketone **26** (214 mg, 0.35 mmol, 1.0 equiv) in anhydrous THF (5 ml) at –15°C. After stirring at –15°C for 30 min, the yellow solution was warmed to 0°C, quenched with aqueous saturated NH_4Cl solution, and extracted with EtOAc (3×15 ml). Combined organic extracts were washed with brine, dried over anhydrous Na_2SO_4, and concentrated under reduced pressure. The residue was purified by column chromatography on silica gel using gradient elution from pure hexane to 50% EtOAc in hexane to afford tertiary alcohol **27** as a mixture of diastereomers. Yield 188 mg (82%), colorless oil ^{1}H NMR spectrum ($CDCl_3$), δ, ppm (*J*, Hz): 8.27 (0.5H, s, NH); 8.24 (0.5H, s, NH); 7.59–7.54 (1H, m, H Ar); 7.02–6.94 (2H, m, H Ar); 6.69–6.62 (1H, m, H Ar); 5.86–5.70 (1H, m, C$\underline{H}$=CH₂); 5.37–5.27 (1H, m, CH=C$\underline{H}_2$); 5.18–5.02 (2H, m, CH=C$\underline{H}_2$); 4.78 (1H, d, *J* = 9.6, C$\underline{H}$NH); 4.66–4.60 (2H, m, C$\underline{H}_2$OH); 3.03 (1H, dt, *J* = 14.7, *J* = 7.5 C$\underline{H}_2$); 2.93–2.79 (1H, m, C$\underline{H}_2$); 1.44 (4.5H, s, OC(CH₃)₃); 1.43 (4.5H, s, OC(CH₃)₃); 1.03 (4.5H, s, C(CH₃)₃); 1.01 (4.5H, s, C(CH₃)₃); 0.92 (4.5H, s, C(CH₃)₃); 0.91 (4.5H, s, C(CH₃)₃); 0.12–0.08 (6H, m, 2CH₃Si). ^{13}C NMR spectrum ($CDCl_3$), δ, ppm (*J*, Hz): 166.5; 162.9 (dd, *J* = 250.6, *J* = 12.0); 156.1; 155.4; 149.3; 149.0; 141.8 (t, *J* = 8.0); 135.6; 132.2; 125.1; 119.2; 108.7–108.4 (m); 103.0 (t, *J* = 25.1); 80.3; 74.5; 58.1; 57.4; 46.0; 45.9; 35.8; 28.4; 26.4; 26.0; –5.2. Found, *m/z*: 648.3294 [M+H]⁺. $C_{33}H_{48}F_2N_3O_6Si$. Calculated, *m/z*: 648.3280.

***tert*-Butyl *N*-{(1*S*)-1-[((1*S*)-1-{5-[1-(3,5-difluorophenyl)-1-hydroxybut-3-en-1-yl]-4-[4-(hydroxymethyl)-1,3-oxazol-2-yl]-1,3-oxazol-2-yl}-2,2-dimethylpropyl)carbamoyl]but-**

3-en-1-yl}carbamate (28) was obtained in a two-step sequence from alcohol **27**.

Step 1. **1-{2-((1*S*)-1-Amino-2,2-dimethylpropyl)-4-[4-(hydroxymethyl)-1,3-oxazol-2-yl]-1,3-oxazol-5-yl}-1-(3,5-difluorophenyl)but-3-en-1-ol**. 4 M HCl solution in 1,4-dioxane (5.1 ml, 20.4 mmol, 50 equiv) was added to a solution of allylic alcohol **27** (265 mg, 0.41 mmol, 1.0 equiv) in 1,4-dioxane (9 ml). The resulting solution was stirred at room temperature for 18 h and concentrated under reduced pressure. The residue was dissolved in EtOAc (10 ml), washed with aqueous saturated $NaHCO_3$ solution and brine, then dried over anhydrous Na_2SO_4 and concentrated under reduced pressure. The residue was purified by column chromatography on silica gel using gradient elution from 1% MeOH in EtOAc to 10% MeOH in EtOAc to afford product as a mixture of diastereomers. Yield 123 mg (69%), yellow oil. ^{1}H NMR spectrum ($CDCl_3$), δ, ppm (*J*, Hz): 8.22 (1H, s, NH₂); 7.65–7.64 (1H, m, H Ar); 7.03–6.95 (2H, m, H Ar); 6.71–6.63 (1H, m, H Ar); 5.85–5.71 (1H, m, C$\underline{H}$=CH₂); 5.18–5.05 (2H, m, CH=C$\underline{H}_2$); 4.63 (2H, d, *J* = 1.1, C$\underline{H}_2$OH); 3.86–3.84 (1H, m, C$\underline{H}$NH₂); 3.08–2.98 (1H, m, C$\underline{H}_2$); 2.93–2.82 (1H, m, CH₂); 1.99–1.70 (3H, br. s, 2OH, NH₂); 1.05–1.00 (9H, m, C(CH₃)₃). ^{13}C NMR spectrum ($CDCl_3$), δ, ppm (*J*, Hz): 165.9; 162.9 (dd, *J* = 248.7, *J* = 12.6); 161.7; 156.5; 155.4; 149.0 (dt, *J* = 7.9, *J* = 3.4); 141.1; 135.7; 132.2; 124.7; 119.4; 108.7–108.3 (m); 103.1 (dt, *J* = 25.4, *J* = 3.6); 74.5; 59.5; 57.1; 45.9; 35.7; 26.4. Found, *m/z*: 434.1896 [M+H]⁺. $C_{22}H_{26}F_2N_3O_4$. Calculated, *m/z*: 434.1891.

Step 2. ***tert*-Butyl *N*-{(1*S*)-1-[((1*S*)-1-{5-[1-(3,5-difluorophenyl)-1-hydroxybut-3-en-1-yl]-4-[4-(hydroxymethyl)-1,3-oxazol-2-yl]-1,3-oxazol-5-yl}-2,2-dimethylpropyl)carbamoyl]but-3-en-1-yl}carbamate (28)** was obtained from 1-{2-((1*S*)-1-amino-2,2-dimethylpropyl)-4-[4-(hydroxy-methyl)-1,3-oxazol-2-yl]-1,3-oxazol-5-yl}-1-(3,5-difluoro-phenyl)but-3-en-1-ol (step 1) (110 mg, 0.25 mmol), EDC·HCl (54 mg, 0.28 mmol), and acid **16A** (55 mg, 0.25 mmol) in anhydrous pyridine following the general method III. Purification by column chromatography on silica gel using gradient elution from 30% EtOAc in hexane to 70% EtOAc in hexane afforded product **28** as a mixture of diastereomers. Yield 114 mg (71%), yellow amorphous solid. ^{1}H NMR spectrum ($CDCl_3$), δ, ppm (*J*, Hz): 8.20 (1H, d, *J* = 12.4, NH); 7.66–7.64 (1H, m, H Ar); 7.19–7.04 (1H, m, NH); 7.02–6.94 (2H, m, H Ar); 6.72–6.60 (1H, m, H Ar); 5.87–5.66 (1H, m, 2CH=CH₂); 5.19–5.03 (5H, m, 2CH=C$\underline{H}_2$, C$\underline{H}$NH); 5.02–4.92 (1H, br. s, OH); 4.66–4.62 (2H, m, C$\underline{H}_2$OH); 4.20–4.13 (1H, m, C$\underline{H}$NH); 3.04 (1H, dt, *J* = 13.4, *J* = 6.4 CH₂); 2.88 (1H, td, *J* = 14.5, *J* = 6.7, CH₂); 2.58–2.46 (2H, m, CH₂, OH); 2.00 (1H, t, *J* = 6.0, CH₂); 1.44 (9H, s, OC(CH₃)₃); 1.03 (4.5H, s, C(CH₃)₃); 1.02 (4.5H, s, C(CH₃)₃). ^{13}C NMR spectrum ($CDCl_3$), δ, ppm (*J*, Hz): 163.0 (dd, *J* = 249.0, *J* = 12.6); 162.0; 161.9; 161.7; 156.4; 155.7; 149.0 (t, *J* = 8.0); 141.1; 135.7; 133.2; 132.1; 125.0; 119.5; 108.7–108.3 (m); 103.1 (dd, *J* = 25.5, *J* = 8.0); 80.6; 74.5; 57.1; 45.9; 45.8; 35.8; 28.4; 26.43; 26.40. Found, *m/z*: 631.2950 [M+H]⁺. $C_{32}H_{41}F_2N_4O_7$. Calculated, *m/z*: 631.2943.

***tert*-Butyl *N*-{(2*S*,5*S*)-2-*tert*-butyl-10-(3,5-difluorophenyl)-10-hydroxy-12-[4-(hydroxymethyl)-1,3-oxazol-2-yl]-4-oxo-14-oxa-3,13-diazabicyclo[9.2.1]tetradeca-1(13),11-dien-**

5-yl}carbamate (29) was synthesized from amide **28** (102 mg, 0.16 mmol) and ruthenium metathesis catalyst **Ru4** (11.9 mg, 0.02 mmol) in anhydrous CH_2Cl_2 following the general method IV. The crude unsaturated macrocycle was obtained as a mixture of *E/Z*-isomers in 2:1 ratio after purification by column chromatography on silica gel using gradient elution from 25% EtOAc in hexane to 100% EtOAc. Yield 80 mg (82%), brown amorphous solid.

A solution of the crude macrocycle (80 mg, 0.13 mmol, 1.0 equiv) in MeOH (10 ml) was stirred for 5 days under H_2 pressure (5 atm) in the presence of 10% Pd on carbon (71 mg, 0.07 mmol, 0.5 equiv). The resulting black suspension was filtered through a pad of Celite®, and the filtrate was concentrated under reduced pressure. The residue was purified by column chromatography on silica gel using gradient elution from 30% EtOAc in hexane to 50% EtOAc in hexane to afford product **29** as a mixture of diastereomers. Yield 52 mg (65%), white amorphous solid. ^{1}H NMR spectrum (CDCl₃), δ, ppm (*J*, Hz): 8.06 (0.67H, s, NH); 7.65–7.62 (0.67H, m, H Ar); 7.61–7.59 (0.33H, m, H Ar); 7.41 (0.33H, s, NH); 6.94–6.86 (1.34H, m, H Ar); 6.85–6.79 (0.66H, m, H Ar); 6.69–6.60 (1H, m, H Ar); 6.26–6.19 (0.33H, m, NHCH); 6.16–6.09 (0.67H, m, NHCH); 5.54–5.42 (1H, m, CH₂OH); 5.18–5.11 (0.33H, m, CHNH); 4.90 (0.67H, d, *J* = 8.0, CHNH); 4.62 (1.34H, br. s, CH₂OH); 4.57–4.51 (0.67H, m, CHCH₂); 4.49 (0.66H, br. s, CH₂OH); 4.31–4.24 (0.33H, m, CHCH₂); 2.41–2.28 (1H, m, CH₂CH); 2.27–2.14 (2H, m, CH₂CH); 2.00–1.72 (4H, m, 2CH₂, CH₂CH); 1.42 (2.97H, s, OC(CH₃)₃); 1.41 (6.03H, s, OC(CH₃)₃); 1.33–1.26 (1H, m, CH₂); 1.24 (2.97H, s, C(CH₃)₃); 1.17 (6.03H, s, C(CH₃)₃). ^{13}C NMR spectrum (CDCl₃), δ, ppm (*J*, Hz): 173.2; 163.0 (dd, *J* = 257.6, *J* = 12.6); 161.9; 161.2; 156.2; 155.3; 155.2; 151.4 (t, *J* = 7.4); 141.2; 135.7; 125.2; 107.8–107.4 (m); 102.9 (t, *J* = 25.3); 74.1; 58.9; 57.1; 53.4; 38.9; 33.6; 30.8; 28.5; 26.9; 21.9; 14.3. Found, *m/z*: 605.2771 [M+H]⁺. C₃₀H₃₉F₂N₄O₇. Calculated, *m/z*: 605.2787.

(2S)-N-{(2S,5S)-2-*tert*-Butyl-10-(3,5-difluorophenyl)-10-hydroxy-12-[4-(hydroxymethyl)-1,3-oxazol-2-yl]-4-oxo-14-oxa-3,13-diazabicyclo[9.2.1]tetradeca-1(13),11-dien-5-yl}-2-hydroxy-3-methylbutanamide (diastereomers 6A and 6B). CF₃CO₂H (0.4 ml, 5.27 mmol, 65 equiv) was dropwise added to a solution of macrocycle **29** (49 mg, 0.081 mmol, 1.0 equiv) in anhydrous CH_2Cl_2 (3 ml) at 0°C. The yellow solution was warmed to room temperature and stirred for 3 h, whereupon all volatiles were removed under reduced pressure. The residue was dissolved in THF (0.5 ml) and MeOH (0.5 ml), and a solution of LiOH (10 mg, 0.40 mmol, 5 equiv) in H₂O (0.5 ml) was added dropwise. The resulting brown solution was stirred for 1 h at room temperature, and all volatiles were concentrated under reduced pressure. The residue was dissolved in Et₂O (10 ml) and washed with 1 M aqueous HCl (2×10 ml), brine, dried over anhydrous Na₂SO₄, and concentrated under reduced pressure. Crude amine was obtained as white amorphous solid, yield 41 mg (100%), which was used in the next reaction without additional purification.

(*S*)-2-Hydroxy-3-methylbutanoic acid (9.6 mg, 0.081 mmol, 1.05 equiv), EDC·HCl (15.6 mg, 0.081 mmol, 1.05 equiv), HOBt (11 mg, 0.081 mmol, 1.05 equiv), and DIPEA (40 µl, 0.23 mmol, 3.0 equiv) were added to a solution of

crude amine (39 mg, 0.077 mmol, 1.0 equiv) in anhydrous DMF (5 ml). The yellow solution was stirred at room temperature for 18 h, whereupon H₂O was added, and the resulting mixture was extracted with EtOAc (3×10 ml). Combined organic extracts were washed with brine, dried over anhydrous Na₂SO₄, and concentrated under reduced pressure. The residue was purified by reversed-phase column chromatography on silica gel using gradient elution from 30 to 50% MeCN in H₂O to afford individual diastereomers.

Diastereomer 6A. Yield 10.5 mg (23%), white amorphous solid, $[\alpha]_D^{20}$ –49.7° (*c* 0.7, MeOH). ^{1}H NMR spectrum (CD₃OD), δ, ppm (*J*, Hz): 8.62 (1H, d, *J* = 7.2, NH); 7.73 (1H, s, H Ar); 6.96–6.86 (2H, m, H Ar); 6.78 (1H, tt, *J* = 8.8, *J* = 2.3, H Ar); 4.99–4.92 (1H, m, CH); 4.74 (1H, dd, *J* = 7.2, *J* = 2.8, CH); 4.37 (2H, s, CH₂OH); 3.87 (1H, d, *J* = 3.4, CHOH); 2.96–2.87 (1H, m, CH₂CH); 2.57–2.40 (1H, m, CH₂CH); 2.16–1.80 (3H, m, CH₂CH, CH(CH₃)₂); 1.34–1.26 (4H, m, 2CH₂); 1.22 (9H, s, C(CH₃)₃); 0.99 (3H, d, *J* = 6.9, CH₃CH); 0.82 (3H, d, *J* = 6.9, CH₃CH). ^{13}C NMR spectrum (CD₃OD), δ, ppm (*J*, Hz): 174.3; 173.4; 163.1 (dd, *J* = 248.0, *J* = 12.6); 156.2; 153.0; 142.9 (t, *J* = 8.1); 137.5; 137.0; 136.3; 126.5; 110.1–109.7 (m); 103.5 (t, *J* = 26.0); 76.5; 73.8; 59.5; 55.3; 51.3; 40.2; 32.9; 31.6; 29.6; 26.9; 22.7; 19.6; 18.2; 15.2. Found, *m/z*: 605.2789 [M+H]⁺. C₃₀H₃₉F₂N₄O₇. Calculated, *m/z*: 605.2787.

Diastereomer 6B. Yield 16.1 mg (34%), white amorphous solid, $[\alpha]_D^{20}$ –27.6° (*c* 0.6, MeOH). ^{1}H NMR spectrum (CD₃OD), δ, ppm (*J*, Hz): 8.67 (1H, d, *J* = 7.2, NH); 7.90 (1H, s, H Ar); 7.06–6.94 (2H, m, H Ar); 6.81 (1H, tt, *J* = 8.8, *J* = 2.3, H Ar); 4.90–4.86 (1H, m, CH); 4.83–4.79 (1H, m, CH); 4.54 (2H, s, CH₂OH); 3.87 (1H, d, *J* = 3.4, CHOH); 2.59–2.42 (1H, m, CH₂CH); 2.27–2.15 (1H, m, CH₂CH); 2.15–2.05 (1H, m, CH(CH₃)₂); 1.98–1.76 (3H, m, CH₂CH, CH₂); 1.46–1.12 (12H, m, C(CH₃)₃, 2CH₂); 0.99 (3H, d, *J* = 6.9, CH₃CH); 0.89–0.69 (3H, m, CH₃CH). ^{13}C NMR spectrum (CD₃OD), δ, ppm (*J*, Hz): 174.4; 173.4; 164.4 (dd, *J* = 248.0, *J* = 12.6); 156.3; 153.0; 143.0 (t, *J* = 8.4); 137.6; 137.0; 136.3; 125.9; 108.7–108.3 (m); 102.2 (t,

6B
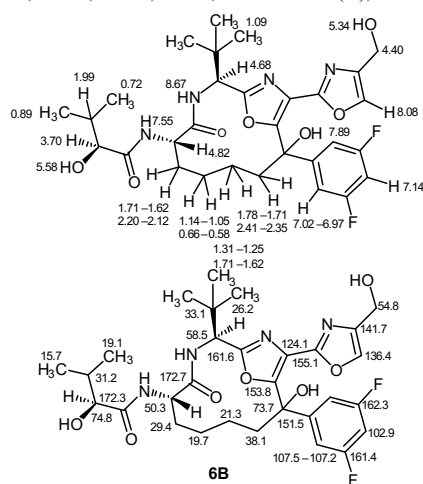
J = 26.0); 75.5; 73.8; 59.3; 55.3; 51.3; 38.1; 33.0; 31.6; 29.6; 25.6; 21.5; 19.9; 18.2; 14.7. ^{1}H NMR spectrum (DMSO-d_6), δ, ppm (J, Hz): 8.67 (1H, d, J = 7.3, NH); 8.08 (1H, s, H oxazole); 7.89 (1H, d, J = 2.2, ArCOH); 7.55 (1H, d, J = 7.7, NH); 7.14 (1H, tt, J = 9.0, J = 2.4, H Ar); 7.02–6.97 (1H, m, H Ar); 5.58 (1H, d, J = 5.7, (CH₃)₂CCHO**H**); 5.34 (1H, t, J = 5.7, CH₂O**H**); 4.82 (1H, ddd, J = 7.9, J = 5.0, J = 2.8, C**H**CH₂); 4.68 (1H, d, J = 7.3, (CH₃)₃C**H**); 4.40 (1H, d, J = 5.7, C**H**₂OH); 3.70 (1H, dd, J = 5.7, J = 3.3, C**H**OH); 2.41–2.35 (1H, m, C**H**₂COH), 2.20–2.12 (1H, m, C**H**₂CH); 1.99 (1H, sept d, J = 6.9, J = 3.3, C**H**(CH₃)₂); 1.78–1.71 (1H, m, C**H**₂COH); 1.71–1.62 (2H, m, C**H**₂CH, CH₂); 1.14–1.05 (10H, m, C(C**H**₃)₃, C**H**₂); 0.89 (3H, d, J = 6.9, C**H**₃CH); 0.72 (3H, d, J = 6.9, C**H**₃CH), 0.66–0.58 (1H, m, CH₂). ^{13}C NMR spectrum (DMSO-d_6), δ, ppm (J, Hz): 172.7; 172.3; 162.3 (dd, J = 248.0, J = 13.2); 161.6; 155.1; 153.8; 151.5 (t, J = 8.4); 141.7; 124.1; 107.5–107.2 (m); 102.9 (t, J = 26.0); 74.8; 73.7; 58.5; 54.8; 50.3; 38.1; 33.1; 31.2; 29.4; 26.2; 21.3; 19.7; 19.1; 15.7. Found, m/z: 605.2792 [M+H]$^+$. C₃₀H₃₉F₂N₄O₇. Calculated, m/z: 605.2787.

Isothermal titration calorimetry. A stock solution of tubulin (5.0 mg/ml, Cytoskeleton Inc., Denver (USA)) was dissolved in the ice-cold 20 mM phosphate (NaPi) 0.1 mM GTP buffer (pH 6.5) just before the experiment and used within 6 h. Prechilled RB3 (STMN4) protein prepared in the same buffer was added to tubulin just before the experiment. Tubulin:RB3 concentration ratio varied from 2:1 to 1:1. Protein sample was stored on ice before loading into the ITC sample cell.

The ITC experiments have been performed in a MicroCal iTC200 calorimeter. The ITC system cleanliness was checked by water-to-water titration before every protein–ligand titration experiment. The temperature of the ITC cell was set up and equilibrated at 10°C. Afterward 280 µl of ice-cold tubulin protein sample was loaded into the cell. ITC syringe was prewashed with the same buffer that was used for the protein and was filled with the ice-cold ligand sample. Next, the ITC titration syringe was put into the sample cell and left for 5–10 min for temperature equilibration.

The titration experiment consisted of 1 × 0.3 µl and 26 × 1.5 µl injections with 125 s spacing in-between and at a stirring rate of 600 rpm. ITC data were analyzed using the Origin 7 SR4 program. The first data point (with the small injection volume) was always removed prior the data fitting. "One Set of Sites" fitting model was applied.

References

1. van Vuuren, R. J.; Visagie, M. H.; Theron, A. E.; Joubert, A. M. *Cancer Chemother. Pharmacol.* **2015**, *76*, 1101.
2. Cruz-Monserrate, Z.; Vervoort, H. C.; Bai, R.; Newman, D. J.; Howell, S. B.; Los, G.; Mullaney, J. T.; Williams, M. D.; Pettit, G. R.; Fenical, W.; Hamel, E. *Mol. Pharmacol.* **2003**, *63*, 1273.
3. Wieczorek, M.; Tcherkezian, J.; Bernier, C.; Prota, A. E.; Chaaban, S.; Rolland, Y.; Godbout, C.; Hancock, M. A.; Arezzo, J. C.; Ocal, O.; Rocha, C.; Olieric, N.; Hall, A.; Ding, H.; Bramoulle, A.; Annis, M. G.; Zogopoulos, G.; Harran, P. G.; Wilkie, T. M.; Brekken, R. A.; Siegel, P. M.; Steinmetz, M. O.; Shore, G. C.; Brouhard, G. J.; Roulston, A. *Sci. Transl. Med.* **2016**, *8*(365), 365ra159.
4. Kazak, M.; Vasilevska, A.; Suna, E. *Chem. Heterocycl. Compd.* **2019**, *56*, 355. [*Khim. Getrotsikl. Soedin.* **2019**, *56*, 355.]
5. Jeong, S.; Chen, X.; Harran, P. G. *J. Org. Chem.* **1998**, *63*, 8640.
6. Prasad Atmuri, N. D.; Lubell, W. D. *J. Org. Chem.* **2015**, *80*, 4904.
7. Mangold, S. L.; Grubbs, R. H. *Chem. Sci.* **2015**, *6*, 4561.
8. Kaul, R.; Surprenant, S.; Lubell, W. D. *J. Org. Chem.* **2005**, *70*, 4901.
9. Shibata, K.; Yoshida, M.; Doi, T.; Takahashi, T. *Tetrahedron Lett.* **2010**, *51*, 1674.
10. Topolovčan, N.; Panov, I.; Kotora, M. *Org. Lett.* **2016**, *18*, 3634.
11. Fürstner, A.; Guth, O.; Dueffels, A.; Seidel, G.; Liebl, M.; Gabor, B.; Mynott, R. J. *Chem.–Eur. J.* **2001**, *7*, 4811.
12. Scholl, M.; Ding, S.; Lee, C. W.; Grubbs, R. H. *Org. Lett.* **1999**, *1*, 953.
13. Grela, K.; Harutyunyan, S.; Michrowska, A. *Angew. Chem., Int. Ed.* **2002**, *41*, 4038.
14. Gradillas, A.; Pérez-Castells, J. *Angew. Chem., Int. Ed.* **2006**, *45*, 6086.
15. Ojima, I.; Lin, S.; Inoue, T.; Miller, M. L.; Borella, C. P.; Geng, X.; Walsh, J. J. *J. Am. Chem. Soc.* **2000**, *122*, 5343.
16. Muthusamy, S.; Azhagan, D. *Eur. J. Org. Chem.* **2014**, 363.
17. Barrett, A. G. M.; Hamprecht, D.; Ohkubo, M. *J. Org. Chem.* **1997**, *62*, 9376.
18. Banister, S. D.; Moir, M.; Stuart, J.; Kevin, R. C.; Wood, K. E.; Longworth, M.; Wilkinson, S. M.; Beinat, C.; Buchanan, A. S.; Glass, M.; Connor, M.; McGregor, I. S.; Kassiou, M. *ACS Chem. Neurosci.* **2015**, *6*, 1546.

Appendix II – DEVELOPMENT OF POTENT MICROTUBULE TARGETING AGENT BY STRUCTURAL SIMPLIFICATION OF NATURAL DIAZONAMIDE

Kalnins. T.; Vitkovska, V.; Kazak, M.; Zelencova-Gopejenko, D.; Ozola, M.; Narvaiss, N.; Makrecka-Kuka, M.; Domraceva, I.; Kinens, A.; Gukalova, B.; Konrad, N.; Aav, R.; Bonato, F.; Lucena-Agell, D.; Díaz, J. F.; Liepinsh, E.; Suna, E. *J. Med. Chem.* **2024**, *67*, 9227–9259.

Development of Potent Microtubule Targeting Agent by Structural Simplification of Natural Diazonamide

Toms Kalnins, Viktorija Vitkovska, Mihail Kazak, Diana Zelencova-Gopejenko, Melita Ozola, Nauris Narvaiss, Marina Makrecka-Kuka, Ilona Domračeva, Artis Kinens, Baiba Gukalova, Nele Konrad, Riina Aav, Francesca Bonato, Daniel Lucena-Agell, J. Fernando Díaz, Edgars Liepinsh,* and Edgars Suna*

Read Online

ACCESS | Metrics & More | Article Recommendations | Supporting Information

Diazonamide A → Structural simplification → Compound 21

✔ Easier to obtain
✔ Diastereoselective synthesis
✔ Potent antiproliferative activity
✔ Proved inhibitor of tubulin assembly
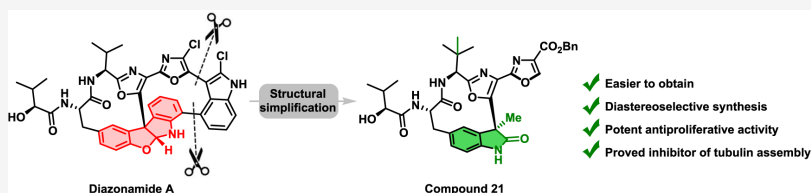
ABSTRACT: The marine metabolite diazonamide A exerts low nanomolar cytotoxicity against a range of tumor cell lines; however, its highly complex molecular architecture undermines the therapeutic potential of the natural product. We demonstrate that truncation of heteroaromatic macrocycle in natural diazonamide A, combined with the replacement of the challenging-to-synthesize tetracyclic hemiaminal subunit by oxindole moiety leads to considerably less complex analogues with improved drug-like properties and nanomolar antiproliferative potency. The structurally simplified macrocycles are accessible in 12 steps from readily available indolin-2-one and *tert*-leucine with excellent diastereoselectivity (99:1 dr) in the key macrocyclization step. The most potent macrocycle acts as a tubulin assembly inhibitor and exerts similar effects on A2058 cell cycle progression and induction of apoptosis as does marketed microtubule-targeting agent vinorelbine.

INTRODUCTION

Cancer is a major public health problem worldwide, with more than 19 million new cases diagnosed and 10 million lethal outcomes in 2020. By 2040, the increase of cancer incidence is expected to rise by 47% and reach 28.4 million cases annualy.[1] Growing incidence and high mortality, together with increasing multidrug resistance toward cancer therapeutics[2] put the development of new effective anticancer treatments among top priorities worldwide. Notably, a considerable number of anticancer medications currently used in clinics originated from natural sources. Thus, about one-third of small molecule anticancer drugs approved for clinical use from 1981 to 2019 are natural products and natural product derivatives.[3] Among them, microtubule-targeting agents (MTAs) such as vinca alkaloids (vinorelbine, vincristine) and taxanes (paclitaxel, docetaxel) have become a standard-of-care treatment in combination chemotherapy regimens.

MTAs of natural origin feature remarkable structural complexity and a high molecular weight that compromise their ADMET and physicochemical properties (leading to, e.g., poor oral bioavailability and solubility) and also limit compound availability due to highly challenging chemical

synthesis and difficulties with large-scale isolation from rare source materials.[4] These shortcomings have been addressed by a structural simplification approach toward less complex and synthetically more accessible molecules with improved drug-likeness.[5] Even though the pharmacological potency of a simplified analogue may be reduced as compared to that of a parent natural product, this is compensated by improved ADMET properties and easier synthetic accessibility. Herein, we report a structural simplification of a highly cytotoxic marine metabolite diazonamide A (**1a**) that resulted in the development of analogues with reduced molecular complexity and cytotoxicity profile comparable to those of parent natural product **1a**.

First isolated in 1991 from rare colonial ascidian *Diazona angulata* (54 mg of **1a** was obtained from 256 g of the

9227

117

lyophilized ascidian),[6] diazonamide A (**1a**) has attracted broad interest owing to its low nanomolar cytotoxicity against a range of tumor cell lines and highly complex molecular architecture. Indeed, diazonamide A contains many synthetically challenging structural elements such as a quaternary C10 stereocenter and two fused macrocycles: 12-membered ring and hetero-aromatic macrocycle, possessing three axially chiral biaryl bonds (Figure 1). Considerable synthetic efforts have
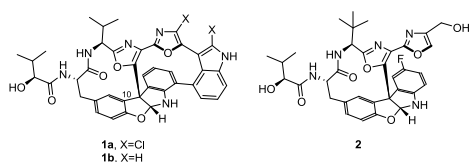

Figure 1. Diazonamide A **1a** and its simplified analogues.

culminated in four completed total syntheses[7] and several formal total syntheses[8] of diazonamide A (**1a**). Unfortunately, these notable synthetic accomplishments did not solve the problem of the poor availability of **1a**. As a consequence, only a limited number of studies on the mechanism of diazonamide A antitumor activity were conducted, generating somewhat controversial data. Thus, it has been demonstrated that the low nanomolar cytotoxicity of diazonamide **1a** arises from the inhibition of mitotic spindle assembly during cell division. Hamel and coworkers proposed binding to tubulin and inhibition of tubulin polymerization as an underlying mechanism for antimitotic activity of **1a**.[9] However, a binding site on heterodimeric tubulin could not be established for diazonamide A. Wang, Harran, et al. suggested an alternative mechanism of action for **1a** that involved the inhibition of mitotic functions of ornithine δ-amino transferase.[10] Later, Harran et al. succeeded in obtaining structurally simplified diazonamide analogue **2** by removing the right-hand heteroaromatic macrocycle.[11] The diazonamide analogue **2** was shown to bind at the vinca domain of tubulin heterodimer and inhibit microtubule growth rate, leading to mitotic arrest and tumor cell apoptosis.[12] Importantly, diazonamide analogues **1b** and **2** featured high safety margins and reduced systemic toxicity in *in vivo* models as compared to other clinically used antimitotic agents such as vinca alkaloids and taxanes.[12,13]

Despite the notable example of successful structural simplification of diazonamide A **1a** by truncation of the right-hand polyaromatic macrocycle, the presence of difficult-to-synthesize tetracyclic hemiaminal subunit[14] with a chiral quaternary stereogenic center confers considerable molecular

complexity to the simplified diazonamide A analogue **2**. We hypothesized that the replacement of the tetracycle by a chiral quaternary center-containing indolin-2-one core, while retaining both bioxazole subunit and peptide macrocycle, would allow easier synthesis of less complex analogues with improved drug-like properties. The respective design is exemplified by macrocycle series **3** and **4** (Scheme 1) that were used to explore SAR and eventually allowed for the development of potent analogues of cytotoxic natural diazonamide **1a** as shown below.

■ RESULTS AND DISCUSSION

Chemistry. The synthesis of macrocycle series **3** and **4** capitalized on an approach developed by Sammakia and coworkers in their formal total synthesis of diazonamide A, where diastereoselective intramolecular S_NAr-type arylation approach was employed to assemble the 12-membered macrocycle with quaternary center of *S* absolute configuration (Scheme 1).[8b] We realized that the base-mediated diastereoselective macrocyclization with concomitant quaternary center formation would be the most efficient strategy toward **3** and **4** provided that bromo-bioxazole subunit in **5** and **6** is sufficiently reactive under S_NAr conditions. We also hypothesized that the desired *S* configuration at the quaternary center could be secured by the stereogenic centers in the peptide backbone. The cyclization precursors **5** and **6** can be readily assembled from 3-substituted indolin-2-ones **7**, **8**, and bromo-bioxazole **9**[15] (Scheme 1).

The synthesis of the macrocyclization precursors **5a–h** commenced by Negishi cross-coupling[16] of known 3-alkyl- or 3-aryl-substituted 5-iodoindolin-2-ones **10a–h** with freshly prepared alkylzinc iodide **11** to afford amino acid esters **7a–h** in good to excellent yields (Scheme 2). Saponification of the ester was followed by EDC-mediated amide coupling with **9** to furnish amides **5a–h**. The synthesis of homologue series **6a,b,i** was accomplished by the decarboxylative coupling[17] between 5-iodoindolin-2-ones **10a,b,i** and *N*-hydroxyphthalimide ester **12** (prepared from *N*-Boc-L-Glu-OBzl and *N*-hydroxyphthalimide).[18] Subsequent hydrogenative cleavage of benzyl ester and amide bond formation with **9** yielded the macrocyclization precursors **6a,b,i** (Scheme 2).

With amides **5a–h** and **6a,b,i** in hand, the macrocyclization reaction was addressed. We were pleased to find that the bromo-bioxazole subunit in **5a–h** is sufficiently reactive to undergo S_NAr-type substitution of bromine by oxindole enolate (formed in situ upon the addition of Na_2CO_3 or K_3PO_4) at elevated temperatures. Under these conditions, macrocycles **3a–h** were obtained in 54–82% yield (Scheme 3A). Notably, the macrocyclization proceeded with excellent diastereoselectivities (from 93:7 dr to 99:1 dr; determined by
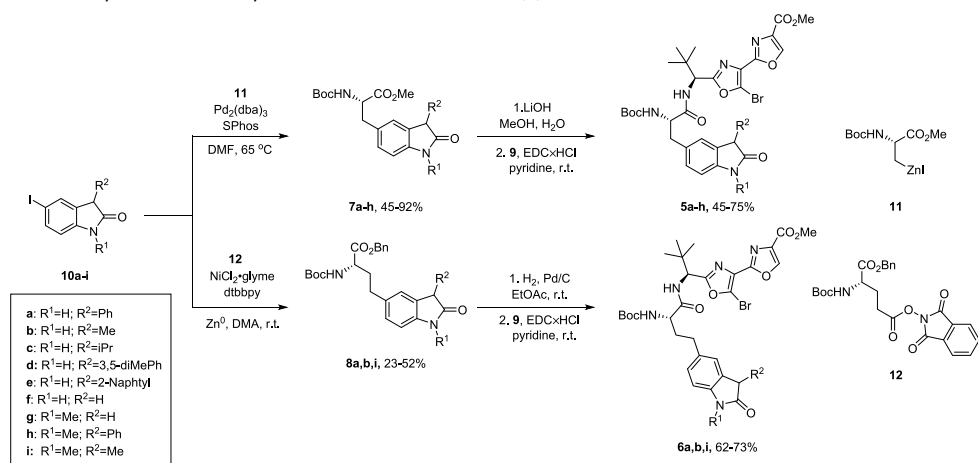
Scheme 1. Retrosynthesis of Macrocycles 3 and 4

3: n=1
4: n=2

5: n=1
6: n=2

7: n=1
8: n=2
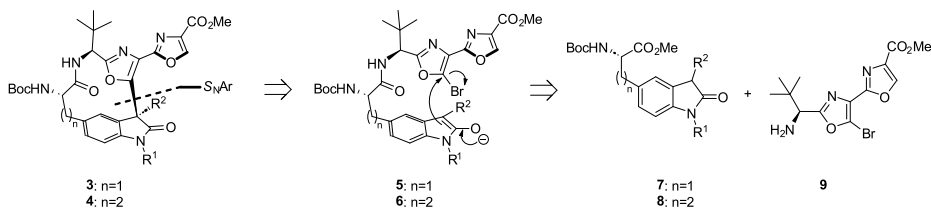
9

Scheme 2. Synthesis of Macrocyclization Precursors 5a−h and 6a,b,i

HPLC-UV/MS assay for the crude reaction mixture) for all substrates **5a−h**, and the corresponding 12-membered macrocycles **3a−h** were obtained as single diastereomers after purification by flash column chromatography (Scheme 3A). The desired *S* configuration at the quaternary stereogenic center was confirmed for the downstream macrocycle **14d** by single crystal X-ray analysis.[19] Hence, *S* configuration was assigned by analogy for all macrocycles **3a−h** in a series (Scheme 3A).

Disappointingly, the macrocyclization of homologue series **6a,b,i** proceeded with markedly reduced diastereoselectivities (62:38 dr for **4a**, 79:21 dr for **4b** and 85:15 dr for **4i**) and lower yields (32−59%, see Scheme 3B). Diastereomers of 13-membered macrocycles **4a,b,i** were not separated at this stage, and individual diastereomers were obtained for the downstream products **15a,b,i** after column chromatography. The assignment of relative configuration at the quaternary stereogenic center in macrocycles **15a,b,i** turned out to be a nontrivial task. NMR methods were not helpful due to the lack of useful H−H or C−H interactions near the stereogenic center in question. All attempts to grow single crystals for X-ray crystallography were also unsuccessful. Finally, the relative configuration at the stereogenic quaternary center in both diastereomers of **15i** was established by comparing experimental electronic circular dichroism (ECD) spectra with those calculated by DFT methods (see Supporting Information, page S19). The major diastereomer of **15i** was formed with *S* absolute configuration. By analogy, *S* configuration was assigned to all major diastereomers of 13-membered macrocycles **15a,b,i**.

Macrocycles **3a−h** and **4a,b,i** were converted into target structures **14a−h** and **15a,b,i**, respectively, in a two-step sequence comprising *N*-Boc cleavage and amide bond formation with (*S*)-hydroxyisovaleric acid (**13**). The methyl ester moiety in the bioxazole subunit of **14** was well-suited for further synthetic transformations, aimed at the increase of structural diversity for SAR studies. Accordingly, the saponification of the ester in **14a** afforded carboxylic acid **16** that was further converted into amide **17**. In the meantime,

direct aminolysis of ester **14a** afforded amides **18,19**. Bioxazole esters **20** and **21** were also obtained from **14b** by titanium isopropoxide-mediated transesterification (Scheme 3A). Aminolysis/amide dehydratation sequence allowed for the synthesis of cyanobioxazole **22** from ester **3a**. Subsequent TFA-mediated *N*-Boc cleavage and amide bond formation with (*S*)-hydroxyisovaleric acid (**13**) yielded cyanobioxazole **23** (Scheme 3C). Benzyl ester **24** was synthesized by Ti(O*i*Pr)$_4$-mediated transeterification, followed by *N*-Boc deprotection and amide coupling with (*S*)-hydroxyisovaleric acid. Finally, hydroxymethyl bioxazole **25** was obtained in a three-step sequence involving the reduction of methyl ester, *N*-Boc cleavage, and amide coupling.

The excellent macrocyclization diastereoselectivities observed for 12-membered series **3a−h** suggest a large energy difference between the two diastereomeric transition states for the S$_N$Ar-type cyclization. Indeed, DFT calculations using b3lyp/6-311++g(2d,p)//b3lyp/6-31+g(d) basis set demonstrated that energy of the TS leading to (*S*)-**3a** is 5 kcal/mol lower than that for the formation of diastereomeric (*R*)-**3a** (see Figure S5, page S23). Importantly, the formation of *S* isomers was also favored by 1 kcal/mol in homologue series **4a,b,i**. Of note, the calculated energy differences for diastereomeric TS of the S$_N$Ar-type cyclization matched perfectly the observed ratios of diastereomers for both macrocycles **3a−h** and **4a,b,i**. Hence, DFT calculation provided additional support for the *S* configuration at the quaternary center for both **3a−h** and **4a,b,i** series.

The highly diastereoselective intramolecular S$_N$Ar-type arylation of oxindoles **5a−h** prompted us to examine the C-alkylation of macrocycle (*S*)-**3g** as a convenient approach to the late-stage formation of quaternary stereogenic center. Gratifyingly, the alkylation of **3g** sodium enolate with a series of alkylating agents proceeded with high diastereoselectivity (from 86:14 dr to 92:8 dr; see Scheme 4). The observed diastereoselectivity matched the calculated energy difference of 1 kcal/mol between diastereomeric TS for the alkylation, with *S* isomer being the favored. The formation of the *S* isomer was later confirmed by the counter-synthesis of **14i** from (*S*)-**3b**
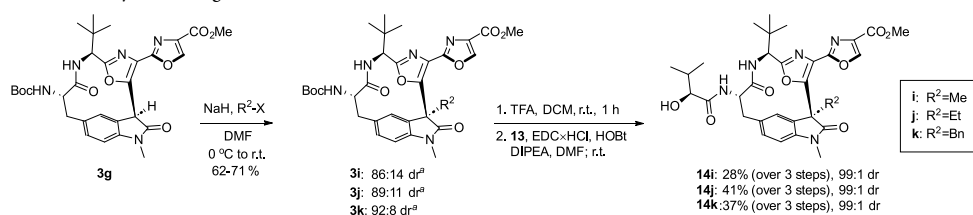
119

Scheme 3. Synthesis of Tubulin Binding Agents using Macrocyclization as the Key Step[ab]
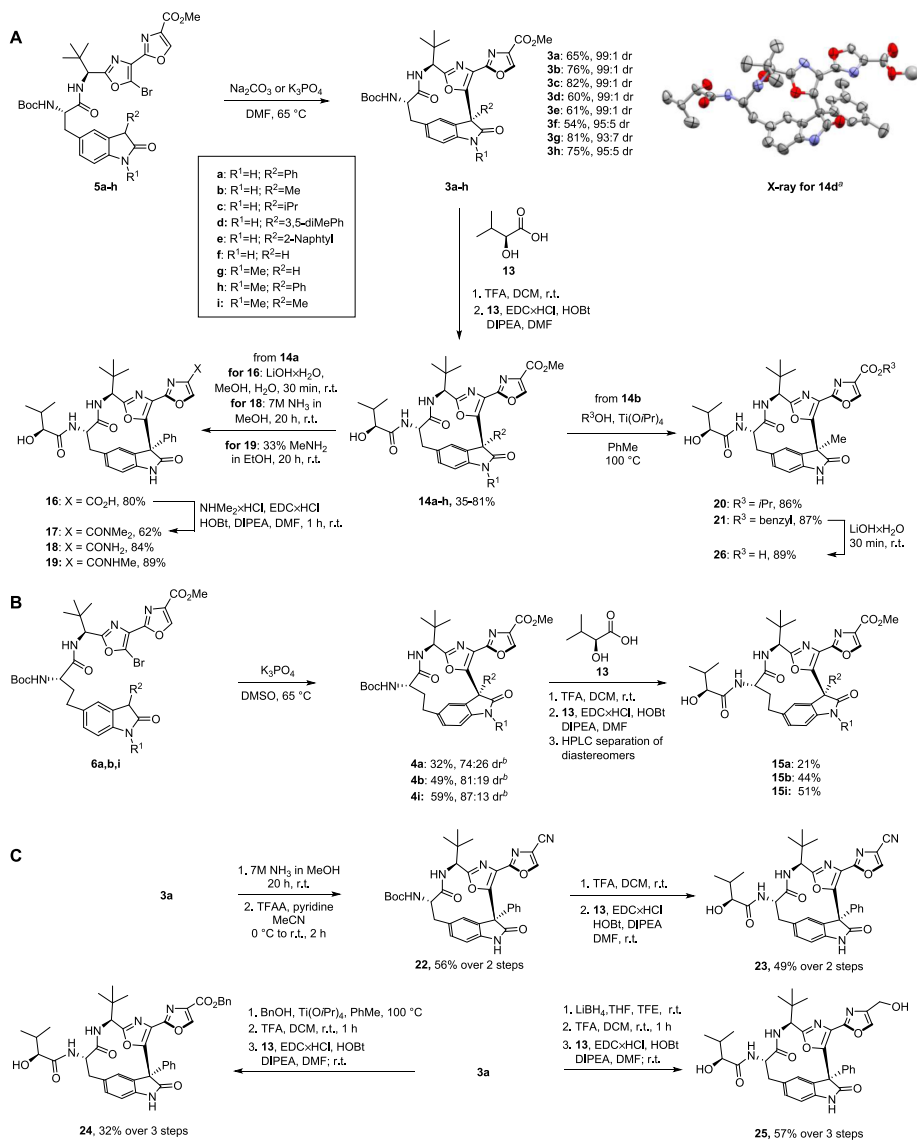
[a]Ellipsoids are shown at 50 probability, with hydrogen atoms omitted for clarity. [b]Diastereomeric purity of isolated product.

involving N-methylation, N-Boc deprotection, and amide bond formation with **13**. Identical NMR spectra for **14i** prepared by the C-alkylation route (from (S)-**3g**) and by the macrocyclization of **5b** provided compelling evidence for the formation of S isomers in the diastereoselective alkylation of **3g** sodium enolate.

Finally, macrocycle **27** with differently disconnected tetracycle was also synthesized for SAR studies using Sammakia's approach (Scheme 5).[8b] Accordingly, magnesium phenoxide

120

Scheme 4. Alkylation of 3g Sodium Enolate[a]

3g

NaH, R²-X
DMF
0 °C to r.t.
62-71 %

3i: 86:14 dr[a]
3j: 89:11 dr[a]
3k: 92:8 dr[a]

1. TFA, DCM, r.t., 1 h
2. **13**, EDC×HCl, HOBt
   DIPEA, DMF; r.t.

14i: 28% (over 3 steps), 99:1 dr
14j: 41% (over 3 steps), 99:1 dr
14k: 37% (over 3 steps), 99:1 dr

i: R²=Me
j: R²=Et
k: R²=Bn

[a]Diastereoselectivity of the alkylation.

Scheme 5. Synthesis of Macrocycle 27

28 + 29

MeMgBr
THF, DCM
50 °C, 20 h

30, 74%

PhN(Tf)₂
TEA
DCM
r.t., 1 h

31, 75 %

1. H₂, Pd/C, TEA
   EtOAc, r.t. 24 h
2. H₂, Pd/C
   MeOH, r.t. 6 d

32, 68% over 2 steps

1. LiOH
   MeOH, H₂O
   r.t., 1 h
2. **9**, EDC×HCl
   Pyridine, r.t., 3 h

33, 63% over 2 steps

Na₂CO₃
DMF
65 °C, 3 h

34, 69%, 85:15 dr

LiBH₄ THF, TFE
0 °C to r.t., 20 h

35, 90%

1. TFA, DCM, r.t., 3 h
2. **13**, EDC×HCl
   HOBt, DIPEA
   DMF, r.t.

27, 45% in two steps
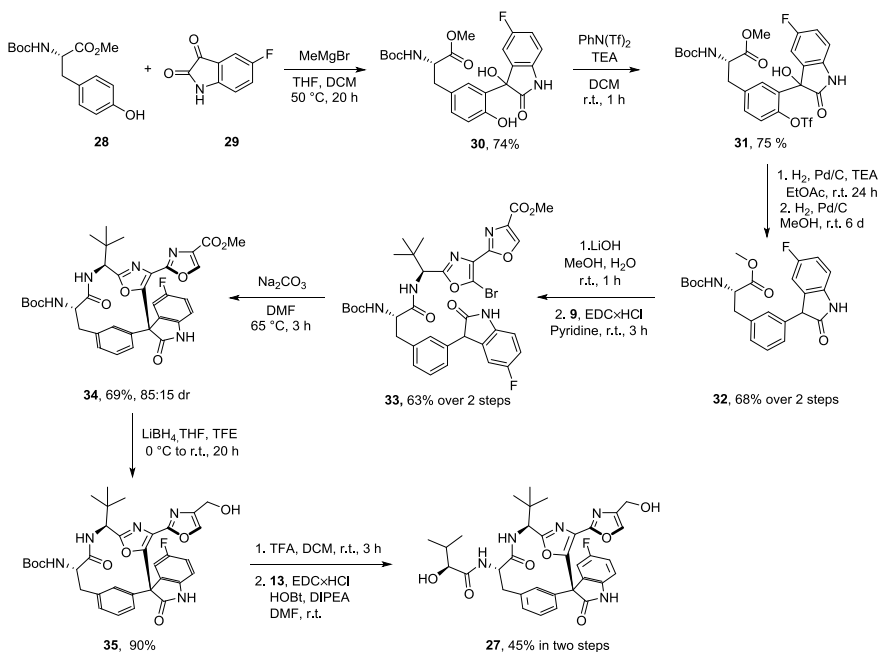
(prepared from **28** and MeMgBr) was added to unprotected isatin **29** to furnish adduct **30** in 74% yield (1:1 dr). Subsequent conversion of phenol **30** into triflate **31** by *N*-phenyl-bis(trifluoromethanesulfonimide (75% yield) was followed by Pd-catalyzed reductive cleavage of triflate (H₂, Pd/C, TEA, EtOAc) and hydrogenolysis of the resulting tertiary alcohol (H₂, Pd/C, MeOH) to deliver ester **32** (68%, 1:1 dr). Saponification with LiOH and coupling with bromo-bioxazole **9** provided macrocyclization precursor **33** (63% over two steps). Gratifyingly, the macrocyclization under Sammakia's conditions (Na₂CO₃ as a base in DMF) afforded the desired 12-membered macrocycle **34** as an 85:15 mixture of diastereomers (69% yield). Major diastereomer was obtained after chromatography, and absolute configuration at the quaternary stereogenic center was assigned *R* by analogy to Sammakia's work. The synthesis end-game involved the

reduction of ester moiety in **34** to alcohol **35**, *N*-Boc cleavage and amide bond formation with (*S*)-hydroxyisovaleric acid (**13**).

Biological Evaluation. *In Vitro Antiproliferative Activities.* All synthesized 12-membered macrocycles **14a–k**, **16–26**, and 13-membered homologues **15a,b,i** as well as *epi*-**15i** and macrocycle **27** were evaluated for their *in vitro* antiproliferative activity against four cancer cell lines (epithelial pancreatic carcinoma PANC-1, pancreatic carcinoma MiaPa-Ca-2, estrogen-positive breast adenocarcinoma MCF-7, and estrogen-negative breast adenocarcinoma MDA-MB-231) by the MTT assay with vinorelbine as the positive control (see Table 1). Noticeably, the antiproliferative activity of the tested compounds was influenced substantially by steric properties of substituent at the chiral quaternary stereogenic center. Thus, GI₅₀ values in the low micromolar to high nanomolar range

121

Table 1. *In Vitro* Antiproliferative Activity Data

14a–k, 16–26
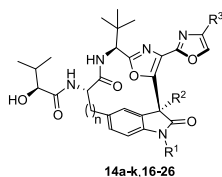
entry	compound	n	R^1	R^2	R^3	GI$_{50}$, μM			
						PANC-1	MiaPaCa-2	MCF-7	MDA-MB-231
1	vinorelbine	-	-	-	-	0.0030 ± 0.0004	0.0008 ± 0.0001	0.0039 ± 0.0004	0.0045 ± 0.0004
2	14a	1	H	Ph	CO$_2$Me	12 ± 2	0.67 ± 0.05	1.2 ± 0.3	8 ± 2
3	14b	1	H	Me	CO$_2$Me	11 ± 2	0.68 ± 0.09	0.53 ± 0.09	1.4 ± 0.3
4	14c	1	H	iPr	CO$_2$Me	>100	39 ± 3	>100	98 ± 11
5	14d	1	H	3,5-diMePh	CO$_2$Me	>100	>100	>100	>100
6	14e	1	H	2-Naphth	CO$_2$Me	36 ± 2	29 ± 5	67 ± 4	28 ± 3
7	14f	1	H	H	CO$_2$Me	>100	>100	89 ± 7	>100
8	14g	1	Me	H	CO$_2$Me	>100	54 ± 2	63 ± 7	>100
9	14h	1	Me	Ph	CO$_2$Me	1.2 ± 0.2	0.42 ± 0.07	0.39 ± 0.08	0.36 ± 0.02
10	14i	1	Me	Me	CO$_2$Me	4.5 ± 1.4	0.55 ± 0.02	0.75 ± 0.07	2.50 ± 0.14
11	14j	1	Me	Et	CO$_2$Me	13 ± 1	3.50 ± 0.62	2.86 ± 0.31	19 ± 4
12	14k	1	Me	Bn	CO$_2$Me	>100	95 ± 5	82 ± 1	54 ± 9
13	15a	2	H	Ph	CO$_2$Me	1.2 ± 0.3	0.46 ± 0.04	7.7 ± 0.3	0.26 ± 0.03
14	15b	2	H	Me	CO$_2$Me	>100	17 ± 2	12 ± 3	21 ± 3
15	15i	2	Me	Me	CO$_2$Me	>100	>100	15 ± 2	4.8 ± 1.3
16	*epi*-15i	2	Me	Me	CO$_2$Me	>100	>100	79 ± 6	75 ± 8
17	16	1	H	Ph	CO$_2$H	>100	38 ± 3	49 ± 1	93 ± 11
18	17	1	H	Ph	CONMe$_2$	>100	56 ± 3	74 ± 13	99 ± 1
19	18	1	H	Ph	CONH$_2$	>100	>100	98 ± 2	99 ± 1
20	19	1	H	Ph	CONHMe	>100	89 ± 13	44 ± 8	88 ± 5
21	20	1	H	Me	CO$_2$i-Pr	2.6 ± 0.1	0.18 ± 0.04	0.24 ± 0.01	21.8 ± 2.3
22	21	1	H	Me	CO$_2$Bn	6.5 ± 1.8	0.081 ± 0.006	0.044 ± 0.015	0.73 ± 0.17
23	23	1	H	Ph	CN	23 ± 3	1.9 ± 0.4	2.2 ± 0.1	6.1 ± 0.3
24	24	1	H	Ph	CO$_2$Bn	1.2 ± 0.1	0.15 ± 0.01	0.26 ± 0.1	2.1 ± 0.5
25	25	1	H	Ph	CH$_2$OH	68 ± 6	20 ± 5	16 ± 4	95 ± 11
26	26	1	H	Me	CO$_2$H	-	-	-	67.1 ± 1.1
27	27	-	-	-	-	>100	45 ± 9	96 ± 6	>100

were observed for phenyl and methyl group-containing macrocycles 14a and 14b (R^2 = Ph and Me; Table 1, entries 2 and 3, respectively). Analogues with sterically more demanding *i*-Pr group (entry 4) and aryl moieties (entries 5 and 6) featured several orders of magnitude weaker potency. On the other hand, tertiary stereogenic center-containing macrocycle 14f (R^2 = H, entry 7) also was virtually inactive. A similar SAR profile was also observed in *N*-Me indolinone series 14g–k (entries 8–12, Table 1), where phenyl and methyl-substituted analogues 14h and 14i showed superior antiproliferative activities (entries 9 and 10). Notably, an order of magnitude drop in potency was observed when going from methyl- (entry 10) to ethyl-substituted macrocycles (entry 11), and further increase of steric demand (R^2 = Bn, entry 12) led to the reduction of antiproliferative activity by another order of magnitude. Consistent with the SAR in *N*-Me indolinone series (entry 7), macrocycle 14g (R^2 = H, entry 8) was virtually inactive, pointing to the importance of quaternary stereogenic center for antiproliferative activity.

Next, SAR around the bioxazole substituent R^3 was explored using macrocycle series 14a, 16–19, and 23–25 with phenyl substituent at the quaternary stereogenic center (entries 2, 17–20, and 23–25, Table 1). The presence of ester functional group in the bioxazole subunit turned out to be critical for the antiproliferative effect with benzyl ester 24 being more potent than methyl ester 14a (entries 2 and 24). Carboxylic acid 16 (entry 17), the corresponding amides 17–19 (entries 18–20), as well as hydroxymethyl-substituted macrocycle 25 (entry 25) exerted 2 orders of magnitude weaker antiproliferative effect with GI$_{50}$ values spanning the low to high micromolar range. Likewise, nitrile 23 also showed inferior efficacy (entry 23, Table 1). The superiority of ester substituent at the bioxazole subunit was also observed in macrocycle series 14b, 20, 21, and 26, having methyl substituent at the quaternary stereogenic center (entries 3, 21, 22, and 26). Thus, benzyl ester 21 (entry 22) possessed the highest antiproliferative activity among all macrocycles tested against MCF-7 and MiaPaCa cancer cell lines. Isopropyl ester 20 (entry 21) featured reduced activity that was comparable to that of methyl ester 14b (entry 3), whereas carboxylic acid 26 (entry 26) showed virtually no antiproliferative activity against MDA-MB-231 cancer cell line.

Ring enlargement to 13-membered homologue 15a (R^2 = Ph, entry 13) helped to increase activity against MDA-MB-231

Table 2. *In Vitro* Antiproliferative Activities of Selected Series against Cancer Cell Lines and Non-cancerous Cells

entry	compound	GI$_{50}$, μM				
		U937	A2058	HCC-44	Hek293	GM08402
1	vinorelbine	0.0041 ± 0.0005	0.0024 ± 0.0002	0.0053 ± 0.0003	0.05 ± 0.01	>100
2	**14b**	0.084 ± 0.007	0.35 ± 0.01	2.38 ± 0.07	44 ± 8	53 ± 9
3	**14h**	0.043 ± 0.001	0.31 ± 0.03	1.25 ± 0.12	1.2 ± 0.3	>100
4	**14i**	0.098 ± 0.01	0.48 ± 0.01	1.52 ± 0.01	0.19 ± 0.01	>100
5	**15a**	0.0087 ± 0.001	0.049 ± 0.001	0.26 ± 0.02	10 ± 1	17 ± 3
6	**20**	0.031 ± 0.004	0.049 ± 0.005	0.22 ± 0.02	3.05 ± 0.02	>100
7	**21**	0.011 ± 0.001	0.0095 ± 0.0004	0.035 ± 0.002	1.67 ± 0.19	33 ± 3
8	**24**	0.014 ± 0.0004	0.080 ± 0.005	0.18 ± 0.01	n.d.	n.d.
9	**26**	12.3 ± 1.2	26.2 ± 1.3	n.d.	43.4 ± 1.2	n.d.

and PANC-1, while keeping comparable efficacy against MCF-7 and MiaPaCa cancer cell lines as compared to the 12-membered congener **14a** (entry 2). In contrast, considerable drop in the antiproliferative activity against all cell lines was observed when going from 12- to 13-membered macrocycles, possessing methyl group at the quaternary center (**15b** vs **14b**, entry 14 vs entry 3). Hence, the phenyl at quaternary center is superior substituent to the methyl group in the 13-membered macrocycle series.

Finally, antiproliferative activity of macrocycle **27** with differently disconnected tetracyclic subunit was compared to that of structurally related indoline congener **25** (Table 1, entries 25 and 27). Marcocycle **27** turned out to be less potent than **25** against all four cancer cell lines with the largest difference in antiproliferative activity measured for MCF-7 cancer cell line.

The influence of substituent at indolinone nitrogen (R^1 = H or Me) was pronounced only for macrocycles possessing Ph group at quaternary center, where *N*−Me analogue **14h** showed superior antiproliferative activity to that of its *N*−H counterpart **14a** (entries 9 vs entry 2). In contrast, similar levels of potency for *N*−Me/*N*−H pairs were observed in 12-membered macrocycle series (**14b** and **14i**; entries 3 and 10) as well as 13-membered homologues **15b** and **15i** (entries 14 and 15). Finally, the considerably higher antiproliferative effect exerted on MDA-MB-231 cell line by **15i** as opposed to its epimer *epi*-**15i** (entry 15 vs 16, respectively) highlighted the importance of configuration at the quaternary stereogenic center for the activity of macrocycles. Overall, the SAR study has helped to identify benzyl ester as the substituent of choice at bioxazole subunit. However, comparable activity of macrocycle series with Ph and Me substituents at quaternary center as well as those at indolinone nitrogen prompted us to continue SAR studies using additional cancer cell lines.

The antiproliferative efficacy of the best-performing macrocycles **14b,h,i**, **15a**, **20**, **21**, **24**, and carboxylic acid **26** as the assay negative control (Table 1) was further evaluated in a series of additional cancer cell lines (histiocytic lymphoma U-937, melanoma A-2058, and lung adenocarcinoma HCC-44) by the MTT assay with vinorelbine as the positive control (see Table 2). Gratifyingly, benzyl ester **21** possessing Me group at the quaternary center demonstrated the highest antiproliferative activity with GI$_{50}$ values in the low nanomolar range for all three cell lines (entry 7). Strikingly, phenyl-substituted benzyl ester **24** turned out to be an order of magnitude less potent against A2058 and HCC-44 cancer cell lines, albeit it was equipotent against U937 cell line (entry 8). As anticipated, isopropyl ester **20** (entry 6) as well as 13-membered macrocycle **15a** (entry 5) were slightly inferior to **21**. Methyl

esters **14b,h,i** (entries 2−4, Table 2) also showed a reduced antiproliferative effect. Consistent with the established SAR, carboxylic acid **26** exerted up to 3 orders of magnitude lower antiproliferative activity than the most efficient macrocyclic benzyl ester **21** (entry 9 vs 7).

The selectivity of toxicity for macrocycles **14b,h,i**, **15a**, **20**, and **21** was also evaluated using noncancerous cell lines such as human embryonic kidney cells (HEK-293) and human dermal fibroblast (GM08402; see Table 2). Surprisingly, *N*-methyl indolinone derivatives **14h,i** showed poor selectivity with antiproliferative activity levels in HEK-293 cells comparable to those in cancer cell lines (PANC-1 and HCC-34; see entries 3 and 4, Table 2). In contrast, *N*−H indolinones **14b**, **15a**, **20**, and **21** featured 1 to 3 orders of magnitude lower activity against noncancerous cells as compared to cancer cell lines. Similarly, high selectivity of toxicity was also observed for all macrocycles when human dermal fibroblast cells GM08402 were used.

Further, 12-membered macrocycles **14b** and **21** as well as 13-membered homologue **15a** were submitted to dose−response screening assay against 60 human tumor cell line panel NCI-60 (US National Cancer Institute) at five concentrations (ranging from 0.01 to 100 μM).[20] Macrocycles **15a** and **21** displayed submicromolar average GI$_{50}$ values whereas **14b** exhibited mean inhibitory activity at the micromolar range (Table 3, entries 1−3). Gratifyingly, despite considerable structural simplification, macrocycle **21** appears to be only ca. 10-fold less active than the natural diazonamide

Table 3. NCI-60 Dose−Response Data

entry	compound	NSC number	mean GI$_{50}$, μM	mean TGI, μM	mean LC$_{50}$, μM
1	**14b**	NSC #830922	4.1	>100[a]	>100[a]
2	**15a**	NSC #830921	0.38	>100[a]	>100[a]
3	**21**	NSC #831032	0.19	>11[b]	>100[a]
4	vinorelbine[c]	NSC #608210	0.018	4.2	52
5	paclitaxel[c]	NSC #125973	0.025	3.9	75
6	diazonamide **1a**[d]	NSC #700089	0.011	>10[e]	>10[e]

[a]TGI and LC$_{50}$ values exceeded the upper concentration limit (100 μM) for more than half of NCI-60 cell lines. [b]TGI values for 11 out of 59 cell lines exceeded the upper concentration limit of 100 μM. [c]Data from ref26. [d]Data from ref25. [e]TGI values exceeded the upper concentration limit (10 μM) for more than half and LC$_{50}$ for 90% of cell lines in NCI-60 panel.
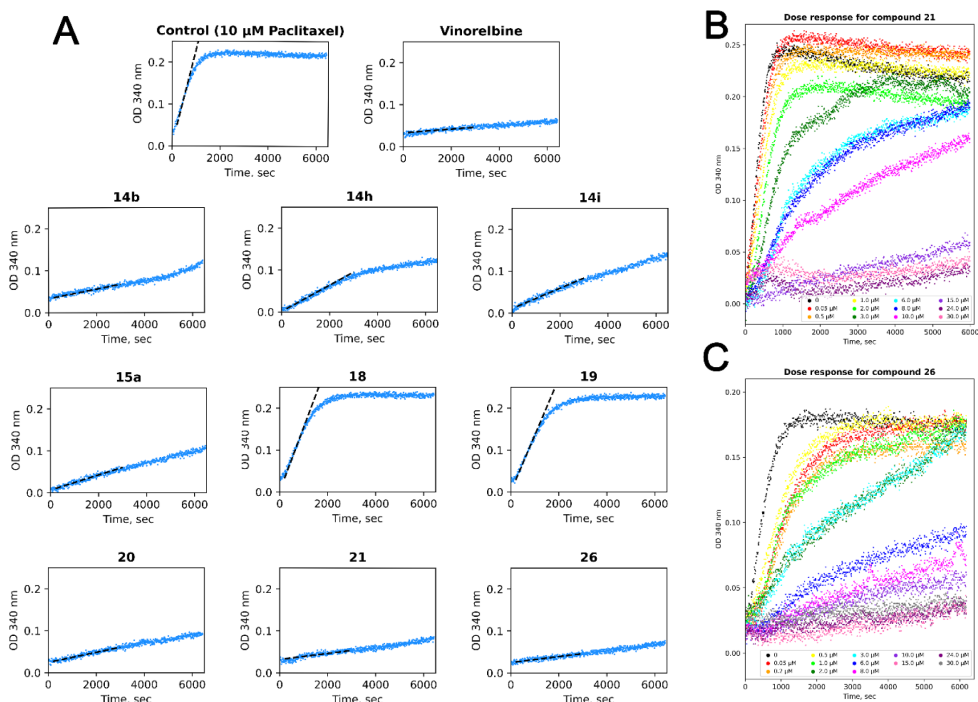
123

Figure 2. Enhancer control tubulin self-polymerization assay results for macrocycles **14b,h,i**, **15a**, **18−20**, **21**, **26**, and vinorelbine (A); dose-dependent inhibition of tubulin polymerization by benzyl ester **21** (B); dose-dependent inhibition of tubulin polymerization by acid **26** (C).

1a as well as marketed MTA vinorelbine and paclitaxel as evidenced by their mean GI_{50} values in NCI-60 panel (entry 3 vs entries 4−6). Moreover, antiproliferative activity within the same order of magnitude was observed for macrocycle **21** and diazonamide **1a** against 19 out of 60 cell lines in the NCI panel (see Table S1, page S15 for complete NCI data). For example, comparable GI_{50} values have been observed for **21** and **1a** in multiple myeloma cell line RPMI-8226 (31.6 nM vs 10.5 nM, respectively), large cell immunoblastic lymphoma SR (<10.0 nM vs 1.9 nM, respectively), human colon adenocarcinoma COLO 205 (50.1 nM vs 17.4 nM, respectively), human brain (astrocytoma) cell line SNB-75 (26.9 nM vs 40.7 nM, respectively), melanoma cancer cell lines MDA-MB-435 (<10.0 nM vs 2.9 nM, respectively), SK-MEL-2 (25.7 nM vs 11.2 nM, respectively), and UACC-62 (28.2 nM vs 19.1 nM, respectively), as well as ovarian cancer cell line OVCAR-8 (49.0 nM vs 14.5 nM, respectively) and renal carcinoma cell lines RXF-393 (21.4 nM vs 5.50 nM, respectively) and SN12C (38.0 nM vs 10.7 nM, respectively). Overall, the results of dose−response screening assay against NCI-60 panel cell lines (Table 3) are in line with our data (Tables 1 and 2) and point to the high antiproliferative potency of macrocycle **21**.

A difference between toxic concentrations of **21** (mean LC_{50} > 100 μM) and the concentration required for total growth inhibition (mean TGI > 11 μM) suggests that macrocycle **21** possibly possesses cytostatic rather than cytotoxic properties

(entry 3, Table 3).[21−23] Similar differences between LC_{50} and TGI concentrations have been determined for marketed tubulin-targeting agents vinorelbine and paclitaxel (entries 4 and 5, Table 3) that are inherently cytostatic because interference with microtubule dynamics leads to proliferation arrest.[24] Hence, NCI-60 data suggest that macrocycle **21** might act in a similar manner. In addition, macrocycle **21** demonstrated a differential cytotoxicity pattern, which was highly similar to that of paclitaxel and vinblastine (correlation coefficients 0.79 and 0.77, respectively as indicated by COMPARE algorithm).[20,25] Overall, the cytotoxicity pattern for macrocycle **21** and marketed MTA paclitaxel and vinblastine suggests that the measured antiproliferative activity of macrocyclic series is associated with their effect on microtubule dynamics.

Tubulin Polymerization Assay. An *in vitro* tubulin polymerization assay was performed to evaluate the effect of macrocycles on microtubule dynamics and stability. In the assay, paclitaxel-induced self-polymerization of soluble α/β-tubulin heterodimer to microtubules under buffered conditions was monitored in the presence or absence of the desired ligands by measuring changes in light scattering at 340 nm.[27,28] A slope was calculated for the linear growth phase of the tubulin polymerization curves to render a comparison vs the positive assembly control containing 10 μM paclitaxel (see Figure 2).[29] Paclitaxel-induced tubulin self-polymerization was

124

measured in the presence of the most cytotoxic macrocyclic esters **14b,h,i**, **15a**, **20**, **21**. In addition, poorly cytotoxic macrocycles such as amides **18,19** as well as carboxylic acid **26** were also examined to verify the correlation between antiproliferative activity of the macrocycles and effect they exert on tubulin polymerization dynamics. Finally, vinorelbine was also tested as a positive control of assembly inhibition (see Figure 2).

A good correlation between the inhibition of tubulin polymerization and *in vitro* antiproliferative activity was observed for macrocycles **14b,h,i**, **15a**, **18−21** (Table 4).

Table 4. Results of the Tubulin Polymerization Assay

entry	ligand[a]	slope[b]	R^2 fit	time span of R^2 fit, s
1	control	1.000	0.99	290−740
2	vinorelbine	0.023	0.83	110−6420
3	**14b**	0.060	0.95	110−5500
4	**14h**	0.155	0.97	516−3000
5	**14i**	0.120	0.99	316−6420
6	**15a**	0.090	0.98	316−6420
7	**18**	0.750	0.97	470−920
8	**19**	0.700	0.98	470−1835
9	**20**	0.060	0.97	110−6420
10	**21**	0.036	0.94	110−6420
11	**26**	0.035	0.94	110−6420

[a]At 15 μM concentration of ligand (2:1 tubulin:ligand ratio). [b]Slope values are relative to that of control (entry 1).

Thus, the most cytotoxic macrocycle **21** turned out to be the most potent inhibitor of tubulin polymerization across the series (entry 10, Table 4). Structurally related 12-membered macrocyclic esters **14b**, **20**, and 13-membered analogue **15a** also inhibited polymerization, albeit they were less efficient than macrocycle **21** (entries 3, 9, and 6, respectively). A further drop in inhibitory efficiency was observed for macrocycles **14h,i** (entries 4 and 5), and this observation is consistent with their reduced antiproliferative effect (cf. Table 2). Not surprisingly, poorly cytotoxic amides **18**, **19** were measured to be the least potent inhibitors in a series (entries 7 and 8, respectively). In striking contrast, acid **26** showed an inhibitory effect similar to that of the most efficient macrocycle **21** (entry 11 vs entry 10, Table 4) despite acid **26** displaying the lowest *in vitro* antiproliferative activity among all tested macrocycles (cf. Tables 1 and 2). The high inhibitory efficiency of tubulin polymerization observed for both **21** and the corresponding acid **26** prompted us to perform a dose-dependent tubulin polymerization assay for both macrocycles (Figure 2B,C). From the assay data, we were able to estimate IC$_{50}$ values for ester **21** (IC$_{50}$ = 2.30 μM) and acid **26** (IC$_{50}$ = 2.74 μM). The similar calculated IC$_{50}$ values confirm that both ester **21** and acid **26** are equally potent inhibitors of tubulin polymerization. The apparent lack of correlation between *in vitro* antiproliferative activity and efficiency in the tubulin polymerization assay for acid **26** led us to hypothesize that poor cell permeability could be responsible for the lack of *in vitro* activity (*vide infra*). Finally, vinorelbine strongly inhibited the polymerization of tubulin (entry 2, Table 4). Overall, the observed inhibition of tubulin polymerization in the presence of macrocycles **14b,h,i**, **15a**, **20**, **21** provides evidence that *in vitro* cytotoxicity effects are to be attributed to binding tubulin and inhibiting the assembly of microtubule networks within cells.

Differential cytotoxicity pattern data (determined from NCI-60 panel by the COMPARE algorithm) and tubulin polymerization assay results provided evidence that the antiproliferative effect for the structurally simplified diazonamide analogue series is exerted through regulation of microtubule dynamics in cells. To determine the binding affinity for tubulin, we employed an ultracentrigation/HPLC assay as described in the Experimental Section. We found that macrocycles **14a,b,h,i** and **15a** bind to tubulin with 20−80 μM affinity, showing a loss of 2 orders of magnitude in binding power in comparison to vinblastine (K_d = 0.54 μM).[30] In order to confirm the binding site of the macrocycles in tubulin, we performed competition experiments of vinblastine with **14a,b,h,i** and **15a** by using the ultracentrifugation/HPLC assay. We found that at equimolar 10 μM concentrations, the macrocycles weakly compete with vinblastine (less than 10% displacement as expected from their 2 orders of magnitude lower binding affinity). This is in agreement with previous reports of biotinylated diazonamide analogue **2**, which binding to tubulin was blocked in a dose−response manner by vinca domain MTA vinorelbine.[12] In addition, in the structural analysis, the apparent overlapping of binding sites for **2** and vinorelbine was confirmed by X-ray crystal structure of **2** bound at vinca domain of the tubulin heterodimer.[12] We also attempted the analysis of the binding site by X-ray crystallography. Unfortunately, very poor diffraction or poorly defined electron density at the tubulin interdimer interface was observed for crystals of T$_2$R-TTL (two α/β-tubulin dimers in complex with the stathmin-like protein RB3 and tubulin tyrosine ligase) that were soaked for different times with the most efficient macrocycles **21** and **26**. Although the density highlights perturbation at the vinca site, it is poorly defined and does not allow modeling of the correct pose of the compounds. Further work is ongoing at our laboratory to establish the binding site of macrocycles to tubulin/microtubules.

Effects of Macrocycle 21 on Cell Morphology. To further investigate the antiproliferative activity of macrocycle **21** and vinorelbine, morphological changes were examined in melanoma A2058 cells. Initially, cells were stained for tubulin (yellow) and DAPI (blue) (Figure 3). When treated with **21** and vinorelbine, the cells detached and became rounded. In the treatment groups, a substantially higher number of cells were stuck in metaphase, which further resulted in apoptosis and degradation (Figures 3 and 5). Thus, **21** and vinorelbine halted cell proliferation, and the cells entering the cell division phase became apoptotic within 4−48 h after the beginning of treatment (see also Figure 4). The remaining cells attached to the plate became substantially larger while polymerized tubulin structure remained intact. Overall, the arrest of the cell cycle and induction of apoptosis were similar in **21**- and vinorelbine-treated cells. Furthermore, the effects of compounds on mitochondria were tested using MitoTracker Deep Red. Both compounds **21** and vinorelbine did not affect the number of mitochondria and their morphology despite substantially increased cell size.

Evaluation of the Effect of Macrocycle 21 on the Cell Cycle. To investigate the antiproliferative mechanisms of **21**, the time-dependent effect on cell cycle distribution in melanoma A2058 cells was examined (Figure 4). In the control group, relative cell count at G1, S and G2 phases remained unchanged over 24 h period. The treatment with **21** and vinorelbine caused strong cell cycle arrest in the G2/M phase. The arrest of the cell cycle induced by both compounds
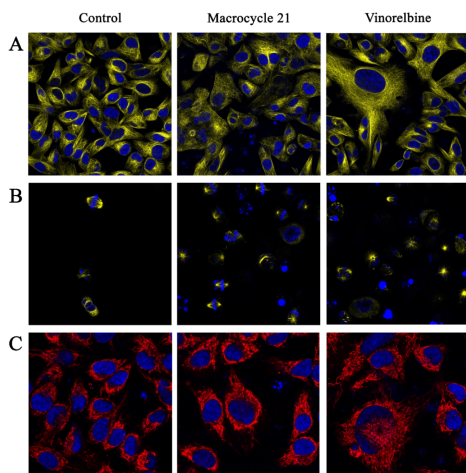
125

Figure 3. Melanoma A2058 cell morphology analysis after incubation with compound 21 (200 nM) and vinorelbine (10 nM). Cells were stained for tubulin (yellow) and Hoechst 33342 (blue) after 24 h incubation with and without compounds. Confocal images show attached cell (A) and floating cell (B) morphology. In the third panel (C), cells are stained with MitoTracker Deep Red to evaluate changes in the number of mitochondria and their structure.

was also time-dependent. A higher number of G2/M cells were evident already after 4 h treatment with **21** while two times more G2/M cells were counted after 24 h incubation period. Thus, after 24 h incubation in the presence of **21** and vinorelbine, approximately 40−50% of cells were arrested at the G2/M phase. Overall, macrocycle **21** (at 200 nM concentration) and vinorelbine (at 10 nM concentration) induced similar effects on the cell cycle.

Evaluation of the Compound-Induced Effects on Apoptosis. In the MTT assay, we observed a time-dependent loss of cell viability. Here, we evaluated apoptotic and necrotic cell death using PI and annexin staining and FACS counting. In the control cells without treatment, 5% necrotic and 15% apoptotic cells were counted. In the presence of **21** and vinorelbine, necrotic cell count gradually increased reaching 10% after 24 h incubation. This indicated that the antiproliferative effect of **21** was not related to the induction of necrotic cell death. Furthermore, incubation with compounds increased both early and late apoptotic cell count in a time-dependent manner. Thus, at the 24 h time point, apoptotic cells are about 40% (10% early and 30% late) of the total cell number in both treatment groups (Figure 5). These results confirm that similarly to vinorelbine, the antiproliferative effect of **21** occurs due to inhibited cell division and induction of apoptotic cell death due to arrested cell cycle.

Evaluation of Intracellular Uptake, Metabolism, and Efflux of Ester 21 and Acid 26. Intracellular uptake of macrocyclic benzyl ester **21** and the corresponding acid **26** was evaluated to address the observed lack of correlation between *in vitro* antiproliferative activity and efficiency in the tubulin polymerization assay for **26** (Figure 2, Table 4). To this end, melanoma A2058 cells were incubated with ester **21** or acid **26**

for up to 16 h. Already during the first 4 h of incubation with ester **21**, acid **26** reached high intracellular levels that decreased gradually over the 16 h incubation period. In sharp contrast, incubation with acid **26** at 5 times higher concentration (1000 nM) resulted in very low intracellular levels. The limited cellular uptake of acid **26** explains its poor antiproliferative effect. However, 2- to 3-fold higher intracellular concentration of the acid **26** as compared to that of the parent benzyl ester **21** at all time points suggests that metabolization of ester **21** to acid **26** occurs *inside* the melanoma A2058 cells that were incubated with ester **21** (Figure 6A). In the meantime, a gradual decrease of intracellular acid **26** concentration points to its slow metabolic degradation. Indeed, a degradation product with an exact mass of 479.18 Da was observed in A2058 cell lysate. The metabolite possibly corresponds to the cleavage of (*S*)-2-hydroxy-3-methylbutanoyl moiety in acid **26**. A small amount of the metabolite was detected already after 4 h of incubation, and the amount increased substantially after 16 h of incubation (see Supporting Information, page S17). In addition, slow efflux of ester **21** and acid **26** from A2058 cells to cell media was also observed (Figure 6B). Importantly, the increase in the concentration of acid **26** in cell media over 4 h is greater than the decrease in ester **21** concentration. This observation rules out the possibility that acid **26** concentration increases only because of ester **21** hydrolysis in cell media. Overall, the metabolism of ester **21** into acid **26** did not reduce the antiproliferative effect of **21** because both **21** and **26** exert a similar effect on tubulin polymerization.

■ CONCLUSIONS

In summary, a series of structurally simplified analogues of highly complex natural product diazonamide A were developed by the replacement of the challenging-to-synthesize tetracyclic subunit and removing the right-hand heteroaromatic macrocycle. The structurally simplified macrocycles are relatively easy to synthesize, and the most potent macrocycle **21** was obtained in 12 steps from readily available indolin-2-one and *tert*-leucine with excellent diastereoselectivity (99:1 dr) in the key macrocyclization step. Despite the considerably reduced structural complexity, macrocyle **21** possesses nanomolar antiproliferative activity against a range of tumor cell lines. In the meantime, **21** featured 1 to 3 orders of magnitude selectivity of toxicity against noncancerous cells such as HEK-293 and GM08402. Macrocycle **21** is a potent inhibitor of tubulin assembly, and it exerts similar effects to the marketed MTA vinorelbine on the cell cycle progression and induction of apoptosis in A2058 cell line. Even though in melanoma A2058 cells, macrocyclic ester **21** metabolizes into the corresponding acid **26**, the latter shows tubulin assembly inhibitory potency similar to that of the parent ester **21**. Taken together, our data provide strong evidence that the antiproliferative effect for the developed structurally simplified diazonamide A analogue series is to be attributed to binding tubulin and inhibiting the assembly of microtubule networks within cells. As such, our work demonstrates that a highly complex natural product can be structurally simplified while retaining the mechanism of action and high antitumor potency. Macrocycle **21** is a promising lead compound that deserves further development as a potential anticancer agent.
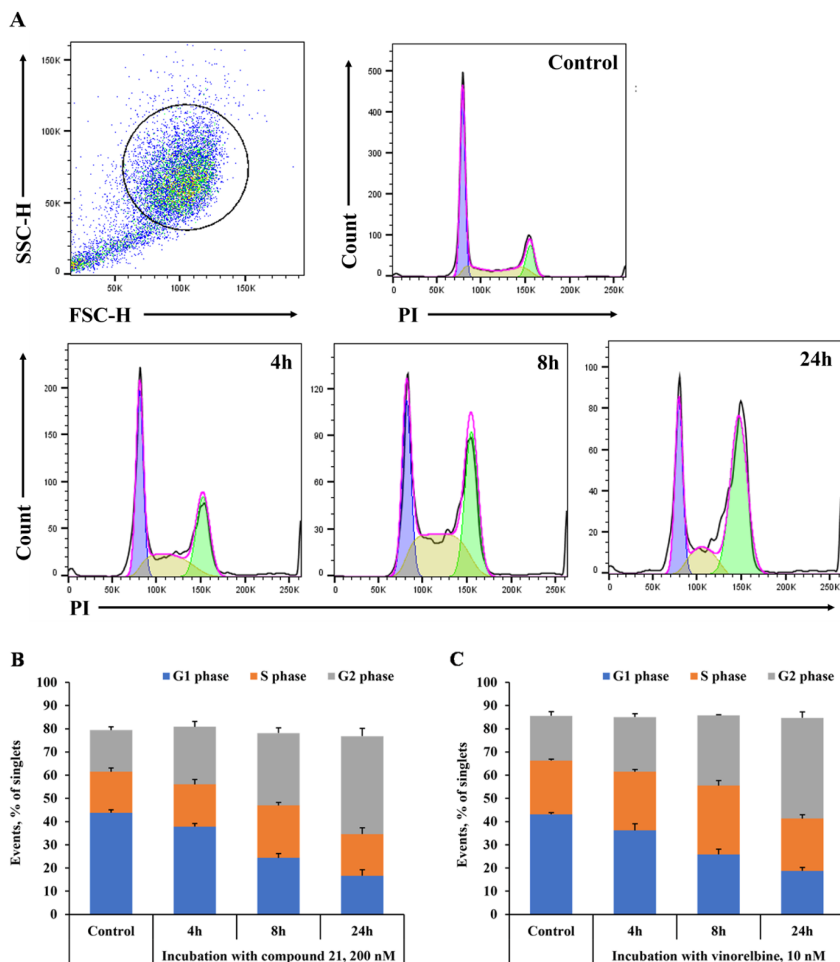
126

Figure 4. Flow cytometry analysis of cell cycle progression of A2058 cells after incubation with compound **21** (200 nM) for up to 24 h (A). Quantitative results of the effects of compound **21** on cell distribution among phases of the cell cycle (B) in comparison with equitoxic concentration (10 nM) of vinorelbine (C). The data are presented as the mean ± SEM of three independent experiments in triplicate.

■ EXPERIMENTAL SECTION

***In Vitro* Antiproliferative Activity.** MCF-7, PANC-1, MDA-MB-231, MIAPaCa-2, Hek293, A2058, and U937 cell lines were obtained from ATCC (Manassas, VA, USA). GM08402 was obtained from the Coriell Institute for Medical Research (Camden, NJ, USA). HCC44 was obtained from the DSMZ-German Collection, Leibniz institute (Braunschweig, Germany). MCF-7, PANC-1, MDA-MB-231, MIAPaCa-2, and A2058 cells were cultured in DMEM with 10% FBS and 1% penicillin−streptomycin. Hek293 and GM08402 cells were cultured in EMEM with 10% FBS and 1% penicillin−streptomycin. HCC44 and U937 cells were cultured in RPMI-1640 medium with 10% FBS and 1% penicillin−

streptomycin. Cells were cultivated in a 37 °C temperature with 5% CO_2, 95% air, and complete humidity. Cells were seeded in a 96-well plate in following concentrations: 5000 cells per well for MCF-7, PANC1, MDA-MB-231, MiaPaCa, Hek293, GM08402; 4000 cells per well for A2058, HCC44; 10000 cells per well for U937. The compounds were added to the cells (n = 6) in a serial dilution fashion. MTT assay was performed after 48 h of incubation.[31] All compounds were tested in two independent experiments for each cell line. The GI$_{50}$ values were calculated using Graph Pad Prism (GraphPad Software, Inc., La Jolla, CA, USA).

NCI-60 Assay. Compounds **14b**, **15a**, and **21** were submitted to NCI-60 human tumor cell line panel at US
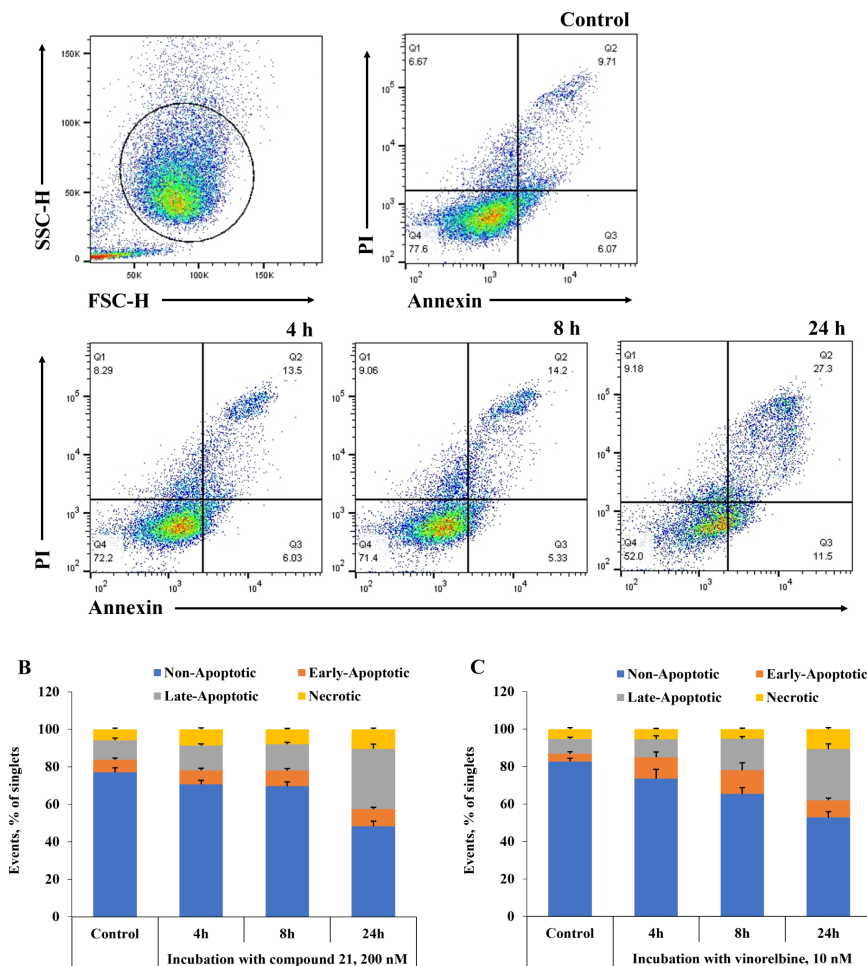
127

Figure 5. Representative plots from flow cytometry analysis of apoptosis after incubation with compound 21 (200 nM) for time points up to 24 h in A2058 cells (A). Effects of compound 21 on induction of apoptosis (B) in comparison with equitoxic concentration (10 nM) of vinorelbine (C). The data are presented as the mean ± SEM of three independent experiments in triplicate.

National Cancer Institute's Division of Cancer Treatment and Diagnosys (Bethesda, MD, USA). The assay was conducted at five doses (from 0.01 to 100 μM) according to the methodology described in literature.[32]

Tubulin Polymerization Assay. The assay was conducted as described in HTS-Tubulin Polymerization Assay Biochem Kit Cat. #BK004P in the presence of 10 μM Paclitaxel.[28] Commercial lyophilized tubulin (>99% pure tubulin protein, porcine brain, catalog number T240-D; Cytoskeleton, Inc.) was employed in the assay. Test compounds as well as control vinorelbine ditartrate (Sigma-Aldrich) were solubilized in DMSO at 2 mM and stored at 4 °C until used. Reagents and buffers: general tubulin buffer (80 mM PIPES pH 6.9, 2

mM $MgCl_2$, 0.5 mM EGTA), GTP (100 mM), G-PEM buffer (1 mM GTP in general tubulin buffer), cushion Buffer (60% v/v glycerol in general tubulin buffer), G-PEM Buffer plus 5% glycerol, paclitaxel (Acros Organics; was solubilized in DMSO at 2 mM and stored at 4 °C until used), tubulin protein (4 mg/mL — each vial of tubulin protein was reconstituted with 1 mL of ice cold G-PEM buffer plus 5% glycerol). Paclitaxel-induced assembly of tubulin was monitored in the presence of 10 μM of the desired ligand, prior to initiating the assay, the spectrophotometer Hidex Sense was set to 340 nm at 37 °C for performing a kinetic measurement. The plate was read kinetically for 60 min.
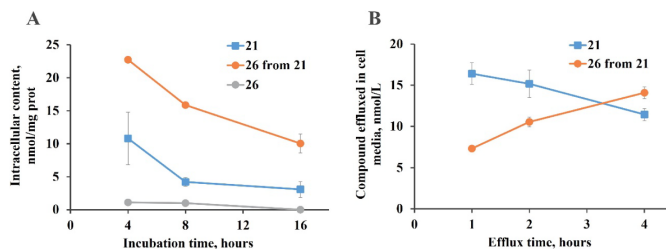
Figure 6. Intracellular uptake of **21** and **26** and the metabolism of **21** (A) as well as efflux from A2058 cells (B). Intracellular uptake of **21** and **26** was measured after incubation with compounds **21** (200 nM) and **26** (1000 nM) for 4−16 h in A2058 cells (A). In the uptake experiment for **21**, metabolism was also evaluated by measuring the concentration of **26** as the main metabolite of **21**. Efflux from A2058 cells was measured in cell media at 1−4 h time points after incubation with ester **21** for 4 h, washing, and addition of fresh cell media (without **21**). The data are presented as the mean ± SEM of three parallels.

Binding of the Compounds to Tubulin. Binding affinity and competition of the compounds for dimeric tubulin were determined using a cosedimentation assay. Briefly, a fixed concentration (10 μM) of the desired compounds was incubated with increasing amounts of dimeric tubulin (up to 100 μM) purified from calf brains as described in the literature[33] and lyophilized for storage. Tubulin was prepared in PEDTA buffer (10 mM NaPi pH 7.0, 1 mM EDTA, 1.5 mM MgCl$_2$, 0.1 mM GTP) and incubated with the compounds for 1/2 h at 25 °C. Samples were centrifuged at 100000 rpm in a TLA-100.2 rotor in an Optima-MAX-XP ultracentrifuge for 2 h at 25 °C. Then, samples were divided into upper (100 μL) and lower (100 μL) parts, and 20 μM noscapine was added to them as internal standard. Samples were subjected three times to an organic extraction using dichloromethane (v:v). Dichloromethane was removed by evaporation, and samples were resuspended in 45% 5 mM NaPi pH 6.0 − 55% acetonitrile. Finally, ligand content was analyzed using an HPLC system (Agilent 1100 Series), and samples were separated using a Zorbax Eclipse XDB C18 column (45% 5 mM NaPi pH 6.0 − 55% acetonitrile isocratic condition; 10 min runs). Competition experiments were performed at fixed concentrations of 10 μM of the desired compounds: 10 μM vinblastine (Sigma-Aldrich) and 10 μM dimeric tubulin.

Data coming out from the HPLC analysis were converted to molar saturation fraction and plotted against the concentration of free tubulin. Then, data were fitted to a one binding site model to obtain the binding constants of the compounds to tubulin.

Cell Morphology Studies. A2058 cells were seeded in ibidi 8-well μ-slides at a density of 1×10^5 cells/mL. The cells were then allowed to rest and adhere to the slides for 5 h. Subsequently, cells were treated with equitoxic concentrations (assessed in the cytotoxicity assay) of vinorelbine and **21** for 24 h. In parallel, cells were stained with SPY555-tubulin live cell fluorescent imaging of microtubules. After incubation and immediately before imaging, cell nuclei were stained with Hoechst 33342 (1 μg/mL final concentration) and MitoTracker Deep Red dye (100 nM final concentration). Live cell imaging was performed with Leica Stellaris 8 confocal microscope.

Cell Cycle Studies. A2058 cells were seeded in 24-well plates at a density of 1×10^5 cells/mL. The cells were then allowed to rest and adhere to the plate for 5 h. Subsequently,

cells were treated with equitoxic concentrations of vinorelbine and **21** for 4, 8, and 24 h.

To assess the distribution of cells between cell cycle phases, we performed cell cycle analysis using quantification of DNA content with the commercially available kit (Abcam, ab139418) according to the manufacturer's instructions. In brief, after incubation with the test compounds, cells were harvested using trypsin, washed with PBS, and fixed with 66% ice-cold ethanol. After fixation, cells were washed with PBS and incubated with propidium iodide (PI) (50 μg/mL) and RNase (550 U/mL) solution for 30 min in the dark at 37 °C. After incubation, the cells were transferred to ice and prepared for flow cytometry analysis using the BD FACS Melody Cell Sorter (BD Biosciences, San Jose, CA, USA). Quantitative results are expressed as the mean ± SEM. All experiments were carried out in triplicate with three technical replicates.

Compound-Induced Apoptosis. A2058 cells were seeded in 24-well plates at a density of 1×10^5 cells/mL. The cells were then allowed to rest and adhere to the plate for 5 h. Subsequently, cells were treated with equitoxic concentrations of vinorelbine and **21** for 4, 8, and 24 h.

To detect the mechanisms of A2058 cell death, we performed double staining using Annexin-V and PI.[34] After incubation with the test compounds, cells were harvested using trypsin, washed with PBS, and resuspended in 100 μL of staining buffer with Annexin V conjugated to APC (1:200) and PI (end concentration 2 μg/mL). The samples were incubated for 20 min in the dark at room temperature and then analyzed by flow cytometry. Quantitative results are expressed as the mean ± SEM. All experiments were carried out in triplicate with three technical replicates.

Intracellular Uptake, Metabolism, and Efflux. A2058 cells were seeded in 24-well plates at a density of 1×10^5 cells/ mL. The cells were then allowed to rest and adhere to the plate for 5 h. The cells were then treated with **21** (200 nM) and **26** (1000 nM) in a time-dependent manner for 4−16 h. After incubation, the cells were washed with PBS buffer solution and lysed with 0.1 N NaOH solution. To assess the potential efflux of compound **21** and its metabolite **26**, A2058 cells were incubated with **21** for 4 h. After the incubation, cells were washed 2 times with PBS, and fresh media were added. Sampling of the media was performed at time points from 1 up to 4 h. Concentrations of **21** and **26** in cell lysate or cell media samples were measured by liquid chromatography-tandem mass spectrometry (LC/MS/MS) in positive electrospray

129

ionization (ESI+) in multiple reaction monitoring (MRM) mode.

All analyses were performed on a Waters Acquity UPLC chromatograph coupled to Waters XEVO TQ-Smicro tandem mass spectrometer. Chromatographic separation was carried out on a Waters Acquity BEH C18 column (2.1 × 50 mm, 1.7 μm). Column temperature was 30 °C, flow rate was 0.4 mL/min. Linear gradient elution was applied, solvent A was 0.1% formic acid solution in water, and solvent B was acetonitrile. The gradient program was: 0 min −5% B; 2.5 min −95% B; 3.5 min −95% B; 3.7 min −5% B; 5 min −5% B. Injection volume was 5 μL.

Mass spectrometry parameters were obtained experimentally by direct infusion of standard solutions of compounds **21** and **26**. The quantification of each analyte was acquired with transitions of the protonated ion at m/z 670.4 → 339.1 (cone voltage 40 V, and collision energy 32 eV) for **21**, and m/z 580.2 → 435.2 (cone voltage 20 V and collision energy 30 eV) for **26**, respectively.

Compounds **21** and **26** were extracted from cell lysate or media by single-step protein precipitation. 500 μL of 3:1 acetonitrile/methanol mixture was added to 100 μL of spiked standard or analytical samples. Samples were vortex mixed for 1 min and centrifuged at 10000g for 10 min. Supernatants were collected, diluted 1:1 with 0.1% formic acid solution in water, and injected into the LCMS system. Data acquisition was carried out using the MassLynx 4.1 software (Waters Corp., Milford, MA, USA). Standardization of the uptake measurements was performed according to protein content in the sample, assessed by Lowry method.

■ CHEMISTRY

General. Unless otherwise noted, all chemicals were used as obtained from commercial sources, and all reactions were performed under argon atmosphere in oven-dried (120 °C) glassware. Anhydrous MeOH, pyridine, DMF, DMA, and DMSO were purchased from Acros. Anhydrous PhMe, Et$_2$O, THF, and DCM were obtained by passing commercially available solvent through activated alumina columns. Reactions were monitored by analytical TLC (precoated silica gel F-254 plates, Merck) or by UPLC-MS assay (Waters Acquity column: Acquity UPLC BEH-C18 (2.1 mm × 50 mm, 1.7 μm (30.0 ± 5.0) °C); gradient, 0.01% TFA in water/CH$_3$CN 90:10 to 0.01% TFA in water/CH$_3$CN 5:95; flow rate, 0.5 mL/min; run time, 8 min; detector, PDA (photodiode matrix), 220−320 nm, SQ detector with an electrospray ion source (APCI). Purification by preparative reverse phase chromatography was performed using a Waters Xbridge BEH C18 OBD column (5 μm, 10 × 150 mm) or Waters Atlantis Prep OBD T3 column (30 mm × 100 mm, 5 μm). All NMR spectra were recorded at 600, 400, or 300 MHz for ^{1}H NMR and 151, 101, or 75 MHz for ^{13}C NMR. Chemical shifts are reported in parts per million (ppm) relative to TMS or with the residual solvent peak as an internal reference. High-resolution mass spectra (HRMS) were recorded on a Waters Synapt G2-Si TOF MS instrument using the ESI technique. Specific rotation was recorded on a Kruss P3000 instrument. The purity of all target inhibitors was confirmed to be ≥95% by the reversed-phase ultrahigh-performance liquid chromatography−mass spectrometry (UPLC-MS) assay.

General Procedure A for the Addition of R^2 MgX to Isatin. A suspension of 5-iodoisatin in anhydrous THF was cooled to 0 °C (crushed ice bath) under argon atmosphere.

NaH (60% suspension in mineral oil) was added, and the resulting dark red slurry was stirred for 15 min. Solution of R^2 MgX was added dropwise, and the resulting red solution was stirred for 10 min at 0 °C, then warmed to room temperature, and left to stir for 18 h. Upon completion of the reaction, aqueous saturated NH$_4$Cl and EtOAc were added. Layers were separated, and water phase was extracted with EtOAc. Combined organic extracts were washed with brine, dried (Na$_2$SO$_4$), and evaporated to dryness under reduced pressure. Purification by column chromatography afforded 3-hydroxy-5-iodooxindole.

General Procedure B for Dehydratation of Hydroxy-Oxindole. Suspension of 3-hydroxy-5-iodooxindole and anhydrous SnCl$_2$ in glacial AcOH was heated at 100 °C with vigorous stirring. Upon full conversion (typically 16−48 h), the orange solution was cooled to room temperature and evaporated to dryness under the reduced pressure. The residue was dissolved in EtOAc, and aqueous saturated NaHCO$_3$ was added. The resulting biphasic suspension was filtered through a plug of Celite, and the filter cake was washed with additional EtOAc. Combined filtrates were separated, and the EtOAc layer was washed with aqueous saturated NaHCO$_3$, brine, dried (Na$_2$SO$_4$), and evaporated to dryness under reduced pressure.

General Procedure C for Negishi Cross-Coupling. Aryl iodide **10a−h**, Pd$_2$(dba)$_3$, and SPhos were dissolved in anhydrous DMF under argon atmosphere, and freshly prepared alkyl zinc iodide **11** (prepared as described in literature)[16] was added. The yellow solution was stirred at 65 °C until complete conversion (typically 2−48 h). Then, the solution was cooled to room temperature, and aqueous saturated NH$_4$Cl and EtOAc were added. Layers were separated, and EtOAc solution was washed with water and brine, dried (Na$_2$SO$_4$), and evaporated under reduced pressure to dryness. Pure products were obtained by column chromatography.

General Procedure D for the Formation of Amide from Methyl Ester. Methyl ester **7a−h** was dissolved in MeOH, and water mixture and stream of argon was passed through the solution for 20 min. Solid LiOH was added, and the clear solution was stirred at room temperature for 2 h, whereupon aqueous HCl (1 M) was added, and MeOH was evaporated under reduced pressure. The resulting suspension was extracted with EtOAc (three times), combined organic extracts were washed with brine, dried (Na$_2$SO$_4$), and concentrated *in vacuo*. To the resulting crude acid was added the corresponding amine, EDC × HCl in anhydrous pyridine. The resulting suspension was stirred at room temperature until complete conversion (typically 1−18 h), and the orange solution was evaporated under reduced pressure to dryness. The residue was dissolved in EtOAc and washed with aqueous HCl (1 M) and brine, dried (Na$_2$SO$_4$), and evaporated under reduced pressure. Pure products were obtained by column chromatography.

General Procedure E for Amide Formation from Benzyl Ester. Benzyl ester **8a,b,i** and Pd on carbon were suspended in EtOAc, and a stream of hydrogen gas was passed through the suspension for 3 h at room temperature. Then, the suspension was filtered through a plug of Celite, the filter cake was washed with EtOAc, and combined filtrates were evaporated under reduced pressure to dryness. To the crude acid was added amine **9**, EDC × HCl in anhydrous pyridine, and the resulting suspension was stirred at room temperature

130

until complete conversion (typically 4−16 h), whereupon the orange solution was evaporated under reduced pressure to dryness. The residue was dissolved in EtOAc and washed with aqueous HCl (1 M) and brine, dried ($MgSO_4$), and concentrated *in vacuo*. Pure products were obtained by column chromatography.

General Procedure F for Macrocyclization. Compound **5a−h** and an oven-dried base (K_2CO_3 or K_3PO_4) were suspended in anhydrous degassed DMF and a stream of argon was passed through the solution for 10 min. Then the suspension was stirred at 65 °C until complete conversion (typically 1−60 h), whereupon it was cooled to room temperature, quenched with aqueous saturated NH_4Cl and extracted with EtOAc (two times). Combined organic extracts were washed with brine, dried (Na_2SO_4) and evaporated under reduced pressure. Pure products were obtained by column chromatography.

General Procedure G (For Alkylation of Macrocycle). To ice ice-cold solution of macrocycle **3g** in anhydrous degassed DMF was added NaH (60% suspension in mineral oil), and the resulting solution was stirred for 15 min (*caution! gas evolution*), whereupon neat alkylating reagent was added dropwise. The resulting solution was left to stir at room temperature for 1 h and then diluted with aqueous saturated NH_4Cl and EtOAc. Layers were separated, and the organic phase was washed with brine, dried (Na_2SO_4), and evaporated under reduced pressure. Pure products were obtained by column chromatography.

General Procedure H for Boc Cleavage and Introduction of HiVA Side Chain. Neat TFA was added to a solution of intermediate **3a−h** or **4a,b,i** in anhydrous DCM. After stirring at room temperature until complete conversion (typically 1−48 h), the reaction mixture was evaporated under reduced pressure to dryness and redissolved in EtOAc. Layers were separated, and organic phase was washed with aqueous saturated $NaHCO_3$ and brine, dried (Na_2SO_4), and evaporated under reduced pressure to dryness. The yellow oily residue was dissolved in anhydrous DMF and (*S*)-2-hydroxy-3-methylbutanoic acid ((*S*)-2-hydroxy-3-methylbutanoic acid; **13**), EDC × HCl and HOBt were added followed by DIPEA. The solution was stirred at room temperature until complete conversion was achieved (typically 1−18 h) and then diluted with aqueous saturated NH_4Cl and EtOAc. Layers were separated, and the organic phase was washed with water and brine, dried (Na_2SO_4), and evaporated. Pure products were obtained by column chromatography.

*5-Iodo-3-phenyl-2,3-dihydro-1H-indol-2-one (**10a**).* Step 1: 3-hydroxy-5-iodo-3-phenyl-2,3-dihydro-1*H*-indol-2-one was prepared according to general procedure A from 5-iodoisatin (1.46 g; 5.33 mmol), NaH (60% suspension in mineral oil; 256 mg; 6.40 mmol; 1.2 equiv), PhMgBr (1 M solution in THF; 8.00 mL; 8.00 mmol; 1.5 equiv), and THF (30 mL) within 18 h. Purification by column chromatography on silica gel (gradient elution from 100% DCM to 10% MeOH in DCM) afforded 3-hydroxy-5-iodo-3-phenyl-2,3-dihydro-1*H*-indol-2-one (1.22 g, 65%) as a pale yellow amorphous solid. Step 2: compound **10a** was prepared according to general procedure B from 3-hydroxy-5-iodo-3-phenyl-2,3-dihydro-1*H*-indol-2-one (1.22 g; 3.48 mmol), $SnCl_2$ (1.65 g; 3.48 mmol; 2.5 equiv), and AcOH (20 mL) within 16 h. Product **10a** was obtained as a white amorphous solid (792 mg, 68%). ^1H NMR (400 MHz, DMSO-d_6): δ 10.65 (s, 1H), 7.56 (ddd, *J* = 8.1, 1.8, 0.9 Hz, 1H), 7.38−7.26 (m, 4H), 7.17−7.11 (m, 2H), 6.76 (d, *J* = 8.1

Hz, 1H), 4.79 (s, 1H). ^{13}C NMR (101 MHz, DMSO-d_6): δ 176.6, 142.5, 137.2, 136.6, 133.0, 132.9, 128.8, 128.3, 127.3, 112.0, 84.4, 51.6. HRMS-ESI (*m/z*) calcd for $C_{14}H_{11}NOI$ [M + H]$^+$ 335.9885; found: 335.9892.

*5-Iodo-3-methyl-2,3-dihydro-1H-indol-2-one (**10b**).* Step 1: 3-hydroxy-5-iodo-3-methyl-2,3-dihydro-1*H*-indol-2-one was prepared according to general procedure A from 5-iodoisatin (5.0 g; 18.3 mmol), NaH (60% suspension in mineral oil; 805 mg; 20.14 mmol; 1.1 equiv), methylmagnesium bromide (3 M in Et_2O; 6.71 mL; 20.14 mmol; 1.1 equiv), and THF (40 mL) within 18 h. Purification by column chromatography on silica gel (gradient elution from 100% DCM to 100% acetone) afforded 3-hydroxy-5-iodo-3-methyl-2,3-dihydro-1*H*-indol-2-one (2.92 g, 55%) as a pale yellow amorphous solid. Step 2: compound **10b** was prepared according to general procedure B from 3-hydroxy-5-iodo-3-methyl-2,3-dihydro-1*H*-indol-2-one (1.39 g; 4.80 mmol), $SnCl_2$ (2.28 g; 12.02 mmol; 2.5 equiv), and AcOH (20 mL) within 12 h. Purification by column chromatography on silica gel (gradient elution from 100% DCM to 60% EtOAc in DCM) afforded **10b** (990 mg, 75%) as a yellow amorphous solid. ^1H NMR (400 MHz, CDCl$_3$): δ 8.64 (s, 1H), 7.57−7.48 (m, 2H), 6.69 (d, *J* = 8.0 Hz, 1H), 3.46 (q, *J* = 7.7 Hz, 1H), 1.48 (d, *J* = 7.7 Hz, 3H). ^{13}C NMR (101 MHz, CDCl$_3$): δ 180.5, 141.0, 136.9, 133.8, 132.9, 111.8, 85.0, 41.0, 15.3. HRMS-ESI (*m/z*) calcd for C_9H_9NOI [M + H]$^+$ 273.9729; found: 273.9733.

*5-Iodo-3-(propan-2-yl)-2,3-dihydro-1H-indol-2-one (**10c**).* Step 1: 3-hydroxy-5-iodo-3-(propan-2-yl)-2,3-dihydro-1*H*-indol-2-one was prepared according to general procedure A from 5-iodoisatin (2.20 g; 8.06 mmol), NaH (60% suspension in mineral oil; 419 mg; 10.48 mmol; 1.3 equiv), isopropylmagnesium chloride (2 M in THF; 6.04 mL; 12.08 mmol; 1.5 equiv), and THF (15 mL) within 18 h. Purification by reverse phase column chromatography (gradient elution from 5% to 95% MeCN in water) afforded 3-hydroxy-5-iodo-3-(propan-2-yl)-2,3-dihydro-1*H*-indol-2-one (900 mg, 35%) as a red amorphous solid. Step 2: compound **10c** was prepared according to general procedure B from 3-hydroxy-5-iodo-3-(propan-2-yl)-2,3-dihydro-1*H*-indol-2-one (900 mg; 2.84 mmol), $SnCl_2$ (2.42 g; 12.77 mmol; 4.5 equiv), and AcOH (15 mL) in 48 h. Purification by reverse phase column chromatography (gradient elution from 5% to 95% MeCN in water) afforded **10c** (465 mg, 54%) as a pale red solid. ^1H NMR (400 MHz, DMSO-d_6): δ 10.43 (s, 1H), 7.55−7.49 (m, 2H), 6.66 (d, *J* = 8.0 Hz, 1H), 3.39 (d, *J* = 3.5 Hz, 1H), 2.32 (sept d, *J* = 6.9, 3.5 Hz, 1H), 0.93 (d, *J* = 6.9 Hz, 3H), 0.87 (d, *J* = 6.9 Hz, 3H). ^{13}C NMR (101 MHz, DMSO-d_6): δ 177.5, 142.9, 136.1, 132.5, 131.4, 111.4, 84.0, 50.9, 29.9, 18.9, 18.3. HRMS-ESI (*m/z*) calcd for $C_{11}H_{13}NOI$ [M + H]$^+$ 302.0042; found: 302.0043.

*3-(3,5-Dimethylphenyl)-5-iodo-2,3-dihydro-1H-indol-2-one (**10d**).* Step 1: 3-(3,5-dimethylphenyl)-3-hydroxy-5-iodo-2,3-dihydro-1*H*-indol-2-one was prepared according to general procedure A from 5-iodoisatin (1.46 g; 5.33 mmol), NaH (60% suspension in mineral oil; 256 mg; 6.40 mmol; 1.2 equiv), 3,5-dimethylphenylmagnesium bromide (1 M in THF; 8.00 mL; 8.00 mmol; 1.5 equiv), and THF (30 mL) within 18 h. Purification by column chromatography on silica gel (gradient elution from 100% DCM to 10% MeOH in DCM) afforded 3-(3,5-dimethylphenyl)-3-hydroxy-5-iodo-2,3-dihydro-1*H*-indol-2-one (1.38 g, 69%) as a pale yellow amorphous solid. Step 2: compound **10d** was prepared according to general procedure B from 3-(3,5-dimethylphenyl)-3-hydroxy-

5-iodo-2,3-dihydro-1*H*-indol-2-one (1.35 g; 3.56 mmol), SnCl₂ (1.55 g; 8.19 mmol; 2.30 equiv), and AcOH (30 mL) within 17 h. Product **10d** was obtained as a white amorphous solid (1.05 g, 81%). ¹H NMR (400 MHz, DMSO-*d₆*): δ 10.61 (s, 1H), 7.55 (ddd, *J* = 8.1, 1.8, 0.9 Hz, 1H), 7.26−7.23 (m, 1H), 6.93−6.91 (m, 1H), 6.75 (d, *J* = 8.1 Hz, 1H), 6.73−6.70 (m, 2H), 4.67 (s, 1H), 2.23 (s, 6H). ¹³C NMR (101 MHz, DMSO-*d₆*): δ 176.7, 142.5, 137.8, 137.1, 136.5, 133.3, 132.7, 128.7, 126.0, 111.9, 84.3, 51.6, 20.8. HRMS-ESI (*m/z*) calcd for C₁₆H₁₃NOI [M − H]⁻ 362.0042; found: 362.0051.

5-Iodo-3-(naphthalen-2-yl)-2,3-dihydro-1H-indol-2-one (10e). Step 1: 3-hydroxy-5-iodo-3-(naphthalen-2-yl)-2,3-dihydro-1*H*-indol-2-one was prepared according to general procedure A from 5-iodoisatin (1.46 g, 5.33 mmol), NaH (60% suspension in mineral oil; 256 mg; 6.40 mmol; 1.2 equiv), 2-naphtylmagnesium bromide (1 M in THF; 8.00 mL; 8.00 mmol; 1.5 equiv), and THF (30 mL) within 18 h. Purification by column chromatography on silica gel (gradient elution from 100% DCM to 10% MeOH in DCM) afforded 3-hydroxy-5-iodo-3-(naphthalen-2-yl)-2,3-dihydro-1*H*-indol-2-one (1.90 g, 89%) as a pale yellow amorphous solid. Step 2: compound **10e** was prepared according to general procedure B from 3-hydroxy-5-iodo-3-(naphthalen-2-yl)-2,3-dihydro-1*H*-indol-2-one (1.87 g; 4.66 mmol), SnCl₂ (2.03 g; 10.72 mmol; 2.3 equiv), and AcOH (25 mL) within 28 h. Product **10e** was obtained as a white amorphous solid (1.03 g, 57%). ¹H NMR (400 MHz, DMSO-*d₆*): δ 10.73 (s, 1H), 7.93−7.85 (m, 3H), 7.77−7.73 (m, 1H), 7.59 (ddd, *J* = 8.1, 1.8, 0.9 Hz, 1H), 7.55−7.47 (m, 2H), 7.35−7.31 (m, 1H), 7.19 (dd, *J* = 8.5, 1.8 Hz, 1H), 6.81 (d, *J* = 8.1 Hz, 1H), 4.98 (s, 1H). ¹³C NMR (101 MHz, DMSO-*d₆*): δ 176.6, 142.6, 136.7, 134.7, 133.04, 132.99, 132.9, 132.1, 128.5, 127.6, 127.5, 127.3, 126.4, 126.2, 126.1, 112.0, 84.5, 51.8. HRMS-ESI (*m/z*) calcd for C₁₈H₁₃INO [M + H]⁺ 386.0042; found: 386.0052.

5-Iodo-2,3-dihydro-1H-indol-2-one (10f). It was synthesized as described in the literature.[35] Thus, a solution of 2-oxindole (300 mg; 2.25 mmol) and NIS (608 mg; 2.70 mmol; 1.2 equiv) in glacial acetic acid (2.5 mL) was stirred at room temperature for 2 h, whereupon water (10 mL) was added. The formed precipitate was filtered, washed with water, and dried on filter. The red powder was then washed with EtOAc to yield **10f** (275 mg, 47%) as a beige amorphous solid. ¹H NMR (300 MHz, DMSO-*d₆*): δ 10.45 (s, 1H), 7.54−7.46 (m, 2H), 6.65 (d, *J* = 8.0 Hz, 1H), 3.48 (s, 2H). ¹³C NMR (101 MHz, DMSO-*d₆*): δ 175.7, 143.5, 135.9, 132.7, 128.8, 111.5, 83.8, 35.5. HRMS-ESI (*m/z*) calcd for C₈H₇NOI [M + H]⁺ 259.9572; found: 259.9573.

5-Iodo-1-methyl-2,3-dihydro-1H-indol-2-one (10g). It was synthesized as described in the literature.[36] Accordingly, NaH (60% in mineral oil; 879 mg; 22.0 mmol; 1.2 equiv) was added to a precooled (0 °C) solution of 5-iodoisatin (5.0 g; 18.3 mmol) in anhydrous DMF (40 mL). The resulting dark purple solution was stirred 10 min, then MeI (1.37 mL; 3.12 mmol; 1.2 equiv) was added, and the reaction mixture was warmed to room temperature. After stirring for 18 h, water was added. The dark red solid was filtered through a sintered glass filter, washed on filter with water, hexanes, and dried on air. The solid was dissolved in hydrazine hydrate (34.0 mL; 0.70 mol; 40.0 equiv), and the clear green solution was heated at 120 °C for 3 h. The appearance of the solution gradually changed to yellow suspension. After cooling to room temperature, water (100 mL) and EtOAc (100 mL) were added, and layers were separated. Organic layer was washed with aqueous 1 M HCl

and brine, dried (MgSO₄), and filtered through a sintered glass filter. The clear red filtrate was evaporated to dryness, redissolved in small amount of hot MeOH, and cooled to room temperature. The formed orange amorphous powder was filtered to afford compound **10g** (3.50 g, 69%). ¹H NMR (400 MHz, DMSO-*d₆*): δ 7.62−7.58 (m, 1H), 7.57−7.54 (m, 1H), 6.81 (d, *J* = 8.2 Hz, 1H), 3.54 (s, 2H), 3.08 (s, 3H). ¹³C NMR (101 MHz, DMSO-*d₆*): δ 173.7, 144.8, 135.9, 132.4, 127.6, 110.6, 84.7, 34.8, 25.9. HRMS-ESI (*m/z*) calcd for C₉H₉NOI [M + H]⁺ 273.9729; found: 273.9735.

5-Iodo-1-methyl-3-phenyl-2,3-dihydro-1H-indol-2-one (10h). 3-Hydroxy-5-iodo-3-phenyl-2,3-dihydro-1*H*-indol-2-one (1.0 g, 3.7 mmol) in anhydrous DMF (15 mL) was cooled to 0 °C (crushed ice bath), and NaH (60% dispersion in mineral oil; 285 mg; 7.1 mmol; 2.5 equiv) was added in one portion turning the suspension into red slurry. After stirring the resulting red slurry for 5 min, iodomethane (0.53 mL; 8.5 mmol; 3.0 equiv) was added, and stirring at 0 °C was continued for 30 min. The suspension turned green and then to yellow over time. The resulting suspension was stirred at room temperature for 18 h. After completion, it was poured into aqueous saturated NH₄Cl and extracted with EtOAc (3 × 50 mL). Combined organic layers were washed with water, brine, dried (MgSO₄), and concentrated under reduced pressure to give crude 5-iodo-3-methoxy-1-methyl-3-phenyl-2,3-dihydro-1*H*-indol-2-one (1.05 g, 99%), which was used in the next step without further purification. The title compound **10h** was prepared according to general procedure B from crude 5-iodo-3-methoxy-1-methyl-3-phenyl-2,3-dihydro-1*H*-indol-2-one (730 mg; 2.00 mmol), SnCl₂ (758 mg; 4.00 mmol; 2.0 equiv), and AcOH (10 mL) within 16 h. Purification by column chromatography on silica gel (gradient elution from 100% DCM to 5% MeOH in DCM) afforded **10h** (500 mg, 72%) as a yellow amorphous solid. ¹H NMR (400 MHz, CDCl₃): δ 7.65 (ddd, *J* = 8.2, 1.8, 0.9 Hz, 1H), 7.44 (t, *J* = 1.5 Hz, 1H), 7.38−7.27 (m, 3H), 7.20−7.14 (m, 2H), 6.68 (d, *J* = 8.2 Hz, 1H), 4.59 (s, 1H), 3.23 (s, 3H). ¹³C NMR (101 MHz, CDCl₃): δ 175.3, 144.3, 137.4, 136.0, 133.8, 131.4, 129.2, 128.5, 128.0, 110.3, 85.3, 51.9, 26.6. HRMS-ESI (*m/z*) calcd for C₁₆H₁₃INO [M + H]⁺ 350.0042; found: 350.0054.

5-Iodo-1,3-dimethyl-2,3-dihydro-1H-indol-2-one (10i). 3-Hydroxy-5-iodo-3-methyl-2,3-dihydro-1*H*-indol-2-one (150 mg, 0.52 mmol) was dissolved in anhydrous DMF (3 mL) and cooled to 0 °C, whereupon NaH (60% dispersion in mineral oil; 52 mg; 1.3 mmol; 2.5 equiv) was added in one portion. The resulting red slurry was stirred for 5 min, and then iodomethane (100 μL; 1.56 mmol; 3 equiv) was added. After stirring at 0 °C for 30 min, the resulting purple suspension was warmed to room temperature and stirred for 18 h. After completion, it was poured into aqueous saturated NH₄Cl and extracted with EtOAc (3 × 20 mL). Combined organic extracts were washed with water, brine, dried (MgSO₄), and concentrated under reduced pressure to give crude 5-iodo-3-methoxy-1,3-dimethyl-2,3-dihydro-1*H*-indol-2-one (160 mg, 97%), which was used in the next step without further purification. The title compound **10i** was prepared according to general procedure B from 5-iodo-3-methoxy-1,3-dimethyl-2,3-dihydro-1*H*-indol-2-one (95 mg; 0.31 mmol), SnCl₂ (149 mg; 0.78 mmol; 2.5 equiv), and AcOH (4 mL) within 48 h. Purification by column chromatography on silica gel (gradient elution from 100% hexanes to 80% EtOAc in hexanes) afforded **10i** (51 mg, 57%) as a yellow amorphous solid. ¹H NMR (400 MHz, CDCl₃): δ 7.58 (ddd, *J* = 8.1, 1.8,

0.8 Hz, 1H), 7.52−7.50 (m, 1H), 6.60 (d, J = 8.1 Hz, 1H), 3.41 (q, J = 7.6 Hz, 1H), 3.17 (s, 3H), 1.45 (d, J = 7.6 Hz, 3H). ^{13}C NMR (101 MHz, CDCl$_3$): δ 177.9, 143.8, 136.8, 133.1, 132.5, 110.1, 85.0, 40.5, 26.3, 15.4. HRMS-ESI (m/z) calcd for C$_{10}$H$_{11}$INO [M + H]$^+$ 287.9885; found: 287.9890.

Methyl (2S)-2-{[(tert-Butoxy)carbonyl]amino}-3-(2-oxo-3-phenyl-2,3-dihydro-1H-indol-5-yl)propanoate (7a). The title compound was prepared according to general procedure C from oxindole **10a** (800 mg; 2.39 mmol), alkyl zincate **11** (0.5 M in DMF; 5.25 mL; 2.63 mmol; 1.1 equiv), Pd$_2$(dba)$_3$ (22 mg; 0.024 mmol; 0.01 equiv), SPhos (39 mg; 0.096 mmol; 0.04 equiv), and DMF (6 mL) in 3 h. Purification by column chromatography on silica gel (gradient elution for 20% to 50% EtOAc in hexanes) afforded **7a** (800 mg, 82%; dr 3:2) as a yellow amorphous solid. ^{1}H NMR (400 MHz, CDCl$_3$): δ 8.51 (s, 1H), 7.39−7.27 (m, 3H), 7.22−7.16 (m, 2H), 7.04−6.96 (m, 1H), 6.90−6.82 (m, 2H), 5.03−4.92 (m, 1H), 4.60 (s, 0.6 H), 4.59 (s, 0.4 H) 4.57−4.45 (m, 1H), 3.64 (s, 1H), 3.53 (s, 2H), 3.09−2.92 (m, 2H), 1.41 (s, 5H), 1.37 (s, 4H). ^{13}C NMR (101 MHz, CDCl$_3$): δ 178.81, 178.79, 172.5, 172.2, 155.2, 155.1, 140.8, 136.54, 136.52, 130.6, 130.5, 130.2, 129.5, 129.4, 129.12, 129.09, 128.62, 128.59, 127.8, 126.2, 110.1, 110.0, 80.1, 54.8, 54.7, 52.82, 52.80, 52.3, 52.2, 38.3, 38.0, 28.4. HRMS-ESI (m/z) calcd for C$_{23}$H$_{26}$N$_2$O$_5$Na [M + Na]$^+$ 433.1739; found 433.1735.

Methyl (2S)-2-{[(tert-Butoxy)carbonyl]amino}-3-(3-methyl-2-oxo-2,3-dihydro-1H-indol-5-yl)propanoate (7b). The title compound was prepared according to general procedure C from oxindole **10b** (415 mg; 1.52 mmol), alkyl zincate **11** (0.5 M in DMF; 8.05 mL; 4.03 mmol; 2.7 equiv), Pd$_2$(dba)$_3$ (28 mg; 0.030 mmol; 0.02 equiv), SPhos (31 mg; 0.076 mmol; 0.05 equiv), and DMF (6 mL) in 2 h. Purification by column chromatography on silica gel (gradient elution from 20% to 70% EtOAc in hexanes) was followed by reverse phase column chromatography (gradient elution from 15% to 70% MeCN in water) afforded **7b** (410 mg, 77%; dr 1:1) as beige amorphous solid. ^{1}H NMR (400 MHz, CDCl$_3$): δ 8.88 (s, 0.5H), 8.79 (s, 0.5H), 7.00−6.91 (m, 2H), 6.82 (s, 0.5H), 6.80 (s, 0.5H), 5.11−4.96 (m, 1H), 4.64−4.48 (m, 1H), 3.71 (s, 3H), 3.48−3.35 (m, 1H), 3.17−2.92 (m, 2H), 1.47 (d, J = 3.6 Hz, 1.5H), 1.46 (d, J = 3.6 Hz, 1.5H), 1.41 (s, 9H). ^{13}C NMR (101 MHz, CDCl$_3$): δ 181.32, 181.26, 172.5, 172.4, 155.13, 155.05, 140.2, 131.6, 131.6, 130.11, 130.07, 128.8, 128.7, 124.8, 109.7, 80.0, 54.7, 52.3, 52.2, 41.0, 38.13, 38.06, 28.3, 15.2. HRMS-ESI (m/z) calcd for C$_{18}$H$_{23}$N$_2$O$_5$ [M − H]$^-$: 347.1607; found 347.1606.

Methyl (2S)-2-{[(tert-Butoxy)carbonyl]amino}-3-[2-oxo-3-(propan-2-yl)-2,3-dihydro-1H-indol-5-yl]propanoate (7c). The title compound was prepared according to general procedure C from oxindole **10c** (380 mg; 1.26 mmol), alkyl zincate **11** (0.5 M in DMF; 3.79 mL; 1.89 mmol; 1.5 equiv), Pd$_2$(dba)$_3$ (12 mg; 0.013 mmol; 0.01 equiv), SPhos (21 mg; 0.051 mmol; 0.04 equiv), and DMF (6 mL) in 2 h. Purification by reverse phase column chromatography (gradient elution from 5% to 95% MeCN in water) afforded **7c** (256 mg, 54%; dr 1:1) as yellow oil. ^{1}H NMR (400 MHz, CDCl$_3$): δ 8.77 (s, 1H), 7.01 (s, 1H), 6.95 (d, J = 7.9 Hz, 1H), 6.80 (d, J = 7.9 Hz, 1H), 5.09−4.97 (m, 1H), 4.61−4.50 (m, 1H), 3.702 (s, 1.5H), 3.699 (s, 1.5H), 3.35 (t, J = 3.7 Hz, 1H), 3.14−2.95 (m, 2H), 2.47 (sept d, J = 7.0, 3.4 Hz, 1H), 1.41 (s, 4.5H), 1.40 (s, 4.5H), 1.14−1.08 (m, 3H), 0.89 (d, J = 7.0, 3H). ^{13}C NMR (101 MHz, CDCl$_3$): δ 180.0, 172.5, 155.2, 155.1, 141.2, 129.7, 128.8, 128.8, 128.7, 125.8, 125.8, 109.63, 109.60, 80.1, 54.8,

54.7, 52.4, 52.2, 38.3, 38.1, 30.9, 28.4, 20.2, 20.1, 18.0. HRMS-ESI (m/z) calcd for C$_{20}$H$_{29}$N$_2$O$_5$ [M + H]$^+$ 377.2076; found 377.2069.

Methyl (2S)-2-{[(tert-Butoxy)carbonyl]amino}-3-[3-(3,5-dimethylphenyl)-2-oxo-2,3-dihydro-1H-indol-5-yl]propanoate (7d). The title compound was prepared according to general procedure C from **10d** (1.00 g; 2.75 mmol), alkyl zincate **11** (0.5 M in DMF; 6.61 mL; 3.30 mmol; 1.2 equiv), Pd$_2$(dba)$_3$ (25 mg; 0.028 mmol; 0.01 equiv), SPhos (57 mg; 0.14 mmol; 0.05 equiv), and DMF (6 mL) in 48 h. Purification by column chromatography on silica gel (gradient elution from 10% to 40% EtOAc in hexanes) afforded **7d** (900 mg, 75%; dr 1:1) as yellow amorphous solid. ^{1}H NMR (300 MHz, CDCl$_3$): δ 8.24 (s, 1H), 7.05−6.95 (m, 1H), 6.91 (s, 1H), 6.88−6.82 (m, 2H), 6.78 (s, 2H), 5.05−4.88 (m, 1H), 4.57−4.43 (m, 2H), 3.63 (s, 1.5 H), 3.53 (s, 1.5 H), 3.10−2.93 (m, 2H), 2.28 (s, 6H), 1.42 (s, 4.5 H), 1.37 (s, 4.5H). ^{13}C NMR (101 MHz, CDCl$_3$): δ 178.9, 178.8, 172.5, 172.2, 155.2, 155.1, 140.7, 138.7, 136.4, 136.3, 130.62, 130.60, 130.5, 130.4, 129.64, 129.59, 129.4, 129.3, 126.41, 126.38, 126.3, 109.93, 109.87, 80.1, 54.9, 54.7, 52.82, 52.77, 52.3, 52.1, 38.4, 38.1, 28.5, 28.4, 21.42, 21.39. HRMS-ESI (m/z) calcd for C$_{25}$H$_{30}$N$_2$O$_5$Na [M + Na]$^+$ 461.2052; found 461.2053.

Methyl (2S)-2-{[(tert-Butoxy)carbonyl]amino}-3-[3-(naphthalen-2-yl)-2-oxo-2,3-dihydro-1H-indol-5-yl]propanoate (7e). The title compound was prepared according to general procedure C from oxindole **10e** (600 mg; 1.56 mmol), alkyl zincate **11** (0.5 M in DMF; 3.43 mL; 1.71 mmol; 1.1 equiv), Pd$_2$(dba)$_3$ (43 mg; 0.047 mmol; 0.03 equiv), SPhos (51 mg; 0.12 mmol; 0.08 equiv), and DMF (16 mL) in 18 h. Purification by column chromatography on silica gel (gradient elution from 20% to 50% EtOAc in hexanes) followed by reverse phase column chromatography (gradient elution from 30% to 70% MeCN in water) afforded **7e** (319 mg, 45%; dr ∼1:1) as white amorphous solid. ^{1}H NMR (400 MHz, CDCl$_3$): δ 8.66 (s, 0.5H), 8.61 (s, 0.5H), 7.87−7.78 (m, 3H), 7.74−7.71 (m, 0.5H), 7.71−7.67 (m, 0.5H), 7.52−7.43 (m, 2H), 7.29−7.23 (m, 1H, overlaps with CDCl$_3$) 7.04−6.97 (m, 1H), 6.91−6.83 (m, 2H), 5.05−4.92 (m, 1H), 4.77 (s, 0.5H), 4.75 (s, 0.5H), 4.57−4.45 (m, 1H), 3.62 (s, 1.5H), 3.46 (s, 1.5H), 3.10−2.90 (m, 2H), 1.40 (s, 5H), 1.29 (s, 4H). ^{13}C NMR (101 MHz, CDCl$_3$): δ 178.4, 178.3, 172.3, 172.1, 155.1, 154.9, 140.7, 140.6, 133.8, 133.7, 133.6, 133.5, 132.9, 132.8, 130.6, 130.5, 129.94, 129.90, 129.5, 129.4, 128.91, 128.87, 127.9, 127.66, 127.65, 127.6, 126.4, 126.3, 126.11, 126.09, 126.0, 109.92, 109.89, 80.0, 79.9, 54.7, 54.5, 52.8, 52.7, 52.2, 52.1, 38.2, 37.9, 28.3, 28.2. HRMS-ESI (m/z) calcd for C$_{27}$H$_{28}$N$_2$O$_5$Na [M + Na]$^+$ 483.1896; found 483.1883.

Methyl (2S)-2-{[(tert-Butoxy)carbonyl]amino}-3-(2-oxo-2,3-dihydro-1H-indol-5-yl)propanoate (7f). The title compound was prepared according to general procedure C from 5-iodo-2-oxindole **10f** (100 mg; 0.39 mmol), alkyl zincate **11** (0.5 M in DMF; 1.16 mL; 0.58 mmol; 1.5 equiv), Pd$_2$(dba)$_3$ (7 mg; 0.008 mmol; 0.02 equiv), SPhos (8 mg; 0.02 mmol; 0.05 equiv), and DMF (2 mL) in 42 h. Purification by column chromatography on silica gel (gradient elution from 0% to 100% EtOAc in hexanes) afforded **7f** (64 mg, 50%) as orange solid. ^{1}H NMR (300 MHz, CDCl$_3$): δ 8.05 (s, 1H), 7.04−6.90 (m, 2H), 6.78 (d, J = 7.9 Hz, 1H), 5.00 (d, J = 8.3 Hz, 1H), 4.59−4.48 (m, 1H), 3.72 (s, 3H), 3.50 (s, 2H), 3.09 (dd, J = 13.9, 5.9 Hz, 1H), 2.98 (dd, J = 13.9, 5.9 Hz, 1H), 1.41 (s, 9H). ^{13}C NMR (101 MHz, CDCl$_3$): δ 177.5, 172.5, 155.2, 141.6, 130.2, 128.9, 125.7, 109.7, 80.2, 54.8, 52.4, 38.2, 36.3,

133

28.4. HRMS-ESI (m/z) calcd for $C_{17}H_{22}N_2O_5Na$ [M + Na]$^+$ 357.1426; found 357.1423. $[\alpha]_D^{20}$ 77.0 (c 1.0, CHCl$_3$).

Methyl (2S)-2-{[(tert-Butoxy)carbonyl]amino}-3-(1-methyl-2-oxo-2,3-dihydro-1H-indol-5-yl)propanoate (7g). The title compound was prepared according to general procedure C from oxindole **10g** (4.00 g; 12.82 mmol), alkyl zincate **11** (0.5 M in DMF; 30.00 mL; 15.00 mmol; 1.2 equiv), Pd$_2$(dba)$_3$ (117 mg; 0.13 mmol; 0.01 equiv), SPhos (132 mg; 0.32 mmol; 0.03 equiv), and DMF (50 mL) in 2 h. Purification by column chromatography on silica gel (gradient elution from 0% to 100% EtOAc in hexanes) afforded **7g** (3.86 g, 86%) as yellow amorphous solid. ^{1}H NMR (400 MHz, CDCl$_3$): δ 7.04−6.99 (m, 2H), 6.72 (d, J = 8.0 Hz, 1H), 5.00 (d, J = 8.3 Hz, 1H), 4.57−4.49 (m, 1H), 3.71 (s, 3H), 3.47 (s, 2H), 3.17 (s, 3H), 3.08 (dd, J = 13.9, 5.7 Hz, 1H), 2.99 (dd, J = 13.9, 6.0 Hz, 1H), 1.40 (s, 9H). ^{13}C NMR (101 MHz, CDCl$_3$): δ 175.0, 172.4, 155.2, 144.3, 130.2, 128.8, 125.4, 124.9, 108.1, 80.1, 54.7, 52.4, 38.2, 35.8, 28.4, 26.3. HRMS-ESI (m/z) calcd for $C_{18}H_{25}N_2O_5$ [M + H]$^+$ 349.1763; found 349.1771. $[\alpha]_D^{20}$ 7.7 (c 1.0, MeOH).

Methyl (2S)-2-{[(tert-Butoxy)carbonyl]amino}-3-(1-methyl-2-oxo-3-phenyl-2,3-dihydro-1H-indol-5-yl)propanoate (7h). The title compound was prepared according to general procedure C from **10h** (490 mg; 1.40 mmol), alkyl zincate **11** (0.5 M in DMF; 3.65 mL; 1.82 mmol; 1.3 equiv), Pd$_2$(dba)$_3$ (19 mg; 0.021 mmol; 0.02 equiv), SPhos (23 mg; 0.056 mmol; 0.04 equiv), and DMF (5 mL) in 2 h. Purification by column chromatography on silica gel (gradient elution from 35% to 65% EtOAc in hexanes) afforded **7h** (550 mg, 92%; dr 1:1) as off-white amorphous solid. ^{1}H NMR (400 MHz, CDCl$_3$): δ 7.36−7.30 (m, 2H), 7.30−7.25 (m, 1H), 7.21−7.15 (m, 2H), 7.12−7.05 (m, 1H), 6.92−6.88 (m, 1H), 6.82 (d, J = 7.9 Hz, 1H), 5.01−4.97 (m, 1H), 4.58 (s, 0.5H), 4.56 (s, 0.5H), 4.56−4.46 (m, 1H), 3.64 (s, 1.5H), 3.53 (s, 1.5H), 3.23 (s, 3H), 3.14−2.94 (m, 2H), 1.42 (s, 4.5H), 1.38 (s, 4.5H). ^{13}C NMR (101 MHz, CDCl$_3$): δ 176.0, 172.4, 172.2, 155.2, 155.1, 143.6, 136.69, 136.67, 130.7, 130.5, 129.5, 129.4, 129.3, 129.1, 129.0, 128.6, 128.5, 127.7, 126.2, 126.1, 108.3, 108.2, 80.11, 80.06, 54.9, 54.7, 52.3, 52.24, 52.18, 52.16, 38.4, 38.0, 28.5, 28.4, 26.7. HRMS-ESI (m/z) calcd for $C_{24}H_{29}N_2O_5$ [M + H]$^+$ 425.2076; found 425.2076.

1-Benzyl 1,3-Dioxo-2,3-dihydro-1H-isoindol-2-yl (2S)-2-{[(tert-butoxy)carbonyl]amino}pentanedioate (12). N-Boc-L-Glu-OBn (2.00 g; 5.93 mmol), N-hydroxyphthalimide (967 mg; 5.93 mmol; 1.0 equiv), and DMAP (72 mg, 0.59 mmol; 0.1 equiv) were suspended in anhydrous DCM (35 mL) under argon atmosphere. N,N'-diisopropylcarbodiimide (1.02 mL; 6.52 mmol, 1.10 equiv) was added, and the light yellow suspension was left to stir for 12 h at room temperature, whereupon the bright yellow heterogeneous mixture was filtered through a plug of Celite. Filter cake was washed with DCM, and combined filtrates were concentrated under reduced pressure. The crude product was purified by column chromatography on silica gel (gradient elution from 100% to 40% Et$_2$O in DCM) to yield **12** (2.32 g, 81%) as a colorless thick oil that solidified upon standing. ^{1}H NMR (400 MHz, CDCl$_3$) δ 7.92−7.85 (m, 2H), 7.82−7.76 (m, 2H), 7.40−7.30 (m, 5H), 5.28−5.15 (m, 3H), 4.52−4.38 (m, 1H), 2.74 (qdd, J = 17.0, 9.3, 6.1 Hz, 2H), 2.43−2.29 (m, 1H), 2.18−2.06 (m, 1H), 1.44 (s, 9H). ^{13}C NMR (101 MHz, CDCl$_3$) δ 171.7, 169.0, 161.9, 155.5, 135.2, 134.9, 129.0, 128.8, 128.7, 128.5, 124.1, 80.4, 67.6, 52.8, 28.4, 27.8, 27.5. HRMS-ESI (m/z)

calcd for $C_{25}H_{26}N_2O_8Na$ [M + Na]$^+$ 505.1587; found 505.1591. $[\alpha]_D^{20}$ +7 (c 2.0, CHCl$_3$).

Benzyl (2S)-2-{[(tert-Butoxy)carbonyl]amino}-4-(2-oxo-3-phenyl-2,3-dihydro-1H-indol-5-yl)butanoate (8a). Aryl iodide **10a** (300 mg; 0.90 mmol), redox-active ester **12** (648 mg; 1.34 mmol; 1.5 equiv), and zinc dust (117 mg; 1.79 mmol; 2 equiv) were suspended in anhydrous DMA (4.5 mL) under argon atmosphere. In a separate vessel, NiCl$_2$ × glyme (20 mg; 0.090 mmol; 0.1 equiv) and dtbbpy (24 mg; 0.090 mmol; 0.1 equiv) were dissolved in anhydrous DMA (0.5 mL) under argon atmosphere and stirred at room temperature for 15 min. Then, the blue-green catalyst solution was added to the reaction mixture, and the resulting green suspension was stirred at room temperature for 18 h, whereupon aqueous saturated NH$_4$Cl and EtOAc were added. Layers were separated, and aqueous layer was extracted with EtOAc. Combined organic extracts were washed with saturated NH$_4$Cl and brine, dried (MgSO$_4$), and evaporated under the reduced pressure. The residue was purified by reverse phase column chromatography (gradient elution from 10% to 100% MeCN in water). Fractions containing product were combined and additionally purified by column chromatography on silica (gradient elution from 100% to 20% Et$_2$O in DCM) to afford **8a** (103 mg, 23%, 1:1 d.r.) as white foam. ^{1}H NMR (400 MHz, CDCl$_3$): δ 8.30 (s, 1H), 7.40−7.27 (m, 8H), 7.23−7.15 (m, 2H), 7.02−6.93 (m, 1H), 6.87−6.82 (m, 1H), 6.81 (d, J = 8.0 Hz, 1H), 5.24−5.02 (m, 3H), 4.56 (d, J = 4.6 Hz, 1H), 4.40−4.31 (m, 1H), 2.63−2.43 (m, 2H), 2.13−2.00 (m, 1H), 1.94−1.79 (m, 1H), 1.43 (s, 9H). ^{13}C NMR (101 MHz, CDCl$_3$): δ 178.4, 172.6, 155.4, 139.8, 136.6, 135.47, 135.46, 135.4, 130.0, 129.11, 129.10, 129.0, 128.7, 128.64, 128.60, 128.55, 128.51, 128.45, 127.8, 125.6, 125.5, 109.8, 80.1, 67.21, 67.18, 53.3, 52.8, 34.9, 34.8, 31.33, 28.4. HRMS-ESI (m/z) calcd for $C_{30}H_{32}N_2O_5Na$ [M + Na]$^+$ 523.2209; found 523.2222.

Benzyl (2S)-2-{[(tert-Butoxy)carbonyl]amino}-4-(3-methyl-2-oxo-2,3-dihydro-1H-indol-5-yl)butanoate (8b). NiCl$_2$ × glyme (40 mg; 0.18 mmol; 0.1 equiv) and dtbbpy (49 mg; 0.18 mmol; 0.1 equiv) were dissolved in anhydrous DMA (2.5 mL) under argon atmosphere, and the resulting blue-colored solution was stirred at room temperature for 20 min. In a separate flask, zinc dust (300 mg; 4.58 mmol; 2.5 equiv) was heated by a heat gun for 2 min and then cooled under argon atmosphere to room temperature. The heating/cooling sequence was repeated twice, whereupon anhydrous DMA (2.5 mL) was added via septa, followed by iodine (47 mg; 0.18 mmol; 0.1 equiv), and the resulting brown suspension was stirred at room temperature until the color faded (approximately 20 min). To the suspension was then added solid aryl iodide **10b** (500 mg; 1.83 mmol), followed by the previously prepared blue-colored catalyst solution. Then, to the yellow suspension was portionwise added redox-active ester **12** (1.06 g; 2.20 mmol; 1.2 equiv) in anhydrous DMA (1.5 mL) within a course of 10 h. After the addition was completed, the moss-green solution was stirred 8 h at room temperature and quenched by aqueous saturated NH$_4$Cl and EtOAc. Layers were separated, and the water layer was extracted with EtOAc. Combined organic extracts were washed with saturated NaHCO$_3$ and brine, dried (MgSO$_4$), and evaporated under reduced pressure. Purification by reverse phase column chromatography (gradient elution from 10% MeCN in water to 100% MeCN) afford **8b** (283 mg, 35%, dr 1:1) as a yellow amorphous solid. ^{1}H NMR (400 MHz, CDCl$_3$): δ 8.16 (s, 1H), 7.40−7.30 (m, 5H), 6.97−6.91 (m, 2H), 6.77 (d, J = 7.8

Hz, 1H), 5.26−5.06 (m, 3H), 4.43−4.34 (m, 1H), 3.39 (q, J = 7.4 Hz, 1H), 2.67−2.50 (m, 2H), 2.17−2.07 (m, 1H), 1.97− 1.86 (m, 1H), 1.51−1.38 (m, 12H). ^{13}C NMR (101 MHz, CDCl$_3$): δ 181.3, 173.0, 155.8, 139.7, 135.8, 135.3, 131.9, 129.1, 129.0, 128.8, 128.2, 124.5, 109.9, 80.5, 67.5, 53.7, 41.4, 35.2, 31.7, 28.8, 15.7. HRMS-ESI (m/z) calcd for C$_{25}$H$_{30}$N$_2$O$_5$Na [M + Na]$^+$ 461.2052; found 461.2053.

Benzyl (2S)-2-{[(tert-Butoxy)carbonyl]amino}-4-(1,3-dimethyl-2-oxo-2,3-dihydro-1H-indol-5-yl)butanoate (8i). NiCl$_2$ × glyme (40 mg; 0.18 mmol; 0.1 equiv) and dtbbpy (49 mg; 0.18 mmol; 0.1 equiv) were dissolved in anhydrous DMA (2.5 mL) under argon atmosphere, and the resulting blue-colored solution was stirred at room temperature for 20 min. In a separate flask, zinc dust (300 mg; 4.58 mmol; 2.5 equiv) under vacuum was heated by a heat gun for 2 min and then cooled under argon atmosphere to room temperature. The heating/cooling sequence was repeated twice, whereupon anhydrous DMA (2.5 mL) was added via septa followed by iodine (47 mg; 0.18 mmol; 0.1 equiv), and the resulting brown suspension was stirred at room temperature until the color faded (approximately 20 min). To the suspension was then added solid aryl iodide 10i (500 mg; 1.83 mmol) followed by the previously prepared blue-colored catalyst solution. Then, to the yellow suspension was portionwise added the redox-active ester 12 (1.06 g; 2.20 mmol; 1.2 equiv) in anhydrous DMA (1.5 mL) within a course of 10 h. After the addition was completed, the moss-green solution was stirred 8 h at room temperature and quenched by aqueous saturated NH$_4$Cl and EtOAC. Layers were separated, and the water layer was extracted with EtOAc. Combined organic extracts were washed with saturated NaHCO$_3$ and brine, dried (MgSO$_4$), and evaporated under reduced pressure. Purification by reverse phase column chromatography (gradient elution from 10% MeCN in water to 100% MeCN) afforded 8i (430 mg, 52%; dr 1:1) as a yellow amorphous solid. ^{1}H NMR (400 MHz, CDCl$_3$): δ 7.40−7.31 (m, 5H), 7.04−6.97 (m, 1H), 6.99−6.94 (m, 1H), 6.71 (d, J = 7.9 Hz, 1H), 5.26−5.04 (m, 3H), 4.43− 4.34 (m, 1H), 3.37 (q, J = 7.4 Hz, 1H), 3.18 (s, 3H), 2.70− 2.51 (m, 2H), 2.16−2.06 (m, 1H), 1.99−1.84 (m, 1H), 1.48− 1.40 (m, 12H). ^{13}C NMR (101 MHz, CDCl$_3$): δ 179.0, 173.0, 171.6, 155.8, 142.7, 135.8, 135.4, 131.4, 129.1, 129.0, 128.8, 128.1, 124.2, 108.3, 80.5, 67.5, 53.6, 41.0, 35.3, 31.7, 28.8, 26.7, 15.8. HRMS (m/z) calcd for C$_{26}$H$_{32}$N$_2$O$_5$Na [M + Na]$^+$ 475.2209; found 475.2206.

Methyl 2-{5-Bromo-2-[(1S)-1-[(2S)-2-{[(tert-butoxy)-carbonyl]amino}-3-(2-oxo-3-phenyl-2,3-dihydro-1H-indol-5-yl)propanamido]-2,2-dimethylpropyl]-1,3-oxazol-4-yl}-1,3-oxazole-4-carboxylate (5a). The title compound was prepared according to general procedure D from ester 7a (520 mg; 1.27 mmol), LiOH (152 mg; 6.33 mmol; 5 equiv) in MeOH/water (3:1 v/v; 8 mL), amine 9 (452 mg; 1.26 mmol; 1 equiv), and EDC × HCl (363 mg; 1.89 mmol; 1.5 equiv) in pyridine (5 mL) in 18 h. Purification by column chromatography on silica gel (gradient elution from 30% to 60% EtOAc in hexanes) afforded 5a (465 mg, 50%, 1:1 d.r.) as a yellow oil. ^{1}H NMR (400 MHz, CDCl$_3$): δ 8.74−8.63 (m, 1H), 8.28 (s, 0.5H), 8.23 (s, 0.5H), 7.37−7.26 (m, 3H), 7.20−7.10 (m, 2H) 7.08−6.88 (m, 2H), 6.84−6.62 (m, 1.5H), 6.54 (d, J = 9.4 Hz, 0.5H), 5.15 (t, J = 8.8 Hz, 1H), 5.03 (d, J = 2.0 Hz, 0.5H), 5.01 (d, J = 2.1 Hz, 0.5H), 4.56 (s, 0.5H), 4.46 (s, 0.5H), 4.30−4.17 (m, 1H), 3.93 (s, 1.5H), 3.90 (s, 1.5H), 3.01−2.86 (m, 2H), 1.40 (s, 9H), 0.92 (s, 9H). ^{13}C NMR (101 MHz, CDCl$_3$): δ 178.3, 178.2, 171.2, 171.1, 164.8, 164.7, 161.42, 161.38, 155.6,

155.5, 154.7, 154.6, 144.21, 144.19, 140.8, 140.7, 136.52, 136.47, 134.64, 134.60, 130.9, 130.8, 130.3, 130.2, 129.4, 129.3, 129.1, 129.0, 128.63, 128.59, 128.5, 128.04, 127.99, 127.8, 127.7, 126.1, 123.1, 123.0, 110.1, 109.9, 80.4, 56.5, 55.7, 55.6, 52.6, 52.5, 52.4, 37.9, 36.1, 35.9, 28.4, 26.2. HRMS-ESI (m/z) calcd for C$_{35}$H$_{38}$BrN$_5$O$_8$Na [M + Na]$^+$ 758.1801; found 758.1810.

Methyl 2-{5-Bromo-2-[(1S)-1-[(2S)-2-{[(tert-butoxy)-carbonyl]amino}-3-(3-methyl-2-oxo-2,3-dihydro-1H-indol-5-yl)propanamido]-2,2-dimethylpropyl]-1,3-oxazol-4-yl}-1,3-oxazole-4-carboxylate (5b). The title compound was prepared according to general procedure D from ester 7b (410 mg; 1.18 mmol), LiOH (141 mg; 5.88 mmol; 5 equiv) in MeOH/water (5:2 v/v; 7 mL), amine 9 (421 mg; 1.18 mmol; 1 equiv), and EDC × HCl (338 mg; 1.76 mmol; 1.5 equiv) in pyridine (10 mL) in 2 h. Purification by column chromatography on silica gel (gradient elution from 50% to 100% EtOAc in hexanes) afforded 5b (435 mg, 55%; dr 1:1) as a yellow oil. ^{1}H NMR (400 MHz, MeOH-d_4): δ 8.64 (s, 1H), 7.09 (s, 0.5H), 7.01−6.96 (m, 1H), 6.88 (d, J = 7.9 Hz, 0.5H), 6.63 (d, J = 8.0 Hz, 0.5H), 6.53 (d, J = 7.9 Hz, 0.5H), 4.98 (s, 0.5H), 4.94 (s, 0.5H), 4.43−4.31 (m, 1H), 3.93 (s, 1.5H), 3.92 (s, 1.5H), 3.35 (s, 1H), 2.89−2.81 (m, 2H), 1.42 (s, 9H), 1.33 (d, J = 1.8 Hz, 1.5H), 1.31 (d, J = 1.8 Hz, 1.5H), 0.97 (s, 9H). ^{13}C NMR (101 MHz, MeOH-d_4): δ 183.0, 182.8, 174.2, 165.9, 165.8, 162.7, 162.6, 157.52, 157.49, 156.1, 156.0, 146.34, 146.31, 141.6, 135.3, 132.9, 132.7, 131.84, 131.76, 129.8, 129.7, 128.8, 128.7, 126.0, 125.9, 124.7, 124.5, 110.3, 109.9, 80.53, 80.51, 57.6, 57.5, 56.9, 56.7, 52.6, 42.2, 42.1, 39.0, 36.79, 36.76, 28.7, 26.6, 26.5, 15.5, 15.3. HRMS-ESI (m/z) calcd for C$_{30}$H$_{36}$N$_5$O$_8$BrNa [M + Na]$^+$ 696.1645; found 696.1661.

Methyl 2-{5-Bromo-2-[(1S)-1-[(2S)-2-{[(tert-butoxy)-carbonyl]amino}-3-[2-oxo-3-(propan-2-yl)-2,3-dihydro-1H-indol-5-yl)propanamido]-2,2-dimethylpropyl]-1,3-oxazol-4-yl}-1,3-oxazole-4-carboxylate (5c). The title compound was prepared according to general procedure D from ester 7c (110 mg; 0.29 mmol), LiOH (21 mg; 0.88 mmol; 3 equiv) in MeOH/water (4:1 v/v; 2.5 mL), amine 9 (105 mg; 0.29 mmol; 1 equiv), and EDC × HCl (67 mg; 0.35 mmol; 1.2 equiv) in pyridine (5 mL) in 3 h. Purification by reverse phase column chromatography (gradient elution from 5% to 95% MeCN in water) afforded 5c (110 mg, 54%; dr 1:1) as a yellow oil. ^{1}H NMR (400 MHz, CDCl$_3$): δ 8.39 (s, 0.5H), 8.33 (s, 0.5H), 8.314 (s, 0.5H), 8.306 (s, 0.5H), 7.10 (s, 0.5H), 7.06 (s, 0.5H), 6.99 (d, J = 8.0 Hz, 0.5H), 6.91 (d, J = 8.0 Hz, 0.5H), 6.83 (d, J = 8.0 Hz, 0.5H), 6.77 (d, J = 8.0 Hz, 0.5H), 6.73 (d, J = 8.0 Hz, 0.5H), 6.67 (d, J = 8.0 Hz, 0.5H), 5.21−5.13 (m, 1H), 5.07 (d, J = 9.4 Hz, 0.5H), 5.06 (d, J = 9.4 Hz, 0.5H), 4.36−4.24 (m, 1H), 3.94 (s, 1.5H), 3.93 (s, 1.5H), 3.29 (d, J = 3.4 Hz, 0.5H), 3.24 (d, J = 3.4 Hz, 0.5H), 3.05−2.93 (m, 2H), 2.41 (sept d, J = 6.9, 3.4 Hz, 1H), 1.42 (s, 4.5H), 1.41 (s, 4.5H), 1.05 (d, J = 1.3 Hz, 3H), 0.95 (s, 9H), 0.88 (d, J = 6.9 Hz, 1.5H), 0.82 (d, J = 6.9 Hz, 1.5H). ^{13}C NMR (101 MHz, CDCl$_3$): δ 179.43, 179.39, 164.9, 164.8, 161.41, 161.38, 155.6, 154.7, 154.7, 144.2, 144.1, 141.0, 134.67, 134.65, 130.3, 130.1, 128.9, 128.8, 128.7, 128.1, 128.0, 125.5, 123.1, 123.0, 109.7, 109.5, 80.4, 56.5, 55.7, 55.6, 52.48, 52.45, 52.1, 52.0, 37.7, 36.1, 36.0, 30.84, 30.79, 28.4, 26.3, 20.0, 19.9, 18.3, 18.1. HRMS-ESI (m/z) calcd for C$_{32}$H$_{40}$N$_5$O$_8$BrNa [M + Na]$^+$ 724.1958; found 724.1967.

Methyl 2-{5-Bromo-2-[(1S)-1-[(2S)-2-{[(tert-butoxy)-carbonyl]amino}-3-[3-(3,5-dimethylphenyl)-2-oxo-2,3-dihydro-1H-indol-5-yl]propanamido]-2,2-dimethylpropyl]-1,3-

135

oxazol-4-yl]-1,3-oxazole-4-carboxylate (5d). The title compound was prepared according to general procedure D from ester **7d** (600 mg; 1.37 mmol), LiOH (164 mg; 6.84 mmol; 5 equiv) in MeOH/water (4:1 v/v; 6 mL), amine **9** (500 mg; 1.40 mmol; 1 equiv), and EDC × HCl (401 mg; 2.09 mmol; 1.5 equiv) in pyridine (5 mL) in 18 h. Purification by column chromatography on silica gel (gradient elution from 30% to 60% EtOAc in hexanes) afforded **5d** (700 mg, 66%; dr 1:1) as a yellow oil. ^{1}H NMR (400 MHz, CDCl$_3$): δ 8.78 (s, 0.5H), 8.73 (s, 0.5H), 8.28 (s, 0.5H), 8.23 (s, 0.5H), 7.04–6.99 (m, 0.5H), 6.96 (s, 0.5), 6.91–6.87 (m, 2H), 6.77 (d, J = 7.9 Hz, 0.5H), 6.75–6.71 (m, 2H), 6.69 (d, J = 7.9 Hz, 0.5 H), 6.63 (d, J = 9.4 Hz, 0.5H), 6.54 (d, J = 9.4 Hz, 0.5 H), 5.15 (t, J = 7.9 Hz, 1H), 5.03 (d, J = 2.7 Hz, 0.5H), 5.01 (d, J = 2.8 Hz, 0.5H), 4.47 (s, 0.5H), 4.35 (s, 0.5H), 4.27–4.17 (m, 1H), 3.93 (s, 1.5H), 3.90 (s, 1.5H), 3.00–2.89 (m, 2H), 2.26 (s, 3H), 2.25 (s, 3H), 1.39 (d, J = 1.9 Hz, 9H), 0.93 (s, 9H). ^{13}C NMR (101 MHz, CDCl$_3$): δ 178.8, 178.7, 171.2, 171.1, 164.8, 164.7, 161.42, 161.37, 155.6, 155.5, 154.7, 154.6, 144.2, 140.7, 140.6, 138.5, 136.3, 134.63, 134.60, 130.84, 130.82, 130.7, 129.6, 129.5, 129.21, 129.19, 128.02, 127.96, 126.40, 126.35, 126.1, 126.0, 123.1, 123.0, 110.0, 109.8, 80.4, 56.5, 55.6, 52.74, 52.71, 52.5, 52.4, 41.0, 37.9, 36.0, 35.9, 28.4, 26.2, 21.4. HRMS-ESI (*m/z*) calcd for C$_{37}$H$_{42}$BrN$_5$O$_8$Na [M + Na]$^+$ 786.2114; found 786.2114.

Methyl 2-{5-Bromo-2-[(1S)-1-[(2S)-2-{[(tert-butoxy)-carbonyl]amino}-3-[3-(naphthalen-2-yl)-2-oxo-2,3-dihydro-1H-indol-5-yl]propanamido]-2,2-dimethylpropyl]-1,3-oxazol-4-yl}-1,3-oxazole-4-carboxylate (5e). The title compound was prepared according to general procedure D from ester **7e** (300 mg; 0.65 mmol), LiOH (78 mg; 3.26 mmol; 5 equiv) in MeOH/water (3:1 v/v; 4 mL), amine **9** (233 mg; 0.65 mmol; 1 equiv), and EDC × HCl (187 mg; 0.98 mmol; 1.5 equiv) in pyridine (10 mL) in 18 h. Purification by column chromatography on silica gel (gradient elution from 10% to 75% EtOAc in hexanes) was followed by reverse phase column chromatography (gradient elution from 40% to 90% MeCN in water) and afforded **5e** (130 mg, 25%; dr 1:1) as a yellow oil. ^{1}H NMR (400 MHz, CDCl$_3$): δ 8.36–8.29 (m, 1H), 8.27 (s, 0.5H), 8.21 (s, 0.5H), 7.85–7.74 (m, 3H), 7.67 (s, 1H), 7.51–7.42 (m, 2H), 7.22 (dd, J = 8.4, 1.8 Hz, 0.5H), 7.18 (dd, J = 8.5, 1.8 Hz, 0.5H), 7.05–6.98 (m, 1H), 6.98–6.92 (m, 1H), 6.80 (d, J = 8.0 Hz, 0.5H), 6.73 (d, J = 7.9 Hz, 0.5H), 6.57 (d, J = 9.4 Hz, 0.5H), 6.44 (d, J = 9.4 Hz, 0.5H), 5.15–5.06 (m, 1H), 5.03 (d, J = 9.4 Hz, 0.5H), 5.00 (d, J = 9.4 Hz, 0.5H), 4.74 (s, 0.5H), 4.62 (s, 0.5H), 4.26–4.18 (m, 1H), 3.95 (s, 1.5H), 3.90 (s, 1.5H), 3.01–2.88 (m, 2H), 1.38 (s, 4.5H), 1.37 (s, 4.5H), 0.93 (s, 4.5H), 0.90 (s, 4.5H). ^{13}C NMR (101 MHz, CDCl$_3$): δ 177.9, 177.8, 171.0, 170.8, 164.7, 164.6, 161.28, 161.26, 155.41, 155.37, 154.6, 154.5, 144.0, 140.6, 140.5, 134.51, 134.49, 133.8, 133.7, 133.51, 133.50, 132.82, 132.80, 130.82, 130.79, 130.19, 130.15, 129.34, 129.30, 128.84, 128.81, 127.92, 127.90, 127.86, 127.74, 127.66, 126.24, 126.21, 126.14, 126.12, 126.03, 125.99, 125.96, 123.0, 122.9, 110.0, 109.8, 80.3, 56.4, 55.49, 55.46, 52.6, 52.4, 52.3, 37.9, 37.8, 35.9, 35.8, 28.2, 26.13, 26.09. HRMS-ESI (*m/z*) calcd for C$_{39}$H$_{40}$BrN$_5$O$_8$Na [M + Na]$^+$ 808.1958; found 808.1940.

Methyl 2-{5-Bromo-2-[(1S)-1-[(2S)-2-{[(tert-butoxy)-carbonyl]amino}-3-(2-oxo-2,3-dihydro-1H-indol-5-yl)-propanamido]-2,2-dimethylpropyl]-1,3-oxazol-4-yl}-1,3-oxazole-4-carboxylate (5f). The title compound was prepared according to general procedure D from ester **7f** (220 mg; 0.66 mmol), LiOH (47 mg; 1.97 mmol; 3 equiv) in MeOH/water

(4:1 v/v; 3.5 mL), amine **9** (237 mg; 0.66 mmol; 1 equiv), and EDC × HCl (165 mg; 0.86 mmol; 1.3 equiv) in pyridine (3 mL) in 18 h. Purification by column chromatography on silica gel (gradient elution from 40% to 70% EtOAc in hexanes) afforded **5f** (135 mg, 31%) as a yellow oil. ^{1}H NMR (400 MHz, CDCl$_3$): δ 8.54 (s, 1H), 8.31 (s, 1H), 7.05 (s, 1H), 6.94 (dd, J = 8.0, 1.7 Hz, 1H), 6.81 (d, J = 9.3 Hz, 1H), 6.67 (d, J = 8.0 Hz, 1H), 5.28 (d, J = 8.2 Hz, 1H), 5.04 (d, J = 9.3 Hz, 1H), 4.34–4.24 (m, 1H), 3.93 (s, 3H), 3.46–3.28 (m, 2H), 2.99 (dd, J = 13.8, 6.8 Hz, 1H), 2.94 (dd, J = 13.8, 8.0 Hz, 1H), 1.43 (s, 9H), 0.94 (s, 9H). ^{13}C NMR (101 MHz, CDCl3) δ 177.4, 171.3, 164.9, 161.4, 155.6, 154.7, 144.2, 141.4, 134.6, 130.6, 128.8, 128.0, 125.8, 125.6, 123.0, 109.8, 80.4, 56.6, 55.7, 52.5, 38.0, 36.2, 36.0, 28.4, 26.3. HRMS-ESI (*m/z*) calcd for C$_{29}$H$_{34}$BrN$_5$O$_8$Na [M + Na]$^+$ 682.1488; found 682.1494 [α]$_D^{20}$ +6 (c 0.9, CHCl$_3$).

Methyl 2-{5-Bromo-2-[(1S)-1-[(2S)-2-{[(tert-butoxy)-carbonyl]amino}-3-(1-methyl-2-oxo-2,3-dihydro-1H-indol-5-yl)propanamido]-2,2-dimethylpropyl]-1,3-oxazol-4-yl}-1,3-oxazole-4-carboxylate (5g). The title compound was prepared according to general procedure D from ester **7g** (2.15 g; 6.17 mmol), LiOH (443 mg; 18.51 mmol; 3 equiv) in MeOH/water (3:2 v/v; 25 mL), amine **9** (2.21 g; 6.17 mmol; 1 equiv), and EDC × HCl (1.42 g; 7.40 mmol; 1.2 equiv) in pyridine (20 mL) in 1 h. Purification by reverse phase column chromatography (gradient elution from 95% to 50% water in MeCN) afforded **5g** (1.80 g, 43%) as a yellow oil. ^{1}H NMR (400 MHz, CDCl$_3$): δ 8.31 (s, 1H), 7.08 (s, 1H), 7.04 (d, J = 8.0 Hz, 1H), 6.60 (d, J = 8.0 Hz, 2H), 5.10–5.05 (m, 1H), 5.03 (d, J = 9.4 Hz, 1H), 4.25 (dd, J = 14.6, 7.2 Hz, 1H), 3.94 (s, 3H), 3.46 (d, J = 22.1 Hz, 1H), 3.38 (d, J = 22.1 Hz, 1H), 3.07 (s, 3H), 3.05–2.94 (m, 2H), 1.42 (s, 9H), 0.94 (s, 9H). ^{13}C NMR (101 MHz, CDCl$_3$): δ 175.0, 171.1, 164.8, 161.3, 155.6, 154.6, 144.2, 144.1, 134.8, 130.5, 128.8, 128.0, 125.5, 125.1, 122.9, 107.9, 80.5, 56.5, 55.7, 52.4, 37.7, 36.01, 35.8, 28.4, 26.3, 26.2. HRMS-ESI (*m/z*) calcd for C$_{30}$H$_{37}$N$_5$O$_8$Br [M + H]$^+$ 674.1826; found 674.1823. [α]$_D^{20}$ −18 (c 1.0, MeOH).

Methyl 2-{5-Bromo-2-[(1S)-1-[(2S)-2-{[(tert-butoxy)-carbonyl]amino}-3-(1-methyl-2-oxo-3-phenyl-2,3-dihydro-1H-indol-5-yl)propanamido]-2,2-dimethylpropyl]-1,3-oxazol-4-yl}-1,3-oxazole-4-carboxylate (5h). The title compound was prepared according to general procedure D from ester **7h** (500 mg; 1.18 mmol), LiOH (141 mg; 5.89 mmol; 5 equiv) in MeOH/water (5:1 v/v; 12 mL), amine **9** (419 mg; 1.17 mmol; 1 equiv), and EDC × HCl (336 mg; 1.75 mmol; 1.5 equiv) in pyridine (10 mL) in 18 h. Purification by column chromatography on silica gel (gradient elution from 40% to 60% EtOAc in hexanes) afforded **5h** (600 mg, 68%; dr 1:1) as a yellow oil. ^{1}H NMR (400 MHz, CDCl$_3$): δ 8.30 (s, 0.5H), 8.23 (s, 0.5H), 7.33–7.21 (m, 3H), 7.17–7.09 (m, 2.5H), 7.05–6.97 (m, 1.5H), 6.71 (d, J = 7.9 Hz, 0.5H) 6.69–6.53 (m, 1.5H), 5.10–4.97 (m, 2H), 4.57 (s, 0.5H), 4.48 (s, 0.5H), 4.27–4.18 (m, 1H), 3.94 (s, 1.5H), 3.92 (s, 1.5H), 3.12 (s, 1.5H), 3.10 (s, 1.5H), 2.01–2.95 (m, 2H), 1.39 (s, 9H), 0.94 (s, 9H). ^{13}C NMR (101 MHz, CDCl$_3$): δ 175.93, 175.86, 171.03, 170.96, 164.8, 164.7, 161.30, 161.25, 155.5, 154.6, 144.14, 144.09, 143.5, 143.4, 136.5, 134.8, 134.7, 131.0, 130.9, 129.6, 129.4, 129.3, 129.0, 128.54, 128.51, 128.02, 127.98, 127.7, 127.6, 126.1, 126.0, 123.0, 122.8, 108.1, 107.8, 80.5, 56.4, 55.7, 55.6, 52.42, 52.39, 52.1, 37.6, 37.5, 36.1, 36.0,

136

28.4, 26.54, 26.48, 26.3. HRMS-ESI (*m/z*) calcd for $C_{36}H_{41}BrN_5O_8$ [M + H]$^+$ 750.2161; found 750.2139.

Methyl 2-{5-Bromo-2-[(1S)-1-[(2S)-2-{[(tert-butoxy)-carbonyl]amino}-4-(2-oxo-3-phenyl-2,3-dihydro-1H-indol-5-yl)butanamido]-2,2-dimethylpropyl]-1,3-oxazol-4-yl}-1,3-oxazole-4-carboxylate (6a). The title compound was prepared according to general procedure E from ester **8a** (115 mg; 0.23 mmol), 5% Pd on carbon (49 mg; 0.023 mmol; 0.1 equiv) in EtOAc (5 mL), amine **9** (94 mg; 0.26 mmol; 1.2 equiv), and EDC × HCl (57 mg; 0.30 mmol; 1.3 equiv) in pyridine (2 mL) in 16 h. Purification by column chromatography on silica gel (gradient elution from 100% DCM to 75% Et$_2$O in DCM) afforded **6a** (114 mg, 66%; dr 1:1) as a white amorphous solid. ^{1}H NMR (400 MHz, CDCl$_3$): δ 8.88 (s, 0.5H), 8.52 (s, 0.5H), 8.29 (s, 0.5H), 8.27 (s, 0.5H), 7.57 (s, 0.5H), 7.35–7.24 (m, 2.5H), 7.28–7.21 (m, 1H), 7.22–7.12 (m, 2H), 7.04–6.95 (m, 1.5H), 6.95–6.88 (m, 1H), 6.78 (d, J = 7.9 Hz, 0.5H), 5.16 (d, J = 7.2 Hz, 1H), 5.11–5.02 (m, 1H), 4.99 (d, J = 8.7 Hz, 0.5H), 4.56 (s, 0.5H), 4.51 (s, 0.5H), 4.17–4.01 (m, 1H), 3.94 (s, 3H), 2.69–2.54 (m, 2H), 2.13–2.02 (m, 1H), 1.93–1.81 (m, 1H), 1.46 (s, 4.5H), 1.43 (s, 4.5H), 0.95 (s, 4.5H), 0.88 (s, 4.5H). ^{13}C NMR (101 MHz, CDCl3): δ 178.2, 178.1, 172.4, 171.9, 165.2, 165.1, 161.43, 161.41, 156.0, 154.92, 154.89, 144.1, 140.4, 140.1, 136.74, 136.66, 135.0, 134.7, 134.6, 130.0, 129.9, 129.2, 129.0, 128.9, 128.7, 128.61, 128.57, 128.1, 128.0, 127.7, 127.6, 125.5, 125.4, 123.14, 123.10, 110.1, 109.6, 80.5, 80.4, 56.3, 56.0, 53.4, 53.0, 52.8, 52.7, 52.5, 35.8, 35.5, 33.1, 32.9, 31.5, 31.3, 28.4, 26.3. HRMS-ESI (*m/z*) calcd for $C_{36}H_{40}N_5O_8BrNa$ [M + Na]$^+$ 772.1958; found 772.1967.

Methyl 2-{5-Bromo-2-[(1S)-1-[(2S)-2-{[(tert-butoxy)-carbonyl]amino}-4-(3-methyl-2-oxo-2,3-dihydro-1H-indol-5-yl)butanamido]-2,2-dimethylpropyl]-1,3-oxazol-4-yl}-1,3-oxazole-4-carboxylate (6b). The title compound was prepared according to general procedure E from ester **8b** (325 mg; 0.74 mmol), 10% Pd on carbon (79 mg; 0.074 mmol; 0.1 equiv) in EtOAc (15 mL), amine **9** (283 mg; 0.79 mmol; 1.1 equiv), and EDC × HCl (179 mg; 0.93 mmol; 1.3 equiv) in pyridine (5 mL) in 4 h. Product **6b** was purified by column chromatography on silica gel (gradient elution from 100% hexanes to 100% EtOAc) to afford 308 mg (62%; dr 1:1) as a white amorphous solid. ^{1}H NMR (400 MHz, MeOH-d_4): δ 8.62 (s, 0.5H), 8.62 (s, 0.5H), 7.05 (d, J = 10.3 Hz, 1H), 6.99 (d, J = 8.0 Hz, 1H), 6.75 (d, J = 8.0 Hz, 1H), 5.03 (s, 0.5H), 5.02 (s, 0.5H), 4.16–4.10 (m, 1H), 3.91 (s, 1.5H), 3.91 (s, 1.5H), 3.42–3.36 (m, 1H), 2.69–2.53 (m, 2H), 2.04–1.93 (m, 1H), 1.92–1.81 (m, 1H), 1.45 (s, 9H), 1.38 (d, J = 4.5 Hz, 1.5H), 1.37 (d, J = 4.5 Hz, 1.5H), 1.06 (s, 9H). ^{13}C NMR (101 MHz, MeOH-d_4): δ 183.3, 175.1, 166.4, 162.6, 157.9, 156.2, 146.2, 141.2, 136.5, 135.3, 133.1, 129.0, 128.9, 125.0, 124.8, 110.6, 80.7, 57.4, 55.3, 52.6, 42.4, 36.4, 35.0, 32.7, 28.7, 26.7, 15.7, 15.6. HRMS-ESI (*m/z*) calcd for $C_{31}H_{38}N_5O_8BrNa$ [M + Na]$^+$ 710.1801; found 710.1805.

Methyl 2-{5-Bromo-2-[(1S)-1-[(2S)-2-{[(tert-butoxy)-carbonyl]amino}-4-(1,3-dimethyl-2-oxo-2,3-dihydro-1H-indol-5-yl)butanamido]-2,2-dimethylpropyl]-1,3-oxazol-4-yl}-1,3-oxazole-4-carboxylate (6i). The title compound was prepared according to general procedure E from ester **8i** (363 mg; 0.80 mmol), 10% Pd on carbon (85 mg; 0.080 mmol; 0.1 equiv) in EtOAc (16 mL), amine **9** (304 mg; 0.85 mmol; 1.1 equiv), and EDC × HCl (193 mg; 1.00 mmol; 1.3 equiv) in pyridine (5 mL) in 4 h. Purification by column chromatography on silica gel (gradient elution from 100% hexanes to

100% EtOAc) afforded **6i** (396 mg, 73%; dr 1:1) as a white amorphous solid. ^{1}H NMR (400 MHz, MeOH-d_4): δ 8.62 (s, 1H), 7.14–7.04 (m, 2H), 6.82 (d, J = 8.3 Hz, 1H), 5.03 (s, 0.5H), 5.03 (s, 0.5H), 4.15 (d, J = 8.4 Hz, 0.5H), 4.13 (d, J = 8.4 Hz, 0.5H), 3.91 (s, 1.5H), 3.90 (s, 1.5H), 3.45–3.36 (m, 1H), 3.16 (s, 3H), 2.70–2.56 (m, 2H), 2.05–1.95 (m, 1H), 1.93–1.82 (m, 1H), 1.45 (s, 9H), 1.38 (d, J = 4.1 Hz, 1.5H), 1.36 (d, J = 4.1 Hz, 1.5H), 1.06 (s, 9H). ^{13}C NMR (101 MHz, MeOH-d_4): δ 180.9, 175.0, 166.5, 162.6, 157.9, 156.2, 146.2, 143.1, 137.1, 135.3, 132.2, 132.1, 129.02, 128.96, 124.8, 109.4, 80.7, 57.4, 55.2, 52.6, 41.9, 36.4, 35.0, 32.6, 28.7, 26.7, 26.5. HRMS-ESI (*m/z*) calcd for $C_{32}H_{40}N_5O_8BrNa$ [M + Na]$^+$ 724.1958; found 724.1948.

Methyl 2-[(1S,6S,9S)-9-{[(tert-Butoxy)carbonyl]amino}-6-tert-butyl-8,16-dioxo-1-phenyl-19-oxa-4,7,15-triazatetracyclo[9.5.2.1^{2,5}.0^{14,17}]nonadeca-2,4,11,13,17-pentaen-3-yl]-1,3-oxazole-4-carboxylate (3a). The title compound was prepared according to general procedure F from amide **5a** (400 mg; 0.54 mmol) and Na$_2$CO$_3$ (173 mg; 1.63 mmol; 3 equiv) in DMF (40 mL) in 4 h. Purification by column chromatography on silica gel (gradient elution from 20% to 50% EtOAc in hexanes) afforded **3a** (230 mg, 65%, dr 99:1) as a white amorphous solid. ^{1}H NMR (400 MHz, CDCl$_3$): δ 9.15 (s, 1H), 7.89 (s, 1H), 7.47–7.37 (m, 2H), 7.32–7.26 (m, 3H), 7.21 (s, 1H), 7.07 (dd, J = 8.0, 1.8 Hz, 1H), 6.77 (d, J = 8.0 Hz, 1H), 6.31 (d, J = 8.6 Hz, 1H), 5.38 (d, J = 9.1 Hz, 1H), 4.94 (d, J = 8.6 Hz, 1H), 3.99 (ddd, J = 12.3, 9.2, 3.5 Hz, 1H), 3.90 (s, 3H), 3.16 (dd, J = 12.3, 12.3 Hz, 1H), 2.80 (dd, J = 12.3, 3.5 Hz, 1H), 1.43 (s, 9H), 1.03 (s, 9H). ^{13}C NMR (101 MHz, CDCl$_3$): δ 175.2, 172.2, 162.7, 161.6, 155.3, 155.2, 150.5, 144.5, 139.6, 135.4, 134.2, 132.5, 131.5, 129.9, 129.7, 129.0, 128.5, 127.6, 127.3, 111.2, 80.4, 59.1, 58.2, 57.3, 52.4, 38.2, 33.3, 28.4, 26.5. HRMS-ESI (*m/z*) calcd for $C_{35}H_{38}N_5O_8$ [M + H]$^+$ 656.2720; found 656.2740. $[\alpha]_D^{20}$ −203 (c 1.0, CHCl$_3$).

Methyl 2-[(1S,6S,9S)-9-{[(tert-Butoxy)carbonyl]amino}-6-tert-butyl-1-methyl-8,16-dioxo-19-oxa-4,7,15-triazatetracyclo[9.5.2.1^{2,5}.0^{14,17}]nonadeca-2,4,11,13,17-pentaen-3-yl]-1,3-oxazole-4-carboxylate (3b). The title compound was prepared according to general procedure F from amide **5b** (810 mg; 1.20 mmol) and Na$_2$CO$_3$ (636 mg; 6.00 mmol; 5 equiv) in DMF (25 mL) in 3 h. Purification by reverse phase column chromatography (gradient elution from 10% to 50% MeCN in water) afforded **3b** (540 mg, 76%) of a single diastereomer as a white amorphous solid. ^{1}H NMR (400 MHz, CDCl$_3$): δ 9.02 (s, 1H), 8.33 (s, 1H), 7.08 (dd, J = 8.0, 1.7 Hz, 1H), 6.81 (d, J = 8.0 Hz, 1H), 6.77 (s, 1H), 6.11 (d, J = 7.4 Hz, 1H), 5.45 (d, J = 9.2 Hz, 1H), 4.64 (d, J = 7.3 Hz, 1H), 4.08–3.98 (m, 1H), 3.94 (s, 3H), 3.04 (dd, J = 12.3 Hz, 1H), 2.85 (dd, J = 12.3, 3.8 Hz, 1H), 1.97 (s, 3H), 1.44 (s, 9H), 0.93 (s, 9H). ^{13}C NMR (101 MHz, CDCl$_3$): δ 177.1, 171.8, 161.5, 161.5, 155.6, 155.3, 150.9, 144.2, 139.8, 134.8, 134.6, 131.2, 129.3, 128.6, 127.9, 111.1, 80.3, 58.3, 58.2, 52.3, 50.6, 38.2, 33.3, 28.3, 26.4, 20.0. HRMS-ESI (*m/z*) calcd for $C_{30}H_{35}N_5O_8Na$ [M + Na]$^+$ 616.2383; found 616.2386. $[\alpha]_D^{20}$ −230 (c 1.5, MeOH).

Methyl 2-[(1S,6S,9S)-9-{[(tert-Butoxy)carbonyl]amino}-6-tert-butyl-8,16-dioxo-1-(propan-2-yl)-19-oxa-4,7,15-triazatetracyclo[9.5.2.1^{2,5}.0^{14,17}]nonadeca-2,4,11,13,17-pentaen-3-yl]-1,3-oxazole-4-carboxylate (3c). The title compound was prepared according to general procedure F from amide **5c** (110 mg; 0.16 mmol) and K$_3$PO$_4$ (166 mg; 0.78

137

mmol; 5 equiv) in DMF (5 mL) in 60 h. Purification by reverse phase column chromatography (gradient elution from 5% to 95% MeCN in water) afforded **3c** (80 mg, 82%) of a single diastereomer as a white amorphous solid. ^{1}H NMR (400 MHz, CDCl$_3$): δ 8.32 (s, 1H), 8.07 (s, 1H), 7.13 (dd, J = 8.0, 1.7 Hz, 1H), 7.04 (d, J = 1.7 Hz, 1H), 6.80 (d, J = 8.0 Hz, 1H), 5.86 (d, J = 8.0 Hz, 1H), 5.22 (d, J = 9.3 Hz, 1H), 4.80 (d, J = 8.0 Hz, 1H), 3.98−3.89 (m, 1H), 3.94 (s, 3H), 3.34 (sept, J = 6.7 Hz, 1H), 3.13 (dd, J = 12.1, 12.1 Hz, 1H), 2.85 (dd, J = 12.1, 3.6 Hz, 1H), 1.44 (s, 9H), 1.07−0.95 (m, 6H), 1.00 (s, 9H). ^{13}C NMR (101 MHz, CDCl$_3$): δ 176.1, 171.7, 161.5, 161.0, 155.6, 155.2, 149.3, 144.3, 140.5, 134.5, 131.1, 130.7, 130.0, 129.3, 127.1, 110.6, 80.4, 59.6, 58.4, 57.5, 52.2, 38.2, 33.4, 31.6, 28.3, 26.4, 18.0, 17.5. HRMS-ESI (m/z) calcd for C$_{32}$H$_{40}$N$_5$O$_8$ [M + H][+] 622.2877; found 622.2886. $[α]_D^{20}$ −18 (c 0.6, CHCl$_3$).

Methyl 2-[(1S,6S,9S)-9-{[(tert-Butoxy)carbonyl]amino}-6-tert-butyl-1-(3,5-dimethylphenyl)-8,16-dioxo-19-oxa-4,7,15-triazatetracyclo[9.5.2.1^{2,5}.0^{14,17}]nonadeca-2,4,11,13,17-pentaen-3-yl]-1,3-oxazole-4-carboxylate (3d). The title compound was prepared according to general procedure F from amide **5d** (600 mg; 0.78 mmol) and Na$_2$CO$_3$ (249 mg; 2.35 mmol; 3 equiv) in DMF (30 mL) in 18 h. Purification by column chromatography on silica gel (gradient elution from 20% to 50% EtOAc in hexanes) afforded **3d** (322 mg, 60%) of a single disetereomer as a white amorphous solid. ^{1}H NMR (400 MHz, CDCl$_3$): δ 9.11 (s, 1H), 7.95 (s, 1H), 7.24−7.18 (m, 1H), 7.07 (dd, J = 8.0, 1.7 Hz, 1H), 6.97 (s, 2H), 6.90 (s, 1H), 6.77 (d, J = 8.0 Hz, 1H), 6.33 (d, J = 8.9 Hz, 1H), 5.35 (d, J = 9.2 Hz, 1H), 5.00 (d, J = 8.9 Hz, 1H), 3.98 (ddd, J = 12.3, 9.2, 3.4 Hz, 1H), 3.91 (s, 3H), 3.18 (dd, J = 12.3, 12.3 Hz, 1H), 2.80 (dd, J = 12.3, 3.4 Hz, 1H), 2.23 (s, 6H), 1.44 (s, 9H), 1.05 (s, 9H). ^{13}C NMR (101 MHz, CDCl$_3$): δ 175.6, 172.3, 162.8, 161.6, 155.33, 155.30, 150.6, 144.6, 139.5, 138.7, 135.0, 134.0, 132.7, 131.4, 130.3, 129.8, 129.7, 127.0, 125.2, 111.2, 80.5, 59.2, 58.2, 57.2, 52.5, 38.3, 33.3, 28.4, 26.5, 21.5. HRMS-ESI (m/z) calcd for C$_{37}$H$_{42}$N$_5$O$_8$ [M + H][+] 684.3033; found 684.3025. $[α]_D^{20}$ −224 (c 1.0, CHCl$_3$).

Methyl 2-[(1S,6S,9S)-9-{[(tert-Butoxy)carbonyl]amino}-6-tert-butyl-1-(naphthalen-2-yl)-8,16-dioxo-19-oxa-4,7,15-triazatetracyclo[9.5.2.1^{2,5}.0^{14,17}]nonadeca-2,4,11,13,17-pentaen-3-yl]-1,3-oxazole-4-carboxylate (3e). The title compound was prepared according to general procedure F from amide **5e** (100 mg) and K$_3$PO$_4$ (108 mg; 0.51 mmol; 4 equiv) in DMF (10 mL) in 48 h. Purification by column chromatography on silica gel (gradient elution from 30% to 70% EtOAc in hexanes) afforded **3e** (55 mg, 61%) of a single diastereomer as a light yellow amorphous solid. ^{1}H NMR (400 MHz, CDCl$_3$): δ 9.17 (d, J = 5.9 Hz, 1H), 7.94 (s, 1H), 7.81−7.71 (m, 4H), 7.50−7.43 (m, 3H), 7.28 (s, 1H), 7.08 (dd, J = 8.1, 1.7 Hz, 1H), 6.80 (d, J = 8.0 Hz, 1H), 6.33 (d, J = 7.2 Hz, 1H), 5.36 (d, J = 9.2 Hz, 1H), 4.97 (d, J = 8.7 Hz, 1H), 4.01 (ddd, J = 12.3, 9.2, 3.5 Hz, 1H), 3.84 (s, 3H), 3.18 (dd, J = 12.3, 12.3 Hz, 1H), 2.81 (dd, J = 12.3, 3.5 Hz, 1H), 1.44 (s, 9H), 1.05 (s, 9H). ^{13}C NMR (101 MHz, CDCl$_3$): δ 175.1, 172.1, 162.7, 161.4, 155.2, 154.9, 150.3, 144.3, 139.5, 134.0, 133.1, 132.9, 132.4, 131.4, 129.9, 129.7, 128.8, 128.2, 127.5, 127.4, 126.9, 126.6, 126.5, 124.7, 111.2, 80.3, 59.1, 58.1, 57.2, 52.3, 38.1, 33.2, 28.3, 26.4. HRMS-ESI (m/z) calcd for C$_{39}$H$_{40}$N$_5$O$_8$ [M + H][+] 706.2877; found 706.2896. $[α]_D^{20}$ −242 (c 0.4, CHCl$_3$).

Methyl 2-[(1S,6S,9S)-9-{[(tert-Butoxy)carbonyl]amino}-6-tert-butyl-8,16-dioxo-19-oxa-4,7,15-triazatetracyclo-[9.5.2.1^{2,5}.0^{14,17}]nonadeca-2,4,11,13,17-pentaen-3-yl]-1,3-oxazole-4-carboxylate (3f). The title compound was prepared according to general procedure F, from amide **5f** (85 mg; 0.13 mmol) and Na$_2$CO$_3$ (41 mg; 0.39 mmol; 3 equiv) in DMF (8 mL) in 60 h. Purification by column chromatography on silica gel (gradient elution from 30% to 60% EtOAc in hexanes) afforded **3f** (40 mg, 54%) of a single diastereomer as a white amorphous solid. ^{1}H NMR (400 MHz, CDCl$_3$): δ 8.76 (s, 1H), 8.32 (s, 1H), 7.12−7.06 (m, 1H), 6.83 (d, J = 8.0 Hz, 1H), 6.58 (s, 1H), 6.06 (d, J = 6.8 Hz, 1H), 5.60 (s, 1H), 5.30 (d, J = 9.3 Hz, 1H), 4.62 (d, J = 6.8 Hz, 1H), 3.97−3.89 (m, 4H), 3.02 (dd, J = 12.2, 12.2 Hz, 1H), 2.76 (dd, J = 12.2, 3.6 Hz, 1H), 1.43 (s, 9H), 0.94 (s, 9H). ^{13}C NMR (101 MHz, CDCl$_3$): δ 174.4, 171.8, 163.6, 161.6, 155.9, 155.4, 148.0, 143.9, 141.7, 134.6, 131.7, 129.7, 129.6, 129.5, 129.4, 111.3, 80.6, 59.2, 58.2, 52.4, 45.9, 37.8, 33.3, 28.4, 26.6. HRMS-ESI (m/z) calcd for C$_{29}$H$_{34}$N$_5$O$_8$ [M + H][+] 580.2407; found 580.2420. $[α]_D^{20}$ −77 (c 0.7, CHCl$_3$).

Methyl 2-[(1S,6S,9S)-9-{[(tert-Butoxy)carbonyl]amino}-6-tert-butyl-15-methyl-8,16-dioxo-19-oxa-4,7,15-triazatetracyclo[9.5.2.1^{2,5}.0^{14,17}]nonadeca-2,4,11,13,17-pentaen-3-yl]-1,3-oxazole-4-carboxylate (3g). The title compound was prepared according to general procedure F from amide **5g** (800 mg; 1.19 mmol) and K$_3$PO$_4$ (755 mg; 3.56 mmol; 3 equiv) in DMF (20 mL) in 1 h. Purification by reverse phase column chromatography (gradient elution from 5% to 95% MeCN in water) afforded **3g** (570 mg, 81%) of a single diastereomer as a white amorphous solid. ^{1}H NMR (300 MHz, CDCl$_3$): δ 8.33 (s, 1H), 7.24 (d, J = 8.0 Hz, 1H), 6.85 (d, J = 8.0 Hz, 1H), 6.63 (s, 1H), 5.75 (d, J = 7.0 Hz, 1H), 5.65 (s, 1H), 5.12 (d, J = 9.3 Hz, 1H), 4.63 (d, J = 7.0 Hz, 1H), 3.93 (s, 3H), 3.85 (ddd, J = 12.2, 9.3, 3.4 Hz, 1H), 3.26 (s, 3H), 3.08 (dd, J = 12.2, 12.2 Hz, 1H), 2.80 (dd, J = 12.2, 3.4 Hz, 1H), 1.43 (s, 9H), 0.95 (s, 9H). ^{13}C NMR (101 MHz, CDCl$_3$): δ 172.4, 171.6, 163.5, 161.6, 155.9, 155.3, 148.1, 144.3, 143.9, 134.7, 132.0, 129.7, 129.6, 129.5, 128.8, 109.9, 80.5, 59.2, 58.5, 52.3, 45.6, 37.7, 33.3, 28.4, 27.0, 26.6. HRMS-ESI (m/z) calcd for C$_{30}$H$_{36}$N$_5$O$_8$ [M + H][+] 594.2564; found 594.2560. $[α]_D^{20}$ −50 (c 1.0, CHCl$_3$).

Methyl 2-[(1S,6S,9S)-9-{[(tert-Butoxy)carbonyl]amino}-6-tert-butyl-15-methyl-8,16-dioxo-1-phenyl-19-oxa-4,7,15-triazatetracyclo[9.5.2.1^{2,5}.0^{14,17}]nonadeca-2,4,11,13,17-pentaen-3-yl]-1,3-oxazole-4-carboxylate (3h). The title compound was prepared according to general procedure F from amide **5h** (600 mg; 0.80 mmol) and Na$_2$CO$_3$ (245 mg; 2.40 mmol; 3 equiv) in DMF (40 mL) in 3 h. Product **3h** was purified by column chromatography on silica gel (gradient elution from 20% to 50% EtOAc in hexanes) to afford 400 mg (75%) of a single diastereomer as a white amorphous solid. ^{1}H NMR (400 MHz, CDCl$_3$): δ 8.12 (s, 1H), 7.43−7.36 (m, 3H), 7.34−7.27 (m, 3H), 7.21 (dd, J = 8.0, 1.7 Hz, 1H), 6.79 (d, J = 8.0 Hz, 1H), 5.65 (d, J = 9.1 Hz, 1H), 5.17 (d, J = 9.1 Hz, 1H), 5.02 (d, J = 9.1 Hz, 1H), 3.89 (s, 3H), 3.79 (ddd, J = 12.3, 9.1, 3.5 Hz, 1H), 3.22 (dd, J = 12.3, 12.3 Hz, 1H), 3.19 (s, 3H), 2.80 (dd, J = 12.3, 3.5 Hz, 1H), 1.43 (s, 9H), 1.06 (s, 9H). ^{13}C NMR (101 MHz, CDCl$_3$): δ 172.4, 171.9, 162.8, 161.5, 155.2, 154.9, 150.8, 144.6, 142.4, 135.6, 134.1, 131.4, 131.1, 129.8, 129.5, 129.0, 128.4, 127.8, 126.5, 109.3, 80.4, 58.6, 58.5, 56.6, 52.2, 38.0, 33.1, 28.4, 27.0, 26.4. HRMS-ESI (m/z) calcd for

138

$C_{36}H_{40}N_5O_8$ $[M + H]^+$ 670.2877; found 670.2883. $[\alpha]_D^{20}$ −247 (c 1.0, CHCl₃).

Methyl 2-[(1S,6S,9S)-9-{[(tert-Butoxy)carbonyl]amino}-6-tert-butyl-1,15-dimethyl-8,16-dioxo-19-oxa-4,7,15-triazatetracyclo[9.5.2.1²,⁵.0¹⁴,¹⁷]nonadeca-2,4,11,13,17-pentaen-3-yl]-1,3-oxazole-4-carboxylate (3i). The title compound was prepared according to general procedure G from macrocycle **3g** (96 mg; 0.16 mmol), NaH (60% suspension in mineral oil; 6.5 mg; 0.16 mmol; 1 equiv), and methyl iodide (30 μL; 0.48 mmol; 3 equiv) in DMF (2 mL). Product **3i** was formed as a mixture of diastereomers (dr 86:14). Purification by column chromatography on silica gel (gradient elution from 30% EtOAc in DCM) afforded the major diastereomer (S,S,S)-**3i** (68 mg, 69%, dr 99:1) as a white amorphous solid. ¹H NMR (400 MHz, CDCl₃): δ 8.36 (s, 1H), 7.24 (d, J = 8.0 Hz, 1H), 6.91 (s, 1H), 6.84 (d, J = 8.0 Hz, 1H), 5.57 (d, J = 7.6 Hz, 1H), 5.17 (d, J = 9.3 Hz, 1H), 4.71 (d, J = 7.6 Hz, 1H), 3.93 (s, 3H), δ 3.87 (ddd, J = 12.0, 9.3, 3.7 Hz, 1H), 3.22 (s, 3H), 3.10 (dd, J = 12.0, 12.0 Hz, 1H), 2.88 (dd, J = 12.0, 3.7 Hz, 1H), 1.98 (s, 3H), 1.43 (s, 9H), 0.95 (s, 9H). ¹³C NMR (101 MHz, CDCl₃): δ 175.0, 171.6, 161.6, 161.3, 155.6, 155.3, 151.0, 144.4, 142.4, 134.7, 133.8, 131.5, 129.4, 128.6, 127.7, 109.2, 80.5, 58.7, 58.1, 52.3, 50.2, 38.2, 33.4, 28.4, 26.9, 26.5, 20.4. HRMS-ESI (m/z) calcd for $C_{31}H_{38}N_5O_8$ $[M + H]^+$ 608.2720; found 608.2722. $[\alpha]_D^{20}$ −42 (c 1.0, CHCl₃).

Methyl 2-[(1S,6S,9S)-9-{[(tert-Butoxy)carbonyl]amino}-6-tert-butyl-1-ethyl-15-methyl-8,16-dioxo-19-oxa-4,7,15-triazatetracyclo[9.5.2.1²,⁵.0¹⁴,¹⁷]nonadeca-2,4,11,13,17-pentaen-3-yl]-1,3-oxazole-4-carboxylate (3j). The title compound was prepared according to general procedure G from macrocycle **3g** (100 mg; 0.17 mmol), NaH (60% suspension in mineral oil; 6.7 mg; 0.17 mmol; 1 equiv), and ethyl iodide (40 μL; 0.51 mmol; 3 equiv) in DMF (2 mL). Product **3j** formed as mixture of diastereomers (dr 89:11) and was purified by column chromatography on silica gel (gradient elution from 20% EtOAc in DCM) to afford of the major diastereomer (S,S,S)-**3j** (65 mg, 62%; dr 99:1) as a white amorphous solid. ¹H NMR (400 MHz, CDCl₃): δ 8.36 (s, 1H), 7.24 (dd, J = 7.9, 1.4 Hz, 1H), 6.96 (d, J = 1.4 Hz, 1H), 6.83 (d, J = 7.9 Hz, 1H), 5.65 (d, J = 7.9 Hz, 1H), 5.20 (d, J = 9.2 Hz, 1H), 4.75 (d, J = 7.9 Hz, 1H), 3.93 (s, 3H), 3.92−3.83 (m, 1H), 3.20 (s, 3H), 3.13 (dd, J = 12.1, 12.1 Hz, 1H), 2.87 (dd, J = 12.1, 3.5 Hz, 1H), 2.75 (dq, J = 14.5, 7.3 Hz, 1H), 2.31 (dq, J = 14.5, 7.3 Hz, 1H), 1.43 (s, 9H), 0.97 (s, 9H), 0.82 (t, J = 7.3 Hz, 3H). ¹³C NMR (101 MHz, CDCl₃): δ 174.2, 171.6, 161.5, 161.1, 155.5, 155.2, 150.2, 144.3, 143.1, 134.5, 131.2, 131.1, 129.3, 129.1, 127.2, 109.0, 80.4, 58.5, 57.7, 55.3, 52.2, 38.1, 33.3, 28.3, 26.7, 26.5, 26.4, 8.9. HRMS-ESI (m/z) calcd for $C_{32}H_{40}N_5O_8$ $[M + H]^+$ 622.2877; found 622.2878. $[\alpha]_D^{20}$ −40 (c 1.0, CHCl₃).

Methyl 2-[(1S,6S,9S)-1-Benzyl-9-{[(tert-butoxy)carbonyl]amino}-6-tert-butyl-15-methyl-8,16-dioxo-19-oxa-4,7,15-triazatetracyclo[9.5.2.1²,⁵.0¹⁴,¹⁷]nonadeca-2,4,11,13,17-pentaen-3-yl]-1,3-oxazole-4-carboxylate (3k). The title compound was prepared according to general procedure G from macrocycle **3g** (55 mg; 0.093 mmol), NaH (60% suspension in mineral oil; 3.7 mg; 0.093 mmol; 1 equiv), and benzyl bromide (33 μL; 0.28 mmol; 3 equiv) in DMF (2 mL). Product **3k** formed as mixture of diastereomers (dr 92:8) and was purified by column chromatography on silica gel (gradient elution from 30% EtOAc in DCM) to afford (S,S,S)-**3k** (45 mg, 71%; dr 99:1) as a white amorphous solid. ¹H NMR (400 MHz,

CDCl₃): δ 8.40 (s, 1H), 7.14 (dd, J = 8.0, 1.4 Hz, 1H), 7.11−7.04 (m, 3H), 7.04−6.99 (m, 3H), 6.58 (d, J = 8.0 Hz, 1H), 5.58 (d, J = 8.0 Hz, 1H), 5.18 (d, J = 9.2 Hz, 1H), 4.77 (d, J = 8.0 Hz, 1H), 4.36 (d, J = 13.0 Hz, 1H), 3.93 (s, 3H), 3.89−3.80 (m, 1H), 3.37 (d, J = 13.0 Hz, 1H), 3.16 (dd, J = 12.1, 12.1 Hz, 1H), 2.94 (m, 3H), 2.86 (dd, J = 12.1, 3.6 Hz, 1H), 1.43 (s, 9H), 0.98 (s, 9H). ¹³C NMR (101 MHz, CDCl₃): δ 173.6, 171.8, 161.6, 161.2, 155.6, 155.3, 150.1, 144.4, 142.8, 134.7, 131.0, 130.8, 130.6, 130.5, 129.4, 129.3, 127.9, 127.7, 127.1, 109.0, 80.5, 58.7, 57.9, 56.2, 52.3, 39.4, 38.2, 33.5, 28.4, 26.6, 26.5. HRMS-ESI (m/z) calcd for $C_{37}H_{42}N_5O_8$ $[M + H]^+$ 684.3033; found 684.3050. $[\alpha]_D^{20}$ −61 (c 1.0, CHCl₃).

Methyl 2-[(1S,6S,9S)-6-tert-Butyl-9-[(2S)-2-hydroxy-3-methylbutanamido]-8,16-dioxo-1-phenyl-19-oxa-4,7,15-triazatetracyclo[9.5.2.1²,⁵.0¹⁴,¹⁷]nonadeca-2,4,11,13,17-pentaen-3-yl]-1,3-oxazole-4-carboxylate (14a). The title compound was prepared according to general procedure H from macrocycle **3a** (50 mg; 0.076 mmol) and TFA (117 μL; 1.53 mmol; 20 equiv) in DCM (0.9 mL) within 2 h, followed by treatment with (S)-2-hydroxy-3-methylbutanoic acid (13 mg; 0.11 mmol; 1.5 equiv), EDC × HCl (26 mg; 0.14 mmol; 1.8 equiv), HOBt (31 mg; 0.23 mmol; 3 equiv), and DIPEA (65 μL; 0.38 mmol; 5 equiv) in DMF (1 mL) for 1 h. Purification by reverse phase column chromatography (gradient elution from 10% to 95% MeCN in water) afforded (S,S,S)-**14a** (35 mg, 71%, dr 99:1) as a white amorphous solid. ¹H NMR (400 MHz, CDCl₃): δ 9.50 (s, 1H), 7.82 (s, 1H), 7.65 (d, J = 8.9 Hz, 1H), 7.45−7.35 (m, 2H), 7.26−7.21 (m, 2H), 7.13 (s, 1H), 7.03 (d, J = 8.1 Hz, 1H), 6.84 (d, J = 7.9 Hz, 1H), 6.75 (d, J = 7.8 Hz, 1H), 4.82 (d, J = 7.8 Hz, 1H), 4.56−4.46 (m, 1H), 4.26 (s, 1H), 4.08 (d, J = 2.7, 1H), 3.89 (s, 3H), 3.25 (dd, J = 12.2, 12.2 Hz, 1H), 2.85−2.71 (m, 1H), 2.25−2.15 (m, 1H), 1.04 (d, J = 6.8 Hz, 3H), 1.00 (s, 9H), 0.87 (d, J = 6.8 Hz, 3H). ¹³C NMR (101 MHz, CDCl₃): δ 175.2, 173.4, 172.2, 162.2, 161.6, 155.2, 150.7, 144.4, 139.9, 135.4, 134.1, 133.0, 130.9, 129.8, 129.7, 129.0, 128.4, 127.7, 127.3, 111.5, 76.1, 59.0, 58.1, 56.1, 52.5, 38.4, 33.4, 32.0, 26.6, 19.3, 15.6. HRMS-ESI (m/z) calcd for $C_{35}H_{38}N_5O_8$ $[M + H]^+$ 656.2720; found 656.2737. $[\alpha]_D^{20}$ −260 (c 1.0, MeOH).

Methyl 2-[(1S,6S,9S)-6-tert-Butyl-9-[(2S)-2-hydroxy-3-methylbutanamido]-1-methyl-8,16-dioxo-19-oxa-4,7,15-triazatetracyclo[9.5.2.1²,⁵.0¹⁴,¹⁷]nonadeca-2,4,11,13,17-pentaen-3-yl]-1,3-oxazole-4-carboxylate (14b). The title compound was prepared according to general procedure H, from macrocycle **3b** (110 mg; 0.185 mmol), TFA (427 μL; 5.56 mmol; 30 equiv) in DCM (2 mL) within 2 h, followed by treatment with (S)-2-hydroxy-3-methylbutanoic acid (24 mg; 0.20 mmol; 1.1 equiv), EDC × HCl (57 mg; 0.30 mmol; 1.6 equiv), HOBt (85 mg; 0.56 mmol; 3 equiv), and DIPEA (128 μL; 0.74 mmol; 4 equiv) in DMF (5 mL) for 18 h. Purification by reverse phase column chromatography (gradient elution from 20% to 100% MeCN in water) afforded (S,S,S)-**14b** (71 mg, 65%; dr 99:1) as a white amorphous solid. ¹H NMR (400 MHz, MeOH-d_4): δ 8.72 (s, 1H), 7.29 (dd, J = 8.0, 1.8 Hz, 1H), 6.96 (d, J = 8.0 Hz, 1H), 6.81 (d, J = 1.6 Hz, 1H), 4.63 (s, 1H), 4.54 (dd, J = 11.6, 4.2 Hz, 1H), 3.94 (s, 3H), 3.88 (d, J = 3.7 Hz, 1H), 3.05 (dd, J = 12.0, 12.0 Hz, 1H), 2.89 (dd, J = 12.5, 4.2 Hz, 1H), 2.15−2.05 (m, 1H), 1.98 (s, 3H), 1.02 (d, J = 7.0 Hz, 3H), 0.98 (s, 9H), 0.91 (d, J = 6.8 Hz, 3H). ¹³C NMR (101 MHz, MeOH-d_4): δ 178.9, 175.8, 173.7, 163.7, 162.8, 156.9, 152.8, 146.5, 141.7, 136.2, 135.3, 132.2, 131.0, 129.4, 128.2, 112.2, 76.8, 60.0, 56.6, 52.6, 52.1, 39.3, 34.2, 33.1,

26.7, 20.5, 19.5, 16.3. HRMS-ESI (*m/z*) calcd for $C_{30}H_{36}N_5O_8$ [M + H]$^+$ 594.2564; found 594.2576. $[\alpha]_D^{20}$ −121 (c 1.1, MeOH).

Methyl 2-[(1S,6S,9S)-6-tert-Butyl-9-[(2S)-2-hydroxy-3-methylbutanamido]-8,16-dioxo-1-(propan-2-yl)-19-oxa-4,7,15-triazatetracyclo[9.5.2.1^{2,5}.0^{14,17}]nonadeca-2,4,11,13,17-pentaen-3-yl]-1,3-oxazole-4-carboxylate (14c). The title compound was prepared according to general procedure H from macrocycle **3c** (80 mg; 0.13 mmol), TFA (99 μL; 1.29 mmol; 10 equiv) in DCM (2 mL) in 3 h and (S)-2-hydroxy-3-methylbutanoic acid (23 mg; 0.19 mmol; 1.5 equiv), EDC × HCl (44 mg; 0.23 mmol; 1.8 equiv), HOBt (52 mg; 0.38 mmol; 3 equiv), and DIPEA (111 μL; 0.64 mmol; 5 equiv) in DMF (2 mL) in 2 h. Purification by reverse phase column chromatography (gradient elution from 5% to 95% MeCN in water) afforded **14c** (28 mg, 35%; dr 99:1) as a white amorphous solid. ^{1}H NMR (400 MHz, MeOH-d_4): δ 8.67 (s, 1H), 7.27 (dd, J = 8.1, 1.8 Hz, 1H), 7.11 (d, J = 1.8 Hz, 1H), 6.90 (d, J = 8.1 Hz, 1H), 4.79 (s, 1H), 4.49 (dd, J = 11.7, 3.9 Hz, 1H), 3.92 (s, 3H), 3.86 (d, J = 3.9 Hz, 1H), 3.34−3.25 (m, 1H, overlapping with MeOH-d_4), 3.15 (dd, J = 12.2, 12.2 Hz, 1H), 2.86 (dd, J = 12.2, 3.9 Hz, 1H), 2.09 (sept d, J = 6.8, 3.1 Hz, 1H), 1.06−0.97 (m, 9H), 1.02 (s, 9H), 0.89 (d, J = 6.8 Hz, 3H). ^{13}C NMR (101 MHz, MeOH-d_4): δ 178.0, 175.8, 173.9, 163.0, 162.8, 157.1, 151.3, 146.5, 143.0, 135.2, 131.8, 131.6, 131.1, 131.0, 127.5, 111.9, 76.8, 61.0, 59.0, 56.8, 52.6, 39.4, 34.3, 33.2, 33.1, 26.7, 19.6, 18.3, 17.8, 16.3. HRMS-ESI (*m/z*) calcd for $C_{32}H_{40}N_5O_8$ [M + H]$^+$ 622.2877; found 622.2875. $[\alpha]_D^{20}$ −114 (c 1.0, MeOH).

Methyl 2-[(1S,6S,9S)-6-tert-Butyl-1-(3,5-dimethylphenyl)-9-[(2S)-2-hydroxy-3-methylbutanamido]-8,16-dioxo-19-oxa-4,7,15-triazatetracyclo[9.5.2.1^{2,5}.0^{14,17}]nonadeca-2,4,11,13,17-pentaen-3-yl]-1,3-oxazole-4-carboxylate (14d). The title compound was prepared according to general procedure H, from macrocycle **3d** (80 mg; 0.12 mmol), TFA (90 μL; 1.17 mmol; 10 equiv) in DCM (1 mL) in 1 h and (S)-2-hydroxy-3-methylbutanoic acid (21 mg; 0.17 mmol; 1.5 equiv), EDC × HCl (40 mg; 0.21 mmol; 1.8 equiv), HOBt (47 mg; 0.35 mmol; 3 equiv), and DIPEA (101 μL; 0.58 mmol; 5 equiv) in DMF (1 mL) in 18 h. Purification by reverse phase column chromatography (gradient elution from 10% to 95% MeCN in water) afforded **14d** (65 mg, 81%; dr 99:1) as a white amorphous solid. ^{1}H NMR (400 MHz, MeOH-d_4): δ 8.49 (d, J = 8.6 Hz, 1H), 8.41 (s, 1H), 7.97 (d, J = 8.2, Hz, 1H), 7.26 (dd, J = 8.0, 1.8 Hz, 1H), 7.22 (d, J = 1.8 Hz, 1H), 6.99 (s, 2H), 6.95 (s, 1H), 6.91 (d, J = 8.0 Hz, 1H), 4.96 (d, J = 8.6 Hz, 1H), 4.50−4.40 (m, 1H), 3.89 (s, 3H), 3.86 (d, J = 3.8 Hz, 1H), 3.18 (t, J = 12.4 Hz, 1H), 2.81 (dd, J = 12.4, 3.8 Hz, 1H), 2.25 (s, 6H), 2.08 (sept d, J = 6.9, 3.9 Hz, 1H), 1.06 (s, 9H), 1.00 (d, J = 6.9 Hz, 3H), 0.89 (d, J = 6.9 Hz, 3H). ^{13}C NMR (101 MHz, MeOH-d_4): δ 176.4, 175.9, 175.8, 174.1, 174.1, 164.6, 162.6, 156.5, 152.6, 146.6, 141.7, 139.8, 136.8, 134.8, 133.8, 132.2, 131.3, 130.8, 130.5, 127.3, 126.4, 112.0, 76.8, 60.4, 58.5, 56.7, 52.6, 39.3, 34.1, 33.1, 26.7, 21.3, 19.5, 16.3. HRMS-ESI (*m/z*) calcd for $C_{37}H_{42}N_5O_8$ [M + H]$^+$ 684.3033; found 684.3031. $[\alpha]_D^{20}$ −218 (c 1.0, CHCl$_3$).

Methyl 2-[(1S,6S,9S)-6-tert-Butyl-9-[(2S)-2-hydroxy-3-methylbutanamido]-1-(naphthalen-2-yl)-8,16-dioxo-19-oxa-4,7,15-triazatetracyclo[9.5.2.1^{2,5}.0^{14,17}]nonadeca-2,4,11,13,17-pentaen-3-yl]-1,3-oxazole-4-carboxylate (14e). The title compound was prepared according to general procedure H, from a macrocycle **3e** (60 mg; 0.085 mmol),

TFA (196 μL; 2.55 mmol; 30 equiv) in DCM (2 mL) in 2 h and (S)-2-hydroxy-3-methylbutanoic acid (11 mg; 0.94 mmol; 1.1 equiv), EDC × HCl (26 mg; 0.14 mmol; 1.6 equiv), HOBt (39 mg; 0.26 mmol; 3 equiv), and DIPEA (59 μL; 0.34 mmol; 4 equiv) in DMF (2 mL) in 18 h. Purification by column chromatography on silica gel (gradient elution from 20% to 80% EtOAc in hexanes) was followed by reverse phase column chromatography (gradient elution from 40% to 80% MeCN in water) and afforded **14e** (32 mg, 53%; dr 99:1) as a white amorphous solid. ^{1}H NMR (400 MHz, CDCl$_3$): δ 9.37 (s, 1H), 7.95 (s, 1H), 7.84−7.65 (m, 4H), 7.60−7.40 (m, 4H), 7.22 (s, 1H), 7.07 (d, J = 7.7 Hz, 1H), 6.87 (d, J = 7.9 Hz, 1H), 6.69−6.54 (m, 1H), 4.94−4.82 (m, 1H), 4.51−4.37 (m, 1H), 4.05 (s, 1H), 3.84 (s, 3H), 3.26 (dd, J = 12.2, 12.2 Hz, 1H), 2.79 (dd, J = 12.3, 3.4 Hz, 1H), 2.24−2.17 (m, 1H), 1.09−0.94 (m, 12H), 0.87 (d, J = 6.8 Hz, 3H). ^{13}C NMR (101 MHz, CDCl$_3$): δ 175.0, 173.2, 171.8, 162.4, 161.3, 155.0, 150.5, 144.2, 139.8, 133.9, 133.1, 132.8, 132.8, 132.3, 130.9, 129.8, 129.7, 128.7, 128.2, 127.6, 127.5, 126.8, 126.6, 126.5, 124.6, 111.4, 76.0, 59.0, 57.7, 56.1, 52.2, 38.2, 33.3, 31.9, 26.4, 19.2, 15.5. HRMS-ESI (*m/z*) calcd for $C_{39}H_{40}N_5O_8$ [M + H]$^+$ 706.2877; found 706.2891. $[\alpha]_D^{20}$ −295 (c 0.5, CHCl$_3$).

Methyl 2-[(1S,6S,9S)-6-tert-Butyl-9-[(2S)-2-hydroxy-3-methylbutanamido]-8,16-dioxo-19-oxa-4,7,15-triazatetracyclo[9.5.2.1^{2,5}.0^{14,17}]nonadeca-2,4,11,13,17-pentaen-3-yl]-1,3-oxazole-4-carboxylate (14f). The title compound was prepared according to general procedure H from macrocycle **3f** (40 mg; 0.069 mmol), TFA (106 μL; 1.38 mmol; 20 equiv) in DCM (1 mL) in 2 h and (S)-2-hydroxy-3-methylbutanoic acid (12 mg; 0.10 mmol; 1.5 equiv), EDC × HCl (24 mg; 0.12 mmol; 1.8 equiv), HOBt (30 mg; 0.21 mmol; 3 equiv), and DIPEA (60 μL; 0.34 mmol; 5 equiv) in DMF (1 mL) in 1 h. Purification by reverse phase column chromatography (gradient elution from 10% to 95% MeCN in water) afforded **14f** (26 mg, 65%; dr 92:8) as a white amorphous solid. ^{1}H NMR (400 MHz, MeOH-d_4): δ 8.68 (s, 1H), 7.28 (dd, J = 8.1, 1.8 Hz, 1H), 6.95 (d, J = 8.1 Hz, 1H), 6.52 (d, J = 1.8 Hz, 1H), 4.55 (s, 1H), 4.51 (dd, J = 12.0, 4.1 Hz, 1H), 3.93 (s, 3H), 3.85 (d, J = 3.6 Hz, 1H), 2.99 (dd, J = 12.0, 12.0 Hz, 1H), 2.80 (dd, J = 12.0, 4.1 Hz, 1H), 2.07 (sept d, J = 6.9, 3.6 Hz, 1H), 0.99 (d, J = 6.9 Hz, 3H), 0.97 (s, 9H), 0.88 (d, J = 6.9 Hz, 3H). ^{13}C NMR (101 MHz, MeOH-d_4): δ 176.5, 175.8, 173.7, 165.7, 162.9, 157.2, 150.2, 146.1, 143.9, 135.3, 132.6, 131.3, 131.1, 130.3, 129.9, 112.4, 76.8, 61.0, 56.5, 52.6, 39.0, 34.1, 33.1, 26.8, 19.5, 16.3. HRMS-ESI (*m/z*) calcd for $C_{29}H_{34}N_5O_8$ [M + H]$^+$ 580.2407; found 580.2411. $[\alpha]_D^{20}$ −96 (c 1.0, MeOH).

Methyl 2-[(1S,6S,9S)-6-tert-Butyl-9-[(2S)-2-Hydroxy-3-methylbutanamido]-15-methyl-8,16-dioxo-19-oxa-4,7,15-triazatetracyclo[9.5.2.1^{2,5}.0^{14,17}]nonadeca-2,4,11,13,17-pentaen-3-yl]-1,3-oxazole-4-carboxylate (14g). The title compound was prepared according to general procedure H from macrocycle **3g** (100 mg; 0.17 mmol), TFA (129 μL; 1.68 mmol; 10 equiv) in DCM (3 mL) in 3 h and (S)-2-hydroxy-3-methylbutanoic acid (30 mg; 0.25 mmol; 1.5 equiv), EDC × HCl (58 mg; 0.30 mmol; 1.8 equiv), HOBt (68 mg; 0.50 mmol; 3 equiv), and DIPEA (146 μL; 0.84 mmol; 5 equiv) in DMF (3 mL) in 2 h. Purification by reverse phase column chromatography (gradient elution from 5% to 50% MeCN in water) afforded **14g** (44 mg, 44%; dr 94:6) as a white amorphous solid. ^{1}H NMR (400 MHz, CDCl$_3$): δ 8.33 (s, 1H), 7.32 (d, J = 8.6 Hz, 1H), 7.25 (d, J = 7.7 Hz, 1H), 6.87

140

(d, J = 7.7 Hz, 1H), 6.61 (s, 1H), 6.04 (d, J = 6.7 Hz, 1H), 5.64 (s, 1H), 4.58 (d, J = 6.7 Hz, 1H), 4.33−4.24 (m, 1H), 4.00 (d, J = 2.8 Hz, 1H), 3.93 (s, 3H), 3.25 (s, 3H), 3.18 (dd, J = 12.0, 12.0 Hz, 1H), 2.77 (dd, J = 12.6, 3.2 Hz, 1H), 2.51 (br s, 1H), 2.17 (sept d, J = 7.0, 2.7 Hz, 1H), 1.00 (d, J = 7.0 Hz, 3H), 0.92 (s, 9H), 0.86 (d, J = 7.0 Hz, 3H). ^{13}C NMR (101 MHz, CDCl$_3$): δ 173.2, 172.4, 171.5, 163.4, 161.6, 155.8, 148.2, 144.5, 144.0, 134.7, 131.5, 129.8, 129.5, 129.4, 128.9, 109.6, 76.2, 59.4, 56.3, 52.4, 45.6, 37.9, 33.3, 32.0, 27.0, 26.7, 19.3, 15.5. HRMS-ESI (m/z) calcd for C$_{30}$H$_{36}$N$_5$O$_8$ [M + H]$^+$ 594.2564; found 594.2561. $[\alpha]_D^{20}$ −90 (c 1.0, CHCl$_3$).

Methyl 2-[(1S,6S,9S)-6-tert-Butyl-9-[(2S)-2-hydroxy-3-methylbutanamido]-15-methyl-8,16-dioxo-1-phenyl-19-oxa-2,4,11,13,17-pentaen-3-yl]-1,3-oxazole-4-carboxylate (14h). The title compound was prepared according to general procedure H from macrocycle **3h** (100 mg; 0.15 mmol), TFA (172 μL; 2.24 mmol; 15 equiv) in DCM (1 mL) in 1 h and (S)-2-hydroxy-3-methylbutanoic acid (26 mg; 0.22 mmol; 1.5 equiv), EDC × HCl (51 mg; 0.27 mmol; 1.8 equiv), HOBt (60 mg; 0.45 mmol; 3 equiv), and DIPEA (129 μL; 0.75 mmol; 5 equiv) in DMF (1 mL) in 3 h. Purification by reverse phase column chromatography (gradient elution from 10% to 95% MeCN in water) afforded **14h** (43 mg, 43%; dr 99:1) as a white amorphous solid. ^{1}H NMR (400 MHz, CD$_3$CN): δ 8.38 (s, 1H), 7.42−7.26 (m, 7H), 7.17 (d, J = 8.3 Hz, 1H), 6.98−6.90 (m, 2H), 5.06−5.02 (m, 1H), 4.28−4.20 (m, 1H), 3.85 (s, 3H), 3.81 (d, J = 3.4 Hz, 1H), 3.60 (s, 1H), 3.19−3.11 (m, 4H), 2.76 (dd, J = 12.6, 3.6 Hz, 1H), 2.05−1.97 (m, 1H), 1.02 (s, 9H), 0.94 (d, J = 6.9 Hz, 3H), 0.80 (d, J = 6.9 Hz, 3H). ^{13}C NMR (101 MHz, CD$_3$CN): δ 173.5, 172.9, 172.9, 165.0, 162.1, 155.4, 151.9, 146.2, 143.4, 137.0, 134.6, 132.5, 131.5, 131.1, 129.9, 129.4, 129.3, 128.9, 126.0, 110.1, 76.2, 59.4, 56.6, 56.4, 52.6, 38.8, 33.7, 32.8, 27.5, 26.5, 19.4, 16.0. HRMS-ESI (m/z) calcd for C$_{36}$H$_{40}$N$_5$O$_8$ [M + H]$^+$ 670.2877; found 670.2874. $[\alpha]_D^{20}$ −347 (c 1.0, MeOH).

Methyl 2-[(1S,6S,9S)-6-tert-Butyl-9-[(2S)-2-hydroxy-3-methylbutanamido]-1,15-dimethyl-8,16-dioxo-19-oxa-4,7,15-triazatetracyclo[9.5.2.1^{2,5}.0^{14,17}]nonadeca-2,4,11,13,17-pentaen-3-yl]-1,3-oxazole-4-carboxylate (14i). The title compound was prepared according to general procedure H from macrocycle **3i** (55 mg; 0.09 mmol), TFA (70 μL; 0.91 mmol; 10 equiv) in DCM (2 mL) in 3 h and (S)-2-hydroxy-3-methylbutanoic acid (16 mg; 0.14 mmol; 1.5 equiv), EDC × HCl (39 mg; 0.20 mmol; 2.2 equiv), HOBt (46 mg; 0.34 mmol; 3.7 equiv), and DIPEA (97 μL; 0.56 mmol; 6.2 equiv) in DMF (2 mL) in 2 h. Purification by reverse phase column chromatography (gradient elution from 5% to 50% MeCN in water) afforded **14i** (22 mg, 40%; dr 99:1) as a white amorphous solid. ^{1}H NMR (400 MHz, MeOH-d_4): δ 8.70 (s, 1H), 8.22 (d, J = 7.4 Hz, 1H), 7.35 (dd, J = 8.1, 1.8 Hz, 1H), 7.04 (d, J = 8.1 Hz, 1H), 6.94 (d, J = 1.8 Hz, 1H), 4.73−4.64 (m, 1H), 4.50 (dd, J = 11.7, 3.9 Hz, 1H), 3.93 (s, 3H), 3.86 (d, J = 3.9 Hz, 1H), 3.23 (s, 3H), 3.09 (dd, J = 12.1, 12.1 Hz, 1H), 2.88 (dd, J = 12.1, 3.9 Hz, 1H), 2.08 (sept d, J = 6.9, 3.9 Hz, 1H), 1.95 (s, 3H), 1.00 (d, J = 6.9 Hz, 3H), 0.97 (s, 9H), 0.89 (d, J = 6.9 Hz, 3H). ^{13}C NMR (101 MHz, MeOH-d_4): δ 176.7, 175.8, 173.8, 163.9, 162.8, 156.7, 152.7, 146.6, 143.5, 135.2, 134.9, 132.8, 131.1, 129.0, 127.7, 110.8, 76.8, 59.6, 56.6, 52.6, 51.6, 39.2, 34.2, 33.1, 27.1, 26.7, 20.3, 19.5, 16.3. HRMS-ESI (m/z) calcd for C$_{31}$H$_{38}$N$_5$O$_8$ [M + H]$^+$ 608.2720; found 608.2720. $[\alpha]_D^{20}$ −94 (c 1.0, MeOH).

Methyl 2-[(1S,6S,9S)-6-tert-Butyl-1-ethyl-9-[(2S)-2-hydroxy-3-methylbutanamido]-15-methyl-8,16-dioxo-19-oxa-4,7,15-triazatetracyclo[9.5.2.1^{2,5}.0^{14,17}]nonadeca-2,4,11,13,17-pentaen-3-yl]-1,3-oxazole-4-carboxylate (14j). The title compound was prepared according to general procedure H from macrocycle **3j** (50 mg; 0.13 mmol), TFA (62 μL; 0.80 mmol; 10 equiv) in DCM (2 mL) in 3 h and (S)-2-hydroxy-3-methylbutanoic acid (14 mg; 0.12 mmol; 1.5 equiv), EDC × HCl (28 mg; 0.15 mmol; 1.8 equiv), HOBt (33 mg; 0.24 mmol; 3 equiv), and DIPEA (70 μL; 0.40 mmol; 5 equiv) in DMF (2 mL) in 2 h. Purification by reverse phase column chromatography (gradient elution from 5% to 50% MeCN in water) afforded **14j** (33 mg, 66%; dr 99:1) as a white amorphous solid. ^{1}H NMR (400 MHz, MeOH-d_4): δ 8.69 (s, 1H), 7.36 (dd, J = 8.1, 1.6 Hz, 1H), 7.05−7.01 (m, 2H), 4.76 (s, 1H), 4.50 (dd, J = 11.8, 4.0 Hz, 1H), 3.93 (s, 3H), 3.87 (d, J = 4.0 Hz, 1H), 3.21 (s, 3H), 3.14 (t, J = 12.2 Hz, 1H), 2.88 (dd, J = 12.2, 4.0 Hz, 1H), 2.69 (dq, J = 7.0, 7.0 Hz, 1H), 2.38 (dq, J = 7.0, 7.0 Hz, 1H), 2.09 (sept d, J = 7.0, 4.0 Hz, 1H), 1.01 (d, J = 7.0 Hz, 3H), 1.00 (s, 9H), 0.89 (d, J = 7.0 Hz, 3H), 0.83 (t, J = 7.0 Hz, 3H). ^{13}C NMR (101 MHz, MeOH-d_4): δ 175.9, 175.8, 173.8, 163.8, 162.7, 156.7, 152.0, 146.6, 144.3, 135.2, 132.7, 132.1, 131.16, 129.6, 127.3, 110.7, 76.8, 59.2, 56.8, 56.7, 52.6, 39.2, 34.2, 33.1, 27.4, 27.0, 26.7, 19.6, 16.3, 9.1. HRMS-ESI (m/z) calcd for C$_{32}$H$_{40}$N$_5$O$_8$ [M + H]$^+$ 622.2877; found 622.2880. $[\alpha]_D^{20}$ −118 (c 1.0, MeOH).

Methyl 2-[(1S,6S,9S)-1-Benzyl-6-tert-butyl-9-[(2S)-2-hydroxy-3-methylbutanamido]-15-methyl-8,16-dioxo-19-oxa-4,7,15-triazatetracyclo[9.5.2.1^{2,5}.0^{14,17}]nonadeca-2,4,11,13,17-pentaen-3-yl]-1,3-oxazole-4-carboxylate (14k). The title compound was prepared according to general procedure H from macrocycle **3k** (45 mg; 0.07 mmol), TFA (51 μL; 0.66 mmol; 10 equiv) in DCM (5 mL) in 3 h and (S)-2-hydroxy-3-methylbutanoic acid (12 mg; 0.10 mmol; 1.5 equiv), EDC × HCl (22 mg; 0.12 mmol; 1.8 equiv), HOBt (27 mg; 0.20 mmol; 3 equiv), and DIPEA (56 μL; 0.33 mmol; 5 equiv) in DMF (2 mL) in 2 h. Purification by reverse phase column chromatography (gradient elution from 5% to 50% MeCN in water) afforded **14k** (23 mg, 52%; dr 99:1) as a white amorphous solid. ^{1}H NMR (400 MHz, MeOH-d_4): δ 8.74 (s, 1H), 7.25 (dd, J = 8.1, 1.7 Hz, 1H), 7.10−7.00 (m, 6H), 6.78 (d, J = 8.1 Hz, 1H), 4.76 (s, 1H), 4.48 (dd, J = 12.1, 4.0 Hz, 1H), 4.26 (d, J = 13.1 Hz, 1H), 3.92 (d, J = 5.4 Hz, 3H), 3.87 (d, J = 4.0 Hz, 1H), 3.49 (d, J = 13.1 Hz, 1H), 3.16 (dd, J = 12.1, 12.1 Hz, 1H), 2.95 (s, 3H), 2.86 (dd, J = 12.1, 4.0 Hz, 1H), 2.09 (sept d, J = 7.0, 4.0 Hz, 1H), 1.01 (d, J = 7.0 Hz, 3H), 1.00 (s, 9H), 0.91 (d, J = 7.0 Hz, 3H). ^{13}C NMR (101 MHz, MeOH-d_4): δ 175.8, 175.4, 173.9, 163.7, 162.8, 156.8, 151.7, 146.7, 143.9, 136.1, 135.2, 132.5, 132.0, 131.4, 131.1, 130.1, 128.8, 128.1, 127.8, 110.5, 76.8, 59.4, 57.6, 56.7, 52.6, 40.0, 39.3, 34.2, 33.1, 26.7, 19.6, 16.3. HRMS-ESI (m/z) calcd for C$_{37}$H$_{42}$N$_5$O$_8$ [M + H]$^+$ 684.3033; found 684.3035. $[\alpha]_D^{20}$ −156 (c 1.0, MeOH).

Methyl 2-[(1S,6S,9S)-6-tert-Butyl-9-[(2S)-2-hydroxy-3-methylbutanamido]-8,17-dioxo-1-phenyl-20-oxa-4,7,16-triazatetracyclo[10.5.2.1^{2,5}.0^{15,18}]icosa-2,4,12,14,18-pentaen-3-yl]-1,3-oxazole-4-carboxylate (15a). A stream of argon was passed for 10 min through light yellow suspension of **6a** (60 mg; 0.080 mmol) and oven-dried K$_3$PO$_4$ (51 mg; 0.24 mmol; 3 equiv) in anhydrous degassed DMSO (3.6 mL). Subsequently, the suspension was left to stir at 65 °C for 6 h, cooled to room temperature, quenched with aqueous saturated

141

NH$_4$Cl, and extracted with EtOAc (two times). Combined organic extracts were washed with brine, dried (MgSO$_4$), and evaporated under the reduced pressure to afford macrocycle **4a** as 62:38 mixture of diastereomers. Purification by reverse phase column chromatography (gradient elution from 10% to 100% MeCN in water) yielded macrocycle **4a** (17 mg, 32%; dr 76:24.) as white amorphous solid.

The cleavage of *N*-Boc protection in macrocycle **4a** and amide bond formation was accomplished as described in general procedure H using TFA (21 μL; 0.27 mmol; 10 equiv) in DCM (1 mL) within 16 h, followed by treatment with (*S*)-2-hydroxy-3-methylbutanoic acid (3.7 mg; 0.032 mmol; 1.5 equiv), EDC × HCl (8.1 mg; 0.042 mmol; 2 equiv), HOBt (5.7 mg; 0.042 mmol; 2 equiv), and DIPEA (11 μL; 0.64 mmol; 3 equiv) in DMF (0.5 mL) for 3 h. Purification by reverse phase preparative HPLC (gradient elution from 10% to 95% MeCN in 0.1% aqueous AcOH) yielded (*S,S,S*)−**15a** (3.0 mg, 21%; dr 99:1) as a white amorphous solid. Absolute configuration of the newly formed quaternary center for the major product was assigned as *S* in analogy to compound **15i** (see Supporting Information, page S19). ^{1}H NMR (400 MHz, MeOH-*d*$_4$): δ 8.23 (s, 1H), 7.40−7.35 (m, 2H), 7.23−7.24 (m, 3H), 7.17 (dd, *J* = 8.0, 1.8 Hz, 1H), 7.14−7.11 (m, 1H), 6.92 (d, *J* = 8.0 Hz, 1H), 4.75 (s, 1H), 4.08 (dd, *J* = 6.4, 3.3 Hz, 1H), 3.87 (s, 3H), 3.84 (d, *J* = 4.0 Hz, 1H), 3.01−2.92 (m, 1H), 2.82−2.69 (m, 2H), 2.11−2.04 (m, 1H), 1.86−1.75 (m, 1H), 1.03 (s, 9H), 0.99 (d, *J* = 6.9 Hz, 3H), 0.87 (d, *J* = 6.9 Hz, 3H). ^{13}C NMR (101 MHz, MeOH-*d*$_4$): δ 176.9, 176.6, 173.9, 163.7, 162.6, 156.8, 151.8, 146.3, 140.4, 138.6, 136.2, 134.8, 133.5, 131.2, 129.9, 129.1, 128.2, 127.8, 127.6, 111.6, 77.0, 59.9, 58.9, 52.7, 52.5, 34.6, 33.1, 32.4, 31.4, 26.7, 19.5, 16.4. HRMS-ESI (*m/z*) calcd for C$_{36}$H$_{40}$N$_5$O$_8$ [M + H]$^+$ 670.2877; found 670.2884. [α]$_D^{20}$ −96 (c 0.4, MeOH).

Methyl 2-[(1S,6S,9S)-6-tert-Butyl-9-[(2S)-2-hydroxy-3-methylbutanamido]-1-methyl-8,17-dioxo-20-oxa-4,7,16-triazatetracyclo[10.5.2.1^{2,5}.0^{15,18}]icosa-2,4,12,14,18-pentaen-3-yl]-1,3-oxazole-4-carboxylate (15b). Compound **6b** (278 mg; 0.40 mmol) and oven-dried K$_3$PO$_4$ (257 mg; 1.21 mmol; 3 equiv) were suspended in anhydrous degassed DMSO (20 mL), and stream of argon was passed through the mixture for 10 min. The light yellow suspension was stirred at 65 °C for 6 h. Compound **4b** was formed as a mixture of diastereomers with ratio 79:21. Vial was cooled to r.t. and reaction was quenched with aqueous saturated NH$_4$Cl and extracted with EtOAc. Combined organic layers were washed with brine, dried (MgSO$_4$), and evaporated. The macrocyclic compound **4b** was purified by reverse phase column chromatography (10% to 100% MeCN in water) to yield 120 mg (49%) of mixture of diastereomers (dr 81:19) as white amorphous solid. The obtained mixture (110 mg; 0.18 mmol) was subjected to general procedure H using TFA (139 μL; 1.81 mmol; 10 equiv) in DCM (3 mL) in 48 h and (*S*)-2-hydroxy-3-methylbutanoic acid (21 mg; 0.18 mmol; 1.5 equiv), EDC × HCl (45 mg; 0.24 mmol; 2 equiv), HOBt (32 mg; 0.24 mmol; 2 equiv), and DIPEA (61 μL; 0.35 mmol; 3 equiv) in DMF (2 mL) in 2 h. Purification by reverse phase column chromatography (gradient elution from 10% to 100% MeCN in water) afforded **15b** (44 mg, 44%; dr 98:2) of white amorphous solid. Absolute configuration of the newly formed quaternary center for the major product was assigned as *S* in analogy to compound **15i** (see Supporting Information, page S19). ^{1}H NMR (400 MHz, MeOH-*d*$_4$): δ 8.70 (s, 1H), 7.16 (dd, *J* = 7.9, 1.7 Hz, 1H), 6.95−6.88 (m, 2H), 4.54 (s, 1H),

4.03 (dd, *J* = 6.2, 3.3 Hz, 1H), 3.92 (s, 3H), 3.82 (d, *J* = 4.1 Hz, 1H), 3.04−2.92 (m, 1H), 2.83−2.67 (m, 2H), 2.08−2.00 (m, 1H), 1.98 (s, 3H), 1.85−1.78 (m, 1H), 0.97 (d, *J* = 6.9 Hz, 3H), 0.95 (s, 9H), 0.87 (d, *J* = 6.9 Hz, 3H). ^{13}C NMR (101 MHz, MeOH-*d*$_4$): δ 179.3, 176.6, 173.9, 163.1, 162.8, 157.1, 152.0, 146.4, 140.4, 135.7, 135.3, 135.2, 131.2, 127.6, 126.4, 111.4, 76.9, 59.6, 52.6, 52.4, 51.5, 34.6, 33.1, 32.9, 31.1, 26.7, 22.0, 19.5, 16.5. HRMS-ESI (*m/z*) calcd for C$_{31}$H$_{38}$N$_5$O$_8$ [M + H]$^+$ 608.2720; found 608.2719. [α]$_D^{20}$ −82 (c 1.4, MeOH).

Methyl 2-[(1S,6S,9S)-6-tert-Butyl-9-[(2S)-2-hydroxy-3-methylbutanamido]-1,16-dimethyl-8,17-dioxo-20-oxa-4,7,16-triazatetracyclo[10.5.2.1^{2,5}.0^{15,18}]icosa-2,4,12,14,18-pentaen-3-yl]-1,3-oxazole-4-carboxylate (15i) and Methyl 2-[(1R,6S,9S)-6-tert-Butyl-9-[(2S)-2-hydroxy-3-methylbutanamido]-1,16-dimethyl-8,17-dioxo-20-oxa-4,7,16-triazatetracyclo[10.5.2.1^{2,5}.0^{15,18}]icosa-2,4,12,14,18-pentaen-3-yl]-1,3-oxazole-4-carboxylate (epi-15i). Compound **6i** (366 mg; 0.52 mmol) and oven-dried K$_3$PO$_4$ (332 mg; 1.56 mmol; 3 equiv) were suspended in anhydrous degassed DMSO (25 mL), and stream of argon was passed through the mixture for 10 min. The light yellow suspension was stirred at 65 °C for 6 h. Compound **4i** was formed as a mixture of diastereomers with ratio 85:15. Vial was cooled to r.t., and reaction was quenched with aqueous saturated NH$_4$Cl and extracted with EtOAc. Combined organic layers were washed with brine, dried (MgSO$_4$), and evaporated. Compound **4i** was purified by reverse phase column chromatography (10% to 100% MeCN in water) to yield 192 mg (59%) of mixture of diastereomers (dr 87:13) as white amorphous solid. The obtained mixture (175 mg; 0.28 mmol) was subjected to general procedure H using TFA (216 μL; 2.81 mmol; 10 equiv) in DCM (3 mL) in 48 h and (*S*)-2-hydroxy-3-methylbutanoic acid (54 mg; 0.46 mmol; 1.5 equiv), EDC × HCl (118 mg; 0.61 mmol; 2 equiv), HOBt (83 mg; 0.61 mmol; 2 equiv), and DIPEA (159 μL; 0.92 mmol; 3 equiv) in DMF (3 mL) in 3 h. Compounds **15i** and *epi*-**15i** were separated and purified by reverse phase column chromatography (gradient elution from 10% to 100% MeCN in water) to afford 97 mg (51%; dr 94:6) of **15i** and 6.9 mg (4%; dr 99:1) of *epi*-**15i** as white amorphous solids. Absolute configuration of the newly formed quaternary centers was determined comparing experimental and calculated CD spectra for both diastereomeric compounds (see Supporting Information, page S19). It was assigned to be *S* for **15i** and *R* for *epi*-**15i**. Data for compound **15i**: ^{1}H NMR (400 MHz, MeOH-*d*$_4$): δ 8.69 (s, 1H), 8.20 (d, *J* = 7.9 Hz, 1H), 7.73 (d, *J* = 7.3 Hz, 1H), 7.25 (dd, *J* = 8.0, 1.7 Hz, 1H), 7.04 (d, *J* = 1.7 Hz, 1H), 7.01 (d, *J* = 8.0 Hz, 1H), 4.63 (d, *J* = 7.3 Hz, 1H), 4.06−4.02 (m, 1H), 3.92 (s, 3H), 3.83 (d, *J* = 4.0 Hz, 1H), 3.23 (s, 3H), 3.05−2.98 (m, 1H), 2.84−2.69 (m, 2H), 2.08−2.01 (m, 1H), 1.97 (s, 3H), 1.83−1.75 (m, 1H), 1.00−0.95 (m, 12H), 0.87 (d, *J* = 6.9 Hz, 3H). ^{13}C NMR (101 MHz, MeOH-*d*$_4$): δ 177.1, 176.5, 173.9, 163.3, 162.8, 157.0, 151.8, 146.5, 142.2, 136.6, 135.2, 134.0, 131.1, 127.2, 126.1, 110.2, 76.9, 59.2, 52.6, 52.5, 50.9, 34.6, 33.1, 32.6, 31.4, 27.1, 26.7, 21.9, 19.5, 16.4. HRMS-ESI (*m/z*) calcd for C$_{32}$H$_{39}$N$_5$O$_8$ [M + H]$^+$ 622.2877; found 622.2875. [α]$_D^{20}$ −121 (c 0.8, MeOH). Data for compound *epi*-**15i**: ^{1}H NMR (400 MHz, MeOH-*d*$_4$): δ 8.65 (s, 1H), 8.27 (d, *J* = 6.2 Hz, 1H), 8.03 (d, *J* = 8.0 Hz, 1H), 7.25 (d, *J* = 1.6 Hz, 1H), 7.14 (dd, *J* = 8.0, 1.6 Hz, 1H), 6.93 (d, *J* = 8.0 Hz, 1H), 4.80−4.71 (m, 1H), 4.44 (d, *J* = 6.2 Hz, 1H), 3.92 (s, 3H), 3.84 (d, *J* = 3.9 Hz, 1H), 3.25 (s, 3H), 2.93−2.75 (m, 2H),

2.50−2.35 (m, 1H), 2.11 (dp, J = 6.8, 3.9 Hz, 1H), 2.05−1.93 (m, 1H), 1.89 (s, 3H), 1.16 (s, 9H), 1.01 (d, J = 6.8 Hz, 3H), 0.91 (d, J = 6.8 Hz, 3H). ^{13}C NMR (101 MHz, MeOH-d_4): 176.4, 175.9, 173.1, 163.9, 162.7, 156.5, 152.3, 146.6, 142.0, 137.7, 134.9, 132.4, 130.5, 125.6, 124.3, 110.4, 76.9, 59.5, 54.5, 52.5, 50.4, 34.4, 34.1, 33.3, 33.0, 27.2, 26.9, 21.0, 19.6, 16.5. HRMS-ESI (m/z) calcd for $C_{32}H_{39}N_5O_8$ [M + H]$^+$ 622.2877; found: 622.2853. $[\alpha]_D^{20}$ −135 (c 0.3, MeOH).

2-[(1S,6S,9S)-6-tert-Butyl-9-[(2S)-2-hydroxy-3-methylbutanamido]-8,16-dioxo-1-phenyl-19-oxa-4,7,15-triazatetracyclo[9.5.2.1^{2,5}.0^{14,17}]nonadeca-2,4,11,13,17-pentaen-3-yl]-1,3-oxazole-4-carboxylic acid (16). To a solution of methyl ester **14a** (130 mg, 0.20 mmol) in MeOH (2 mL) and water (1 mL) was added LiOH × H$_2$O (25 mg, 0.60 mmol, 3.0 equiv), and the resulting suspension was stirred at room temperature for 30 min. Then, the solution was acidified with aqueous 1 M HCl to pH 2, and the resulting suspension was extracted with EtOAc (three times). Combined organic extracts were washed with brine, dried (Na$_2$SO$_4$) and evaporated under reduced pressure. Purification by reverse phase column chromatography (gradient elution from 10% to 50% MeCN in 0.01% aqueous TFA) provided carboxylic acid **16** (100 mg, 80%) as a white amorphous solid. ^{1}H NMR (400 MHz, MeOH-d_4): δ 8.37 (s, 1H), 7.45−7.39 (m, 2H), 7.38−7.30 (m, 3H), 7.29−7.25 (m, 2H), 6.92 (d, J = 8.4 Hz, 1H), 4.96 (s, 1H), 4.45 (dd, J = 11.8, 3.8 Hz, 1H), 3.86 (d, J = 3.8 Hz, 1H), 3.18 (dd, J = 12.2, 12.2 Hz, 1H), 2.82 (dd, J = 12.7, 3.8 Hz, 1H), 2.07 (sept d, J = 6.9, 3.8 Hz, 1H), 1.06 (s, 9H), 1.00 (d, J = 6.9 Hz, 3H), 0.89 (d, J = 6.9 Hz, 3H).^{13}C NMR (101 MHz, MeOH-d_4): δ 176.2, 175.8, 174.0, 164.5, 163.5, 156.3, 152.2, 146.5, 141.8, 137.2, 135.5, 133.5, 132.2, 131.4, 130.5, 130.0, 129.4, 128.7, 127.5, 112.0, 76.8, 60.5, 58.3, 56.7, 39.3, 34.1, 33.1, 26.7, 19.5, 16.3. HRMS-ESI (m/z) calcd for $C_{34}H_{36}N_5O_8$ [M + H]$^+$ 642.2564; found: 642.2571. $[\alpha]_D^{20}$ −226 (c 1.0, MeOH).

2-[(1S,6S,9S)-6-tert-Butyl-9-[(2S)-2-hydroxy-3-methylbutanamido]-8,16-dioxo-1-phenyl-19-oxa-4,7,15-triazatetracyclo[9.5.2.1^{2,5}.0^{14,17}]nonadeca-2,4,11,13,17-pentaen-3-yl]-N,N-dimethyl-1,3-oxazole-4-carboxamide (17). EDC × HCl (36 mg, 0.19 mmol, 2.0 equiv), HOBt (38 mg, 0.28 mmol, 3.0 equiv), NHMe$_2$ × HCl (38 mg, 0.47 mmol, 5 equiv), and DIPEA (80 μL, 0.47 mmol, 5.0 equiv) were sequentially added to a solution of carboxylic acid **16** (60 mg, 0.094 mmol) in anhydrous DMF (0.5 mL) at room temperature. After stirring for 2 h, the resulting yellow solution was diluted with aqueous saturated NH$_4$Cl and EtOAc. The layers were separated, and the organic phase was washed with water, brine, dried (Na$_2$SO$_4$), and evaporated under reduced pressure. Purification by reverse phase column chromatography (gradient elution from 10% to 50% MeCN in 0.01% aqueous TFA) provided amide **17** (39 mg, 62%) as a white amorphous solid. ^{1}H NMR (400 MHz, MeOH-d_4): δ 8.23 (s, 1H), 7.45−7.40 (m, 2H), 7.37−7.29 (m, 3H), 7.27 (dd, J = 8.0, 1.8 Hz, 1H), 7.22 (d, J = 1.8 Hz, 1H), 6.92 (d, J = 8.0 Hz, 1H), 4.91 (s, 1H), 4.47 (dd, J = 11.7, 3.8 Hz, 1H), 3.86 (d, J = 3.8 Hz, 1H), 3.28 (s, 3H), 3.16 (dd, J = 12.1, 12.1 Hz, 1H), 3.05 (s, 3H), 2.82 (dd, J = 12.6, 3.8 Hz, 1H), 2.08 (sept d, J = 6.9, 3.8 Hz, 1H), 1.06 (s, 9H), 1.00 (d, J = 6.9 Hz, 3H), 0.89 (d, J = 6.9 Hz, 3H). ^{13}C NMR (101 MHz, MeOH-d_4): δ 176.2, 175.8, 174.0, 164.3, 151.9, 144.7, 141.7, 137.4, 133.9, 132.2, 131.3, 130.6, 129.9, 129.3, 128.6, 128.1, 112.0, 76.8, 60.5, 58.6, 56.7, 39.2, 36.6, 34.2, 33.2, 26.7, 19.5, 16.3. HRMS-ESI (m/z

calcd for $C_{36}H_{41}N_6O_7$ [M + H]$^+$ 669.3037; found: 669.3029. $[\alpha]_D^{20}$ −229 (c 1.0, MeOH).

2-[(1S,6S,9S)-6-tert-Butyl-9-[(2S)-2-hydroxy-3-methylbutanamido]-8,16-dioxo-1-phenyl-19-oxa-4,7,15-triazatetracyclo[9.5.2.1^{2,5}.0^{14,17}]nonadeca-2,4,11,13,17-pentaen-3-yl]-1,3-oxazole-4-carboxamide (18). A clear solution of methyl ester **14a** (22 mg, 0.034 mmol) in anhydrous ammonia (7 N solution in MeOH, 0.24 mL, 1.68 mmol, 50 equiv) was stirred at room temperature for 20 h and evaporated to dryness under the reduced pressure. The residue was purified by reverse phase column chromatography (gradient elution from 10% to 50% MeCN in 0.01% aqueous TFA) to provide amide **18** (18 mg, 84%) as a white amorphous solid. ^{1}H NMR (400 MHz, MeOH-d_4): δ 8.21 (s, 1H), 7.49−7.41 (m, 2H), 7.37−7.29 (m, 3H), 7.28 (dd, J = 8.0, 1.7 Hz, 1H), 7.18 (d, J = 1.7 Hz, 1H), 6.93 (d, J = 8.0 Hz, 1H), 4.86 (s, 1H), 4.50 (dd, J = 11.7, 4.0 Hz, 1H), 3.86 (d, J = 3.8 Hz, 1H), 3.14 (dd, J = 12.1, 12.1 Hz, 1H), 2.83 (dd, J = 12.6, 4.0 Hz, 1H), 2.09 (sept d, J = 6.9, 3.8 Hz, 1H), 1.05 (s, 9H), 1.00 (d, J = 6.9 Hz, 3H), 0.89 (d, J = 6.9 Hz, 3H). ^{13}C NMR (101 MHz, MeOH-d_4): δ 176.5, 175.8, 174.0, 164.8, 164.4, 155.4, 152.2, 143.7, 141.6, 138.0, 137.3, 134.4, 132.3, 131.3, 130.5, 129.9, 129.3, 128.6, 128.3, 112.1, 76.8, 60.6, 59.0, 56.6, 39.2, 34.2, 33.2, 26.7, 19.5, 16.3. HRMS-ESI (m/z) calcd for $C_{34}H_{37}N_6O_7$ [M + H]$^+$ 641.2724; found: 641.2726. $[\alpha]_D^{20}$ −192 (c 1.0, MeOH).

2-[(1S,6S,9S)-6-tert-Butyl-9-[(2S)-2-hydroxy-3-methylbutanamido]-8,16-dioxo-1-phenyl-19-oxa-4,7,15-triazatetracyclo[9.5.2.1^{2,5}.0^{14,17}]nonadeca-2,4,11,13,17-pentaen-3-yl]-N-methyl-1,3-oxazole-4-carboxamide (19). A clear solution of methyl ester **14a** (35 mg, 0.053 mmol) in anhydrous MeNH$_2$ (33% solution in EtOH, 0.56 mL, 5.34 mmol, 100 equiv) was stirred at room temperature for 20 h and evaporated to dryness under reduced pressure. The residue was purified by reverse phase column chromatography (gradient elution from 10% to 50% MeCN in water) to provide amide **19** (31 mg, 89%) as a white amorphous solid. ^{1}H NMR (400 MHz, MeOH-d_4): δ 8.18 (s, 1H), 7.44−7.40 (m, 2H), 7.36−7.26 (m, 4H), 7.17 (d, J = 1.7 Hz, 1H), 6.93 (d, J = 8.0 Hz, 1H), 4.85 (s, 1H), 4.49 (dd, J = 11.7, 4.0 Hz, 1H), 3.86 (d, J = 3.8 Hz, 1H), 3.14 (dd, J = 12.2, 12.2 Hz, 1H), 2.88 (s, 3H), 2.84 (dd, J = 12.6, 4.0 Hz, 1H), 2.09 (sept d, J = 6.9, 3.8 Hz, 1H), 1.04 (s, 9H), 1.00 (d, J = 6.9 Hz, 3H), 0.89 (d, J = 6.9 Hz, 3H). ^{13}C NMR (101 MHz, MeOH-d_4): δ 176.6, 175.8, 174.0, 164.4, 163.1, 155.3, 152.1, 142.9, 141.6, 138.1, 137.3, 134.4, 132.3, 131.3, 130.5, 129.9, 129.2, 128.6, 128.4, 112.1, 76.8, 60.7, 59.0, 56.6, 39.2, 34.2, 33.2, 26.7, 25.9, 19.5, 16.3. HRMS-ESI (m/z) calcd for $C_{35}H_{39}N_6O_7$ [M + H]$^+$ 655.2880; found: 655.2877. $[\alpha]_D^{20}$ −176 (c 1.0, MeOH).

Propan-2-yl 2-[(1S,6S,9S)-6-tert-butyl-9-[(2S)-2-hydroxy-3-methylbutanamido]-1-methyl-8,16-dioxo-19-oxa-4,7,15-triazatetracyclo[9.5.2.1^{2,5}.0^{14,17}]nonadeca-2,4,11,13,17-pentaen-3-yl]-1,3-oxazole-4-carboxylate (20). To a solution of methyl ester **14b** (50 mg, 0.084 mmol) in anhydrous toluene (0.5 mL) was added iPrOH (258 μL, 3.37 mmol, 40 equiv), followed by dropwise addition of neat Ti(OiPr)$_4$ (25 μL, 0.084 mmol, 1.0 equiv). After addition was completed, the vial was placed in preheated oil bath and stirred at 100 °C for 20 h. After cooling to room temperature, the reaction mixture was quenched with aqueous 1 M HCl and extracted with EtOAc (two times). Combined organic extracts were washed with brine, dried (Na$_2$SO$_4$), and evaporated under reduced

pressure. The resulting yellow oily residue was purified by reverse phase column chromatography (gradient elution from 10% to 50% MeCN in water) to give ester **20** (45 mg, 86%) as a white amorphous solid. ^{1}H NMR (400 MHz, MeOH-d_4): δ 8.66 (s, 1H), 7.27 (dd, J = 8.0, 1.7 Hz, 1H), 6.94 (d, J = 8.0 Hz, 1H), 6.80 (d, J = 1.7 Hz, 1H), 5.25 (hept, J = 6.3 Hz, 1H), 4.61 (s, 1H), 4.52 (dd, J = 11.6, 4.2 Hz, 1H), 3.86 (d, J = 3.7 Hz, 1H), 3.04 (t, J = 12.0 Hz, 1H), 2.87 (dd, J = 12.5, 4.2 Hz, 1H), 2.08 (sept d, J = 6.9, 3.5 Hz, 1H), 1.96 (s, 3H), 1.38 (d, J = 6.3 Hz, 6H), 1.00 (d, J = 6.9 Hz, 3H), 0.96 (s, 9H), 0.89 (d, J = 6.9 Hz, 3H). ^{13}C NMR (101 MHz, MeOH-d_4): δ 178.9, 175.8, 173.7, 163.6, 161.9, 156.8, 152.8, 146.3, 141.7, 136.2, 135.9, 132.2, 131.0, 129.4, 128.2, 112.1, 76.8, 70.3, 60.0, 56.6, 52.1, 39.3, 34.2, 33.1, 26.7, 22.1, 20.5, 19.5, 16.3. HRMS-ESI (m/z) calcd for $C_{32}H_{40}N_5O_8$ [M + H]$^+$ 622.2877; found: 622.2874. [α]$_D^{20}$ −120 (c 1.0, MeOH).

Benzyl 2-[(1S,6S,9S)-6-tert-Butyl-9-[(2S)-2-hydroxy-3-methylbutanamido]-1-methyl-8,16-dioxo-19-oxa-4,7,15-triazatetracyclo[9.5.2.1^{2,5}.0^{14,17}]nonadeca-2,4,11,13,17-pentaen-3-yl]-1,3-oxazole-4-carboxylate (21). To a solution of methyl ester **14b** (130 mg, 0.22 mmol) in anhydrous toluene (1 mL), BnOH (0.9 mL, 8.8 mmol, 40 equiv), and neat Ti(OiPr)$_4$ (65 μL, 0.22 mmol, 1.0 equiv) were added dropwise. After addition the vial was placed in preheated oil bath at 100 °C and stirred for 2 h. After cooling to room temperature, reaction was quenched with aqueous HCl (1 M) and extracted with EtOAc. The combined organic layers were washed with brine, dried (Na$_2$SO$_4$), and evaporated under reduced pressure. The resulting yellow oil was purified with reverse phase column chromatography (10% to 70% MeCN in water) to give 127 mg (87%) of ester **21** as white amorphous solid. ^{1}H NMR (400 MHz, MeOH-d_4): δ 8.71 (s, 1H), 8.17 (d, J = 7.0 Hz, 1H), 7.51−7.45 (m, 2H), 7.42−7.30 (m, 3H), 7.27 (dd, J = 8.1, 1.7 Hz, 1H), 6.94 (d, J = 8.0 Hz, 1H), 6.79 (d, J = 1.7 Hz, 1H), 5.39 (s, 2H), 4.64−4.57 (m, 1H), 4.52 (dd, J = 11.6, 4.2 Hz, 1H), 3.86 (d, J = 3.7 Hz, 1H), 3.03 (dd, J = 12.0, 12.0 Hz, 1H), 2.86 (dd, J = 12.5, 4.2 Hz, 1H), 2.08 (sept d, J = 6.8, 3.3 Hz, 1H), 1.96 (s, 3H), 1.00 (d, J = 6.9 Hz, 3H), 0.96 (s, 9H), 0.89 (d, J = 6.9 Hz, 3H). ^{13}C NMR (101 MHz, MeOH-d_4): δ 178.9, 175.8, 173.8, 173.7, 163.7, 162.1, 156.9, 152.8, 146.7, 141.7, 137.2, 136.3, 135.4, 132.2, 131.0, 129.6, 129.4, 128.2, 112.2, 76.8, 67.8, 60.1, 56.7, 52.1, 39.3, 34.2, 33.1, 26.7, 20.5, 19.5, 16.3. HRMS-ESI (m/z) calcd for $C_{36}H_{40}N_6O_8$ [M + H]$^+$ 670.2877; found: 670.2885. [α]$_D^{20}$ −99 (c 1.0, MeOH).

tert-Butyl N-[(1S,6S,9S)-6-tert-Butyl-3-(4-cyano-1,3-oxazol-2-yl)-8,16-dioxo-1-phenyl-19-oxa-4,7,15-triazatetracyclo[9.5.2.1^{2,5}.0^{14,17}]nonadeca-2,4,11,13,17-pentaen-9-yl]carbamate (22). A solution of N-Boc-protected ester **3a** (110 mg, 0.17 mmol, 1 equiv) in anhydrous ammonia (7 M solution in MeOH, 0.72 mL, 5.0 mmol, 30 equiv) was stirred at room temperature for 20 h and was evaporated to dryness under reduced pressure. The resulting white amorphous solid (50 mg, 0.08 mmol, 1 equiv) was dissolved in anhydrous MeCN (0.5 mL), and anhydrous pyridine (32 μL, 0.23 mmol, 3 equiv) was added. The vial was cooled to 0 °C, and TFAA (22 μL, 0.16 mmol, 2 equiv) was added. The reaction mixture was warmed to room temperature and stirred for 2 h. The reaction mixture was quenched with saturated aqueous NaHCO$_3$ and extracted with EtOAc two times. Organics were combined, washed with brine, dried over Na$_2$SO$_4$, and evaporated under reduced pressure. The yellow

amorphous solid residue was purified by reverse phase column chromatography (gradient elution from 10% to 50% MeCN in water) to give nitrile **22** (27 mg, 56%) as a white amorphous solid. ^{1}H NMR (400 MHz, MeOH-d_4): δ 8.58 (s, 1H), 7.44−7.39 (m, 2H), 7.38−7.30 (m, 3H), 7.28−7.22 (m, 2H), 6.90 (d, J = 8.0 Hz, 1H), 4.96 (s, 1H), 4.05 (dd, J = 12.3, 3.7 Hz, 1H), 3.12 (dd, J = 12.3, 12.3 Hz, 1H), 2.78 (dd, J = 12.3, 3.7 Hz, 1H), 1.43 (s, 9H), 1.08 (s, 9H). ^{13}C NMR (101 MHz, MeOH-d_4): δ 176.1, 174.9, 164.8, 157.1, 156.9, 152.8, 149.6, 141.6, 137.2, 133.4, 132.8, 131.4, 130.6, 130.0, 129.4, 128.7, 126.7, 116.5, 112.5, 112.0, 80.5, 60.4, 58.5, 58.3, 38.8, 34.1, 28.7, 26.7. HRMS-ESI (m/z) calcd for $C_{34}H_{35}N_6O_6$ [M + H]$^+$ 623.2618; found: 623.2609. [α]$_D^{20}$ −228 (c 1.0, MeOH).

(2S)-N-[(1S,6S,9S)-6-tert-Butyl-3-(4-cyano-1,3-oxazol-2-yl)-8,16-dioxo-1-phenyl-19-oxa-4,7,15-triazatetracyclo-[9.5.2.1^{2,5}.0^{14,17}]nonadeca-2,4,11,13,17-pentaen-9-yl]-2-hydroxy-3-methylbutanamide (23). The title compound was prepared according to general procedure H from macrocycle **22** (27 mg, 0.043 mmol), TFA (33 μL, 0.43 mmol; 10 equiv) in DCM (0.5 mL) within 3 h, followed by treatment with (S)-2-hydroxy-3-methylbutanoic acid (8 mg; 0.065 mmol; 1.5 equiv), EDC × HCl (17 mg; 0.09 mmol; 2.0 equiv), HOBt (17 mg; 0.13 mmol; 3.0 equiv), and DIPEA (37 μL; 0.22 mmol; 5 equiv) in DMF (0.5 mL) for 1 h. Purification by reverse phase column chromatography (gradient elution from 10% to 95% MeCN in 0.1% TFA in water) afforded amide **23** (13 mg, 49%; dr 99:1) as a white amorphous solid. ^{1}H NMR (400 MHz, MeOH-d_4): δ 8.57 (s, 1H), 7.45−7.40 (m, 2H), 7.39−7.32 (m, 3H), 7.28 (dd, J = 8.0, 1.7 Hz, 1H), 7.24 (d, J = 1.7 Hz, 1H), 6.93 (d, J = 8.0 Hz, 1H), 4.93 (s, 1H), 4.46 (dd, J = 11.7, 3.8 Hz, 1H), 3.86 (d, J = 3.8 Hz, 1H), 3.18 (dd, J = 12.2, 12.2 Hz, 1H), 2.82 (dd, J = 12.6, 3.8 Hz, 1H), 2.07 (sept d, J = 6.9, 3.8 Hz, 1H), 1.06 (s, 9H), 1.00 (d, J = 6.9 Hz, 3H), 0.89 (d, J = 6.9 Hz, 3H). ^{13}C NMR (101 MHz, MeOH-d_4): δ 176.1, 175.8, 174.0, 164.6, 156.8, 152.9, 149.6, 141.8, 137.1, 133.6, 132.3, 131.5, 130.6, 130.0, 129.4, 128.7, 126.9, 116.5, 112.5, 112.1, 76.8, 60.4, 58.5, 56.7, 39.2, 34.2, 33.2, 26.7, 19.5, 16.3. HRMS-ESI (m/z) calcd for $C_{34}H_{35}N_6O_6$ [M + H]$^+$ 623.2618; found: 623.2629. [α]$_D^{20}$ −256 (c 1.0, MeOH).

Benzyl 2-[(1R,6S,9R)-6-tert-Butyl-9-(2-hydroxy-3-methylbutanamido)-8,16-dioxo-1-phenyl-19-oxa-4,7,15-triazatetracyclo[9.5.2.1^{2,5}.0^{14,17}]nonadeca-2,4,11,13,17-pentaen-3-yl]-1,3-oxazole-4-carboxylate (24). To a solution of methyl ester **3a** (133 mg, 0.20 mmol) in anhydrous toluene (2 mL), BnOH (0.83 mL, 8.0 mmol, 40 equiv) and neat Ti(OiPr)$_4$ (60 μL, 0.2 mmol, 1.0 equiv) were added dropwise. After addition the vial was placed in preheated oil bath at 100 °C and stirred for 2 h. After cooling to room temperature reaction was quenched with aqueous HCl (1M) and extracted with EtOAc. The combined organic layers were washed with brine, dried (Na$_2$SO$_4$), and evaporated under reduced pressure. The resulting yellow oil was purified with reverse phase column chromatography (10% to 90% MeCN in water) to give 80 mg of benzyl ester as white amorphous solid. The crude benzyl ester was converted into the title compound according to general procedure H, involving N-Boc cleavage by TFA (335 μL; 4.37 mmol; 10 equiv) in DCM (2 mL) within 3 h, followed by amide bond formation with (S)-2-hydroxy-3-methylbutanoic acid (19 mg; 0.16 mmol; 1.5 equiv) in the presence of EDC × HCl (42 mg; 0.22 mmol; 1.8 equiv), HOBt (44 mg; 0.33 mmol; 3 equiv) and DIPEA (94 μL; 0.55 mmol; 5 equiv) in DMF (3 mL) within 2 h. Purification by

144

reverse phase column chromatography (10% to 50% MeCN in water) afforded 48 mg (32%; dr 99:1) of macrocycle **24** as a yellowish amorphous solid. ^{1}H NMR (400 MHz, MeOH-d_4): 8.42 (s, 1H), 7.52−7.21 (m, 12H), 6.90 (d, J = 8.6 Hz, 1H), 5.34 (s, 2H), 5.01−4.93 (m, 1H), 4.44 (dd, J = 11.7, 3.8 Hz, 1H), 3.86 (d, J = 3.8 Hz, 1H), 3.18 (dd, J = 12.2, 12.2 Hz, 1H), 2.81 (dd, J = 12.6, 3.8 Hz, 1H), 2.07 (sept d, J = 6.8, 3.7 Hz, 1H), 1.06 (s, 9H), 1.00 (d, J = 6.8 Hz, 3H), 0.89 (d, J = 6.8 Hz, 3H). ^{13}C NMR (101 MHz, MeOH-d_4) δ 176.1, 175.7, 174.1, 174.0, 164.5, 162.0, 156.4, 152.3, 146.8, 141.7, 137.1, 134.9, 133.4, 132.2, 131.4, 130.6, 129.9, 129.6, 129.5, 129.4, 129.3, 128.7, 127.3, 112.0, 76.8, 67.8, 60.4, 58.3, 56.7, 39.2, 34.1, 33.1, 26.7, 19.5, 16.3. HRMS-ESI (m/z) calcd for $C_{41}H_{42}N_5O_8$ [M + H]$^+$ 732.3028; found: 732.3057. $[\alpha]_D^{20}$ −204 (c 1.0, MeOH).

(2S)-N-[(1S,6S,9S)-6-tert-Butyl-3-[4-(hydroxymethyl)-1,3-oxazol-2-yl]-8,16-dioxo-1-phenyl-19-oxa-4,7,15-triazatetracyclo[9.5.2.1^{2,5}.0^{14,17}]nonadeca-2,4,11,13,17-pentaen-9-yl]-2-hydroxy-3-methylbutanamide (25). Macrocycle **3a** (53 mg; 0.08 mmol) was dissolved in anhydrous THF (1 mL) and trifluoroethanol (57 μL) was added. The resulting solution was cooled to 0 °C (crushed ice bath), and LiBH$_4$ (9 mg; 0.40 mmol; 5 equiv) was added portionwise. The resulting suspension was warmed to room temperature and stirred for 3 h, whereupon it was poured into aqueous saturated NH$_4$Cl and extracted with EtOAc (two times). Combined organic extracts were washed with brine, dried (Na$_2$SO$_4$), and concentrated under reduced pressure. The yellow oily residue was purified by reverse phase column chromatography (gradient elution from 10% to 50% MeCN in water) to give alcohol (48 mg) as white amorphous solid. The crude alcohol was converted into the title compound **25** according to general procedure H, involving N-Boc cleavage by TFA (117 μL; 1.54 mmol; 10 equiv) in DCM (1 mL) within 3 h, followed by amide bond formation with (S)-2-hydroxy-3-methylbutanoic acid (13 mg; 0.11 mmol; 1.5 equiv) in the presence of EDC × HCl (26 mg; 0.14 mmol; 1.8 equiv), HOBt (31 mg; 0.23 mmol; 3 equiv), and DIPEA (66 μL; 0.38 mmol; 5 equiv) in DMF (2 mL) within 2 h. Purification by reverse phase column chromatography (10% to 95% MeCN in water) afforded 27 mg (57%; dr 99:1) of compound **25** as a white amorphous solid. ^{1}H NMR (400 MHz, MeOH-d_4): δ 7.64 (s, 1H), 7.45−7.38 (m, 2H), 7.37−7.29 (m, 3H), 7.29−7.20 (m, 2H), 6.91 (dd, J = 8.0, 2.3 Hz, 1H), 4.94−4.91 (m, 1H), 4.54−4.40 (m, 3H), 3.88−3.82 (m, 1H), 3.33−3.11 (m, 1H), 2.86−2.78 (m, 1H), 2.15−2.02 (m, 1H), 1.06 (s, 9H), 1.00 (d, J = 6.9, 3H), 0.89 (d, J = 6.9, 3H). ^{13}C NMR (101 MHz, MeOH-d_4): δ 176.3, 175.8, 174.0, 164.3, 155.8, 151.4, 143.1, 141.7, 137.9, 137.4, 133.9, 132.2, 131.3, 130.5, 129.9, 129.2, 128.7, 128.4, 112.0, 76.8, 60.5, 58.5, 57.1, 56.6, 39.2, 34.2, 33.1, 26.7, 19.5, 16.3. HRMS-ESI (m/z) calcd for $C_{34}H_{38}N_5O_7$ [M + H]$^+$ 628.2771; found 628.2786. $[\alpha]_D^{20}$ −233 (c 1.0, MeOH).

2-[(1S,6S,9S)-6-tert-Butyl-9-[[(2S)-2-hydroxy-3-methylbutanamido]-1-methyl-8,16-dioxo-19-oxa-4,7,15-triazatetracyclo[9.5.2.1^{2,5}.0^{14,17}]nonadeca-2,4,11,13,17-pentaen-3-yl]-1,3-oxazole-4-carboxylic acid (26). To a solution of methyl ester **14b** (150 mg, 0.25 mmol) in MeOH (2 mL) and water (1 mL) was added LiOH × H$_2$O (32 mg, 0.76 mmol, 3.0 equiv), and the resulting suspension was stirred at room temperature for 30 min. Then, aqueous 1 M HCl was added, and the resulting suspension was extracted with EtOAc (three times) Combined organic layers were washed with

brine, dried (Na$_2$SO$_4$), and evaporated under reduced pressure. Purification by reverse phase column chromatography (gradient elution from 10% to 50% MeCN in 0.01% aqueous TFA) provided carboxylic acid **26** (130 mg, 89%) as a white amorphous solid. ^{1}H NMR (400 MHz, MeOH-d_4): δ 8.67 (s, 1H), 7.28 (dd, J = 8.1, 1.7 Hz, 1H), 6.95 (d, J = 8.1 Hz, 1H), 6.79 (d, J = 1.7 Hz, 1H), 4.60 (s, 1H), 4.53 (dd, J = 11.6, 4.2 Hz, 1H), 3.86 (d, J = 3.6 Hz, 1H), 3.03 (dd, J = 12.0, 12.0 Hz, 1H), 2.87 (dd, J = 12.4, 4.2 Hz, 1H), 2.09 (sept d, J = 6.9, 3.8 Hz, 1H), 1.96 (s, 3H), 1.00 (d, J = 6.9 Hz, 3H), 0.96 (s, 9H), 0.89 (d, J = 6.9 Hz, 3H). ^{13}C NMR (75 MHz, MeOH-d_4): δ 179.0, 175.9, 173.7, 163.7, 152.7, 146.5, 141.8, 136.2, 132.23 131.0, 129.4, 128.4, 112.2, 76.8, 60.0, 56.6, 52.1, 39.3, 34.2, 33.1, 26.7, 20.4, 19.5, 16.3. HRMS-ESI (m/z) calcd for $C_{29}H_{34}N_5O_8$ [M + H]$^+$ 580.2407; found: 580.2415. $[\alpha]_D^{20}$ −120 (c 1.0, MeOH).

Methyl (2S)-2-{[(tert-Butoxy)carbonyl]amino}-3-[3-(5-fluoro-3-hydroxy-2-oxo-2,3-dihydro-1H-indol-3-yl)-4-hydroxyphenyl]propanoate (30). The title compound was synthesized according to literature procedure.[14] MeMgBr (3.0 M solution in Et$_2$O; 4.85 mL; 14.5 mmol, 1.6 equiv) was added dropwise via syringe to an ice cold (0 °C) solution of N-Cbz-L-tyrosine methyl ester (**28**, 3.48 g; 11.8 mmol; 1.3 equiv) in anhydrous THF (30 mL) under argon atmosphere. The crushed ice bath was removed, the yellow solution was warmed to room temperature and left to stir for 30 min. Concentration under reduced pressure provided yellow solid magnesium phenoxide to which 5-fluoroisatin (**29**, 1.50 g; 9.1 mmol; 1.0 equiv) was added, followed by anhydrous DCM (60 mL). The resulting heterogeneous dark brown reaction mixture was heated under reflux for 20 h, then cooled to room temperature, and quenched by addition of aqueous 1 M HCl (50 mL). Layers were separated, and the aqueous layer was extracted with EtOAc (3 × 40 mL). Combined organic extracts were washed with brine (50 mL), dried (MgSO$_4$), and concentrated under reduced pressure to provide a yellow foam. Purification by column chromatography on silica gel (gradient elution from 10% to 70% EtOAc in hexanes) afforded **30** (3.07 g; 74%; dr 3:2) as a yellowish foam. ^{1}H NMR (600 MHz, MeOH-d_4): δ 7.51−7.47 (m, 1H), 7.02−6.97 (m, 1H), 6.97−6.92 (m, 1H), 6.88−6.83 (m, 1H), 6.79 (dd, J = 7.7, 2.1 Hz, 0.6H), 6.75 (dd, J = 7.7, 2.1 Hz, 0.4H), 6.66−6.61 (m, 1H), 4.40 (dd, J = 7.9, 5.9 Hz, 0.6H), 4.34 (dd, J = 7.9, 5.9 Hz, 0.4H), 3.71 (s, 2H), 3.70 (s, 1H), 3.09 (dd, J = 13.8, 5.7 Hz, 0.4H), 3.04 (dd, J = 13.8, 5.7 Hz, 0.6H), 2.94 (dd, J = 13.8, 8.4 Hz, 0.4H), 2.87 (dd, J = 13.8, 8.4 Hz, 0.6H), 1.42 (s, 3H), 1.39 (s, 6H). ^{13}C NMR (151 MHz, MeOD) (no [13]C−{[19]F} was possible, signals are listed as they appear) δ 181.83, 181.79, 174.3, 161.3, 159.7, 157.84, 157.77, 154.6, 139.94, 139.88, 135.8, 135.73, 135.68, 131.0, 130.9, 128.9, 128.7, 128.63, 128.58, 127.4, 116.5, 116.3, 116.34, 116.32, 116.19, 116.17, 112.99, 112.9, 111.53, 111.48, 111.4, 80.70, 80.65, 78.01, 77.96, 56.8, 56.7, 52.6, 38.2, 38.1, 28.7. HRMS-ESI (m/z) calcd for $C_{23}H_{25}N_2O_7F$ [M + Na]$^+$ 483.1543; found: 483.1562.

Methyl (2S)-2-{[(tert-Butoxy)carbonyl]amino}-3-[3-(5-fluoro-3-hydroxy-2-oxo-2,3-dihydro-1H-indol-3-yl)-4-(trifluoromethanesulfonyloxy)phenyl]propanoate (31). The title compound was synthesized according to literature procedure.[8b] Thus, phenol **30** (1.00 g; 2.20 mmol; 1.0 equiv) and PhN(Tf)$_2$ (970 mg; 2.70 mmol; 1.25 equiv) were dissolved in anhydrous DCM (20 mL) under argon atmosphere. Et$_3$N (908 μL, 6.50 mmol, 3.0 equiv) was added, and the resulting yellow solution was stirred at room

145

temperature for 2 h, whereupon it was concentrated under reduced pressure. Purification of a yellow oily residue by column chromatography on silica gel (gradient elution from 10% to 40% EtOAc in hexanes) provided triflate **31** (970 mg; 75%; dr 2:3) as a colorless oil. ^{1}H NMR (600 MHz, MeOH-d_4): δ 8.07 (s, 0.5H), 8.04 (s, 0.5H), 7.37 (d, J = 8.5 Hz, 0.5H), 7.34 (d, J = 8.5 Hz, 0.5H), 7.31−7.26 (m, 1H), 7.06−6.99 (m, 1H), 6.96−6.92 (m, 1H), 6.85 (d, J = 7.8 Hz, 0.5H), 6.76 (d, J = 7.8 Hz, 0.5H), 4.58 (dd, J = 9.5, 5.2 Hz, 0.5H), 4.45 (dd, J = 8.9, 5.2 Hz, 1H), 3.78 (s, 1.8H), 3.75 (s, 1.2H), 3.35−3.31 (m, 0.5H, overlapping with MeOH-d_4), 3.25 (dd, J = 13.8, 5.4 Hz, 0.5H), 3.12 (dd, J = 13.8, 9.5 Hz, 0.5H), 3.00 (dd, J = 13.8, 9.5 Hz, 0.5H), 1.42 (s, 4H), 1.35 (s, 5H). ^{13}C NMR (151 MHz, MeOH-d_4): (no[13]C−{[19]F} was possible, signals are listed as they appear) δ 210.1, 179.7, 173.8, 173.7, 161.43, 161.40, 159.84, 159.81, 157.8, 157.7, 147.2, 139.9, 139.8, 138.8, 138.7, 134.30, 134.25, 134.22, 134.18, 133.0, 132.2, 131.9, 131.4, 131.2, 122.8, 120.7, 120.6, 120.3, 118.6, 117.5, 117.4, 117.3, 117.2, 113.5, 113.3, 113.2, 113.0, 112.93, 112.87, 112.80, 112.75, 80.8, 80.7, 76.7, 56.3, 56.1, 52.83, 52.78, 38.4, 37.9, 30.7, 28.68, 28.65. HRMS-ESI (m/z) calcd for $C_{24}H_{24}F_4N_2O_9S$ [M + Na]$^+$ 615.1046; found: 615.1036.

Methyl (2S)-2-{[(tert-Butoxy)carbonyl]amino}-3-[3-(5-fluoro-2-oxo-2,3-dihydro-1H-indol-3-yl)phenyl]propanoate (32). The title compound was synthesized according to literature procedure.[8b] Accordingly, 10% Pd on carbon (162 mg; 0.15 mmol; 0.1 equiv) was added to a solution of triflate **31** (900 mg; 1.52 mmol; 1.0 equiv) and Et$_3$N (740 μL; 5.32 mmol; 3.5 equiv) in MeOH (15 mL). The black suspension was stirred under 5 atm hydrogen pressure at room temperature for 24 h, then filtered through a short pad of Celite, and rinsed with MeOH (50 mL). Combined filtrates were evaporated under reduced pressure to give crude alcohol as a yellow foam (675 mg) that was used in the next step without additional purification. 10% Pd on carbon (323 mg; 0.30 mmol; 0.2 equiv) was added to a solution of tertiary alcohol (675 mg; 1.52 mmol; 1.0 equiv) in MeOH (20 mL). The black suspension was stirred under 10 atm hydrogen pressure at room temperature for 6 days. The heterogeneous mixture was filtered through a short pad of Celite and rinsed with MeOH (50 mL). Purification by column chromatography on silica gel (gradient elution from 0% to 5% MeOH in DCM) provided **32** (440 mg, 68%; dr 1:1) as a white foam. ^{1}H NMR (400 MHz, CDCl$_3$): δ 9.04 (s, 1H), 7.29 (t, J = 7.7 Hz, 1H), 7.13−7.06 (m, 2H), 6.97−6.90 (m, 2H), 6.88−6.83 (m, 2H), 5.04−4.98 (m, 1H), 4.61−4.52 (m, 2H), 3.65 (s, 1.4H), 3.63 (s, 1.6H), 3.18−2.97 (m, 2H), 1.40 (s, 9H). [13]C−{^{19}F} NMR (151 MHz, CDCl$_3$): δ 178.5, 172.4, 172.3, 159.3, 155.2, 137.7, 137.6, 137.14, 137.07, 136.22, 136.17, 131.2, 129.41, 129.39, 129.3, 129.1, 129.0, 127.4, 127.3, 122.4, 115.1, 113.3, 113.2, 110.7, 80.1, 54.5, 54.4, 53.0, 52.3, 38.4, 38.2, 28.4. HRMS-ESI (m/z) calcd for $C_{23}H_{25}N_2O_5F$ [M + Na]$^+$ 451.1645; found: 451.1645.

Methyl 2-{5-Bromo-2-[(1S)-1-[(2S)-2-{[(tert-butoxy)-carbonyl]amino}-3-[3-(5-fluoro-2-oxo-2,3-dihydro-1H-indol-3-yl)phenyl]propanamido}-2,2-dimethylpropyl]-1,3-oxazol-4-yl}-1,3-oxazole-4-carboxylate (33). The title compound was synthesized according to literature procedure.[8b] Thus, ester **32** (440 mg; 1.03 mmol; 1.0 equiv) was dissolved in 2:1 THF/water mixture (33 mL) and solid LiOH (74 mg; 3.08 mmol; 3.0 equiv) was added. The clear solution was stirred at room temperature for 1 h, then aqueous 1 M HCl was added until pH 2, and the resulting suspension was extracted with

EtOAc (three times). Combined organic extracts were washed with brine, dried (Na$_2$SO$_4$), and evaporated under reduced pressure. To the resulting crude acid (yellow oil; 426 mg) were added bioxazole **9** (368 mg; 1.03 mmol; 1.0 equiv), EDC × HCl (394 mg; 2.00 mmol; 2.0 equiv), and anhydrous pyridine (15 mL). The resulting suspension was stirred at room temperature for 2 h, and then the orange solution was evaporated to dryness under reduced pressure. The residue was dissolved in EtOAc, washed with aqueous 1 M HCl, brine, dried (Na$_2$SO$_4$), and evaporated under reduced pressure. Purification by reverse phase column chromatography (gradient elution from 0% to 70% MeCN in 0.1% TFA in water) provided **33** (490 mg, 63%; dr 1:1) as a yellow foam. ^{1}H NMR (400 MHz, CDCl$_3$): δ 8.71(s, 0.5H), 8.59(s, 0.5H), 8.30 (s, 0.5H), 8.29 (s, 0.5H), 7.21−7.05 (m, 3H), 7.02−6.79 (m, 5H), 5.19−5.11 (m, 1H), 5.05 (dd, J = 9.3, 8.5 Hz, 1H), 4.56 (s, 0.5H), 4.52 (s, 0.5H), 4.41−4.29 (m, 1H), 3.92 (s, 3H), 3.10−2.95 (m, 2H), 1.40 (s, 9H), 0.94 (s, 9H). [13]C−{^{19}F} NMR (151 MHz, CDCl$_3$): δ 178.10, 178.05, 171.2, 164.9, 164.8, 161.4, 159.3, 159.2, 155.7, 154.9, 154.8, 144.1, 137.73, 137.65, 136.3, 134.64, 134.61, 131.1, 129.6, 129.4, 129.3, 129.2, 128.9, 128.0, 127.0, 126.8, 123.2, 123.1, 115.0, 115.0, 113.3, 113.2, 110.68, 110.65, 80.52, 80.46, 55.8, 55.7, 52.9, 52.4, 37.7, 37.4, 35.89, 35.85, 28.4, 26.30, 26.28. HRMS-ESI (m/z) calcd for $C_{35}H_{37}N_5O_8BrF$ [M + Na]$^+$ 776.1721; found: 776.1707.

Methyl 2-[(3R,7′S,10′S)-10′-{[(tert-Butoxy)carbonyl]-amino}-7′-tert-butyl-5-fluoro-2,9′-dioxo-1,2-dihydro-17′-oxa-5′,8′-diazaspiro[indole-3,2′-tricyclo[10.3.1.1^{3,6}]-heptadecane]-1′(16′),3′,5′,12′,14′-pentaen-4′-yl]-1,3-oxazole-4-carboxylate (34). The title compound was synthesized according to literature procedure.[8b] A suspension of amide **33** (490 mg; 0.65 mmol; 1.0 equiv) and anhydrous Na$_2$CO$_3$ (206 mg; 1.95 mmol; 3.0 equiv) in anhydrous DMF (25 mL) was stirred at 65 °C for 3 h under argon atmosphere. After cooling to room temperature, saturated aqueous NH$_4$Cl solution (50 mL) and EtOAc (100 mL) were added, and layers were separated. The aqueous layer was extracted with EtOAc (3 × 50 mL), and combined organic extracts were washed with brine (50 mL), dried (Na$_2$SO$_4$), and concentrated under reduced pressure to provide a yellow oil. Purification by reverse phase column chromatography (gradient elution from 0% to 70% MeCN in 0.1% TFA in water) provided macrocycle **34** (300 mg, 69%; dr 99:1) as a white amorphous solid. ^{1}H NMR (400 MHz, CDCl$_3$): δ 9.32 (s, 1H), 7.98 (s, 1H), 7.28−7.19 (m, 2H), 7.13 (d, J = 7.8 Hz, 1H), 6.95 (dd, J = 8.7, 4.2 Hz, 1H), 6.89 (s, 1H), 6.83 (td, J = 8.7, 2.6 Hz, 1H), 6.73 (dd, J = 7.8, 2.6 Hz, 1H), 6.65 (d, J = 7.0 Hz, 1H), 5.40 (d, J = 9.2 Hz, 1H), 4.75 (d, J = 7.0 Hz, 1H), 4.26−4.18 (m, 1H), 3.83 (s, 3H), 3.25 (t, J = 11.9 Hz, 1H), 2.85 (dd, J = 12.6, 3.2 Hz, 1H), 1.47 (s, 9H), 0.95 (s, 9H). ^{13}C NMR (101 MHz, CDCl$_3$): δ 175.0, 172.4, 163.3, 161.1, 159.1 (J_{CF} = 241.5 Hz), 155.4, 154.8, 150.5, 143.9, 139.4, 137.9 (J_{CF} = 2.0 Hz), 136.5, 134.1, 132.0, 131.2 (J_{CF} = 8.0 Hz), 129.2, 128.7, 127.1, 124.7, 115.6 (J_{CF} = 23.0 Hz), 111.8 (J_{CF} = 25.2 Hz), 111.3 (J_{CF} = 7.8 Hz), 80.6, 59.1, 58.5, 57.2, 52.1, 38.6, 33.4, 28.5, 26.6. HRMS-ESI (m/z) calcd for $C_{35}H_{36}N_5O_8F$ [M + Na]$^+$ 696.2438; found: 696.2446. [α]$_D^{20}$ −354 (c 1.0, CHCl$_3$).

(2S)-N-[(3R,7′S,10′S)-7′-tert-Butyl-5-fluoro-4′-[4-(hydroxy-methyl)-1,3-oxazol-2-yl]-2,9′-dioxo-1,2-dihydro-17′-oxa-5′,8′-diazaspiro[indole-3,2′-tricyclo[10.3.1.1^{3,6}]-heptadecane]-1′(16′),3′,5′,12′,14′-pentaen-10′-yl]-2-hy-

146

droxy-3-methylbutanamide (27). Macrocycle **34** (290 mg; 0.43 mmol) was dissolved in anhydrous THF (3 mL) under argon atmosphere and cooled to 0 °C (crushed ice bath). Then, TFE (310 μL, 4.31 mmol, 10 equiv) was added dropwise, followed by solid LiBH$_4$ (47 mg, 2.16 mmol, 5.0 equiv). The resulting suspension was warmed to room temperature and stirred for 18 h. Saturated aqueous NH$_4$Cl solution (20 mL) was then added, and after stirring for 10 min, the white suspension was poured into aqueous 1 M HCl (30 mL) and extracted with EtOAc (3 × 50 mL). Combined organic extracts were washed with brine (50 mL), dried (Na$_2$SO$_4$), and concentrated under reduced pressure to provide alcohol **35** (250 mg; 90%) as a white amorphous solid, which was used in the next step without additional purification. The primary alcohol **35** (100 mg; 0.16 mmol) was dissolved in anhydrous DCM (2 mL), and TFA (120 μL; 1.55 mmol; 10 equiv) was added. The solution was stirred at room temperature for 3 h, then evaporated to dryness under reduced pressure, and redissolved in EtOAc. Organic layer was washed with aqueous saturated NaHCO$_3$ and brine, dried (Na$_2$SO$_4$), and evaporated to dryness under reduced pressure to give amine (84 mg; 0.15 mmol) as a yellow oil that was dissolved in anhydrous DCM (2 mL). (*S*)-2-Hydroxy-3-methylbutanoic acid (**13**, 22 mg; 0.19 mmol; 1.2 equiv), EDC × HCl (59 mg; 0.31 mmol; 2.0 equiv), and HOBt (62 mg; 0.46 mmol; 3.0 equiv) were added to the solution, followed by DIPEA (160 μL; 0.92 mmol; 6.0 equiv). The resulting mixture was stirred at room temperature for 3 h, whereupon the yellow solution was diluted with aqueous saturated NH$_4$Cl and EtOAc. Layers were separated, and the organic phase was washed with water, brine, dried (Na$_2$SO$_4$), and evaporated under reduced pressure. Purification by reverse phase column chromatography (gradient elution from 10% to 95% MeCN in 0.1% TFA in water) provided **27** (40 mg; 40%; dr 99:1) as a white solid. ¹H NMR (400 MHz, MeOH-*d*$_4$): δ 7.52 (t, *J* = 1.0 Hz, 1H), 7.32−7.30 (m, 1H), 7.29 (d, *J* = 1.0 Hz, 1H), 7.14−7.09 (m, 1H), 7.00−6.89 (m, 2H), 6.87 (s, 1H), 6.82 (dd, *J* = 8.2, 2.4 Hz, 1H), 4.72 (dd, *J* = 11.4, 3.5 Hz, 1H), 4.67 (s, 1H), 4.32 (d, *J* = 1.0 Hz, 2H), 3.89 (d, *J* = 3.5 Hz, 1H), 3.21 (t, *J* = 12.0 Hz, 1H), 2.83 (dd, *J* = 12.6, 3.5 Hz, 1H), 2.12 (sept d, *J* = 6.9, 3.8 Hz, 1H), 1.06−1.00 (m, 12H), 0.91 (d, *J* = 6.9 Hz, 3H). ¹³C NMR (101 MHz, MeOH-*d*$_4$): δ 177.1, 175.8, 174.4, 165.1, 160.5 (*J*$_{CF}$ = 239.6 Hz), 155.4, 151.1, 143.6, 141.5, 139.7 (*J*$_{CF}$ = 2.4 Hz), 137.7, 137.3, 133.4 (*J*$_{CF}$ = 8.4 Hz), 133.1, 129.93, 129.90, 128.7, 125.3, 116.4 (*J*$_{CF}$ = 23.8 Hz), 112.4 (*J*$_{CF}$ = 26.1 Hz), 112.2 (*J*$_{CF}$ = 8.3 Hz), 76.9, 60.9, 60.0, 57.3, 55.7, 39.6, 34.3, 33.2, 26.9, 19.6, 16.3. HRMS-ESI (*m/z*) calcd for C$_{34}$H$_{36}$N$_5$O$_7$F [M + H]$^+$ 646.2680; found: 646.2677. [α]$_D^{20}$ −354 (c 1.0, MeOH).

■ ASSOCIATED CONTENT

Ⓢ Supporting Information

The Supporting Information is available free of charge at https://pubs.acs.org/doi/10.1021/acs.jmedchem.4c00388

> NCI-60 assay results for macrocycles **14b**, **15a**, and **21**; acid **26** metabolite identification in A2058 cell lysate; ECD spectra for macrocycle **15i**; crystal data and structure refinement for macrocycle **14d**; geometries and energies of the DFT calculated stationary points; HPLC traces of macrocycles **14a-k**, **15a,b,i**, **16−21**, **23−27**; copies of NMR spectra (PDF)

Crystallographic data for **14d** deposited at the Cambridge Crystallographic Data Centre as Supplementary Publication Number CCDC 2295669 (CSV)

■ AUTHOR INFORMATION

Corresponding Authors

Edgars Liepinsh − *Latvian Institute of Organic Synthesis, Riga LV-1006, Latvia;* ⊙ orcid.org/0000-0003-2213-8337; Email: ledgars@farm.osi.lv

Edgars Suna − *Latvian Institute of Organic Synthesis, Riga LV-1006, Latvia;* ⊙ orcid.org/0000-0002-3078-0576; Email: edgars@osi.lv

Authors

Toms Kalnins − *Latvian Institute of Organic Synthesis, Riga LV-1006, Latvia*

Viktorija Vitkovska − *Latvian Institute of Organic Synthesis, Riga LV-1006, Latvia*

Mihail Kazak − *Latvian Institute of Organic Synthesis, Riga LV-1006, Latvia*

Diana Zelencova-Gopejenko − *Latvian Institute of Organic Synthesis, Riga LV-1006, Latvia;* ⊙ orcid.org/0000-0002-6931-2294

Melita Ozola − *Latvian Institute of Organic Synthesis, Riga LV-1006, Latvia;* ⊙ orcid.org/0000-0002-3453-0099

Nauris Narvaiss − *Latvian Institute of Organic Synthesis, Riga LV-1006, Latvia*

Marina Makrecka-Kuka − *Latvian Institute of Organic Synthesis, Riga LV-1006, Latvia*

Ilona Domračeva − *Latvian Institute of Organic Synthesis, Riga LV-1006, Latvia*

Artis Kinens − *Latvian Institute of Organic Synthesis, Riga LV-1006, Latvia;* ⊙ orcid.org/0000-0003-1992-525X

Baiba Gukalova − *Latvian Institute of Organic Synthesis, Riga LV-1006, Latvia*

Nele Konrad − *Department of Chemistry and Biotechnology, Tallinn University of Technology, Tallinn, Harju Maakon 12618, Estonia*

Riina Aav − *Department of Chemistry and Biotechnology, Tallinn University of Technology, Tallinn, Harju Maakon 12618, Estonia;* ⊙ orcid.org/0000-0002-...

Francesca Bonato − *Unidad BICS, Centro de Investigaciones Biologicas Margarita Salas, Consejo Superior de Investigaciones Científicas, Madrid 28040, Spain*

Daniel Lucena-Agell − *Unidad BICS, Centro de Investigaciones Biologicas Margarita Salas, Consejo Superior de Investigaciones Científicas, Madrid 28040, Spain*

J. Fernando Díaz − *Unidad BICS, Centro de Investigaciones Biologicas Margarita Salas, Consejo Superior de Investigaciones Científicas, Madrid 28040, Spain;* ⊙ orcid.org/0000-0003-2743-3319

Complete contact information is available at:
https://pubs.acs.org/10.1021/acs.jmedchem.4c00388

Author Contributions

All authors have given approval to the final version of the manuscript.

Notes

The authors declare no competing financial interest.

◼ REFERENCES

(1) Sung, H.; Ferlay, J.; Siegel, R. L.; Laversanne, M.; Soerjomataram, I.; Jemal, A.; Bray, F. Global Cancer Statistics 2020: GLOBOCAN Estimates of Incidence and Mortality Worldwide for 36 Cancers in 185 Countries. *Ca-Cancer J. Clin.* **2021**, *71*, 209−249.

(2) (a) Vaidya, F. U.; Sufiyan Chhipa, A.; Mishra, V.; Gupta, V. K.; Rawat, S. G.; Kumar, A.; Pathak, C. Molecular and Cellular Paradigms of Multidrug Resistance in Cancer. *Cancer Rep.* 2022, *5.* . (b) Cree, I. A.; Charlton, P. Molecular Chess? Hallmarks of Anti-Cancer Drug Resistance. *BMC Cancer* **2017**, *17* (1), 10.

(3) Newman, D. J.; Cragg, G. M. Natural Products as Sources of New Drugs over the Nearly Four Decades from 01/1981 to 09/2019. *J. Nat. Prod.* **2020**, *83*, 770−803.

(4) Huang, M.; Lu, J.-J.; Ding, J. Natural Products in Cancer Therapy: Past, Present and Future. *Nat. Prod. Bioprospect.* **2021**, *11*, 5−13.

(5) Wang, S.; Dong, G.; Sheng, C. Structural Simplification: An Efficient Strategy in Lead Optimization. *Acta Pharm. Sin. B* **2019**, *9*, 880−901.

(6) Lindquist, N.; Fenical, W.; Van Duyne, G. D.; Clardy, J. Isolation and Structure Determination of Diazonamides A and B, Unusual Cytotoxic Metabolites from the Marine Ascidian Diazona Chinensis. *J. Am. Chem. Soc.* **1991**, *113*, 2303−2304.

(7) (a) Burgett, A. W. G.; Li, Q.; Wei, Q.; Harran, P. G. A Concise and Flexible Total Synthesis of (−)-Diazonamide A. *Angew. Chem., Int. Ed.* **2003**, *42*, 4961−4966. (b) Nicolaou, K. C.; Bella, M.; Chen, D. Y.-K.; Huang, X.; Ling, T.; Snyder, S. A. Total Synthesis of Diazonamide A. *Angew. Chem., Int. Ed.* **2002**, *41*, 3495−3499. (c) Nicolaou, K. C.; Chen, D. Y.-K.; Huang, X.; Ling, T.; Bella, M.; Snyder, S. A. Chemistry and Biology of Diazonamide A: First Total Synthesis and Confirmation of the True Structure. *J. Am. Chem. Soc.* **2004**, *126*, 12888−12896. (d) Nicolaou, K. C.; Chen, D. Y.-K.; Huang, X.; Ling, T.; Bella, M.; Snyder, S. A. The Second Total Synthesis of Diazonamide A. *Angew. Chem., Int. Ed.* **2003**, *42*, 1753−1758. (e) Nicolaou, K. C.; Chen, D. Y.-K.; Huang, X.; Ling, T.; Bella, M.; Snyder, S. A. Chemistry and Biology of Diazonamide A: Second Total Synthesis and Biological Investigations. *J. Am. Chem. Soc.* **2004**, *126*, 12897−12906. (f) Knowles, R. R.; Carpenter, J.; Blakey, S. B.; Kayano, A.; Mangion, I. K.; Sinz, C. J.; MacMillan, D. W. C. Total Synthesis of Diazonamide A. *Chem. Sci.* **2011**, *2*, 308−311.

(8) (a) Cheung, C.-M.; Goldberg, F. W.; Magnus, P.; Russell, C. J.; Turnbull, R.; Lynch, V. An Expedient Formal Total Synthesis of (−)-Diazonamide A via a Powerful, Stereoselective O-Aryl to C-Aryl Migration To Form the C10 Quaternary Center. *J. Am. Chem. Soc.* **2007**, *129*, 12320−12327. (b) Mai, C.-K.; Sammons, M. F.; Sammakia, T. A Concise Formal Synthesis of Diazonamide A by the Stereoselective Construction of the C10 Quaternary Center. *Angew. Chem, Int. Ed.* **2010**, *49*, 2397−2400.

(9) (a) Cruz-Monserrate, Z.; Vervoort, H. C.; Bai, R.; Newman, D. J.; Howell, S. B.; Los, G.; Mullaney, J. T.; Williams, M. D.; Pettit, G. R.; Fenical, W.; Hamel, E. Diazonamide A and a Synthetic Structural Analog: Disruptive Effects on Mitosis and Cellular Microtubules and Analysis of Their Interactions with Tubulin. *Mol. Pharmacol.* **2003**, *63*, 1273−1280. (b) Bai, R.; Cruz-Monserrate, Z.; Fenical, W.; Pettit, G. R.; Hamel, E. Interaction of Diazonamide A with Tubulin. *Arch. Biochem. Biophys.* **2020**, *680*, 108217.

(10) Wang, G.; Shang, L.; Burgett, A. W. G.; Harran, P. G.; Wang, X. Diazonamide Toxins Reveal an Unexpected Function for Ornithine δ-Amino Transferase in Mitotic Cell Division. *Proc. Natl. Acad. Sci. U. S. A.* **2007**, *104*, 2068−2073.

(11) Ding, H.; DeRoy, P. L.; Perreault, C.; Larivée, A.; Siddiqui, A.; Caldwell, C. G.; Harran, S.; Harran, P. G. Electrolytic Macro-cyclizations: Scalable Synthesis of a Diazonamide-Based Drug Development Candidate. *Angew. Chem., Int. Ed.* **2015**, *54*, 4818−4822.

(12) Wieczorek, M.; Tcherkezian, J.; Bernier, C.; Prota, A. E.; Chaaban, S.; Rolland, Y.; Godbout, C.; Hancock, M. A.; Arezzo, J. C.; Ocal, O.; et al. The Synthetic Diazonamide DZ-2384 has Distinct Effects on Microtubule Curvature and Dynamics without Neuro-toxicity. *Sci. Transl. Med.* **2016**, *8* (365), ra365159.

(13) Williams, N. S.; Burgett, A. W. G.; Atkins, A. S.; Wang, X.; Harran, P. G.; McKnight, S. L. Therapeutic Anticancer Efficacy of a Synthetic Diazonamide Analog in the Absence of Overt Toxicity. *Proc. Natl. Acad. Sci. U. S. A.* **2007**, *104*, 2074−2079.

(14) (a) Stereoselective construction of chiral, non-racemic quaternary center has been a challenge in the total synthesis of diazonamide A (**1a**): Lachia, M.; Moody, C. J. The Synthetic Challenge of Diazonamide A, a Macrocyclic Indole Bis-Oxazole Marine Natural Product. *Nat. Prod. Rep.* **2008**, *25*, 227−253. (b) Peris, G.; Vedejs, E. Enantiocontrolled Synthesis of a Tetracyclic Aminal Corresponding to the Core Subunit of Diazonamide A. *J. Org. Chem.* **2015**, *80*, 3050−3057. (c) Mutule, I.; Kalnins, T.; Vedejs, E.; Suna, E. Diazonamide Synthetic Studies. Reactivity of N-Unsub-stituted Benzofuro[2,3-b]Indolines. *Chem. Heterocycl. Compd.* **2015**, *51*, 613−620.

(15) Kazak, M.; Vasilevska, A.; Suna, E. Preparative Scale Synthesis of Functionalized Bioxazole. *Chem. Heterocycl. Compd.* **2020**, *56*, 355−364.

(16) Ross, A. J.; Lang, H. L.; Jackson, R. F. W. Much Improved Conditions for the Negishi Cross-Coupling of Iodoalanine Derived Zinc Reagents with Aryl Halides. *J. Org. Chem.* **2010**, *75*, 245−248.

(17) Huihui, K. M. M.; Caputo, J. A.; Melchor, Z.; Olivares, A. M.; Spiewak, A. M.; Johnson, K. A.; DiBenedetto, T. A.; Kim, S.; Ackerman, L. K. G.; Weix, D. J. Decarboxylative Cross-Electrophile Coupling of *N*-Hydroxyphthalimide Esters with Aryl Iodides. *J. Am. Chem. Soc.* **2016**, *138*, 5016−5019.

(18) Toriyama, F.; Cornella, J.; Wimmer, L.; Chen, T.-G.; Dixon, D. D.; Creech, G.; Baran, P. S. Redox-Active Esters in Fe-Catalyzed C−C Coupling. *J. Am. Chem. Soc.* **2016**, *138*, 11132−11135.

(19) Even though the configuration at quaternary center could be established, the correct analysis of the bond lengths and valence angles was not possible due to small sizes of the single crystals of **14d**. For further details, see Supporting Information, page S27 and crystallographic data for **14d** deposited at the Cambridge Crystallo-graphic Data Centre as Supplementary Publication Number CCDC 2295669.

(20) Shoemaker, R. H. The NCI60 Human Tumour Cell Line Anticancer Drug Screen. *Nat. Rev. Cancer* **2006**, *6*, 813−823.

(21) Sisco, E.; Barnes, K. L. Design, Synthesis, and Biological Evaluation of Novel 1,3-Oxazole Sulfonamides as Tubulin Polymer-ization Inhibitors. *ACS Med. Chem. Lett.* **2021**, *12*, 1030−1037.

(22) An additional cell proliferation rate experiment was performed to investigate cytostatic vs. cytotoxic properties of macrocyclic ester **21**. Melanoma A2058 cells treated with **21** exhibited an approximately two-fold decrease in proliferation rate as compared to untreated control cells suggesting that the effects of compound **21** should be considered as cytostatic rather than cytotoxic (see SI, Figure S1, page S18).

(23) (a) It has been proposed that cytostatic (antiproliferative) anticancer agents are prone to fewer resistance mechanisms than are cytotoxic agents: ref. 2b. (b) Krause, W. Resistance to Anti-Tubulin

148

Agents: From Vinca Alkaloids to Epothilones. *Cancer Drug Resist.* **2019**, *2* (1), 82−106. (c) Cortes, J.; Vidal, M. Beyond Taxanes: The next Generation of Microtubule-Targeting Agents. *Breast Cancer Res. Treat* **2012**, *133* (3), 821−830.

(24) Rixe, O.; Fojo, T. Is Cell Death a Critical End Point for Anticancer Therapies or Is Cytostasis Sufficient? *Clin. Cancer Res.* **2007**, *13*, 7280−7287.

(25) National Cancer Institute; *Publicly accessible database of NCI-60 panel screening results and COMPARE analysis*, 2021, https://dtp.cancer.gov/public_compare/.

(26) Holbeck, S. L.; Collins, J. M.; Doroshow, J. H. Analysis of Food and Drug Administration−Approved Anticancer Agents in the NCI60 Panel of Human Tumor Cell Lines. *Mol. Cancer Ther.* **2010**, *9*, 1451−1460.

(27) Gaskin, F.; Cantor, C. R.; Shelanski, M. L. Turbidimetric Studies of the in Vitro Assembly and Disassembly of Porcine Neurotubules. *J. Mol. Biol.* **1974**, *89*, 737−755.

(28) *The assay was conducted following Enhancer Control Polymerization Assay Method described in Tubulin Polymerization Assay Kit manual by Cytoskeleton*, Cytoskeleton Inc, https://www.cytoskeleton.com/pdf-storage/datasheets/bk004p.pdf.

(29) (a) The slope values derived from the tubulin polymerization assay have been used in quantification of functional activity and comparison across analog series: ref. 21. (b) Argirova, M.; Guncheva, M.; Momekov, G.; Cherneva, E.; Mihaylova, R.; Rangelov, M.; Todorova, N.; Denev, P.; Anichina, K.; Mavrova, A.; Yancheva, D. Modulation Effect on Tubulin Polymerization, Cytotoxicity and Antioxidant Activity of 1H-Benzimidazole-2-Yl Hydrazones. *Molecules* **2023**, *28* (1), 291.

(30) Safa, A. R.; Hamel, E.; Felsted, R. L. Photoaffinity Labeling of Tubulin Subunits with a Photoactive Analog of Vinblastine. *Biochemistry* **1987**, *26*, 97−102.

(31) Mosmann, T. Rapid Colorimetric Assay for Cellular Growth and Survival: Application to Proliferation and Cytotoxicity Assays. *J. Immunol. Methods* **1983**, *65*, 55−63.

(32) *NCI-60 Screening Methodology | NCI-60 Human Tumor Cell Lines Screen | Discovery & Development Services | Developmental Therapeutics Program (DTP)*, https://dtp.cancer.gov/discovery_development/nci-60/methodology.htm. (accessed 2023−06−13).

(33) Andreu, J. M. Large Scale Purification of Brain Tubulin With the Modified Weisenberg Procedure. *Methods Mol. Med.* **2007**, 17−28.

(34) Cornelissen, M.; Philippé, J.; De Sitter, S.; De Ridder, L. Annexin V Expression in Apoptotic Peripheral Blood Lymphocytes: An Electron Microscopic Evaluation. *Apoptosis* **2002**, *7* (1), 41−47.

(35) Alanine, A.; Buettelmann, B.; Heitz, N. M.-P.; Jaeschke, G.; Pinard, E.; Wyler, R.; *Pyrrolidine and Piperidine Derivatives and Their Use for the Treament of Neurodegenerative Disorders*, 2001, WO 0,181,303 A1.

(36) Zhang, J.-Q.; Li, S.-M.; Wu, C.-F.; Wang, X.-L.; Wu, T.-T.; Du, Y.; Yang, Y.-Y.; Fan, L.-L.; Dong, Y.-X.; Wang, J.-T.; Tang, L. The Synthesis of Symmetrical 3,3-Disubstituted Oxindoles by Phosphine-Catalyzed γ/γ-Addition of Oxindoles with Allenates. *Catal. Commun.* **2020**, *138*, 105838.

149

Appendix III – STRUCTURALLY SIMPLIFIED DIAZONAMIDE ANALOGS AS ANTIMITOTIC AGENTS

Suna, E.; Kalnins, T.; Kazak, M.; Vitkovska, V.; Narvaiss N.; Zelencova D.; Jaudzems K. WO2021130515A1, Jul. 1, 2021.

(54) Title: STRUCTURALLY SIMPLIFIED DIAZONAMIDE ANALOGS AS ANTIMITOTIC AGENTS

Formula I

(57) Abstract: The present invention relates to medicine and in particular to the treatment of metastatic tumors, more particularly to antimitotic agents and microtubule polymerization inhibitors. Even more particularly, the invention relates to novel analogs of natural antimitotic agent diazonamide A and pharmaceutical compositions thereof and the use of the novel analogs as inhibitors of microtubule polymerization. Formula (I):
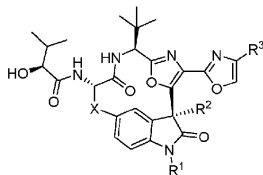
Appendix IV – MACROCYCLIC TUBULIN POLYMERIZATION INHIBITORS AS ANTICANCER AGENTS

Vitkovska V., Kazak M., Suna E.
Application number: PCT/IB2024/059899, Oct. 10, 2024.

FIELD OF THE INVENTION

The present invention relates to the field of chemistry and biochemistry and in particular to the novel anticancer compounds, more particularly to antiproliferative agents and microtubule polymerization inhibitors. Even more particularly, the invention relates to novel analogs of natural antimitotic agent diazonamide A and to salts, pharmaceutical compositions, conjugates and a process of manifacture thereof and the potential use of the novel compounds for treatment of melanoma.

BACKGROUND OF THE INVENTION

Cancer is a major public health problem worldwide with more than 19 million new cancer cases diagnosed and 10 million lethal outcomes in 2020 [1]. Growing incidence and high mortality together with increasing multidrug resistance towards cancer therapeutics [2] puts the development of new effective anticancer treatment among top priorities worldwide. Chemotherapeutics are the most effective means for the treatment of tumors. However, a majority of cancer chemotherapeutic agents currently used in clinics develops resistance overtime. Therefore, there still is high medical need for effective anticancer chemotherapeutic medicines.

The marine metabolite diazonamide A exerts nanomolar cytotoxicity against a range of human tumor cell lines. It has been demonstrated that diazonamide A prevents formation of the mitotic spindle during cell division by inhibition of microtubules assembly and, consequently, tubulin polymerization [3]. However, high structural complexity of diazonamide A precludes its use in cancer therapy.

diazonamide A

DZ-2384

A   X-Y= trans-CH=CH-
B   X-Y = -CH₂-CH₂-

C (X=NR, CR¹R²)

D

E
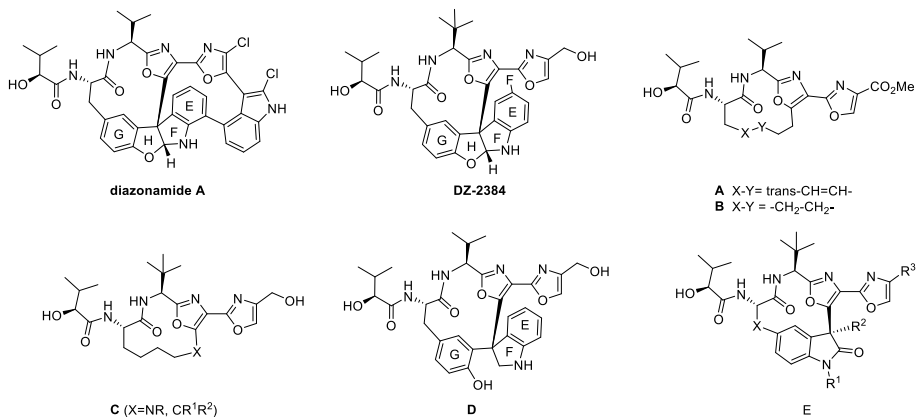
Decrease of structural complexity of diazonamide A without affecting its anticancer activity profile is possible as was demonstrated by the development of anticancer agent DZ-2384 [4, 5]. A notable feature of DZ-2384 as a cancer chemotherapeutic agent is that in animal models it does not cause

1

systemic toxicity typical for other antimitotic such as taxanes (paclitaxel), and vinca alkaloids (vinorelbine) [5]. Although being structurally less complex as compared to diazonamide A, DZ-2384 still contains remarkable structural complexity with the chiral tetracyclic subunit EFGH imposing most of the synthetic challenges. Thus, the highly optimized synthesis of DZ-2384 required 13 synthetic steps with the key transformation being electrochemical macrocyclization to form the tetracycle EFGH that proceeded with poor 35% yield (48% based on recovered starting material) and afforded 2.7:1 mixture of diastereomers that required separation by silica gel columnm chromatography [6].

The development of less-complex analogs of diazonamide A that lacks chiral tetracyclic subunit EFGH is highly desirable. Among numerous analogs of diazonamide A reported in the literature, there is a handful of macrocycles that lack the tetracyclic subunit EFGH (compounds **A**,**B**) [4]. One example of diazonamide analog (compound **D**) with a tricyclic moiety EFG instead of the tetracycle EFGH has been also disclosed [4].

Recently we found that the replacement of the difficult-to-synthesize tetracycle subunit EFGH by aliphatic chain leads to the loss of activity as evidenced by remarkable reduction of tubulin binding afinity for the resulting macrocycles **C** as compared to DZ-2384 [7]. On the other hand, the incorporation of oxindole subunit instead of the tetracycle subunit EFGH afforded macrocycles E that are potent tubulin polymerization inhibitors with nanomolar citotoxicity against a series of cancer cell lines [8]. Unfortunately, oxindole moiety-containing macrocycles **B** feature poor metabolic stability that hampers their application as anti-cancer agents.

SUMMARY OF THE INVENTION

In a first aspect, the invention features a method for the treatment of tumours, comprising administering to the human in need thereof a therapeutically effective amount of a compound or prodrug thereof, or pharmaceutically acceptable salt, hydrate, solvate, or polymorph of said compound or prodrug, wherein the compound is an inhibitor of microtubules assembly and tubulin polymerization.

In another aspect, the invention features a pharmaceutical composition for the treatment of tumors, comprising a therapeutically effective amount of a composition comprising (i) a compound or prodrug thereof, or pharmaceutically acceptable salt, hydrate, solvate, or polymorph of said compound or prodrug; and (ii) a pharmaceutically acceptable carrier, wherein the compound is an inhibitor of microtubules assembly and tubulin polymerization

2

In another aspect, the invention features the use of a compound or prodrug thereof, or pharmaceutically acceptable salt, hydrate, solvate, or polymorph of said compound or prodrug, wherein the compound is an inhibitor of microtubules assembly and tubulin polymerization, in the manufacture of medicament for the treatment of tumors.

In another aspect, the invention features a compound or prodrug thereof, or pharmaceutically acceptable salt, hydrate, solvate, or polymorph of said compound or prodrug for the use in the treatment of tumors, wherein the compound is an inhibitor of microtubules assembly and tubulin polymerization.

In one embodiment the inhibitor of microtubules assembly and tubulin polymerization is a compound of general formula (I) or a pharmaceutically acceptable salt or conjugate thereof.

DETAILED DESCRIPTION OF THE INVENTION

Definitions

Unless otherwise stated, the following terms used in the specification and claims have the following meanings set out below.

It is to be appreciated that references to "treating" or "treatment" include prophylaxis as well as the alleviation of established symptoms of a condition. "Treating" or "treatment" of a state, disorder or condition therefore includes: (1) preventing or delaying the appearance of clinical symptoms of the state, disorder or condition developing in a human that may be afflicted with or predisposed to the state, disorder or condition but does not yet experience or display clinical or subclinical symptoms of the state, disorder or condition, (2) inhibiting the state, disorder or condition, Le., arresting, reducing or delaying the development of the disease or a relapse thereof (in case of maintenance treatment) or at least one clinical or subclinical symptom thereof, or (3) relieving or attenuating the disease, i.e., causing regression of the state, disorder or condition or at least one of its clinical or subclinical symptoms.

The term "alkyl" as used herein refers to a straight or branched alkyl chain having one to six (inclusive) carbon atoms. For example, the alkyl group may be part cyclic (cyclopropylmethyl), linear or branched (ethyl, *n*-propyl, *iso*-propyl, *n*-butyl, *sec*-butyl, *tert*-butyl).

The terms "alkylene," "alkenylene," or "alkynylene" as used herein refers to an alkyl, alkenyl, or alkynyl group that is positioned between and serves to connect two other chemical groups. For example, the term "C_{1-6}alkylene" means a linear saturated divalent hydrocarbon radical of one to six carbon atoms or a branched saturated divalent hydrocarbon radical of three to six carbon atoms, such as methylene, ethylene, propylene, 2-methylpropylene, pentylene, and the like. The term "C_{2-}

3

₆alkenylene" means a linear divalent hydrocarbon radical of two to six carbon atoms or a branched divalent hydrocarbon radical of three to six carbon atoms, containing at least one double bond, for example, as in ethenylene, 2,4-pentadienylene, and the like. The term "C_{2-6}alkynylene" means a linear divalent hydrocarbon radical of two to six carbon atoms or a branched divalent hydrocarbon radical of three to six carbon atoms, containing at least one triple bond, for example, as in ethynylene, propynylene, and butynylene and the like.

The term "cycloalkyl" as used herein refers to nonaromatic, saturated or partially unsaturated cyclic, bicyclic, tricyclic or polycyclic hydrocarbon groups having three to 12 carbon atoms. Cycloalkyl groups can contain fused rings. Fused rings are rings that share one or more common carbon atoms. Any ring atom can be substituted (e.g., with one or more substituents). Examples of C_{3-8}cycloalkyl groups include, but are not limited to, cyclopropyl, cyclobutyl, cyclopentyl, cyclohexyl, cyclohexenyl, cyclohexadienyl, methylcyclohexyl, adamantyl, norbornyl and norbornenyl.

The term "alkenyl" refers to a straight or branched alkyl chain having two to six (inclusive) carbon atoms and one or more double bonds. Examples of alkenyl groups include, but are not limited to, allyl, propenyl, 2-butenyl and 3-hexenyl groups. One of the double bond carbons may optionally be the point of attachment of the alkenyl substituent.

The term "alkynyl" refers to a straight or branched hydrocarbon chain having two to six (inclusive) carbon atoms and one or more triple bonds. Examples of alkynyl groups include, but are not limited to, ethynyl, propargyl, and 3-hexynyl. One of the triple bond carbons may optionally be the point of attachment of the alkynyl substituent.

The term "aryl" means a cyclic or polycyclic aromatic ring having from 5 to 12 carbon atoms. The term aryl includes both monovalent species and divalent species. Examples of aryl groups include, but are not limited to, phenyl, biphenyl, naphthyl and the like. In particular embodiment, an aryl is phenyl.

The term "arylC_{1-6}alkyl" means an aryl group covalently attached to a C_{1-6}alkylene group, both of which are defined herein. Examples of arylC_{1-6}alkyl groups include benzyl, phenylethyl, and the like.

The term "heteroaryl" means an aromatic mono-, or bi-cyclic ring incorporating one or more (for example 1-4, particularly 1, 2 or 3) heteroatoms selected from nitrogen, oxygen or sulfur. The term heteroaryl includes both monovalent species and divalent species. Examples of heteroaryl groups are monocyclic and bicyclic groups containing from five to twelve ring members, and more usually from five to ten ring members. The heteroaryl group can be, for example, a 5- or 6-membered monocyclic ring or a 9- or 10-membered bicyclic ring, for example a bicyclic structure formed from fused five

4

and six membered rings or two fused six membered rings. Each ring may contain up to about four heteroatoms typically selected from nitrogen, sulfur and oxygen. Typically the heteroaryl ring will contain up to 3 heteroatoms, more usually up to 2, for example a single heteroatom. In one embodiment, the heteroaryl ring contains at least one ring nitrogen atom. The nitrogen atoms in the heteroaryl rings can be basic, as in the case of an imidazole or pyridine, or essentially non-basic as in the case of an indole or pyrrole nitrogen. In general the number of basic nitrogen atoms present in the heteroaryl group, including any amino group substituents of the ring, will be less than five.

Examples of heteroaryl include furyl, pyrrolyl, thienyl, oxazolyl, isoxazolyl, imidazolyl, pyrazolyl, thiazolyl, isothiazolyl, oxadiazolyl, thiadiazolyl, triazolyl, tetrazolyl, pyridyl, pyridazinyl, pyrimidinyl, pyrazinyl, 1,3,5-triazenyl, benzofuranyl, indolyl, isoindolyl, benzothienyl, benzoxazolyl, benzimidazolyl, benzothiazolyl, benzothiazolyl, indazolyl, purinyl, benzofurazanyl, quinolyl, isoquinolyl, quinazolinyl, quinoxalinyl, cinnolinyl, pteridinyl, naphthyridinyl, carbazolyl, phenazinyl, benzisoquinolinyl, pyridopyrazinyl, thieno[2,3-b]furanyl, 2H-furo[3,2-b]-pyranyl, 5H-pyrido[2,3-d]-o-oxazinyl, 1H-pyrazolo[4,3-d]-oxazolyl, 4H-imidazo[4,5-d]thiazolyl, pyrazino[2,3-d]pyridazinyl, imidazo[2,1-b]thiazolyl, imidazo[1,2-b][1,2,4]triazinyl. "Heteroaryl" also covers partially aromatic bi- or polycyclic ring systems wherein at least one ring is an aromatic ring and one or more of the other ring(s) is a non-aromatic, saturated or partially saturated ring, provided at least one ring contains one or more heteroatoms selected from nitrogen, oxygen or sulfur. Examples of partially aromatic heteroaryl groups include for example, tetrahydroisoquinolinyl, tetrahydroquinolinyl, 2-oxo-1,2,3,4-tetrahydroquinolinyl, dihydrobenzthienyl, dihydrobenzfuranyl, 2,3-dihydrobenzo[1,4]dioxinyl, benzo[1,3]dioxolyl, 2,2-dioxo-1,3-dihydro-2-benzothienyl, 4,5,6,7-tetrahydrobenzofuranyl, indolinyl, 1,2,3,4-tetrahydro-1,8-naphthpyridinyl, 1,2,3,4-tetrahydropyrido[2,3-b]pyrazinyl and 3,4-dihydro-2H-pyrido[3,2-b][1,4]oxazinyl.

The term "heteroaryl$C_{1–6}$alkyl" means a heteroaryl group covalently attached to a $C_{1–6}$alkylene group, both of which are defined herein. Examples of heteroarylalkyl groups include pyridin-2-ylmethyl, 3-(benzofuran-2-yl)propyl, and the like.

Where optional substituents are chosen from "one or more" groups it is to be understood that this definition includes all substituents being chosen from one of the specified groups or the substituents being chosen from two or more of the specified groups.

The phrase "compound of the invention" means those compounds which are disclosed herein, both generically and specifically.

Compounds of the invention

5

In one aspect, the present invention relates to a compound of general formula (I) or a pharmaceutically acceptable salt or solvate thereof, as shown below:
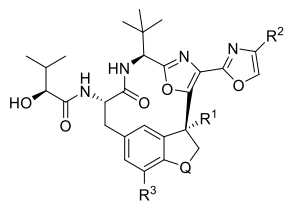
general formula (I)

wherein

R^1 represents optional substituent at quaternary carbon;

R^2 represents optional substituent at oxazole;

R^3 represents optional substituent at aromatic subunit;

Q represents C_{1-2} alkylene group or C_{1-2} heteroalkylene group;

Compound with general formula (I),

wherein:

R^1 is $-CN$, $-C(=O)R^4$, $-C(=O)OR^4$, $-C(=O)N(R^4)R^5$, $-CH_2N(R^4)R^5$,
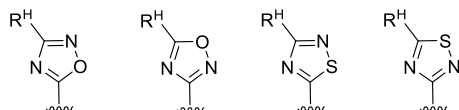
wherein:

R^4, R^5, independently represent, on each occasion when used herein, H, alkyl, cycloalkyl, alkenyl, alkynyl, aryl, arylC$_{1-6}$alkyl, heteroaryl, heteroarylC$_{1-6}$alkyl,

R^4 and R^5 taken together represent $-V^A-W^A-X^A-Y^A-Z^A-$, or $-V^A-W^A-X^A-Y^A-$, $-V^A-W^A-X^A-$, $-V^A-W^A-$,

wherein:

V^A represents, oxygen, sulfur, $-NR^6$, $-CR^6R^7$

W^A represents oxygen, sulfur, $-NR^6$, $-CR^6R^7$

X^A represents oxygen, sulfur, $-NR^6$, $-CR^6R^7$

Y^A represents oxygen, sulfur, $-NR^6$, $-CR^6R^7$

Z^A represents oxygen, sulfur, $-NR^6$, $-CR^6R^7$,

6

162

wherein:

R^6, R^7, independently represent, on each occasion when used herein, H, alkyl, cycloalkyl, alkenyl, alkynyl, aryl, arylC$_{1-6}$alkyl, heteroaryl, heteroarylC$_{1-6}$alkyl,

R^2 is –F, –Cl, –Br, –I, –L–CF$_3$, –L–CHF$_2$, –L–CH$_2$F, –L–F, –L–OR^8, –L–NR^{8}R^9, –L–C(=O)R^8, –L–C(=N-OR^8)R^9, –L–C(=O)OR^8, –L–C(=O)OCR^{8}R^{9}OC(=O)–L-R^{10}, –L–C(=O)NR^{8}R^9, –L–C(=O)NR^8–OR^9, –L–CN, –L–NO$_2$, –L–aryl, –L–arylC$_{1-6}$alkyl, –L–heteroaryl

wherein:

(a) Heteroaryl is selected from:

wherein:

R^H represent H, alkyl, cycloalkyl, alkenyl, alkynyl, aryl, arylC$_{1-6}$alkyl, heteroaryl, heteroarylC$_{1-6}$alkyl,

(b) R^8, R^9 and R^{10} independently represent, on each occasion when used herein, H, alkyl, cycloalkyl, alkenyl, alkynyl, aryl, arylC$_{1-6}$alkyl, heteroaryl, heteroarylC$_{1-6}$alkyl

R^8 and R^9 taken together represent –V^B–W^B–X^B–Y^B–Z^B–, or –V^B–W^B–X^B–Y^B–, –V^B–W^B–X^B–, –V^B–W^B–

wherein:

V^B represents, oxygen, sulfur, –NR^{11}, –CR^{11}R^{12}

W^B represents oxygen, sulfur, –NR^{11}, –CR^{11}R^{12}

X^B represents oxygen, sulfur, –NR^{11}, –CR^{11}R^{12}

Y^B represents oxygen, sulfur, –NR^{11}, –CR^{11}R^{12}

Z^B represents oxygen, sulfur, –NR^{11}, –CR^{11}R^{12}

wherein:

R^{11}, R^{12}, independently represent, on each occasion when used herein, H, alkyl, cycloalkyl, alkenyl, alkynyl, aryl, arylC$_{1-6}$alkyl, heteroaryl, heteroarylC$_{1-6}$alkyl

L represents –W^C–X^C–Y^C–, or –W^C–X^C–, or –W^C–

7

wherein:

W^C is absent or represents oxygen, sulfur, $-NR^{13}$, $=CR^{13}$, $-CR^{13}R^{14}$

X^C represents oxygen, sulfur, $-NR^{13}$, $=CR^{13}$, $-CR^{13}R^{14}$

Y^C represents oxygen, sulfur, $-NR^{13}$, $=CR^{13}$, $-CR^{13}R^{14}$

wherein:

R^{13}, R^{14} independently represent, on each occasion when used herein, H, alkyl, cycloalkyl, alkenyl, alkynyl, aryl, arylC$_{1-6}$alkyl, heteroaryl, heteroarylC$_{1-6}$alkyl

R^{13} and R^{14} taken together represent $-V^D-W^D-X^D-Y^D-Z^D-$, or $-V^D-W^D-X^D-Y^D-$, $-V^D-W^D-X^D-$, $-V^D-W^D-$,

wherein:

V^D represents, oxygen, sulfur, $-NR^{15}$, $-CR^{15}R^{16}$

W^D represents oxygen, sulfur, $-NR^{15}$, $-CR^{15}R^{16}$

X^D represents oxygen, sulfur, $-NR^{15}$, $-CR^{15}R^{16}$

Y^D represents oxygen, sulfur, $-NR^{15}$, $-CR^{15}R^{16}$

Z^D represents oxygen, sulfur, $-NR^{15}$, $-CR^{15}R^{16}$

wherein:

R^{15}, R^{16} independently represent, on each occasion when used herein, H, alkyl, cycloalkyl, alkenyl, alkynyl, aryl, arylC$_{1-6}$alkyl, heteroaryl, heteroarylC$_{1-6}$alkyl

R^3 is $-H$, $-F$, $-Cl$, $-Br$, $-I$, C$_{1-6}$alkyl;

Q represents $-W^E-X^E-$, or $-W^E-$

wherein:

W^E represents oxygen, sulfur, $-S(=O)-$, $-SO_2-$, $-CH_2-$

X^E represents oxygen, sulfur, $-S(=O)-$, $-SO_2-$, $-CH_2-$

Compounds of formula (I) and disclosed embodiments thereof possess four or more asymmetric centers and therefore exist in different enantiomeric and diastereomeric forms. All optical isomers and stereoisomers of the compounds described herein, and mixtures thereof, are considered to be within the scope of the invention, including racemate, one or more enantiomeric forms, one or more diastereomeric forms, or mixtures thereof.

8

164

In one preferred embodiment, compound with general formula (I) possesses all four stereogenic centers with (*S*) absolute configuration.

In another aspect, the invention features compounds with general formula (I) obtainable by a method of synthesis as described herein, or a method of synthesis as described herein.

In another aspect, the invention features novel intermediates for the compound with general formula (I), as described herein, which are suitable for use in the methods of synthesis described herein.

In another aspect, the invention features the use of such novel intermediates, for the compound with general formula (I) according to the claim 1 as described herein, in the methods of synthesis described herein.

As will be appreciated by one of skill in the art, features and preferred embodiments of one aspect of the invention will also pertain to other aspects of the invention.

Description of the Invention

Natural marine metabolite diazonamide A is a highly potent cancer chemotherapy agent, which exerts its anti-tumor activity by preventing the formation of the mitotic spindle during cell division by inhibition of microtubules assembly and, consequently, tubulin polymerization [3]. A structurally simplified diazonamide analog DZ-2384 is highly effective chemotherapy agent in the treatment of triple-negative breast cancer [9].

It has been surprisingly found that the tetracyclic subunit EFGH in the diazonamide A could be replaced by indane subunit to provide a novel class of macrocyclic diazonamide analogs of general formula (I) that displays nanomolar to low micromolar cytotoxicity against a wide panel of human tumor cell lines, including A2058 (metastatic melanoma), MDA-MB-435 (metastatic melanoma), U937 (myeloid leukemia) and MDA-MB-231 (breast adenocarcinoma). At the same time, compounds of General formula (I) are not cytotoxic towards normal human cell lines (such as human embryonic kidney cells (HEK-293). Furthermore, some of the compounds of general formula (I) show high plasma stability (see Table 4).

Results from tubulin polymerization experiments demonstrate that the compounds of general formula (I) bind to tubulin and disrupts tubulin polymerization dinamics in the same manner as other marketed tubulin polymerization inhibitors (vinblastine, vinorelbine). Flow cytometry analysis shows that compounds of general formula (I) induce strong cell cycle arrest in the G2/M phase, possessing identical effect to known antimitotic drugs such as vinorelbine (see Figure 2).

9

Compounds of general formula (I) are useful as cancer chemotherapy agents in the treatment of tumors including melanoma and metastatic melanoma. These macrocycles can be used for manufacturing of various pharmaceutical compositions, wherein they are present together with one or more pharmaceutically acceptable diluents, carriers or excipients.
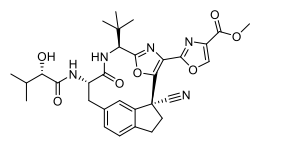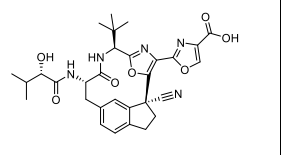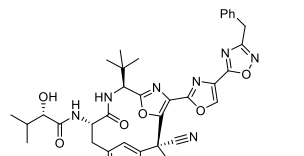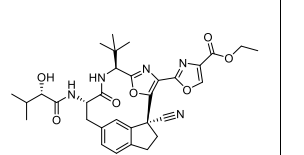
Stereochemistry
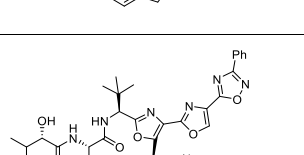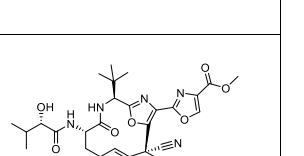
Compounds of general formula (I) and disclosed embodiments thereof possess four or more asymmetric centers and therefore exist in different enantiomeric and diastereomeric forms. All optical isomers and stereoisomers of the compounds described herein, and mixtures thereof, are considered to be within the scope of the invention, including racemate, one or more enantiomeric forms, one or more diastereomeric forms, or mixtures thereof.
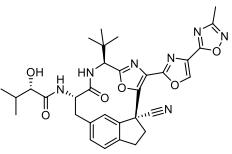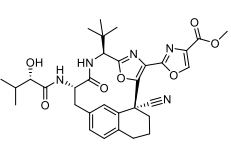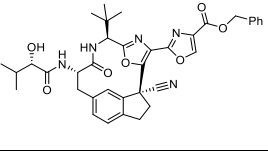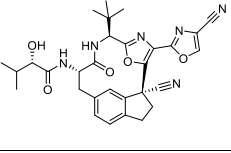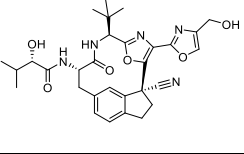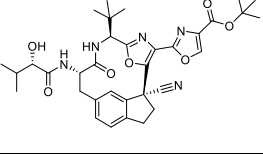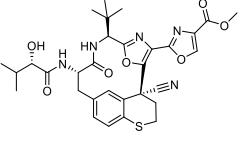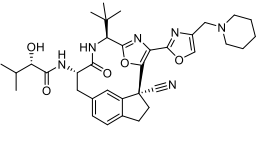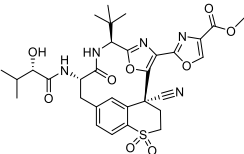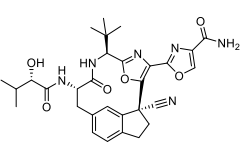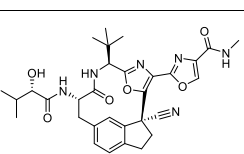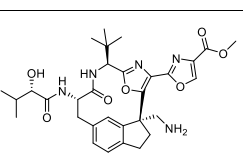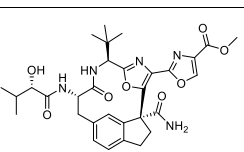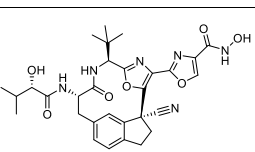
Examples of specific embodiments
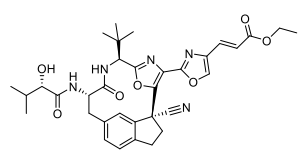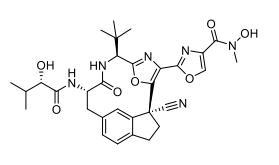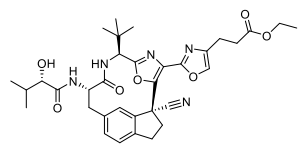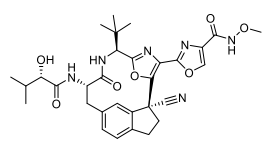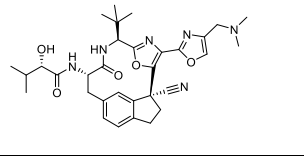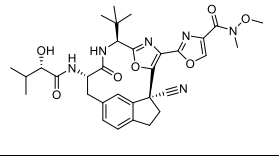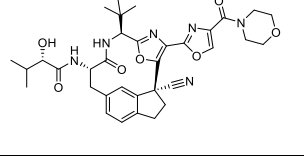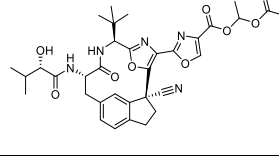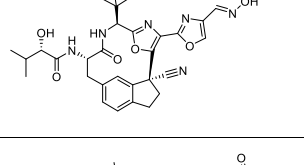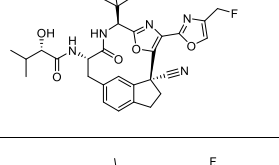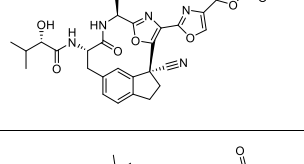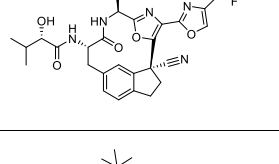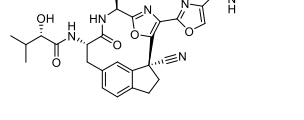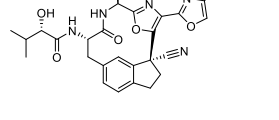
The following examples further illustrate the invention, but should not be construed to limit the scope of the invention in any way.

The following compounds were prepared as an examples of the current invention:

Table 1

#	Cmpnd	Structure	#	Cmpnd	Structure
1	DZA-129		6	DZA-138	
2	DZA-132		7	DZA-139	
3	DZA-133		8	DZA-140	

10

#	ID	Structure	#	ID	Structure
4	DZA-134		9	DZA-141	
5	DZA-135		10	DZA-142	
11	DZA-137		18	DZA-143	
12	DZA-144		19	DZA-152	
13	DZA-145		20	DZA-153	
14	DZA-146		21	DZA-154	
15	DZA-147		22	DZA-156	

11

16	DZA-148		23	DZA-157	
17	DZA-149		24	DZA-158	
25	DZA-150		32	DZA-159	
26	DZA-151		33	DZA-165	
27	DZA-160		34	DZA-168	
28	DZA-161		35	DZA-174	
29	DZA-162		36	DZA-175	

12

30	DZA-163		37	DZA-176	
31	DZA-164				

General Synthesis

The synthesis of diazonamide A analog DZA-129 is shown in Scheme 1.

Accordingly, nitrile **1** was reacted with freshly prepared organozinc species **2** in Pd-catalyzed Negishi cross-coupling with quantitative yield. Ester hydrolysis in **3** was followed by amide coupling with corresponding amine **4** giving amide **5**. The key macrocyclization step in presence of K_3PO_4 furnished macrocycle **6** with diastereomeric ratio 98:2. After *N*-Boc cleavage with TFA the resulting amine was coupled with (*S*)-2-hydroxy-3-methylbutanoic acid (*S*-H*i*VA; **7**) to give analog **DZA-129** (Scheme 1).
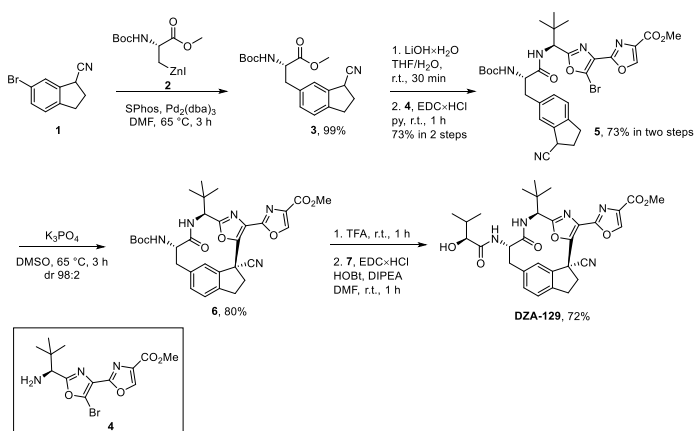
Scheme 1. Synthesis of analog **DZA-129**

Methyl (2*S*)-2-{[(*tert*-butoxy)carbonyl]amino}-3-(3-cyano-2,3-dihydro-1*H*-inden-5-yl)propanoate (3). Aryl bromide 1 (1.50 g; 6.75 mmol), Pd$_2$(dba)$_3$ (93 mg; 0.10 mmol; 0.02 equiv.) and SPhos (111 mg; 0.27 mmol; 0.04 equiv.) were dissolved in anhydrous DMF (5 mL) under argon

13

atmosphere and freshly prepared solution of alkyl zinc iodide 2 (0.5 M in DMF; 20.3 mL; 10.13 mmol; 1.5 equiv.) (prepared as described in [10]) was added. The dark red solution was stirred at 65 °C for 3 h. Then the solution was cooled to room temperature and aqueous saturated NH$_4$Cl and EtOAc were added. Layers were separated and EtOAc was washed with 1N HCl aqueous solution and brine, dried (Na$_2$SO$_4$) and evaporated to dryness. The residue was purified by column chromatography on silica (10% to 50% EtOAc in hexanes) to afford 2.30 g (99%; dr ~1:1) of **DZA-129** as a yellow amorphous solid.

^{1}H NMR (400 MHz, CDCl$_3$) δ 7.22 – 7.11 (m, 2H), 7.08 – 7.00 (m, 1H), 5.00 (d, J = 8.3 Hz, 1H), 4.63 – 4.51 (m, 1H), 4.11 – 4.03 (m, 1H), 3.75 (s, 1.5H), 3.73 (s, 1.5H), 3.21 – 2.98 (m, 3H), 2.98 – 2.83 (m, 1H), 2.65 – 2.52 (m, 1H), 2.42 – 2.29 (m, 1H), 1.42 (s, 4.5H), 1.43 (s, 4.5H). ^{13}C NMR (101 MHz, CDCl$_3$) δ 172.4, 172.2, 155.2, 155.1, 141.84, 141.81, 138.2, 138.1, 135.6, 129.84, 129.79, 125.3, 125.2, 125.12, 121.13, 121.08, 80.2, 80.1, 54.7, 54.6, 52.53, 52.45, 38.23, 38.16, 34.54, 31.45, 31.4, 31.3, 28.42, 28.37. HRMS (m/z): C$_{19}$H$_{24}$N$_2$O$_4$Na [M+Na]$^+$ found: 367.1644. Calculated: 367.1634.

General procedure A (amide formation):

Methyl ester was dissolved in THF. Separately solid LiOH×H$_2$O was dissolved in water and added to the reaction mixture. Emulsion was stirred at room temperature for 30 min, then aqueous HCl (1 N) was added. The resulting mixture was extracted with EtOAc (×3), combined organic layers were washed with brine, dried (Na$_2$SO$_4$) and evaporated. To the resulting crude acid was added the corresponding amine (prepared as described in [11]), EDC×HCl and anhydrous pyridine. The resulting orange suspension was stirred at room temperature to full conversion (1 h) and the orange solution was evaporated to dryness. The residue was dissolved in EtOAc and washed with 1N aqueous HCl (x2) and brine, dried (Na$_2$SO$_4$) and evaporated. Pure products were obtained after column chromatography.

Methyl 2-{5-bromo-2-[(1*S*)-1-[(2*S*)-2-{[(*tert*-butoxy)carbonyl]amino}-3-(3-cyano-2,3-dihydro-1*H*-inden-5-yl)propanamido]-2,2-dimethylpropyl]-1,3-oxazol-4-yl}-1,3-oxazole-4-carboxylate (5). Compound was prepared according to General procedure A from ester 3 (1.90 g; 5.52 mmol), LiOH×H$_2$O (1.16 g; 27.58 mmol; 5 equiv.) in THF/water (1:1 v/v; 15 mL) and amine 4 (1.95 g; 5.44 mmol; 1 equiv.), EDC×HCl (1.57 g; 8.17 mmol; 1.5 equiv.) in pyridine (15 mL) in 1 h. Product 5 was purified by reverse phase flash chromatography (from 10% to 70% MeCN in 0.01% TFA in water) to afford 2.65 g (73%) of a 1:1 mixture of diastereomers as a white solid.

^{1}H NMR (400 MHz, CDCl$_3$) δ 8.34 (s, 0.5H), 8.32 (s, 0.5H), 7.28 – 7.24 (m, 1H), 7.16 – 7.04 (m, 2H), 6.77 (d, J = 9.4 Hz, 0.5H), 6.68 (d, J = 9.4 Hz, 0.5H), 5.07 (d, J = 9.4 Hz, 0.5H), 5.04 (d, J = 9.4

14

Hz, 0.5H), 5.05 – 4.95 (m, 1H), 4.34 – 4.26 (m, 1H), 4.09 – 4.02 (m, 1H), 3.94 (s, 3H), 3.15 – 3.00 (m, 2H), 3.01 – 2.91 (m, 1H), 2.88 – 2.75 (m, 1H), 2.58 – 2.41 (m, 1H), 2.38 – 2.23 (m, 1H), 1.43 (s, 9H), 0.97 (s, 4.5H), 0.95 (s, 4.5H). ^{13}C NMR (101 MHz, CDCl$_3$) δ 170.95, 170.93, 164.8, 161.38, 161.36, 155.7, 154.81, 154.76, 144.14, 144.05, 141.73, 141.68, 138.2, 136.1, 136.0, 134.7, 129.8, 129.6, 128.1, 125.5, 125.24, 125.22, 125.1, 123.12, 123.09, 121.1, 121.0, 80.6, 56.2, 55.8, 55.7, 52.4, 37.4, 37.2, 36.0, 35.8, 34.5, 31.41, 31.39, 31.19, 31.15, 28.4, 26.32, 26.29. HRMS (m/z): C$_{31}$H$_{35}$N$_5$O$_7$Br [M-H]$^-$ found: 668.1722. Calculated: 668.1720.

General procedure B (macrocyclization)

Compound **5** and an oven dried K$_3$PO$_4$ were suspended in anhydrous DMSO. Then the suspension was stirred at 65 °C to full conversion (typically 3–6 h) upon which it was cooled to r.t., quenched with aqueous saturated NH$_4$Cl and extracted with EtOAc (×2). Combined organic layers were washed with brine, dried (Na$_2$SO$_4$) and evaporated. Pure products were obtained after reverse phase flash column chromatography.

Methyl 2-[(1*S*,6*S*,9*S*)-9-{[(*tert*-butoxy)carbonyl]amino}-6-*tert*-butyl-1-cyano-8-oxo-19-oxa-4,7-diazatetracyclo[9.5.2.1^{2,5}.0^{14,17}]nonadeca-2,4,11,13,17-pentaen-3-yl]-1,3-oxazole-4-carboxylate (6).

Compound was prepared according to General procedure B from amide 5 (2.65 g; 3.95 mmol) and K$_3$PO$_4$ (4.19 g; 19.76 mmol; 5 equiv.) in DMSO (120 mL) in 5 h. Product 6 was purified by reverse phase flash chromatography (from 10% to 70% MeCN in 0,01% TFA in water) to afford 1.865 g (80%, 99:1 d.r.) of title compound as a white amorphous solid.

^{1}H NMR (400 MHz, CDCl$_3$) δ 8.37 (s, 1H), 7.23 – 7.21 (m, 2H), 7.12 (s, 1H), 5.73 (d, J = 7.8 Hz, 1H), 5.24 (d, J = 9.2 Hz, 1H), 4.81 (d, J = 7.8 Hz, 1H), 3.94 (s, 3H), 3.89 (ddd, J = 12.0, 9.2, 3.2 Hz, 1H), 3.32 – 3.12 (m, 3H), 2.99 – 2.89 (m, 2H), 2.86 (dd, J = 12.4, 3.4 Hz, 1H), 1.43 (s, 9H), 1.00 (s, 9H). ^{13}C NMR (101 MHz, CDCl$_3$) δ 171.9, 162.0, 161.4, 155.3, 154.8, 148.9, 144.6, 141.4, 140.9, 135.6, 134.8, 130.3, 129.3, 127.1, 125.5, 118.2, 80.5, 58.3, 57.8, 52.4, 46.4, 38.5, 37.9, 33.5, 31.1, 28.4, 26.6. HRMS (m/z): C$_{31}$H$_{36}$N$_5$O$_7$ [M+H]$^+$ found: 590.2617. Calculated: 590.2615. [α]$_D^{20}$ -129 (c 1.0, CHCl$_3$).

General procedure C (cleavage of *N*-Boc and introduction of HiVA sidechain)

N-Boc protected macrocyle was dissolved in anhydrous DCM and TFA was added. The solution was stirred at room temperature to full conversion (typically 1–2 h). The flask was placed in ice bath and aqueous saturated NaHCO$_3$ was added slowly. CO$_2$ evolution! Organic layer was washed with brine, dried (Na$_2$SO$_4$) and evaporated to dryness. The yellow amorphous solid was dissolved in anhydrous DMF and (*S*)-2-hydroxy-3-methylbutanoic acid (*S*-HiVA; 7), EDC×HCl and HOBt were added

15

followed by DIPEA. The solution was stirred at room temperature until full conversion was achieved (typically 1 h). The solution was diluted with aqueous saturated NH$_4$Cl and EtOAc. The layers were separated and the organic phase was washed with brine, dried (Na$_2$SO$_4$) and evaporated. Pure products were obtained by reverse phase flash column chromatography.

Methyl 2-[(1S,6S,9S)-6-*tert*-butyl-1-cyano-9-[(2S)-2-hydroxy-3-methylbutanamido]-8-oxo-19-oxa-4,7-diazatetracyclo[9.5.2.1^2,^5.0^14,^17]nonadeca-2,4,11,13,17-pentaen-3-yl]-1,3-oxazole-4-carboxylate (DZA-129). Compound was prepared according to General procedure C from macrocycle **6** (250 mg; 0.42 mmol), TFA (650 μL; 8.48 mmol; 20 equiv.) in DCM (2 mL) in 1 h and *S*-H*i*VA (75 mg; 0.64 mmol; 1.5 equiv.), EDC×HCl (163 mg; 0.85 mmol; 2 equiv.), HOBt (172 mg; 1.27 mmol; 3 equiv.), DIPEA (367 μL; 2.12 mmol; 5 equiv.) in DMF (2 mL) in 1 h . Purification by reverse phase flash chromatography (10% to 50% MeCN in 0.01% TFA in water) afforded 180 mg (72%) of the title compound **DZA-129** as a white amorphous solid.

^{1}H NMR (400 MHz, MeOD) δ 8.75 (s, 1H), 7.44 – 7.21 (m, 2H), 6.97 (d, J = 1.5 Hz, 1H), 4.74 (s, 1H), 4.54 (dd, J = 11.8, 3.8 Hz, 1H), 3.94 (s, 3H), 3.86 (d, J = 3.8 Hz, 1H), 3.29 – 3.10 (m, 3H), 3.05 – 2.80 (m, 3H), 2.09 (sept d, J = 6.9, 3.8 Hz, 1H), 1.01 (s, 9H), 1.00 (d, J = 6.8 Hz, 3H), 0.89 (d, J = 6.8 Hz, 3H). ^{13}C NMR (101 MHz, MeOD) δ 175.8, 173.9, 164.4, 162.7, 156.2, 150.7, 146.8, 142.9, 142.5, 136.8, 135.4, 131.9, 129.6, 127.7, 126.6, 119.3, 76.8, 59.6, 56.2, 52.7, 47.8, 39.2, 39.1, 34.3, 33.2, 31.8, 26.8, 19.5, 16.3. HRMS (m/z): C$_{31}$H$_{36}$N$_5$O$_7$ [M+H]$^+$ found: 590.2619. Calculated: 590.2615. $[\alpha]_D^{20}$ -182 (c 1.0, MeOH).

The synthesis of diazonamide A analogs DZA-135, 139, 164-165 is shown in Scheme 2.

Ester analogs **DZA-135**, **DZA-139, DZA-164** and **DZA-165** were synthesized from **DZA-129**. Accordingly, ethyl ester (**DZA-139**) and benzyl ester (**DZA-135**) were prepared from methyl ester **DZA-129** by Lewis acid–catalyzed transesterification reaction in the presence of EtOH or BnOH, respectively. Macrocycles **DZA-164** and DZA-165 were obtained by initial hydrolysis of **DZA-129** in the presence of LiOH×H$_2$O and subsequent alkylation of the resulting acid with iodomethyl pivalate to give ester **DZA-164** or with 1-bromoethyl acetate to give analog **DZA-165** (Scheme 2).

16
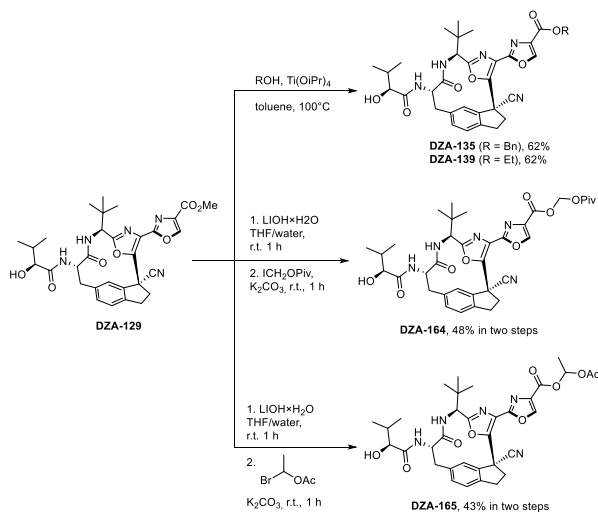
Scheme 2. Synthesis of diazonamide A analogs **DZA-135, DZA-139, DZA-164**, and **DZA-165**

Benzyl 2-[(1*S*,6*S*,9*S*)-6-*tert*-butyl-1-cyano-9-[(2*S*)-2-hydroxy-3-methylbutanamido]-8-oxo-19-oxa-4,7-diazatetracyclo[9.5.2.1²,⁵.0¹⁴,¹⁷]nonadeca-2,4,11,13,17-pentaen-3-yl]-1,3-oxazole-4-carboxylate (DZA-135). To methyl ester **DZA-129** (50 mg; 0.085 mmol) in toluene (1 mL) was added benzyl alcohol (350 µL; 3.39 mmol; 40 equiv.) followed by the addition of Ti(O*i*Pr)₄ (25 µL; 0.085 mmol; 1 equiv.). The resulting yellow solution was stirred at 100˚C in mineral oil bath for 2 h. Then the vial was cooled to room temperature and diluted with EtOAc. The resulting solution was washed with aqueous 1N HCl (×2), then brine. The organic layer was dried (Na₂SO₄) and evaporated. The resulting yellow oil was purified with reverse phase flash chromatography (10% to 70% MeCN in water) to give benzyl ester **DZA-135** (35 mg; 62%) as a white amorphous solid.

^{1}H NMR (400 MHz, MeOD) δ 8.77 (s, 1H), 7.51 – 7.46 (m, 2H), 7.43 – 7.29 (m, 5H), 6.97 (s, 1H), 5.40 (s, 2H), 4.74 (s, 1H), 4.54 (dd, *J* = 11.8, 3.8 Hz, 1H), 3.86 (d, *J* = 3.8 Hz, 1H), 3.28 – 3.11 (m, 3H), 3.01 – 2.91 (m, 2H), 2.88 (d, *J* = 12.4, 3.8 Hz, 1H), 2.08 (sept d, *J* = 6.9, 3.8 Hz, 1H), 1.01 (s, 9H), 1.00 (d, *J* = 6.9 Hz, 3H), 0.89 (d, *J* = 6.9 Hz, 3H). ^{13}C NMR (101 MHz, MeOD) δ 175.8, 173.9, 164.4, 162.0, 156.3, 150.7, 147.0, 142.9, 142.5, 137.1, 136.8, 135.5, 131.9, 129.6, 129.6, 129.4, 129.4, 127.7, 126.6, 119.4, 76.8, 67.9, 59.6, 56.3, 47.8, 39.2, 39.1, 34.3, 33.2, 31.8, 26.7, 19.5, 16.3. HRMS (m/z): C₃₇H₄₀N₅O₇ [M+H]$^+$ found: 666.2934. Calculated: 666.2928. [α]$_D^{20}$ -128 (c 1.0, MeOH).

Ethyl 2-[(1*S*,6*S*,9*S*)-6-*tert*-butyl-1-cyano-9-[(2*S*)-2-hydroxy-3-methylbutanamido]-8-oxo-19-oxa-4,7-diazatetracyclo[9.5.2.1²,⁵.0¹⁴,¹⁷]nonadeca-2,4,11,13,17-pentaen-3-yl]-1,3-oxazole-4-carboxylate (DZA-139). To methyl ester **DZA-129** (38 mg; 0.064 mmol) in toluene (0.5 mL) was

17

added ethanol (188 µL; 3.22 mmol; 50 equiv.) followed by the addition of Ti(O*i*Pr)$_4$ (19 µL; 0.065 mmol; 1 equiv.). The resulting yellow solution was stirred at 100°C in mineral oil bath for 20 h. Then the vial was cooled to room temperature and diluted with EtOAc. The resulting solution was washed with aqueous 1N HCl (×2), then brine. The organic layer was dried (Na$_2$SO$_4$) and evaporated. The resulting yellow oil was purified with reverse phase flash chromatography (10% to 70% MeCN in water) to give ethyl ester **DZA-139** (24 mg; 62%) as a white amorphous solid.

^{1}H NMR (400 MHz, MeOD) δ 8.74 (s, 1H), 8.37 (d, *J* = 7.6 Hz, 1H), 7.42 – 7.26 (m, 2H), 6.97 (s, 1H), 4.78 – 4.71 (m, 1H), 4.54 (dd, *J* = 11.8, 3.8 Hz, 1H), 4.41 (q, *J* = 7.1 Hz, 2H), 3.86 (d, *J* = 3.8 Hz, 1H), 3.29 – 3.10 (m, 3H), 3.03 – 2.91 (m, 2H), 2.88 (dd, *J* = 12.2, 3.8 Hz, 1H), 2.09 (sept d, *J* = 6.9, 3.8 Hz, 1H), 1.40 (t, *J* = 7.1 Hz, 3H), 1.01 (s, 9H), 1.00 (d, *J* = 6.8 Hz, 3H), 0.89 (d, *J* = 6.8 Hz, 3H). ^{13}C NMR (101 MHz, MeOD) δ 175.8, 173.9, 164.4, 162.3, 156.2, 150.6, 146.7, 142.9, 142.5, 136.8, 135.7, 131.9, 129.6, 127.7, 126.6, 119.4, 76.8, 62.5, 59.6, 56.3, 47.8, 39.3, 39.2, 34.3, 33.2, 31.8, 26.7, 19.5, 16.3, 14.6. HRMS (m/z): C$_{32}$H$_{38}$N$_5$O$_7$ [M+H]$^+$ found: 604.2783. Calculated: 604.2771. [α]$_D^{20}$ -147 (c 1.0, MeOH).

{2-[(1*S*,6*S*,9*S*)-6-*tert*-Butyl-1-cyano-9-[(2*S*)-2-hydroxy-3-methylbutanamido]-8-oxo-19-oxa-4,7-diazatetracyclo[9.5.2.1^{2,5}.0^{14,17}]nonadeca-2,4,11,13,17-pentaen-3-yl]-1,3-oxazole-4-carbonyloxy}methyl 2,2-dimethylpropanoate (DZA-164). Methyl ester **DZA-129** (45 mg; 0.076 mmol) was dissolved in THF (0.5 mL). Separately solid LiOH×H$_2$O (10 mg; 0.23 mmol; 3 equiv.) was dissolved in water (0.2 mL) and added to the reaction mixture. Emulsion was stirred at room temperature for 30 min, then aqueous 1N HCl was added. The resulting mixture was extracted with EtOAc (×2), combined organic layers were washed with brine, dried (Na$_2$SO$_4$) and evaporated. The crude carboxylic acid was used in the next step without additional purification. The crude acid was dissolved in dry DMF (0.5 mL), then K$_2$CO$_3$ (21 mg; 0.15 mmol; 2 equiv.) was added at room temperature followed by iodomethyl pivalate (43 µL; 0.15 mmol; 2 equiv.). The suspension was stirred for 1 h, then it was diluted with EtOAc and washed with aqueous saturated NH$_4$Cl (×2). Organic layer was washed with brine, dried (Na$_2$SO$_4$), evaporated. The resulting dark brown oil was purified with reverse phase flash chromatography (10% to 70% MeCN in 0.01% TFA in water) to give ester **DZA-164** (25 mg; 48%) as a white amorphous solid.

^{1}H NMR (400 MHz, MeOD) δ 8.83 (s, 1H), 8.36 (d, *J* = 7.6 Hz, 1H), 7.38 – 7.29 (m, 2H), 7.98 (s, 1H), 6.01 (d, *J* = 7.6 Hz, 1H), 6.00 (d, *J* = 7.6 Hz, 1H), 4.79 – 4.71 (m, 1H), 4.54 (dd, *J* = 11.8, 3.8 Hz, 1H), 3.86 (d, *J* = 3.8 Hz, 1H), 3.29 – 3.09 (m, 3H), 3.04 – 2.92 (m, 2H), 2.89 (dd, *J* = 12.4, 3.8 Hz, 1H), 2.08 (sept d, *J* = 6.9, 3.8 Hz, 1H), 1.23 (s, 9H), 1.01 (s, 9H), 1.00 (d, *J* = 6.8 Hz, 3H), 0.89 (d, *J* = 6.8 Hz, 3H). ^{13}C NMR (101 MHz, MeOD) δ 178.3, 175.8, 174.0, 164.4, 160.7, 156.5, 150.8,

18

174

147.8, 142.9, 142.4, 136.8, 134.6, 131.9, 129.6, 127.6, 126.6, 119.3, 81.1, 76.8, 59.7, 56.3, 47.8, 39.8, 39.22, 39.15, 34.3, 33.2, 31.8, 27.2, 26.7, 19.5, 16.3. HRMS (m/z): $C_{36}H_{44}N_5O_9$ [M+H]$^+$ found: 690.3152. Calculated: 690.3139. $[\alpha]_D^{20}$ -161 (c 1.0, MeOH).

1-{2-[(1S,6S,9S)-6-*tert*-Butyl-1-cyano-9-[(2S)-2-hydroxy-3-methylbutanamido]-8-oxo-19-oxa-4,7-diazatetracyclo[9.5.2.1^{2,5}.0^{14,17}]nonadeca-2,4,11,13,17-pentaen-3-yl]-1,3-oxazole-4-carbonyloxy}ethyl acetate (DZA-165). Methyl ester **DZA-129** (130 mg; 0.22 mmol) was dissolved in THF (1 mL). Separately solid LiOH×H₂O (28 mg; 0.66 mmol; 3 equiv.) was dissolved in water (0.5 mL) and added to the reaction mixture. Emulsion was stirred at room temperature for 30 min, then aqueous 1N HCl was added. The resulting mixture was extracted with EtOAc (×2), combined organic layers were washed with brine, dried (Na₂SO₄) and evaporated. The crude carboxylic acid was used in the next step without additional purification. The crude acid was dissolved in dry DMF (1 mL), then K₂CO₃ (61 mg; 0.44 mmol; 2 equiv.) was added at room temperature followed by 1-bromoethylacetate (74 µL; 0.44 mmol; 2 equiv.). The suspension was stirred for 1 h, then it was diluted with EtOAc and washed with aqueous saturated NH₄Cl (×2). Organic layer was washed with brine, dried (Na₂SO₄), evaporated. The resulting dark brown oil was purified with reverse phase flash chromatography (10% to 70% MeCN in 0.01% TFA in water) to give ester **DZA-165** (62 mg; 43%) as a white amorphous solid.

^{1}H NMR (400 MHz, MeOD) δ 8.81 (d, J = 1.8 Hz, 1H), 8.36 (d, J = 7.6 Hz, 1H), 7.40 – 7.22 (m, 2H), 7.09 (q, J = 5.4 Hz, 1H), 6.98 (s, 1H), 4.79 – 4.69 (m, 1H), 4.54 (dd, J = 11.8, 3.8 Hz, 1H), 3.86 (d, J = 3.8 Hz, 1H), 3.30 – 3.10 (m, 3H), 3.02 – 2.91 (m, 2H), δ 2.89 (dd, J = 12.5, 3.8 Hz, 1H), 2.13 – 2.04 (m, 1H), 2.09 (s, 3H), 1.61 (d, J = 5.4 Hz, 3H), 1.01 (s, 9H), 1.00 (d, J = 6.8 Hz, 3H), 0.89 (d, J = 6.8 Hz, 3H). ^{13}C NMR (101 MHz, MeOD) δ 175.8, 174.0, 173.9, 170.6, 164.4, 160.1, 156.4, 150.8, 147.6, 142.9, 142.4, 136.8, 134.9, 131.9, 129.6, 127.6, 126.6, 119.4, 90.4, 76.8, 59.6, 56.3, 47.8, 39.2, 34.3, 33.2, 31.8, 26.8, 20.7, 19.7, 19.5, 16.3. HRMS (m/z): $C_{34}H_{39}N_5O_9Na$ [M+Na]$^+$ found: 684.2657. Calculated: 684.2645.

The synthesis of diazonamide A analog DZA-143 is shown in Scheme 3.

Accordingly, the crude acid **8** (prepared as described in [11]) was reacted with L-serine *tert*-butyl ester hydrochloride in the presence of EDC hydrochloride in pyridine to furnish amide 9. The cyclization of **9** into bisoxazole **10** was accomplished by DAST reagent in the presence of DBU and BrCCl₃. The final step of the synthesis was the cleavage of *N*-Boc protecting group to afford the building block **11**. Accordingly, ester hydrolysis in **12** was followed by amide coupling with corresponding amine **11** giving amide **13**. The key macrocyclization step in presence of K₃PO₄ furnished macrocycle **14** with diastereomeric ratio 97:3. After *N*-Boc cleavage with MsOH the

19

resulting amine was coupled with (*S*)-2-hydroxy-3-methylbutanoic acid (*S*-H*i*VA; **7**) to give analog **DZA-143** (Scheme 3).
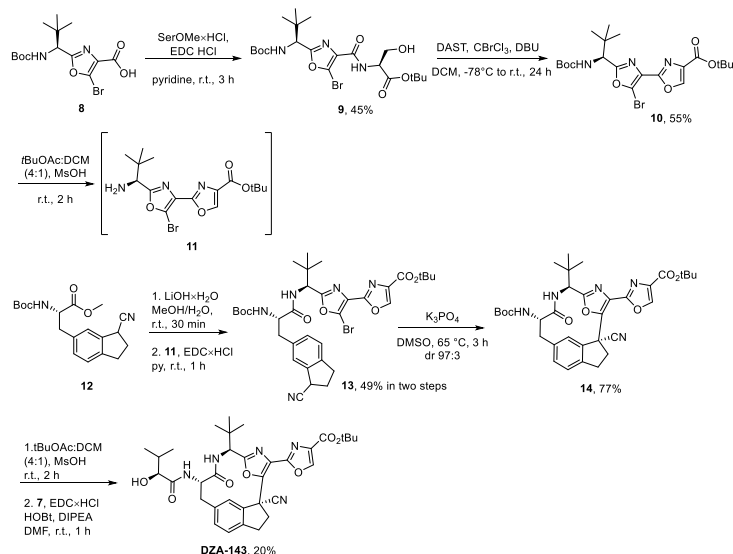
Scheme 3. Synthesis of diazonamide A analog **DZA-143**

***tert*-Butyl (2*S*)-2-({5-bromo-2-[(1*S*)-1-{[(*tert*-butoxy)carbonyl]amino}-2,2-dimethylpropyl]-1,3-oxazol-4-yl}formamido)-3-hydroxypropanoate (9).** Carboxylic acid **8** (500 mg; 1.33 mmol) was dissolved in dry pyridine (5 mL), EDC×HCl (356 mg; 1.86 mmol; 1.4 equiv.) and L-SerO*t*Bu (328 mg; 1.66 mmol; 1.25 equiv.) were added at room temperature. The resulting solution was stirred at room temperature for 1 h, then pyridine was evaporated and the resulting orange oil was redissolved in EtOAc and washed with aqueous 1N HCl (×2). Combined organic layers were washed with brine, dried (Na$_2$SO$_4$) and evaporated. The resulting orange oil was purified with direct phase flash chromatography (20% to 40% EtOAc in hexanes) to give amide **9** (310 mg; 45%) as a yellow oil.

^{1}H NMR (400 MHz, CDCl$_3$) δ 7.72 (d, *J* = 7.2 Hz, 1H), 5.19 (d, *J* = 9.9 Hz, 1H), 4.71 – 4.64 (m, 2H), 4.06 – 3.97 (m, 2H), 1.50 (s, 9H), 1.44 (s, 9H), 0.98 (s, 9H). ^{13}C NMR (101 MHz, CDCl$_3$) δ 169.1, 164.2, 160.2, 155.4, 131.3, 125.1, 83.3, 80.5, 64.1, 57.5, 55.6, 35.7, 28.4, 28.2, 26.3. HRMS (m/z): C$_{21}$H$_{34}$N$_3$O$_7$NaBr [M+Na]$^+$ found: 542.1487. Calculated: 542.1478. [α]$_D^{20}$ -7 (c 1.0, CHCl$_3$).

***tert*-Butyl 2-{5-bromo-2-[(1*S*)-1-{[(*tert*-butoxy)carbonyl]amino}-2,2-dimethylpropyl]-1,3-oxazol-4-yl}-1,3-oxazole-4-carboxylate (10).** To alcohol **9** (800 mg; 1.54 mmol) in dry DCM (7 mL) DAST (207 µL; 1.69 mmol; 1.1 equiv.) was added dropwise after the flask was cooled to -78°C. The

20

orange solution was gradually warmed to 0 °C and K_2CO_3 (850 mg; 6.15 mmol; 4 equiv.) was added in one portion. The resulting suspension was stirred for 30 minutes at the same temperature. Then the flask was shielded from the light with aluminum foil and neat $BrCCl_3$ (378 µL; 3.84 mmol; 2.5 equiv.) was added followed by DBU (574 µL; 3.84 mmol; 2.5 equiv.). The dark red reaction mixture was stirred at room temperature for 20 h. The dark red suspension was quenched by the addition of aqueous 4N HCl (Caution! CO_2 evolution) and extracted with EtOAc (×3). Organic layers were combined, washed with water, brine, dried (Na_2SO_4), evaporated. The resulting dark oil was purified with direct phase flash chromatography (0% to 20% EtOAc in hexanes) to give bioxazole **10** (420 mg; 55%) as colourless oil.

^{1}H NMR (400 MHz, $CDCl_3$) δ 8.18 (s, 1H), 5.34 (d, J = 9.9 Hz, 1H), 4.74 (d, J = 9.9 Hz, 1H), 1.59 (s, 9H), 1.42 (s, 9H), 1.00 (s, 9H). ^{13}C NMR (101 MHz, $CDCl_3$) δ 165.8, 160.1, 155.4, 154.7, 143.4, 136.1, 128.2, 122.9, 82.6, 80.3, 57.5, 36.0, 28.4, 28.3, 26.3. HRMS (m/z): $C_{21}H_{30}N_3O_6NaBr$ [M+Na]$^+$ found: 522.1218. Calculated: 522.1216. $[\alpha]_D^{20}$ -34 (c 1.0, $CHCl_3$).

***tert*-Butyl 2-{5-bromo-2-[(1*S*)-1-[(2*S*)-2-{[(*tert*-butoxy)carbonyl]amino}-3-(3-cyano-2,3-dihydro-1*H*-inden-5-yl)propanamido]-2,2-dimethylpropyl]-1,3-oxazol-4-yl}-1,3-oxazole-4-carboxylate (13).** Compound was prepared according to General procedure C from ester **12** (290 mg; 0.84 mmol), LiOH×H_2O (177 mg; 4.21 mmol; 5 equiv.) in THF/water (1:1 v/v; 3 mL) and amine **11** (337 mg; 0.84 mmol; 1 equiv.), EDC×HCl (242 mg; 1.26 mmol; 1.5 equiv.) in pyridine (6 mL) in 1 h. Product **13** was purified by reverse phase flash chromatography (from 10% to 70% MeCN in 0,01% TFA in water) to afford **13** (230 mg, 49%) of a 1:1 mixture of diastereomers as a white amorphous solid.

^{1}H NMR (400 MHz, $CDCl_3$) δ 8.20 (s, 0.5H), 8.19 (s, 0.5H), 7.27 (s, 1H), 7.14 – 7.05 (m, 2H), 6.73 (d, J = 8.4 Hz, 0.5H), 6.64 (d, J = 8.4 Hz, 0.5H), 5.06 (t, J = 9.6 Hz, 1H), 5.07 – 4.96 (m, 1H), 4.34 – 4.26 (m, 1H), 4.08 – 4.03 (m, 1H), 3.14 – 3.02 (m, 2H), 3.01 – 2.92 (m, 1H), 2.87 – 2.74 (m, 1H), 2.55 – 2.44 (m, 1H), 2.37 – 2.25 (m, 1H), 1.60 (s, 9H), 1.43 (s, 9H), 0.96 (s, 4.5H), 0.95 (s, 4.5H). ^{13}C NMR (101 MHz, $CDCl_3$) δ 171.0, 170.9, 164.7, 160.1, 160.0, 155.7, 155.6, 154.52, 154.47, 143.43, 143.36, 141.7, 138.2, 136.1, 136.0, 129.8, 129.6, 128.2, 125.5, 125.2, 125.1, 123.0, 121.1, 121.0, 82.7, 80.6, 56.2, 55.8, 55.7, 37.5, 37.3, 36.0, 35.9, 34.5, 31.4, 31.2, 28.4, 28.3, 26.3. HRMS (m/z): $C_{34}H_{42}N_5O_7NaBr$ [M+Na]$^+$ found: 734.2167. Calculated: 734.2165.

***tert*-Butyl 2-[(1*S*,6*S*,9*S*)-9-{[(*tert*-butoxy)carbonyl]amino}-6-*tert*-butyl-1-cyano-8-oxo-19-oxa-4,7-diazatetracyclo[9.5.2.1^{2,5}.0^{14,17}]nonadeca-2,4,11,13,17-pentaen-3-yl]-1,3-oxazole-4-carboxylate (14).** Compound was prepared according to General procedure B from amide **13** (220 mg; 0.31 mmol) and K_3PO_4 (328 mg; 1.54 mmol; 5 equiv.) in DMF (10 mL) in 4 h. Product 14 was

21

purified by reverse phase flash chromatography (from 10% to 70% MeCN in 0,01% TFA in water) to afford 150 mg (77%) of a single diastereomer **14** as a white amorphous solid.

^{1}H NMR (400 MHz, CDCl₃) δ 8.25 (s, 1H), 7.24 – 7.19 (m, 2H), 7.15 (s, 1H), 5.69 (d, *J* = 7.9 Hz, 1H), 5.22 (d, *J* = 9.2 Hz, 1H), 4.83 (d, *J* = 7.9 Hz, 1H), 3.89 (ddd, *J* = 12.3, 9.2, 3.3 Hz, 1H), 3.32 – 3.21 (m, 2H), 3.19 – 3.11 (m, 1H), 3.03 – 2.91 (m, 2H), 2.90 – 2.83 (m, 1H), 1.60 (s, 9H), 1.43 (s, 9H), 1.01 (s, 9H). ^{13}C NMR (101 MHz, CDCl₃) δ 171.9, 161.9, 160.1, 155.3, 154.6, 148.6, 144.0, 141.4, 140.9, 136.2, 135.5, 130.3, 129.4, 127.2, 125.5, 118.3, 82.5, 80.5, 58.3, 57.7, 46.4, 38.2, 37.9, 33.5, 31.1, 28.4, 28.4, 26.6. HRMS (m/z): $C_{34}H_{42}N_5O_7$ [M+H]⁺ found: 632.3085. Calculated: 632.3084. $[\alpha]_D^{20}$ -115 (c 1.0, CHCl₃).

***tert*-Butyl 2-[(1*S*,6*S*,9*S*)-6-*tert*-butyl-1-cyano-9-[(2*S*)-2-hydroxy-3-methylbutanamido]-8-oxo-19-oxa-4,7-diazatetracyclo[9.5.2.1²,⁵.0¹⁴,¹⁷]nonadeca-2,4,11,13,17-pentaen-3-yl]-1,3-oxazole-4-carboxylate (DZA-143).** Compound was prepared according to General procedure C from macrocycle **14** (120 mg; 0.19 mmol), MsOH (43 μL; 0.66 mmol; 3.5 equiv.) in DCM/*t*BuOAc (4:1 v/v; 0.5 mL) in 2 h and *S*-H*i*VA (34 mg; 0.29 mmol; 1.5 equiv.), EDC×HCl (73 mg; 0.38 mmol; 2 equiv.), HOBt (77 mg; 0.57 mmol; 3 equiv.), DIPEA (164 μL; 0.95 mmol; 5 equiv.) in DMF (2 mL) in 1 h . Product **DZA-143** was purified by reverse phase flash chromatography (10% to 95% MeCN in water) to afford 21 mg (20%) as a white amorphous solid.

^{1}H NMR (400 MHz, MeOD) δ 8.58 (s, 1H), 7.37 – 7.30 (m, 2H), 7.00 (s, 1H), 4.75 (s, 1H), 4.52 (dd, *J* = 11.8, 3.8 Hz, 1H), 3.86 (d, *J* = 3.8 Hz, 1H), 3.29 – 3.08 (m, 3H), 3.02 – 2.83 (m, 3H), 2.09 (sept d, *J* = 6.8, 3.8 Hz, 1H), 1.61 (s, 9H), 1.01 (s, 9H), 1.00 (d, *J* = 6.8 Hz, 3H), 0.90 (d, *J* = 6.8 Hz, 3H). ^{13}C NMR (101 MHz, MeOD) δ 175.8, 173.9, 164.3, 161.6, 156.1, 150.6, 146.2, 142.9, 142.5, 136.89, 136.87, 131.9, 129.7, 127.9, 126.5, 119.5, 83.7, 77.0, 59.7, 56.4, 47.8, 39.3, 39.2, 34.3, 33.2, 31.8, 28.5, 26.8, 19.4, 16.4. HRMS (m/z): $C_{34}H_{41}N_5O_7Na$ [M+Na]⁺ found: 654.2922. Calculated: 654.2904. $[\alpha]_D^{20}$ -144 (c 1.0, MeOH).

The synthesis of diazonamide A analog DZA-163 is shown in Scheme 4.

Accordingly, ketone **15** was transformed into nitrile **16** in the presence of TosMIC and KO*t*Bu, then the resulting nitrile **16** was reacted with freshly prepared organozinc species **2** in Pd-catalyzed Negishi cross-coupling. Ester hydrolysis in **17** was followed by amide coupling with corresponding amine **4** giving amide **18**. The key macrocyclization step in presence of K₃PO₄ furnished macrocycle **19** with diastereomeric ratio 98:2. After *N*-Boc cleavage with TFA the resulting amine was coupled with (*S*)-2-hydroxy-3-methylbutanoic acid (*S*-H*i*VA; **7**) to give analog **DZA-163** (Scheme 4).
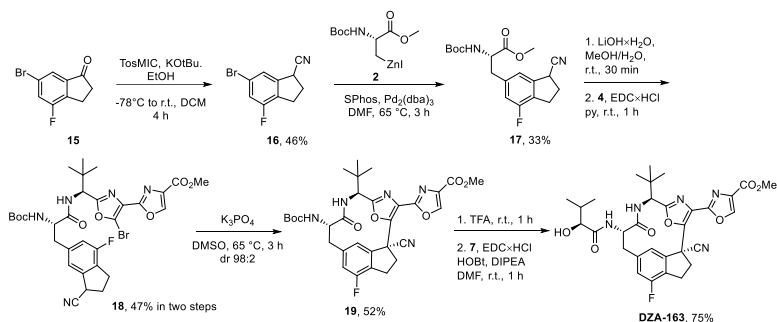
Scheme 4. Synthesis of diazonamide A analog **DZA-163**

6-Bromo-4-fluoro-2,3-dihydro-1*H*-indene-1-carbonitrile (16). Ketone **15** (650 mg; 2.84 mmol) and TosMIC (665 mg; 3.41 mmol; 1.2 equiv.) were dissolved in dry THF (7 mL) and cooled to -78 °C. EtOH (200 µL; 3.41 mmol; 1.2 equiv.) and *t*-BuOK (446 mg; 3.97 mmol; 1.40 equiv.) were added sequentially and stirring was continued for 2 h while the cold bath was allowed to warm to room temperature gradually. The cold bath was removed and the mixture was stirred at room temperature for 20 h. Dark red thick solution. The solution was diluted with water, then 1N HCl was added and the mixture was extracted with EtOAc (×2). Organic layers were combined, washed with brine, dried (Na$_2$SO$_4$) and evaporated. Dark red solid. The residue was purified with column chromatography (10% EtOAc in hexanes) to give the product **16** (310 mg, 46%) as yellowish oil.

^{1}H NMR (400 MHz, CDCl$_3$) δ 7.38 (s, 1H), 7.16 (d, J = 8.2 Hz, 1H), 4.13 (t, J = 8.2 Hz, 1H), 3.15 – 3.06 (m, 1H), 2.98 – 2.84 (m, 1H), 2.70 – 2.55 (m, 1H), 2.47 – 2.37 (m, 1H). ^{13}C NMR (101 MHz, CDCl$_3$) δ 158.8 (d, J = 252.6 Hz), 142.4 (d, J = 6.8 Hz), 128.8 (d, J = 19.8 Hz), 123.6 (d, J = 3.8 Hz), 121.3 (d, J = 7.9 Hz), 119.9 (s), 119.1 (d, J = 23.7 Hz), 34.7 (d, J = 2.3 Hz), 31.2, 27.4. HRMS (m/z): C$_{10}$H$_6$NBrF [M+H]$^+$ found: 237.9662. Calculated: 237.9668.

Methyl (2*S*)-2-{[(*tert*-butoxy)carbonyl]amino}-3-(3-cyano-7-fluoro-2,3-dihydro-1*H*-inden-5-yl)propanoate (17). Aryl bromide **15** (130 mg; 0.54 mmol), Pd$_2$(dba)$_3$ (7 mg; 0.008 mmol; 0.02 equiv.) and SPhos (9 mg; 0.022 mmol; 0.04 equiv.) were dissolved in anhydrous DMF (1 mL) under argon atmosphere and freshly prepared solution of alkyl zinc iodide **2** (0.5 M in DMF; 2.2 mL; 1.08 mmol; 2.0 equiv.) (prepared as described in [10]) was added. The dark red solution was stirred at 65 °C for 3 h. Then the solution was cooled to room temperature and aqueous saturated NH$_4$Cl and EtOAc were added. Layers were separated and EtOAc was washed with 1N HCl aqueous solution and brine, dried (Na$_2$SO$_4$) and evaporated to dryness. Product **17** was purified by column

chromatography on silica (30% EtOAc in hexanes) to afford 65 mg (33%; dr ~1:1) as a orange oil that solidifies upon standing.

^{1}H NMR (400 MHz, MeOD) δ 7.11 (s, 0.5H), 7.09 (s, 0.5H), 6.94 – 6.88 (m, 1H), 4.44 – 4.26 (m, 2H), 3.72 (s 1.5H), 3.70 (s, 1.5H), 3.19 – 3.10 (m, 1H), 3.11 – 3.02 (m, 1H), 3.00 – 2.84 (m, 2H), 2.68 – 2.58 (m, 1H), 2.39 – 2.25 (m, 1H), 1.39 (s, 4.5H), 1.37 (s, 4.5H). ^{13}C-$\{^{19}$F$\}$ NMR (151 MHz, MeOD) δ 173.8, 173.7, 160.3, 160.2, 157.7, 142.9, 140.9, 129.04, 128.97, 122.02, 121.96, 121.84, 121.81, 117.0, 116.9, 80.7, 56.4, 56.2, 52.8, 52.7, 38.2, 38.1, 35.5, 32.4, 28.64, 28.60, 28.0. HRMS (m/z): $C_{19}H_{23}N_2O_4FNa$ [M+Na]$^{+}$ found: 385.1536. Calculated: 385.1540.

Methyl 2-{5-bromo-2-[(1S)-1-[(2S)-2-{[(*tert*-butoxy)carbonyl]amino}-3-(3-cyano-7-fluoro-2,3-dihydro-1H-inden-5-yl)propanamido]-2,2-dimethylpropyl]-1,3-oxazol-4-yl}-1,3-oxazole-4-carboxylate (18). Compound was prepared according to General procedure A from ester **17** (50 mg; 0.14 mmol), LiOH×H$_2$O (29 mg; 0.69 mmol; 5 equiv.) in THF/water (1:1 v/v; 1 mL) and amine **4** (49 mg; 0.14 mmol; 1 equiv.), EDC×HCl (40 mg; 0.21 mmol; 1.5 equiv.) in pyridine (1 mL) in 1 h. Product was purified by reverse phase flash chromatography (from 10% to 70% MeCN in 0,01% TFA in water) to afford 45 mg (47%) of a 1:1 mixture of diastereomers of **18** as a yellow amorphous solid.

^{1}H NMR (600 MHz, MeOD) δ 8.69 (s, 1H), 7.09 (s, 1H), 6.84 (d, J = 10.0 Hz, 0.5H), 6.82 (d, J = 9.8 Hz, 0.5H), 5.02 (d, J = 9.4 Hz, 1H), 4.44 – 4.37 (m, 1H), 4.27 (dd, J = 8.1, 8.1 Hz, 0.5H), 4.22 (dd, J = 8.1, 8.1 Hz, 0.5H), 3.93 (s, 1.5H), 3.92 (s, 1.5H), 3.03 – 2.83 (m, 3H), 2.81 – 2.68 (m, 1H), 2.56 – 2.48 (m, 1H), 2.28 – 2.19 (m, 1H), 1.41 (s, 4.5H), 1.40 (s, 4.5H), 1.02 (s, 4.5H), 1.01 (s, 4.5H). ^{13}C-$\{^{19}$F$\}$ NMR (151 MHz, MeOD) δ 174.0, 173.9, 166.1, 162.6, 160.1, 157.5, 156.3, 156.2, 146.3, 142.74, 142.67, 140.7, 140.6, 135.34, 135.30, 128.9, 128.73, 128.7, 124.9, 124.8, 122.2, 122.1, 121.73, 121.68, 116.99, 116.95, 80.7, 57.1, 57.0, 52.7, 38.6, 38.5, 36.7, 36.6, 35.5, 32.29, 32.25, 28.6, 27.92, 27.88, 26.6. HRMS (m/z): $C_{31}H_{35}N_5O_7FNaBr$ [M+Na]$^{+}$ found: 710.1603. Calculated: 710.1602.

Methyl 2-[(1S,6S,9S)-9-{[(*tert*-butoxy)carbonyl]amino}-6-*tert*-butyl-1-cyano-13-fluoro-8-oxo-19-oxa-4,7-diazatetracyclo[9.5.2.1^{2,5}.0^{14,17}]nonadeca-2,4,11,13,17-pentaen-3-yl]-1,3-oxazole-4-carboxylate (19). Compound was prepared according to General procedure B from amide **18** (46 mg; 0.067 mmol) and K$_3$PO$_4$ (71 mg; 0.34 mmol; 5 equiv.) in DMF (2 mL) in 8 h. Product **19** was purified by reverse phase flash chromatography (from 10% to 70% MeCN in 0,01% TFA in water) to afford 21 mg (52%; dr 98:2) of a single diastereomer as a white amorphous solid.

^{1}H NMR (400 MHz, CDCl$_3$) δ 8.68 (s, 1H), 7.57 (s, 1H), 7.28 – 7.25 (m, 2H), 6.16 (d, J = 7.7 Hz, 1H), 5.51 (d, J = 9.3 Hz, 1H), 5.11 (d, J = 7.7 Hz, 1H), 4.25 (s, 3H), 4.24 – 4.19 (m, 1H), 3.62 – 3.45

24

(m, 3H), 3.40 – 3.25 (m, 2H), 3.13 (dd, J = 12.3, 3.3 Hz, 1H), 1.74 (s, 9H), 1.33 (s, 9H). ^{13}C NMR (101 MHz, CDCl$_3$) δ 171.6, 162.1, 161.3, 159.1 (d, J = 250.4 Hz), 155.3, 154.7, 148.1, 144.6, 143.6 (d, J = 6.5 Hz), 138.2 (d, J = 6.1 Hz), 134.8, 128.2 (d, J = 20.6 Hz), 127.3, 125.3 (d, J = 3.6 Hz), 117.7, 116.3 (d, J = 20.3 Hz), 80.7, 58.0, 57.9, 52.4, 46.6, 38.3, 37.7, 33.5, 28.4, 27.6, 26.6. HRMS (m/z): C$_{31}$H$_{34}$N$_5$O$_7$FNa [M+Na]$^+$ found: 630.2361. Calculated: 630.2340. [α]$_D^{20}$ -121 (c 1.0, CHCl$_3$).

Methyl 2-[(1S,6S,9S)-6-tert-butyl-1-cyano-13-fluoro-9-[(2S)-2-hydroxy-3-methylbutanamido]-8-oxo-19-oxa-4,7-diazatetracyclo[9.5.2.1^2,^{5}.0^{14},^{17}]nonadeca-2,4,11,13,17-pentaen-3-yl]-1,3-oxazole-4-carboxylate (DZA-163). Compound was prepared according to General procedure C from macrocycle **19** (20 mg; 0.033 mmol), TFA (50 μL; 0.66 mmol; 20 equiv.) in DCM (0.5 mL) in 1 h and S-HiVA (6 mg; 0.049 mmol; 1.5 equiv.), EDC×HCl (19 mg; 0.099 mmol; 3 equiv.), HOBt (13 mg; 0.099 mmol; 3 equiv.), DIPEA (29 μL; 0.17 mmol; 5 equiv.) in DMF (0.5 mL) in 1 h . Product **DZA-163** was purified by reverse phase flash chromatography (10% to 70% MeCN in 0,01% TFA in water) to afford 15 mg (75%) as a white amorphous solid.

^{1}H NMR (400 MHz, MeOD) δ 8.75 (s, 1H), 7.15 (dd, J = 9.8, 1.3 Hz, 1H), 6.83 (d, J = 1.3 Hz, 1H), 4.74 (s, 1H), 4.57 (dd, J = 11.8, 3.8 Hz, 1H), 3.94 (s, 3H), 3.86 (d, J = 3.8 Hz, 1H), 3.28 – 3.13 (m, 3H), 3.12 – 2.97 (m, 2H), 2.89 (dd, J = 12.4, 3.8 Hz, 1H), 2.08 (sept d, J = 6.9, 3.8 Hz, 1H), 1.02 (s, 9H), 0.99 (d, J = 6.8 Hz, 3H), 0.89 (d, J = 6.8 Hz, 3H). ^{13}C NMR (101 MHz, MeOD) δ 175.9, 173.7, 164.4, 162.7, 160.5 (d, J = 248.9 Hz), 156.1, 149.8, 146.9, 145.3 (d, J = 6.4 Hz), 139.8 (d, J = 6.6 Hz), 135.4, 129.4 (d, J = 20.6 Hz), 127.9, 125.8 (d, J = 3.2 Hz), 118.9, 117.9 (d, J = 21.0 Hz), 76.8, 59.6, 56.1, 52.7, 48.0, 38.9, 34.4, 33.2, 30.8, 28.0, 26.7, 19.5, 16.4. HRMS (m/z): C$_{31}$H$_{35}$N$_5$O$_7$F [M+H]$^+$ found: 608.2537. Calculated: 608.2521. [α]$_D^{20}$ -154 (c 1.0, MeOH).

The synthesis of diazonamide A analogs DZA-140-141, 144-145 is shown in Scheme 5.

Accordingly, ketones **20a-c** were converted into corresponding nitriles **21a-c** in the presence of TosMIC and KOtBu. Then nitriles **21a-c** were reacted with freshly prepared organozinc species **2** in Pd-catalyzed Negishi cross-coupling. Ester hydrolysis in **22a-c** was followed by amide coupling with corresponding amine **4** giving amides **23a-c**. The key macrocyclization step in presence of K$_3$PO$_4$ furnished macrocycles **24a-c** with diastereomeric ratio 96:4 to 99:1. After N-Boc cleavage with TFA the resulting amine was coupled with (S)-2-hydroxy-3-methylbutanoic acid (S-HiVA; **7**) to give analogs **DZA-140, 141, 144**. Analog **DZA-145** was furnished from **DZA-144** after oxidation with mCPBA (Scheme 5).

25
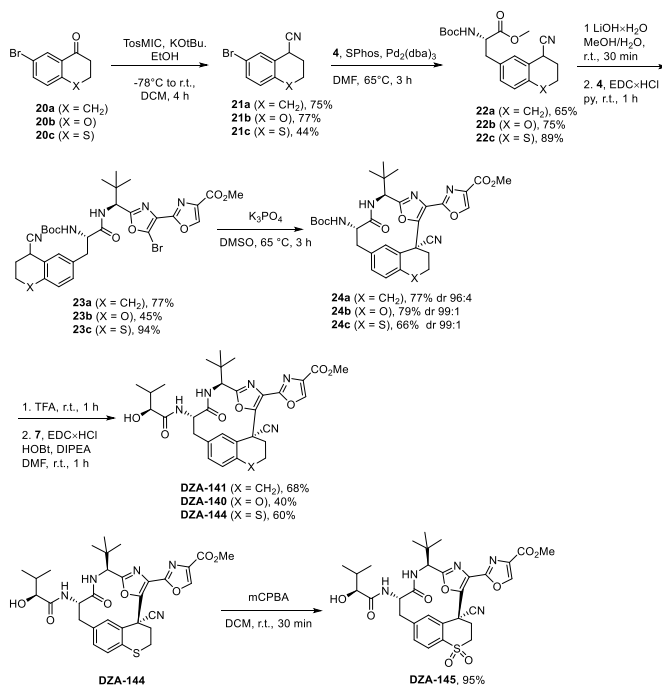
Scheme 5. Synthesis of diazonamide A analogs **DZA-140–141, 144–145**.

7-Bromo-1,2,3,4-tetrahydronaphthalene-1-carbonitrile (21a). Ketone **20a** (1 g; 4.44 mmol) and TosMIC (1.04 g; 5.33 mmol; 1.2 equiv.) were dissolved in dry THF (10 mL) and cooled to -78 ˚C. EtOH (311 µL; 5.33 mmol; 1.2 equiv.) and *t*-BuOK (698 mg; 6.22 mmol; 1.4 equiv.) were added sequentially and stirring was continued for 2 h while the cold bath was allowed to warm to room temperature gradually. The cold bath was removed and the mixture was stirred at room temperature for 20 h. Dark red thick solution. The solution was diluted with water, then 1N HCl was added and the mixture was extracted with EtOAc (×2). Organic layers were combined, washed with brine, dried (Na$_2$SO$_4$) and evaporated. Dark red solid. The residue was purified with column chromatography (10% EtOAc in hexanes) to give the product **21a** (786 mg, 75%) as white solid.

^{1}H NMR (400 MHz, CDCl$_3$) δ 7.51 (d, *J* = 2.1 Hz, 1H), 7.34 (dd, *J* = 8.2, 2.1 Hz, 1H), 7.00 (d, *J* = 8.2 Hz, 1H), 3.94 (dd, *J* = 6.3, 6.3 Hz, 1H), 2.86 – 2.65 (m, 2H), 2.19 – 2.09 (m, 2H), 2.09 – 1.97 (m, 1H), 1.90 – 1.78 (m, 1H). ^{13}C NMR (101 MHz, CDCl$_3$) δ 135.5, 132.0, 131.7, 131.5, 131.3, 121.2, 120.0, 30.7, 28.1, 27.2, 20.7. HRMS (m/z): C$_{11}$H$_9$NBr [M-H]$^-$ found: 233.9919. Calculated: 233.9918.

26

182

6-Bromo-3,4-dihydro-2*H*-1-benzopyran-4-carbonitrile (21b). Ketone **20b** (1 g; 4.40 mmol) and TosMIC (1.03 g; 5.29 mmol; 1.2 equiv.) were dissolved in dry DCM (10 mL) and cooled to -78 ˚C. EtOH (310 µL; 5.30 mmol; 1.2 equiv.) and *t*-BuOK (692 mg; 6.17 mmol; 1.4 equiv.) were added sequentially and stirring was continued for 2 h while the cold bath was allowed to warm to room temperature gradually. The cold bath was removed and the mixture was stirred at room temperature for 20 h. Dark red thick solution. The solution was diluted with water, then 1N HCl was added and the mixture was extracted with EtOAc (×2). Organic layers were combined, washed with brine, dried (Na$_2$SO$_4$) and evaporated. Dark red solid. The residue was purified with column chromatography (10% EtOAc in hexanes) to give the product **21b** (810 mg, 77%) as white solid.

^{1}H NMR (400 MHz, CDCl$_3$) δ 7.42 (dd, *J* = 2.4, 0.8 Hz, 1H), 7.32 (ddd, *J* = 8.7, 2.4, 0.8 Hz, 1H), 6.75 (d, *J* = 8.8 Hz, 1H), 4.36 – 4.30 (m, 1H), 4.28 – 4.17 (m, 1H), 4.00 (t, *J* = 5.9 Hz, 1H), 2.35 – 2.29 (m, 2H). ^{13}C NMR (101 MHz, CDCl$_3$) δ 153.3, 133.1, 132.0, 120.0, 119.7, 117.2, 113.2, 63.8, 26.8, 25.9. HRMS (m/z): C$_{10}$H$_8$NOBr [M+H]$^+$ found: 236.9790. Calculated: 236.9789.

6-Bromo-3,4-dihydro-2*H*-1-benzothiopyran-4-carbonitrile (21c). Ketone **20c** (900 mg; 3.70 mmol) and TosMIC (867 mg; 2.63 mmol; 1.1 equiv.) were dissolved in dry THF (10 mL) and cooled to -78 ˚C. EtOH (259 µL; 4.44 mmol; 1.2 equiv.) and *t*-BuOK (582 mg; 5.18 mmol; 1.4 equiv.) were added sequentially and stirring was continued for 2 h while the cold bath was allowed to warm to room temperature gradually. The cold bath was removed and the mixture was stirred at room temperature for 20 h. Dark red thick solution. The solution was diluted with water, then 1N HCl was added and the mixture was extracted with EtOAc (×2). Organic layers were combined, washed with brine, dried (Na$_2$SO$_4$) and evaporated. Dark red solid. The residue was purified with column chromatography (10% EtOAc in hexanes) to give the product **21c** (412 mg, 44%) as white solid.

^{1}H NMR (400 MHz, CDCl$_3$) δ 7.48 (d, *J* = 2.2 Hz, 1H), 7.31 (dd, *J* = 8.5, 2.2 Hz, 1H), 7.03 (d, *J* = 8.5 Hz, 1H), 3.99 (dd, *J* = 6.6, 4.5 Hz, 1H), 3.24 (ddd, *J* = 13.1, 9.0, 4.1 Hz, 1H), 3.09 – 3.02 (m, 1H), 2.50 – 2.33 (m, 2H). ^{13}C NMR (101 MHz, CDCl$_3$) δ 132.4, 132.3, 132.0, 129.0, 128.8, 119.5, 118.1, 30.9, 26.5, 24.4. HRMS (m/z): C$_{10}$H$_7$NSBr [M-H]$^-$ found: 251.9491. Calculated: 251.9483.

Methyl (2*S*)-2-{[(*tert*-butoxy)carbonyl]amino}-3-(8-cyano-5,6,7,8-tetrahydronaphthalen-2-yl)propanoate (22a). Aryl bromide **21a** (1.26 g; 5.32 mmol), Pd$_2$(dba)$_3$ (97 mg; 0.11 mmol; 0.02 equiv.) and SPhos (87 mg; 0.21 mmol; 0.04 equiv.) were dissolved in anhydrous DMF (1 mL) under argon atmosphere and freshly prepared solution of alkyl zinc iodide **2** (0.5 M in DMF; 16.0 mL; 7.98 mmol; 1.5 equiv.) was added. The dark red solution was stirred at 65 °C for 3 h. Then the solution was cooled to room temperature and aqueous saturated NH$_4$Cl and EtOAc were added. Layers were separated and EtOAc was washed with 1N HCl aqueous solution and brine, dried (Na$_2$SO$_4$) and

27

evaporated to dryness. Product **22a** was purified by column chromatography on silica (30% EtOAc in hexanes) to afford 1.24 g (65%; dr ~1:1) as a orange oil.

^{1}H NMR (400 MHz, CDCl$_3$) δ 7.17 – 6.94 (m, 3H), 5.00 (d, *J* = 8.3 Hz, 1H), 4.66 – 4.46 (m, 1H), 4.00 – 3.88 (m, 1H), 3.76 (s, 1.5H), 3.74 (s, 1.5H), 3.19 – 2.96 (m, 2H), 2.87 – 2.70 (m, 2H), 2.25 – 2.07 (m, 2H), 2.07 – 1.95 (m, 1H), 1.91 – 1.74 (m, 1H), 1.43 (s, 9H). ^{13}C NMR (101 MHz, CDCl$_3$) δ 172.4, 172.2, 155.2, 135.3, 134.61, 134.55, 130.13, 130.05, 129.7, 129.3, 129.1, 121.83, 121.76, 80.2, 80.1, 54.6, 54.5, 52.6, 52.5, 38.1, 37.8, 30.9, 28.4, 28.3, 28.2, 27.5, 27.4, 21.0, 20.9. HRMS (m/z): C$_{20}$H$_{26}$N$_2$O$_4$Na [M+Na]$^+$ found: 381.1793. Calculated: 381.1790.

Methyl (2*S*)-2-{[(*tert*-butoxy)carbonyl]amino}-3-(4-cyano-3,4-dihydro-2*H*-1-benzothiopyran-6-yl)propanoate (22c). Aryl bromide **21c** (380 mg; 1.50 mmol), Pd$_2$(dba)$_3$ (21 mg; 0.022 mmol; 0.02 equiv.) and SPhos (25 mg; 0.060 mmol; 0.04 equiv.) were dissolved in anhydrous DMF (5 mL) under argon atmosphere and freshly prepared solution of alkyl zinc iodide **2** (0.5 M in DMF; 4.49 mL; 2.24 mmol; 1.5 equiv.) was added. The dark red solution was stirred at 65 °C for 3 h. Then the solution was cooled to room temperature and aqueous saturated NH$_4$Cl and EtOAc were added. Layers were separated and EtOAc was washed with 1N HCl aqueous solution and brine, dried (Na$_2$SO$_4$) and evaporated to dryness. Product **22c** was purified by column chromatography on silica (30% EtOAc in hexanes) to afford 500 mg (89%; dr ~1:1) as a orange oil.

^{1}H NMR (400 MHz, CDCl$_3$) δ 7.11 – 7.04 (m, 2H), 7.01 – 6.93 (m, 1H), 5.00 (d, *J* = 8.2 Hz, 1H), 4.61 – 4.51 (m, 1H), 4.01 – 3.95 (m, 1H), 3.75 (s, 1.5H), 3.74 (s, 1.5H), 3.28 – 3.16 (m, 1H), 3.14 – 2.95 (m, 3H), 2.46 – 2.34 (m, 2H), 1.43 (s, 9H). ^{13}C NMR (101 MHz, CDCl$_3$) δ 172.3, 172.1, 155.1, 133.23, 133.18, 131.7, 131.6, 130.6, 130.5, 130.0, 129.9, 127.8, 127.7, 127.1, 127.0, 120.1, 120.0, 80.2, 54.5, 54.4, 52.6, 52.5, 37.9, 37.8, 31.13, 31.11, 28.43, 28.37, 27.0, 26.9, 24.6, 24.5. HRMS (m/z): C$_{19}$H$_{24}$N$_2$O$_4$SNa [M+Na]$^+$ found: 399.1365. Calculated: 399.1354.

Methyl 2-{5-bromo-2-[(1*S*)-1-[(2*S*)-2-{[(*tert*-butoxy)carbonyl]amino}-3-(4-cyano-3,4-dihydro-2*H*-1-benzopyran-6-yl)propanamido]-2,2-dimethylpropyl]-1,3-oxazol-4-yl}-1,3-oxazole-4-carboxylate (23b). Aryl bromide **21b** (480 mg; 2.00 mmol), Pd$_2$(dba)$_3$ (36 mg; 0.039 mmol; 0.02 equiv.) and SPhos (33 mg; 0.081 mmol; 0.04 equiv.) were dissolved in anhydrous DMF (3 mL) under argon atmosphere and freshly prepared solution of alkyl zinc iodide **2** (0.5 M in DMF; 6.0 mL; 3.00 mmol; 1.5 equiv.) was added. The dark red solution was stirred at 65 °C for 8 h. Then the solution was cooled to room temperature and aqueous saturated NH$_4$Cl and EtOAc were added. Layers were separated and EtOAc was washed with 1N HCl aqueous solution and brine, dried (Na$_2$SO$_4$) and evaporated to dryness. Negishi coupling product **22b** was semi-purified by filtering throug short pad

of silica (30% EtOAc in hexanes) to afford 546 mg (75%; dr ~1:1) as a colourless oil and used in the next step without further purification.

Then compound **23b** was prepared according to General procedure A from crude ester **22b** (570 mg; 1.58 mmol), LiOH×H$_2$O (332 mg; 7.91 mmol; 5 equiv.) in THF/water (3:1 v/v; 6 mL) and amine **4** (567 mg; 1.58 mmol; 1 equiv.), EDC×HCl (455 mg; 2.37 mmol; 1.5 equiv.) in pyridine (10 mL) in 1 h. Product **23b** was purified by reverse phase flash chromatography (from 10% to 70% MeCN in 0.01% TFA in water) to afford 490 mg (45%) of a 1:1 mixture of diastereomers as a white amorphous solid.

^{1}H NMR (400 MHz, CDCl$_3$) δ 8.34 (s, 0.5H), 8.32 (s, 0.5H), 7.14 – 7.06 (m, 1.5H), 7.03 (dd, J = 8.4, 2.2 Hz, 0.5H), 6.74 (d, J = 8.4 Hz, 0.5H), 6.73 – 6.68 (m, 0.5H), 6.68 (d, J = 8.4 Hz, 0.5H), 6.54 (d, J = 7.4 Hz, 0.5H), 5.13 – 4.94 (m, 2H), 4.33 – 4.16 (m, 2.5H), 4.16 – 4.03 (m, 1H), 4.00 – 3.95 (m, 0.5H), 3.94 (s, 3H), 3.05 – 2.92 (m, 2H), 2.32 – 2.18 (m, 2H), 1.43 (s, 9H), 0.96 (s, 4.5H), 0.93 (s, 4.5H). ^{13}C NMR (101 MHz, CDCl$_3$) δ 170.96, 170.94, 164.9, 164.8, 161.4, 155.6, 154.9, 154.8, 153.1, 153.0, 144.2, 144.0, 134.7, 131.0, 130.7, 130.6, 130.2, 129.5, 129.4, 128.13, 128.10, 123.2, 123.1, 120.6, 120.4, 118.2, 118.0, 115.5, 115.4, 80.6, 63.62, 63.59, 56.1, 55.9, 55.7, 52.4, 37.0, 36.7, 36.0, 35.7, 28.4, 26.81, 26.78, 26.32, 26.25, 26.1. HRMS (m/z): C$_{31}$H$_{36}$N$_5$O$_8$NaBr [M+Na]$^+$ found: 708.1663. Calculated: 708.1645.

Methyl 2-{5-bromo-2-[(1S)-1-[(2S)-2-{[(*tert*-butoxy)carbonyl]amino}-3-(8-cyano-5,6,7,8-tetrahydronaphthalen-2-yl)propanamido]-2,2-dimethylpropyl]-1,3-oxazol-4-yl}-1,3-oxazol-4-carboxylate (23a). Compound was prepared according to General procedure A from ester **22a** (980 mg; 2.73 mmol), LiOH×H$_2$O (574 mg; 13.7 mmol; 5 equiv.) in THF/water (3:1 v/v; 15 mL) and amine **4** (980 mg; 2.74 mmol; 1 equiv.), EDC×HCl (787 mg; 4.10 mmol; 1.5 equiv.) in pyridine (20 mL) in 1 h. Product **23a** was purified by reverse phase flash chromatography (from 10% to 70% MeCN in 0.01% TFA in water) to afford 1.44 g (77%) of a 1:1 mixture of diastereomers as a white amorphous solid.

^{1}H NMR (400 MHz, CDCl$_3$) δ 8.34 (s, 0.5H), 8.32 (s, 0.5H), 7.19 (s, 0.5H), 7.15 (s, 0.5H), 7.10 – 6.93 (m, 2H), 6.81 (d, J = 7.6 Hz, 0.5H), 6.63 (d, J = 7.6 Hz, 0.5H), 5.09 (d, J = 9.3 Hz, 0.5H), 5.09 – 5.02 (m, 0.5H), 5.03 (d, J = 9.3 Hz, 0.5H), 5.06 (dd, J = 23.8, 9.3 Hz, 2H), 5.00 – 4.92 (m, 0.5H), 4.35 – 4.25 (m, 1H), 4.00 – 3.95 (m, 0.5H), 3.94 (s, 3H), 3.93 – 3.88 (m, 0.5H), 3.12 – 2.96 (m, 2H), 2.82 – 2.60 (m, 2H), 2.15 – 2.03 (m, 2H), 2.00 – 1.89 (m, 1H), 1.86 – 1.70 (m, 1H), 1.42 (s, 9H), 0.97 (s, 4.5H), 0.94 (s, 4.5H). ^{13}C NMR (101 MHz, CDCl$_3$) δ 170.96, 170.95, 164.89, 164.85, 161.4, 155.69, 155.65, 154.83, 154.79, 144.2, 144.0, 135.21, 135.16, 135.1, 134.7, 130.3, 130.2, 130.1, 129.7, 129.1, 128.9, 128.10, 128.07, 123.14, 123.11, 121.9, 121.6, 80.6, 55.9, 55.7, 52.4, 37.2, 36.8,

29

36.0, 35.7, 30.81, 30.75, 28.4, 28.2, 28.1, 27.4, 26.33, 26.27, 20.81, 20.79. HRMS (m/z): $C_{32}H_{38}N_5O_7NaBr$ [M+Na]$^+$ found: 706.1858. Calculated: 706.1852.

Methyl 2-{5-bromo-2-[(1S)-1-[(2S)-2-{[(*tert*-butoxy)carbonyl]amino}-3-(4-cyano-3,4-dihydro-2H-1-benzothiopyran-6-yl)propanamido]-2,2-dimethylpropyl]-1,3-oxazol-4-yl}-1,3-oxazole-4-carboxylate (23c). Compound was prepared according to General procedure A from ester **22c** (1 g; 2.66 mmol), LiOH×H₂O (557 mg; 13.28 mmol; 5 equiv.) in THF/water (3:1 v/v; 15 mL) and amine **4** (952 g; 2.66 mmol; 1 equiv.), EDC×HCl (764 mg; 3.99 mmol; 1.5 equiv.) in pyridine (15 mL) in 1 h. Product **23c** was purified by reverse phase flash chromatography (from 10% to 70% MeCN in 0.01% TFA in water) to afford 1.75 g (94%) of a 1:1 mixture of diastereomers as a white amorphous solid.

^{1}H NMR (400 MHz, CDCl₃) δ 8.34 (s, 0.5H), 8.32 (s, 0.5H), 7.16 (s, 1H), 7.08 – 6.95 (m, 2H), 6.71 (d, *J* = 8.4 Hz, 0.5H), 6.59 (d, *J* = 8.4 Hz, 0.5H), 5.11 – 5.00 (m, 1H), 5.05 (d, *J* = 9.4 Hz, 0.5H), 5.00 (d, *J* = 9.1 Hz, 0.5H), 5.11 – 5.00 (m, 1H), 4.32 – 4.23 (m, 1H), 4.09 (dd, *J* = 6.2, 4.3 Hz, 0.5H), 4.03 (dd, *J* = 6.2, 4.3 Hz, 0.5H), 3.94 (s, 3H), 3.26 – 3.12 (m, 1H), 3.05 – 2.96 (m, 2H), 2.96 – 2.89 (m, 1H), 2.48 – 2.35 (m, 1H), 2.33 – 2.23 (m, 1H), 1.43 (s, 9H), 0.96 (s, 4.5H), 0.94 (s, 4.5H). ^{13}C NMR (101 MHz, CDCl₃) δ 170.84, 170.81, 164.9, 164.8, 161.4, 155.6, 154.9, 154.8, 144.1, 144.0, 134.72, 134.68, 133.6, 133.5, 131.5, 131.4, 131.2, 130.8, 129.8, 129.6, 128.2, 127.8, 127.6, 127.13, 127.06, 123.13, 123.11, 120.1, 119.9, 80.6, 55.9, 55.7, 52.4, 37.2, 37.0, 36.0, 35.8, 30.9, 30.8, 28.4, 26.7, 26.6, 26.30, 26.25, 24.4, 24.3. HRMS (m/z): $C_{31}H_{36}N_5O_7NaSBr$ [M+Na]$^+$ found: 724.1418. Calculated: 724.1417.

Methyl 2-[(1S,6S,9S)-9-{[(*tert*-butoxy)carbonyl]amino}-6-*tert*-butyl-1-cyano-8-oxo-20-oxa-4,7-diazatetracyclo[9.6.2.1²,⁵.0¹⁴,¹⁸]icosa-2,4,11,13,18-pentaen-3-yl]-1,3-oxazole-4-carboxylate (24a). Compound was prepared according to General procedure B from amide **23a** (1.34 g; 0.54 mmol) and K₃PO₄ (2.078 g; 9.79 mmol; 5 equiv.) in DMF (100 mL) in 3 h. Product **24a** was purified by reverse phase flash chromatography (from 10% to 70% MeCN in 0.01% TFA in water) to afford 905 mg (77%; dr 96:4) of a single diastereomer as a white amorphous solid.

^{1}H NMR (400 MHz, CDCl₃) δ 8.38 (s, 1H), 7.20 (dd, *J* = 7.9, 1.8 Hz, 1H), 7.13 (d, *J* = 7.9 Hz, 1H), 6.81 (d, *J* = 1.8 Hz, 1H), 5.77 (d, *J* = 6.4 Hz, 1H), 5.17 (d, *J* = 9.2 Hz, 1H), 4.63 (d, *J* = 6.4 Hz, 1H), 3.98 (ddd, *J* = 12.3, 6.7, 3.1 Hz, 1H), 3.93 (s, 3H), 3.11 (dd, *J* = 12.1, 12.1 Hz, 1H), 3.08 – 3.00 (m, 1H), 2.95 – 2.86 (m, 1H), 2.86 – 2.76 (m, 2H), 2.28 (ddd, *J* = 13.5, 11.2, 2.4 Hz, 1H), 2.18 – 2.06 (m, 1H), 1.97 – 1.87 (m, 1H), 1.44 (s, 9H), 0.95 (s, 9H). ^{13}C NMR (101 MHz, CDCl₃) δ 171.9, 161.9, 161.4, 155.3, 154.8, 150.5, 144.6, 135.5, 134.8, 134.1, 133.4, 131.9, 130.1, 129.6, 127.5, 119.1, 80.5,

59.0, 57.8, 52.3, 41.1, 38.0, 34.5, 33.4, 28.4, 28.3, 26.6, 20.0. HRMS (m/z): $C_{32}H_{38}N_5O_7$ [M+H]$^+$ found: 604.2778. Calculated: 604.2771. $[\alpha]_D^{20}$ -134 (c 1.0, CHCl$_3$).

Methyl 2-[(1S,6S,9S)-9-{[(*tert*-butoxy)carbonyl]amino}-6-*tert*-butyl-1-cyano-8-oxo-15,20-dioxa-4,7-diazatetracyclo[9.6.2.1^2,^{5}.0^{14},^{18}]icosa-2,4,11,13,18-pentaen-3-yl]-1,3-oxazole-4-carboxylate (24b). Compound was prepared according to General procedure B from amide **23b** (360 mg; 0.52 mmol) and K$_3$PO$_4$ (557 mg; 2.62 mmol; 5 equiv.) in DMF (30 mL) in 2 h. Product **24b** was purified by reverse phase flash chromatography (from 10% to 70% MeCN in 0.01% TFA in water) to afford 251 mg (79%; dr 99:1) of a single diastereomer as a white amorphous solid.

^{1}H NMR (400 MHz, CDCl$_3$) δ 8.37 (s, 1H), 7.19 (dd, J = 8.4, 2.2 Hz, 1H), 6.87 (d, J = 8.4 Hz, 1H), 6.81 (d, J = 2.2 Hz, 1H), 5.91 (d, J = 6.3 Hz, 1H), 5.16 (d, J = 9.2 Hz, 1H), 4.65 (d, J = 6.3 Hz, 1H), 4.48 – 4.30 (m, 2H), 4.00 (ddd, J = 12.2, 9.2, 3.2 Hz, 1H), 3.93 (s, 3H), 3.26 (d, J = 14.3 Hz, 1H), 3.13 (dd, J = 12.1, 12.1 Hz, 1H), 2.74 (dd, J = 12.5, 3.2 Hz, 1H), 2.39 (ddd, J = 14.3, 10.4, 4.7 Hz, 1H), 1.44 (s, 9H), 0.97 (s, 9H). ^{13}C NMR (101 MHz, CDCl$_3$) δ 172.1, 162.0, 161.3, 155.4, 154.6, 153.6, 148.6, 144.7, 134.7, 133.7, 131.6, 128.6, 128.1, 118.2, 118.1, 117.3, 80.6, 63.0 59.0, 57.7, 52.4, 37.4, 37.3, 33.52, 33.49, 28.4, 26.7. HRMS (m/z): $C_{31}H_{35}N_5O_8Na$ [M+Na]$^+$ found: 628.2388. Calculated: 628.2383. $[\alpha]_D^{20}$ -151 (c 1.0, CHCl$_3$).

Methyl 2-[(1S,6S,9S)-9-{[(*tert*-butoxy)carbonyl]amino}-6-*tert*-butyl-1-cyano-8-oxo-20-oxa-15-thia-4,7-diazatetracyclo[9.6.2.1^2,^{5}.0^{14},^{18}]icosa-2,4,11,13,18-pentaen-3-yl]-1,3-oxazole-4-carboxylate (24c). Compound was prepared according to General procedure B from amide **23c** (1.20 g; 1.71 mmol) and K$_3$PO$_4$ (1.81 g; 8.54 mmol; 5 equiv.) in DMF (80 mL) in 2 h. Product **24c** was purified by reverse phase flash chromatography (from 10% to 70% MeCN in 0.01% TFA in water) to afford 705 mg (66%; dr 99:1) of a single diastereomer as a white amorphous solid.

^{1}H NMR (400 MHz, CDCl$_3$) δ 8.37 (s, 1H), 7.17 – 7.09 (m, 2H), 6.79 (d, J = 1.6 Hz, 1H), 5.92 (d, J = 6.1 Hz, 1H), 5.15 (d, J = 9.2 Hz, 1H), 4.64 (d, J = 6.0 Hz, 1H), 4.00 (ddd, J = 12.1, 9.1, 3.1 Hz, 1H), 3.93 (s, 3H), 3.53 (ddd, J = 13.9, 5.8, 1.9 Hz, 1H), 3.46 (ddd, J = 13.9, 12.1, 1.9 Hz, 1H), 3.09 (dd, J = 12.1, 12.1 Hz, 1H), 3.01 (ddd, J = 13.9, 5.8, 1.9 Hz, 1H), 2.74 (dd, J = 12.4, 3.1 Hz, 1H), 2.46 (ddd, J = 13.9, 12.1, 2.3 Hz, 1H), 1.44 (s, 9H), 0.97 (s, 9H). ^{13}C NMR (101 MHz, CDCl$_3$) δ 172.0, 162.3, 161.3, 155.3, 154.5, 149.3, 144.7, 134.8, 134.7, 132.4, 132.1, 130.1, 128.0, 127.8, 127.8, 117.9, 80.6, 59.2, 57.5, 52.3, 40.7, 37.7, 34.5, 33.4, 28.4, 26.7, 23.6. HRMS (m/z): $C_{31}H_{35}N_5O_7NaS$ [M+Na]$^+$ found: 644.2174. Calculated: 644.2155. $[\alpha]_D^{20}$ -82 (c 1.0, CHCl$_3$).

Methyl 2-[(1S,6S,9S)-6-*tert*-butyl-1-cyano-9-[(2S)-2-hydroxy-3-methylbutanamido]-8-oxo-20-oxa-4,7-diazatetracyclo[9.6.2.1^2,^{5}.0^{14},^{18}]icosa-2,4,11,13,18-pentaen-3-yl]-1,3-oxazole-4-carboxylate (DZA-141). Compound was prepared according to General procedure C from

31

macrocycle **24a** (135 mg; 0.22 mmol), TFA (172 μL; 2.24 mmol; 10 equiv.) in DCM (1 mL) in 1 h and *S*-H*i*VA (29 mg; 0.25 mmol; 1.5 equiv.), EDC×HCl (63 mg; 0.33 mmol; 2 equiv.), HOBt (67 mg; 0.50 mmol; 3 equiv.), DIPEA (143 μL; 0.82 mmol; 5 equiv.) in DMF (2 mL) in 1 h . Product **DZA-141** was purified by reverse phase flash chromatography (10% to 50% MeCN in 0.01% TFA in water) to afford 68 mg (68%) as a white amorphous solid.

^{1}H NMR (400 MHz, MeOD) δ 8.76 (s, 1H), 8.43 (d, *J* = 6.1 Hz, 1H), 7.31 (dd, *J* = 7.9, 1.8 Hz, 1H), 7.22 (d, *J* = 7.9 Hz, 1H), 6.69 (d, *J* = 1.8 Hz, 1H), 4.64 (dd, *J* = 11.8, 3.7 Hz, 1H), 4.54 (d, *J* = 6.1 Hz, 1H), 3.94 (s, 3H), 3.86 (d, *J* = 3.7 Hz, 1H), 3.11 – 3.00 (m, 2H), 2.97 – 2.84 (m, 2H), 2.82 (d, *J* = 12.4, 3.7 Hz, 1H), 2.31 (ddd, *J* = 13.7, 11.0, 2.8 Hz, 1H), 2.15 – 2.03 (m, 2H), 2.03 – 1.94 (m, 1H), 1.00 (d, *J* = 6.9 Hz, 3H), 0.98 – 0.94 (m, 9H), 0.89 (d, *J* = 6.9 Hz, 3H). ^{13}C NMR (101 MHz, MeOD) δ 175.9, 174.1, 164.4, 162.8, 156.2, 152.2, 146.8, 137.0, 135.5, 135.3, 134.0, 133.2, 131.2, 131.1, 128.0, 120.5, 76.8, 61.1, 55.9, 52.7, 42.4, 39.2, 35.3, 34.2, 33.2, 29.0, 26.7, 21.0, 19.5, 16.3. HRMS (m/z): $C_{32}H_{38}N_5O_7$ [M+H]$^+$ found: 604.2783. Calculated: 604.2771. $[\alpha]_D^{20}$ -165 (c 1.0, MeOH).

Methyl 2-[(1*S*,6*S*,9*S*)-6-*tert*-butyl-1-cyano-9-[(2*S*)-2-hydroxy-3-methylbutanamido]-8-oxo-15,20-dioxa-4,7-diazatetracyclo[9.6.2.1^{2,5}.0^{14,18}]icosa-2,4,11,13,18-pentaen-3-yl]-1,3-oxazole-4-carboxylate (DZA-140). Compound was prepared according to General procedure C from macrocycle **24b** (100 mg; 0.17 mmol), TFA (127 μL; 1.65 mmol; 10 equiv.) in DCM (1 mL) in 1 h and *S*-H*i*VA (29 mg; 0.25 mmol; 1.5 equiv.), EDC×HCl (63 mg; 0.33 mmol; 2 equiv.), HOBt (67 mg; 0.49 mmol; 3 equiv.), DIPEA (142 μL; 0.82 mmol; 5 equiv.) in DMF (1 mL) in 1 h . Product **DZA-140** was purified by reverse phase flash chromatography (10% to 50% MeCN in 0.01% TFA in water) to afford 40 mg (40%) as a white amorphous solid.

^{1}H NMR (400 MHz, MeOD) δ 8.76 (s, 1H), 7.31 (dd, *J* = 8.5, 2.1 Hz, 1H), 6.92 (d, *J* = 8.5 Hz, 1H), 6.67 (d, *J* = 2.1 Hz, 1H), 4.65 (dd, *J* = 11.8, 3.7 Hz, 1H), 4.57 (s, 1H), 4.46 (ddd, *J* = 11.8, 3.3, 3.3 Hz, 1H), 4.32 (ddd, *J* = 11.8, 11.8, 1.6 Hz, 1H), 3.94 (s, 3H), 3.86 (d, *J* = 3.8 Hz, 1H), 3.22 (ddd, *J* = 14.6, 3.3, 1.6 Hz, 1H), 3.06 (dd, *J* = 12.2, 12.2 Hz, 1H), 2.77 (dd, *J* = 12.6, 3.8 Hz, 1H), 2.42 (ddd, *J* = 14.6, 11.8, 3.3 Hz, 1H), 2.09 (sept d, *J* = 6.9, 3.8 Hz, 1H), 1.00 (d, *J* = 6.9 Hz, 3H), 0.99 (s, 9H), 0.88 (d, *J* = 6.9 Hz, 3H). ^{13}C NMR (101 MHz, MeOD) δ 175.9, 174.2, 164.4, 162.8, 155.9, 155.0, 150.5, 146.9, 135.5, 134.2, 133.1, 129.8, 128.6, 119.5, 119.2, 118.8, 76.8, 63.9, 60.9, 55.8, 52.7, 38.8, 38.6, 34.3, 34.2, 33.2, 26.8, 19.5, 16.3. HRMS (m/z): $C_{31}H_{36}N_5O_8$ [M+H]$^+$ found: 606.2565. Calculated: 606.2564. $[\alpha]_D^{20}$ -194 (c 1.0, MeOH).

Methyl 2-[(1*S*,6*S*,9*S*)-6-*tert*-butyl-1-cyano-9-[(2*S*)-2-hydroxy-3-methylbutanamido]-8-oxo-20-oxa-15-thia-4,7-diazatetracyclo[9.6.2.1^{2,5}.0^{14,18}]icosa-2,4,11,13,18-pentaen-3-yl]-1,3-oxazole-4-carboxylate (DZA-144). Compound was prepared according to General procedure C from

32

macrocycle **24c** (200 mg; 0.32 mmol), TFA (247 μL; 3.22 mmol; 10 equiv.) in DCM (2 mL) in 1 h and *S*-H*i*VA (57 mg; 0.48 mmol; 1.5 equiv.), EDC×HCl (124 mg; 0.64 mmol; 2 equiv.), HOBt (131 mg; 0.97 mmol; 3 equiv.), DIPEA (279 μL; 1.61 mmol; 5 equiv.) in DMF (2 mL) in 1 h . Product **DZA-144** was purified by reverse phase flash chromatography (10% to 50% MeCN in 0.01% TFA in water) to afford 120 mg (60%) as a white amorphous solid.

^{1}H NMR (400 MHz, MeOD) δ 8.76 (s, 1H), 8.57 (d, *J* = 6.0 Hz, 1H), 7.27 (dd, *J* = 8.2, 1.8 Hz, 1H), 7.18 (d, *J* = 8.2 Hz, 1H), 6.68 (d, *J* = 1.8 Hz, 1H), 4.65 (dd, *J* = 11.8, 3.7 Hz, 1H), 4.60 – 4.55 (m, 1H), 3.94 (s, 3H), 3.86 (d, *J* = 3.7 Hz, 1H), 3.50 (ddd, *J* = 14.2, 5.7, 1.8 Hz, 1H), 3.40 (ddd, *J* = 13.7, 12.0, 1.8 Hz, 1H), 3.12 (ddd, *J* = 13.7, 5.7, 2.3 Hz, 1H), 3.04 (dd, *J* = 12.1, 12.1 Hz, 1H), 2.77 (dd, *J* = 12.5, 3.7 Hz, 1H), 2.48 (ddd, *J* = 14.2, 12.0, 2.3 Hz, 1H), 2.09 (sept d, *J* = 6.9, 3.7 Hz, 1H), 1.00 (d, *J* = 6.9 Hz, 3H), 0.99 (s, 9H), 0.88 (d, *J* = 6.9 Hz, 3H). ^{13}C NMR (101 MHz, MeOD) δ 175.9, 174.1, 164.6, 162.8, 155.9, 151.1, 146.9, 135.5, 135.4, 133.53, 133.49, 131.6, 129.4, 128.7, 128.4, 119.2, 76.8, 61.1, 55.6, 52.7, 42.0, 39.0, 35.3, 34.2, 33.1, 26.8, 24.2, 19.5, 16.3. HRMS (m/z): $C_{31}H_{36}N_5O_7S$ [M+H]$^+$ found: 622.2345. Calculated: 622.2335. [α]$_D^{20}$ -129 (c 1.0, MeOH).

Methyl 2-[(1*S*,6*S*,9*S*)-6-*tert*-butyl-1-cyano-9-[(2*S*)-2-hydroxy-3-methylbutanamido]-8,15,15-trioxo-20-oxa-15λ⁶-thia-4,7-diazatetracyclo[9.6.2.1²,⁵.0¹⁴,¹⁸]icosa-2,4,11,13,18-pentaen-3-yl]-1,3-oxazole-4-carboxylate (DZA-145). To a sulfide **DZA-144** (45 mg; 0.072 mmol) in dry DCM (0.5 mL) was added *m*-chloroperoxybenzoic acid (73%; 51 mg; 0.22 mmol; 3 equiv.) and stirred for 30 minutes at room temperature. The reaction mixture was diluted with DCM and washed with saturated NaHCO₃ and brine. The organic layer was dried (Na₂SO₄) and evaporated. White amorphous solid was purified with reverse phase flash chromatography (10% to 50% MeCN in 0.01% TFA in water) to give sulfone **DZA-145** (45 mg; 95%) as a white amorphous solid.

^{1}H NMR (400 MHz, MeOD) δ 8.78 (s, 1H), 8.51 (d, *J* = 5.8 Hz, 1H), 7.98 (d, *J* = 8.2 Hz, 1H), 7.75 (dd, *J* = 8.2, 1.6 Hz, 1H), 7.02 (d, *J* = 1.6 Hz, 1H), 4.72 (dd, *J* = 11.8, 3.9 Hz, 1H), 4.55 – 4.52 (m, 1H), 3.95 (s, 3H), 3.87 (d, *J* = 3.7 Hz, 1H), 3.82 – 3.65 (m, 2H), 3.59 – 3.51 (m, 1H), 3.40 – 3.32 (m, 1H), 3.17 (dd, *J* = 12.0, 12.0 Hz, 1H), 3.00 (dd, *J* = 12.2, 3.9 Hz, 1H), 2.09 (sept d, *J* = 6.9, 3.9 Hz, 1H), 1.00 (d, *J* = 6.9 Hz, 3H), 0.98 (s, 9H), 0.89 (d, *J* = 6.9 Hz, 3H). ^{13}C NMR (101 MHz, MeOD) δ 175.9, 173.5, 164.8, 162.8, 155.7, 148.5, 147.0, 142.9, 138.8, 135.6, 135.0, 133.4, 133.0, 129.2, 125.3, 118.0, 76.9, 61.2, 55.4, 52.8, 47.8, 42.1, 39.2, 34.3, 33.2, 32.0, 26.7, 19.5, 16.3. HRMS (m/z): $C_{31}H_{36}N_5O_9S$ [M+H]$^+$ found: 654.2247. Calculated: 654.2234. [α]$_D^{20}$ -130 (c 1.0, MeOH).

The synthesis of diazonamide A analogs DZA-147, 154-155 is shown in Scheme 6.

Modifications in the quaterinary position of macrocycle are depicted in Scheme 6. Accordingly, amide **25** was obtained from corresponding macrocycle **6** after conversion of nitrile to amide in the

33

presence of K_2CO_3 and hydrogen peroxide. The resulting amide **25** was converted into analog **DZA-147** after *N*-Boc cleavage and following amide coupling with carboxylic acid **7**. Primary amine containing analog **DZA-154** was obtained from analog **DZA-129** after reduction of nitrile in the presence of $InCl_3$ and $NaBH_4$. Methyl ester containing analog **DZA-155** was synthesized from analog **DZA-129** in two steps. In the first step **DZA-129** was treated with $LiOH \times H_2O$ in methanol/water mixture to produce methyl ester at the quaterinary position. In the second step methyl ester at the oxazole moiety was restored with $TMSCHN_2$ after it was hydrolyzed during the first step (Scheme 6).
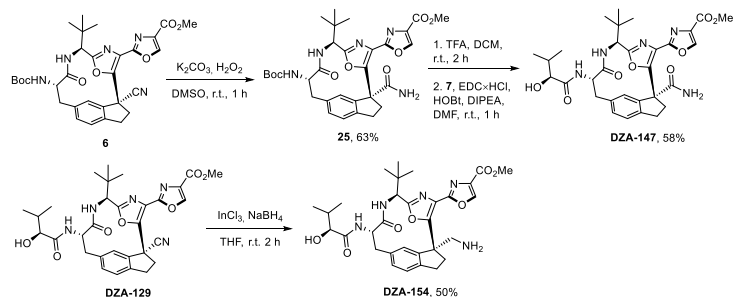
Scheme 6. Synthesis of diazonamide A analogs **DZA-147** and **DZA-154**.

Methyl 2-[(1*R*,6*S*,9*S*)-9-{[(*tert*-butoxy)carbonyl]amino}-6-*tert*-butyl-1-carbamoyl-8-oxo-19-oxa-4,7-diazatetracyclo[9.5.2.1²,⁵.0¹⁴,¹⁷]nonadeca-2,4,11,13,17-pentaen-3-yl]-1,3-oxazole-4-carboxylate (25). To nitrile **6** (115 mg; 0.20 mmol) in dry DMSO (0.5 mL) K_2CO_3 (54 mg; 0.39 mmol; 2 equiv.) was added and the flask was cooled to 0˚C. Then H_2O_2 (50% in water; 117 µL; 1.95 mmol; 10 equiv.) was added dropwise and the resulting suspension was warmed to room temperature and stirred for 3 h. Then the suspension was quenched by the addition of aqueous 1N $Na_2S_2O_3$ and extracted with EtOAc (×2). Organic layer was washed with brine, dried (Na_2SO_4) and evaporated. The resulting yellow oil was purified with reverse phase flash chromatography (from 10% to 50% MeCN in 0.01% TFA in water) to give amide **25** (58 mg; 49%) as a yellowish solid.

^{1}H NMR (400 MHz, CDCl₃) δ 8.31 (s, 1H), 7.47 (s, 1H), 7.16 – 7.09 (m, 2H), 5.69 (d, *J* = 9.1 Hz, 1H), 5.27 (d, *J* = 9.2 Hz, 1H), 4.97 (d, *J* = 9.2 Hz, 1H), 3.93 (s, 3H), 3.87 (ddd, *J* = 12.3, 9.2, 3.3 Hz, 1H), 3.30 (dd, *J* = 12.1, 12.1 Hz, 1H), 3.16 – 3.06 (m, 1H), 3.04 – 2.80 (m, 3H), 2.79 – 2.69 (m, 1H), 1.72 (s, 2H), 1.43 (s, 9H), 1.09 (s, 9H). ^{13}C NMR (101 MHz, CDCl₃) δ 172.6, 172.3, 161.3, 160.8, 156.4, 155.3, 153.2, 144.2, 142.5, 142.2, 134.3, 134.2, 131.6, 129.3, 125.2, 125.0, 80.4, 60.9, 58.7, 56.7, 52.4, 38.4, 34.7, 33.4, 31.3, 28.4, 26.6. HRMS (m/z): $C_{31}H_{38}N_5O_8$ [M+H]⁺ found: 608.2712. Calculated: 608.2720. [α]$_D^{20}$ -55 (c 1.0, CHCl₃).

34

Methyl 2-[(1*R*,6*S*,9*S*)-6-*tert*-butyl-1-carbamoyl-9-[(2*S*)-2-hydroxy-3-methylbutanamido]-8-oxo-19-oxa-4,7-diazatetracyclo[9.5.2.1²,⁵.0¹⁴,¹⁷]nonadeca-2,4,11,13,17-pentaen-3-yl]-1,3-oxazole-4-carboxylate (DZA-147). Compound was prepared according to General procedure C from macrocycle **25** (50 mg; 0.082 mmol), TFA (63 μL; 82 mmol; 10 equiv.) in DCM (1 mL) in 1 h and *S*-H*i*VA (15 mg; 0.12 mmol; 1.5 equiv.), EDC×HCl (32 mg; 0.17 mmol; 2 equiv.), HOBt (34 mg; 0.25 mmol; 3 equiv.), DIPEA (72 μL; 0.41 mmol; 5 equiv.) in DMF (1 mL) in 1 h. Product **DZA-147** was purified by reverse phase flash chromatography (10% to 50% MeCN in 0.01% TFA in water) to afford 32 mg (64%) as a white amorphous solid.

^{1}H NMR (400 MHz, MeOD) δ 8.64 (s, 1H), 7.29 – 7.13 (m, 3H), 4.87 – 4.82 (m, 1H), 4.52 (dd, J = 11.8, 3.6 Hz, 1H), 3.92 (s, 3H), 3.86 (d, J = 3.8 Hz, 1H), 3.26 – 3.13 (m, 3H), 2.84 (dd, J = 12.4, 3.7 Hz, 1H), 2.82 – 2.67 (m, 2H), 2.09 (sept d, J = 6.9, 3.8 Hz, 1H), 1.06 (s, 9H), 1.01 (d, J = 6.9 Hz, 3H), 0.90 (d, J = 6.9 Hz, 3H). ^{13}C NMR (101 MHz, MeOD) δ 175.7, 175.5, 174.3, 162.8, 162.7, 157.7, 155.3, 146.2, 145.2, 143.6, 135.5, 135.1, 130.8, 130.6, 126.6, 125.9, 76.8, 62.2, 58.9, 56.6, 52.6, 39.6, 36.4, 34.4, 33.2, 32.5, 26.8, 19.5, 16.3. HRMS (m/z): $C_{31}H_{38}N_5O_8$ $[M+H]^+$ found: 608.2711. Calculated: 608.2720. $[\alpha]_D^{20}$ -60 (c 1.0, MeOH).

Methyl 2-[(1S,6S,9S)-1-(aminomethyl)-6-tert-butyl-9-[(2S)-2-hydroxy-3-methylbutanamido]-8-oxo-19-oxa-4,7-diazatetracyclo[9.5.2.1²,⁵.0¹⁴,¹⁷]nonadeca-2,4,11,13,17-pentaen-3-yl]-1,3-oxazole-4-carboxylate (DZA-154). Anhydrous InCl$_3$ (30 mg; 0.14 mmol, 1 equiv.) and NaBH$_4$ (15 mg; 0.41 mmol; 3 equiv.) were suspended in dry THF (1) at room temperature under argon atmosphere. The green suspension was stirred for 1 h at room temperature, then macrocycle **DZA-129** (80 mg; 0.14 mmol; 1 equiv.) was added in one portion. The resulting suspension was stirred for another 2 h at the same temperature. Then the reaction mixture was quenched by the addition of aqueous 1N HCl, then NH$_4$OH was added dropwise until the mixture reached basic pH. The resulting mixture was extracted with EtOAc, organic layer was washed witn brine, dried (Na$_2$SO$_4$) and evaporated. The residue was purified with reverse phase flash chromatography (from 10% to 40% MeCN in aqueous 0,1% TFA) to give amine **DZA-154** (40 mg; 50%) as a white amorphous solid.

^{1}H NMR (400 MHz, MeOD) δ 8.73 (s, 1H), 8.44 (d, J = 8.2 Hz, 1H), 7.31 – 7.23 (m, 2H), 7.04 (d, J = 1.4 Hz, 1H), 4.89 – 4.82 (m, 1H), 4.48 (dd, J = 11.7, 3.7 Hz, 1H), 4.09 (d, J = 13.3 Hz, 1H), 3.96 (s, 3H), 3.91 (d, J = 13.3 Hz, 1H), 3.87 (d, J = 3.7 Hz, 1H), 3.25 – 3.08 (m, 2H), 2.91 – 2.81 (m, 2H), 2.81 – 2.72 (m, 1H), 2.58 – 2.47 (m, 1H), 2.09 (sept d, J = 6.8, 3.7 Hz, 1H), 1.06 (s, 9H), 1.01 (d, J = 6.8 Hz, 3H), 0.89 (d, J = 6.8 Hz, 3H). ^{13}C NMR (101 MHz, MeOD) δ 175.8, 174.2, 163.8, 163.2, 157.5, 154.2, 146.6, 144.8, 143.5, 136.0, 134.9, 131.2, 129.9, 127.0, 126.6, 76.8, 58.8, 56.5, 54.5,

52.9, 45.0, 39.5, 36.0, 34.2, 33.2, 31.3, 26.7, 19.5, 16.3. HRMS (m/z): $C_{31}H_{40}N_5O_7$ $[M+H]^+$ found: 594.2935. Calculated: 594.2928. $[\alpha]_D^{20}$ -142 (c 1.0, MeOH).

The synthesis of diazonamide A analogs DZA-137 and DZA-142 is shown in Scheme 7.

Accordingly, analog **DZA-137** was prepared in three steps from macrocycle **6**. Methyl ester was reduced with LiBH4 in TFE/THF and then after *N*-Boc cleavage, crude amine was coupled with (*S*)-2-hydroxy-3-methylbutanoic acid (*S*-H*i*VA; **7**) to give analog **DZA-137**. Nitrile moiety containing analog **DZA-142** was prepared from ester **6**. Methyl ester first was converted into amide in the presence of NH3 and then resulting amide was treated with TFAA and pyridine to give nitrile **27**. NBoc cleavage and following amide coupling with *S*-H*i*VA **7** gave analog **DZA-142** (Scheme 7).
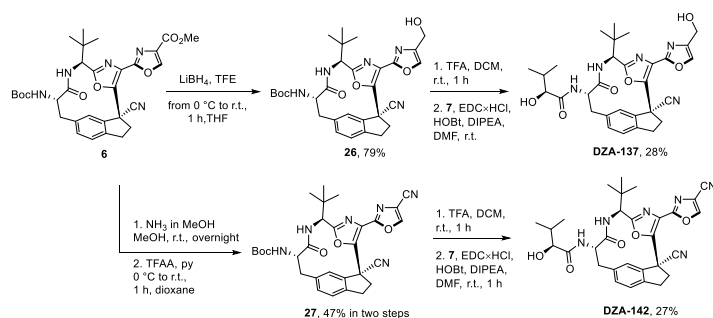
Scheme 7. Synthesis of diazonamide A analogs **DZA-137** and **DZA-142**.

***tert*-Butyl *N*-[(1*S*,6*S*,9*S*)-6-*tert*-butyl-1-cyano-3-[4-(hydroxymethyl)-1,3-oxazol-2-yl]-8-oxo-19-oxa-4,7-diazatetracyclo[9.5.2.1²,⁵.0¹⁴,¹⁷]nonadeca-2,4,11,13,17-pentaen-9-yl]carbamate (26).** To a solution of ester **6** (120 mg; 0.20 mmol) in dry THF (1 mL) TFE (146 µL, 2.04 mmol, 10 equiv.) was added and flask was cooled to 0°C. Then LiBH4 (22 mg; 1.02 mmol; 5 equiv.) was added in one portion and resulting suspension was stirred for 1 h at 0°C, then gradually warmed to room temperature and stirred for 2 h. The reaction mixture was quenched by the addition of aqueous 1N HCl and extracted with EtOAc (×2). Organic layers were combined, dried (Na2SO4), evaporated. The off-white amorphous solid was purified with reverse flash column chromatography (10% to 70% MeCN in 0.01% TFA in water) to give alcohol **26** (90 mg; 79%) as a white amorphous solid.

¹H NMR (400 MHz, MeOD) δ 7.99 (t, *J* = 1.1 Hz, 1H), 7.35 – 7.27 (m, 1H), 7.01 (s, 1H), 4.75 (s, 1H), 4.63 (d, *J* = 1.1 Hz, 2H), 4.13 (dd, *J* = 11.9, 3.6 Hz, 1H), 3.28 – 3.21 (m, 1H), 3.18 – 3.04 (m, 2H), 2.99 – 2.89 (m, 2H), 2.85 (dd, *J* = 12.4, 3.6 Hz, 1H), 1.44 (s, 9H), 1.03 (s, 9H). ¹³C NMR (101 MHz, MeOD) δ 174.8, 164.2, 157.2, 155.7, 149.3, 144.0, 142.6, 142.4, 138.0, 137.2, 131.8, 129.7,

36

128.4, 126.5, 119.6, 80.6, 59.5, 58.1, 57.3, 47.7, 39.2, 38.8, 34.3, 31.7, 28.7, 26.8. HRMS (m/z): $C_{30}H_{36}N_5O_6$ [M+H]$^+$ found: 562.2677. Calculated: 562.2666. [α]$_D^{20}$ -139 (c 1.0, MeOH).

(2*S*)-*N*-[(1*S*,6*S*,9*S*)-6-*tert*-Butyl-1-cyano-3-[4-(hydroxymethyl)-1,3-oxazol-2-yl]-8-oxo-19-oxa-4,7-diazatetracyclo[9.5.2.1²,⁵.0¹⁴,¹⁷]nonadeca-2,4,11,13,17-pentaen-9-yl]-2-hydroxy-3-methylbutanamide (DZA-137). Compound was prepared according to General procedure C from macrocycle **26** (90 mg; 0.16 mmol), TFA (123 μL; 1.60 mmol; 10 equiv.) in DCM (1 mL) in 1 h and *S*-H*i*VA (29 mg; 0.24 mmol; 1.5 equiv.), EDC×HCl (62 mg; 0.32 mmol; 2 equiv.), HOBt (65 mg; 0.48 mmol; 3 equiv.), DIPEA (139 μL; 0.80 mmol; 5 equiv.) in DMF (2 mL) in 1 h. Product **DZA-137** was purified by reverse phase flash chromatography (10% to 50% MeCN in 0.01% TFA in water) to afford 25 mg (28%) as a white amorphous solid.

^{1}H NMR (400 MHz, MeOD) δ 7.99 (t, *J* = 1.1 Hz, 1H), 7.41 – 7.27 (m, 2H), 6.99 (s, 1H), 4.73 (s, 1H), 4.63 (d, *J* = 1.1 Hz, 2H), 4.55 (dd, *J* = 11.8, 3.8 Hz, 1H), 3.86 (d, *J* = 3.8 Hz, 1H), 3.27 – 3.04 (m, 3H), 3.01 – 2.81 (m, 3H), 2.09 (sept d, *J* = 6.9, 3.8 Hz, 1H), 1.01 (s, 9H), 1.00 (d, *J* = 6.9 Hz, 3H), 0.89 (d, *J* = 6.9 Hz, 3H). ^{13}C NMR (101 MHz, MeOD) δ 175.8, 173.9, 164.1, 155.7, 149.4, 144.0, 142.8, 142.6, 138.1, 136.8, 131.8, 129.7, 128.5, 126.6, 119.6, 76.8, 59.6, 57.3, 56.3, 47.7, 39.3, 39.2, 34.3, 33.2, 31.7, 26.8, 19.5, 16.3. HRMS (m/z): $C_{30}H_{36}N_5O_6$ [M+H]$^+$ found: 562.2675. Calculated: 562.2666. [α]$_D^{20}$ -142 (c 1.0, MeOH).

***tert*-Butyl *N*-[(1*S*,6*S*,9*S*)-6-*tert*-butyl-1-cyano-3-(4-cyano-1,3-oxazol-2-yl)-8-oxo-19-oxa-4,7-diazatetracyclo[9.5.2.1²,⁵.0¹⁴,¹⁷]nonadeca-2,4,11,13,17-pentaen-9-yl]carbamate (27).** To a solution of ester **6** (250 mg; 0.42 mmol) in dry MeOH (2 mL) NH$_3$ (7M in MeOH; 1.82 mL; 12.72 mmol, 30 equiv.) was added dropwise at room temperature. The yellowish solution was stirred for 18 h, then evaporated. Crude amide (220 mg; 90%) was used in the next step without additional purification. To a crude amide (150 mg; 0.26 mmol) in dry dioxane (1 mL) was added pyridine (106 μL; 1.31 mmol, 5 equiv.) and the resulting solution was cooled to 0˚C. Then TFAA (109 μL; 0.78 mmol; 3 equiv.) was added dropwise and the flask was warmed to room temperature gradually. Solution became red after 1 h of stirring. Then the red solution was quenched by the addition of aqueous saturated NH$_4$Cl and extracted with EtOAc (×2). Organic layers were combined, washed with brine, dried (Na$_2$SO$_4$), evaporated. The resulting red amorphous material was purified with reverse phase column chromatography (10% to 70% MeCN in 0.01% TFA in water) to give nitrile **27** (75 mg; 52%) as a white amorphous solid.

^{1}H NMR (400 MHz, CDCl$_3$) δ 8.31 (s, 1H), 7.26 (s, 2H), 7.11 (s, 1H), 5.82 (d, *J* = 7.5 Hz, 1H), 5.26 (d, *J* = 9.2 Hz, 1H), 4.76 (d, *J* = 7.5 Hz, 1H), 3.92 (ddd, *J* = 12.3, 9.2, 3.4 Hz, 1H), 3.35 – 3.12 (m,

37

3H), 3.01 – 2.91 (m, 1H), 2.91 – 2.77 (m, 2H), 1.43 (s, 9H), 1.00 (s, 9H). ^{13}C NMR (101 MHz, CDCl$_3$) δ 171.9, 162.1, 155.6, 155.4, 149.8, 146.6, 141.4, 140.4, 135.6, 130.4, 129.5, 126.4, 125.6, 118.0, 116.7, 111.5, 80.6, 58.2, 58.1, 46.4, 38.5, 37.8, 33.6, 31.1, 28.4, 26.6. HRMS (m/z): C$_{30}$H$_{32}$N$_6$O$_5$Na [M+Na]$^+$ found: 579.2327. Calculated: 579.2332. [α]$_D^{20}$ -152 (c 1.0, CHCl$_3$).

(2S)-N-[(1S,6S,9S)-6-*tert*-Butyl-1-cyano-3-(4-cyano-1,3-oxazol-2-yl)-8-oxo-19-oxa-4,7-diazatetracyclo[9.5.2.1^{2,5}.0^{14,17}]nonadeca-2,4,11,13,17-pentaen-9-yl]-2-hydroxy-3-methylbutanamide (DZA-142). Compound was prepared according to General procedure C from macrocycle **27** (70 mg; 0.13 mmol), TFA (97 μL; 1.26 mmol; 10 equiv.) in DCM (0.5 mL) in 1 h and S-H*i*VA (19 mg; 0.16 mmol; 1.5 equiv.), EDC×HCl (41 mg; 0.22 mmol; 2 equiv.), HOBt (44 mg; 0.32 mmol; 3 equiv.), DIPEA (93 μL; 0.54 mmol; 5 equiv.) in DMF (1 mL) in 1 h. Product **DZA-142** was purified by reverse phase flash chromatography (10% to 50% MeCN in 0.01% TFA in water) to afford 16 mg (27%) as a white amorphous solid.

^{1}H NMR (400 MHz, MeOD) δ 8.90 (s, 1H), 7.42 – 7.26 (m, 2H), 6.98 (s, 1H), 4.71 (s, 1H), 4.56 (dd, J = 11.8, 3.8 Hz, 1H), 3.86 (d, J = 3.8 Hz, 1H), 3.35 – 3.26 (m, 1H), 3.23 – 3.10 (m, 2H), 3.04 – 2.95 (m, 1H), 2.94 – 2.86 (m, 2H), 2.08 (sept d, J = 6.9, 3.8 Hz, 1H), 1.00 (s, 9H), 1.00 (d, J = 6.8 Hz, 3H), 0.90 (d, J = 6.8 Hz, 3H). ^{13}C NMR (101 MHz, MeOD) δ 175.8, 173.9, 164.3, 156.8, 151.3, 149.8, 142.9, 142.1, 136.8, 131.9, 129.8, 127.2, 126.6, 119.3, 117.0, 112.5, 76.8, 59.8, 56.3, 47.8, 39.3, 39.1, 34.4, 33.2, 31.8, 26.7, 19.5, 16.3. HRMS (m/z): C$_{30}$H$_{33}$N$_6$O$_5$ [M+H]$^+$ found: 557.2521. Calculated: 557.2512. [α]$_D^{20}$ -153 (c 1.0, MeOH).

The synthesis of diazonamide A analogs DZA-166, DZA-174 and DZA-175 is shown in Scheme 8.

The synthesis of fluorinated analogs is depicted in Scheme 8. Mono-fluorinated analog **DZA-166** was obtained from corresponding alcohol **26**. Alcohol was treated with MsCl under basic conditions to give mesylate, which was subjected to S$_N$2-type reaction in the presence of TBAF. Fluorinated macrocycle **28** was then subjected into *N*-Boc deprotection followed by amide bond formation with S-H*i*VA **7** to give analog **DZA-166**. Di-fluorinated analog **DZA-174** was obtained from alcohol **26**. Alcohol was oxidized to aldehyde with DMP and then treated with DAST reagent to furnish di-fluoride **29**. After *N*-Boc cleavage with TFA the resulting amine was coupled with (*S*)-2-hydroxy-3-methylbutanoic acid (S-H*i*VA; **7**) to give analog **DZA-174**. Tri-fluorinated analog **DZA-175** was obtained starting from ester **3**. Ester **3** was hydrolyzed with LiOH×H$_2$O to produce carboxylic acid, which was coupled with corresponding amine **30** to give amide **31**. Amide **31** was then subjected into macrocyclization under basic conditions to give macrocycle **32** with diastereomeric ratio 99:1. Methyl ester of **32** was then hydrolyzed and coupled with 2-amino-3,3,3-trifluoropropan-1-ol to give amide

38

33. Primary alcohol of **33** was oxidized to aldehyde and after futher oxazole cyclization reaction in the presence of PPh$_3$ and 1,2-dibromotetrachloroethane under basic conditions was converted into tri-fluorinated bioxazole **34**. After *N*-Boc cleavage with TFA the resulting amine was coupled with (*S*)-2-hydroxy-3-methylbutanoic acid (*S*-H*i*VA; **7**) to give analog **DZA-175** (Scheme 8).

Scheme 8. Synthesis of diazonamide A analogs **DZA-166**, **DZA-174** and **DZA-175**.

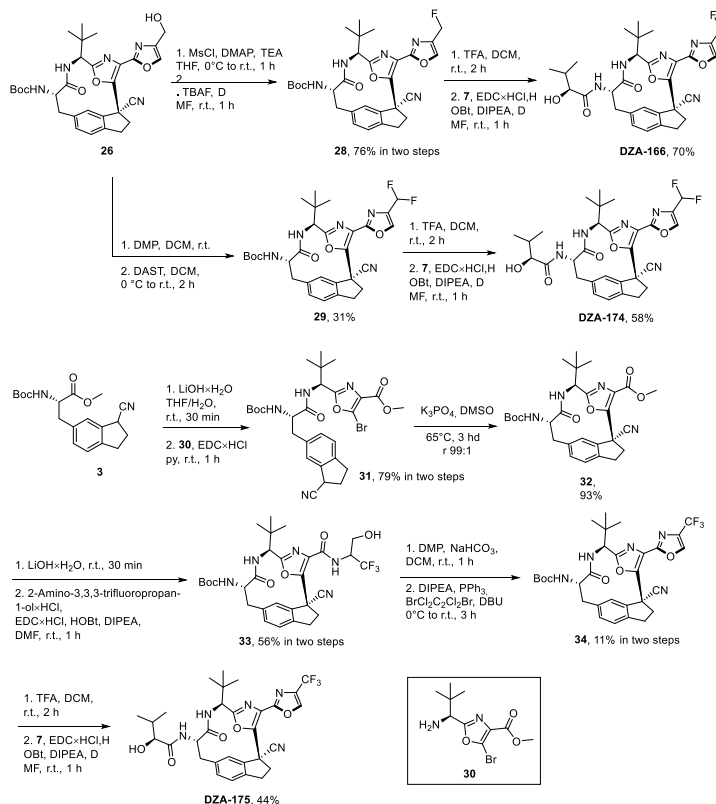***tert*-Butyl *N*-[(1*S*,6*S*,9*S*)-6-*tert*-butyl-1-cyano-3-[4-(fluoromethyl)-1,3-oxazol-2-yl]-8-oxo-19-oxa-4,7-diazatetracyclo[9.5.2.1²,⁵.0¹⁴,¹⁷]nonadeca-2,4,11,13,17-pentaen-9-yl]carbamate (28).** To alcohol **26** (178 mg; 0.32 mmol) in dry THF (1 mL) TEA (88 µL; 0.63 mmol; 2 equiv.) was added followed by DMAP (1 mg; 0.01 mmol; 0.03 equiv.). Then flask was cooled to 0°C and MsCl (37 µL; 0.48 mmol; 1.5 equiv.) was added dropwise. The orange solution was warmed to room temperature and stirred for 1 h. Then the solution was diluted with EtOAc and washed with 1N HCl (×2). The

39

organic layer was washed with brine, dried (Na$_2$SO$_4$) and evaporated. The resulting yellow oil was used in the next step without additional purification. To a crude mesylate (203 mg; 0.32 mmol) in dry THF (1 mL) TBAF (1M in THF; 3.17 mL; 3.17 mmol; 10 equiv.) was added dropwise at room temperature. The resulting yellow solution was stirred for 2 h. Then the solution was diluted with EtOAc and washed with aqueous saturated NH$_4$Cl (×2). Organic layers were washed with brine, dried (Na$_2$SO$_4$) and evaporated. The yellow oil was purified with reverse phase flash chromatograhy (10% to 70% MeCN in 0.01% TFA in water) to give fluoride **28** (135 mg; 76%) as a white amorphous solid.

^{1}H NMR (400 MHz, CDCl$_3$) δ 7.88 (d, J = 4.3 Hz, 1H), 7.25 – 7.20 (m, 2H), 7.11 (s, 1H), 5.78 (d, J = 7.8 Hz, 1H), 5.51 – 5.43 (m, 1H), 5.39 – 5.32 (m, 1H), 5.27 (d, J = 9.2 Hz, 1H), 4.77 (d, J = 7.8 Hz, 1H), 3.92 (ddd, J = 12.4, 9.2, 3.4 Hz, 1H), 3.33 – 3.21 (m, 2H), 3.21 – 3.12 (m, 1H), 3.01 – 2.90 (m, 1H), 2.90 – 2.79 (m, 2H), 1.43 (s, 9H), 1.00 (s, 9H). ^{13}C NMR (101 MHz, CDCl$_3$) δ 171.9, 161.8, 155.3, 154.9, 148.1, 141.4, 140.9, 138.1, 138.0 (d, J = 19.7 Hz), 135.5, 130.2, 129.5, 127.7, 125.5, 118.3, 80.5, 76.4 (d, J = 165.2 Hz), 58.3, 58.0, 46.4, 38.7, 37.9, 33.5, 31.1, 28.4, 26.6. HRMS (m/z): C$_{30}$H$_{34}$N$_5$O$_5$FNa [M+Na]$^+$ found: 586.2439. Calculated: 586.2442. [α]$_D^{20}$ -126 (c 1.0, MeCN).

(2S)-N-[(1S,6S,9S)-6-tert-Butyl-1-cyano-3-[4-(fluoromethyl)-1,3-oxazol-2-yl]-8-oxo-19-oxa-4,7-diazatetracyclo[9.5.2.1^{2,5}.0^{14,17}]nonadeca-2,4,11,13,17-pentaen-9-yl]-2-hydroxy-3-methylbutanamide (DZA-166). Compound was prepared according to General procedure C from macrocycle **28** (100 mg; 0.16 mmol), TFA (122 μL; 1.59 mmol; 10 equiv.) in DCM (1 mL) in 1 h and S-HiVA (28 mg; 0.24 mmol; 1.5 equiv.), EDC×HCl (61 mg; 0.32 mmol; 2 equiv.), HOBt (64 mg; 0.48 mmol; 3 equiv.), DIPEA (137 μL; 0.79 mmol; 5 equiv.) in DMF (2 mL) in 1 h. Product **DZA-166** was purified by reverse phase flash chromatography (10% to 50% MeCN in 0.01% TFA in water) to afford 70 mg (70%) as a white amorphous solid.

^{1}H NMR (400 MHz, MeOD) δ 8.35 (d, J = 7.6 Hz, 1H), 8.24 (d, J = 4.9 Hz, 1H), 7.40 – 7.26 (m, 2H), 6.98 (s, 1H), 5.45 (s, 1H), 5.33 (s, 1H), 4.76 – 4.69 (m, 1H), 4.55 (dd, J = 11.8, 3.8 Hz, 1H), 3.86 (d, J = 3.8 Hz, 1H), 3.28 – 3.06 (m, 3H), 3.02 – 2.82 (m, 3H), 2.09 (septd, J = 6.8, 3.8 Hz, 1H), 1.01 (s, 9H), 1.00 (d, J = 6.8 Hz, 3H), 0.89 (d, J = 6.8 Hz, 3H). ^{13}C NMR (101 MHz, MeOD) δ 175.8, 174.0, 164.2, 156.1, 149.9, 142.8, 142.5, 140.7 (d, J = 8.2 Hz), 139.2 (d, J = 19.7 Hz), 136.8, 131.8, 129.7, 128.2, 126.6, 119.5, 77.4, 76.6 (d, J = 163.7 Hz), 59.8, 56.3, 47.7, 39.3, 39.2, 34.4, 33.2, 31.8, 26.8, 19.5, 16.3. HRMS (m/z): C$_{30}$H$_{35}$N$_5$O$_5$F [M+H]$^+$ found: 564.2625. Calculated: 564.2622. [α]$_D^{20}$ -155 (c 1.0, MeOH).

***tert*-Butyl N-[(1S,6S,9S)-6-*tert*-butyl-1-cyano-3-[4-(difluoromethyl)-1,3-oxazol-2-yl]-8-oxo-19-oxa-4,7-diazatetracyclo[9.5.2.1^{2,5}.0^{14,17}]nonadeca-2,4,11,13,17-pentaen-9-yl]carbamate (29).** To

40

a solution of alcohol **26** (476 mg; 0.85 mmol) in dry DCM (5 mL) DMP (395 mg; 0.93 mmol, 1.1 equiv.) was added in one portion. The resulting suspension was stirred at room temperature for 1 h. Then the suspension was diluted with EtOAc and washed with aqueous 1M $Na_2S_2O_3$ and aqueous saturated $NaHCO_3$. Organic layer was washed with brine, dried (Na_2SO_4), evaporated. The crude aldehyde was used in the next step without additional purification. To a crude aldehyde (474 mg; 0.85 mmol) in dry DCM (2 mL) DAST (491 µL; 3.81 mmol; 4.5 equiv.) was added after the flask was cooled to -78˚C in dry ice-acetone bath. The resulting solution was stirred for 30 minutes at the same temprature and then warmed to room temperature and stirred for 2 h. Then the solution was diluted with EtOAc and washed with aqueous saturated $NaHCO_3$ (×2). The organic layer was washed with brine, dried (Na_2SO_4), evaporated. The resulting yellow amorphous material was purified with column chromatography (30% to 50% EtOAc in hexanes) to give difluoride **29** (154 mg; 31%) as a white amorphous material.

^{1}H NMR (400 MHz, MeOD) δ 8.42 (t, J = 2.5 Hz, 1H), 7.38 – 7.25 (m, 2H), 7.02 (s, 1H), 6.89 (s, J = 54 Hz, 1H), 4.79 – 4.71 (m, 1H), 4.14 (dd, J = 11.9, 3.7 Hz, 1H), 3.29 – 3.19 (m, 1H), 3.19 – 3.03 (m, 2H), 3.01 – 2.80 (m, 3H), 1.44 (s, 9H), 1.03 (s, 9H). ^{13}C NMR (101 MHz, MeOD) δ 174.8, 164.4, 157.2, 156.6, 150.2, 142.6, 142.2, 140.5 (t, J = 6.7 Hz), 138.3 (t, J = 27.8 Hz), 137.3, 131.9, 129.7, 127.8, 126.5, 119.5, 111.2 (t, J = 234.1 Hz), 80.6, 59.5, 58.1, 47.7, 39.1, 38.8, 34.3, 31.7, 28.7, 26.8. HRMS (m/z): $C_{30}H_{33}N_5O_5F_2Na$ [M+Na]$^+$ found: 604.2371. Calculated: 604.2347. [α]$_D^{20}$ -127 (c 1.0, MeOH).

(2*S*)-*N*-[(1*S*,6*S*,9*S*)-6-*tert*-butyl-1-cyano-3-[4-(difluoromethyl)-1,3-oxazol-2-yl]-8-oxo-19-oxa-4,7-diazatetracyclo[9.5.2.1²,⁵.0¹⁴,¹⁷]nonadeca-2,4,11,13,17-pentaen-9-yl]-2-hydroxy-3-methylbutanamide (DZA-174). Compound was prepared according to General procedure C from macrocycle **29** (120 mg; 0.21 mmol), TFA (158 µL; 2.06 mmol; 10 equiv.) in DCM (1 mL) in 2 h and *S*-H*i*VA (37 mg; 0.31 mmol; 1.5 equiv.), EDC×HCl (119 mg; 0.62 mmol; 3 equiv.), HOBt (84 mg; 0.62 mmol; 3 equiv.), DIPEA (179 µL; 1.03 mmol; 5 equiv.) in DMF (2 mL) in 1 h. Product **DZA-174** was purified by reverse phase flash chromatography (10% to 50% MeCN in 0.01% TFA in water) to afford 70 mg (58%) as a white amorphous solid.

^{1}H NMR (400 MHz, MeOD) δ 8.42 (t, J = 2.5 Hz, 1H), 8.35 (d, J = 7.6 Hz, 1H), 7.38 – 7.30 (m, 2H), 7.00 (s, 1H), 6.90 (t, J = 54.2 Hz, 1H), 4.76 – 4.70 (m, 1H), 4.55 (dd, J = 11.8, 3.8 Hz, 1H), 3.86 (d, J = 3.8 Hz, 1H), 3.29 – 3.07 (m, 3H), 3.01 – 2.86 (m, 3H), 2.09 (septd, J = 6.9, 3.8 Hz, 1H), 1.01 (s, 9H), 1.00 (d, J = 6.8 Hz, 3H), 0.89 (d, J = 6.8 Hz, 3H). ^{13}C NMR (101 MHz, MeOD) δ 175.8, 174.0, 164.2, 156.6, 150.3, 142.8, 142.4, 140.5 (t, J = 6.7 Hz), 138.3 (t, J = 27.8 Hz), 136.8, 131.9, 129.7, 127.9, 126.6, 119.4, 111.2 (t, J = 234 Hz), 76.83, 59.73, 56.31, 47.73, 39.22, 39.16, 34.36, 33.17,

41

31.75, 26.75, 19.53, 16.34. HRMS (m/z): $C_{30}H_{34}N_5O_5F_2$ [M+H]$^+$ found: 582.2537. Calculated: 582.2528. $[\alpha]_D^{20}$ -163 (c 1.0, MeOH).

Methyl 5-bromo-2-[(1*S*)-1-[(2*S*)-2-{[(*tert*-butoxy)carbonyl]amino}-3-(3-cyano-2,3-dihydro-1*H*-inden-5-yl)propanamido]-2,2-dimethylpropyl]-1,3-oxazole-4-carboxylate (31). Compound was prepared according to General procedure A from ester **3** (460 mg; 1.34 mmol), LiOH×H$_2$O (280 mg; 6.68 mmol; 5 equiv.) in THF/water (1:1 v/v; 10 mL) and amine **30** (389 mg; 1.34 mmol; 1 equiv.), EDC×HCl (384 mg; 2.00 mmol; 1.5 equiv.) in pyridine (4 mL) in 1 h. Product **31** was purified by direct phase flash chromatography (from 20% to 70% EtOAc in hexanes) to afford 476 mg (59%) of a 1:1 mixture of diastereomers as a white solid.

^{1}H NMR (400 MHz, CDCl$_3$) δ 7.24 (s, 0.5H), 7.23 (s, 0.5H), 7.15 – 7.04 (m, 2H), 6.75 (d, *J* = 8.2 Hz, 0.5H), 6.68 (d, *J* = 8.2 Hz, 0.5H), 5.06 – 4.97 (m, 2H), 4.33 – 4.24 (m, 1H), 4.10 – 3.98 (m, 1H), 3.93 (s, 1.5H), 3.92 (s, 1.5H), 3.12 – 2.95 (m, 3H), 2.93 – 2.80 (m, 1H), 2.58 – 2.48 (m, 1H), 2.38 – 2.27 (m, 1H), 1.42 (s, 9H), 0.94 (s, 4.5H), 0.93 (s, 4.5H). ^{13}C NMR (101 MHz, CDCl$_3$) δ 170.99, 170.97, 164.02, 163.99, 160.9, 155.6, 141.7, 138.2, 136.1, 136.0, 130.49, 130.47, 129.8, 129.6, 128.3, 125.4, 125.2, 125.1, 121.1, 121.0, 80.6, 56.1, 55.8, 55.7, 52.54, 52.51, 37.2, 35.9, 35.8, 34.5, 31.4, 31.17, 31.15, 28.4, 26.3. HRMS (m/z): $C_{28}H_{35}N_4O_6BrNa$ [M+Na]$^+$ found: 625.1649. Calculated: 625.1638.

Methyl (1*S*,6*S*,9*S*)-9-{[(*tert*-butoxy)carbonyl]amino}-6-*tert*-butyl-1-cyano-8-oxo-19-oxa-4,7-diazatetracyclo[9.5.2.1^{2,5}.0^{14,17}]nonadeca-2,4,11,13,17-pentaene-3-carboxylate (32). Compound was prepared according to General procedure B from amide **31** (476 mg; 0.79 mmol) and K$_3$PO$_4$ (837 mg; 3.94 mmol; 5 equiv.) in DMSO (15 mL) in 5 h. Product **32** was purified by reverse phase flash chromatography (from 10% to 70% MeCN in 0,01% TFA in water) to afford 385 mg (93%; dr 99:1) of a single diastereomer as a white amorphous solid.

^{1}H NMR (400 MHz, CDCl$_3$) δ 7.26 – 7.22 (m, 2H), 7.06 (s, 1H), 5.70 (d, *J* = 7.3 Hz, 1H), 5.23 (d, *J* = 9.2 Hz, 1H), 4.67 (d, *J* = 7.3 Hz, 1H), 4.01 (s, 3H), 3.93 (ddd, *J* = 12.1, 8.1, 3.3 Hz, 1H), 3.35 – 3.25 (m, 1H), 3.21 (dd, *J* = 12.1, 12.1 Hz, 1H), 3.18 – 3.10 (m, 1H), 3.01 – 2.92 (m, 1H), 2.87 (dd, *J* = 12.1, 3.4 Hz, 1H), 2.60 (dt, *J* = 13.5, 8.2 Hz, 1H), 1.42 (s, 9H), 0.96 (s, 9H). ^{13}C NMR (101 MHz, CDCl$_3$) δ 171.8, 161.2, 160.7, 155.3, 153.5, 141.5, 140.5, 135.5, 130.8, 130.2, 129.8, 125.4, 118.3, 80.5, 58.3, 58.2, 52.5, 46.7, 39.1, 37.8, 33.6, 31.1, 28.4, 26.6. HRMS (m/z): $C_{28}H_{34}N_4O_6Na$ [M+Na]$^+$ found: 545.2369. Calculated: 545.2376. $[\alpha]_D^{20}$ -116 (c 1.0, MeOH).

***tert*-Butyl *N*-[(1*S*,6*S*,9*S*)-6-*tert*-butyl-1-cyano-8-oxo-3-[(1,1,1-trifluoro-3-hydroxypropan-2-yl)carbamoyl]-19-oxa-4,7-diazatetracyclo[9.5.2.1^{2,5}.0^{14,17}]nonadeca-2,4,11,13,17-pentaen-9-yl]carbamate (33).** Methyl ester **32** (385 mg; 0.74 mmol) was dissolved in THF (4 mL). Separately solid LiOH×H$_2$O (93 mg; 0.2.21 mmol; 3 equiv.) was dissolved in water (2 mL) and added to the

42

reaction mixture. Emulsion was stirred at room temperature for 30 min, then aqueous 1N HCl was added. The resulting mixture was extracted with EtOAc (×2), combined organic layers were washed with brine, dried (Na_2SO_4) and evaporated. The crude carboxylic acid was used in the next step without additional purification. The off-white amorphous solid was dissolved in anhydrous DMF (5 mL) and 2-amino-3,3,3-trifluoropropan-1-ol hydrochloride (183 mg; 1.11 mmol; 1.5 equiv.), EDC×HCl (212 mg; 1.11 mmol; 1.5 equiv.) and HOBt (199 mg; 1.47 mmol; 2 equiv.) were added followed by DIPEA (382 µL; 2.21 mmol; 3 equiv.). The solution was stirred at room temperature for 1 h. The solution was diluted with aqueous saturated NH_4Cl and EtOAc. The layers were separated and the organic phase was washed with brine, dried (Na_2SO_4) and evaporated. Product **33** was purified by reverse phase flash chromatography (10% to 70% MeCN in 0.01% TFA in water) to afford 257 mg (56%) as a white amorphous solid.

^{1}H NMR (400 MHz, $CDCl_3$) δ 7.54 (d, J = 9.7 Hz, 1H), 7.25 – 7.21 (m, 2H), 7.12 (s, 1H), 5.95 (d, J = 7.7 Hz, 1H), 5.41 (d, J = 9.3 Hz, 1H), 4.96 – 4.77 (m, 1H), 4.66 (d, J = 7.7 Hz, 1H), 4.09 (dd, J = 12.1, 3.9 Hz, 1H), 3.98 – 3.85 (m, 2H), 3.30 – 3.17 (m, 2H), 3.16 – 3.05 (m, 1H), 2.97 – 2.80 (m, 3H), 2.70 (brs, 1H), 1.42 (s, 9H), 0.97 (s, 9H). ^{13}C NMR (101 MHz, $CDCl_3$) δ 172.2, 160.3, 160.2, 155.4, 151.3, 141.6, 140.5, 135.4, 131.8, 130.3, 129.6, 125.6, 124.7 (q, J = 282.5 Hz), 118.4, 80.6, 59.7, 58.3, 57.8, 51.3 (q, J = 29.7 Hz), 46.5, 38.2, 37.8, 33.5, 31.0, 28.4, 26.5. HRMS (m/z): $C_{30}H_{36}N_5O_6F_3Na$ [M+Na]$^+$ found: 642.2545. Calculated: 642.2515.

***tert*-Butyl *N*-[(1*S*,6*S*,9*S*)-6-*tert*-butyl-1-cyano-8-oxo-3-[4-(trifluoromethyl)-1,3-oxazol-2-yl]-19-oxa-4,7-diazatetracyclo[9.5.2.1^2,^{5}.0^{14},^{17}]nonadeca-2,4,11,13,17-pentaen-9-yl]carbamate (34).** To a stirred solution of amide **33** (240 mg; 0.39 mmol) in DCM (3 mL) was added $NaHCO_3$ (65 mg; 0.78 mmol; 2 equiv.) followed by DMP (197 mg; 0.47 mmol). The reaction mixture was stirred at room temperature for 1 h before being quenched with aqueous saurated $NaHCO_3$ (5 mL) and $Na_2S_2O_3$ (5 mL). The mixture was stirred vigorously for 1 h before being extracted with DCM (×2). The combined organic extracts were then dried (Na_2SO_4) and evaporated to afford a crude aldehyde, which was used without further purification. To a stirred solution of the crude aldehyde in DCM (3 mL) at 0 °C was added sequentially DIPEA (268 µL, 1.55 mmol; 4 equiv.), PPh$_3$ (203 mg, 0.78 mmol; 2 equiv.) and $Br_2C_2Cl_4$ (252 mg, 0.78 mmol; 2 equiv.). The reaction mixture was allowed to warm to room temperature and stirred for 1 h before being recooled to 0°C and DBU (231 µL, 1.55 mmol; 4 equiv.) added. The reaction mixture was then stirred for 2 h at room temperature before being quenched with H_2O and extracted with DCM (×2). The combined organic extracts were then dried (Na_2SO_4) and evaporated. The   resulting orange oil was purified with direct phase flash

43

chromatography (10% to 50% EtOAc in hexanes) to give bioxazole **34** (25 mg; 11%) as a white amorphous solid.

^{1}H NMR (400 MHz, CDCl$_3$) δ 8.13 (q, J = 1.4 Hz, 1H), 7.26 – 7.22 (m, 2H), 7.10 (s, 1H), 5.79 (d, J = 7.7 Hz, 1H), 5.25 (d, J = 9.2 Hz, 1H), 4.78 (d, J = 7.7 Hz, 1H), 3.92 (ddd, J = 12.3, 9.1, 3.4 Hz, 1H), 3.34 – 3.12 (m, 3H), 3.02 – 2.91 (m, 1H), 2.90 – 2.78 (m, 2H), 1.43 (s, 9H), 1.00 (s, 9H). HRMS (m/z): C$_{30}$H$_{32}$N$_5$O$_5$F$_3$Na [M+Na]$^+$ found: 622.2245. Calculated: 622.2253.

(2S)-N-[(1S,6S,9S)-6-$tert$-Butyl-1-cyano-8-oxo-3-[4-(trifluoromethyl)-1,3-oxazol-2-yl]-19-oxa-4,7-diazatetracyclo[9.5.2.1^{2},^{5}.0^{14},^{17}]nonadeca-2,4,11,13,17-pentaen-9-yl]-2-hydroxy-3-methylbutanamide (DZA-175). Compound was prepared according to General procedure C from macrocycle **34** (23 mg; 0.038 mmol), TFA (30 μL; 0.38 mmol; 10 equiv.) in DCM (0.5 mL) in 2 h and S-HiVA (7 mg; 0.058 mmol; 1.5 equiv.), EDC×HCl (22 mg; 0.12 mmol; 3 equiv.), HOBt (16 mg; 0.12 mmol; 3 equiv.), DIPEA (33 μL; 0.19 mmol; 5 equiv.) in DMF (0.5 mL) in 1 h. Product **DZA-175** was purified by reverse phase flash chromatography (10% to 50% MeCN in 0.01% TFA in water) to afford 10 mg (44%) as a white amorphous solid.

^{1}H NMR (400 MHz, MeOD) δ 8.70 (q, J = 1.5 Hz, 1H), 8.36 (d, J = 7.5 Hz, 1H), 8.01 (d, J = 8.5 Hz, 1H), 7.39 – 7.31 (m, 2H), 6.99 (s, 1H), 4.73 (d, J = 7.5 Hz, 1H), 4.61 – 4.51 (m, 1H), 3.86 (d, J = 3.8 Hz, 1H), 3.29 – 3.08 (m, 3H), 3.05 – 2.85 (m, 3H), 2.08 (sept d, J = 8.4, 3.8 Hz, 1H), 1.01 (s, 9H), 1.00 (d, J = 6.8 Hz, 3H), 0.90 (d, J = 6.8 Hz, 3H). ^{13}C NMR (101 MHz, MeOD) δ 175.8, 174.0, 164.3, 157.0, 150.9, 142.9, 142.3, 141.8 (q, J = 4.2 Hz), 136.8, 134.3 (q, J = 40.2 Hz), 131.9, 129.8, 127.6, 126.6, 122.0 (q, J = 266.5 Hz), 119.3, 76.8, 59.7, 56.3, 47.8, 39.3, 39.1, 34.4, 33.2, 31.8, 26.8, 19.5, 16.3. HRMS (m/z): C$_{30}$H$_{33}$N$_5$O$_5$F$_3$ [M+H]$^+$ found: 600.2433. Calculated: 600.2434. [α]$_D^{20}$ -141 (c 1.0, MeOH).

The synthesis of diazonamide A analogs DZA-146, DZA-150, DZA-151, DZA-152 and DZA-153 is shown in Scheme 9.

Amide analogs **DZA-151**, **DZA-146** and **DZA-153** and amine analogs **DZA-150** and **DZA-152** have been prepared as follows. Morpholine moiety containing amide was prepared from macrocycle **6**. In the first step methyl ester was hydrolized and then coupled with corresponding morpholine in the presence of EDC hydrochloride, HOBt and DMAP. In the second step the resulting amide 35 was converted into analog **DZA-151** in the two-step transformation. Amines **DZA-150** and **DZA-152** were synthesized from alcohol **26**. After alcohol mesylation reaction followed S$_N$2 process in order to substitute mesylate to corresponding amine under basic conditions. Amine **36** was prepared from

44

dimethylamine and amine **37** was prepared from piperidine. Then after *N*-Boc deprotection and coupling with *S*-H*i*VA **7** analogs **DZA-150** and **DZA-152** were furnished. Amides **DZA-146** and **DZA-153** were prepared from analog **DZA-129** in one-step amynolysis process with corresponding ammonia or dimethyl amine (Scheme 9).
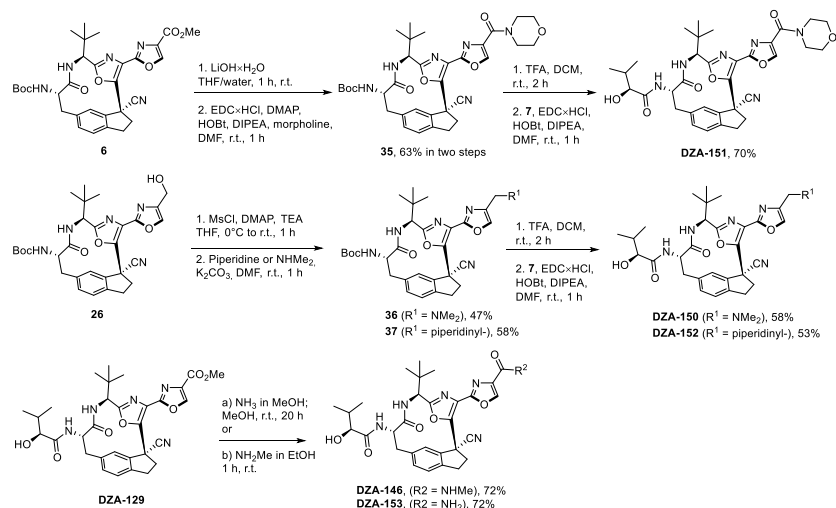
Scheme 9. Synthesis of diazonamide A analogs **DZA-146, DZA-150, DZA-151, DZA-152** and **DZA-153**.

tert-**Butyl** *N*-**[(1*S*,6*S*,9*S*)-6-*tert*-butyl-1-cyano-3-[4-(morpholine-4-carbonyl)-1,3-oxazol-2-yl]-8-oxo-19-oxa-4,7-diazatetracyclo[9.5.2.1²,⁵.0¹⁴,¹⁷]nonadeca-2,4,11,13,17-pentaen-9-yl]carbamate** (**35**). Methyl ester **6** (120 mg; 0.20 mmol) was dissolved in THF (1 mL). Separately solid LiOH×H$_2$O (26 mg; 0.61 mmol; 3 equiv.) was dissolved in water (0.5 mL) and added to the reaction mixture. Emulsion was stirred at room temperature for 30 min, then aqueous 1N HCl was added. The resulting mixture was extracted with EtOAc (×2), combined organic layers were washed with brine, dried (Na$_2$SO$_4$) and evaporated. The crude carboxilyc acid was used in the next step without additional purification. To crude carboxylic acid (117 mg; 0.20 mmol) in DMF (1 mL) EDC×HCl (78 mg; 0.41 mmol; 2 equiv.), HOBt (82 mg; 0.61 mmol; 3 equiv.) and morpholine (88 µL; 1.02 mmol; 5 equiv.) were added at room temperature followed by DIPEA (352 µL; 2.03 mmol; 10 equiv.). The resulting yellow solution was stirred for 20 h at room temperature and then diluted with EtOAc and washed with aqueous saturated NH$_4$Cl, water and brine. Organic layer were dried (Na$_2$SO$_4$) and evaporated. The resulting orange oil was purified with reverse phase flash chromatography (10% to 60% MeCN in 0.01% TFA in water) to give amide **35** (70 mg; 63%) as a white amorphous solid.

45

<superscript>1</superscript>H NMR (400 MHz, CDCl$_3$) δ 8.33 (s, 1H), 7.26 (s, 2H, overlapping with CDCl$_3$), 7.11 (s, 1H), 5.81 (d, J = 7.5 Hz, 1H), 5.23 (d, J = 9.3 Hz, 1H), 4.73 (d, J = 7.4 Hz, 1H), 4.39 – 4.22 (m, 2H), 3.95 (ddd, J = 12.4, 9.3, 3.4 Hz, 1H), 3.85 – 3.71 (m, 6H), 3.36 – 3.19 (m, 2H), 3.09 (ddd, J = 13.1, 8.3, 4.6 Hz, 1H), 2.98 (ddd, J = 15.8, 8.3, 4.6 Hz, 1H), 2.89 (dd, J = 12.4, 3.4 Hz, 1H), 2.80 – 2.71 (m, 1H), 1.43 (s, 9H), 0.99 (s, 9H). ^{13}C NMR (101 MHz, CDCl$_3$) δ 171.9, 161.6, 160.4, 155.4, 153.3, 148.2, 144.4, 141.4, 140.5, 138.3, 135.7, 130.4, 129.8, 127.6, 125.5, 118.5, 80.6, 67.5, 67.0, 58.3, 47.4, 46.4, 43.2, 38.8, 37.9, 33.6, 31.1, 28.4, 26.6. HRMS (m/z): C$_{34}$H$_{41}$N$_6$O$_7$ [M+H]$^+$ found: 645.3036. Calculated: 645.3037. [α]$_D^{20}$ -119 (c 1.0, CHCl$_3$).

(2*S*)-*N*-[(1*S*,6*S*,9*S*)-6-*tert*-butyl-1-cyano-3-[4-(morpholine-4-carbonyl)-1,3-oxazol-2-yl]-8-oxo-19-oxa-4,7-diazatetracyclo[9.5.2.1²,⁵.0¹⁴,¹⁷]nonadeca-2,4,11,13,17-pentaen-9-yl]-2-hydroxy-3-methylbutanamide (DZA-151). Compound was prepared according to General procedure C from macrocycle **35** (60 mg; 0.094 mmol), TFA (72 μL; 0.93 mmol; 10 equiv.) in DCM (0.5 mL) in 1 h and *S*-H*i*VA (17 mg; 0.14 mmol; 1.5 equiv.), EDC×HCl (36 mg; 0.19 mmol; 2 equiv.), HOBt (38 mg; 0.28 mmol; 3 equiv.), DIPEA (81 μL; 0.47 mmol; 5 equiv.) in DMF (1 mL) in 1 h. Product **DZA-151** was purified by reverse phase flash chromatography (10% to 50% MeCN in 0.01% TFA in water) to afford 50 mg (83%) as a white amorphous solid.

^{1}H NMR (400 MHz, MeOD) δ 8.55 (s, 1H), 7.40 – 7.33 (m, 2H), 6.96 (s, 1H), 4.66 (s, 1H), 4.59 (dd, J = 11.8, 3.9 Hz, 1H), 4.26 (s, 2H), 3.83 – 3.72 (m, 6H), 3.36 – 3.26 (m, 1H), 3.18 (dd, J = 12.1, 12.1 Hz, 1H), 3.14 – 3.07 (m, 1H), 3.06 – 2.96 (m, 1H), 2.91 (dd, J = 12.4, 3.9 Hz, 1H), 2.88 – 2.79 (m, 1H), 2.09 (sept d, J = 6.9, 3.9 Hz, 1H), 1.01 (d, J = 6.8 Hz, 3H), 1.00 (s, 9H), 0.90 (d, J = 6.8 Hz, 3H). ^{13}C NMR (101 MHz, MeOD) δ 175.8, 173.9, 164.0, 162.2, 154.9, 150.2, 145.6, 143.0, 142.1, 138.7, 136.8, 131.9, 130.0, 128.1, 126.6, 119.7, 76.8, 68.3, 67.8, 60.0, 56.3, 47.8, 44.3, 39.7, 39.2, 34.4, 33.2, 31.8, 26.8, 19.5, 16.3. HRMS (m/z): C$_{34}$H$_{41}$N$_6$O$_7$ [M+H]$^+$ found: 645.3039. Calculated: 645.3037. [α]$_D^{20}$ -139 (c 1.0, MeOH).

***tert*-Butyl *N*-[(1*S*,6*S*,9*S*)-6-*tert*-butyl-1-cyano-3-{4-[(dimethylamino)methyl]-1,3-oxazol-2-yl}-8-oxo-19-oxa-4,7-diazatetracyclo[9.5.2.1²,⁵.0¹⁴,¹⁷]nonadeca-2,4,11,13,17-pentaen-9-yl]carbamate (36).** To alcohol **26** (265 mg; 0.47 mmol) in dry THF (4 mL) TEA (132 μL; 0.94 mmol; 2 equiv.) was added dropwise followed by DMAP (1 mg; 0.009 mmol; 0.02 equiv.) and the resulting solution was cooled to 0°C in ice bath. Then MsCl (55 μL; 0.71 mmol; 1.5 equiv.) was added dropwise to the solution and the resulting orange solution was stirred at the same temperature for 30 minutes. Then the solution was diluted with EtOAc and washed with 1N HCl, water and brine. Organic layer was dried (Na$_2$SO$_4$) and evaporated. The crude mesylate was used in the next step without additional purification. To crude meslate (145 mg; 0.23 mmol) in dry THF (1 mL) TEA (158 μL; 1.13 mmol; 5

46

equiv.) was added dropwise at room temperature followed by Me$_2$NH×HCl (92 mg; 1.13 mmol; 5 equiv.). The resulting yellow solution was stirred for 20 h, white precipitate was formed. The suspension was diluted with EtOAc and washed with aqueous saturated NH$_4$Cl, water and brine. Organic layer was dried (Na$_2$SO$_4$) and evaporated. The resulting yellow oil was purified with reverse phase flash chromatography (10% to 70% MeCN in 0.01% TFA in water) to give amine **36** (63 mg; 47%) as a white amorphous solid.

^{1}H NMR (400 MHz, MeOD) δ 8.34 (s, 1H), 8.20 (d, *J* = 7.2 Hz, 1H), 7.38 – 7.31 (m, 2H), 6.88 (s, 1H), 4.71 – 4.65 (m, 1H), 4.45 (d, *J* = 19.7 Hz, 1H), 4.41 (d, *J* = 19.7 Hz, 1H), 4.17 (dd, *J* = 11.8, 3.7 Hz, 1H), 3.34 – 3.26 (m, 1H), 3.18 – 3.03 (m, 3H), 3.01 (s, 6H), 2.90 – 2.76 (m, 2H), 1.44 (s, 9H), 1.01 (s, 9H). ^{13}C NMR (101 MHz, MeOD) δ 174.8, 164.5, 157.2, 156.7, 150.5, 142.8, 142.2, 137.3, 133.4, 131.9, 129.7, 128.2, 126.5, 119.7, 80.7, 60.2, 60.1, 58.1, 52.8, 47.8, 43.4, 39.9, 38.7, 34.4, 31.8, 28.7, 26.8. HRMS (m/z): C$_{32}$H$_{41}$N$_6$O$_5$ [M+H]$^+$ found: 589.3149. Calculated: 589.3138. [α]$_D^{20}$ -95 (c 1.0, MeOH).

(2*S*)-*N*-[(1*S*,6*S*,9*S*)-6-*tert*-Butyl-1-cyano-3-{4-[(dimethylamino)methyl]-1,3-oxazol-2-yl}-8-oxo-19-oxa-4,7-diazatetracyclo[9.5.2.1^{2,5}.0^{14,17}]nonadeca-2,4,11,13,17-pentaen-9-yl]-2-hydroxy-3-methylbutanamide (DZA-150). Compound was prepared according to General procedure C from macrocycle **36** (40 mg; 0.068 mmol), TFA (52 µL; 0.68 mmol; 10 equiv.) in DCM (0.5 mL) in 1 h and *S*-H*i*VA (12 mg; 0.10 mmol; 1.5 equiv.), EDC×HCl (26 mg; 0.14 mmol; 2 equiv.), HOBt (27 mg; 0.20 mmol; 3 equiv.), DIPEA (58 µL; 0.34 mmol; 5 equiv.) in DMF (1 mL) in 1 h. Product **DZA-150** was purified by reverse phase flash chromatography (10% to 50% MeCN in 0.01% TFA in water) to afford 23 mg (58%) as a white amorphous solid.

^{1}H NMR (400 MHz, MeOD) δ 8.37 (d, *J* = 7.2 Hz, 1H), 8.34 (s, 1H), 7.40 – 7.34 (m, 2H), 6.86 (m, 1H), 4.68 – 4.64 (m, 1H), 4.58 (dd, *J* = 11.7, 3.9 Hz, 1H), 4.44 (d, *J* = 19.9 Hz, 1H), 4.41 (d, *J* = 19.9 Hz, 1H), 3.87 (d, *J* = 3.8 Hz, 1H), 3.36 – 3.27 (m, 1H, overlapping with MeOD), 3.20 – 3.11 (m, 2H), 3.09 – 3.03 (m, 1H), 3.01 (s, 6H), 2.90 (dd, *J* = 12.4, 3.8 Hz, 1H), 2.84 – 2.75 (m, 1H), 2.09 (sept d, *J* = 6.9, 3.8 Hz, 1H), 1.01 (d, *J* = 6.8 Hz, 3H) 1.00 (s, 9H), 0.89 (d, *J* = 6.8 Hz, 3H). ^{13}C NMR (101 MHz, MeOD) δ 175.8, 174.0, 164.4, 156.6, 150.6, 143.0, 142.8, 142.3, 136.9, 133.4, 131.9, 129.7, 128.3, 126.6, 119.7, 76.8, 60.2, 56.2, 52.8, 47.8, 43.4, 40.0, 39.1, 34.4, 33.2, 31.9, 26.8, 19.5, 16.3. HRMS (m/z): C$_{32}$H$_{41}$N$_6$O$_5$ [M+H]$^+$ found: 589.3143. Calculated: 589.3138. [α]$_D^{20}$ -134 (c 1.0, MeOH).

***tert*-Butyl *N*-[(1*S*,6*S*,9*S*)-6-*tert*-butyl-1-cyano-8-oxo-3-{4-[(piperidin-1-yl)methyl]-1,3-oxazol-2-yl}-19-oxa-4,7-diazatetracyclo[9.5.2.1^{2,5}.0^{14,17}]nonadeca-2,4,11,13,17-pentaen-9-yl]carbamate (37).** To alcohol **26** (70 mg; 0.13 mmol) in dry THF (1 mL) TEA (35 µL; 0.25 mmol; 2 equiv.) was

47

added dropwise followed by DMAP (3 mg; 0.03 mmol; 0.2 equiv.) and the resulting solution was cooled to 0°C in ice bath. Then MsCl (15 μL; 0.19 mmol; 1.5 equiv.) was added dropwise to the solution and the resulting orange solution was stirred at the same temperature for 30 minutes. Then the solution was diluted with EtOAc and washed with 1N HCl, water and brine. Organic layer was dried (Na$_2$SO$_4$) and evaporated. The crude mesylate was used in the next step without additional purification. To crude meslate (80 mg; 0.13 mmol) in dry DMF (1 mL) K$_2$CO$_3$ (86 mg; 0.63 mmol; 5 equiv.) was added in one portion at room temperature followed by piperidine (124 μL; 1.25 mmol; 10 equiv.). The resulting yellow suspesnion was stirred for 1 h. The suspension was diluted with EtOAc and washed with aqueous 1N HCl (×2) and brine. Organic layer was dried (Na$_2$SO$_4$) and evaporated. The resulting yellow oil was purified with reverse phase flash chromatography (10% to 70% MeCN in 0.01% TFA in water) to give amine **37** (40 mg; 51%) as a white amorphous solid.

^{1}H NMR (400 MHz, MeOD) δ 8.33 (s, 1H), 8.20 (d, *J* = 7.1 Hz, 1H), 7.42 – 7.30 (m, 2H), 6.86 (d, *J* = 1.2 Hz, 1H), 4.70 – 4.64 (m, 1H), 4.45 – 4.34 (m, 2H), 4.17 (dd, *J* = 11.9, 3.7 Hz, 1H), 3.76 – 3.69 (m, 1H), 3.66 – 3.60 (m, 1H), 3.33 – 3.26 (m, 1H, overlapping with MeOD), 3.21 – 3.10 (m, 3H), 3.08 – 2.99 (m, 2H), 2.87 (dd, *J* = 12.3, 3.6 Hz, 1H), 2.82 – 2.74 (m, 1H), 2.01 – 1.94 (m, 2H), 1.86 – 1.75 (m, 3H), 1.55 – 1.50 (m, 1H), 1.44 (s, 9H), 1.01 (s, 9H). ^{13}C NMR (101 MHz, MeOD) δ 174.8, 164.5, 157.2, 156.6, 150.4, 142.8, 142.2, 137.3, 133.1, 131.9, 129.8, 128.2, 126.6, 119.8, 80.7, 60.1, 58.1, 54.4, 52.1, 47.8, 40.0, 38.7, 34.4, 31.8, 28.7, 26.8, 24.4, 22.4. HRMS (m/z): C$_{35}$H$_{45}$N$_6$O$_5$ [M+H]$^+$ found: 629.3452. Calculated: 629.3451. [α]$_D^{20}$ -97 (c 1.0, MeOH).

(2*S*)-*N*-[(1*S*,6*S*,9*S*)-6-*tert*-butyl-1-cyano-8-oxo-3-{4-[(piperidin-1-yl)methyl]-1,3-oxazol-2-yl}-19-oxa-4,7-diazatetracyclo[9.5.2.1^{2,}⁵.0^{14,}¹⁷]nonadeca-2,4,11,13,17-pentaen-9-yl]-2-hydroxy-3-methylbutanamide (DZA-152). Compound was prepared according to General procedure C from macrocycle **37** (38 mg; 0.06 mmol), TFA (46 μL; 0.60 mmol; 10 equiv.) in DCM (0.5 mL) in 1 h and *S*-H*i*VA (11 mg; 0.091 mmol; 1.5 equiv.), EDC×HCl (23 mg; 0.12 mmol; 2 equiv.), HOBt (25 mg; 0.18 mmol; 3 equiv.), DIPEA (52 μL; 0.30 mmol; 5 equiv.) in DMF (0.5 mL) in 1 h. Product **DZA-152** was purified by reverse phase flash chromatography (10% to 50% MeCN in 0.01% TFA in water) to afford 20 mg (53%) as a white amorphous solid.

^{1}H NMR (400 MHz, MeOD) δ 8.33 (s, 1H), 7.40 – 7.33 (m, 2H), 6.85 (s, 1H), 4.66 – 4.63 (m, 1H), 4.59 (dd, *J* = 11.8, 3.9 Hz, 1H), 4.41 (d, *J* = 23.3 Hz, 1H), 4.37 (d, *J* = 23.3 Hz, 1H), 3.87 (d, *J* = 3.9 Hz, 1H), 3.73 (d, *J* = 12.3 Hz, 1H), 3.63 (d, *J* = 12.0 Hz, 1H), 3.36 – 3.28 (m, 1H, overlapping with MeOD), 3.22 – 3.11 (m, 3H), 3.10 – 3.00 (m, 2H), 2.90 (dd, *J* = 12.5, 3.9 Hz, 1H), 2.83 – 2.74 (m, 1H), 2.09 (sept d, *J* = 6.9, 3.9 Hz, 1H), 2.01 – 1.93 (m, 2H), 1.86 – 1.72 (m, 3H), 1.59 – 1.47 (m, 1H), 1.01 (d, *J* = 6.8 Hz, 3H), 1.00 (s, 9H), 0.89 (d, *J* = 6.8 Hz, 3H). ^{13}C NMR (101 MHz, MeOD) δ 175.8,

48

174.0, 164.3, 156.5, 150.5, 143.0, 142.8, 142.4, 136.9, 133.2, 131.9, 129.8, 128.3, 126.6, 119.7, 76.8, 60.2, 56.2, 54.4, 52.1, 47.8, 40.1, 39.1, 34.4, 33.2, 31.9, 26.8, 24.2, 22.4, 19.5, 16.3. HRMS (m/z): $C_{35}H_{45}N_6O_5$ [M+H]$^+$ found: 629.3464. Calculated: 629.3451. $[\alpha]_D^{20}$ -115 (c 1.0, MeOH).

2-[(1S,6S,9S)-6-tert-Butyl-1-cyano-9-[(2S)-2-hydroxy-3-methylbutanamido]-8-oxo-19-oxa-4,7-diazatetracyclo[9.5.2.1²,⁵.0¹⁴,¹⁷]nonadeca-2,4,11,13,17-pentaen-3-yl]-1,3-oxazole-4-carboxamide (153). To a solution of ester **DZA-129** (56 mg; 0.096 mmol) in dry MeOH (0.5 mL) NH$_3$ (7M in MeOH; 543 µL; 3.80 mmol, 40 equiv.) was added dropwise at room temperature. The yellowish solution was stirred for 20 h, then evaporated. The resulting yellow amorphous material was purified with reverse phase flash chromatography (10% to 40% MeCN in water) to give amide **DZA-153** (39 mg; 72%) as a white amorphous material.

^{1}H NMR (400 MHz, MeOD) δ 8.58 (s, 1H), 7.40 – 7.30 (m, 2H), 6.96 (d, J = 1.4 Hz, 1H), 4.71 (s, 1H), 4.56 (dd, J = 11.8, 3.8 Hz, 1H), 3.86 (d, J = 3.8 Hz, 1H), 3.35 – 3.25 (m, 1H, overlapping with MeOD), 3.23 – 3.13 (m, 2H), 3.03 – 2.94 (m, 1H), 2.93 – 2.84 (m, 2H), 2.09 (sept d, J = 6.8, 3.8 Hz, 1H), 1.01 (s, 9H), 1.00 (d, J = 6.8 Hz, 3H), 0.90 (d, J = 6.8 Hz, 3H). ^{13}C NMR (101 MHz, MeOD) δ 175.8, 174.0, 164.8, 164.3, 155.5, 150.5, 144.0, 142.9, 142.5, 138.5, 136.8, 131.9, 129.7, 127.9, 126.6, 119.5, 76.8, 59.8, 56.3, 47.8, 39.6, 39.1, 34.4, 33.2, 31.8, 26.8, 19.5, 16.3. HRMS (m/z): $C_{30}H_{35}N_6O_6$ [M+H]$^+$ found: 575.2632. Calculated: 575.2618. $[\alpha]_D^{20}$ -171 (c 1.0, MeOH).

2-[(1S,6S,9S)-6-tert-Butyl-1-cyano-9-[(2S)-2-hydroxy-3-methylbutanamido]-8-oxo-19-oxa-4,7-diazatetracyclo[9.5.2.1²,⁵.0¹⁴,¹⁷]nonadeca-2,4,11,13,17-pentaen-3-yl]-N-methyl-1,3-oxazole-4-carboxamide (DZA-146). To a solution of ester **DZA-129** (36 mg; 0.061 mmol) MeNH$_2$ (33% in EtOH; 320 µL; 3.05 mmol, 50 equiv.) was added dropwise at room temperature. The yellowish solution was stirred for 1 h, then evaporated. The resulting yellow amorphous material was purified with reverse phase flash chromatography (10% to 50% MeCN in water) to give amide **DZA-146** (26 mg; 72%) as a white amorphous material.

^{1}H NMR (400 MHz, MeOD) δ 8.55 (s, 1H), 7.38 – 7.30 (m, 2H), 6.97 (s, 1H), 4.72 (s, 1H), 4.55 (dd, J = 11.8, 3.8 Hz, 1H), 3.86 (d, J = 3.8 Hz, 1H), 3.34 – 3.24 (m, 1H, overlapping with MeOD), 3.23 – 3.14 (m, 2H), 3.01 – 2.92 (m, 1H), 2.96 (s, 3H), 2.92 – 2.85 (m, 2H), 2.09 (sept d, J = 6.9, 3.8 Hz, 1H), 1.01 (s, 9H), 1.00 (d, J = 6.9 Hz, 3H), 0.89 (d, J = 6.9 Hz, 3H). ^{13}C NMR (101 MHz, MeOD) δ 175.8, 174.0, 164.3, 163.1, 155.5, 150.4, 143.3, 142.9, 142.5, 138.6, 136.8, 131.9, 129.7, 127.9, 126.6, 119.5, 76.8, 59.7, 56.3, 47.8, 39.5, 39.1, 34.4, 33.2, 31.8, 26.8, 26.2, 19.5, 16.3. HRMS (m/z): $C_{31}H_{37}N_6O_6$ [M+H]$^+$ found: 589.2775. Calculated: 589.2775. $[\alpha]_D^{20}$ -164 (c 1.0, MeOH).

The synthesis of diazonamide A analogs DZA-160 and DZA-162 is shown in Scheme 10.

49

Accordingly, oxime **DZA-160** and acetamide **DZA-162** were prepared starting from alcohol **26**. To synthesize oxime **38** alcohol was oxidized to aldehyde and then in the presence of hydroxyamine was converted into oxime **38**. Then, after *N*-Boc deprotection and coupling with *S*-H*i*VA **7** analog **DZA-160** was furnished. Acetamide **DZA-162** was prepared from alcohol 26 in mesylation and futher S$_N$2 reaction with sodium azide to give **39**. Azide was then reduced to primary amine. Acylation of amine gave acetamide **40**, which was converted into analog **DZA-162** in deprotection-amidation reaction sequence (Scheme 10).
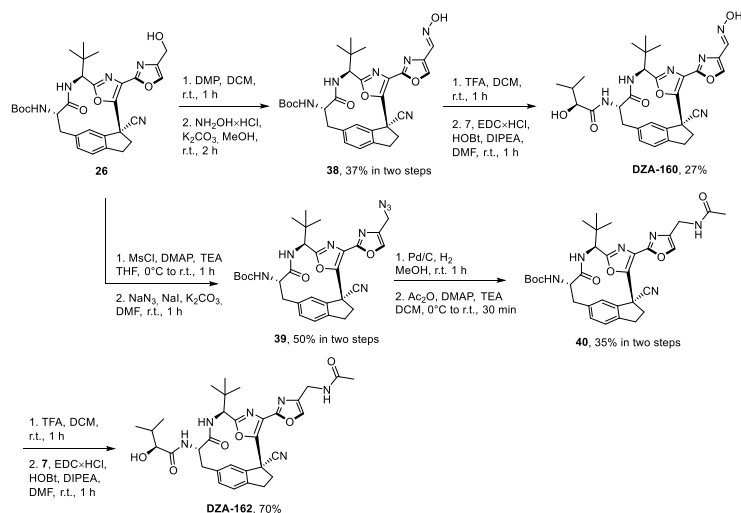
Scheme 10. Synthesis of diazonamide A analogs **DZA-160** and **DZA-162**.

***tert*-Butyl** ***N*-[(1*S*,6*S*,9*S*)-6-*tert*-butyl-1-cyano-3-{4-[(*E*)-(hydroxyimino)methyl]-1,3-oxazol-2-yl}-8-oxo-19-oxa-4,7-diazatetracyclo[9.5.2.1^2,^{5}.0^1^{4},^{1}^{7}]nonadeca-2,4,11,13,17-pentaen-9-yl]carbamate (38).** To a solution of alcohol **26** (225 mg; 0.40 mmol) in dry DCM (2 mL) DMP (187 mg; 0.44 mmol, 1.1 equiv.) was added in one portion. The resulting suspension was stirred at room temperature for 1 h. Then the suspension was diluted with EtOAc and washed with aqueous 1M Na$_2$S$_2$O$_3$ and aqueous saturated NaHCO$_3$. Organic layer was washed with brine, dried (Na$_2$SO$_4$), evaporated. The crude aldehyde was used in the next step without additional purification. To a crude aldehyde (224 mg; 0.40 mmol) in MeOH (2 mL) hydroxylamine HCl (84 mg; 1.20 mmol, 3 equiv.) was added in one portion followed by K$_2$CO$_3$ (166 mg; 1.20 mmol; 3 equiv.). The resulting suspension was stirred for 2 h at room temperature. The reaction mixture was quenched by the addition of aqueous saturated NH$_4$Cl and extracted with EtOAc (×2). Organic layers were combined, washed

50

with brine, dried (Na_2SO_4) and evaporated. The off-white amorphous solid was purified with reverse phase flash chromatograhy (10% to 50% MeCN in 0.01% TFA in water) to give oxime **38** (85 mg; 37%) as a mixture of *E* and *Z* isomers as a white amorphous solid.

^{1}H NMR (400 MHz, MeOD) δ 8.76 (s, 1H), 8.18 (d, *J* = 7.6 Hz, 1H), 7.54 (s, 1H), 7.36 – 7.27 (m, 2H), 7.02 (s, 1H), 4.79 – 4.74 (m, 1H), 4.20 – 4.09 (m, 1H), 3.29 – 3.20 (m, 1H), 3.20 – 3.02 (m, 2H), 3.02 – 2.80 (m, 3H), 1.44 (s, 9H), 1.03 (s, 9H). ^{13}C NMR (101 MHz, MeOD) δ 174.8, 164.3, 157.2, 154.8, 149.8, 144.9, 142.6, 142.3, 139.5, 137.3, 133.6, 131.8, 129.7, 128.0, 126.5, 119.6, 80.6, 59.6, 58.1, 47.7, 39.2, 38.8, 34.3, 31.7, 28.7, 26.8. HRMS (m/z): $C_{30}H_{35}N_6O_6$ [M+H]+ found: 575.2632. Calculated: 575.2618.

(2*S*)-*N*-[(1*S*,6*S*,9*S*)-6-*tert*-Butyl-1-cyano-3-{4-[(*E*)-(hydroxyimino)methyl]-1,3-oxazol-2-yl}-8-oxo-19-oxa-4,7-diazatetracyclo[9.5.2.1²,⁵.0¹⁴,¹⁷]nonadeca-2,4,11,13,17-pentaen-9-yl]-2-hydroxy-3-methylbutanamide (DZA-160). Compound was prepared according to General procedure C from macrocycle **38** (62 mg; 0.11 mmol), TFA (166 µL; 2.16 mmol; 20 equiv.) in DCM (1 mL) in 1 h and *S*-H*i*VA (19 mg; 0.16 mmol; 1.5 equiv.), EDC×HCl (41 mg; 0.22 mmol; 2 equiv.), HOBt (44 mg; 0.32 mmol; 3 equiv.), DIPEA (93 µL; 0.54 mmol; 5 equiv.) in DMF (2 mL) in 1 h. Product **DZA-160** was purified by reverse phase flash chromatography (10% to 50% MeCN in 0.01% TFA in water) to afford 17 mg (27%) as a white amorphous solid.

^{1}H NMR (400 MHz, MeOD) δ 8.77 (s, 1H), 7.55 (s, 1H), 7.43 – 7.26 (m, 2H), 7.00 (s, 1H), 4.74 (s, 1H), 4.55 (dd, *J* = 11.8, 3.8 Hz, 1H), 3.87 (d, *J* = 3.8 Hz, 1H), 3.30 – 3.08 (m, 3H), 3.02 – 2.84 (m, 3H), 2.09 (sept d, *J* = 6.9, 3.8 Hz, 1H), 1.01 (s, 9H), 1.00 (d, *J* = 6.8 Hz, 3H), 0.90 (d, *J* = 6.8 Hz, 3H). ^{13}C NMR (101 MHz, MeOD) δ 175.8, 173.9, 164.2, 154.8, 149.9, 144.9, 142.8, 142.5, 139.5, 136.8, 133.6, 131.9, 129.7, 128.1, 126.6, 119.5, 76.8, 59.7, 56.3, 47.7, 39.3, 39.2, 34.4, 33.2, 31.8, 26.8, 19.5, 16.3. HRMS (m/z): $C_{30}H_{35}N_6O_6$ [M+H]+ found: 575.2621. Calculated: 575.2618. [α]$_D^{20}$ -149 (c 1.0, MeOH).

***tert*-Butyl *N*-[(1*S*,6*S*,9*S*)-3-[4-(azidomethyl)-1,3-oxazol-2-yl]-6-*tert*-butyl-1-cyano-8-oxo-19-oxa-4,7-diazatetracyclo[9.5.2.1²,⁵.0¹⁴,¹⁷]nonadeca-2,4,11,13,17-pentaen-9-yl]carbamate (39).** To alcohol **26** (400 mg; 0.71 mmol) in dry THF (5 mL) TEA (199 µL; 0.142 mmol; 2 equiv.) was added dropwise followed by DMAP (2 mg; 0.014 mmol; 0.02 equiv.) and the resulting solution was cooled to 0°C in ice bath. Then MsCl (83 µL; 1.07 mmol; 1.5 equiv.) was added dropwise to the solution and the resulting orange solution was stirred at the same temperature for 30 minutes. Then the solution was diluted with EtOAc and washed with aqueous 1N HCl, water and brine. Organic layer was dried (Na_2SO_4) and evaporated. The crude mesylate was used in the next step without additional purification. To crude meslate (465 mg; 0.71 mmol) in dry DMF (5 mL) K_2CO_3 (493 mg; 3.56 mmol;

51

5 equiv.) was added in one portion at room temperature followed by NaI (11 mg; 0.071 mmol; 0.1 equiv.) and NaN_3 (139 mg; 2.14 mmol; 3 equiv.). The resulting yellow suspesnion was stirred for 1 h. The suspension was diluted with EtOAc and washed with water and brine. Organic layer was dried (Na_2SO_4) and evaporated. The resulting yellow oil was purified with direct phase flash chromatography (10% to 80% EtOAc in hexanes) to give azide **39** (180 mg; 50%) as a white amorphous solid.

^{1}H NMR (400 MHz, $CDCl_3$) δ 7.79 (s, 1H), 7.25 – 7.21 (m, 2H), 7.12 (s, 1H), 5.78 (d, J = 7.7 Hz, 1H), 5.27 (d, J = 9.3 Hz, 1H), 4.78 (d, J = 7.7 Hz, 1H), 4.41 (d, J = 28.9 Hz, 1H), 4.37 (d, J = 28.9 Hz, 1H), 3.93 (ddd, J = 12.4, 9.3, 3.4 Hz, 1H), 3.33 – 3.20 (m, 2H), 3.20 – 3.11 (m, 1H), 2.99 – 2.93 (m, 1H), 2.93 – 2.82 (m, 2H), 1.43 (s, 9H), 1.00 (s, 9H). ^{13}C NMR (101 MHz, $CDCl_3$) δ 171.9, 161.7, 155.4, 154.9, 148.1, 141.4, 140.9, 137.7, 136.8, 135.5, 130.2, 129.5, 127.7, 125.5, 118.3, 80.6, 58.3, 58.0, 46.4, 46.3, 38.6, 37.9, 33.5, 31.1, 28.4, 26.6. HRMS (m/z): $C_{30}H_{34}N_8O_5Na$ [M+Na][+] found: 609.2571. Calculated: 609.2550. $[α]_D^{20}$ -146 (c 1.0, $CHCl_3$).

***tert*-Butyl *N*-[(1*S*,6*S*,9*S*)-6-*tert*-butyl-1-cyano-3-[4-(acetamidomethyl)-1,3-oxazol-2-yl]-8-oxo-19-oxa-4,7-diazatetracyclo[9.5.2.1[2],[5].0[1][4],[1][7]]nonadeca-2,4,11,13,17-pentaen-9-yl]carbamate (40).**
To azide **39** (471 mg; 0.80 mmol) in dry MeOH (12 mL) Pd/C (10%; 43 mg; 0.040 mmol; 0.05 equiv.) was added in one portion and H_2 was barbotated through the suspension for 1 h at room temperature. Then the suspension was filtered through celite, evaporated. The crude amine was used in the next step without additional purification. To the crude amine (450 mg; 0.80) in DCM (10 mL) TEA (224 μL; 1.61 mmol; 2 equiv.) was added dropwise followed by DMAP (10 mg; 0.08 mmol; 0.1 equiv.) and the flask was cooled to 0°C in ice bath. Then acetic anhydride (76 μL; 0.80 mmol; 1 equiv.) was added dropwise to the solution. The yellow solution was stirred for 10 minutes at the same temperature and 30 minutes at room temperature. The reaction was diluted with EtOAc and washed with saturated aqueous $NaHCO_3$, 1 N HCl, water, and brine. Organic layer was dried (Na_2SO_4) and evaporated. The resulting yellow oil was purified with direct phase flash chromatography (10% to 50% EtOAc in hexanes) to afford amide **40** (171 mg; 35%) as a white amorphous solid.

^{1}H NMR (400 MHz, $CDCl_3$) δ 7.74 (s, 1H), 7.26 – 7.22 (m, 2H), 6.96 (s, 1H), 6.34 (s, 1H), 5.86 (d, J = 6.9 Hz, 1H), 5.23 (d, J = 9.3 Hz, 1H), 4.72 (d, J = 7.3 Hz, 1H), 4.51 (dd, J = 15.1, 5.8 Hz, 1H), 4.35 (dd, J = 15.1, 4.6 Hz, 1H), 3.94 (ddd, J = 12.1, 9.3, 3.4 Hz, 1H), 3.38 – 3.28 (m, 1H), 3.24 – 3.14 (m, 2H), 3.01 (ddd, J = 15.6, 8.4, 3.4 Hz, 1H), 2.85 (dd, J = 12.3, 3.4 Hz, 1H), 2.65 (ddd, J = 13.4, 8.4, 8.4 Hz, 1H), 2.00 (s, 3H), 1.43 (s, 9H), 0.98 (s, 9H). ^{13}C NMR (101 MHz, $CDCl_3$) δ 171.9, 170.6, 162.0, 155.4, 154.5, 148.2, 141.5, 141.1, 138.6, 136.2, 135.6, 130.2, 129.4, 128.1, 125.5, 118.5, 80.6,

58.4, 58.1, 46.6, 39.7, 37.9, 35.6, 33.5, 31.2, 28.4, 26.6, 23.1. HRMS (m/z): $C_{32}H_{39}N_6O_6$ [M+H]$^+$ found: 603.2939. Calculated: 603.2931. [α]$_D^{20}$ -101 (c 1.0, CH_2Cl_2).

(2S)-N-[(1S,6S,9S)-6-*tert*-Butyl-1-cyano-3-[4-(acetamidomethyl)-1,3-oxazol-2-yl]-8-oxo-19-oxa-4,7-diazatetracyclo[9.5.2.1²,⁵.0¹⁴,¹⁷]nonadeca-2,4,11,13,17-pentaen-9-yl]-2-hydroxy-3-methylbutanamide (DZA-162). Compound was prepared according to General procedure C from macrocycle **40** (171 mg; 0.28 mmol), TFA (436 μL; 5.67 mmol; 20 equiv.) in DCM (2 mL) in 2 h and S-H*i*VA (50 mg; 0.43 mmol; 1.5 equiv.), EDC×HCl (109 mg; 0.57 mmol; 2 equiv.), HOBt (115 mg; 0.85 mmol; 3 equiv.), DIPEA (246 μL; 1.42 mmol; 5 equiv.) in DMF (3 mL) in 1 h. Product **DZA-162** was purified by reverse phase flash chromatography (10% to 50% MeCN in 0.01% TFA in water) to afford 120 mg (70%) as a white amorphous solid.

^{1}H NMR (400 MHz, MeOD) δ 7.97 (s, 1H), 7.39 – 7.25 (m, 2H), 6.97 (s, 1H), 4.72 (s, 1H), 4.55 (dd, J = 11.8, 3.8 Hz, 1H), 4.38 (s, 2H), 3.86 (d, J = 3.8 Hz, 1H), 3.28 – 3.05 (m, 3H), 3.01 – 2.84 (m, 3H), 2.09 (sept d, J = 6.8, 3.8 Hz, 1H), 2.00 (s, 3H), 1.00 (s, 9H), 1.00 (d, J = 6.8 Hz, 3H), 0.89 (d, J = 6.8 Hz, 3H). ^{13}C NMR (101 MHz, MeOD) δ 175.8, 173.9, 173.4, 164.1, 155.6, 149.5, 142.8, 142.6, 140.8, 138.3, 136.8, 131.8, 129.7, 128.4, 126.6, 119.6, 76.8, 59.7, 56.3, 47.8, 39.4, 39.2, 36.3, 34.3, 33.2, 31.8, 26.8, 22.5, 19.5, 16.3. HRMS (m/z): $C_{32}H_{39}N_6O_6$ [M+H]$^+$ found: 603.2955. Calculated: 603.2931. [α]$_D^{20}$ -133 (c 1.0, MeOH).

The synthesis of diazonamide A analogs DZA-149 and DZA-161 is shown in Scheme 11.

Accordingly, carbonate **41** was prepared from alcohol **26** after reaction with methylchloroformate under basic conditions. Analog **DZA-161** was obtained after *N*-Boc deprotection and amidation reaction sequence. Accordingly, analog **DZA-148** was prepared from alcohol **26**. After alcohol oxidation to aldehyde it was subjected into Horner-Wadsworth–Emmons reaction to give *E*-alkene **42**. The resulting alkene was converted into analog **DZA-148** in two steps. Analog **DZA-149** was obtained from analog **DZA-148** after alkene Pd-catalyzed hydrogenation (Scheme 11).

53
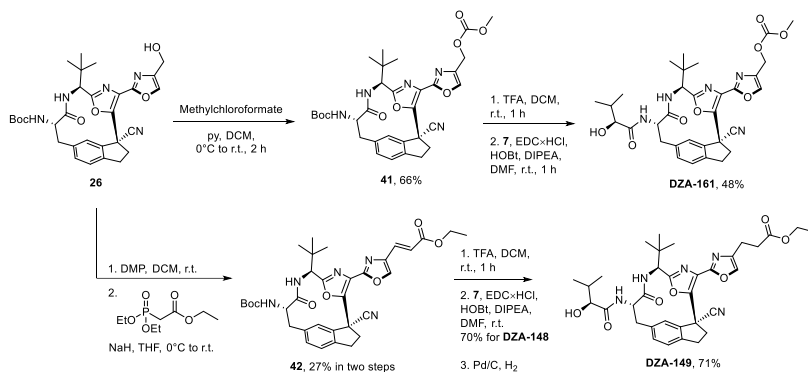
Scheme 11. Synthesis of diazonamide A analogs **DZA-148–149** and **DZA-161**.

{2-[(1*S*,6*S*,9*S*)-9-{[(***tert*-Butoxy)carbonyl]amino}-6-*tert*-butyl-1-cyano-8-oxo-19-oxa-4,7-diazatetracyclo[9.5.2.1²,⁵.0¹⁴,¹⁷]nonadeca-2,4,11,13,17-pentaen-3-yl]-1,3-oxazol-4-yl}methyl methyl carbonate (41).** To alcohol **26** (200 mg; 0.36 mmol) in dry DCM (2 mL) pyridine (32 µL; 0.39 mmol; 1.1 equiv.) was added dropwise at room temperature. Then the flask was cooled to 0˚C and methyl chloroformate (50 µL; 0.64 mmol; 1.8 equiv.) was added in one portion. The yellow solution was stirred for 2 h while gradually warming to room temperature. The solution was quenched by the addition of aqueous saturated NH₄Cl and extracted with EtOAc (×2). Organic layers were combined, washed with brine, dried (Na₂SO₄) and evaporated. The yellow oil was purified with reverse phase flash chromatograhy (10% to 70% MeCN in 0.01% TFA in water) to give carbonate **41** (145 mg; 66%) as a white amorphous solid.

¹H NMR (400 MHz, CDCl₃) δ 7.86 (s, 1H), 7.25 – 7.21 (m, 2H), 7.11 (s, 1H), 5.77 (d, *J* = 7.7 Hz, 1H), 5.24 (dd, *J* = 9.4 Hz, 1H), 5.20 (dd, *J* = 3.8, 0.9 Hz, 2H), 4.78 (d, *J* = 7.7 Hz, 1H), 3.95 – 3.87 (m, 1H), 3.81 (s, 3H), 3.33 – 3.19 (m, 2H), 3.19 – 3.11 (m, 1H), 3.00 – 2.90 (m, 1H), 2.89 – 2.78 (m, 2H), 1.43 (s, 9H), 1.00 (s, 9H). ¹³C NMR (101 MHz, CDCl₃) δ 171.9, 161.7, 155.7, 155.4, 154.6, 148.0, 141.4, 141.0, 138.2, 137.2, 135.5, 130.2, 129.5, 127.7, 125.5, 118.3, 80.6, 61.5, 58.2, 58.0, 55.2, 46.4, 38.7, 37.9, 33.5, 31.1, 28.4, 26.6. HRMS (m/z): C₃₂H₃₈N₅O₈ [M+H]⁺ found: 620.2731. Calculated: 620.2720. [α]ᴅ²⁰ -126 (c 1.0, CHCl₃).

{2-[(1*S*,6*S*,9*S*)-6-*tert*-Butyl-1-cyano-9-[(2***S*)-2-hydroxy-3-methylbutanamido]-8-oxo-19-oxa-4,7-diazatetracyclo[9.5.2.1²,⁵.0¹⁴,¹⁷]nonadeca-2,4,11,13,17-pentaen-3-yl]-1,3-oxazol-4-yl}methyl methyl carbonate (DZA-161).** Compound was prepared according to General procedure C from macrocycle **41** (135 mg; 0.22 mmol), TFA (335 µL; 4.36 mmol; 20 equiv.) in DCM (1 mL) in 2 h and *S*-H*i*VA (39 mg; 0.33 mmol; 1.5 equiv.), EDC×HCl (84 mg; 0.44 mmol; 2 equiv.), HOBt (88

54

mg; 0.66 mmol; 3 equiv.), DIPEA (189 µL; 1.09 mmol; 5 equiv.) in DMF (1 mL) in 1 h. Product **DZA-161** was purified by reverse phase flash chromatography (10% to 50% MeCN in 0.01% TFA in water) to afford 65 mg (48%) as a white amorphous solid.

^{1}H NMR (400 MHz, MeOD) δ 8.16 (s, 1H), 7.37 – 7.30 (m, 2H), 6.98 (s, 1H), 5.20 (d, J = 15.1 Hz, 1H), 5.17 (d, J = 15.1 Hz, 1H), 4.75 – 4.72 (m, 1H), 4.55 (dd, J = 11.8, 3.8 Hz, 1H), 3.86 (d, J = 3.8 Hz, 1H), 3.79 (s, 3H), 3.28 – 3.05 (m, 3H), 3.00 – 2.83 (m, 3H), 2.09 (sept d, J = 6.8, 3.8 Hz, 1H), 1.01 (s, 9H), 1.00 (d, J = 6.8 Hz, 3H), 0.89 (d, J = 6.8 Hz, 3H). ^{13}C NMR (101 MHz, MeOD) δ 175.8, 173.9, 164.2, 157.0, 155.9, 149.8, 142.8, 142.5, 140.4, 138.5, 136.8, 131.8, 129.7, 128.2, 126.6, 119.5, 76.8, 61.9, 59.6, 56.3, 55.5, 47.7, 39.3, 39.2, 34.3, 33.2, 31.7, 26.8, 19.5, 16.3. HRMS (m/z): $C_{32}H_{38}N_5O_8$ [M+H]$^+$ found: 620.2736. Calculated: 620.2720. $[\alpha]_D^{20}$ -143 (c 1.0, MeOH).

Ethyl (2*E*)-3-{2-[(1*S*,6*S*,9*S*)-9-{[(*tert*-butoxy)carbonyl]amino}-6-*tert*-butyl-1-cyano-8-oxo-19-oxa-4,7-diazatetracyclo[9.5.2.1^2,^{5}.0^{14},^{17}]nonadeca-2,4,11,13,17-pentaen-3-yl]-1,3-oxazol-4-yl}prop-2-enoate (42). To a solution of alcohol **26** (380 mg; 0.68 mmol) in dry DCM (4 mL) DMP (316 mg; 0.74 mmol, 1.1 equiv.) was added in one portion. The resulting suspension was stirred at room temperature for 1 h. Then the suspension was diluted with EtOAc and washed with aqueous 1M $Na_2S_2O_3$ and aqueous saturated $NaHCO_3$. Organic layer was washed with brine, dried (Na_2SO_4), evaporated. The crude aldehyde (288 mg; 76%) was used in the next step without additional purification.

To a solution of triethyl phosphonoacetate (255 µL; 1.29 mmol, 2.5 equiv.) in THF (1 mL) was added sodium hydride (60% in mineral oil; 52 mg; 1.29 mmol, 2.5 equiv.) at 0 °C. The solution was stirred for 1 h at room temperature before being added to a solution of the crude aldehyde (288 mg; 0.52 mmol) in THF (1 mL) at 0 °C. The mixture was stirred at room temperature for 15 min. Then the reaction mixture was quenched with aqueous saturated NH_4Cl and extracted with EtOAc (×2). Organic layers were combined, washed with brine, dried (Na_2SO_4) and evaporated. The residue was purified with reverse phase column chromatography (from 10% to 50% MeCN in 0.01% TFA in water) to give ester **42** (115 mg; 36%) as a white amorphous solid.

^{1}H NMR (400 MHz, CDCl$_3$) δ 7.91 (s, 1H), 7.55 (d, J = 15.5 Hz, 1H), 7.25 – 7.22 (m, 2H), 7.13 (d, J = 1.1 Hz, 1H), 6.79 (d, J = 15.5 Hz, 1H), 5.82 (d, J = 7.7 Hz, 1H), 5.28 (d, J = 9.2 Hz, 1H), 4.79 (d, J = 7.7 Hz, 1H), 4.26 (q, J = 7.1 Hz, 2H), 3.94 (ddd, J = 12.3, 9.2, 3.4 Hz, 1H), 3.35 – 3.14 (m, 3H), 3.01 – 2.84 (m, 3H), 1.43 (s, 9H), 1.34 (t, J = 7.1 Hz, 3H), 1.00 (s, 9H). ^{13}C NMR (101 MHz, CDCl$_3$) δ 171.9, 166.9, 161.7, 155.4, 154.9, 148.5, 141.4, 140.8, 139.4, 138.8, 135.5, 131.8, 130.2, 129.5, 127.5, 125.5, 121.4, 118.2, 80.6, 60.7, 58.2, 58.0, 46.5, 38.6, 37.9, 33.6, 31.1, 28.4, 26.6, 14.5. HRMS (m/z): $C_{34}H_{40}N_5O_7$ [M+H]$^+$ found: 630.2919. Calculated: 630.2928. $[\alpha]_D^{20}$ -117 (c 1.0, CHCl$_3$).

55

Ethyl (2*E*)-3-{2-[(1*S*,6*S*,9*S*)-6-*tert*-butyl-1-cyano-9-[(2*S*)-2-hydroxy-3-methylbutanamido]-8-oxo-19-oxa-4,7-diazatetracyclo[9.5.2.1²,⁵.0¹⁴,¹⁷]nonadeca-2,4,11,13,17-pentaen-3-yl]-1,3-oxazol-4-yl}prop-2-enoate (DZA-148). Compound was prepared according to General procedure C from macrocycle **42** (100 mg; 0.16 mmol), TFA (122 µL; 1.59 mmol; 10 equiv.) in DCM (1 mL) in 1 h and *S*-H*i*VA (28 mg; 0.24 mmol; 1.5 equiv.), EDC×HCl (61 mg; 0.32 mmol; 2 equiv.), HOBt (64 mg; 0.48 mmol; 3 equiv.), DIPEA (137 µL; 0.79 mmol; 5 equiv.) in DMF (2 mL) in 1 h. Product **DZA-148** was purified by reverse phase flash chromatography (10% to 50% MeCN in 0.01% TFA in water) to afford 70 mg (70%) as a white amorphous solid.

^{1}H NMR (400 MHz, MeOD) δ 8.33 (d, J = 7.5 Hz, 1H), 8.33 (s, 1H, overlapping with 8.33 doublet), 7.63 (d, J = 15.6 Hz, 1H), 7.40 – 7.30 (m, 2H), 6.99 (s, 1H), 6.73 (d, J = 15.6 Hz, 1H), 4.76 – 4.67 (m, 1H), 4.56 (dd, J = 11.8, 3.8 Hz, 1H), 4.26 (q, J = 7.1 Hz, 2H), 3.87 (d, J = 3.8 Hz, 1H), 3.36 – 3.26 (m, 1H, overlapping with MeOD), 3.24 – 3.08 (m, 2H), 3.04 – 2.90 (m, 2H), 2.90 (dd, J = 12.4, 3.9 Hz, 1H), 2.09 (sept d, J = 6.9, 3.8 Hz, 1H), 1.34 (t, J = 7.1 Hz, 3H), 1.01 (s, 9H), 1.00 (d, J = 6.9 Hz, 3H), 0.90 (d, J = 6.9 Hz, 3H). ^{13}C NMR (101 MHz, MeOD) δ 175.8, 174.0, 168.2, 164.1, 156.2, 150.3, 142.9, 142.4, 142.1, 139.7, 136.8, 133.4, 131.8, 129.8, 128.1, 126.6, 121.6, 119.4, 76.8, 61.8, 59.8, 56.3, 47.8, 39.5, 39.2, 34.4, 33.2, 31.8, 26.8, 19.5, 16.3, 14.6. HRMS (m/z): $C_{34}H_{40}N_5O_7$ [M+H]⁺ found: 630.2957. Calculated: 630.2928. [α]$_D^{20}$ -148 (c 1.0, MeOH).

Ethyl 3-{2-[(1*S*,6*S*,9*S*)-6-*tert*-butyl-1-cyano-9-[(2*S*)-2-hydroxy-3-methylbutanamido]-8-oxo-19-oxa-4,7-diazatetracyclo[9.5.2.1²,⁵.0¹⁴,¹⁷]nonadeca-2,4,11,13,17-pentaen-3-yl]-1,3-oxazol-4-yl}propanoate (DZA-149). To a solution of alkene (35 mg; 0.056 mmol) in dry MeOH (1 ML) was added Pd/C (10%; 6 mg; 0.006 mmol, 0.1 equiv.) in one portion at room temperature. Then H_2 was barbotated through the suspension for 30 minutes. The resulting suspension was filtrated through celite and evaporated. The resulting yellowish amorphous solid was purified with reverse phase flash chromatography (10% to 50% MeCN in 0.01% TFA in water) to give ester **DZA-149** (25 mg; 71%) as a white amorphous solid.

^{1}H NMR (400 MHz, MeOD) δ 8.34 (d, J = 7.5 Hz, 1H), 7.86 (s, 1H), 7.39 – 7.28 (m, 2H), 6.96 (d, J = 1.4 Hz, 1H), 4.74 – 4.69 (m, 1H), 4.55 (dd, J = 11.8, 3.8 Hz, 1H), 4.15 (q, J = 7.1 Hz, 2H), 3.86 (d, J = 3.8 Hz, 1H), 3.29 – 3.05 (m, 3H), 3.01 – 2.84 (m, 5H), 2.82 – 2.69 (m, 2H), 2.09 (sept d, J = 6.9, 3.8 Hz, 1H), 1.25 (t, J = 7.1 Hz, 3H), 1.00 (s, 9H), 1.00 (d, J = 6.9 Hz, 3H), 0.89 (d, J = 6.9 Hz, 3H). ^{13}C NMR (101 MHz, MeOD) δ 175.8, 174.3, 174.0, 164.1, 155.3, 149.4, 142.8, 142.7, 142.3, 137.4, 136.7, 131.8, 129.7, 128.5, 126.5, 119.5, 76.8, 61.7, 59.7, 56.3, 47.8, 39.4, 39.2, 34.3, 33.8, 33.2, 31.8, 26.8, 22.5, 19.5, 16.3, 14.5. HRMS (m/z): $C_{34}H_{42}N_5O_7$ [M+H]⁺ found: 632.3087. Calculated: 632.3084. [α]$_D^{20}$ -149 (c 1.0, MeOH).

56

The synthesis of diazonamide A analog DZA-176 is shown in Scheme 12.

Accordingly, methyl ester of **32** was hydrolyzed and coupled with (*S*)-(+)-2-amino-propan-1-ol to give amide **43**. Primary alcohol of **43** was oxidized to aldehyde and after further oxazole cyclization reaction in the presence of PPh$_3$ and 1,2-dibromotetrachloroethane under basic conditions was converted into methyl bioxazole **44**. After *N*-Boc cleavage with TFA the resulting amine was coupled with (*S*)-2-hydroxy-3-methylbutanoic acid (*S*-H*i*VA; **7**) to give analog **DZA-176** (Scheme 12).
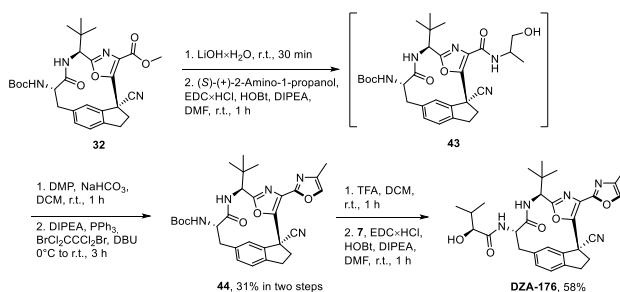
Scheme 12. Synthesis of diazonamide A analog **DZA-176**.

tert-Butyl *N*-[(1*S*,6*S*,9*S*)-6-*tert*-butyl-1-cyano-3-(4-methyl-1,3-oxazol-2-yl)-8-oxo-19-oxa-4,7-diazatetracyclo[9.5.2.1²,⁵.0¹⁴,¹⁷]nonadeca-2,4,11,13,17-pentaen-9-yl]carbamate (**44**). Methyl ester **32** (385 mg; 0.74 mmol) was dissolved in THF (4 mL). Separately solid LiOH×H$_2$O (93 mg; 0.2.21 mmol; 3 equiv.) was dissolved in water (2 mL) and added to the reaction mixture. Emulsion was stirred at room temperature for 30 min, then aqueous 1N HCl was added. The resulting mixture was extracted with EtOAc (×2), combined organic layers were washed with brine, dried (Na$_2$SO$_4$) and evaporated. The crude carboxylic acid was used in the next step without additional purification. The off-white amorphous solid was dissolved in anhydrous DMF (5 mL) and 2-amino-3,3,3-trifluoropropan-1-ol hydrochloride (183 mg; 1.11 mmol; 1.5 equiv.), EDC×HCl (212 mg; 1.11 mmol; 1.5 equiv.) and HOBt (199 mg; 1.47 mmol; 2 equiv.) were added followed by DIPEA (382 µL; 2.21 mmol; 3 equiv.). The solution was stirred at room temperature for 1 h. The solution was diluted with aqueous saturated NH$_4$Cl and EtOAc. The layers were separated and the organic phase was washed with brine, dried (Na$_2$SO$_4$) and evaporated. The resulting amide **43** was used in the next step without additional purification.

To a stirred solution of amide **43** (135 mg; 0.24 mmol) in DCM (1.5 mL) was added NaHCO$_3$ (40 mg; 0.48 mmol; 2 equiv.) followed by DMP (122 mg; 0.29 mmol; 1.2 equiv). The reaction mixture was stirred at room temperature for 1 h before being quenched with aqueous saturated NaHCO$_3$ and Na$_2$S$_2$O$_3$. The mixture was stirred vigorously for 1 h before being extracted with DCM (×2). The

57

combined organic extracts were then dried (Na$_2$SO$_4$) and evaporated to afford a crude aldehyde, which was used without further purification. To a stirred solution of the crude aldehyde in DCM (2 mL) at 0°C was added sequentially DIPEA (165 µL, 0.96 mmol; 4 equiv.), PPh$_3$ (125 mg, 0.96 mmol; 2 equiv.) and Br$_2$C$_2$Cl$_4$ (155 mg, 0.48 mmol; 2 equiv.). The reaction mixture was allowed to warm to room temperature and stirred for 1 h before being recooled to 0°C and DBU (143 µL, 0.96 mmol; 4 equiv.) added. The reaction mixture was then stirred for 2 h at room temperature before being quenched with H$_2$O and extracted with DCM (×2). The combined organic extracts were then dried (Na$_2$SO$_4$) and evaporated. The resulting orange oil was purified with direct phase flash chromatography (10% to 50% EtOAc in hexanes) to give bioxazole **44** (40 mg; 31%) as a white amorphous solid.

^{1}H NMR (400 MHz, CDCl$_3$) δ 7.53 (q, J = 1.2 Hz, 1H), 7.25 – 7.19 (m, 2H), 7.12 (s, 1H), 5.67 (d, J = 7.9 Hz, 1H), 5.22 (d, J = 9.3 Hz, 1H), 4.79 (d, J = 7.9 Hz, 1H), 3.90 (ddd, J = 12.3, 9.3, 3.4 Hz, 1H), 3.34 – 3.07 (m, 3H), 3.01 – 2.79 (m, 3H), 2.27 (d, J = 1.3 Hz, 3H), 1.43 (s, 9H), 1.00 (s, 9H). ^{13}C NMR (101 MHz, CDCl$_3$) δ 171.8, 161.6, 155.3, 153.9, 147.2, 141.3, 141.1, 138.4, 135.5, 135.3, 130.2, 129.5, 128.2, 125.4, 118.5, 80.5, 58.3, 57.9, 46.4, 38.7, 38.0, 33.5, 31.1, 28.4, 26.6, 11.9. HRMS (m/z): C$_{30}$H$_{36}$N$_5$O$_5$ [M+H]$^+$ found: 546.2720. Calculated: 546.2716. [α]$_D^{20}$ -125 (c 1.0, CHCl$_3$).

(2*S*)-*N*-[(1*S*,6*S*,9*S*)-6-*tert*-butyl-1-cyano-3-(4-methyl-1,3-oxazol-2-yl)-8-oxo-19-oxa-4,7-diazatetracyclo[9.5.2.1²,⁵.0¹⁴,¹⁷]nonadeca-2,4,11,13,17-pentaen-9-yl]-2-hydroxy-3-methylbutanamide (DZA-176). Compound was prepared according to General procedure C from macrocycle **44** (40 mg; 0.073 mmol), TFA (56 µL; 0.73 mmol; 10 equiv.) in DCM (0.5 mL) in 2 h and *S*-H*i*VA (13 mg; 0.11 mmol; 1.5 equiv.), EDC×HCl (42 mg; 0.22 mmol; 3 equiv.), HOBt (30 mg; 0.22 mmol; 3 equiv.), DIPEA (63 µL; 0.37 mmol; 5 equiv.) in DMF (0.5 mL) in 1 h. Product **DZA-176** was purified by reverse phase flash chromatography (10% to 50% MeCN in 0.01% TFA in water) to afford 28 mg (70%) as a white amorphous solid.

^{1}H NMR (400 MHz, MeOD) δ 8.34 (d, J = 7.5 Hz, 1H), 8.00 (d, J = 8.5 Hz, 1H), 7.82 (s, 1H), 7.42 – 7.26 (m, 2H), 6.94 (s, 1H), 4.71 (d, J = 7.5 Hz, 1H), 4.62 – 4.45 (m, 1H), 3.86 (d, J = 3.8 Hz, 1H), 3.26 (dd, J = 15.5, 7.7 Hz, 1H), 3.18 (dd, J = 12.1, 12.1 Hz, 1H), 3.15 – 3.07 (m, 1H), 3.00 – 2.92 (m, 1H), 2.91 – 2.82 (m, 2H), 2.27 (d, J = 1.3 Hz, 3H), 2.09 (sept d, J = 6.9, 3.8 Hz, 1H), 1.01 (d, J = 6.9 Hz, 3H), 1.00 (s, 9H), 0.89 (d, J = 6.9 Hz, 3H). ^{13}C NMR (101 MHz, MeOD) δ 175.8, 173.9, 164.1, 155.2, 149.3, 142.8, 142.7, 139.3, 137.3, 136.7, 131.8, 129.6, 128.5, 126.5, 119.5, 76.8, 59.7, 56.3, 47.7, 39.5, 39.2, 34.3, 33.2, 31.7, 26.8, 19.5, 16.3, 11.4. HRMS (m/z): C$_{30}$H$_{36}$N$_5$O$_5$ [M+H]$^+$ found: 546.2725. Calculated: 546.2716. [α]$_D^{20}$ -109 (c 1.0, MeOH).

58

The synthesis of diazonamide A analogs DZA-156-159 is shown in Scheme 13.

Accordingly, hydroxamic acid **DZA-156** and its derivatives **DZA-157–159** were obtained from analog **DZA-129** in two-step reaction sequence. After methyl ester hydrolysis the resulting acid was coupled with corresponding hydroxy/alkoxyamine to give analogs **DZA-156-159** (Scheme 13).
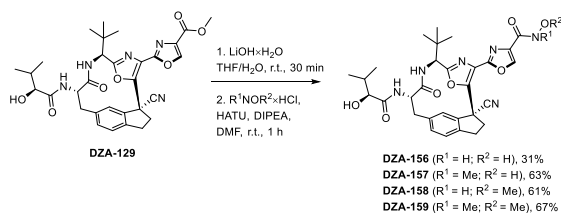
Scheme 13. Synthesis of diazonamide A analogs **DZA-156–159**

General procedure D (hydroxamic acid formation):

Methyl ester **DZA-129** was dissolved in THF. Separately solid LiOH×H$_2$O was dissolved in water and added to the reaction mixture. Emulsion was stirred at room temperature for 30 min, then aqueous HCl (1 N) was added. The resulting mixture was extracted with EtOAc (×3), combined organic layers were washed with brine, dried (Na$_2$SO$_4$) and evaporated. To the resulting crude acid was added the corresponding hydroxylamine and dissolved in dry DMF. Then HATU was added followed by DIPEA. The resulting solution was stirred at room temperature to full conversion (1 h). The solution was diluted with aqueous saturated NH$_4$Cl and EtOAc. The layers were separated and the organic phase was washed with brine, dried (Na$_2$SO$_4$) and evaporated. Pure products were obtained after column chromatography.

2-[(1S,6S,9S)-6-*tert*-Butyl-1-cyano-9-[(2S)-2-hydroxy-3-methylbutanamido]-8-oxo-19-oxa-4,7-diazatetracyclo[9.5.2.1^2,^{5}.0^{14},^{17}]nonadeca-2,4,11,13,17-pentaen-3-yl]-N-hydroxy-1,3-oxazole-4-carboxamide (DZA-156). Compound was prepared according to General procedure D from macrocycle **DZA-129** (134 mg; 0.23 mmol), LiOH×H$_2$O (51 mg; 0.68 mmol; 3 equiv.) in THF/water (1:1 v/v; 1.5 mL) in 30 minutes and hydroxylamine×HCl (79 mg; 1.14 mmol; 5 equiv.), HATU (112 mg; 0.30 mmol; 1.3 equiv.), DIPEA (275 μL; 1.59 mmol; 7 equiv.) in DMF (2 mL) in 1 h. Product **DZA-156** was purified by reverse phase flash chromatography (10% to 50% MeCN in 0.01% TFA in water) to afford 42 mg (31%) as a white amorphous solid.

^{1}H NMR (400 MHz, MeOD) δ 8.59 (s, 1H), 7.42 – 7.26 (m, 2H), 6.97 (s, 1H), 4.74 – 4.70 (m, 1H), 4.55 (dd, J = 11.8, 3.8 Hz, 1H), 3.86 (d, J = 3.8 Hz, 1H), 3.30 – 3.24 (m, 1H, overlapping with MeOD), 3.22 – 3.13 (m, 2H), 3.02 – 2.94 (m, 1H), 2.94 – 2.85 (m, 2H), 2.09 (sept d, J = 6.9, 3.8 Hz, 1H), 1.01

59

(s, 9H), 1.00 (d, J = 6.9 Hz, 3H), 0.89 (d, J = 6.9 Hz, 3H). ^{13}C NMR (101 MHz, MeOD) δ 175.8, 174.0, 164.4, 160.2, 155.7, 150.5, 143.6, 142.9, 142.5, 136.8, 131.9, 129.7, 127.8, 126.6, 119.5, 76.8, 59.7, 56.2, 47.8, 39.4, 39.1, 34.4, 33.2, 31.8, 26.7, 19.5, 16.3. HRMS (m/z): $C_{30}H_{35}N_6O_7$ [M+H]$^+$ found: 591.2579. Calculated: 591.2567. $[α]_D^{20}$ -147 (c 1.0, MeOH).

2-[(1S,6S,9S)-6-tert-Butyl-1-cyano-9-[(2S)-2-hydroxy-3-methylbutanamido]-8-oxo-19-oxa-4,7-diazatetracyclo[9.5.2.1^2,^{5}.0^{14},^{17}]nonadeca-2,4,11,13,17-pentaen-3-yl]-N-hydroxy-N-methyl-1,3-oxazole-4-carboxamide (DZA-157). Compound was prepared according to General procedure D from macrocycle **DZA-129** (50 mg; 0.087 mmol), LiOH×H$_2$O (11 mg; 0.26 mmol; 3 equiv.) in THF/water (1:1 v/v; 1.5 mL) in 30 minutes and N-methylhydroxylamine×HCl (36 mg; 0.43 mmol; 5 equiv.), HATU (43 mg; 0.11 mmol; 1.3 equiv.), DIPEA (180 μL; 1.04 mmol; 12 equiv.) in DMF (1 mL) in 1 h. Product **DZA-157** was purified by reverse phase flash chromatography (10% to 50% MeCN in 0.01% TFA in water) to afford 33 mg (63%) as a white amorphous solid.

^{1}H NMR (400 MHz, MeOD) δ 8.70 (s, 1H), 7.38 – 7.29 (m, 2H), 6.98 (s, 1H), 4.76 (s, 1H), 4.54 (dd, J = 11.8, 3.8 Hz, 1H), 3.86 (d, J = 3.8 Hz, 1H), 3.43 (s, 3H), 3.29 – 3.09 (m, 3H), 3.01 – 2.91 (m, 2H), 2.88 (dd, J = 12.5, 3.8 Hz, 1H), 2.09 (sept d, J = 6.9, 3.8 Hz, 1H), 1.01 (s, 9H), 1.00 (d, J = 6.8 Hz, 3H), 0.89 (d, J = 6.8 Hz, 3H). ^{13}C NMR (101 MHz, MeOD) δ 175.8, 174.0, 164.3, 162.2, 154.9, 150.3, 145.7, 142.8, 142.6, 136.8, 135.6, 131.8, 129.6, 128.0, 126.6, 119.4, 76.8, 59.6, 56.2, 47.8, 39.2, 37.1, 34.3, 33.2, 31.8, 26.8, 19.5, 16.3. HRMS (m/z): $C_{31}H_{37}N_6O_7$ [M+H]$^+$ found: 605.2744. Calculated: 605.2724. $[α]_D^{20}$ -161 (c 1.0, MeOH).

2-[(1S,6S,9S)-6-tert-Butyl-1-cyano-9-[(2S)-2-hydroxy-3-methylbutanamido]-8-oxo-19-oxa-4,7-diazatetracyclo[9.5.2.1^2,^{5}.0^{14},^{17}]nonadeca-2,4,11,13,17-pentaen-3-yl]-N-methoxy-1,3-oxazole-4-carboxamide (DZA-158). Compound was prepared according to General procedure D from macrocycle **DZA-129** (134 mg; 0.23 mmol), LiOH×H$_2$O (51 mg; 0.68 mmol; 3 equiv.) in THF/water (1:1 v/v; 1.5 mL) in 30 minutes and O-methylhydroxylamine×HCl (36 mg; 0.43; 5 equiv.), HATU (112 mg; 0.30 mmol; 1.3 equiv.), DIPEA (180 μL; 1.04 mmol; 12 equiv.) in DMF (2 mL) in 1 h. Product **DZA-158** was purified by reverse phase flash chromatography (10% to 50% MeCN in 0.01% TFA in water) to afford 42 mg (31%) as a white amorphous solid.

^{1}H NMR (400 MHz, MeOD) δ 8.64 (s, 1H), 7.39 – 7.28 (m, 2H), 6.97 (s, 1H), 4.73 (s, 1H), 4.55 (dd, J = 11.8, 3.8 Hz, 1H), 3.86 (d, J = 3.7 Hz, 1H), 3.84 (s, 3H), 3.30 – 3.24 (m, 1H), 3.24 – 3.12 (m, 2H), 3.01 – 2.83 (m, 3H), 2.09 (sept d, J = 6.9, 3.8 Hz, 1H), 1.01 (s, 9H), 1.00 (d, J = 6.9 Hz, 3H), 0.89 (d, J = 6.9 Hz, 3H). ^{13}C NMR (101 MHz, MeOD) δ 175.8, 174.0, 164.4, 160.0, 155.8, 150.6, 144.3, 142.8, 142.5, 136.8, 136.7, 131.9, 129.7, 127.8, 126.6, 119.5, 76.8, 64.7, 59.7, 56.2, 47.8, 39.3,
60

216

39.1, 34.3, 33.2, 31.8, 26.7, 19.5, 16.3. HRMS (m/z): $C_{31}H_{37}N_6O_7$ $[M+H]^+$ found: 605.2737. Calculated: 605.2724. $[\alpha]_D^{20}$ -137 (c 1.0, MeOH).

2-[(1S,6S,9S)-6-*tert*-Butyl-1-cyano-9-[(2S)-2-hydroxy-3-methylbutanamido]-8-oxo-19-oxa-4,7-diazatetracyclo[9.5.2.1²,⁵.0¹⁴,¹⁷]nonadeca-2,4,11,13,17-pentaen-3-yl]-*N*-methoxy-*N*-methyl-1,3-oxazole-4-carboxamide (DZA-159). Compound was prepared according to General procedure D from macrocycle **DZA-129** (50 mg; 0.087 mmol), LiOH×H₂O (11 mg; 0.26 mmol; 3 equiv.) in THF/water (1:1 v/v; 1.5 mL) in 30 minutes and *N,O*-dimethylhydroxylamine (43 mg; 0.43 mmol; 5 equiv.), HATU (43 mg; 0.11 mmol; 1.3 equiv.), DIPEA (105 μL; 0.61 mmol; 7 equiv.) in DMF (1 mL) in 1 h. Product **DZA-159** was purified by reverse phase flash chromatography (10% to 50% MeCN in 0.01% TFA in water) to afford 36 mg (67%) as a white amorphous solid.

^{1}H NMR (400 MHz, MeOD) δ 8.70 (s, 1H), 7.39 – 7.25 (m, 2H), 6.97 (s, 1H), 4.74 (s, 1H), 4.55 (dd, *J* = 11.8, 3.8 Hz, 1H), 3.87 (d, *J* = 3.8 Hz, 1H), 3.86 (s, 3H), 3.45 (s, 3H), 3.29 – 3.22 (m, 1H), 3.22 – 3.09 (m, 2H), 3.04 – 2.92 (m, 2H), 2.89 (dd, *J* = 12.4, 3.8 Hz, 1H), 2.09 (sept d, *J* = 6.9, 3.8 Hz, 1H), 1.01 (s, 9H), 1.00 (d, *J* = 6.8 Hz, 3H), 0.89 (d, *J* = 6.8 Hz, 3H). ^{13}C NMR (101 MHz, MeOD) δ 175.8, 173.9, 164.3, 162.1, 155.3, 150.4, 146.0, 142.9, 142.5, 136.8, 135.5, 131.9, 129.6, 127.9, 126.6, 119.4, 76.8, 62.1, 59.6, 56.3, 55.1, 47.8, 39.2, 39.2, 34.3, 33.2, 31.8, 26.8, 19.5, 16.3. HRMS (m/z): $C_{32}H_{39}N_6O_7$ $[M+H]^+$ found: 619.2890. Calculated: 619.2880. $[\alpha]_D^{20}$ -140 (c 1.0, MeOH).

The synthesis of diazonamide A analogs DZA-132–134 and DZA-138 is shown in Scheme 14.

1,2,4-Oxadiazole-containing analogs **DZA-132–134** were prepared from analog **DZA-129** in one step in reaction with corresponding hydroxyamidine in the presence of K_2CO_3. Accordingly, analog **DZA-138** was obtained after methyl ester hydrolysis in the presence of LiOH×H₂O (Scheme 14).
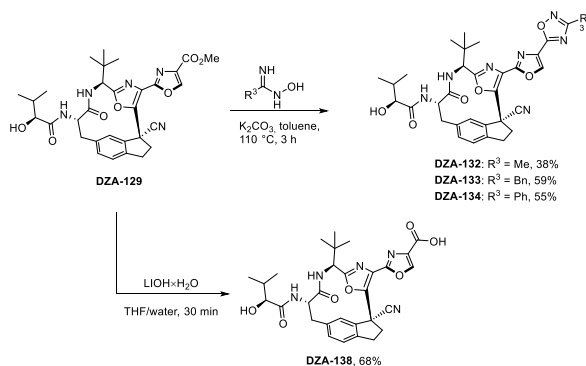
Scheme 14. Synthesis of diazonamide A analogs **DZA-132–134** and **DZA-138**

61

General procedure E (1,2,4-oxadiazole formation):

Methyl ester DZA-129 was dissolved in dry toluene and K_2CO_3, *N*-hydroxyamidine were added to the reaction mixture. The resulting suspension was stirred at 110°C to full conversion (4-10 h). The solution was diluted with aqueous saturated NH_4Cl and EtOAc. The layers were separated and the organic phase was washed with brine, dried (Na_2SO_4) and evaporated. Pure products were obtained after column chromatography.

(2*S*)-*N*-[(1*S*,6*S*,9*S*)-6-*tert*-Butyl-1-cyano-3-[4-(3-methyl-1,2,4-oxadiazol-5-yl)-1,3-oxazol-2-yl]-8-oxo-19-oxa-4,7-diazatetracyclo[9.5.2.1²,⁵.0¹⁴,¹⁷]nonadeca-2,4,11,13,17-pentaen-9-yl]-2-hydroxy-3-methylbutanamide (DZA-132). Compound was prepared according to General procedure E from macrocycle **DZA-129** (60 mg; 0.10 mmol), K_2CO_3 (42 mg; 0.31 mmol; 3 equiv.) and *N*-hydroxyacetamidine (38 mg; 0.51 mmol; 5 equiv.) in toluene (1 mL) in 4 h. Product **DZA-132** was purified by reverse phase flash chromatography (10% to 70% MeCN in water) to afford 24 mg (38%) as a white amorphous solid.

^{1}H NMR (400 MHz, MeOD) δ 8.99 (s, 1H), 7.39 – 7.31 (m, 2H), 7.02 (s, 1H), 4.76 (s, 1H), 4.56 (dd, *J* = 11.8, 3.8 Hz, 1H), 3.87 (d, *J* = 3.8 Hz, 1H), 3.36 – 3.25 (m, 1H, overlapping with MeOD), 3.24 – 3.11 (m, 2H), 3.06 – 2.94 (m, 2H), 2.90 (dd, *J* = 12.4, 3.8 Hz, 1H), 2.47 (s, 3H), 2.09 (sept d, *J* = 6.9, 3.8 Hz, 1H), 1.02 (s, 9H), 1.01 (d, *J* = 6.9 Hz, 3H), 0.90 (d, *J* = 6.9 Hz, 3H). ^{13}C NMR (101 MHz, MeOD) δ 175.8, 174.0, 170.3, 169.1, 164.3, 157.1, 150.9, 144.6, 142.9, 142.3, 136.8, 131.9, 130.3, 129.7, 127.6, 126.6, 119.4, 76.8, 59.6, 56.3, 47.8, 39.19, 39.15, 34.4, 33.2, 31.8, 26.8, 19.5, 16.3, 11.3. HRMS (m/z): $C_{32}H_{36}N_7O_6$ [M+H]$^+$ found: 614.2766. Calculated: 614.2727. $[\alpha]_D^{20}$ -164 (c 1.0, MeOH).

(2*S*)-*N*-[(1*S*,6*S*,9*S*)-3-[4-(3-Benzyl-1,2,4-oxadiazol-5-yl)-1,3-oxazol-2-yl]-6-*tert*-butyl-1-cyano-8-oxo-19-oxa-4,7-diazatetracyclo[9.5.2.1²,⁵.0¹⁴,¹⁷]nonadeca-2,4,11,13,17-pentaen-9-yl]-2-hydroxy-3-methylbutanamide (DZA-133). Compound was prepared according to General procedure E from macrocycle **DZA-129** (55 mg; 0.093 mmol), K_2CO_3 (39 mg; 0.28 mmol; 3 equiv.) and *N*-hydroxy-2-phenylethanimidamide (70 mg; 0.47 mmol; 5 equiv.) in toluene (1 mL) in 10 h. Product **DZA-133** was purified by reverse phase flash chromatography (10% to 70% MeCN in water) to afford 38 mg (59%) as a white amorphous solid.

^{1}H NMR (400 MHz, DMSO-*d₆*) δ 9.38 (s, 1H), 8.40 (d, *J* = 7.9 Hz, 1H), 7.62 (d, *J* = 8.4 Hz, 1H), 7.38 – 7.34 (m, 4H), 7.32 – 7.29 (m, 2H), 7.30 – 7.25 (m, 1H), 6.99 (s, 1H), 5.42 (d, *J* = 6.1 Hz, 1H), 4.74 (d, *J* = 7.8 Hz, 1H), 4.52 (ddd, *J* = 11.9, 8.4, 3.9 Hz, 1H), 4.21 (s, 2H), 3.72 (dd, *J* = 6.1, 3.9 Hz, 1H), 3.26 – 3.14 (m, 1H), 3.10 – 2.96 (m, 3H), 2.93 – 2.76 (m, 2H), 1.99 (sept d, *J* = 6.8, 3.8 Hz, 1H), 0.96 (s, 9H), 0.90 (d, *J* = 6.8 Hz, 4H), 0.79 (d, *J* = 6.8 Hz, 4H). ^{13}C NMR (101 MHz, DMSO-*d₆*) δ
62

172.4, 171.8, 170.0, 168.7, 162.9, 155.0, 148.3, 144.5, 140.9, 140.2, 135.6, 135.5, 130.7, 129.0, 128.7, 128.2, 128.1, 127.0, 125.3, 125.3, 118.6, 74.8, 57.0, 54.3, 45.7, 38.1, 36.5, 33.1, 31.5, 31.3, 30.5, 26.2, 19.1, 16.2. HRMS (m/z): $C_{38}H_{40}N_7O_6$ [M+H]$^+$ found: 690.3021. Calculated: 690.3040. $[\alpha]_D^{20}$ -126 (c 1.0, MeOH).

(2S)-N-[(1S,6S,9S)-6-tert-Butyl-1-cyano-8-oxo-3-[4-(3-phenyl-1,2,4-oxadiazol-5-yl)-1,3-oxazol-2-yl]-19-oxa-4,7-diazatetracyclo[9.5.2.1²,⁵.0¹⁴,¹⁷]nonadeca-2,4,11,13,17-pentaen-9-yl]-2-hydroxy-3-methylbutanamide (DZA-134). Compound was prepared according to General procedure E from macrocycle **DZA-129** (60 mg; 0.10 mmol), K_2CO_3 (42 mg; 0.31 mmol; 3 equiv.) and benzamidoxime (69 mg; 0.51 mmol; 5 equiv.) in toluene (1 mL) in 10 h. Product **DZA-134** was purified by reverse phase flash chromatography (10% to 70% MeCN in water) to afford 38 mg (55%) as a white amorphous solid.

^{1}H NMR (400 MHz, DMSO-d_6) δ 9.50 (s, 1H), 8.42 (d, J = 7.9 Hz, 1H), 8.16 – 8.02 (m, 2H), 7.70 – 7.55 (m, 4H), 7.39 – 7.24 (m, 2H), 7.01 (s, 1H), 5.43 (d, J = 6.1 Hz, 1H), 4.76 (d, J = 7.8 Hz, 1H), 4.54 (ddd, J = 11.9, 8.4, 3.9 Hz, 1H), 3.73 (dd, J = 6.1, 3.9 Hz, 1H), 3.28 – 3.17 (m, 1H), 3.13 – 3.06 (m, 2H), 3.02 (dd, J = 11.9, 11.9 Hz, 1H), 2.96 – 2.85 (m, 1H), 2.82 (dd, J = 12.3, 3.9 Hz, 1H), 2.06 – 1.92 (m, 1H), 0.97 (s, 9H), 0.91 (d, J = 6.9 Hz, 3H), 0.80 (d, J = 6.9 Hz, 3H). ^{13}C NMR (101 MHz, DMSO-d_6) δ 172.5, 171.8, 169.1, 168.3, 162.9, 155.2, 148.4, 144.7, 140.9, 140.2, 135.5, 131.9, 130.7, 129.4, 128.18, 128.16, 127.2, 125.8, 125.4, 125.3, 118.7, 74.9, 57.1, 54.3, 45.8, 38.1, 36.6, 33.1, 31.5, 30.5, 26.2, 19.1, 16.2. HRMS (m/z): $C_{37}H_{38}N_7O_6$ [M+H]$^+$ found: 676.2897. Calculated: 676.2884. $[\alpha]_D^{20}$ -121 (c 1.0, MeOH).

2-[(1S,6S,9S)-6-tert-Butyl-1-cyano-9-[(2S)-2-hydroxy-3-methylbutanamido]-8-oxo-19-oxa-4,7-diazatetracyclo[9.5.2.1²,⁵.0¹⁴,¹⁷]nonadeca-2,4,11,13,17-pentaen-3-yl]-1,3-oxazole-4-carboxylic acid (DZA-138). Methyl ester **DZA-129** (33 mg; 0.056 mmol) was dissolved in THF (0.5 mL). Separately solid LiOH×H_2O (7 mg; 0.17 mmol; 3 equiv.) was dissolved in water (0.2 mL) and added to the reaction mixture. Emulsion was stirred at room temperature for 30 min, then aqueous 1N HCl was added. The resulting mixture was extracted with EtOAc (×2), combined organic layers were washed with brine, dried (Na_2SO_4) and evaporated. The resulting white amorphous solid was purified with reverse phase flash chromatography (10% to 50% MeCN in 0.01% TFA in water) to give carboxylic acid **DZA-138** (22 mg; 68%) as a white amorphous solid.

^{1}H NMR (400 MHz, MeOD) δ 8.71 (s, 1H), 7.43 – 7.25 (m, 2H), 6.98 (s, 1H), 4.75 (s, 1H), 4.54 (dd, J = 11.8, 3.8 Hz, 1H), 3.86 (d, J = 3.8 Hz, 1H), 3.29 – 3.10 (m, 3H), 3.02 – 2.92 (m, 2H), 2.88 (dd, J = 12.4, 3.8 Hz, 1H), 2.08 (sept d, J = 13.4, 6.9, 3.8 Hz, 1H), 1.01 (s, 9H), 1.00 (d, J = 6.9 Hz, 3H), 0.89 (d, J = 6.9 Hz, 3H). ^{13}C NMR (101 MHz, MeOD) δ 175.8, 174.0, 164.4, 163.6, 156.2, 150.5,

63

146.7, 142.9, 142.5, 136.8, 136.0, 131.9, 129.6, 127.8, 126.6, 119.4, 76.8, 59.6, 56.2, 47.8, 39.18, 39.15, 34.3, 33.2, 31.8, 26.8, 19.5, 16.3. HRMS (m/z): $C_{30}H_{34}N_5O_7$ [M+H]$^+$ found: 576.2470. Calculated: 576.2458. $[\alpha]_D^{20}$ -135 (c 1.0, MeOH).

Antiproliferative activity *in vitro*

Anticancer activity of all synthesized compounds above was tested *in vitro* using cytotoxicity assay. Thus, monolayer tumor cell lines A2058 (metastatic melanoma), U937 (myeloid leukemia), MDA-MB-231 (breast adenocarcinoma), MDA-MB-435 (metastatic melanoma) and non-cancer HEK-293 (human embryonic kidney cells) were cultured in standard medium DMEM (Dulbecco' s modified Eagle's medium) ("Sigma") supplemented with 10% fetal bovine serum ("Sigma"). About 2-9 10^4 cells/mL (depending on line nature) were placed in 96-well plates immediately after compounds were added to the wells. Untreated cells were used as a control. The plates were incubated for 72 h, 37 °C, 5% CO_2. The number of surviving cells was determined using 3-(4,5-dimethylthiazol-2-yl)-2,5-diphenyltetrazolinium bromide (MTT). MTT-test: after incubating culture medium was removed and 200 μL fresh medium with 10 mM HEPES was added in each well of the plate, than 20 μL MTT (2mg/mL in HBSS) was added. After incubation (3 hr, 37°C, 5% CO_2), the medium with MTT was removed and 200 μL DMSO were added at once to each sample. The samples were tested at 540 nm on Anthos HT II photometer. The results of cell culture-based studies are summarized in Table 2.

All compounds were tested on A2058 (metastatic melanoma) cell line. Then compounds with highest cytotoxicity against this line were further tested on U937 (myeloid leukemia), MDA-MB-231 (breast adenocarcinoma), MDA-MB-435 (metastatic melanoma) and non-cancer HEK-293 (human embryonic kidney cells). In general, tested compounds showed medium or low cytotoxicity against tumor cells. In partucular the series of compounds were most cytotoxic against melanoma cell lines. Notably, almost all derivatives are low toxic to normal HEK-293 cells showing high selectivity ($\geq$ 10-fold). Compounds containing ester moiety at the oxazole have lower IC_{50} compaired to those with different functional groups. **DZA-129** has the lowest IC_{50} values against all cancer cells. However, the compound also has low selectivity against normal cell line. Compound **DZA-174** in partucular has highest selectivity against cancer cells compared to normal cell line indicating potential for future preclinical studies. Overall the selectivity against melanoma cancer cell lines makes the series of compounds very promising as anticancer agents.

65

Table 2. Cell viability data. In vitro cytotoxicity of diazonamide analogs on human tumor cell lines: A2058 (metastatic melanoma), U937 (myeloid leukemia), MDA-MB-231 (breast adenocarcinoma), MDA-MB-435 (metastatic melanoma) and non-cancer HEK-293 (human embryonic kidney cells).

#	Compound #	Cytotoxicity IC$_{50}$, nM				
		A2058	U937	MDA-MB-231	MDA-MB-435	HEK-293
1	Vinorelbine	2.41±0.21	4.21±0.61	4.50±0.42	n/a	48.0±11.3
2	DZA-129	12.9±1.9	1.93±0.7	130.6±20.7	40.09±6.0	190.9±24.3
3	DZA-132	186±16	157±2	n/a	n/a	>1000
4	DZA-133	687±79	729±75	n/a	n/a	>1000
5	DZA-134	156±18	110±8	n/a	n/a	>1000
6	DZA-135	20.4±1.3	22.2±1.2	n/a	n/a	>1000
7	DZA-137	167.4±16.5	64.94±9.3	>1000	299.4±59.9	>1000
8	DZA-138	>1000	>1000	>1000	>1000	>1000
9	DZA-139	12.37±1.5	9.71±2.1	290.2±42.5	n/a	324.9±79.0
10	DZA-140	>1000	261±65.9	>1000	n/a	>1000

11	DZA-141	958.7±130.4	214±47	>1000	n/a	>1000
12	DZA-142	643.4±91.7	692.3±20.2	>1000	n/a	>1000
13	DZA-143	68.19±10.8	22.45±4.6	n/a	n/a	540.4±66.7
14	DZA-144	574.2±76.1	100.8±22.6	n/a	n/a	>1000
15	DZA-145	>1000	>1000	n/a	n/a	>1000
16	DZA-146	>1000	177.9±40.6	>1000	n/a	n/a
17	DZA-147	792.5±223.3	40.86±10.3	>1000	n/a	n/a
18	DZA-148	541.0±182.1	94.7±17.5	>1000	n/a	n/a
19	DZA-149	202.7±53.0	136.3±45.0	>1000	n/a	n/a
20	DZA-150	>1000	n/a	n/a	n/a	n/a
21	DZA-151	>1000	175	>1000	n/a	n/a
22	DZA-152	>1000	n/a	n/a	n/a	n/a
23	DZA-153	>1000	n/a	n/a	n/a	n/a

24	DZA-154	>1000	n/a	>1000	n/a	>1000
25	DZA-156	>1000	n/a	>1000	n/a	>1000
26	DZA-157	212.3±54.6	n/a	>1000	n/a	>1000
27	DZA-158	864.6±190.8	n/a	>1000	n/a	>1000
28	DZA-159	220.9±51.6	n/a	>1000	n/a	>1000
29	DZA-160	319.4±105.2	n/a	>1000	n/a	>1000
30	DZA-161	60.1±8.9	n/a	432.9±54.5	62.05±8.9	>1000
31	DZA-162	>1000	n/a	>1000	n/a	n/a
32	DZA-163	100.3±10.0	n/a	736.2±176.1	n/a	n/a
33	DZA-164	>1000	n/a	>1000	n/a	n/a
34	DZA-165	>1000	n/a	>1000	n/a	n/a
35	DZA-168	235.3±35.3	n/a	526.7±57.2	130.5±19.2	>1000
36	DZA-174	90.78±16.52	n/a	n/a	80.8±10.88	>1000

| 37 | DZA-175 | 480.1±86.7 | n/a | n/a | 402.9±85.9 | 902.7±188.6 |
| 38 | DZA-176 | 328.8±104.0 | n/a | n/a | 334.8±36.8 | 591.8±135.0 |

Tubulin polymerization assay

An *in vitro* tubulin polymerization assay was performed to evaluate the effect of the series on microtubule dynamics. In the assay, enhancer (paclitaxel) control self-polymerization of soluble α/β-tubulin dimer to insoluble oligomers under buffered conditions is monitored by measuring changes in light scattering at 340 nm. A slope was calculated for the linear growth phase of the tubulin polymerization curve to render a comparison across the series more convenient (see Table 3). Enhancer control tubulin self-polymerization was measured in the presence of the previously synthesized analogs DZA.[1] To verify the correlation between antiproliferative activity of the macrocycles and effect they exert on tubulin polymerization dynamics, poorly cytotoxic macrocycles and analogs with the highest antiproliferative activities were examined. Finally, vinorelbine was also tested as the assay positive control (see Figure 1 Enhancer control tubulin self-polymerization assay results for macrocycles DZA-129, DZA-137, DZA-138, DZA-141, DZA-145, DZA-147, DZA-156, DZA-161, DZA-163, DZA-165, DZA-168, DZA-174, DZA-175 and vinorelbine (VNB) as a positive conrol of the assay.).

Table 3. Tubulin polymerization assay results.

Entry	Ligand[a]	Slope[b]	R^2 fit
1	Control	1.000	0.999
2	Vinorelbine (VNB)	0.010	0.999
3	DZA-129	0.021	0.999
4	DZA-137	0.061	0.998
5	DZA-138	0.019	0.999
6	DZA-141	0.058	0.998
7	DZA-145	0.551	0.999
8	DZA-147	0.075	0.999
9	DZA-156	0.040	0.999
10	DZA-161	0.040	0.999
11	DZA-163	0.033	0.999
12	DZA-165	0.0198	0.999
13	DZA-168	0.1979	0.999
14	DZA-174	0.0074	0.999
15	DZA-175	0.0459	0.979

[a] 2:1 tubulin:ligand ratio;

[b] Slope values are relative to that of control (entry 1)

---

[1] The assay was conducted following Enhancer Control Polymerization Assay Method from Tubulin Polymerization Assay Kit manual by Cytoskeleton, Inc. (https://www.cytoskeleton.com/pdf-storage/datasheets/bk004p.pdf)

70

226

Plasma stability assay

Stock solutions (100 μM) of test compound, propantheline bromide (positive control) and verapamil (negative control) are prepared in dimethyl sulfoxide (DMSO).

The assay procedure is performed in microcentrifuge tubes (1.5 mL). Mouse plasma with heparin (Innovative Research, Inc., Cat # IGMSCD1PLANAH50ML-36650, 495 μL in each tube) was pre-incubated at 37 °C for 10 minutes. Afterwards, 5 μL of stock solution (100 μM) was added. The spiked plasma samples containing 1 μM of a compound and 1 % of DMSO were incubated at 37 °C for 2 hours. Aliqouts of 20 μL were collected at 0, 15, 30, 60 and 120 min and added to 180 μL of 3:1 acetonitrile:methanol, containing reserpine as an internal standard. The samples were centrifuged at 10000 rpm for 10 min and 150 μL of supernatant was diluted with 300 μL of 0.1 % formic acid for LC-MS/MS analysis.

The samples were analyzed by LC-MS/MS according to standard procedures on the Waters XevoTQ-Smicro system. Mass spectrometric settings were optimized for each of test compound. Chromatographic separation was performed on C18 BEH 1.7μm column (2×50mm).

The calculated peak area response ratio (peak area corresponding to test compound divided by that of an analytical internal standard) was normalized (% of response at 0h) and plotted against the incubation time.

Table 4. Plasma stability data

	% of a compound found				
	0 min	15 min	30 min	60 min	120 min
% of **DZA-174** found	100. 0	95.8	94.2	96.9	96.4
% of **DZA-161** found	100.0	0.2	-	-	-
% of **DZA-143** found	100.0	55.3	27.6	10.2	1.0
% of **DZA-137** found	100.0	100.4	103.2	103.3	104.8
% of **DZA-129** found	100.0	-	-	-	-

Cell cycle studies. MDA-MB-435 cells were seeded in 24-well plates at a density of 1×10^5 cells/mL. The cells were then allowed to rest and adhere to the plate for 5 hours. Subsequently, cells were treated with equitoxic concentrations (IC_{90}) of vinorelbine and **DZA-174** for 4, 8 and 24 hours.

Flow cytometry analysis of cell cycle progression of MDA-MB-435 cells after incubation with **DZA-174** (200 nM) for up to 24 hours. Quantitative results of the effects of **DZA-174** on cell distribution among phases of the cell cycle in comparison with equitoxic concentration (30 nM) of vinorelbine

71

(bottom) (Fig.2). The data are presented as the mean ± SEM of three independent experiments in triplicate.

To assess the distribution of cells between cell cycle phases, we performed cell cycle analysis using quantification of DNA content with the commercially available kit (Abcam, ab139418) according to the manufacturer's instructions. In brief, after incubation with the test compounds, cells were harvested using trypsin, washed with PBS, and fixed with 66% ice-cold ethanol. After fixation, cells were washed with PBS, and incubated with propidium iodide (PI) (50 μg/mL) and RNase (550 U/mL) solution for 30 min in the dark at 37 ° C. After incubation, the cells were transferred to ice and prepared for flow cytometry analysis using the BD FACS Melody Cell Sorter (BD Biosciences, San Jose, CA, USA). Quantitative results are expressed as the mean ± SEM. All experiments were carried out in triplicate with three technical replicates.

References

[1] Sung, H.; Ferlay, J.; Siegel, R. L.; Laversanne, M.; Soerjomataram, I.; Jemal, A.; Bray, F. Global Cancer Statistics 2020: GLOBOCAN Estimates of Incidence and Mortality Worldwide for 36 Cancers in 185 Countries. *CA A Cancer J Clin* **2021**, *71* (3), 209–249.

[2] Vaidya, F. U.; Sufiyan Chhipa, A.; Mishra, V.; Gupta, V. K.; Rawat, S. G.; Kumar, A.; Pathak, C. Molecular and Cellular Paradigms of Multidrug Resistance in Cancer. *Cancer Reports* **2022**, *5* (12). https://doi.org/10.1002/cnr2.1291.

[3] Cruz-Monserrate, Z. Diazonamide A and a Synthetic Structural Analog: Disruptive Effects on Mitosis and Cellular Microtubules and Analysis of Their Interactions with Tubulin. *Molecular Pharmacology* **2003**, *63* (6), 1273–1280.

[4] Wei, Q.; Zhou, M.; Xu, X.; Caldwell, C.; Harran, S.; Wang, L. Diazonamide Analogs. US8846734B2, September 30, 2014.

[5] Wieczorek, M.; Tcherkezian, J.; Bernier, C.; Prota, A. E.; Chaaban, S.; Rolland, Y.; Godbout, C.; Hancock, M. A.; Arezzo, J. C.; Ocal, O.; et al. The Synthetic Diazonamide DZ-2384 Has Distinct Effects on Microtubule Curvature and Dynamics without Neurotoxicity. *Science Transl. Med.* **2016**, *8* (365), 365ra159.

[6] Ding, H.; DeRoy, P. L.; Perreault, C.; Larivée, A.; Siddiqui, A.; Caldwell, C. G.; Harran, S.; Harran, P. G. Electrolytic Macrocyclizations: Scalable Synthesis of a Diazonamide-Based Drug Development Candidate. *Angew. Chem. Int. Ed.* **2015**, *54* (16), 4818-4822.

[7] Vitkovska, V.; Zogota, R.; Kalnins, T.; Zelencova, D.; Suna, E. Aliphatic chain-containing macrocycles as diazonamide A analogs. *Chem. Heterocycl. Comp.* **202**0, *56*, 586–602.

[8] Kalnins, T.; Kazak, M.; Vitkovska, V.; Narvaiss, N.; Zelencova, D.; Jaudzems, K.; Suna, E. WO/2021/130515, PCT/IB2019/061264.

[9] Bernier, C.; Soliman, A.; Gravel, M.; Dankner, M.; Savage, P.; Petrecca, K.; Park, M.; Siegel, P. M.; Shore, G. C.; Roulston, A. DZ-2384 Has a Superior Preclinical Profile to Taxanes for the Treatment of Triple-Negative Breast Cancer and Is Synergistic with Anti-CTLA-4 Immunotherapy. *Anticancer Drugs* **2018**, *29* (8), 774–785.

[10] Tuttle, J. B.; Azzarelli, J. M.; Bechle, B. M.; Dounay, A. B.; Evrard, E.; Gan, X.; Ghosh, S.; Henderson, J.; Kim, J.-Y.; Parikh, V. D.; Verhoest, P. R. Synthesis of Ortho-Substituted Nitroaromatics via Improved Negishi Coupling Conditions. *Tetrahedron Letters* **2011**, *52* (41), 5211–5213.

[11] Kazak, M.; Vasilevska, A.; Suna, E. Preparative scale synthesis of functionalized bioxazole. *Chem. Heterocycl. Comp.* **2020**, *56*, 355–364.

73

Abstract

The present invention relates to the field of chemistry and biochemistry and in particular to the novel anticancer compounds, more particularly to antiproliferative agents and microtubule polymerization inhibitors. Even more particularly, the invention relates to novel analogs of natural antimitotic agent diazonamide A and to salts, pharmaceutical compositions, conjugates and a process of manifacture thereof and the potential use of the novel compounds for treatment of melanoma. A new series of compounds with high activity against cancer cells has been developed. The most active compounds from the series show cytotoxicity against several cancer cell lines with $IC_{50} = 12$–90 nM.

I hereby declare and confirm with my signature that the doctoral thesis "Simplified analogs of diazonamide A as anticancer agents" is exclusively the result of my own autonomous work based on my research and literature published, which is seen in the notes and bibliography used. I also declare that no part of the submitted doctoral thesis has been made in an inappropriate way, whether by plagiarizing or infringing on any third person's copyright. Finally, I declare that no part of the submitted doctoral thesis has been used for any other thesis in another higher education institution, research institution or educational institution.

Author: Viktorija Vitkovska

Signature _____

Supervisor: Dr. chem., prof. Edgars Sūna

Signature _____

Thesis submitted in the Promotion Council in Chemistry of University of Latvia for the commencement of the degree of Doctor of Chemistry on _____.

Secretary of the Promotion Council: Vita Rudoviča _____

Thesis defended at the session of Promotion Council in Chemistry of University of Latvia for the commencement of the degree of Doctor of Chemistry on _____, protocol No. _____.

Secretary of the Promotion Council: Vita Rudoviča _____

Viktorija was born in 1994 in Riga, Latvia. She obtained a Bachelor's degree in Chemical Technology from Riga Technical University (2017) and a Master's degree in Chemistry from University of Latvia (2019), where she defended her thesis on the "Synthesis of Macrocyclic Diazonamide A Analogs" under the supervision of Prof. E. Suna. During her Master's studies, Viktorija spent a semester at Ruhr University Bochum (Germany) in the Faculty of Chemistry and Biochemistry as a part of the ERASMUS+ program. In 2019, Viktorija began her PhD studies at University of Latvia, conducting research under the supervision of Prof. E. Suna at the Latvian Institute of Organic Synthesis. From 2019 to 2022, Viktorija was awarded the "MikroTik" scholarship for PhD students in the fields of Natural Sciences, Medicine, and Life Sciences, administered by the University of Latvia Foundation. Her research focuses on medicinal chemistry, specifically on developing new structural analogs of natural compounds with the potential to become novel anticancer drugs. The results of her work have been published in two internationally cited journals, and she has received multiple awards at both local and international conferences.